Methods in Molecular Biology 2178

Springer Protocols

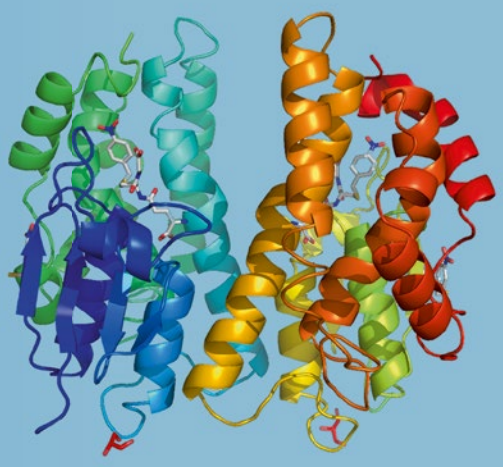

Nikolaos E. Labrou *Editor*

Protein Downstream Processing

Design, Development, and Application of High and Low-Resolution Methods

Second Edition

Humana Press

METHODS IN MOLECULAR BIOLOGY

Series Editor
John M. Walker
School of Life and Medical Sciences
University of Hertfordshire
Hatfield, Hertfordshire, UK

For further volumes:
http://www.springer.com/series/7651

For over 35 years, biological scientists have come to rely on the research protocols and methodologies in the critically acclaimed *Methods in Molecular Biology* series. The series was the first to introduce the step-by-step protocols approach that has become the standard in all biomedical protocol publishing. Each protocol is provided in readily-reproducible step-by-step fashion, opening with an introductory overview, a list of the materials and reagents needed to complete the experiment, and followed by a detailed procedure that is supported with a helpful notes section offering tips and tricks of the trade as well as troubleshooting advice. These hallmark features were introduced by series editor Dr. John Walker and constitute the key ingredient in each and every volume of the *Methods in Molecular Biology* series. Tested and trusted, comprehensive and reliable, all protocols from the series are indexed in PubMed.

Protein Downstream Processing

Design, Development, and Application of High and Low-Resolution Methods

Second Edition

Edited by

Nikolaos E. Labrou

Laboratory of Enzyme Technology, Department of Biotechnology, School of Applied Biology and Biotechnology, Agricultural University of Athens, Athens, Greece

Humana Press

Editor
Nikolaos E. Labrou
Laboratory of Enzyme Technology
Department of Biotechnology
School of Applied Biology
and Biotechnology
Agricultural University of Athens
Athens, Greece

ISSN 1064-3745 ISSN 1940-6029 (electronic)
Methods in Molecular Biology
ISBN 978-1-0716-0774-9 ISBN 978-1-0716-0775-6 (eBook)
https://doi.org/10.1007/978-1-0716-0775-6

This Humana imprint is published by the registered company Springer Science+Business Media, LLC, part of Springer Nature.
The registered company address is: 1 New York Plaza, New York, NY 10004, U.S.A.

Preface

Proteins are the most diverse group of biomolecules that are vital for cellular structure and function. The technological advances in the omics area and the efforts in proteomics research have increased the rate of discovering many new proteins with unknown structure and function. These newly discovered proteins present enormous opportunities for research and industrial application. The key factor for their commercial exploitation depends on the development of an efficient and effective purification procedure. However, with thousands of proteins—each displaying unique characteristics—the development of purification strategies that deliver the required purity needed for downstream applications is important. The challenge, therefore, is to separate the protein of interest from all of the other components in the cell, especially the unwanted contaminating proteins, with reasonable efficiency, speed, and yield, while retaining the biological activity and chemical integrity of the polypeptide. The increasing requirement for the production of pure proteins is forcing scientists to gain a thorough understanding of protein purification methods and gain abilities and knowledge to improve current and develop new and more effective purification methods and protocols.

This volume, which is the second edition of Vol. 1129 (2014), is designed to give the laboratory worker the information needed to design and implement a successful purification strategy. It presents reliable and robust protocols in a concise form, emphasizing the critical aspects on practical problems and questions encountered at the lab bench. Written in the highly successful Methods in Molecular Biology series format, each chapter provides introductory material with an overview of the topic of interest; a description of methods, materials, and reagents; readily reproducible step-by-step protocols, a Notes section for tips on troubleshooting; and a collection of published data with an extensive list of references for further details.

This volume consists of thirty chapters. It is divided in five parts (I–V), each of which dealing with different approaches and methods. Part I starts with an overview of screening and design of purification strategies and covers initial aspects on high-throughput screening, methods development, and media selection. Parts II and III of this volume concentrate on low- and high-resolution protein purification methods that currently enjoy frequent citation in the literature with the emphasis being on affinity chromatography. Information on scale-up considerations is given where appropriate. Aside from methods related directly to purification, this volume includes a description of analytical techniques of value in protein preparation. For example, much space has been allowed in Part IV on cutting-edge analytical techniques of purified proteins. The last section (Part V) presents a few selected examples and case studies.

It is impossible for a single book volume to cover all of the different methods, techniques, and applications of protein purification in which scientists have made significant progress. Thus, I have selected key examples covering a wide range of diverge scientific disciplines and state-of-the-art experimental approaches, in order to provide the reader with a representative sample of current status of the field.

The present book would definitely be an ideal source of scientific information to advanced students, junior researchers, and scientists involved in health sciences, cellular and molecular biology, biochemistry, biotechnology, and other related areas in both academia and industry.

I sincerely hope that the reader will enjoy the information provided in this book and find its contents interesting and scientifically stimulating. I also hope that I have established a successful compilation of chapters within the exciting area of protein purification. I would like to thank all contributing authors for their enthusiasm and for the time they spent preparing the chapters for this book. I would also like to thank Dr. John Walker, the series editor, for putting forward the idea of the book and for his help and encouragement, and everybody at Springer for their helpful advice, support, and professionalism. Without their cooperation, this volume would have not seen the light. Last but not least, I would especially like to thank my family for their understanding and patience during the editing and organization of the chapters.

Athens, Greece *Nikolaos E. Labrou*

Contents

Contributors

Shilpi Agrawal • *Department of Chemistry and Biochemistry, University of Arkansas, Fayetteville, AR, USA*

Oscar Aguilar • *Tecnologico de Monterrey, Escuela de Ingenieria y Ciencias, Monterrey, Mexico*

Musaab Al-Ameer • *Department of Chemistry and Biochemistry, University of Arkansas, Fayetteville, AR, USA*

F. Albericio • *Peptide Science Laboratory, School of Chemistry and Physics, University of KwaZulu-Natal, Durban, South Africa; CIBER-BBN, Networking Centre on Bioengineering, Biomaterials & Nanomedicine, Department of Organic Chemistry, University of Barcelona, Barcelona, Spain*

Mikael Åstrand • *Division of Protein Technology, School of Engineering Sciences in Chemistry, Biotechnology and Health, KTH/AlbaNova University Center, Stockholm, Sweden*

Dev Baines • *Astrea Bioseparations Ltd, Cambridge, UK*

G. R. Barredo • *Cátedra de Biotecnología, Facultad de Farmacia y Bioquímica, Universidad de Buenos Aires, Buenos Aires, Argentina; Instituto de Nanobiotecnología (NANOBIOTEC), Facultad de Farmacia y Bioquímica, CONICET-Universidad de Buenos Aires, Buenos Aires, Argentina*

Íris L. Batalha • *UCIBIO, Departamento de Química, Faculdade de Ciências e Tecnologia, Universidade Nova de Lisboa, Caparica, Portugal; Nanoscience Centre, Department of Engineering, University of Cambridge, Cambridge, UK*

R. Bhambure • *Department of Chemical Engineering, Indian Institute of Technology, New Delhi, India*

Mariachiara Bianco • *Dipartimento di Chimica, Università degli Studi di Bari "Aldo Moro", Bari, Italy*

Charlotte Cabanne • *Bordeaux INP, CBMN, UMR 5248, Pessac, France*

Cosima D. Calvano • *Centro Interdipartimentale di Ricerca SMART, Dipartimento di Farmacia- Scienze del Farmaco, Università degli Studi di Bari "Aldo Moro", Bari, Italy*

S. A. Camperi • *Cátedra de Biotecnología, Facultad de Farmacia y Bioquímica, Universidad de Buenos Aires, Buenos Aires, Argentina; Instituto de Nanobiotecnología (NANOBIOTEC), Facultad de Farmacia y Bioquímica, CONICET-Universidad de Buenos Aires, Buenos Aires, Argentina*

O. Cascone • *Cátedra de Biotecnología, Facultad de Farmacia y Bioquímica, Universidad de Buenos Aires, Buenos Aires, Argentina; Instituto de Nanobiotecnología (NANOBIOTEC), Facultad de Farmacia y Bioquímica, CONICET-Universidad de Buenos Aires, Buenos Aires, Argentina*

Tommaso R. I. Cataldi • *Centro Interdipartimentale di Ricerca SMART, Università degli Studi di Bari "Aldo Moro", Bari, Italy; Dipartimento di Chimica, Università degli Studi di Bari "Aldo Moro", Bari, Italy*

Tao Chen • *Technology and Process Development (TPD), WuXi Biologics, Shanghai, China*

Paul Christakopoulos • *Biochemical Process Engineering, Chemical Engineering, Department of Civil, Environmental and Natural Resources Engineering, Luleå University of Technology, Luleå, Sweden*

Evangelia G. Chronopoulou • *Laboratory of Enzyme Technology, Department of Biotechnology, School of Applied Biology and Biotechnology, Agricultural University of Athens, Athens, Greece*

Karolina Corin • *Department of Chemistry and Biochemistry, UCLA-DOE Institute, Molecular Biology Institute, University of California, Los Angeles, CA, USA*

Ario de Marco • *University of Nova Gorica (UNG), Rožna Dolina (Nova Gorica), Slovenia*

Salvatore G. De-Simone • *FIOCRUZ, Center for Technological Development in Health (CDTS)/National Institute of Science and Technology for Innovation on Neglected of Population Diseases (INCT-INDP), Rio de Janeiro, RJ, Brazil; FIOCRUZ, Oswaldo Cruz Institute, Laboratory of Experimental and Computational Biochemistry of Pharmaceuticals, Rio de Janeiro, RJ, Brazil; Department of Cellular and Molecular Biology, Biology Institute, Federal Fluminense University, Niterói, RJ, Brazil*

Ana M. G. C. Dias • *UCIBIO, Departamento de Química, Faculdade de Ciências e Tecnologia, Universidade Nova de Lisboa, Caparica, Portugal*

Eduarda Dráberová • *Laboratory of Biology of Cytoskeleton, Institute of Molecular Genetics of the Czech Academy of Sciences, Prague, Czech Republic*

Pavel Dráber • *Laboratory of Biology of Cytoskeleton, Institute of Molecular Genetics of the Czech Academy of Sciences, Prague, Czech Republic*

Pierpaolo Falcicchio • *Laboratory of Microbiology, Wageningen University, Wageningen, The Netherlands*

Manasia Gaikwad • *Institute of Clinical Chemistry and Laboratory Medicine, Mass Spectrometric Proteomics Group, University Medical Center Hamburg-Eppendorf, Hamburg, Germany*

Nikolaos Georgakis • *Laboratory of Enzyme Technology, Department of Biotechnology, School of Applied Biology and Biotechnology, Agricultural University of Athens, Athens, Greece*

S. L. Giudicessi • *Cátedra de Biotecnología, Facultad de Farmacia y Bioquímica, Universidad de Buenos Aires, Buenos Aires, Argentina; Instituto de Nanobiotecnología (NANOBIOTEC), Facultad de Farmacia y Bioquímica, CONICET-Universidad de Buenos Aires, Buenos Aires, Argentina*

Jessica J. Gomez-Lugo • *Facultad de Ciencias Quimicas, Universidad Autonoma de Nuevo Leon, San Nicolas de los Garza, NL, Mexico*

Ravi Kumar Gundampati • *Department of Chemistry and Biochemistry, University of Arkansas, Fayetteville, AR, USA*

Gaili Guo • *Technology and Process Development (TPD), WuXi Biologics, Shanghai, China*

My Hedhammar • *KTH Royal Institute of Technology, School of Engineering Sciences in Chemistry, Biotechnology and Health (CBH), Department of Protein Science, AlbaNova University Centre, Stockholm, Sweden*

Laura Heikaus • *Institute of Clinical Chemistry and Laboratory Medicine, Mass Spectrometric Proteomics Group, University Medical Center Hamburg-Eppendorf, Hamburg, Germany*

Erick Heredia-Olea • *Tecnologico de Monterrey, Escuela de Ingenieria y Ciencias, Monterrey, Mexico*

Siti Hidayah • *Institute of Clinical Chemistry and Laboratory Medicine, Mass Spectrometric Proteomics Group, University Medical Center Hamburg-Eppendorf, Hamburg, Germany*

Sophia Hober • *Department of Protein Science, KTH Royal Institute of Technology, School of Engineering Sciences in Chemistry, Biotechnology and Health (CBH), AlbaNova University Centre, Stockholm, Sweden*
Elisavet Ioannou • *Laboratory of Enzyme Technology, Department of Biotechnology, School of Applied Biology and Biotechnology, Agricultural University of Athens, Athens, Greece*
Sara Kanje • *Department of Protein Science, KTH Royal Institute of Technology, School of Engineering Sciences in Chemistry, Biotechnology and Health (CBH), AlbaNova University Centre, Stockholm, Sweden*
Anthi Karnaouri • *Industrial Biotechnology and Biocatalysis Group, Biotechnology Laboratory, Department of Synthesis and Development of Industrial Processes, School of Chemical Engineering, National Technical University of Athens, Athens, Greece*
Servé W. M. Kengen • *Laboratory of Microbiology, Wageningen University, Wageningen, The Netherlands*
E. G. Korzhikova-Vlakh • *Institute of Macromolecular Compounds, Russian Academy of Sciences, St. Petersburg, Russia*
Marta Kotasinska • *Institute of Clinical Chemistry and Laboratory Medicine, Mass Spectrometric Proteomics Group, University Medical Center Hamburg-Eppendorf, Hamburg, Germany*
Sotirios Koutsopoulos • *Center for Biomedical Engineering, Massachusetts Institute of Technology, Cambridge, MA, USA*
Frank A. Kovacs • *Chemistry Department, University of Nebraska at Kearney, Kearney, NE, USA*
Sunil Kumar • *Postdoctoral Research Associate, Lineberger Comprehensive Cancer Center, University of North Carolina at Chapel Hill, Chapel Hill, NC, USA*
Thallapuranam Krishnaswamy Suresh Kumar • *Department of Chemistry and Biochemistry, University of Arkansas, Fayetteville, AR, USA*
Marcel Kwiatkowski • *Institute of Clinical Chemistry and Laboratory Medicine, Mass Spectrometric Proteomics Group, University Medical Center Hamburg-Eppendorf, Hamburg, Germany*
Nikolaos E. Labrou • *Laboratory of Enzyme Technology, Department of Biotechnology, School of Applied Biology and Biotechnology, Agricultural University of Athens, Athens, Greece*
Mark Levisson • *Laboratory of Microbiology, Wageningen University, Wageningen, The Netherlands*
Yifeng Li • *Technology and Process Development (TPD), WuXi Biologics, Shanghai, China*
Ilario Losito • *Centro Interdipartimentale di Ricerca SMART, Università degli Studi di Bari "Aldo Moro", Bari, Italy; Dipartimento di Chimica, Università degli Studi di Bari "Aldo Moro", Bari, Italy*
Sanhita Maity • *Department of Chemistry and Biochemistry, University of Arkansas, Fayetteville, AR, USA*
M. M. Marani • *Instituto Patagónico para el Estudio de Ecosistemas Continentales (IPEEC), CONICET, Puerto Madryn, Chubut, Argentina*
M. C. Martínez-Ceron • *Cátedra de Biotecnología, Facultad de Farmacia y Bioquímica, Universidad de Buenos Aires, Buenos Aires, Argentina; Instituto de Nanobiotecnología (NANOBIOTEC), Facultad de Farmacia y Bioquímica, CONICET-Universidad de Buenos Aires, Buenos Aires, Argentina*
Jesse Mattsson • *Turku Bioscience Centre, University of Turku and Åbo Akademi University, BioCity, Turku, Finland*

Megan M. McEvoy • *Institute for Society & Genetics, Department of Microbiology, Immunology, & Molecular Genetics, University of California, Los Angeles, CA, USA*
Jorge M. Montfort-Gardeazabal • *Facultad de Ciencias Quimicas, Universidad Autonoma de Nuevo Leon, San Nicolas de los Garza, NL, Mexico*
Phil Morton • *Albumedix Ltd. Head Office, Nottingham, UK*
Annette C. Moser • *Chemistry Department, University of Nebraska at Kearney, Kearney, NE, USA*
S. Muthukumar • *Department of Chemical Engineering, Indian Institute of Technology, New Delhi, India*
Johan Nilvebrant • *Division of Protein Technology, School of Engineering Sciences in Chemistry, Biotechnology and Health, KTH/AlbaNova University Centre, Stockholm, Sweden*
Anastassios C. Papageorgiou • *Turku Bioscience Centre, University of Turku and Åbo Akademi University, BioCity, Turku, Finland*
Esther Perez-Carrillo • *Tecnologico de Monterrey, Escuela de Ingenieria y Ciencias, Monterrey, Mexico*
David A. Perez-Perez • *Facultad de Ciencias Quimicas, Universidad Autonoma de Nuevo Leon, San Nicolas de los Garza, NL, Mexico*
Ana Sofia Pina • *UCIBIO, Departamento de Química, Faculdade de Ciências e Tecnologia, Universidade Nova de Lisboa, Caparica, Portugal*
G. A. Platonova • *Institute of Macromolecular Compounds, Russian Academy of Sciences, St. Petersburg, Russia*
Nirmal Poudel • *Turku Bioscience Centre, University of Turku and Åbo Akademi University, BioCity, Turku, Finland*
Georgios Premetis • *Laboratory of Enzyme Technology, Department of Biotechnology, School of Applied Biology and Biotechnology, Agricultural University of Athens, Athens, Greece*
Narayan S. Punekar • *Biotechnology Group, Department of Biosciences and Bioengineering, Indian Institute of Technology Bombay, Mumbai, India*
Anurag S. Rathore • *Department of Chemical Engineering, Indian Institute of Technology, New Delhi, India*
Verena Richter • *Institute of Clinical Chemistry and Laboratory Medicine, Mass Spectrometric Proteomics Group, University Medical Center Hamburg-Eppendorf, Hamburg, Germany*
Marco Rito-Palomares • *Tecnologico de Monterrey, Escuela de Medicina y Ciencias de la Salud, Monterrey, Mexico*
Ana Cecília A. Roque • *UCIBIO, Departamento de Química, Faculdade de Ciências e Tecnologia, Universidade Nova de Lisboa, Caparica, Portugal*
S. L. Saavedra • *Cátedra de Biotecnología, Facultad de Farmacia y Bioquímica, Universidad de Buenos Aires, Buenos Aires, Argentina; Instituto de Nanobiotecnología (NANOBIOTEC), Facultad de Farmacia y Bioquímica, CONICET-Universidad de Buenos Aires, Buenos Aires, Argentina*
Xavier Santarelli • *Bordeaux INP, CBMN, UMR 5248, Pessac, France*
Bryan D. Santos • *Facultad de Ciencias Quimicas, Universidad Autonoma de Nuevo Leon, San Nicolas de los Garza, NL, Mexico*
Julia Scheffel • *Department of Protein Science, KTH Royal Institute of Technology, School of Engineering Sciences in Chemistry, Biotechnology and Health (CBH), AlbaNova University Centre, Stockholm, Sweden*

Hartmut Schlüter • *Institute of Clinical Chemistry and Laboratory Medicine, Mass Spectrometric Proteomics Group, University Medical Center Hamburg-Eppendorf, Hamburg, Germany*

Peter M. Schmidt • *CSL Behring GmbH, R&D, Marburg, Germany; CSL Limited, BIO21 Institute, Parkville, VIC, Australia*

Isabel T. Sousa • *iBB–Institute for Bioengineering and Biosciences, Instituto Superior Té cnico, University of Lisbon, Lisboa, Portugal*

Tetyana Sulimenko • *Laboratory of Biology of Cytoskeleton, Institute of Molecular Genetics of the Czech Academy of Sciences, Prague, Czech Republic*

Vadym Sulimenko • *Laboratory of Biology of Cytoskeleton, Institute of Molecular Genetics of the Czech Academy of Sciences, Prague, Czech Republic*

M. Ângela Taipa • *iBB–Institute for Bioengineering and Biosciences, Instituto Superior Té cnico, University of Lisbon, Lisboa, Portugal; Department of Bioengineering, Instituto Superior Técnico, University of Lisbon, Lisboa, Portugal*

Guoqing Tan • *Technology and Process Development (TPD), WuXi Biologics, Shanghai, China*

Lotta T. Tegler • *Center for Biomedical Engineering, Massachusetts Institute of Technology, Cambridge, MA, USA*

T. B. Tennikova • *Institute of Chemistry, Saint-Petersburg State University, St. Petersburg, Russia*

Evangelos Topakas • *Industrial Biotechnology and Biocatalysis Group, Biotechnology Laboratory, Department of Synthesis and Development of Industrial Processes, School of Chemical Engineering, National Technical University of Athens, Athens, Greece; Biochemical Process Engineering, Chemical Engineering, Department of Civil, Environmental and Natural Resources Engineering, Luleå University of Technology, Luleå, Sweden*

John van der Oost • *Laboratory of Microbiology, Wageningen University, Wageningen, The Netherlands*

Christina Varotsou • *Laboratory of Enzyme Technology, Department of Biotechnology, School of Applied Biology and Biotechnology, Agricultural University of Athens, Athens, Greece*

Ying Wang • *Technology and Process Development (TPD), WuXi Biologics, Shanghai, China*

Benjamin White • *Chemistry Department, University of Nebraska at Kearney, Kearney, NE, USA*

David W. Provance Jr. • *FIOCRUZ, Center for Technological Development in Health (CDTS)/National Institute of Science and Technology for Innovation on Neglected of Population Diseases (INCT-INDP), Rio de Janeiro, RJ, Brazil; FIOCRUZ, Oswaldo Cruz Institute, Interdisciplinar Laboratory of Medical Research, Rio de Janeiro, RJ, Brazil*

Sharon Williams • *Astrea Bioseparations Ltd., Cambridge, UK*

Xristo Zarate • *Facultad de Ciencias Quimicas, Universidad Autonoma de Nuevo Leon, San Nicolas de los Garza, NL, Mexico*

Anastasia Zerva • *Industrial Biotechnology and Biocatalysis Group, Biotechnology Laboratory, Department of Synthesis and Development of Industrial Processes, School of Chemical Engineering, National Technical University of Athens, Athens, Greece*

Part I

Screening and Design Purification Strategies

Chapter 1

Protein Purification Technologies

Nikolaos E. Labrou

Abstract

Protein Biotechnology is an exciting and fast- growing area of research, with numerous industrial applications. The growing demand for developing efficient and rapid protein purification methods is driving research and growth in this area. Advances and progress in the techniques and methods of protein purification have been such that one can reasonably expect that any protein of a given order of stability may be purified to currently acceptable standards of homogeneity. However, protein manufacturing cost remains extremely high, with downstream processing constituting a substantial proportion of the overall cost. Understanding of the methods and optimization of the experimental conditions have become critical to the manufacturing industry in order to minimize production costs while satisfying the quality as well as all regulatory requirements. New purification processes exploiting specific, effective and robust methods and chromatographic materials are expected to guide the future of the protein purification market.

Key words Chromatography, Downstream processing, Protein purification, Protein manufacturing, quality and safety

1 Introduction

As scientists now have completed the sequencing of the genomes of hundreds of species, they have embarked on the next great challenge: understanding the biology of the cell at the molecular level [1–4]. As researchers attempt to understand the vast amount of genetic information, proteomics has become a major focus in the biotechnology industry. If sequencing the human genome has been a major technological challenge, characterizing the proteome promises to be an even great one [1–6]. With thousands of potential genes identified from sequencing projects, protein biochemistry seeks to define the role and biological function of the gene products. Biotechnology seeks to develop new protein-based applications and their commercial exploitation. The first requirement for achieving these goals is the development of efficient and effective purification methods [7, 8].

Nikolaos E. Labrou (ed.), *Protein Downstream Processing: Design, Development, and Application of High and Low-Resolution Methods*, Methods in Molecular Biology, vol. 2178, https://doi.org/10.1007/978-1-0716-0775-6_1,

Table 1
Physicochemical basis of common bioseparation methods

Separation	Basis of separation	Resolution
Precipitation		
Ammonium sulfate	Solubility	Low
Organic solvents	Solubility	Low
Polyethyleneimine	Charge, size	Low
Polyethylene glycol	Solubility	Low
Isoelectric	Solubility, p*I*	Low
Affinity precipitation	Molecular recognition, Solubility	Low
Phase partitioning		
Aqueous two-phase partition	Solubility/hydrophobicity	Low/medium
Three-phase partitioning	Solubility/hydrophobicity	Low/medium
Chromatography		
Ion exchange	Charge, charge distribution	High
Hydrophobic interaction	Hydrophobicity	High
Reverse-phase HPLC	Hydrophobicity, size	High
Affinity chromatography	Molecular recognition	High
Gel filtration/size exclusion	Size, shape	High

The various steps in the downstream processing protocol separate the protein and nonprotein parts of the mixture and finally separate the desired protein from all other proteins while retaining the biological activity and chemical integrity of the polypeptide [9–18]. The last step is typically the most laborious and difficult aspect of protein purification. The purified protein should be free not only of contaminants (e.g., nucleic acids, viruses, pyrogens, residual host cell proteins, cell culture media, and leachates from the separation media) but also of the various isoforms, originating from post-translational modifications [12–14].

Separation steps may exploit differences in chemical/structural/functional properties between the target protein and other proteins in the crude mixture (Table 1). These properties include size, shape, charge, isoelectric point, charge distribution, hydrophobicity, solubility, density, ligand binding affinity, metal binding, reversible association, post-translational modifications, and specific sequences or structures. By exploiting these variations in physical and chemical properties among proteins, several different fractionation or chromatographic steps can be designed for the development of a workable purification Scheme [9, 10, 12, 13, 16, 19].

However, some proteins may be very challenging to be purified in an active and stable form, for example, integral membrane proteins, unstable protein complexes, proteins produced as insoluble aggregates, and proteins with a specific set of post-translational modifications. The challenges and difficulties in protein purification make worthwhile the in-depth study of the available methods so that they can be selected and applied in an optimal way [9, 10, 12, 13, 16, 19].

2 Historical Aspects

Techniques for protein isolation and purification were developed by Edwin Joseph Cohn, during World War II [20]. He carried out pioneering work on fractionation of plasma proteins. The solubility properties, precipitation, and crystallization dominated the design of early purification studies. The next major milestone in protein purification was chromatography [21]. Ion exchangers began to be used and have become indispensable in protein purification. Whatman introduced cellulose-based ion exchangers followed by introduction of dextran-based ion exchangers by Pharmacia. In 1910, Emil Starkenstein described the concept of affinity chromatography [22]. This was an important milestone. He studied the separation of a macromolecule (liver α-amylase) via its interactions with an immobilized substrate (starch). The term affinity chromatography introduced in 1968 by Pedro Cuatecasas, Chris Anfinsen, and Meir Wilchek in an article that briefly described the technique of enzyme purification via immobilized substrates and inhibitors [23]. This progress was some kind of a mini-revolution in protein purification area. For a couple of decades, a typical protein purification protocol invariably consisted of precipitation by ammonium sulfate, one or two ion-exchange steps, gel filtration, and finally an affinity chromatography step.

3 Low- and High-Resolution Protein Purification Methods

Downstream processing has been challenged with demands of high yields, resolving power, and cost efficiency. This has triggered remarkable developments in improving process tools and innovative strategies for protein separation. A wide variety of protein purification methods that can be combined to generate a suitable purification scheme are available [7–14]. Usually, one executes a series of purification steps, and only a few proteins can be purified in a single step, even when this step is based on exquisitely specific biological characteristics [24, 25]. Early steps combine low-resolution and high-capacity methods (when large amounts of protein are present) with higher-resolution and lower-capacity ones (when less protein is present) at later stages of the purification

scheme. For low-resolution protein purification, methods such as fractional precipitation and two-phase partition systems are usually employed [26–30]. For applications requiring the highest purity and relatively small amounts of protein, chromatographic techniques can be chosen to selectively purify the target proteins [15, 31].

Chromatography is certainly the principal and commonly used method in downstream processing [32]. This can be explained by certain advantages of chromatography over other methods. For example, chromatography displays high-resolution efficiencies, which allows the resolution of complex crude mixtures with very similar molecular properties. In addition, chromatography is ideal for capturing molecules from the dilute solutions encountered in bioprocessing. Among all chromatographic techniques, affinity chromatography plays a major role [33–41]. In fact, this technique is very specific and effective since it exploits the principle of biomolecular recognition, that is, the ability of proteins to form specific and reversible complexes with their ligands. As conventional purification protocols for high-value proteins are replaced by more sophisticated procedures based on affinity chromatography, the focus is shifted toward designing and selecting ligands of high affinity and specificity [42–46]. Affinity ligands can be classified as biological and synthetic. The former, although they display high affinity and binding capacity, they suffer seriously from low chemical and biological stability and unfavorable economics since they show low adsorbent lifetime and high manufacturing costs. Synthetic ligands appear to tackle effectively most of the problems mentioned above [37, 42–46].

The accumulated knowledge of structures obtained by X-ray crystallography, NMR, and molecular modeling studies and the technological advances in high-throughput screening have made the design and selection of high-affinity synthetic ligands faster and more effective [37, 42, 43, 45–48]. There are three main methods for generating a ligand [17]: (1) the rational, (2) the combinatorial, and (3) the structure-guided combinatorial. The decision depends primarily on the available information.

4 Current Trends

The gap between upstream and downstream processing is a big problem for the biotechnology industry [44]. This is because the progress toward producing more protein per unit volume of culture medium has improved more rapidly than increases in the rates at which these materials can be possessed and purified. Therefore, the biotechnology industry is suffering from a severe shortage of purification capacity for proteins.

The essential goal of the development and optimization of the downstream processing protocol is the production of quality

products with sufficient purity while maintaining the biological activity in a consistent manner and satisfying all regulatory requirements. Quality and safety guidelines for biotechnology products have grown increasingly stringent [11–13, 48]. For certain applications, proteins can be used as crude extracts with little purification. However, pharmaceutical proteins typically require exceptional purity, making downstream processing a critical component of the overall process with high costs [11–13, 49, 50]. These costs are estimated to be about 50–80% of the total costs, and the largest part of them is due to chromatography. This is owing to the stringent quality criteria imposed on protein products, such as defined purity, efficacy, potency, stability, toxicity, and immunogenicity [12, 13]. It is noteworthy that the steps of the downstream processing procedure are further complicated and influenced by commercial conditions, business plans, and patent rights [51, 52]. The commercial competition to develop new protein products or to decrease the production cost of the patented product becomes very important than ever, and cost reduction is now often more critical than speed-to-market.

Recombinant DNA technology impacts the development of protein purification methods in two ways: First, the development and availability of several different protein expression systems meant that sources of proteins are not limited to naturally occurring animals, plants, and microbes [53, 54]. Protein expression systems are used to produce wild-type proteins in biotechnology and industry, and more recently to produce novel engineered variants of proteins that display improved properties [16, 25, 48]. Commonly used protein expression systems include those derived from bacteria, yeast, baculovirus/insect, mammalian cells, and transgenic plants and animals. Second, the use of "affinity tags" and production of proteins in the form of fusion proteins became possible [47, 55]. The efficiency gained by the generic purification approaches based on affinity tagging of the target protein has simplified protein purification. Biotechnology companies have commercialized several different protein-fusion systems available for biochemical research. It should be noted, however, that these methods do not always provide sufficient purity, and additional physicochemical-based chromatography methods (e.g., gel filtration, ion exchange, etc.) may thus have to be included to the protocol [35, 38, 39].

Over the last decade, numerous authors have demonstrated significant potential that multimode chromatography offers as a protein purification tool [56–59]. Multimodal chromatography has emerged as an alternative to the traditional modes. It is based on the use of more than one mode of separation, such as ion-exchange and hydrophobic interactions, to achieve selectivity and sensitivity.

5 Conclusions

The progress in the commercial exploitation of high value-added proteins depends mainly on their availability in high purity. Downstream processing has thus been challenged with demands of high yields, resolving power, and cost efficiency. This has triggered remarkable developments in improving process tools and innovative strategies for protein separation. Therefore, a plethora of emerging technologies for the development and optimization of the protein purification challenge are anticipated to help address these needs. Innovations, possibly combined with cost savings, exploiting specific, effective, and robust methods and materials, are expected to guide the future of the protein purification area.

Acknowledgments

This work was supported by the grant AlgaCeuticals funded by the European Union.

References

1. Shendure J, Lieberman AE (2012) The expanding scope of DNA sequencing. Nat Biotechnol 30:1084–1094
2. Ing-Simmons E, Vaquerizas JM (2019) Visualising three-dimensional genome organisation in two dimensions. Development 146(19):pii: dev177162
3. Beigh MM (2016) Next-generation sequencing: the translational medicine approach from "bench to bedside to population". Medicines (Basel) 3(2):14. https://doi.org/10.3390/medicines3020014
4. Park ST, Kim J (2016) Trends in next-generation sequencing and a new era for whole genome sequencing. Int Neurourol J 20(Suppl 2):S76–S83
5. Henry RJ, Edwards M, Waters DL et al (2012) Application of large-scale sequencing to marker discovery in plants. J Biosci 37:829–841
6. Vaudel M, Sickmann A, Martens L (2012) Current methods for global proteome identification. Expert Rev Proteomics 9:519–532
7. Marichal-Gallardo PA, Alvarez MM (2012) State-of-the-art in downstream processing of monoclonal antibodies: process trends in design and validation. Biotechnol Prog 28:899–916
8. Kalyanpur M (2002) Downstream processing in the biotechnology industry. Mol Biotechnol 22:87–98
9. Łojewska E, Kowalczyk T, Olejniczak S, Sakowicz T (2016) Extraction and purification methods in downstream processing of plant-based recombinant proteins. Protein Expr Purif 2016(120):110–117
10. Owczarek B, Gerszberg A, Hnatuszko-Konka K (2019) A brief reminder of systems of production and chromatography-based recovery of recombinant protein biopharmaceuticals. Biomed Res Int 2019:4216060
11. Schiermeyer A (2019) Optimizing product quality in molecular farming. Curr Opin Biotechnol 4(61):15–20
12. Gervais D (2019) Quality control and downstream processing of therapeutic enzymes. Adv Exp Med Biol 1148:55–80
13. Taipa MÂ, Fernandes P, de Carvalho CCCR (2019) Production and purification of therapeutic enzymes. Adv Exp Med Biol 1148:1–24
14. Li Y, Stern D, Lock LL, Mills J, Ou SH, Morrow M, Xu X, Ghose S, Li ZJ, Cui H (2019) Emerging biomaterials for downstream manufacturing of therapeutic proteins. Acta Biomater 1(95):73–90
15. Shekhawat LK, Rathore AS (2019) An overview of mechanistic modeling of liquid chromatography. Prep Biochem Biotechnol 49:623–638

16. Oliveira C, Domingues L (2018) Guidelines to reach high-quality purified recombinant proteins. Appl Microbiol Biotechnol 102:81–92
17. Jacquemart R, Vandersluis M, Zhao M, Sukhija K, Sidhu N, Stout J (2016) A single-use strategy to enable manufacturing of affordable biologics. Comput Struct Biotechnol J 5 (14):309–318
18. Steinebach F, Müller-Späth T, Morbidelli M (2016) Continuous counter-current chromatography for capture and polishing steps in biopharmaceutical production. Biotechnol J 11:1126–1141
19. Kallberg K, Johansson HO, Bulow L (2012) Multimodal chromatography: an efficient tool in downstream processing of proteins. Biotechnol J 7:1485–1495
20. Cohn EJ, Edsall JT (1943) Proteins, amino acids and peptides as ions and dipolar ions. Reinhold Publishing, New York, NY
21. Lucy CA (2003) Evolution of ion-exchange: from Moses to the Manhattan Project to modern times. J Chromatogr A 1000:711–724
22. Starkenstein E (1910) Ferment action and the influence upon it of neutral salts. Biochem Z 24:210–218
23. Cuatrecasas P, Wilcheck M, Anfinsen CB (1968) Selective enzyme purification by affinity chromatography. Proc Natl Acad Sci U S A 61:636–643
24. Butler M, Meneses-Acosta A (2012) Recent advances in technology supporting biopharmaceutical production from mammalian cells. Appl Microbiol Biotechnol 96:885–894
25. Wilken LR, Nikolov ZL (2012) Recovery and purification of plant-made recombinant proteins. Biotechnol Adv 30:419–433
26. Hekmat D (2015) Large-scale crystallization of proteins for purification and formulation. Bioprocess Biosyst Eng 38:1209–1231
27. McQueen L, Lai D (2019) Ionic liquid aqueous two-phase systems from a pharmaceutical perspective. Front Chem 7:135
28. Li Y (2019) The application of caprylic acid in downstream processing of monoclonal antibodies. Protein Expr Purif 153:92–96
29. Wong FWF, Ariff AB, Stuckey DC (2018) Downstream protein separation by surfactant precipitation: a review. Crit Rev Biotechnol 38:31–46
30. Rosa PA, Azevedo AM, Sommerfeld S et al (2011) Aqueous two-phase extraction as a platform in the biomanufacturing industry: economical and environmental sustainability. Biotechnol Adv 29:559–567
31. Chon JH, Zarbis-Papastoitsis G (2011) Advances in the production and downstream processing of antibodies. Nat Biotechnol 28:458–463
32. Freitag R, Horváth C (1996) Chromatography in the downstream processing of biotechnological products. Adv Biochem Eng Biotechnol 53:17–59
33. Ramos-de-la-Peña AM, González-Valdez J, Aguilar O (2019) Protein A chromatography: challenges and progress in the purification of monoclonal antibodies. J Sep Sci 42:1816–1827
34. Arora S, Saxena V, Ayyar BV (2017) Affinity chromatography: a versatile technique for antibody purification. Methods 1(116):84–94
35. Singh N, Herzer S (2018) Downstream processing technologies/capturing and final purification: opportunities for innovation, change, and improvement. A review of downstream processing developments in protein purification. Adv Biochem Eng Biotechnol 165:115–178
36. Kruljec N, Bratkovič T (2017) Alternative affinity ligands for immunoglobulins. Bioconjug Chem 28:2009–2030
37. Fang YM, Lin DQ, Yao SJ (2018) Review on biomimetic affinity chromatography with short peptide ligands and its application to protein purification. J Chromatogr A 1571:1–15
38. Burgess RR (2018) A brief practical review of size exclusion chromatography: rules of thumb, limitations, and troubleshooting. Protein Expr Purif 150:81–85
39. Rathore AS, Kumar D, Kateja N (2018) Recent developments in chromatographic purification of biopharmaceuticals. Biotechnol Lett 40:895–905
40. Perret G, Santambien P, Boschetti E (2015) The quest for affinity chromatography ligands: are the molecular libraries the right source? J Sep Sci 38:2559–2572
41. Roque AC, Silva CS, Taipa MA (2007) Affinity-based methodologies and ligands for antibody purification: advances and perspectives. J Chromatogr A 1160:44–55
42. Labrou NE (2003) Design and selection of ligands for affinity chromatography. J Chromatogr B Analyt Technol Biomed Life Sci 790:67–78
43. Clonis YD (2006) Affinity chromatography matures as bioinformatic and combinatorial tools develop. J Chromatogr A 1101:1–24
44. Gottschalk U (2008) Bioseparation in antibody manufacturing: the good, the bad and the ugly. Biotechnol Prog 24:496–503

45. Maltezos A, Platis D, Vlachakis D, Kossida S, Marinou M, Labrou NE (2014) Design, synthesis and application of benzyl-sulfonate biomimetic affinity adsorbents for monoclonal antibody purification from transgenic corn. J Mol Recognit 27:19–31
46. Marinou M, Platis D, Ataya FS, Chronopoulou E, Vlachakis D, Labrou NE (2018) Structure-based design and application of a nucleotide coenzyme mimetic ligand: application to the affinity purification of nucleotide dependent enzymes. J Chromatogr A 1535:88–100
47. Dias AM, Roque AC (2017) The future of protein scaffolds as affinity reagents for purification. Biotechnol Bioeng 114:481–491
48. Wingfield PT (2015) Overview of the purification of recombinant proteins. Curr Protoc Protein Sci 80:6.1.1–6.135
49. Rasmussen SK, Næsted H, Müller C et al (2012) Recombinant antibody mixtures: production strategies and cost considerations. Arch Biochem Biophys 526:139–145
50. Kelley B (2009) Industrialization of mAb production technology: the bioprocessing industry at a crossroads. MAbs 5:443–452
51. Dranitsaris G, Amir E, Dorward K (2011) Biosimilars of biological drug therapies: regulatory, clinical and commercial considerations. Drugs 71:1527–1536
52. Davies HM (2010) Commercialization of whole-plant systems for biomanufacturing of protein products: evolution and prospects. Plant Biotechnol J 8:845–861
53. Huang CJ, Lin H, Yang X (2012) Industrial production of recombinant therapeutics in *Escherichia coli* and its recent advancements. J Ind Microbiol Biotechnol 39:383–399
54. Chen R (2012) Bacterial expression systems for recombinant protein production: *E. coli* and beyond. Biotechnol Adv 30:1102–1107
55. Young CL, Britton ZT, Robinson AS (2012) Recombinant protein expression and purification: a comprehensive review of affinity tags and microbial applications. Biotechnol J 7:620–634
56. Cabanne C, Santarelli X (2019) Mixed mode chromatography, complex development for large opportunities. Curr Protein Pept Sci 20:22–27
57. Santarelli X, Cabanne C (2019) Mixed mode chromatography: a novel way toward new selectivity. Curr Protein Pept Sci 20:14–21
58. Arakawa T (2019) Review on the application of mixed-mode chromatography for separation of structure isoforms. Curr Protein Pept Sci 20:56–60
59. Zhang K, Liu X (2016) Mixed-mode chromatography in pharmaceutical and biopharmaceutical applications. J Pharm Biomed Anal 5 (128):73–88

Chapter 2

High-Throughput Process Development: I—Process Chromatography

Anurag S. Rathore and R. Bhambure

Abstract

Chromatographic separation serves as "a workhorse" for downstream process development and plays a key role in the removal of product-related, host-cell-related, and process-related impurities. Complex and poorly characterized raw materials and feed material, low feed concentration, product instability, and poor mechanistic understanding of the processes are some of the critical challenges that are faced during the development of a chromatographic step. Traditional process development is performed as a trial-and-error-based evaluation and often leads to a suboptimal process. A high-throughput process development (HTPD) platform involves the integration of miniaturization, automation, and parallelization and provides a systematic approach for time- and resource-efficient chromatographic process development. Creation of such platforms requires the integration of mechanistic knowledge of the process with various statistical tools for data analysis. The relevance of such a platform is high in view of the constraints with respect to time and resources that the biopharma industry faces today.

This protocol describes the steps involved in performing the HTPD of chromatography steps. It describes the operation of a commercially available device (PreDictor™ plates from GE Healthcare). This device is available in 96-well format with 2 or 6 μL well size. We also discuss the challenges that one faces when performing such experiments as well as possible solutions to alleviate them. Besides describing the operation of the device, the protocol also presents an approach for statistical analysis of the data that are gathered from such a platform. A case study involving the use of the protocol for examining ion exchange chromatography of the Granulocyte Colony Stimulating Factor (GCSF), a therapeutic product, is briefly discussed. This is intended to demonstrate the usefulness of this protocol in generating data that are representative of the data obtained at the traditional lab scale. The agreement in the data is indeed very significant (regression coefficient 0.93). We think that this protocol will be of significant value to those involved in performing the high-throughput process development of the chromatography process.

Key words High-throughput process development (HTPD), PreDictor™ plates, Miniaturization, Ion-exchange chromatography (IEX), Design of experiments (DOE), Design space

1 Introduction

Downstream process development for manufacturing biopharmaceutical proteins typically involves the integration of at least two to three chromatography steps, each with differential selectivity with

Nikolaos E. Labrou (ed.), *Protein Downstream Processing: Design, Development, and Application of High and Low-Resolution Methods*, Methods in Molecular Biology, vol. 2178, https://doi.org/10.1007/978-1-0716-0775-6_2,

respect to the separation of numerous product-related, host-cell-related, and process-related impurities that are present in the feed material of downstream processing. During early-stage process development, separations are mostly performed on a trial-and-error basis primarily due to the complex interactions between the vast variety of resin matrices that are available in the market and the product under consideration. However, this leads to processes that are suboptimal with respect to their efficiency, robustness, and efficacy. A high-throughput chromatography platform offers a potential solution to gain process and product understanding [1–6]. The available literature on the HTPD of chromatography steps for various biopharmaceutical proteins focuses primarily on the identification of operating conditions for obtaining higher product recovery and purity [7–18]. This is especially relevant in today's paradigm of Quality by Design and Process Analytical Technology, where the requirement of a thorough process understanding is more than ever [19–29].

1.1 Steps for Optimization of Process Chromatography

Chromatography optimization is performed in multiple steps.

1. Identification of a suitable resin matrix: A wide variety of resins are available in the market today, with several new ones that have been introduced in the last decade. The type of resin base matrix, particle size, pore diameter, type of the ligand, ligand density, pressure-flow characteristics, suitability for scale-up, and reusability are some of the critical attributes of a resin that need to be considered while selecting an optimal resin [30–32].
2. Optimization of binding conditions: Optimization of binding conditions for a specific combination of the product and the resin matrix is a key activity of chromatography process development and involves the identification of suitable buffer conditions (pH, buffer molarity, buffer salt, etc.) that would result in optimum binding [3, 30, 32]. Design-of-experiment (DOE)-based approaches are commonly used for exploring different combinations of these parameters.
3. Optimization of elution conditions: Elution of the product from the ion exchange matrix is achieved either by increasing the salt concentration or by changing the pH. With the recent advent of mixed-mode chromatography, more complex elution strategies involving a combination of pH and salt gradients are also being practiced [33, 34].
4. Examination of process robustness: It is important that the developed chromatography step is robust for the intended purification. The quality standards for biotech therapeutic products are quite rigid, and hence, the developed step should be reasonably robust with respect to typical variations that occur in the various process parameters during routine manufacturing [5].

1.2 Steps Toward Establishing an HTPD Platform

Step I: Pre-experimental Planning: This step involves the identification of a suitable resin matrix, selection of the process parameters that need to be examined, and the appropriate levels that need to be evaluated. Once these inputs were known, the appropriate DOE can be chosen, and the experiments are performed [28].

Step II: Experimentation: This step involves the creation of a sample preparation protocol that generates the product in the various conditions (pH, buffer molarity, etc.) as required by the DOE protocol. Product concentration and buffer exchange are typically used to achieve this. Experiments are performed according to the protocol and include equilibration, protein loading, and elution cycles. As mentioned above, the availability of analytical instrumentation with the necessary sensitivity and the ability to analyze HTPD formats is essential for achieving satisfactory mass balance and accurate estimation of recovery and product quality.

Step III: Data Analysis: Automation and parallelization of experiments in an HTPD platform make data analysis a complex task [30]. Statistical data analysis is required for defining optimum operating conditions. Care should be taken to appropriately recognize the various errors that can come from working at such micro volumes.

Step IV: Validation of the statistical model: While HTPD is capable of generating significantly large amounts of data in a relatively short duration, it is important to verify the validity of the data by comparing the results with those obtained at the more conventional lab scale. Several statistical approaches exist, and an appropriate one can be used for establishing this comparability.

2 Materials

2.1 Equipments

PreDictor™ plates prefilled with chromatography medium from GE Healthcare.

A Minimate™ tangential flow filtration device from Pall Corporation USA for the concentration of protein.

A multichannel Eppendorf Research® pro electronic pipette for achieving automation in liquid handling.

An Ika MTS 2/4 digital shaker for suspending the sample/buffer in the medium during incubation at various stages of the experiment.

Whatman® vacuum manifold for vacuum filtration of the sample and buffer from the 96-well PreDictor plates.

An Epoch microplate spectrophotometer (BioTek® Instruments Inc. Winooski, VT, USA) for the quantitative estimation of the protein using UV absorbance.

2.2 Buffer Preparation

Prepare all the buffers using ultrapure water. Prepare and store all the reagents at room temperature. For the selected case studies, acetate buffer of varying buffer molarity and pH was used. Glacial acetic acid, sodium acetate (anhydrous), sodium chloride, and sodium hydroxide were purchased from Merck Chemicals, India. Buffer selection was done as per the selected design of experimental strategy.

3 Methods

3.1 Sample Preparation

The sample has to be clarified before use in the HTPD platform. An unclarified sample can cause clogging of the filter plates at the bottom of the wells. Sample volume to be applied depends on the estimated dynamic binding capacity of the product for the resin under consideration. The concentration of the input sample has to be adjusted in such a way so that the output can be analyzed for detecting the impurities at various wash and elution steps. Two different sample cleaning protocols can be applied for sample clarification, namely microfiltration and centrifugation. Preprocess the protein sample using buffer exchange to achieve the desired pH and buffer molarity.

3.2 Preprocessing of the Plates Before Starting the Experiment

1. For prepacked plates, preprocessing is essential for uniform distribution of the resin beads. Hold the plate with both hands and keep the thumbs on the bottom side of the PreDictor plate and the other fingers on the top side. Rotate the plate to bottom side up while thrusting it downward in a swift, controlled movement. This protocol ensures the formation of a uniform suspension of resin beads. After resuspnesion of the resin beads, remove the storage solution from the repacked plate by applying a vacuum or the centrifugation protocol (*see* **Note 1**).
2. For manual resin filling in plates, prepare 50% resin slurry in an appropriate buffer. Place the plate on a vacuum manifold with a collection plate at the bottom side. Quickly pipette out the 0.2 mL of uniform suspension of the resin slurry into the collection plate. Apply the vacuum to settle the resin bed.
3. After preprocessing of the resin containing plate, place the plate on the collection plate. It is possible to partially open the plate if less than 96 experiments are to be performed and the user wishes to reuse the remaining wells later.
4. Add 0.2 mL of equilibration buffer into each well of the plate. Cover the PreDictor™ plate and incubate it at 1100 rpm (156 × *g*) for 5 min at room temperature (RT). After shaking the plate, keep it for 2 min to allow the resin to settle uniformly. Remove the equilibration buffer using a

vacuum at 25 cmHg for 15–20 s using the vacuum manifold. In the case of partial use of the plate, cover all the nonused wells using aluminum foil. This improves the efficiency of the vacuum application. Alternatively, the equilibration buffer can be removed using centrifugation. Perform at least three cycles of the equilibration to ensure resin equilibration (*see* **Notes 1** and **2**).

5. Upto 0.3 mL of preprocessed protein sample can be added into each well. Cover the PreDictor™ plate and incubate it at 1100 rpm (156 × *g*) for 60 min at RT. After 60 min, collect the unbound proteins in the flow through (FT) fraction using a vacuum or centrifugation.
6. Add 0.2 mL of equilibration buffer in each well and incubate for 3 min and remove the fluid to wash away any residual unbound proteins. Repeat the step at least two times to ensure that there is no unbound protein left in the wells.
7. Elute the bound protein using step gradient of either pH or salt. Add 0.2 mL of elution buffer to each well and incubate for 5 min. Avoid dilution by appropriately selecting the elution buffer volume.
8. Perform the analysis using UV-visible spectroscopy or any other analytical test (*see* **Note 3**).
9. Correct for path length, if required, to get an accurate determination of the sample volume collected in the collection plate (*see* **Note 4**).
10. Analyze the data using appropriate statistical tools for identifying the process parameters that have the most significant effect on the step performance as well as build empirical models to aid in process optimization (*see* **Note 5**).
11. Validate portion of the data from the HTPD platform with that from the traditional lab-scale column chromatography (*see* **Note 6**).

3.3 Case Study Illustrating the Application of the HTPD Platform

Figure 1 illustrates the outcome of a Case Study involving the application of the HTPD platform presented here for examining the effect of different process parameters on the purification of the Granulocyte Colony Stimulating Factor (GCSF) on SP Sepharose Fast Flow resin. Percent product binding was chosen as the response in this case study, and the effect of pH and buffer molarity was examined. As seen in Fig. 1, the data from the HTPD protocol are in very good agreement with those from the traditional laboratory-scale column chromatography (regression coefficient 0.93). Impact of the two process variables under consideration, pH and buffer molarity, on the recovery of GCSF in HTPD and lab-scale is evident from the leverage plots (Fig. 1). The presented data validate the HTPD platform presented in this protocol.

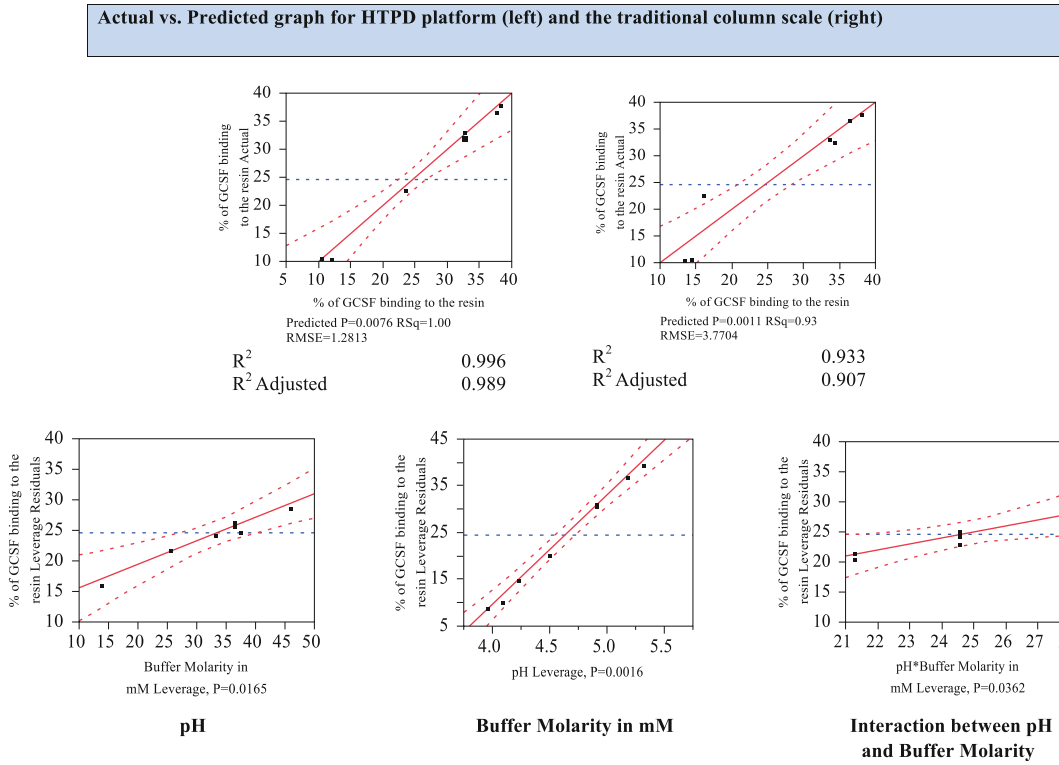

Fig. 1 Optimization of the recovery of GCSF in cation-exchange chromatography using SP Sepharose FF resin—comparison of data from the HTPD platform to those from the traditional lab-scale column chromatography. Adapted from Ref. 17

4 Notes

1. Partial use of the 96-well chromatography resin plate. It is possible to partially use the 96-well plate. However, this requires extra precaution while performing buffer or product collection in the collection plate during the equilibration or the loading cycle. Cover the nonused wells using aluminum foil for appropriate vacuum application. Selectively remove the cover seal depending upon the number of experiments.
2. Overcoming the errors in liquid handling. Accurate liquid handling is the key to the successful implementation of high-throughput process development for chromatography. Two critical liquid handling steps are dispensing of the buffer and the product into the PreDictor™ plate and the collection of the samples in collection plates by applying vacuum or centrifugation. It is essential that the errors are minimized during HTPD experimentation so as to allow for appropriate predictive statistical data analysis. This can be achieved by minimizing the error when dispensing the sample as well as selecting the appropriate

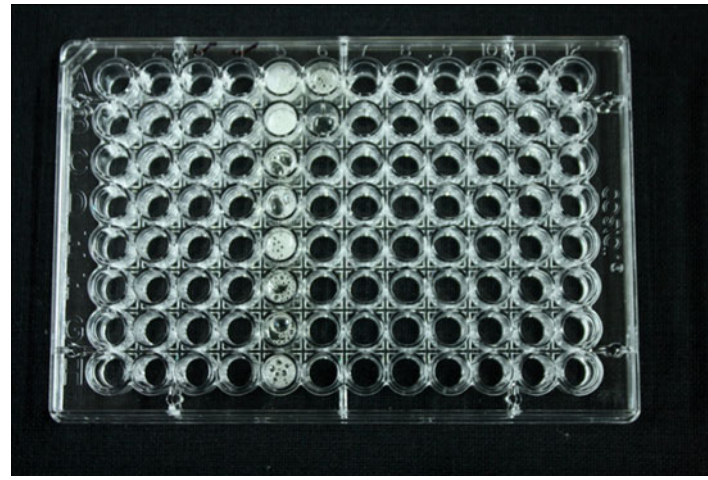

Fig. 2 Formation of the foam during vacuum application while processing the sample in the HTPD platform

method for collection of the sample or buffer from the plate. In the case where vacuum is being used for collection, optimization of the magnitude of the vacuum applied is essential for avoiding any droplet formation at the bottom of the plate. The latter can otherwise lead to product loss and result in lower mass balance values.

3. Foam formation in the collection plate and the resulting interference during measurement of UV-visible absorbance. Figure 2 shows foam generated in the collection plate after the application of vacuum for the removal of the protein solution from the PreDictor™ plate. Five microliter of absolute ethanol was used as a foam reducing agent, which helps in lowering the interferences in the absorbance values of the protein solutions.
4. Accurate determination of the sample volume in 96-well collection plates. It is important to know the actual sample volume collected in the collection plate. The volume of the sample collected in 96-well collection plates should be calculated using the path length correction option that is commonly available in commercial microplate spectrophotometers. The path length of each sample obtained is multiplied by the area of a single well of the 96-well UV readable plate, leading to accurate determination of the sample volume collected in the collection plate accounting for the losses during liquid dispensing and liquid collection by applying vacuum.
5. Statistical analysis of HTPD data. Statistical data analysis is necessary for reaching accurate conclusions. Regression analysis can be performed using least-squares fitting for identifying the relationships between the various responses and the

independent process variables. Analysis of Variance (ANOVA) at 95% confidence interval can be performed to check the statistical validity of the data. Leverage plots can be used for identifying the impact of each process variable as well as interaction among them on the related performance parameters. Finally, the optimization function using a counter profiler can be used by setting constraints on the response variables as per the process needs to estimate the "design space [28, 30, 35, 36].

6. Validation of the HTPD platform with conventional column chromatography. Once the HTPD platform is established, a detailed comparison of the HTPD experiments and the conventional column-scale experiments is essential for validation of the platform. The HTPD platform is capable of generating a lot of data in a very short time. Not all data need to be examined at the traditional scale but it is important that the platform is validated before the conclusions from the analysis are applied toward commercialization of the product. Once the platform has been validated, it may be possible to use it for other molecules using similar chromatographic separations.

Acknowledgments

Financial assistance from the Department of Biotechnology, Government of India, New Delhi, is gratefully acknowledged. We are also thankful to GE Healthcare (Uppsala, Sweden) for providing us with financial support and some of the consumable items used in this investigation. We also thank Dionex Corporation, USA, for donating some of the equipment for this project.

References

1. Bhambure R, Kumar K, Rathore AS (2011) High-throughput process development for biopharmaceutical drug substances. Trends Biotechnol 29:127–135
2. Allen L (2017) The evolution of platform technologies for the downstream processing of antibodies. In: Gottschalk U (ed) Process scale purification of antibodies. John Wiley & Sons Inc., Hoboken, NJ, p 365
3. Rathore AS, Kumar D, Kateja N (2018) Recent developments in chromatographic purification of biopharmaceuticals. Biotechnol Lett 40:1–11
4. Rathore AS, Singh SK (2016) Production of protein therapeutics in the quality by design (QbD) paradigm. In: Sauna ZE, Kimchi-Sarfaty C (eds) Protein therapeutics. Springer, Cham, p 41
5. Rathore AS (2016) Quality by design (QbD)-based process development for purification of a biotherapeutic. Trends Biotechnol 34:358–370
6. Petroff MG, Bao H, Welsh JP et al (2016) High throughput chromatography strategies for potential use in the formal process characterization of a monoclonal antibody. Biotechnol Bioeng 113:1273–1283
7. Wiendahl M, Wierling PS, Nielsen J et al (2008) High throughput screening for the design and optimization of chromatographic processes – miniaturization, automation and parallelization of breakthrough and elution studies. Chem Eng Technol 31:893–903
8. Wierling PS, Bogumil R, Knieps-Grunhagen E et al (2007) High-throughput screening of packed-bed chromatography coupled with

SELDI-TOF MS analysis: monoclonal antibodies versus host cell protein. Biotechnol Bioeng 98:440–450

9. Susanto A, Treier K, Knieps-Grunhagen E et al (2009) High throughput screening for the design and optimization of chromatographic processes: automated optimization of chromatographic phase systems. Chem Eng Technol 32:140–154
10. Bergander T, Nilsson-Valimaa K, Oberg K et al (2008) High-throughput process development: determination of dynamic binding capacity using microtiter filter plates filled with chromatography resin. Biotechnol Prog 24:632–639
11. Kramarczyk JF, Kelley BD, Coffman JL (2008) High-throughput screening of chromatographic separations: II. Hydrophobic interaction. Biotechnol Bioeng 100:702–720
12. Kelley BD, Switzer M, Bastek P et al (2008) High-throughput screening of chromatographic separations: IV. Ion-exchange. Biotechnol Bioeng 100:950–963
13. Bailey MJ, Hooker AD, Adams CS et al (2005) A platform for high-throughput molecular characterization of recombinant monoclonal antibodies. J Chromatogr B 826:177–187
14. Nfor BK, Noverraz M, Chilamkurthi S et al (2010) High-throughput isotherm determination and thermodynamic modeling of protein adsorption on mixed mode adsorbents. J Chromatogr B 1217:6829–6850
15. Chhatre S, Bracewell DG, Titchener-Hooker NJ (2009) A microscale approach for predicting the performance of chromatography columns used to recover therapeutic polyclonal antibodies. J Chromatogr A 1216:7806–7815
16. Titchener-Hooker NJ, Dunnill P, Hoare M (2008) Micro biochemical engineering to accelerate the design of industrial–scale downstream processes for biopharmaceutical proteins. Biotechnol Bioeng 100:473–487
17. Bhambure R, Rathore AS (2013) Chromatography process development in the QbD paradigm I. Establishing a high throughput process development (HTPD) platform as a tool for establishing "characterization space" for an ion exchange chromatography step. Biotechnol Prog 29:403–414
18. Diederich P, Hoffmann M, Hubbuch J (2015) High-throughput process development of purification alternatives for the protein avidin. Biotechnol Prog 31:957–973
19. Rathore AS, Winkle H (2009) Quality by design for biopharmaceuticals: regulatory perspective and approach. Nat Biotechnol 27:26–34
20. Rathore AS (2009) A roadmap for implementation of quality by design (QbD) for biotechnology products. Trends Biotechnol 27:546–553
21. Read EK, Park JT, Shah RB et al (2010) Process analytical technology (PAT) for biopharmaceutical products: concepts and applications – part I. Biotechnol Bioeng 105:276–284
22. Read EK, Park JT, Shah RB et al (2010) Process analytical technology (PAT) for biopharmaceutical products: concepts and applications – part II. Biotechnol Bioeng 105:285–295
23. Rathore AS, Bhambure R, Ghare V (2010) Process analytical technology (PAT) for biopharmaceutical products. Anal Bioanal Chem 398:137–154
24. Rathore AS, Ghare V, Bhambure R (2011) Process analytical technology (PAT) for bioseparation unit operations. In: Undey C, Low D, De Menezes JMC (eds) Process analytical technology applied in biopharmaceutical process development and manufacturing. Taylor and Francis, Boca Raton, FL, pp 179–200
25. Roch P, Mandenius CF (2016) On-line monitoring of downstream bioprocesses. Curr Opin Chem Eng 14:112–120
26. Patel BA, Pinto ND, Gospodarek A et al (2017) On-line ion exchange liquid chromatography as a process analytical technology for monoclonal antibody characterization in continuous bioprocessing. Anal Chem 89:11357–11365
27. Joshi VS, Kumar V, Rathore AS (2017) Optimization of ion exchange sigmoidal gradients using hybrid models: implementation of quality by design in analytical method development. J Chromatogr A 1491:145–152
28. Kumar V, Bhalla A, Rathore AS (2014) Design of experiments applications in bioprocessing: concepts and approach. Biotechnol Prog 30:86–99
29. Rathore AS, Pathak M, Godara A (2016) Process development in the QbD paradigm: role of process integration in process optimization for production of biotherapeutics. Biotechnol Prog 32:355–362
30. Shekhawat LK, Godara A, Kumar V, Rathore AS (2018) Design of experiments applications in bioprocessing: chromatography process development using split DOE. Biotechnol Prog. https://doi.org/10.1002/btpr.2730

31. Tustian AD, Laurin L, Ihre H et al (2018) Development of a novel affinity chromatography resin for platform purification of bispecific antibodies with modified protein a binding avidity. Biotechnol Prog. https://doi.org/10.1002/btpr.2622
32. Rodriguez-Aller M, Guillarme D, Beck A, Fekete S (2016) Practical method development for the separation of monoclonal antibodies and antibody-drug-conjugate species in hydrophobic interaction chromatography, part 1: optimization of the mobile phase. J Pharm Biomed Anal 118:393–403
33. Gagnon P, CheungCW LEJ et al (2010) Minibodies and multimodal chromatography methods. BioProcess Int 8:26–35
34. Joshi VS, Kumar V, Rathore AS (2015) Role of organic modifier and gradient shape in RP-HPLC separation: analysis of GCSF variants. J Chromatogr Sci 53:417–423
35. Rathore AS, Sharma C, Malhotra D (2012) Computational fluid dynamics (CFD) as a tool for establishing design space for mixing in a bioreactor. Biotechnol Prog 28:382–391
36. Harms J, Wang X, Kim T et al (2008) Defining design space for biotech products: case study of *Pichia pastoris* fermentation. Biotechnol Prog 24:655–662

Chapter 3

High-Throughput Process Development: II—Membrane Chromatography

Anurag S. Rathore and S. Muthukumar

Abstract

Membrane chromatography is gradually emerging as an alternative to conventional column chromatography. It alleviates some of the major disadvantages associated with the latter, including high-pressure drop across the column bed and dependence on intraparticle diffusion for the transport of solute molecules to their binding sites within the pores of separation media. In the last decade, it has emerged as a method of choice for final polishing of biopharmaceuticals, in particular, monoclonal antibody products. The relevance of such a platform is high in view of the constraints with respect to time and resources that the biopharma industry faces today.

This protocol describes the steps involved in performing HTPD of a membrane chromatography step. It describes the operation of a commercially available device (AcroPrep™ Advance filter plate with Mustang S membrane from Pall Corporation). This device is available in 96-well format with a 7 μL membrane in each well. We will discuss the challenges that one faces when performing such experiments as well as possible solutions to alleviate them. Besides describing the operation of the device, the protocol also presents an approach for statistical analysis of the data that are gathered from such a platform. A case study involving the use of the protocol for examining ion-exchange chromatography of the Granulocyte Colony Stimulating Factor (GCSF), a therapeutic product, is briefly discussed. This is intended to demonstrate the usefulness of this protocol in generating data that are representative of the data obtained at the traditional lab scale. The agreement in the data is indeed very significant (regression coefficient 0.9866). We think that this protocol will be of significant value to those involved in performing high-throughput process development of membrane chromatography.

Key words High-throughput process development (HTPD), Membrane chromatography, AcroPrep™ Advance filter plate with Mustang S membrane, Miniaturization, Ion-exchange chromatography (IEX), Design of experiments (DOE), Design space

1 Introduction

Chromatography is by far the most widely used technique for purification of therapeutic proteins [1–4]. Conventionally, chromatography is carried out using packed beds. However, some key limitations that are associated with packed-bed chromatography include high-pressure drop across the bed and dependence on

Nikolaos E. Labrou (ed.), *Protein Downstream Processing: Design, Development, and Application of High and Low-Resolution Methods*, Methods in Molecular Biology, vol. 2178, https://doi.org/10.1007/978-1-0716-0775-6_3,

intraparticle diffusion for the transport of solute molecules to their binding sites within the pores of such media. Membrane chromatography offers a viable and efficient alternative to traditional packed-bed chromatography [5–11]. The convective flow across the membrane module facilitates the binding of the solute molecules to the ligand, thus overcoming the diffusion-related limitations associated with the traditional resin beads [12–16]. Development of this step for the recombinant protein typically involves optimization of the various parameters that would affect the performance of the step. However, screening optimal process conditions can be time-consuming and tedious (as mentioned in Part I). Miniaturization and automation are bringing new tools and strategies to biotech process development for the production of therapeutic proteins [17–20]. This protocol describes the creation of a high-throughput process development (HTPD) approach using membrane chromatography. The steps for optimization of membrane chromatography are similar to those discussed earlier in Part I for resin-based conventional chromatography. The steps toward establishing an HTPD platform are also similar to those discussed earlier in Part I for resin-based conventional chromatography.

2 Materials

2.1 Equipment

An AcroPrep™ Advance filter plate with a Mustang S membrane.

A multichannel Eppendorf Research® pro electronic pipette for achieving automation in liquid handling.

An Ika MTS 2/4 digital shaker for suspending the sample/buffer in the medium during incubation at various stages of the experiment.

Whatman® vacuum manifold for vacuum filtration of the sample and buffer from 96-well plates.

2.2 Buffer Preparation

Prepare all the buffers using ultrapure water. Prepare and store all the reagents at room temperature.

3 Methods

3.1 High-Throughput Process Development (HTPD)

1. Place an appropriately sized collection plate into the vacuum manifold.
2. Place an AcroPrep™ Advance filter plate with a Mustang S membrane onto the vacuum manifold (*see* **Note 6**).
3. Add 0.2 ml of equilibration/loading buffer into the well of the plate (depending on the plate capacity) and incubate for 5 min at room temperature (25 °C). Apply vacuum at 25 cm Hg for

15 s to remove the fluid from the filter plate using the vacuum manifold. The same should be performed for all fluid removing steps (*see* **Notes 3**, **4**, and 7).

4. Discard the equilibration buffer from the collection plate and repeat the step two more times.
5. Load 0.3 ml of protein sample into each well and incubate for 15 min under continuous shaking at room temperature (RT).
6. Collect the unbound proteins in the flow-through (FT) fraction using vacuum.
7. Add 0.2 ml of equilibration buffer in each well and incubate for 2 min and remove the fluid to wash away residual unbound proteins and repeat the step two times.
8. Elute bound proteins using salt or pH elution.
9. Fractions can be eluted by adding 0.2 ml of elution buffers to avoid dilution of the sample. The incubation time for each elution would be 8 min (*see* **Notes 1** and **2**).
10. After the final NaCl or pH elution step, tightly bound proteins can be eluted with 1% (w/v) sodium dodecyl sulfate (SDS) in water.
11. Perform the analysis using UV-visible spectroscopy or any other analytical test.
12. Analyze the data using appropriate statistical tools for identifying the process parameters that have the most significant effect on the step performance as well as build empirical models to aid in process optimization (*see* **Notes 5** and **8**).
13. Validate portion of the data from the HTPD platform with that from the traditional lab-scale column chromatography (*see* **Note 9**).

3.2 Case Study Illustrating the Application of the HTPD Platform

An AcroPrep Advance 96-well filter plate with a Mustang S 7 μl membrane volume per well was used for the HTPD platform to study the binding behavior of the Granulocyte Colony Stimulating Factor (GCSF). Process steps for ion-exchange chromatography in the HTPD platform are identical to the column chromatography and involve equilibration, protein loading, and elution. A full factorial experimental design was used to investigate the effect of these two process parameters on the recovery of the GCSF across the cation-exchange membrane chromatography. Considering the pH range, the acetate buffer system was selected and buffers of varying molarities were prepared. The experimental design was created and the results were analyzed using JMP® 8.0 (SAS Institute Inc., Cary NC). Acetate buffer of varying pH (4.00, 4.85 and 5.70) and molarity values (20, 35, 50) were used for equilibration in cation-exchange membrane chromatography. A salt-based elution strategy was selected in this study (*see* **Note 9**). Leverage plots were used to

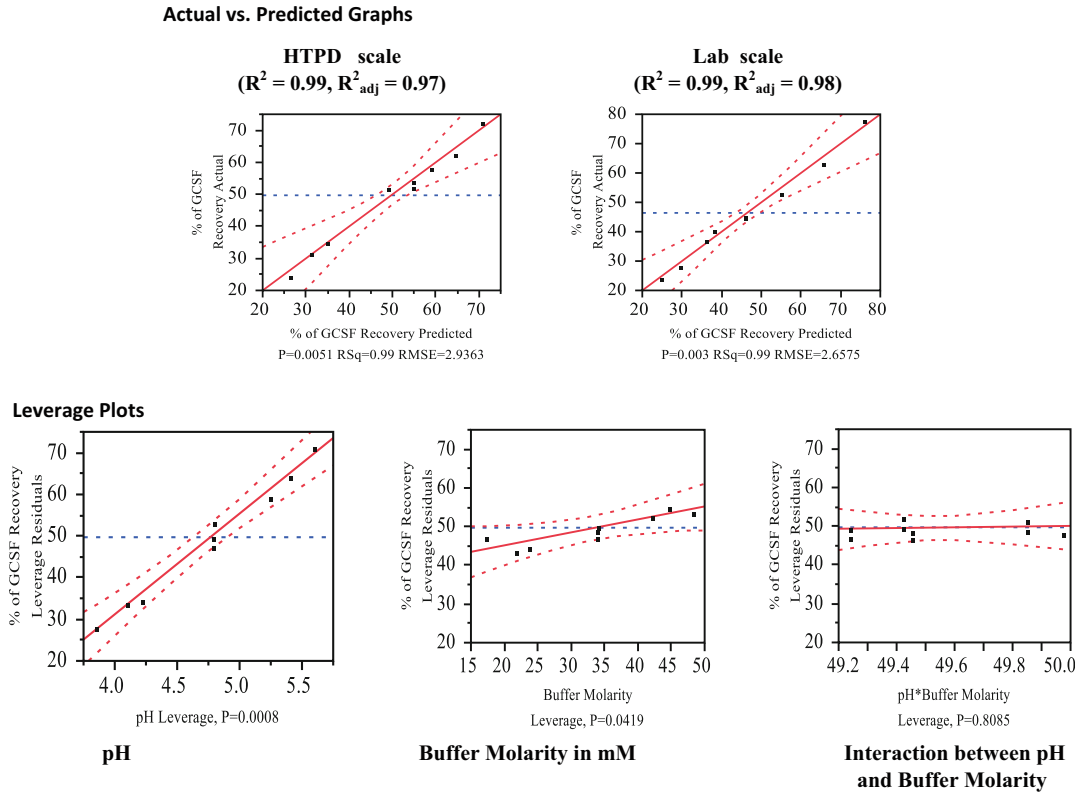

Fig. 1 Statistical comparison of data obtained from the HTPD platform and the traditional lab-scale membrane chromatography and leverage plots based on data from HTPD experimentation for ion-exchange membrane chromatography of the GCSF (Adapted from Ref. 19)

assess the impact of each process parameter on the process outcome. It is evident from Fig. 1 that the HTPD platform is capable of estimating the effect of different process parameters on step performance. Furthermore, as seen in Fig. 1, it can be concluded that the data generated by the HTPD platform is representative of the data generated with the traditionally used lab-scale membrane chromatography systems.

4 Notes

1. The volume of the sample collected in 96-well collection plates was calculated using the path length correction option of Gen 5 software in a Biotek® Epoch microplate spectrophotometer. The path length of each sample obtained was multiplied by the area of the single well of 96-well UV readable plates, leading to accurate determination of the sample volume collected in the collection plate accounting for the losses during liquid dispensing and liquid collection using vacuum application.

2. Recovery of the ion-exchange process step is the amount of protein recovered in the elution fraction divided by the amount loaded into the 96-well plate/lab-scale device.
3. Two methods are currently available for removal of liquid solutions from the AcroPrep™ Advance filter plate with a Mustang S membrane, namely the use of vacuum and the use of the centrifugation technique. The vacuum technique was chosen for our current study. Optimization of the magnitude of vacuum is essential for avoiding droplet formation at the bottom of the plate, which can otherwise lead to loss of the protein solution and result in lower mass balance values.
4. The samples include equilibration buffer, elution buffer, and protein that has to be filtered using a 0.2 μm membrane before loading it in the membrane chromatography column.
5. Even though the recovery is by performing singular measurements, replication of experiments is generally recommended in order to increase the robustness of the process.
6. When choosing the AcroPrep™ Advance filter plate with a Mustang S membrane, consider the amount of material, target protein, and impurities required for final analysis. If a large amount of sample is needed, a larger medium volume and/or an increased number of sample aliquots in the loading step is necessary.
7. The buffers can be stored at 4 °C for a week. Before starting the experiment, bring it to room temperature.
8. Statistical data analysis is necessary in order to reach accurate conclusions. Regression analysis can be performed using least-squares fitting for identifying the relationships between the various responses and the independent process variables. Analysis of Variance (ANOVA) at a 95% confidence interval can be performed to check the statistical validity of the data. Leverage plots can be used for identifying the impact of each process variable as well as interaction among them on the related performance parameters. Finally, the optimization function using a counter profiler can be used by setting constraints on the response variables as per the process needs to estimate the "design space" [21–23].
9. Once the HTPD platform is established, a detailed comparison of the HTPD experiments and the conventional column-scale experiments is essential for validation of the platform. The HTPD platform is capable of generating a lot of data in a very short time. Not all data need to be examined at the traditional scale, but it is important that the platform is validated before the conclusions from the analysis are applied toward commercialization of the product. Once the platform has been validated, it may be possible to use it for other molecules using similar chromatographic separations.

References

1. Frerick C, Kreis P, Gorak A et al (2008) Simulation of a human serum albumin downstream process incorporating ion-exchange membrane adsorbers. Chem Eng Prog 47:1128–1138
2. Gottschalk U et al (2012) The need for innovation in biomanufacturing. Nat Biotechnol 30:489–492
3. Hanke AT, Ottens M (2014) Purifying biopharmaceuticals: knowledge-based chromatographic process development. Trends Biotechnol 32:210–220
4. Fekete S, Veuthey JL, Guillarme D (2017) Achievable separation performance and analysis time in current liquid chromatographic practice for monoclonal antibody separations. J Pharm Biomed Anal 141:59–69
5. Rathore AS, Shirke A (2011) Recent developments in membrane-based separations in biotechnology processes. Prep Biochem Biotechnol 41:307–315
6. Rao CS (2001) Purification of large proteins using ion-exchange membranes. Process Biochem 37:247–256
7. Anspach FB, Petsch D (2000) Membrane adsorbers for selective endotoxin removal from protein solutions. Process Biochem 35:1005–1012
8. Boi C (2007) Membrane adsorbers as purification tools for monoclonal antibody purification. J Chromatogr B 848:19–27
9. Liu Z, Wickramasinghe SR, Qian X (2017) Membrane chromatography for protein purifications from ligand design to functionalization. Sep Sci Technol 52:299–319
10. Muthukumar S, Muralikrishnan T, Mendhe R, Rathore AS (2017) Economic benefits of membrane chromatography versus packed bed column purification of therapeutic proteins expressed in microbial and mammalian hosts. J Chem Technol Biotechnol 92:59–68
11. Shekhawat LK, Manvar AP, Rathore AS (2016) Enablers for QbD implementation: mechanistic modeling for ion-exchange membrane chromatography. J Membr Sci 500:86–98
12. Labanda J, Sabate J, Llorens J (2009) Modeling of the dynamic adsorption of an anionic dye through ion-exchange membrane adsorber. J Membr Sci 340:234–240
13. Van Reis R, Brake JM, Charkoudian J et al (1999) High performance tangential flow filtration using charged membranes. J Membr Sci 159:133–142
14. Ghosh R (2002) Protein separation using membrane chromatography: opportunities and challenges. J Chromatogr A 952:13–27
15. Demmer W, Nussbaumer D (1999) Large-scale membrane adsorbers. J Chromatogr A 852:73–81
16. Teepakorn C, Fiaty K, Charcosset C (2016) A review on some recent advances on membrane chromatography for biomolecules purification. J Colloid Sci Biotechnol 5:32–44
17. Chandler M, Zydney A (2004) High throughput screening for membrane process development. J Membr Sci 237:181–188
18. Rege K, Pepsin M, Steele BF et al (2006) High-throughput process development for recombinant protein purification. Biotechnol Bioeng 93:618–630
19. Muthukumar S, Rathore AS (2013) High throughput process development (HTPD) platform for membrane chromatography. J Membr Sci 442:245–253
20. González-González M, Ruiz-Ruiz F (2017) Aqueous two-phase systems for the recovery of bioparticles. In: Rito-Palomares M, Benavides J (eds) Aqueous two-phase systems for bioprocess development for the recovery of biological products. Springer, Cham, pp 55–78
21. Rathore AS, Sharma C, Malhotra D (2012) Computational fluid dynamics (CFD) as a tool for establishing design space for mixing in a bioreactor. Biotechnol Prog 28:382–391
22. Harms J, Wang X, Kim T et al (2008) Defining design space for biotech products: case study of *Pichia pastoris* fermentation. Biotechnol Prog 24:655–662
23. Shekhawat LK, Godara A, Kumar V, Rathore AS (2018) Design of sDOE. Biotechnol Prog. https://doi.org/10.1002/btpr.2730

Chapter 4

Media Selection in Ion Exchange Chromatography in a Single Microplate

Charlotte Cabanne and Xavier Santarelli

Abstract

High-throughput process development is more and more used in chromatography. Limitations are the tools provided by the manufacturers. Here, we describe a method to select ion exchange chromatographic media using a 96-well filter microplate.

Key words Ion exchange chromatography, Screening, Chromatographic media, Process development

1 Introduction

96-Well microplates are often used in analytical research and clinical diagnostic laboratories because of their speed, accuracy, and efficiency further enhanced by using robotic systems [1]. Their use in chromatographic process development named High-Throughput Process Development (HTPD) is a timeliness approach to avoid complex operations of traditional development methods that relied on trial-and-error approaches. When HTS is associated with Design of Experiment and modeling, it allows having a considerable amount of information. Most studies relate the development of separation methods using 96-well microplates [1–5]. Rege et al. described the high-throughput development of a purification process of α-amylase from a cell-culture broth based on screening of a wide variety of chromatography media and conditions. Studies of dynamic binding capacity under various binding conditions, including various pH and ionic strength levels, have also been done [6, 7]. We have done the screening of chromatographic conditions in a microplate with a design-of-experiment approach to purify antibody from a CHO cell culture. We tested both different resins and different conditions for wash and elution steps [8]. Unfortunately, resin manufacturers do not provide microplates with different resins made by them and by competitors. We propose

Nikolaos E. Labrou (ed.), *Protein Downstream Processing: Design, Development, and Application of High and Low-Resolution Methods*, Methods in Molecular Biology, vol. 2178, https://doi.org/10.1007/978-1-0716-0775-6_4,

here a methodology to screen four ion exchange chromatographic media in a single 96-well microplate. This protocol can be transposed to other techniques such as mixed-mode chromatography with some adaptations [9]. We describe the preparation of four chromatographic resins (or media) of your choice in the 96-well microplate and then the different chromatographic steps (equilibration, protein loading, wash and elution). This is a rapid and accurate technique for choosing the more efficient media in one step.

2 Materials

2.1 Equipment

1. A vacuum manifold compatible with a microplate and a vacuum/filtration pump.
2. A microplate shaker with a circular movement and with a speed of 136 × *g*.
3. A multichannel pipettor.
4. An elastic to tie two plates together.
5. A timer.
6. An AcroWell™ 96-well filter plate with a 0.45 μm hydrophilic polypropylene (GHP) pore membrane and 350 μl wells from Pall Life Sciences (Saint Germain en Laye, France).
7. Nine standard 96-well plates (*see* **Note 1**).
8. A 48 deep well plate.

2.2 Media, Buffers, and Protein

1. Chose four chromatographic media to compare (*see* **Note 2**).
2. Prepare equilibration and elution buffers (*see* **Note 3**).
3. Prepare your protein solution in equilibration buffer (*see* **Note 4**).

3 Methods

3.1 Preparation and Equilibration of Microplates

Carry out all procedures at room temperature or at 4 °C if necessary.

1. Prepare eight empty standard microplates: FT (flowthrough), W1 (wash), W2, W3, E1 (elution), E2, E3, CAL (calibration). Locate the top right corner of the microplates noting these letters in the top right. Prepare a 48-deep-well plate denoted by T (trash). Prepare a standard microplate denoted by T (trash) (*see* **Note 5**).
2. Prepare a mix of each chromatographic media with equilibration buffer (ratio 1:1) in a beaker.

Resin 1	Resin 1	Resin 1	Resin 2	Resin 2	Resin 2	Resin 3	Resin 3	Resin 3	Resin 4	Resin 4	Resin 4
Resin 1	Resin 1	Resin 1	Resin 2	Resin 2	Resin 2	Resin 3	Resin 3	Resin 3	Resin 4	Resin 4	Resin 4
Resin 1	Resin 1	Resin 1	Resin 2	Resin 2	Resin 2	Resin 3	Resin 3	Resin 3	Resin 4	Resin 4	Resin 4
Resin 1	Resin 1	Resin 1	Resin 2	Resin 2	Resin 2	Resin 3	Resin 3	Resin 3	Resin 4	Resin 4	Resin 4
Resin 1	Resin 1	Resin 1	Resin 2	Resin 2	Resin 2	Resin 3	Resin 3	Resin 3	Resin 4	Resin 4	Resin 4
Resin 1	Resin 1	Resin 1	Resin 2	Resin 2	Resin 2	Resin 3	Resin 3	Resin 3	Resin 4	Resin 4	Resin 4
Resin 1	Resin 1	Resin 1	Resin 2	Resin 2	Resin 2	Resin 3	Resin 3	Resin 3	Resin 4	Resin 4	Resin 4
Resin 1	Resin 1	Resin 1	Resin 2	Resin 2	Resin 2	Resin 3	Resin 3	Resin 3	Resin 4	Resin 4	Resin 4

Fig. 1 Distribution of chromatographic media in the 96-well filter plate

3. Shake gently to obtain a homogeneous mixture. Drop 200 μl per well of this mixture in the 96-well filter plate, which corresponds to 100 μl of preequilibrated chromatographic sorbent. This deposit can follow the plan designed for the screening of four resins (Fig. 1). Allow the gel to sediment for 1 min (*see* **Note 6**).
4. Place the plate with 48 deep wells T in the filtration vacuum system and place the microplate with resins on top. Eliminate the equilibration buffer under vacuum aspiration. Turn on the pump within 0.15–0.5 bar and vacuum for 10 s or until all solution is removed. Wipe the plate and put gel on the microplate T (*see* **Notes** 7 and **8**).
5. Fill a rack with equilibration buffer (~60 ml). Using a multichannel pipettor, add 200 μl of equilibration buffer to each well. Mix for 1 min at 1100 rpm. Place the microplate with resins on top of the filtration vacuum system. Turn on the pump within 0.15–0.5 bar and vacuum for 10 s or until all solution is removed. Wipe the plate and put gel on the microplate T. Repeat two times.

3.2 Sample Loading

1. Remove the plate P of the filtration vacuum system. Place the microplate FT in the filtration vacuum system. Fill the sample rack with the protein solution (~25 ml). Using the multichannel pipettor, add 200 μl of the protein solution to each well. Mix for 1 h at 1100 rpm.

2. Place the plate in the filtration vacuum system. Turn on the pump within 0.15–0.5 bar and vacuum for 10 s or until all solution is removed. Wipe the plate and put gel on the plate diameter. Remove the microplate FT from the filtration vacuum system and it is stored for analysis (*see* **Note 8**).

3.3 Wash

1. Place the microplate W1 in the filtration vacuum system. Fill the rack with equilibration buffer (~60 ml). Using the multichannel pipettor, add 200 µl of equilibration buffer to each well. Mix for 1 min at 1100 rpm. Place the microplate with resins on top of the filtration vacuum system. Turn on the pump within 0.15–0.5 bar and vacuum for 10 s or until all solution is removed. Wipe the plate and put on the microplate T. Remove the plate W1 from the filtration vacuum system and stored for analysis.
2. Place the microplate W2 in the filtration vacuum system. Fill the rack with equilibration buffer (~60 ml). Using the multichannel pipettor, add 200 µl of equilibration buffer to each well. Mix for 1 min at 1100 rpm. Place the microplate with resins on top of the filtration vacuum system. Turn on the pump within 0.15–0.5 bar and vacuum for 10 s or until all solution is removed. Wipe the plate and put on the microplate T. Remove the plate W2 from the filtration vacuum system and stored for analysis.
3. Place the microplate W3 in the vacuum filtration system. Fill the rack with equilibration buffer (~60 ml). Using the multichannel pipettor, add 200 µl of equilibration buffer to each well. Mix for 1 min at 1100 rpm. Place the microplate with resins on top of the filtration vacuum system Turn on the pump within 0.15–0.5 bar and vacuum for 10 s or until all solution is removed. Wipe the plate and put on the microplate T. Remove the plate W3 from the filtration vacuum system and stored for analysis.

3.4 Elution

1. Place the microplate E1 in the vacuum filtration system. Fill the rack with elution buffer (~60 ml). Using the multichannel pipettor, add 200 µl of elution buffer to each well. Mix for 1 min at 1100 rpm. Place the microplate with resins on top of the filtration vacuum system. Turn on the pump within 0.15–0.5 bar and vacuum for 10 s or until all solution is removed. Wipe the plate and put on the microplate T. Remove the plate E1 from the filtration vacuum system and stored for analysis.
2. Place the microplate E2 in the vacuum filtration system. Fill the rack with elution buffer (~60 ml). Using the multichannel pipettor, add 200 µl of elution buffer to each well. Mix for 1 min at 1100 rpm. Place the microplate with resins on top of

the filtration vacuum system. Turn on the pump within 0.15–0.5 bar and vacuum for 10 s or until all solution is removed. Wipe the plate and put on the microplate T. Remove the plate E2 from the filtration vacuum system and stored for analysis (*see* **Note 9**).

3. Place the microplate E3 in the vacuum filtration system. Fill the rack with elution buffer (~60 ml). Using the multichannel pipettor, add 200 µl of elution buffer to each well. Mix for 1 min at 1100 rpm. Place the microplate with resins on top of the filtration vacuum system. Turn on the pump within 0.15–0.5 bar and vacuum for 10 s or until all solution is removed. Wipe the plate and put on the microplate T. Remove the plate E3 from the filtration vacuum system and stored for analysis (*see* **Notes 10** and **11**).

3.5 Calibration and Analysis

1. Prepare dilutions of the protein solution in the equilibration buffer and add 200 µl per well of each dilution in the microplate for calibration (CAL) (Fig. 2). Add 200 µl per well of equilibration and elution buffer to do the blank of spectrophotometric measurements (*see* **Note 3**).
2. Analyze the microplates FT, W1, W2, W3, E1, E2, E3, and CAL (*see* **Note 12**).

Protein solution 1 :1	Protein solution 1 :1	Protein solution 1 :1	Eq. buffer	Eq. buffer	El. buffer	El. buffer						
Protein solution 1 :2	Protein solution 1 :2	Protein solution 1 :2	Eq. buffer	Eq. buffer	El. buffer	El. buffer						
Protein solution 1 :4	Protein solution 1 :4	Protein solution 1 :4	Eq. buffer	Eq. buffer	El. buffer	El. buffer						
Protein solution 1 :5	Protein solution 1 :5	Protein solution 1 :5	Eq. buffer	Eq. buffer	El. buffer	El. buffer						
Protein solution 1 :8	Protein solution 1 :8	Protein solution 1 :8	Eq. buffer	Eq. buffer	El. buffer	El. buffer						
Protein solution 1 :10	Protein solution 1 :10	Protein solution 1 :10	Eq. buffer	Eq. buffer	El. buffer	El. buffer						
			Eq. buffer	Eq. buffer	El. buffer	El. buffer						
			Eq. buffer	Eq. buffer	El. buffer	El. buffer						

Fig. 2 Distribution of the microplate CAL (*Eq. Buffer* equilibration buffer, *El. Buffer* elution buffer)

4 Notes

1. Standard or UV microplates can be used according to the subsequent spectrophotometric readings performed.
2. Chose cationic or anionic exchangers as a function of your protein p*I* and its stability. If the protein is most stable below its p*I*, cation exchangers should be used and if it is most stable above its p*I*, anion exchangers should be used. Preferably select media whose bead size is comparable.
3. Chose buffer as a function of the exchanger type, the highest ionic strength, which allows binding to be used. Operate within at least one pH unit above the p*I* of the protein.
   Cationexchange chromatography: (example).

   Equilibration buffer: sodium citrate buffer 35 mM pH 5.5.

   First prepare acidic (A) and basic (B) solutions:

   A: citric acid (0.1 M, 1.05 g) in 50 ml of distilled water.

   B: sodium citrate (0.1 M, 1.47 g) in 50 ml of distilled water.

   Mix 3 ml of A and 7 ml of B with 100 ml of distilled water. Adjust pH at 5.5 with A or B and make up with distilled water to 200 ml.

   Elution buffer: sodium citrate buffer, 35 mM, pH 5.5, NaCl 1 M.

   Prepare as for equilibration buffer, just add 1 M NaCl prior to adjusting pH.

   Anionexchange chromatography: (example).

   Equilibration buffer: Tris–HCl buffer 20 mM pH 8.

   Dissolve 0.48 g of Tris base in 150 ml of distilled water. Adjust pH to 8 with 0.1 M HCl and make up to 200 ml. Elution buffer is prepared by adding 1 M of NaCl in this equilibration buffer.

   Elution buffer: Tris–HCl buffer 20 mM pH 8 NaCl 1 M.

   Prepare as for equilibration buffer, just add 1 M of NaCl prior to adjusting pH.
4. Prepare 30 ml of protein solution in equilibration buffer at a concentration adjusted to the dynamic binding capacities of selected resins. Keep the surplus for the microplate CAL.
5. Wear gloves when handling microplates. Do not touch the bottom of the microplate gel with your fingers to not disturb the subsequent spectrophotometric readings.
6. Place the 96-well filter plate on the microplate T after each use.
7. The gel volume can range from 10 to 100 µl according to the requirements.

8. The distance between the bottom of the microplate with resins and the top of the collection plate in the vacuum manifold should be about 5 mm to avoid cross contamination during vacuum filtration.
9. Wipe the 96-well filter plate after each gel filtration step with a paper towel.
10. Cover the microplate during the incubation time.
11. At half time, the content of the wells can be homogenized gently using a multichannel pipettor.
12. Measurements can be made by reading the absorbance at 280, by an ELISA assay, a protein assay, etc. Data analysis will show how experimental conditions affect yield, binding capacity, recovery, etc. Ensure that the calibration curve is linear and covers the range of concentrations to be measured. Use standard procedures to compensate for the blank absorbance and path length. The FT, W1, W2, and W3 microplates give the amount of unbound protein. The E1, E2, and E3 microplates give the amount of bound/eluted protein. Determine the yield using the ratio of the amount of bound/eluted protein on the amount of protein initially charged. Determine the recovery using the ratio of the amount of bound and unbound proteins to the amount of proteins initially charged.

References

1. Charlton H, Galarza B, Beacon B, LeRiche K, Jones R (2006) Chromatography process development using 96-well microplate formats. BioPharm Int 19:20–27
2. Bensch M, Schulze Wierling P, von Lieres E, Hubbuch J (2005) High throughput screening of chromatographic phases for rapid process development. Chem Eng Technol 28:1274–1284
3. Mazza CB, Rege K, Breneman CM, Sukumar N, Dordick JS, Cramer SM (2002) High-throughput screening and quantitative structure-efficacy relationship models of potential displacer molecules for ion-exchange systems. Biotechnol Bioeng 80:60–72
4. Rege K, Pepsin M, Falcon B, Steele L, Heng M (2006) High-throughput process development for recombinant protein purification. Biotechnol Bioeng 93:618–630
5. Thiemann J, Jankowski J, Rykl J, Kurzawski S, Pohl T, Wittmann-Lievold B, Schluter H (2004) Principle and applications of the protein-purification-parameter screening system. J Chromatogr A 1043:73–80
6. Bergander T, Nilsson-Välimaa K, Öberg KM, Lacki K (2008) High-throughput process development: determination of dynamic binding capacity using microtiter filter plates filled with chromatography resin. Biotechnol Prog 24:632–639
7. Linden T (2001) Untersuchungen zum inneren transport bei der proteinadsorption an poröse medien mittels konfokaler laser-rester-mikroskopie. Heinrich-Heine University, Dusseldorf, p 227
8. Pezzini J, Joucla G, Gantier R, Toueille M, Lomenech A-M, Le Sénéchal C, Garbay B, Santarelli X, Cabanne C (2011) Antibody capture by mixed-mode chromatography: a comprehensive study from determination of optimal purification conditions to identification of contaminating host cell proteins. J Chromatogr A 1218:8197–8208
9. Cabanne C, Santarelli X (2018) Mixed mode chromatography, complex development for large opportunities (Review). Curr Protein Pept Sci 19:1–7

Chapter 5

High-Throughput Screening of Dye-Ligands for Chromatography

Sunil Kumar and Narayan S. Punekar

Abstract

Dye-ligand-based chromatography has become popular after Cibacron Blue, the first reactive textile dye, found application for protein purification. Many other textile dyes have since been successfully used to purify a number of proteins and enzymes. While the exact nature of their interaction with target proteins is often unclear, dye-ligands are thought to mimic the structural features of their corresponding substrates, cofactors, etc. The dye-ligand affinity matrices are therefore considered pseudo-affinity matrices. In addition, dye-ligands may simply bind with proteins due to electrostatic, hydrophobic, and hydrogen bonding interactions. Because of their low cost, ready availability, and structural stability, dye-ligand affinity matrices have gained much popularity. The choice of a large number of dye structures offers a range of matrices to be prepared and tested. When presented in the high-throughput screening mode, these dye-ligand matrices serve as a formidable tool for protein purification. One could pick from the list of dye-ligands already available or build a systematic library of such structures for use. A high-throughput screen may be set up to choose the best dye-ligand matrix as well as ideal conditions for binding and elution, for a given protein. The mode of operation could be either manual or automated. The technology is available to test the performance of dye-ligand matrices in small volumes in an automated liquid handling workstation. Screening a systematic library of dye-ligand structures can help establish a structure-activity relationship. While the origins of dye-ligand chromatography lie in exploiting pseudo-affinity, it is now possible to design very specific biomimetic dye structures. High-throughput screening will be of value in this endeavor as well.

Key words Dye-ligand chromatography, Cibacron blue, Biomimetic ligands, Protein purification, High-throughput screening, Dye-ligand library

1 Introduction

The serendipitous discovery that some proteins bound to blue dextran during gel-permeation chromatography brought Cibacron Blue F3G-A® (abbreviated henceforth as CB, a textile dye from Ciba-Geigy) into the limelight [1, 2]. This specific interaction was subsequently exploited in the successful purification of lactate dehydrogenase [3], blood coagulating factors [4], pyruvate kinase [5, 6], and phosphofructokinase [7]. These initial discoveries led to

Nikolaos E. Labrou (ed.), *Protein Downstream Processing: Design, Development, and Application of High and Low-Resolution Methods*, Methods in Molecular Biology, vol. 2178, https://doi.org/10.1007/978-1-0716-0775-6_5,

the development of textile dyes as ligands for affinity chromatography [8, 9]. Riding on this success, many dye-ligand matrices derived from various textile dyes were explored. These developments positioned dye-ligand chromatography as an important tool in protein purification strategies. The technique has since evolved concurrent with other separation techniques.

Twenty-seven plasma proteins were fractionated by affinity chromatography on CB immobilized on cross-linked agarose beads, simply by varying the elution pH [10]. Thus, a single dye-ligand resin could be used to purify multiple proteins by suitable design of binding and elution conditions. The dye-ligands also score over their protein or nucleic acid counterparts in terms of their ease of synthesis and manipulation [11]. Most dyes in use today show significant stability and resistance to both chemical and biological degradation [12, 13]. The vast structural diversity of textile dyes offers a readily available chemical-library for screening, at least for analytical purification purposes.

1.1 Diversity of Dye-Ligand Matrices

The dye structures: Cibacron Blue is the most popular dye-ligand used for protein purification and this has been reviewed periodically [8, 14, 15]. It belongs to the category of textile dyes known as reactive triazine dyes. Typically, such dyes consist of an anthraquinone chromophore linked to a reactive group (mostly a mono- or di-chlorotriazine ring). Besides the choice of chromophores (and hence different colors!), diversity is generated by a variety of structural moieties A and B (Fig. 1). The sulfonate group on the aniline ring (B, in Fig. 1) may be in the *ortho* position (Cibacron series) or the *meta/para* position (Procion H series). Similarly, the aromatic rings A and B of the dye-ligands may have other substituents like the carboxyl-, amino-, chloro-, or metal-complexing groups. Dyes containing nitrogen in the aromatic ring are also known. Generally, these substituent groups provide improved specificity of interaction with a given protein. Negatively charged sulfonic acid groups make the dye-ligands water soluble [16]. Other variations in presenting a given dye-ligand for chromatography include the length of spacer used and the ligand densities achieved on the matrix.

Immobilization of dye-ligands: Proper presentation of the dye-ligand to the protein of interest is crucial for a successful purification effort. This depends on—(a) the nature of inert support on which the ligand is immobilized, (b) the coupling (attachment) chemistry used, and (c) the final ligand densities available on the matrix for binding. These three features mutually influence each other. The popular inert matrices in use include cross-linked polymeric beads of dextran, agarose, cellulose, methacrylate, polystyrene, etc. Many routes are available for immobilization of dye-ligands on the matrix. The coupling of the ligands to the matrix is either achieved by direct covalent linkage to the matrix surface or via a spacer arm. Direct coupling of the reactive dyes to matrices is

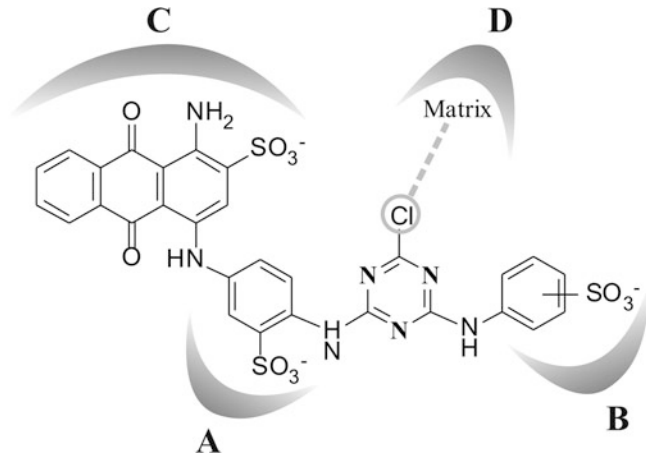

Fig. 1 Structure of Cibacron Blue F-3GA. The structural variety is possible by introducing different bridging groups (A), ring substitutions (B), chromophores (C), and spacers and matrices (D)

well studied [17, 18]. Besides structural variations in the dye structure, a systematic library of matrices could include the same dyes immobilized differently, through a choice of spacer lengths. The length of a spacer arm can be controlled and the spacers may be built in with various diaminoalkanes, bisoxiranes, epichlorohydrin, or dextran. Such a variation may also endow these dye-ligand resins with differential binding abilities [19–21].

Systematic dye-ligand libraries: Attempts have been made in the past to generate novel dye-ligands for better selectivity [20–23]. A rational design of a dye-ligand as an affinity bait requires detailed structural information and computational analysis [24, 25]. Ligand binding can be targeted to the active site or other solvent-exposed regions of the target protein [23, 26–29]. However, rational design is tricky and involved as conformational flexibility (of the ligand and the protein) is an important consideration [28]. A library screening-based approach works best when rational design is not feasible, either due to limited information or investment. A systematic library of dye-ligand affinity resins can be screened to find the most selective adsorbent matrix. Such a library may be constructed by—(a) choosing from a set of readily available entities (from major suppliers like Bio-Rad, GE Healthcare, Prometic, and Tosoh Bioscience) selected either randomly or rationally (based on structures) and (b) systematic combinatorial chemical synthesis (manual or automated) [15, 20, 30]. The library could contain variety, both in the dye structure and spacer length. Screening of dye-ligand diversity has found application in the purification and/or resolution of a range of proteins (Table 1). Whenever a dye-ligand library with systematic structural information is available, it should be possible to generate structure-activity correlations.

Table 1
Dye-ligand libraries tested for protein purification

Target protein(s)	Library size	Operation	References
Glucose-6-phosphate dehydrogenase	65	Column	[48]
Recombinant human clotting factor VII	50	Column	[49]
Enzymes (glucose-6-phosphate dehydrogenase, glucokinase, and fructokinase)	50	Column	[50]
IgG2-enriched fraction	69	Frontal chromatography	[33]
Enzymes (NADP-glutamate dehydrogenase, laccase, glutamine synthetase, arginase, and bovine pancreatic trypsin) and serum proteins (human serum albumin and IgG)	96	Batch	[20]
Enzymes (glycerol dehydrogenase, 6-phosphogluconate dehydrogenase, and glucose-6-phosphate dehydrogenase)	96	Microtitre plate	[37]

1.2 High-Throughput Screening

With a large structural diversity, it becomes necessary to effectively screen and choose a suitable adsorbent. The best way to exploit the rich structural range is the high-throughput screening approach.

Mode of operation: A chromatographic matrix is traditionally chosen for its ability to bind the protein of interest. However, occasionally negative binding feature is employed to eliminate some contaminants [31]. Protein binding to the dye-ligand matrix is tested in a batch or column mode.

When choosing from fewer dye adsorbents, the column mode of evaluation and/or screening may be suitable. This method quickly gets cumbersome when dealing with difficult-to-pack matrices with variable flow properties and poor mechanical strength. Certain beads shrink and/or deform with changing pressure, ionic strength, etc. Handling many columns simultaneously demands automation in process parameter control. Protein chromatography systems like Äkta Explorer (GE Healthcare), BioCAD 700E Workstation (Applied Biosystems), and Bio-Logic DuoFlow (Bio-Rad) can handle one column at a time; hence, each dye-ligand adsorbent has to be individually tested for its efficacy to bind the protein of interest. However, screening based on automated parallel column chromatography is possible with the availability of automated instruments: (a) The multi-module Äktaxpress set up (GE Healthcare), (b) Protein Maker (Emerald Bio, MA, USA; capable of handling 24 chromatography columns (1–5 ml) in parallel), and (c) Freedom EVO® Protein Chromatography system (Tecan Group Ltd., Männedorf, Switzerland; able to handle 96 Atoll's MediaScout® RoboColumn array (ATOLL GmbH

Weingarten, Germany) and PreDictor RoboColumn™ units (GE Healthcare, Uppsala, Sweden)) [32]. Other MultiPROBE liquid-handling workstations (e.g., from PerkinElmer in Boston, MA, USA) may also be adopted for multicolumn screening. All the column-based approaches still place limits on the number of dye adsorbents tested at one time. Frontal chromatography was used to screen 69 immobilized dyes for effective enrichment of IgG2 fractions [33]. For this, four dye-ligand matrices were processed in parallel at a time using a multi-channel peristaltic pump and a four-channel fraction collector.

The batch operation is more scalable than the column mode when screening a large number of dye-ligands. The batch mode helps in quickly finalizing the binding and elution conditions. However, plain retardation on the adsorbent of the target protein cannot be easily scored. Simple adsorption isotherms were used to screen many dyes for their ability to bind yeast alcohol dehydrogenase [34]. Rapid, batch mode screening of a large number of dyes to purify proteases [35] and penicillin-binding protein [36] is reported. In a microtitre-plate-based operation, dye-affinity matrices were screened and selected to resolve and purify three different dehydrogenases from *Aspergillus nidulans*. The enzyme fractions were also assayed in the microtitre plates [37]. Although automated platforms are available for microtitre plate-based screens in a 96-well format (Table 1 in Ref. 20), the method of microcentrifuge tube-based batch binding and elution is less resource intensive yet very effective.

Dye-ligand adsorbents could be offered for high-throughput screening in a 96 pre-packed, small column screening kit. It is also possible to encapsulate and trap very small quantities of the adsorbent at the very end of a pipette tip (PhyTips from PhyNexus, San Jose, CA, USA) [38]. A combination of tips, adsorbents, and an automated platform provides exquisite control on the screening process. Kits based on filtration in a spin-column format allow for faster processing. Spin-column kits with membrane matrix adsorbents (developed by Vivascience, Hanover, Germany) are another option. The simplicity of kits and set protocols make protein purification less formidable to a molecular biologist. A library of 2688 triazine compounds was immobilized on a glass surface and the interaction of IgG with this small molecule microarray was monitored by Surface Plasmon Resonance [39]. A similar high-throughput approach could be adopted to screen a dye-ligand library.

Binding and elution strategies: The aromatic triazine moiety of CB was thought to mimic the structure of nicotinamide adenine dinucleotide (NAD^+) and proteins and enzymes possessing a 'dinucleotide fold' could therefore bind with CB [40]. However, it is difficult to rationalize how so many other proteins (like albumin, aldolases, hemoglobin, and cytochrome C) lacking a dinucleotide fold can also bind to CB. It is more likely that several functional

groups (and the conformational freedom enjoyed by them) endow a dye-ligand with the ability to maximize favorable interactions with proteins. These interactions could be at the active sites (often specific) or less specific ones at the crevices, cavities, or patches on the protein surface. The components may include a combination of ionic, hydrophobic, hydrogen bonding, and electrostatic forces [41]. This in turn determines the optimal binding and the elution strategy is to be employed. A more selective binding to the adsorbent is desirable and should be encouraged through suitably defined process parameters [10, 29, 42].

A CB-bound adsorbent is known to act as a cation exchanger (due to sulfonate groups) and a hydrophobic matrix (due to its aromatic rings). With ionic interactions, binding and elution are best controlled by varying the ionic strength and/or pH. The hydrophobic interactions can be modulated by the addition of an organic solvent or a detergent to the elution buffer. Elution of a protein bound to the dye-ligand matrix can be made either selective or generic. Nucleotide cofactors like NAD^+, NADPH, ATP, etc. are used to selectively elute bound dehydrogenases and kinases from the matrix [43]. The 'kinetic locking-on' is an important strategy in selective enzyme binding and elution—it has been successfully used to purify some dehydrogenases [11]. If and when a dye-ligand mimics a substrate or a cofactor (like NAD^+ or $NADP^+$), then the enzyme could be locked on to the dye adsorbent, by including another substrate in the loading and equilibration buffers. Similar approaches could also be incorporated into the screening strategy.

For nonselective elution, one may normally employ an ionic strength gradient (linear or step), a pH gradient, or both. In addition, elution can also be achieved by including nonaqueous solvents, detergents, and chaotropic agents. The binding of proteins to a number of immobilized triazine dye-ligand adsorbents is enhanced in the presence of low concentrations of divalent metal ions like Zn^{2+}, Co^{2+}, Mn^{2+}, Ni^{2+}, and Cu^{2+} [13, 44, 45].

In high-throughput screening, binding and/or elution steps can be conveniently optimized for the target protein. This may include permutations of multiple elution routines in a sequential manner. The procedure thereby permits us to choose quickly from a large number of dye-ligand adsorbents.

2 Materials

Use analytical-grade chemicals to prepare various reagents. Unless specified, store all reagents and chemicals at room temperature. Dispose waste materials properly following standard guidelines.

1. Ultrapure water (resistivity of 20 MΩ cm, at 25 °C) (for preparation of various reagents).

2. Extraction buffer: 200 mM imidazole-HCl, pH 7.5; 1 mM PMSF; 12 mM $MnSO_4$; and 2 mM 2-mercaptoethanol (*see* **Note 1**).
3. Binding/wash buffer: 25 mM imidazole-HCl, pH 7.5; 1.2 mM $MnSO_4$; and 2 mM 2-mercaptoethanol (*see* **Note 1**).
4. Elution buffer: 25 mM imidazole-HCl, pH 7.5; 1.2 mM $MnSO_4$; and 2 mM 2-mercaptoethanol with KCl (0.3 M for elution 1 and elution 2; 0.6 M for elution 3) (*see* **Note 1**).
5. A library of 96 dye-ligand adsorbents (*see* **Note 2**).
6. Refrigerated centrifuge.
7. Miscellaneous: microcentrifuge tubes (1.5 ml capacity), micropipettes, disposable tips, and a scalpel blade.

3 Method

3.1 High-Throughput Screening: Binding and Elution of 4-Guanidinobutyrase

We describe a microcentrifuge tube-based manual method (batch mode) to rapidly screen 96 dye-ligand adsorbents [20] for their ability to bind (and elute) 4-guanidinobutyrase from *Aspergillus niger* (*see* **Note 3**).

1. Extract 4-guanidinobutyrase from *A. niger* according to the protocol reported for arginase (*see* **Note 4**).
2. Cut the sharp end of a 1-ml *p*ipette tip (with a scalpel blade) to pipette out the adsorbent suspension from a stock. Pipette out the suspension into a microcentrifuge tube (*see* **Note 5**). Spin down the adsorbent (0.3 ml when settled) by brief centrifugation (5000 × *g* for 2 min) and discard the supernatant solution.
3. Add 1 ml of the binding/wash buffer to the settled adsorbent, gently mix, and centrifuge (5000 × *g* for 2 min). Discard the supernatant solution. Repeat this washing step two more times (*see* **Note 6**).
4. Add 0.5 ml of 4-guanidinobutyrase (0.5 U of activity) to the equilibrated resins and mix gently. Incubate on ice for 30 min with occasional mixing and centrifuge (5000 × *g* for 2 min). Carefully pipette out the supernatant and this is the unbound fraction (*see* **Note 7**).
5. Wash the affinity resins twice with 0.5 ml of binding/wash buffer. Each time centrifuge (5000 × *g* for 2 min) and collect the supernatant separately. These are the two wash fractions (wash 1 and wash 2).
6. Elute the bound proteins from the adsorbent in three consecutive steps.

(a) Add elution buffer containing 0.3 M KCl (0.5 ml), gently mix and incubate on ice for 10 min. Centrifuge (5000 × *g* for 2 min) and collect the supernatant (eluate 1).

(b) Repeat step (a) once more and collect the supernatant (eluate 2).

(c) Add elution buffer containing 0.6 M KCl (0.5 ml), gently mix and incubate on ice for 10 min. Centrifuge (5000 × *g* for 2 min) and collect the supernatant (eluate 3) (*see* **Note 8**).

7. Estimate the 4-guanidinobutyrase activity in each fraction (unbound, wash 1, wash 2, eluate 1, eluate 2, and eluate 3) (*see* **Note 9**).
8. Calculate the percent 4-guanidinobutyrase activity recovered by using the following formula (*see* **Note 10**).

$$\text{Enzyme U recovered } (\%) = \frac{\text{Enzyme U (eluate 1 + eluate 2 + eluate 3)}}{\text{Enzyme U loaded}} \times 100.$$

3.2 Data Interpretation

A library of 96 dye-ligand adsorbents used here shows significant discriminatory binding with 4-guanidinobutyrase (Fig. 2). Under a set of binding/elution conditions tested, few adsorbents bound arginase (another ureohydrolase from *A. niger* [20]) better than 4-guanidinobutyrase. The library also contains representative resins that (a) bound both the enzymes, (b) bound neither one, and

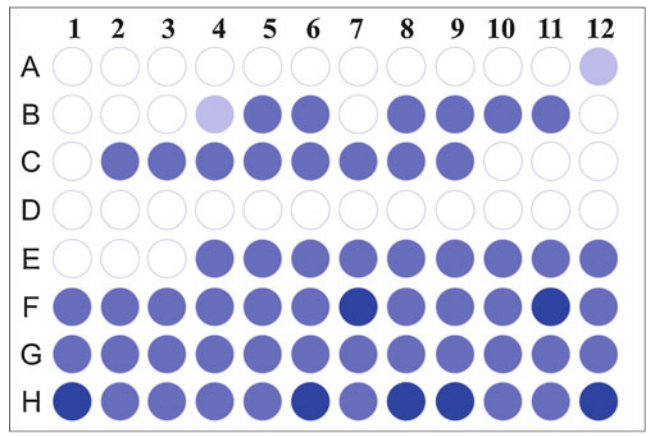

Fig. 2 Discriminatory binding of dye-ligand adsorbents to 4-guanidinobutyrase. The adsorbents were screened for their ability to bind and elute 4-guanidinobutyrase. Enzyme recovered in the eluate (relative to the amount loaded) ranged from 0% to 100%. The affinity resins were grouped into four categories according to percent 4-guanidinobutyrase recovered as—none (<10%; ○), poor (10–33%; ●), intermediate (34–66%; ●), and high (>66%; ●). Affinity resins (CR-085, CR-090, CR-092, and CR-093) showed more than 70% enzyme recovery

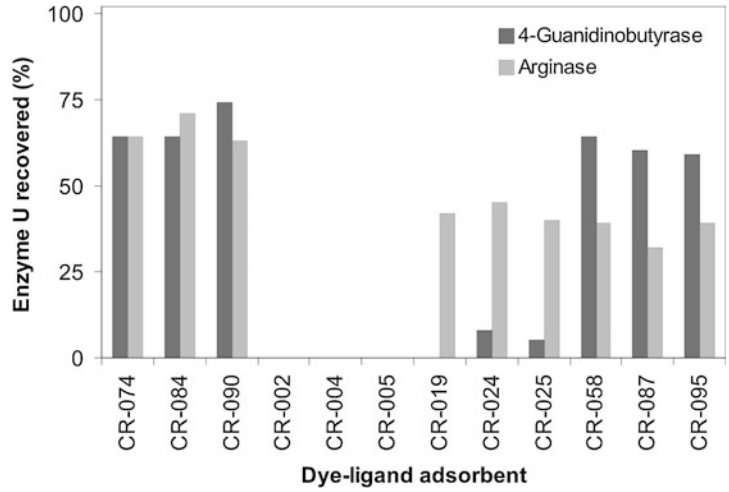

Fig. 3 Differential binding of 4-guanidinobutyrase and arginase with select dye-ligand adsorbents. Representative examples of adsorbents that bound (a) both the enzymes (CR-074, CR-084, and CR-090), (b) neither enzyme (CR-002, CR-004, and CR-005), (c) arginase preferentially (CR-019, CR-024, and CR-025), and (d) 4-guanidinobutyrase better than arginase (CR-058, CR87, and CR-095) are shown (Arginase activity data for comparison is from Ref. 20)

(c) bound 4-guanidinobutyrase better (like CR-058, CR-087, and CR-095; *see* Fig. 3). Promising resins from this analysis can be chosen for further standardization and scale-up (*see* **Note 11**) to purify 4-guanidinobutyrase.

4 Notes

1. Storage conditions: Store the extraction buffer, binding/wash buffer, and elution buffer at 4 °C and use it within a month. Add 2-mercaptoethanol and PMSF, freshly to the buffer as required, just before use. Note that PMSF in water is very unstable [46].
2. Chromatography adsorbents (CibaFix® resins CR-001 to CR-096 [20]) are best stored at 4 °C in 20% ethanol. Similarly, other adsorbent libraries (synthesized or commercially available from suppliers like Bio-Rad, GE Healthcare, Prometic, and Tosoh Bioscience) can also be defined and screened.
3. The batch mode protocol can easily be adopted for any target protein of choice as well as for other dye-ligand matrices. Initial buffer conditions suitable for efficient handling of the protein (enzyme) and a simple procedure to follow its activity would be helpful. We show here the data for 4-guanidinobutyrase from *A. niger* as a representative example. The number of resins

handled in one round of experimentation will depend on the centrifuge rotor capacity. A centrifuge rotor with a 24-tube holder was used.

4. Add filter-sterilized 4-guanidinobutyrate to the autoclaved fungal growth medium. Ensure that the final pH is between 5.5 and 6.0. Grow *A. niger* on this medium and extract 4-guanidinobutyrase essentially as done for arginase [20]. The protein fractionating between 30% and 60% ammonium sulfate saturation is further enriched on a DEAE Sephacel column (a linear gradient of 0–0.8 M KCl). Pool active fractions, desalt, and use this 4-guanidinobutyrase preparation for screening.
5. Use dedicated tips for each adsorbent. A larger opening in pipette tips allows free movement of the gel suspension during pipetting. Pipette out a suitably larger volume of the suspension in the 1.5 ml graduated microcentrifuge tube such that there is 0.3 ml of dye-ligand adsorbent when settled. Graduated microcentrifuge tubes are better suited to visually note the actual packed volume of the resin bed.

   Dye-ligand adsorbents could also be packed into commercially available empty spin columns with filters (MICROCON® Centrifugal Filter Devices, Millipore and Nanosep® MF Centrifugal Devices, PALL Life Sciences). This approach is user friendly. However, reproducibility/protein-stability issues related to adsorbent deformation/drying upon centrifugation need to be resolved. These technical hurdles can be overcome with some effort.
6. The dye adsorbents should be equilibrated with binding/wash buffer before use. This removes the ethanol used to store the adsorbent. Ensure that the pH of the supernatant after the third wash is the same as that of the binding/wash buffer (check this with a strip of pH paper). Three washes of 1 ml each suffice to equilibrate 0.3 ml of the adsorbent.
7. 4-Guanidinobutyrase activity is quantified by measuring urea formed in the reaction by the Archibald method [47]. One unit of 4-guanidinobutyrase activity is the amount of enzyme required to produce 1 μmol of urea per min in the standard assay. The ideal quantity of sample load is an empirical decision governed by the binding capacity of the adsorbent and the sensitivity of the assay method. Overloading even a good adsorbent can lead to difficulties in interpretation, as excess enzyme will appear in the unbound and wash fractions.

   Gentle mixing of the adsorbent and the sample is critical. Ensure minimal protein inactivation while maintaining optimal sample contact with the resin. An end-on mixer (with multiple holders) operated in a cold room could also be used for incubations.

8. Although we demonstrate the elution of 4-guanidinobutyrase by a simple-step gradient of KCl, other parameters like pH, solvent, substrate, inhibitors, etc. could also be attempted.
9. Store all enzyme fractions (from different steps) carefully on ice to avoid any loss of enzyme activity. Any inactivation due to storage will also influence percent recovery.
10. A quick alternative to monitor just the 4-guanidinobutyrase binding is to compare the enzyme units loaded with those recovered in the unbound fraction. However, this does not take into account for inactivation, if any.
11. Evaluation of the binding capacity of an adsorbent should be the first step once it has been shortlisted through a screen. Although binding capacity measurements can be performed with 0.3 ml of the adsorbent (*see* **Note 5**), working with a larger volume provides better reproducibility. Take 2 ml (settled volume) of the dye-ligand adsorbent in 15 ml conical bottom centrifuge tubes and equilibrate with 10 ml of binding/wash buffer. Load increasing amounts of the sample (use separate tubes for each concentration) to determine the maximum binding that can be achieved [20].

Acknowledgements

We thank Ciba Research (India) Pvt. Ltd., for providing the ninety-six novel-affinity resins (CibaFix® Resins CR-001–CR-096). This work was supported by a research fellowship (to Sunil Kumar) from the University Grant Commission, India, and the Board of Research in Nuclear Sciences, Department of Atomic Energy, India.

References

1. Kopperschlager G, Freyer R, Diezel W et al (1968) Some kinetic and molecular properties of yeast phosphofructokinase. FEBS Lett 1:137–141
2. Haeckel R, Hess B, Lauterborn W et al (1968) Purification and allosteric properties of yeast pyruvate kinase. Hoppe Seylers Z Physiol Chem 349:699–714
3. Ryan LD, Vestling CS (1974) Rapid purification of lactate dehydrogenase from rat liver and hepatoma: a new approach. Arch Biochem Biophys 160:279–284
4. Swart AC, Hemker HC (1970) Separation of blood coagulation factors II, VII, IX and X by gel filtration in the presence of dextran blue. Biochim Biophys Acta 222:692–695
5. Blume KG, Hoffbauer RW, Busch D et al (1971) Purification and properties of pyruvate kinase in normal and in pyruvate kinase deficient human red blood cells. Biochim Biophys Acta 227:364–372
6. Staal GE, Koster JF, Kamp H et al (1971) Human erythrocyte pyruvate kinase. Its purification and some properties. Biochim Biophys Acta 227:86–96
7. Bohme HJ, Kopperschlager G, Schulz J et al (1972) Affinity chromatography of phosphofructokinase using Cibacron blue F3G-A. J Chromatogr 69:209–214
8. Subramanian S (1984) Dye-ligand affinity chromatography: the interaction of Cibacron

Blue F3GA with proteins and enzymes. CRC Crit Rev Biochem 16:169–205

9. El Khoury G, Khogeer B, Chen C et al (2015) Bespoke affinity ligands for the purification of therapeutic proteins. Pharm Bioprocess 3:139–152
10. Gianazza E, Arnaud P (1982) Chromatography of plasma proteins on immobilized Cibacron Blue F3-GA. Mechanism of the molecular interaction. Biochem J 203:637–641
11. Forde J, Oakey L, Jennings L et al (2005) Fundamental differences in bioaffinity of amino acid dehydrogenases for N6- and S6-linked immobilized cofactors using kinetic-based enzyme-capture strategies. Anal Biochem 338:102–112
12. Burton SJ (1992) Dye-ligand affinity chromatography. Methods Mol Biol 11:91–103
13. Lowe CR, Pearson JC (1984) Affinity chromatography on immobilized dyes. In: William BJ (ed) Methods in enzymology part C: enzyme purification and related techniques. Academic, New York, NY, pp 97–113
14. Denizli A, Piskin E (2001) Dye-ligand affinity systems. J Biochem Biophys Methods 49:391–416
15. Curling J (2004) Affinity chromatography – from textile dyes to synthetic ligands by design, part I. BioPharm Int 17:34–42
16. Lascu I, Porumb H, Porumb T et al (1984) Ion-exchange properties of Cibacron Blue 3G-A Sepharose (Blue Sepharose) and the interaction of proteins with Cibacron Blue 3G-A. J Chromatogr 283:199–210
17. Baird JK, Sherwood RF, Carr RJ et al (1976) Enzyme purification by substrate elution chromatography from procion dye-polysaccharide matrices. FEBS Lett 70:61–66
18. Burton SJ, Stead CV, Lowe CR (1990) Design and applications of biomimetic anthraquinone dyes. III. Anthraquinone-immobilised C.I. reactive blue 2 analogues and their interaction with horse liver alcohol dehydrogenase and other adenine nucleotide-binding proteins. J Chromatogr 508:109–125
19. Ekkundi VS, Punekar NS, Roentgen G et al (2006) Adsorbents comprising anthraquinone dye-ligands for the separation of biological materials. WO/2006/108760, EP20060725379
20. Kumar S, Dalvi DB, Moorthy M et al (2009) Discriminatory protein binding by a library of 96 new affinity resins: a novel dye-affinity chromatography tool-kit. J Chromatogr B Analyt Technol Biomed Life Sci 877:3610–3618
21. Felle MF, Granström M, Linder D et al (2016) Method for purification of antibodies, antibody fragments or engineered variants thereof using specific anthraquinone dye-ligand structures. US 2016/0347789 A1
22. Garg N, Galaev IY, Mattiasson B (1996) Dye-affinity techniques for bioprocessing: recent developments. J Mol Recognit 9:259–274
23. Lowe CR, Lowe AR, Gupta G (2001) New developments in affinity chromatography with potential application in the production of biopharmaceuticals. J Biochem Biophys Methods 49:561–574
24. Labrou NE (2003) Design and selection of ligands for affinity chromatography. J Chromatogr B Analyt Technol Biomed Life Sci 790:67–78
25. Labrou NE, Eliopoulos E, Clonis YD (1999) Molecular modeling for the design of a biomimetic chimeric ligand. Application to the purification of bovine heart L-lactate dehydrogenase. Biotechnol Bioeng 63:322–332
26. Clonis YD, Labrou NE, Kotsira VP et al (2000) Biomimetic dyes as affinity chromatography tools in enzyme purification. J Chromatogr A 891:33–44
27. Lowe CR (2001) Combinatorial approaches to affinity chromatography. Curr Opin Chem Biol 5:248–256
28. Carlson HA (2002) Protein flexibility and drug design: how to hit a moving target. Curr Opin Chem Biol 6:447–452
29. Liang-Schenkelberg J, Fieg F, Waluga T (2017) Molecular insight into affinity interaction between Cibacron Blue and proteins. Ind Eng Chem Res 56:9691–9697
30. Curling J (2004) Affinity chromatography – from textile dyes to synthetic ligands by design, Part II. BioPharm Int 17:60–66
31. Lee MFX, Chan ES, Tey BT (2014) Negative chromatography: progress, applications and future perspectives. Process Biochem 49:1005–1011
32. Wiendahl M, Schulze Wierling P, Nielsen J et al (2008) High throughput screening for the design and optimization of chromatographic processes – miniaturization, automation and parallelization of breakthrough and elution studies. Chem Eng Technol 31:893–903
33. Hasnaoui MH, Debbia M, Cochet S et al (1997) Screening of a large number of dyes for the separation of human immunoglobulin G2 from the other immunoglobulin G subclasses immunoglobulin G2 enrichment on immobilized Procion Yellow HE-4R. J Chromatogr A 766:49–60

34. Raya-Tonetti G, Perotti N (1999) Rapid screening of textile dyes employed as affinity ligands to purify enzymes from yeast. Biotechnol Appl Biochem 29:151–156
35. Ibrahim-Granet O, Bertrand O (1996) Separation of proteases: old and new approaches. J Chromatogr B Biomed Appl 684:239–263
36. Mottl H, Keck W (1992) Rapid screening of a large number of immobilized textile dyes for the purification of proteins: use of penicillin-binding protein 4 of *Escherichia coli* as a model enzyme. Protein Expr Purif 3:403–409
37. Hondmann DH, Visser J (1990) Screening method for large numbers of dye-adsorbents for enzyme purification. J Chromatogr 510:155–164
38. Chapman T (2005) Protein purification: pure but not simple. Nature 434:795–798
39. Uttamchandani M, Walsh DP, Khersonsky SM et al (2004) Microarrays of tagged combinatorial triazine libraries in the discovery of small-molecule ligands of human IgG. J Comb Chem 6:862–868
40. Stellwagen E (1977) Use of blue dextran as a probe for the nicotinamide adenine dinucleotide domain in proteins. Acc Chem Res 10:92–98
41. Kopperschläger G, Bohme HJ, Hofmann E (1982) Cibacron blue F3G-A and related dyes as ligands in affinity chromatography. In: Fiechter A (ed) . Springer, Berlin, pp 101–138
42. Gallant SR, Koppaka V, Zecherle N (2008) Dye ligand chromatography. Methods Mol Biol 421:61–69
43. Thompson ST, Cass KH, Stellwagen E (1975) Blue dextran-sepharose: an affinity column for the dinucleotide fold in proteins. Proc Natl Acad Sci U S A 72:669–672
44. Small DAP, Atkinson T, Lowe CR (1981) High-performance liquid affinity chromatography of enzymes on silica-immobilised triazine dyes. J Chromatogr A 216:175–190
45. Hughes P, Lowe CR, Sherwood RF (1982) Metal ion-promoted binding of proteins to immobilized triazine dye affinity adsorbents. Biochim Biophys Acta 700:90–100
46. James GT (1978) Inactivation of the protease inhibitor phenylmethylsulfonyl fluoride in buffers. Anal Biochem 86:574–579
47. Dave K, Ahuja M, Jayashri TN et al (2012) A novel selectable marker based on *Aspergillus niger* arginase expression. Enzyme Microb Technol 51:53–58
48. Hey Y, Dean PD (1983) Tandem dye-ligand chromatography and biospecific elution applied to the purification of glucose-6-phosphate dehydrogenase from *Leuconostoc mesenteroides*. Biochem J 209:363–371
49. Morrill PR, Gupta G, Sproule K et al (2002) Rational combinatorial chemistry-based selection, synthesis and evaluation of an affinity adsorbent for recombinant human clotting factor VII. J Chromatogr B Analyt Technol Biomed Life Sci 774:1–15
50. Scopes RK, Testolin V, Stoter A et al (1985) Simultaneous purification and characterization of glucokinase, fructokinase and glucose-6-phosphate dehydrogenase from *Zymomonas mobilis*. Biochem J 228:627–634

Chapter 6

Technical Optimization for the High-Throughput Purification of Antibodies on Automated Liquid Handlers

Peter M. Schmidt

Abstract

Monoclonal antibodies (mAbs) are the fastest-growing segment in the drug market with eight of the top 20 selling drugs being mAbs and combined sales of close to 60 billion US$/year. The development of new therapeutic mAbs requires the purification of a large number of candidate molecules during initial screenings, subsequent affinity maturation campaigns, and finally the engineering of variants to improve half-life, functionality, or biophysical properties of potential lead molecules. A successful strategy to purify this ever-increasing number of mAbs in a timely manner has been the miniaturization and automation of the purification process using automatic liquid handlers (ALHs) such as Tecan's Evo or PerkinElmer's Janus platforms. These systems can be equipped with miniaturized columns, which are available in a wide variety of sizes and affinity matrices to cater to the need of the respective application. Various publications have described the setup of ALHs including the respective purification procedure. However, despite being very precise regarding the overall approach, most publications do not focus on the technical optimization and potential pitfalls, which can be crucial to obtain a robust process. To fill this gap, the present publication is aiming to point at some technical difficulties and suggesting potential ways to overcome these problems in order to facilitate the setup of new ALH systems for the purification of antibodies.

Key words Monoclonal antibody, Affinity purification, High throughput, Liquid handling, Robotics

1 Introduction

Monoclonal antibodies are the fastest-growing segment in the drug market with eight of the top 20 selling drugs being mAbs and combined sales of close to 60 billion US$/year [1]. The initial screening of antibodies that bind specifically a target protein as well as the subsequent optimization of such binders regarding their affinity [2], expression levels [3, 4], and biophysical characteristics [5–7] relies on the expression and subsequent purification of large numbers of mAb variants at each stage of development. Commercially available high titer transient expression systems such as Expi293 or ExpiCHO [8] enable early research labs to produce sufficient amounts of material in volumes small enough

Nikolaos E. Labrou (ed.), *Protein Downstream Processing: Design, Development, and Application of High and Low-Resolution Methods*, Methods in Molecular Biology, vol. 2178, https://doi.org/10.1007/978-1-0716-0775-6_6,

to be handled in automated liquid handlers (ALHs) such as Freedom EVO (Tecan Deutschland GmbH, Crailsheim, Germany) or Janus (PerkinElmer, MA, USA) [9–11]. These robotic systems in combination with miniaturized affinity columns represent a versatile and powerful approach to purify larger numbers of mAbs in an automated fashion. With the development of new affinity Protein A affinity matrices that have an increased dynamic binding capacity at short residence times [12], these systems usually obtain enough material to cater for initial screening assays such as ELISA, Surface Plasmon Resonance (SPR), or Differential Scanning Fluorimetry (DSF).

Various publications have described the setup of such ALH instruments and their respective purification procedures [9, 13] but despite the fact that these papers describe the overall purification approach in substantial detail, there is not much information available on the technical optimization steps. In general, automated procedures have to be carefully optimized to ensure that protocols run robustly in the absence of an operator (e.g., overnight). In addition, and in contrast to lab-scale chromatographic systems, mAb purification on ALHs has opened liquid flow paths and requires therefore careful optimization and testing to prevent cross-contamination of samples [9]. To fill this gap, the present publication is aiming to point at some technical difficulties and suggesting potential ways to overcome these problems. The focus is therefore not on the quantity or quality of the purified mAbs but rather on supporting new ALH users to successfully set up a robust purification protocol whilst avoiding already known pitfalls. Although the current manuscript is mainly focused on the Janus ALH system, some of the strategies presented apply to robotics-based mAb purification in general and might therefore be considered useful for the larger community of ALH users.

2 Materials

2.1 Buffers for ALH mAb Purification

1. *Phosphate buffered saline (PBS)*: PBS is used to equilibrate Protein A columns prior to sample loading and to wash columns before mAb elution. PBS is prepared by adding 1.8 L of MilliQ water to a measuring cylinder and, under constant stirring, adding 4.34 g of Na_2HPO_4 (8.1 mM), 0.4 g of KH_2PO_4 (1.47 mM), 16 g of NaCl (137 mM), and 0.4 g of KCl (2.7 mM). The pH is adjusted to 7.3 using NaOH (1 M).
2. *Arginine wash buffer*: The buffer for the pre-elution arginine wash (*see* **Note 10**) is prepared by adding 1.21 g of Tris (10 mM), 8.77 g of NaCl (150 mM), and 87.1 g of arginine to 900 mL of MilliQ water under constant stirring. The pH is adjusted to 7.5 by adding 48 mL of concentrated HCl (32%), and MilliQ water is added to a final volume of 1 L.

3. *Antibody elution buffer*: Acetate buffer for eluting mAbs from the Protein A column is made by dissolving 8.2 g of sodium acetate (100 mM) in 900 mL of MilliQ water. pH is adjusted to 3.0 by adding 9 mL of concentrated HCl (32%). MilliQ water is added to a final volume of 1 L.
4. NaOH (0.25 M) for column sanitization is prepared by diluting 50 mL NaOH stock solution (5 M) into 950 mL MilliQ water.
5. *Column storage solution:* 20% ethanol for column storage and instrument sanitization is prepared by diluting 400 mL of ethanol with MilliQ water to a final volume of 2 L.
6. *Antibody neutralization buffer*: The buffer for the pH neutralization of eluted mAbs is prepared by adding 12.1 g of Tris (1 M) to 90 mL of MilliQ water under constant stirring. The pH is adjusted to 9.0 by adding HCl (1 M). MilliQ water is added to a final volume of 100 mL.
7. To prevent column blockage, all working buffers and solutions except ethanol (20%) are filtered through a 0.22 μM filter to remove potential particles.

2.2 Antibody Samples for Purification

1. Depending on the depth of the 48-deep-well plate used to store the samples on the cooling block on the ALH deck, 4.5 or 7.5 mL of conditioned media from the transient mAb expression are filtered through a 0.22 μm filter into the storage plate (*see* **Note 1**).

2.3 Instrumentation and Columns

1. *Automated liquid handler (ALH)*: Antibody purification is performed on a JANUS VariSpan automated liquid handler (PerkinElmer, MA, USA) equipped with a plate shuttle and an external valve, which allows switching between six different solutions to be used as system liquid. The instrument is controlled using WinPrep V4.7 software [9]. The deck layout and the labware used for the procedure are shown in Fig. 1.
2. *Protein A micro column*: The ALH system is equipped with 100 μL OPUS RoboColumns (Repligen, Waltham, MA, USA; bed height: 5 mm, inner diameter: 5 mm) packed with a MabSelect PCC Protein A matrix [12] (GE Healthcare Bio-Sciences, PA, USA).
3. *Protein desalting:* Subsequent to the protein A affinity purification, mAb samples are desalted into a buffer of choice (e.g., PBS, TBS, HBS) using a CentriPure P96 gel filtration column array (emp BIOTECH GmbH, Berlin, Germany).
4. *Concentration measurement:* The concentration of purified mAbs is measured by their optical density at 280 nm using a Trinean DropSense96 system (Trinean, Gentbrugge, Belgium).

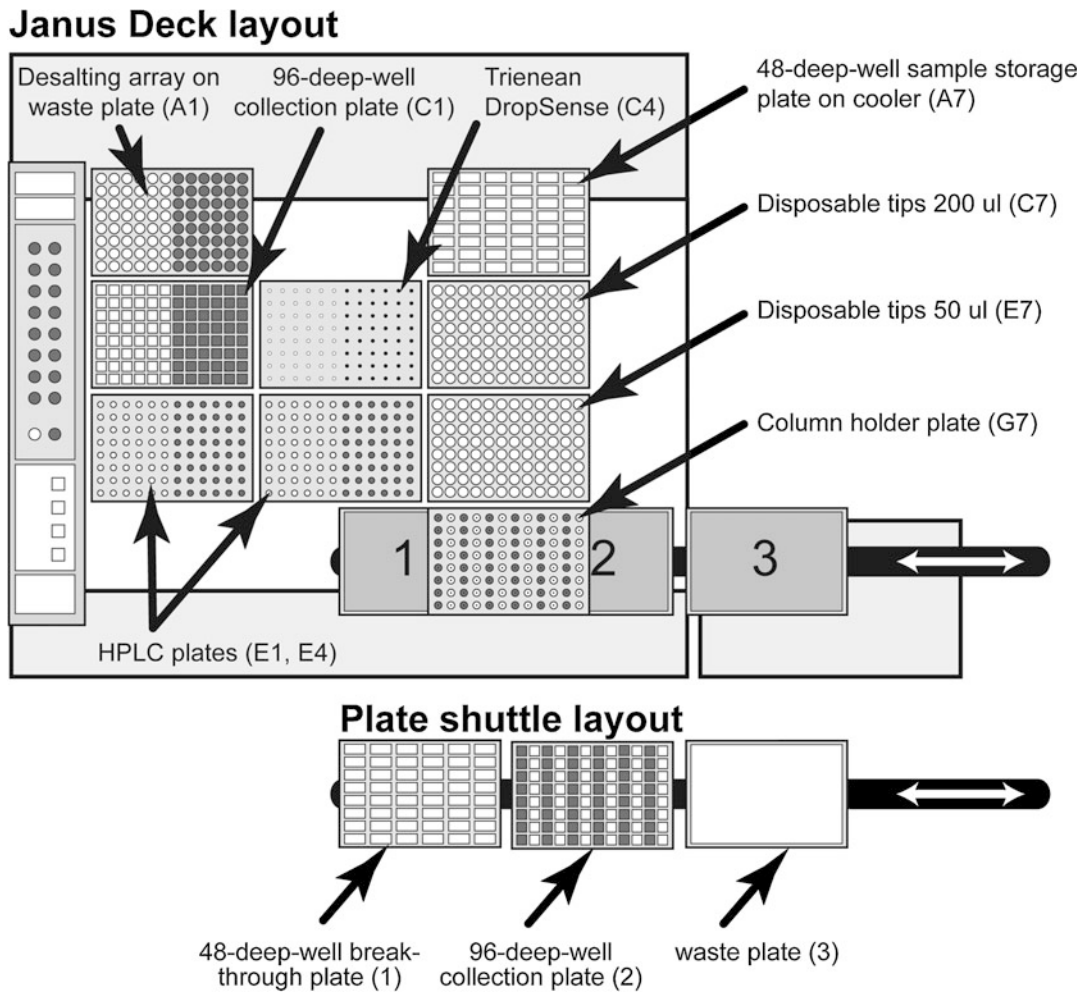

Fig. 1 The Janus deck layout. (A1) A metal system waste plate with the desalting array (emp BIOTECH) on top (*see* Subheading 3.1.3). (A4) Empty. (A7) An Inheco thermoshake with a 48-deep-well plate for sample storage (4.5 or 7.5 mL, pyramid bottom; e.g., Seahorse). (C1) A 96-deep well collection plate (2 mL, square well, V-bottom; e.g., SSIBio). (C4) A Trinean DropSense plate. (C7) 200 μL non-conductive disposable tips (PerkinElmer Roborack). (E1, E4) 96-well plates for SDS-PAGE (optional) and HPLC SEC analysis (e.g., Eppendorf 96-well 150 μL PCR plates). (E7) 50 μL conductive disposable tips (PerkinElmer Roborack). (G7) Column holder (PerkinElmer). The plate shuttle was holding: Position 1: a 48-deep-well plate for breakthrough storage (4.5 mL, pyramid bottom; e.g., Seahorse), Position 2: a 96-deep well collection plate (2 mL, square well, V-bottom; e.g., SSIBio), and Position 3: a system metal waste plate (*see* Subheading 3.1.1)

3 Methods

3.1 General Modifications of the ALH Instrument

3.1.1 Removing Droplets from the Tip of the Microcolumns

All buffers from column wash steps are discarded via a metal system waste plate positioned on the plate shuttle (position 3), which is connected via a tube to a liquid waste tank. At the end of a column wash step, droplets of various volumes (≈ 5–50 μL) remain hanging from the tips of the columns (Fig. 3b). As the waste plate's height is about 2–3 mm lower compared to a standard 96-deep-well plate (≈39 mm) used for sample collection, it hardly collects any droplets from the column tips when moving under the column holder. Therefore, as the collection plate (shuttle position 2) is higher than the waste plate, its surface gets in contact with the remaining hanging droplets. The wet surface of the collection plate interferes with the optimized strategy described below (*see* Subheading 3.2.2) to reliably collect the column eluate into the correct well, which results in potential cross-contaminations. To overcome this problem, the wall of the system waste plate on the shuttle (position 3) is extended with an adhesive plastic foil, which bridges the gap to the column tips (Fig. 2a) and allows picking up all droplets from the tips by moving the waste plate under the column holder (*see* **Note 2**).

3.1.2 Reducing the Width of the ALH Tips

The ALH-based mAb purification protocol can be adapted to load up to 7 mL of conditioned media per column, which, in combination with optimized Protein A matrices, significantly increases the total yield [12]. However, 48-deep-well plates with a capacity of 7.5 mL per well have a depth of about 63 mm, which means that the ALH tip has to fully enter the well to be able to aspirate the entire volume down to the bottom of the well. As the Janus ALH mechanism responsible for dropping of disposable tips from each system tip thickens at the top end (Fig. 2b), the tips get stuck in the wells of the high capacity 48-well plates once they fully enter the plate (Fig. 2c left). To allow the Janus ALH to work with these high-volume storage plates, the plastic of the drop-off mechanism needs to be thinned by about 1–2 mm at its top end (Fig. 2b, c; *see* **Note 3**).

3.1.3 Adding a Bracket to the System Waste Plate

The desalting array used in the mAb purification protocol is washed multiple times during the procedure to equilibrate the desalting columns or to sanitize the array after purification. To allow all buffers to be drained directly into the liquid waste container, the desalting array is placed manually onto the system waste plate (position A1). However, although the footprint of both labware is identical, the desalting array tends to slightly move horizontally on the waste plate. This movement results in a misalignment, which in turn can lead to the ALH tips crashing into the labware when dispensing buffers into the desalting array. To circumvent this issue, four sturdy pieces of flat plastic are glued to the outer walls of the waste plate extending its height by 2–3 mm and forming a

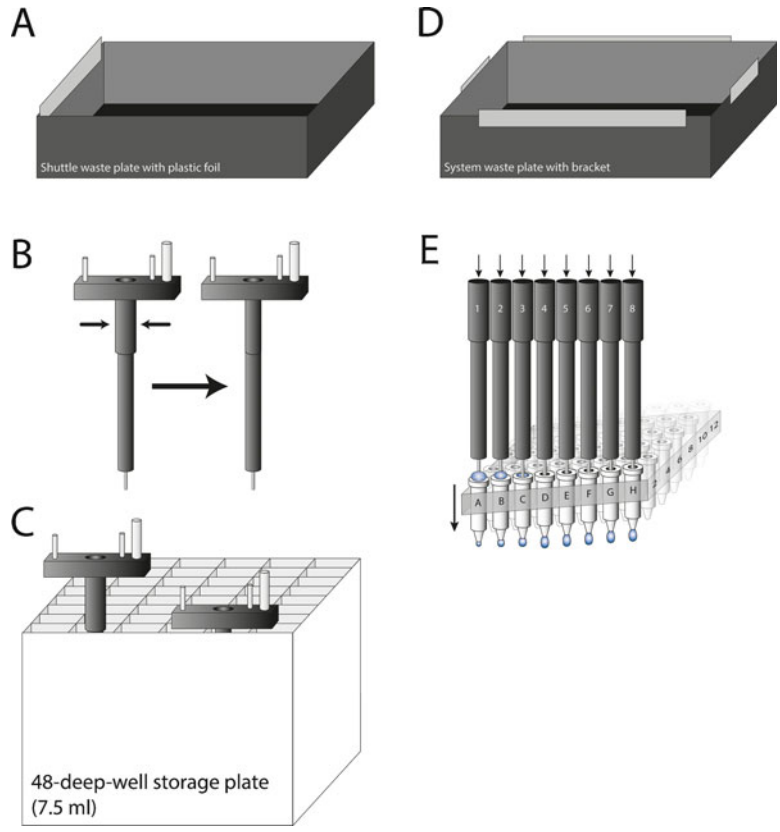

Fig. 2 (**a**) The system waste plate on the plate shuttle was extended on the inside with a self-adhesive plastic foil to allow removing droplets from the microcolumns in the column holder (*see* Subheading 3.1.1). (**b**) The disposable tip drop-off mechanism of the Janus ALH is thickened at the top (left) end preventing it from entering 7.5 mL 48-deep well plates (**c** left). After sanding down the plastic (**b** right) the tip can fully enter high volume storage plates (**c** right; *see* Subheading 3.1.2). (**d**) To hold the desalting array, the system waste plate (deck position A1) is extended on the outside with a bracket (*see* Subheading 3.1.3). (**e**) The column holder plate can move down once the system tip applies pressure. This vertical movement gets more with increasing distance from the column holder support (adjacent to row H, not depicted; *see* Subheading 3.2.1)

bracket that helps to align the desalting array on the waste plate (Fig. 2d; *see* **Note 4**).

3.2 General Optimizations Before the Start of the Purification Protocol

3.2.1 Optimizing the Z-Movement into the Column O-Ring Seal

Dispensing liquid through the microcolumns installed on the ALH column holder results in a significant pressure buildup, which is aggravated by the age of the column and the deterioration of the O-ring seal over time. The ALH tips need to enter the columns deep enough to create a tight seal with the column O-ring that is able to withstand the backpressure. To achieve this, the tips have to be moved into the columns to the lowest possible Z-position using the control software and this position needs to be saved as new dispensing height (Fig. 2e; *see* **Note 5**).

3.2.2 Adjusting the Shuttle Position to Prevent Cross-Contamination and Sample Loss

By default, the Janus ALH plate shuttle is set up in a way that the tip of each column is centered over the respective well. This is problematic, as a droplet that is building up at the tip of the column (e.g., at 2 μL/s) has to reach a certain volume to reliably drip into the well, which is usually at about 50 μL (Fig. 3a). However, smaller droplets are likely to remain hanging from the tip (Fig. 3b). Depending on the size of the droplets, this might lead to various outcomes once the shuttle moves the collection plate: (1) The droplet will be picked up by the wall of the correct well and run down to the bottom of the well (Fig. 3c well I); (2) the droplet gets picked up by the wall, but due to its small volume, it sticks at the wall and potentially might dry out if this happens overnight (Fig. 3c well IV); (3) smaller droplets stay connected to the tip and can be shifted to the adjacent wells once the plate is moved (Fig. 3c well III); and (4) very small droplets do not get in touch with the collection plate at all (Fig. 3c well II). All but example 1 lead to sample loss or, even worse, to cross-contamination. To overcome this issue, the shuttle position is modified in a way that the wall of a well is in close proximity to the tip of the column (Fig. 3e). In this setup, a droplet forming at the column tip is attracted to the wall of the well and reliably collected. Once a 'flow path' has been formed (plastic got wetted), even small droplets (e.g., 10–20 μL) are efficiently captured. However, this optimized alignment works only if the surface of the 96-deep-well collection plate is dry as a wetted surface changes the droplet attraction to the plastic surface (*see* also **Note 2**). By optimizing the alignment, virtually the entire eluate can be reliably collected without cross-contamination or sample loss [9].

3.3 Optimization of the mAb Purification Procedure

3.3.1 Priming the System Liquid Input Lines

The Janus ALH is equipped with six independent buffer lines connected to the instrument via a software-controlled switching valve. This setup allows using up to six different solutions that can be dispensed directly from external buffer reservoirs. This is a crucial feature, as the buffer volumes required for mAb purification exceed by far the available space on the ALH deck. Buffer lines are placed into: line 1—5 L MilliQ water, line 2—2 L PBS, line 3—500 mL NaOH, line 4—2 L PBS or alternative desalting buffer, and line 6—2 L Ethanol (20%). Line 5 is still available to extend the protocol if needed. All lines are primed before purification (*see* **Note 6**).

3.3.2 Placing Labware on the ALH Deck

The deck of the Janus mini ALH has 12 available deck positions (Fig. 1) and is equipped with the following labware: (A1) a system waste plate holding the desalting array; (A7) an Inheco thermoshake holding a 48-deep-well plate (4.5 or 7.5 mL); (C1) a 96-square-deep-well plate; (C4) a 96-well Trinean dropsense plate; (C7) disposable tips (200 μL); (E1) a 96-well HPLC plate for SDS-PAGE (optional); (E4) a 96-well HPLC plate for SEC; and

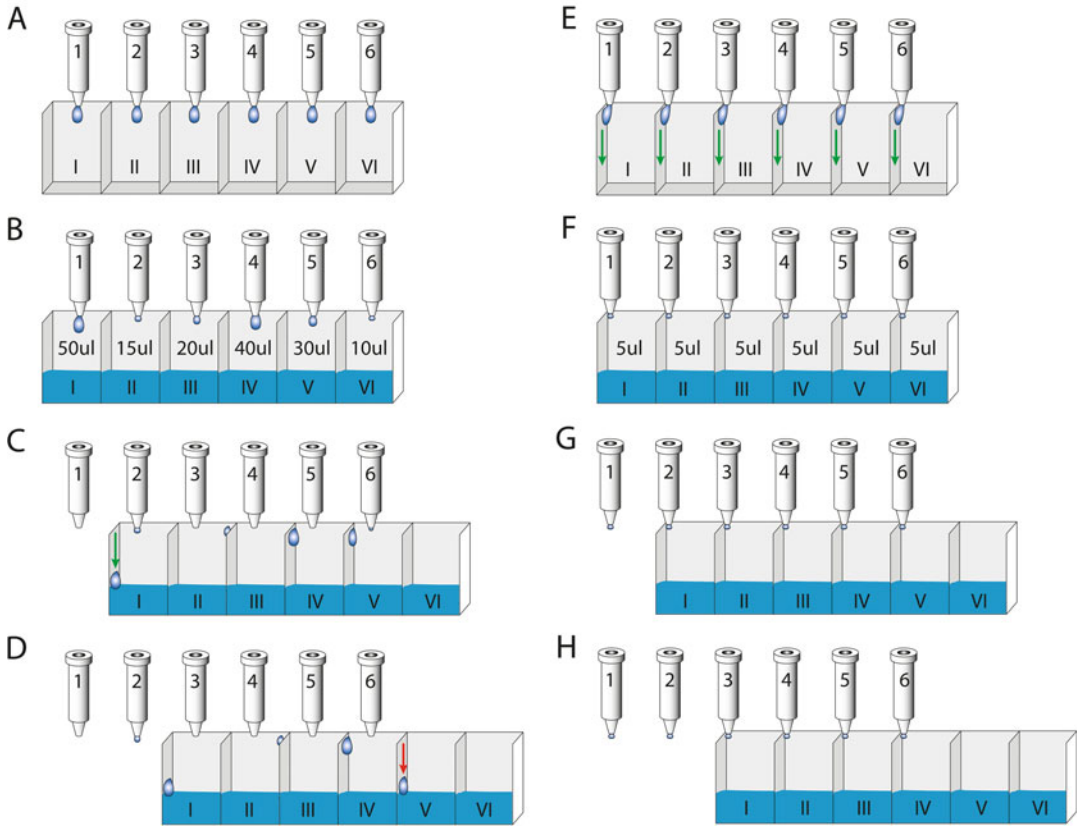

Fig. 3 (**a**–**d**) Droplet collection using the standard system setting. After liquid dispensing (**a**), droplets of all sizes remain hanging from the tips of the columns (**b**). (**c**, **d**) Depending on their size, these droplets can behave differently once the shuttle moves the collection plate: Droplet 1 is collected in well I. Droplet 2 is too small and remains at the tip of column 2. Droplet 3 makes contact with the plate but is shifted from well III to well II. Droplets 4 and 5 get collected but are too small to run to the bottom of the wells. Droplet 6 is too small to be collected but can combine with droplet 5 that is sticking at the wall of the well. The combined droplets 5 and 6 are heavy enough and runs down to the bottom of well V. With the optimized alignment (**e**–**h**), the droplets of all columns get in contact with the wall of the respective well while building up at the tip of the columns. Once the first droplets have been collected at the bottom of the respective well, all further liquid is collected in the correct well even before droplets are built up

(E7) disposable tips (50 µL). The column-holder plate of the plate shuttle is on deck position G7. The plate shuttle is equipped with a 48-deep-well plate to collect column breakthrough (position 1), a 96-square-deep-well plate to collect the column eluate (position 2), and a metal system waste plate connected to a waste line to drain the buffer used to wash the columns (position 3).

3.3.3 Confirming Labware Alignment

Before starting the priming of the buffer lines and subsequent to sample loading, the ALH protocol performs an XYZ move of all tips to the final position for each labware. After successfully completing this step, the purification protocol starts (*see* **Note 7**).

3.3.4 Equilibrating Columns Before Sample Loading

The system waste plate (position 3) on the shuttle is moved under the column holder. System liquid is switched to MilliQ water (line 1), lines are primed with 20 syringe strokes, and 5 column volumes (CV) are pumped through the columns at 5 μL/s to remove the ethanol (20%) storage solution. Subsequently, system liquid is switched to PBS, lines are primed, and columns are equilibrated with 5 CV PBS prior to sample loading (*see* **Note 8**).

3.3.5 Overnight Sample Loading

Due to the small bed volume of the Protein A columns, longer residence times can only be achieved by loading the media at a low flow rate. With 1 mL syringes being installed, 2 μL/s is a realistic sample-loading rate resulting in a residence time of 50 s (*see* **Note 9**). At this speed, loading of 7 mL of conditioned media takes close to 1 h. Purification of 48 mAbs on a 4-tip system requires 12 independent sample loading cycles resulting in 12 h of sample loading time. Although an 8-tip system would half this time, it is still recommended to load samples overnight.

3.3.6 Overnight mAb Elution from the Affinity Matrix

After overnight sample loading, the respective breakthrough is stored in the 48-deep-well plate located on the shuttle (position 1) for subsequent quantification of unbound mAb (only possible for 4 mL sample loading, as the shuttle cannot accommodate 7.5 mL 48-dep-well plates). Subsequently, all columns are washed with 6 CV arginine buffer (*see* **Note 10**) and 10 CV PBS. Prior to eluting bound mAbs, the ALH dispenses 33 μL of Tris buffer (1 M, pH 9.0) to all wells of the collection plate (shuttle position 2) required for mAb collection. The plate shuttle moves the collection plate (position 2) under the column holder and mAbs are eluted with 300 μL acetate buffer at a flow rate of 2 μL/s resulting in a final sample volume of about 330 μL. Affinity-purified mAbs are stored overnight in the collection plate for desalting.

3.3.7 Overnight CIP of Affinity Columns

Sanitization of the affinity columns is a slow process and is therefore performed overnight once mAbs have been successfully eluted and stored at neutral pH. Affinity columns are subjected to the CIP procedure by washing with 1× 9 CV MilliQ water, 1× 9 CV NaOH (0.25 M), 4× 9 CV PBS, 1× 1 CV MilliQ water, and 2× 9 CV ethanol (20%). All dispensing steps are performed at a flow rate of 5 μL/s. Sanitized columns are capped and stored at 4 °C (*see* **Note 11**).

3.3.8 Desalting of Protein A-Purified mAbs

The desalting array consists of 96 individual desalting columns in a standard SBS 8 × 12 format. The columns can be uncapped individually, which allows using the exact amount of columns needed. After uncapping, the desalting array is placed on top of the system waste plate (position A1) until the storage solution is fully drained (*see* also Subheading 3.1.3). In the meantime, the system liquid is set to MilliQ water and lines are primed (20 syringe strokes). The

remaining storage solution in the gel matrix of the desalting columns is displaced by dispensing 900 µl of MilliQ water into each column. Subsequently, system liquid is set to line 4 (desalting buffer) and system lines are primed. The desalting columns are equilibrated with 5× 900 µL desalting buffer with a 10 min pause between each liquid transfer to allow the buffer to drain by gravity flow. After successful equilibration of the desalting array, 330 µL of neutralized mAbs are transferred from the 96-square-deep-well collection plate on the plate shuttle (position 2) to the desalting array using 200 µL nonconductive disposable tips. The samples are allowed to enter the gel matrix for 5 min. Afterward, the desalting array is manually placed onto a 96-square-deep-well collection plate (position C1) and mAbs are eluted by dispensing 500 µL of desalting buffer into each column. After eluting the antibodies, the desalting array is manually placed back onto the waste plate (position A1) for sanitization.

3.3.9 Analysis of Final Purified mAb Samples

After successful two-step purification of the antibodies, the ALH transfers 20 µL of each sample into an HPLC plate for SEC analysis (15 µL) as well as into a Trinean DropSense plate (5 µL) to determine the concentration of the samples. The transfer is done with 50 µL conductive disposable tips using a multi-dispensing step (aspirate 20 µL, dispense 15 µL + 5 µL) as this allows dispensing into both plates without changing the disposable tips (*see* **Note 12**).

3.3.10 CIP of Desalting Array

As the last step of the mAb purification protocol, the desalting array is sanitized by dispensing 0.9 mL of MilliQ water, 0.9 mL of NaOH, 5× 0.9 mL of PBS, 1× 0.9 mL of MilliQ water, and 1× 0.9 mL of ethanol (20%). Between every dispensing step, the desalting array is allowed to fully drain for 10 min. After the ethanol transfer, the bottom cap-mat is put back onto the nozzles of the desalting columns to prevent further draining and the array is filled up with 0.9 mL of ethanol (20%) before sealing the columns with the top caps.

4 Notes

1. The conditioned media is filtered through a 0.22 µm filter to prevent column blockage due to potential precipitate in the media. So far, there is no high-volume 48-well filtration plate commercially available with a 0.22 µm membrane. Therefore, standard 10 mL syringes equipped with 33-mm 0.22-µm Luer lock filters (e.g., Millex Durapore PVDF) are used to filter the samples directly into the 48-deep-well storage plate. As the samples need to be manually transferred from 50 mL tubes

into the 48-deep-well storage plate, the filtration step adds only limited extra work.

2. To bridge the gap between the top end of the waste plate and the tip of the columns in the column holder, a self-adhesive plastic film can be cut to size and glued to the inner wall of the waste plate (Fig. 2a). A more sturdy and self-adhesive plastic foil such as 96-well plate seals worked very well for this.
3. This note might only apply to the Janus ALH system. The plastic part that is needed to drop off disposable tips from the fixed metal ALH tips is slightly thicker at its top end (Fig. 2b left). In order to transfer the full volume from a high-capacity 48-well plate (holding up to 7.5 mL per well), the tip has to fully enter the well (Fig. 2c). To make this possible, the drop-off mechanism can be manually pulled off the fixed metal ALH tips and thinned using standard fine grade sand paper (Fig. 2b). As the tips need to be only thinned on two sides (the width of the rectangular 48-well plates is sufficient to enter the well), the stability of the drop-off mechanism is not affected.
4. This bracket can be made from any material. The sturdy plastic that is used for the lids of the disposable tip boxes worked fine but other available materials can be used equally well.
5. The optimization of the dispensing height can be very problematic. The pressure buildup is significant and without a tight seal between O-ring and ALH tip leakage at the top of the column is likely to occur. To ensure a tight seal, the tip has to enter the column as deep as possible without creating a Z-move error due to increased resistance. As the column holder of the Janus ALH system is supported only at the front (next to row H), the backside of the column holding plate tends to be slightly pushed down when the tips are applying pressure while entering the columns (Fig. 2e). This slight movement of the column holding plate can be sufficient to create a difference in the absolute Z-position of the installed columns in relation to the deck. Therefore, a dispensing height that has been optimized using a column in row A (back) can trigger a Z-move error for columns in row H (front). Vice versa, an optimal penetration depth for columns in row H (front) might not be sufficient for columns in row A (back) to create a proper seal. To facilitate this optimization, it has been helpful to increase the resistance detection limit of the tips, which allows pushing harder into the columns without triggering a Z-move error.
6. It is important that all buffer lines are fully primed from the reservoir bottle to the tip of the dispensing arm and that all bubbles are fully flushed out of the lines. This priming needs to be done by the system syringes and, depending on the volume

(recommended: 1 mL; dispensing speed 500 μL/s) and the length of the buffer lines, priming can easily take 20 syringe strokes or even more.

7. This trial run of the tip movement is an essential step, which increased the robustness of the protocol significantly. The width of the Janus ALH dispensing tips including the drop off mechanism for disposable tips fits exactly into the wells of a 96-square-deep-well plate without much additional space. Similarly, the wells of the Trinean DropSense plate are very narrow. Small misalignment of the tips during the run will cause the protocol to stop most likely at night. If the XYZ trial run works without any problems, the alignment is within the required accuracy range.
8. It is highly recommended to carefully watch the column equilibration steps at the beginning of the protocol. The column O-ring seal has only a limited half-life and fails on average after using a column for 20–30 purifications. This results in leakage at the column head, which, in turn, is likely to result in a cross-contamination of all samples with spilled media. If both equilibration steps (MilliQ water and PBS) work without liquid buildup on top of a column, sample loading overnight is likely to work fine. In the case of leakage, the faulty column can be replaced and the protocol can be started again (without priming the lines).
9. Slower sample loading rates are possible by installing 250 μL syringes. However, as the syringes are also required to prime the system liquid lines, reducing the syringe volume automatically increase the time needed for priming the buffer lines (e.g., 80 instead of 20 syringe strokes). 1 mL syringes offer a good compromise between the priming speed, the sample loading rate, and the required accuracy when pipetting out small volumes.
10. An arginine wash step as part of the mAb purification procedure has been published by Ritzen and co-workers in order to reduce the Endotoxin load of the eluted antibodies [14]. This wash step is added to the standard protocol as it is easy to implement and ensures low Endotoxin levels in the purified sample. However, this additional wash step can also be omitted to simplify the purification protocol.
11. The first ethanol wash step in the CIP procedure is the last dispensing step that occurred at night before the purification protocol pauses and waits for the operator to return. This is to ensure that columns are stored in ethanol overnight to prevent bacterial growth. Once the operator is back, the protocol initiates a second ethanol wash to make sure all columns are filled bubble free with ethanol before being capped and stored

at 4 °C. These steps are set up this way to maximize the lifetime of the Protein A affinity columns.

12. The 20 μL disposable tips for the Janus ALH cannot be recommended as they hold only about 11 μL volume (the rest is dead volume) and their short and stubby shape make it very problematic to enter 96-square-deep-well plates down to the bottom. In contrast, the 50 μL tips have a long slim shape, which allows easy aspiration of small sample volumes from the bottom of deep-well plates. In addition, their extended volume facilitates pre-transfer sample mixing as well as multi-dispensing steps.

Acknowledgments

The author would like to thank R. Butcher and her team for the continuous interest and enthusiasm in the area of protein purification and characterization, especially while setting up and troubleshooting the protocols for the ALH-mAb purification.

References

1. Iervolino A, Urquhart L (2017) World preview 2017, Outlook 2022. www.evaluate.com/PharmaWorldPreview2017
2. Strohl WR (2014) Antibody discovery: sourcing of monoclonal antibody variable domains. Curr Drug Discov Technol 11(1):3–19
3. Frenzel A, Hust M, Schirrmann T (2013) Expression of recombinant antibodies. Front Immunol 4:217
4. Haryadi R, Ho S, Kok YJ, Pu HX, Zheng L, Pereira NA, Li B, Bi X, Goh LT, Yang Y, Song Z (2015) Optimization of heavy chain and light chain signal peptides for high level expression of therapeutic antibodies in CHO cells. PLoS One 10(2):e0116878
5. Dudgeon K, Rouet R, Christ D (2013) Rapid prediction of expression and refolding yields using phage display. Protein Eng Design Select 26(10):671–674
6. Dudgeon K, Rouet R, Kokmeijer I, Schofield P, Stolp J, Langley D, Stock D, Christ D (2012) General strategy for the generation of human antibody variable domains with increased aggregation resistance. Proc Natl Acad Sci U S A 109(27):10879–10884
7. Zalevsky J, Chamberlain AK, Horton HM, Karki S, Leung IW, Sproule TJ, Lazar GA, Roopenian DC, Desjarlais JR (2010) Enhanced antibody half-life improves in vivo activity. Nat Biotechnol 28(2):157–159
8. Jain NK, Barkowski-Clark S, Altman R, Johnson K, Sun F, Zmuda J, Liu CY, Kita A, Schulz R, Neill A, Ballinger R, Patel R, Liu J, Mpanda A, Huta B, Chiou H, Voegtli W, Panavas T (2017) A high density CHO-S transient transfection system: comparison of ExpiCHO and Expi293. Protein Expr Purif 134:38–46
9. Schmidt PM, Abdo M, Butcher RE, Yap MY, Scotney PD, Ramunno ML, Martin-Roussety-G, Owczarek C, Hardy MP, Chen CG, Fabri LJ (2016) A robust robotic high-throughput antibody purification platform. J Chromatogr A 1455:9–19
10. Treier K, Hansen S, Richter C, Diederich P, Hubbuch J, Lester P (2012) High-throughput methods for miniaturization and automation of monoclonal antibody purification processes. Biotechnol Prog 28(3):723–732
11. Wiendahl M, Schulze Wierling P, Nielsen J, Fomsgaard Christensen D, Krarup J, Staby A, Hubbuch J (2008) High throughput screening for the design and optimization of chromatographic processes – miniaturization, automation and parallelization of breakthrough and elution studies. Chem Eng Technol 37 (6):893–903
12. Butcher RE, Martin-Roussety G, Bradford RA, Tester A, Owczarek C, Hardy MP, Chen CG, Sansome G, Fabri LJ, Schmidt PM (2019) Optimizing high throughput antibody purification by using continuous chromatography media. Protein Expr Purif 159:75–82

13. Chhatre S, Bracewell DG, Titchener-Hooker NJ (2009) A microscale approach for predicting the performance of chromatography columns used to recover therapeutic polyclonal antibodies. J Chromatogr A 1216 (45):7806–7815

14. Ritzen U, Rotticci-Mulder J, Stromberg P, Schmidt SR (2007) Endotoxin reduction in monoclonal antibody preparations using arginine. J Chromatogr B Analyt Technol Biomed Life Sci 856(1–2):343–347

Part II

Low-Resolution Protein Purification Methods

Chapter 7

Aqueous Two-Phase Systems for Cleanup and Recovery of Enzymes from Plants and Plant-Derived Extracts

Oscar Aguilar, Erick Heredia-Olea, Esther Perez-Carrillo, and Marco Rito-Palomares

Abstract

The increasing interest of the biopharmaceutical industry to exploit plants as a commercially viable production system is demanding the development of new strategies to maximize product recovery. Aqueous two-phase systems (ATPSs) are a primary recovery technique that has shown great potential for the efficient extraction and purification of biological products, from organelles to proteins and low-molecular-weight compounds. The evaluation of different system parameters upon the partitioning behavior can provide the conditions that favor the concentration of contaminants and the desired target protein in opposite phases. The protocols described here provide the basic strategy to explore the use of ATPSs for the isolation and partial purification of native and recombinant proteins from plants and plant-derived extracts.

Key words Aqueous two-phase systems, Plant proteins, Soybean, Sorghum, Green-tissue proteins

1 Introduction

Green leafy crops as well as plant-derived products have been identified as economically attractive alternatives to bulk, recombinant, or functional protein production, as well as for new additive formulations [1, 2]. This is demanding the development of new downstream strategies to maximize product recovery. Aqueous two-phase partitioning has emerged as a practical technique that allows recovery and purification of biological products. This technique, which was first described by Albertsson in 1958, exploits mild hydrophobic interactions between proteins and polymers in aqueous environments [3]. ATPSs are formed when two water-soluble polymers (e.g., polyethyleneglycol, dextran) or a polymer and a salt (e.g., potassium phosphate, sodium citrate, sodium sulfate, etc.) are mixed in aqueous solutions at a given proportion beyond the critical concentration. Distribution of proteins between the two phases is achieved by manipulating the partition coefficient

Nikolaos E. Labrou (ed.), *Protein Downstream Processing: Design, Development, and Application of High and Low-Resolution Methods*, Methods in Molecular Biology, vol. 2178, https://doi.org/10.1007/978-1-0716-0775-6_7,

of the proteins, varying the molecular weight of the polymers, the ionic strength of the salts, the relative proportion of each component, the pH, etc. [4, 5].

A typical approach is used to evaluate the effect of system parameters, such as polyethylene glycol (PEG) and phosphate concentrations and the nominal molecular weight of PEG, on the partition behavior of proteins. This approach has been followed traditionally to establish the potential conditions under which the target protein and the contaminant proteins concentrate preferentially to opposite phases. This practical strategy can be useful as a starting point to be applied in the recovery of recombinant and native proteins, but novel ionic liquids, thermo-separating polymers, and volatile solvents, such as alcohols, are being explored in order to facilitate further purification steps [6–8]. In the particular case of products of plant origin, early success has demonstrated the potential application of ATPS-based strategies to address the major disadvantages of the traditional recovery and purification techniques. Chow and Ow evaluated the use of ethanol-phosphate systems to purify α-amylase from pitaya [9, 10]. Previous studies [11–14] have shown the potential of traditional downstream processing operations applied to seed-produced recombinant proteins and the use of genetic engineering strategies to recover them from the bulk storage proteins in which the product of interest is immersed. Additionally, ATPSs have demonstrated to be useful as a cleanup step prior to the downstream processing of a green tissue protein extract [2]. The potential economic benefits of substitution of costly unit operations, such as chromatography, by ATPSs without commitment of the yield, have previously been addressed and the same strategies can be applied to plant-made products [10, 14]. Recently, the potential applicability of ATPSs in integrated extractive partitioning applied to the recovery of a model recombinant protein expressed in maize and tobacco has been demonstrated [11, 14]. This chapter discloses the relevant contribution of ATPSs to facilitate the establishment of bioprocesses in the growing field of high-value products from plants by presenting a simple methodology for the efficient use of ATPS-based strategies for the isolation and partial purification of bioparticles of plant origin. Selected examples of the use of ATPSs are presented to demonstrate the versatility of such a strategy as pretreatment as well as a primary recovery technique.

2 Materials

All buffers and solutions were prepared using distilled water and were analytical grade reagents, stored at room temperature (25 °C), unless indicated otherwise.

2.1 Protein Extraction

1. Seed protein extraction buffer: 0.03 M Tris-HCl buffer, pH 8. Add 100 mL of water to a graduated cylinder to pre-dissolve Tris–HCl. In a fume hood, add 0.781 g of 2-mercaptoethanol, equivalent to 0.701 mL considering a density of 1.114 g/mL. Weigh 4.73 g of Tris–HCl and transfer to the cylinder, add water to a volume of 900 mL. Adjust the pH to 8.0 using 1 M sodium hydroxide and make up to 1.0 L with water. Store at 4 °C protected from sunlight to avoid 2-mercaptoethanol degradation.
2. Green-tissue protein extraction buffer: TBE (Tris-borate-EDTA) buffer, pH 8. 0.45 M Tris–HCl, 0.45 M H_3BO_3, 10 mM EDTA, pH 8.0. In a 1.0 L graduated cylinder, place 300 mL of water. Add 70.92 g of Tris–HCl and dissolve it in the cylinder. Weigh 27.83 g of boric acid (H_3BO_3) and 2.92 g of ethylenediaminetetraacetic acid and dissolve it in the cylinder. Add water to a volume of 900 mL, adjust the pH to 8.0 using 1 M sodium hydroxide and make up to 1 L with water. Store at room temperature.
3. Green-tissue protein extraction buffer 2 (for chlorophyll cleanup):
4. Liquid nitrogen.

2.2 Aqueous Two-Phase Systems

1. Polyethylene glycol (PEG) and ethanol stock solutions.
   (a) 80% w/w PEG 1000. Weigh 80 g of polyethylene glycol nominal molecular weight 1000 g/mol and add 20 g of water. Agitate overnight with a magnetic stirrer at room temperature or until complete dissolution of PEG. Do not store under cold conditions since PEG will precipitate due to high concentration.
   (b) 50% w/w PEG 1450. Weigh 50 g of polyethylene glycol with a nominal molecular weight of 1450 g/mol and add 50 g of water. Agitate overnight with a magnetic stirrer at room temperature or until complete dissolution of PEG.
   (c) Stock solutions of PEG 3350 and PEG 8000 can be prepared at the same concentration as described in step b (*see* **Note 1**).
   (d) Ethanol as a phase-forming compound can be used preferably in absolute form or >95% reagent grade with no denaturants added.
2. Potassium phosphate and sodium citrate as phase-forming salts. Prepare a 40% w/w potassium phosphate solution with a proportion of 7:18 monobasic:dibasic potassium phosphate by weighing 22.4 g of anhydrous monobasic potassium phosphate and 57.6 g of anhydrous dibasic potassium phosphate. Place 100 g of water in a container and add the potassium salts until complete dissolution. Adjust the pH to 7.0 using 1 M

potassium hydroxide or 1 M orthophosphoric acid. Make up to 200 g with water. Do not store under cold conditions since phosphate salts will easily precipitate due to high concentration. In the case of sodium citrate, anhydrous powder form can be used directly without the need for the preparation of stock solution (*see* **Note 2**).

2.3 Protein Detection by Electrophoresis

1. Separating Buffer. Mix 1.415 mL of 40% w/v 97:3 acrylamide: bisacrylamide commercial solution (available from many suppliers) with 1.4 mL of 1.5 M Tris buffer pH 8.8, 0.011 g of SDS, and 2.74 mL of water. Store at 4 °C protected from sunlight (*see* **Note 3**).
2. Stacking Buffer. Mix 0.25 mL of 40% w/v 97:3 acrylamide: bisacrylamide commercial solution with 0.67 mL of 0.5 M Tris buffer pH 6.8, 0.0018 g of SDS, and 1.4 mL of water. Store at 4 °C protected from sunlight.
3. 10% APS solution. Weigh 0.1 g of ammonium persulfate (APS) and dissolve it in 1 mL of water (*see* **Note 4**).
4. TEMED. *N*,*N*,*N*,*N*′-tetramethylethylenediamine, 100% pure, liquid. Store at 4 °C protected from sunlight.
5. Running buffer. Weigh 6.06 g of Tris base, and mix with 28.8 g of glycine and 2 g of SDS, and make up to 2 L with water. Store at 4 °C when not in use (*see* **Note 5**).
6. Sample buffer. 0.3 M Tris–HCl, pH 6.8, 0.1% w/v SDS, 2% w/v DTT, 0.1% w/v bromophenol blue (BPB), 10% glycerol. Leave one aliquot at 4 °C for current use and store remaining aliquots at −20 °C.
7. Coomassie Blue G-250. Prepare a 0.1% w/v Coomassie Blue solution by dissolving 0.1 g of Coomassie Brilliant Blue G-250 in destaining solution. Filter using 0.45 μm filter paper. Store at 4 °C in the dark.
8. Destaining solution: 40% v/v methanol, 10% v/v acetic acid solution, 50% water.
9. Hoefer MiniVE vertical electrophoresis system (GE Healthcare): 10.5 cm × 10 cm × 1.5 mm glass plates with gel caster.

3 Methods

All procedures can be carried out at room temperature, unless specified otherwise.

3.1 Protein Extracts from Seed Material

Among the crops, soybeans (*Glycine max*) represent an attractive alternative since potentially they can produce high levels of recombinant proteins [16, 17]. The methodology described in the next section is to obtain soybean extracts to evaluate ATPSs as a first step to recover recombinant proteins expressed in seeds [17].

1. Rinse soybean seeds briefly (no more than 5 min) with tap water to remove soil and other materials. Let the seeds dry at room temperature, or place in an oven at 40 °C for 10–15 min.
2. Weigh the desired amount of seeds and grind to a fine powder using a household grinder in 20 s intervals to avoid overheating. Ground powder can be passed through mesh US No. 100 to obtain flour.
3. Soybean flour is suspended in 0.03 M Tris–HCl buffer pH 8.0, containing 0.01 M 2-mercaptoethanol at a proportion of 1.0 g solids/20 mL buffer. The slurry is stirred for 1 h and then centrifuged at 10,000 × *g* for 20 min at 2–5 °C to discard solids. An optional isoelectric precipitation can be performed at this step (*see* **Note 6**).

The potential use of ATPSs for the extraction of industrially relevant enzymes from plant-derived extracts, such as fermented flours, has also been explored. The following procedure can be used for the partial purification of enzymes from *Aspergillus*-fermented sorghum or other cereals.

1. Waxy sorghum flour is inoculated with *Aspergillus* sp. mycelium (obtained by growing 1×10^7 spores/mL in PDA plates for 72 h at 28 °C) and incubated at 28 °C for 4 days and adding Yeast Mold Broth (YMB) at a proportion of 4.0 g solids/mL YMB (*see* **Note 7**).
2. 10 g of the fermented sorghum mixture is mixed with distilled water at a proportion of 1:4 mixture:water and stirred at 180 rpm at 30 °C for 30 min. The slurry is then centrifuged at 10,000 × *g* for 10 min at 4 °C. Solids can be discarded and the clarified protein extract is used for ATPS extraction or stored at 4 °C for further use [18].

3.2 Green Tissue Protein Extracts

The possibility to use green tissues for the constitutive expression of glycosylated therapeutic proteins represents a real challenge for downstream processing given the high concentration of contaminant proteins and the presence of the highly abundant protein rubisco [19]. The following procedure can be used for the extraction of soluble protein from alfalfa leaves or any other green tissue with minimal or non-woody stems. For recombinant protein extraction, **steps 1** and **2** can be followed:

1. Collect the aerial parts (first and second stem and leaves) of the plant before flowering and immediately ground using liquid nitrogen with a previously frozen mortar and pestle (*see* **Note 8**), adding glass powder to improve cell wall breaking (approx. 1:1 ratio). Powdered tissues can be stored at this point immediately at −86 °C to avoid moisture capture from air and protease activation.
2. Protein extraction is performed using Tris-borate-ethylenediaminetetraacetic acid (EDTA) buffer (TBE) at a proportion of 1.0 g of powdered alfalfa per 10 mL buffer. The slurry is stirred for 1.0 h and then centrifuged at 12,000 × *g* for 10 min at room temperature. The supernatant is then filtered using a 0.45 μm syringe filter [20].

In the case of fresh tissue protein extraction for protein primary recovery or chlorophyll depletion pretreatment, the following steps can be followed:

1. 30 g of fresh tissue alfalfa (first and second stem and leaves) are mixed with 300 mL of TBE buffer. The mixture is homogenized for 5 min at mid to high speed using a tissue homogenizer and stirred in a tube rotator for 1 h. After this, the slurry is centrifuged at 3100 × *g* for 10 min at room temperature. The supernatant is then filtered using a 0.45 μm syringe filter and recovered for storage at 4 °C for further use (*see* **Note 9**) [20].

3.3 Aqueous Two-Phase Partitioning

The use of ATPS for the recovery and purification from plant tissues follows a similar procedure to that previously reported for different hosts [2, 4, 11, 13, 15]. The practical strategies for the development of primary recovery processes can be divided into four main stages: (1) initial physicochemical characterization of the feedstock; (2) selection of the type of ATPS; (3) selection of system parameters; and (4) evaluation of the influence of process parameters upon product recovery/purity.

Different system parameters such as molecular weight of the polymer, salt composition, volume ratio, or pH have a great impact on the protein distribution (Kp, partition coefficient) and total yield.

The following procedure focuses on the selection of the type of ATPS for maximizing the recovery of a particular protein from protein feedstock, providing that certain knowledge exists regarding the nature of the contaminant proteins or as described later, here the presence of chlorophyll in plant protein samples.

1. Calculate the amount of the PEG solution or absolute ethanol that has to be weighted according to the concentration of the stock solution and the final desired composition of the system. The strategy behind the selection of an experimental system is

Table 1
Systems selected for the evaluation of the partition behavior of the proteins from the alfalfa extracts

System	PEG MW (g/mol)	% PEG (w/w)	% Phosphate (w/w)	TLL (%)
1	600	14.5	17.5	32.0
2		15.5	18.0	37.1
3		15.8	19.5	41.5
4		17.0	20.5	45.2
5	1000	15.6	18.0	47.2
6		17.6	18.0	49.9
7		19.8	18.5	53.6
8		22.2	23.0	67.7
9	1450	13.7	13.1	27.1
10		15.7	13.9	34.4
11		18.6	15.2	41.9
12		21.0	16.0	47.8
13	3350	16.9	14.5	42.3
14		18.7	15.0	46.2
15		21.0	15.7	51.3
16		22.1	17.0	56.2
17	8000	12.0	7.7	21.0
18		16.1	10.0	35.7
19		20.0	11.6	42.6
20		21.9	12.3	47.5

Systems prepared on a weight basis. The volume ratio (estimated from blank systems as the ratio of volumes of the phases), and the pH values of these systems are kept constant and are equal to 1.0 and 7.0

well described elsewhere, but Table 1 is a good starting point for initial screening in the case of PEG/salt systems and Table 2 in the case of ethanol/salt systems, which are suggested for some systems, in this case, amylase recovery from fermented sorghum extract. The system tie-line length (TLL), which represents the length of the line that connects the compositions of the top and bottom phases in a phase diagram for a defined system, was calculated as described before [15]. A large collection of phase diagrams for a large variety of phase-forming polymers and salts can be found on Zaslavsky and Ooi et al. [21, 22]. In the same manner, calculate the amount (in g) of potassium phosphate stock solution or sodium citrate to be weighted according to the desired composition and the total weight of the system (*see* Tables 1 and 2) (*see* **Note 10**).

2. In a test tube, mix the predetermined quantities of phase-forming components to give the desired PEG/salt or ethanol/salt composition with the protein sample (0.1 g of protein per gram of system) approximately 10% of the total system. Add the required amount of distilled water to complete the final weight.

Table 2
Systems selected for the evaluation of the partition behavior of proteins from fermented sorghum extracts

System	Ethanol (% w/w)	Salt
1	45	15% Sodium citrate
2	45	10% Sodium citrate
3	35	13% Sodium citrate
4	30	18% Sodium citrate
5	35	10% Potassium phosphate
6	25	17% Potassium phosphate
7	20	25% Potassium phosphate

Systems prepared on a weight basis. The volume ratio (estimated from blank systems as the ratio of volumes of the phases) is highly variable and dependent on the concentration of solids in the fermented extracts. The pH of these systems is kept constant and is equal to 7.0

3. Adjustment of the pH to 7.0 can be made (if needed) by addition of 1 M orthophosphoric acid or potassium hydroxide.
4. All the test tubes are gently mixed for 1 h at 22 °C.
5. To achieve complete phase separation, a low-speed batch centrifugation at 1500 × *g* for 10 min is performed.
6. Estimate the volumes of top and bottom phases using graduated tubes and calculate the experimental volume ratio (Vr = volume of the top phase/volume of the bottom phase).
7. Separate the phases by pipetting top and bottom phases carefully to avoid cross-contamination (*see* **Note 11**). Estimate the amount of protein by the traditional Bradford Method [23] or by 280 nm UV absorption using appropriate solvents for blank corrections and dilutions. The top and bottom phase recoveries are estimated as the amount of the target product present in the phase (volume of the phase × product concentration in the phase) and expressed relative to the original amount loaded into the system (Fig. 1).

3.4 Target Protein Detection/Analysis

An electrophoresis analysis is the preferred method to identify low abundant proteins present in any of the phases previously isolated. A typical electrophoresis following the Laemmli method (1970) [24] can be performed.

1. Prepare the resolving gel by mixing 5.66 mL of separating buffer with 50 μL of APS solution and 5 μL of TEMED. Degas for 3 min in an ultrasonic bath and cast within a gel cassette leaving approx. 1.5 cm space for the stacking gel. Overlay with isobutanol and allow to polymerize for 10–20 min.

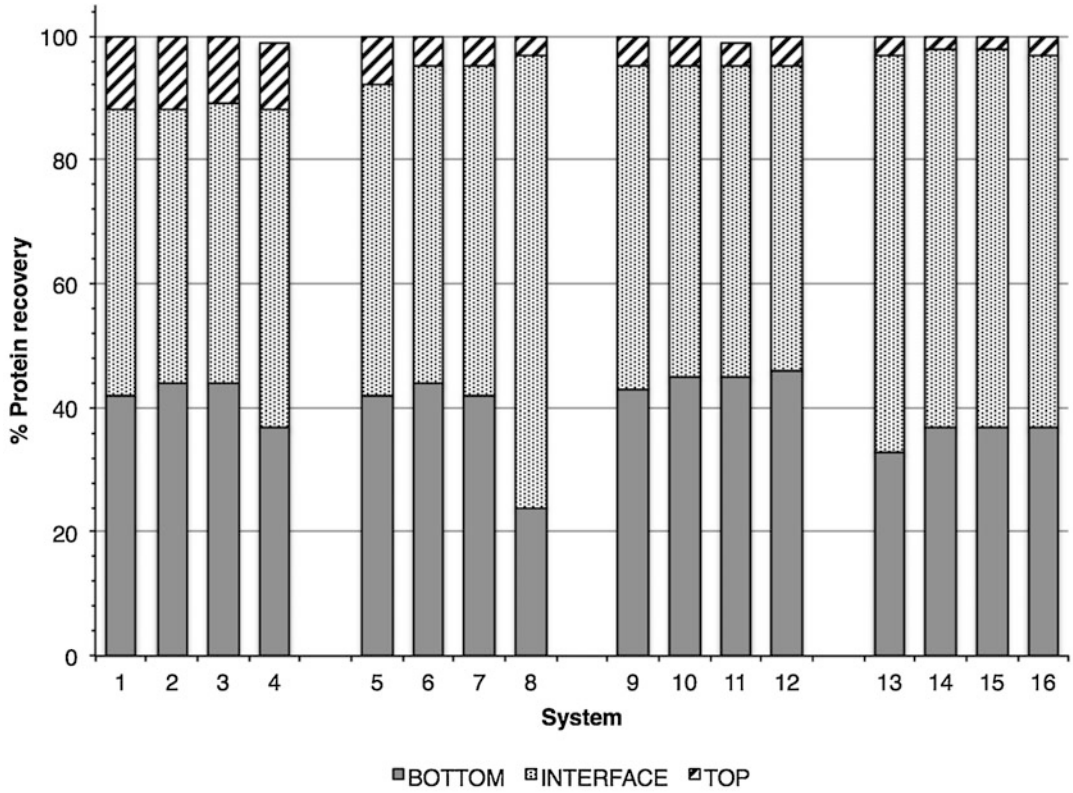

Fig. 1 Distribution of soybean protein in ATPS of different compositions, 16 systems as listed in Table 1. Concentration of protein in all systems was 10% w/w. Top and bottom recovery are expressed relative to the original amount of protein added to the systems. Interface recovery is the necessary amount of protein to complete the mass balance

2. Mix 2.08 mL of stacking buffer with 12.2 μL of APS solution and 1.8 μL of TEMED. Degas for 3 min in an ultrasonic bath and cast within the gel cassette previously removed of isopropanol. Insert a 10-well gel comb immediately without introducing air bubbles and allow to polymerize for 10–20 min.
3. Samples from top or bottom phases can be used directly into each well diluted with sample buffer to 1:1, 1:2, or 1:3 parts, depending on the protein content of the sample. Heat the samples at 95 °C for 5 min and apply into the wells. Run at 150 V for 2.0 h in a Hoefer miniVE vertical electrophoresis system filled with running buffer (GE Healthcare) (*see* **Note 12**).
4. Remove the gel from the cassette and reveal the protein bands by staining it with Coomassie Blue G-250 solution. After 1 h staining, the gel is destained with the same methanol-acetic acid-water solution (without Coomassie dye) for 3 h. The protein bands should be visible at different intensities

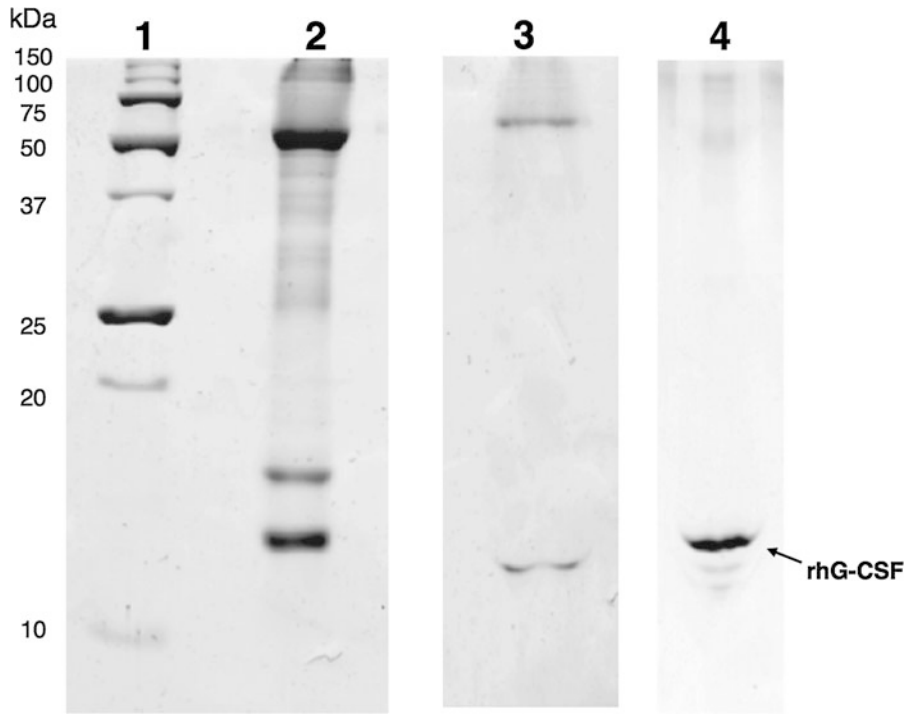

Fig. 2 Electrophoresis analysis of the protein products obtained from a sample of alfalfa protein containing the granulocyte-colony stimulating factor (rhG-CSF) in an ATPS. Samples from system 18 (Table 1) are the PEG 8000/phosphate system. Lane 1 is the molecular weight standard. Lane 2 alfalfa protein sample containing rhG-CSF (0.1 mg/g ATPS) showing Rubisco subunits. Lane 3 is the bottom phase sample showing faint bands of Rubisco subunits. Lane 4 is the top phase sample corresponding to rhG-CSF (Reproduced from [13] with permission from Elsevier)

depending on the protein content of the sample (Fig. 2; Fig. 3). Scan the gels at 300 dpi in transmissive mode using a flatbed scanner.

3.5 Quantification of the Protein Content in Each Phase

Quantification of the protein content in each phase can be performed by spectroscopic measurements at 280 nm.

1. Place 250 μL of the top/bottom phase in a microplate well and 250 μL of the top/bottom phase from a blank system (a system prepared exactly as the others but adding water instead of the protein sample).
2. Read absorbance at 280 nm subtracting blank absorbance lecture. Use bovine serum albumin to run the calibration curve from 0 to 2 mg/mL of protein.

3.6 Quantification of α-Amylase Content in Each Phase

For the quantification of α-amylase from the original extract and phases, several reported methods can be used, for example, the Megazyme K-CERA® kit based on the AOAC 2002.01 standard method [25] (*see* Table 3).

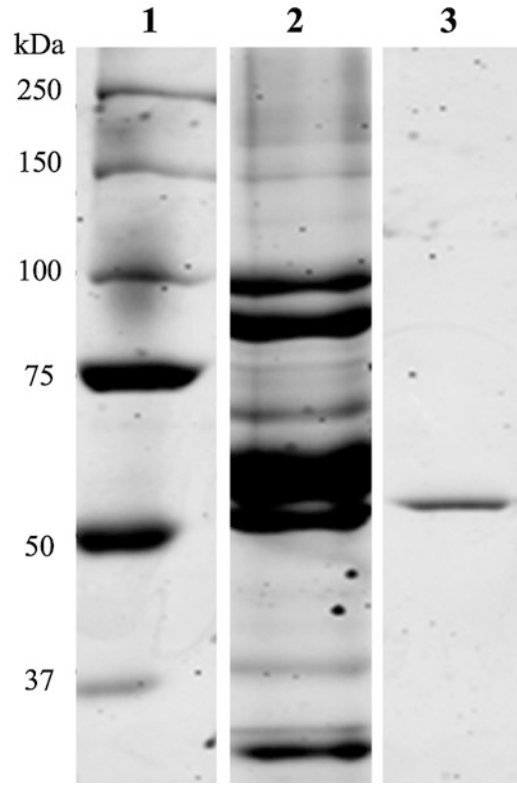

Fig. 3 Primary extraction of α-amylase from the soybean protein extract using an ATPS. System 5 (*see* Table 1) loaded with 10% w/w of soybean protein extract containing α-amylase (60 mU/mL). Lane 1 is the molecular weight standard. Lane 2 is the bottom phase sample, showing the majority of soybean proteins. Lane 3 is the top phase sample showing a band corresponding to α-amylase as the only protein present in the phase (verified from the enzymatic activity)

4 Notes

1. Polyethylene glycol or PEG is a highly water-soluble polymer that can be prepared at concentrations up to 80% w/w in the case of PEG 1000. To our experience, PEG stock solutions must be prepared at the highest possible concentration in order to increase the amount of sample that can be added to the system. 80% w/w is still possible for PEG 1000 and 1450 g/mol; however, as the molecular weight of the polymer increases, the solubility decreases up to 70% w/w for PEG 3350 g/mol and 50% w/w for PEG 8000 g/mol and 20,000 g/mol. In the case of PEG lower than 1000 g/mol, liquid pure form is preferably used.

Table 3
Recovery of α-amylase from fermented sorghum extracts for selected ATPSs (*see* Table 2)

		α-Amylase (U/L)		Specific activity (U/mg)		α-Amilase recovery yield (%)	
System	Composition	Top phase	Bottom phase	Top phase	Bottom phase	Top phase	Bottom phase
1	45% Ethanol 15% Sodium citrate	464.9 ± 3^{a}	N.D.	194.1 ± 2^{a}	N.D.	48.7 ± 2^{b}	N.D.
3	35% Ethanol 13% Sodium citrate	246.3 ± 9^{b}	N.D.	97.0 ± 4^{b}	N.D.	91.9 ± 1^{a}	N.D.
4	30% Ethanol 18% Sodium citrate	224.1 ± 2^{c}	N.D.	75.2 ± 5^{c}	N.D.	31.4 ± 1^{c}	N.D.
5	35% Ethanol 10% Potassium phosphate	52.6 ± 1^{d}	N.D.	26.2 ± 3^{d}	N.D.	28.0 ± 1^{d}	N.D.

Values with different letters within a column indicate a statistical difference ($p \leq 0.05$). One U is defined as the amount of enzyme, in the presence of excess thermostable α-glucosidase, required to release one micromole of *p*-nitrophenol from *Benzylidene-G7-α-PNP* in 1 min under the defined assay conditions

2. The use of potassium phosphate as a phase-forming salt is advantageous since binodal curves (two-phase diagrams) are widely available. However, a common problem is the limit of solubility of phosphate in water. The potassium phosphate stock solution (40% w/w) is prepared as a buffer solution with a composition of monobasic and dibasic phosphate salts at a proportion of 7:18, respectively. Such solution must be prepared adding slowly the salt to a container with the previously weighed water with continuous magnetic stirring. Failure to do so may result in the formation of hard phosphate clumps due to rehydration of the crystals that may take days to dissolve. A suggestion is to weigh the empty containers before, in order to add the exact amount of water needed to complete 200 g after pH adjustments and obtain the desired 40% w/w solution. For the use of citrate salt, it is recommended to add salt into the water volume first, before adding ethanol or the protein sample to facilitate citrate dissolution.
3. Separating and stacking gel formulations described herein are meant to prepare gels with 10% acrylamide. If a higher percentage is desired, the amount of acrylamide stock solution has to be increased accordingly, reducing the amount of water proportionally.
4. To our experience, this solution should be prepared a few minutes before its use.

5. Running buffer can be stored and reused up to ten times, depending on the amount of residual gel debris and conductivity. We find that a typical 1.5 mm-thick gel could take 2.5 or 3 h maximum to reach the bottom, if longer times are required, it may be necessary to prepare new fresh running buffer.
6. Tanah and Shibasaki [16] have reported a simple procedure for the fractionation of soybean seed proteins. Isoelectric precipitation yields fractionated extracts enriched with one of the two main storage proteins in soybeans, glycinin, and b-conglycinin. The extract pH is carefully adjusted drop wise to 6.4 with 2 M HCl and centrifuged at 10,000 × *g* for 20 min at 2–5 °C. The precipitate collected is referred to as the 11S fraction (11S fractionated soybean extract). The supernatant is further adjusted dropwise to pH 4.8, and the resulting precipitate is referred to as the 7S fraction (or 7S fractionated soybean extract). Both precipitates can be resuspended in 0.03 M Tris-HCl buffer at pH 8.0, and any trace of precipitate, if present, can be removed by centrifugation (5 min at 10,000 × *g*). These two fractionated extracts can be further used for ATP partitioning experiments.
7. Previously sterilized YMB medium must be used for *Aspergillus* sp. inoculation of sorghum flour. Water activity should be maintained during fermentation (c.a. A_w 0.9) by adding 0.25 mL of YMB/g of flour before the incubation; later, the same proportion of water is added every 24 h during the entire incubation time.
8. We find that grinding can be performed inside a cold room to decrease moisture capture during grinding and avoid protease activation once the cells are broken. However, freezing the mortar at −20 °C for 15 min before the operation helps to keep green powder dry during the grinding operations and decrease overheating due to friction.
9. Use the same TBE buffer previously described and preferably place the container in an ice bath to avoid overheating or perform homogenization in 30 s intervals. The use of protease inhibitors such as ascorbic acid, EDTA, and phenylmethylsulfonyl fluoride should be considered; however, the toxicity and final use of the extract should be a primary concern.
10. Calculate the amount of each stock solution to be weighed depending on the concentration of the stocks and the desired concentration of the system to be prepared.

    g of PEG solution = (weight of system) × (% polymer/100)/(% w/w stock solution).

    g of phosphate solution = (weight of system) × (% phosphate/100)/(% w/w stock solution).

g of ethanol = (weight of system) × (% ethanol/100).

g of citrate = (weight of system) × (% citrate/100),

where (*% polymer/100*) is the total composition of PEG in the system and (*% w/w stock solution*) represents the concentration weight basis (w/w) of the polymer stock solution. Similarly, (*% phosphate/100*) is the total composition of potassium phosphate in the system and (*% w/w stock solution*) represents the concentration weight basis (w/w) of the potassium phosphate stock solution. Ethanol and sodium citrate are used in its pure form as absolute reagent and anhydrous powder form, respectively.

11. Phase separation is a critical step for the recovery of the target product. In our experience, at lab scales, ATPSs can be performed in plastic conical tubes, which can be punctured to allow lower phase separation by gravity. First, the top phase can be pipetted out without disruption of the interphase, and then a pushpin is used to make a small hole at the bottom; the lower phase can be recovered dropwise before the interphase reaches the end of the tube. In the case of fermented sorghum extracts, the thickness of the interphase is an important factor, since it can affect the final volume of recovered phases. Larger systems, no less than 5 g, are recommended to avoid small volume manipulation problems and cross contamination.
12. The length of the electrophoresis run is highly dependent on the conductivity of the sample applied. Usually the high salt content of the ATPS samples allows running 2–2.5 h at the suggested voltage. Power supply is set at 80 V for the first 15 min of the run to allow the sample to enter into the gel and then to 150 V until the bromophenol blue reaches the end of the glass plates. If an irregular dye front is observed, maybe due to precipitation of phosphates from ATPS samples, in these cases, ultrafiltration using centricon units is recommended.

Acknowledgments

The authors wish to acknowledge the financial support from Tecnológico de Monterrey Bioprocesses Research Chair (Grant 0020209I13).

References

1. Melnik S, Stoger E (2013) Green factories for biopharmaceuticals. Curr Med Chem 20:1038–1046
2. Vázquez-Villegas P, Acuña-González E, Mejía-Manzano LA, Rito-Palomares M, Aguilar O (2016) Production and optimization of a chlorophyll-free leaf protein concentrate from alfalfa (*Medicago sativa*) through aqueous two-phase system. Rev Mex Ing Quim 14 (2):383–392

3. Albertsson P-A (1999) Partition of proteins in liquid polymer–polymer two-phase systems. Nature 182:709–711
4. Benavides J, Rito-Palomares M (2008) Practical experiences from the development of aqueous two-phase processes for the recovery of high value biological products. J Chem Technol Biotechnol 83:133–142
5. Rito-Palomares M (2004) Practical application of aqueous two-phase partition to process development for the recovery of biological products. J Chromatogr B 807:3–11
6. McQueen L, Lai D (2019) Ionic liquid aqueous two-phase systems from a pharmaceutical perspective. Front Chem 15(7):135
7. Hernandez-Vargas G, González-González M, Rito-Palomares M, Benavides J, González-Valdez J (2019) Thermo-separating polymer-based aqueous two-phase systems for the recovery of PEGylated lysozyme species. J Chromatogr B 1105:120–128
8. Zhou L, Tao Zhang BJ, Li S (2019) Ultrasound-assisted aqueous two-phase extraction of resveratrol from the enzymatic hydrolysates of *Polygonum cuspidatum*. Food Biosci 31:100442
9. Aguilar O, Rito-Palomares M (2010) Aqueous two-phase systems strategies for the recovery and characterization of biological products from plants. J Sci Food Agric 90:1385–1392
10. Chow YH, Ow JL (2018) Selective recovery of amylase from pitaya (*Hylocereus polyrhizus*) peel using alcohol/salt aqueous two-phase system. J Eng Sci Technol 8:123–136
11. Gu Z, Glatz CE (2007) Aqueous two-phase extraction for protein recovery from corn extracts. J Chromatogr B 845:38–50
12. Zhang C, Glatz CE (1999) Process engineering strategy for recombinant protein recovery from canola by cation exchange chromatography. Biotechnol Prog 15:12–18
13. Zhang C, Love RT, Jilka JM, Glatz CE (2001) Genetic engineering strategies for purification of recombinant proteins from canola by anion exchange chromatography: an example of β-glucuronidase. Biotechnol Prog 17:161–167
14. Platis D, Labrou NE (2006) Development of an aqueous two-phase partitioning system for fractionating therapeutic proteins from tobacco extract. J Chromatogr A 1128:114–124
15. Aguilar O, Albiter V, Serrano-Carreon L, Rito-Palomares M (2006) Direct comparison between ion-exchange chromatography and aqueous two-phase processes for the partial purification of penicillin acylase produced by *E. coli*. J Chromatogr B 835:77–83
16. Thanh VH, Shibasaki K (1976) Major proteins of soybean seeds. A straightforward fractionation and characterization. J Agric Food Chem 24:1117–1121
17. Aguilar O, Rito-Palomares M (2008) Processing of soybean (*Glycine max*) extracts in aqueous two-phase systems as a first step for the potential recovery of recombinant proteins. J Chem Technol Biotechnol 83:286–293
18. Sandhya C, Sumantha A, Szakacs G, Pandey A (2005) Comparative evaluation of neutral protease production by *Aspergillus oryzae* in submerged and solid-state fermentation. Process Biochem 40(8):2689–2694
19. Aguilar O, Glatz CE, Rito-Palomares M (2009) Characterization of green-tissue protein extract from alfalfa (*Medicago sativa*) exploiting a 3-D technique. J Sep Sci 32:3223–3231
20. Ibarra-Herrera CC, Aguilar O, Rito-Palomares M (2011) Application of an aqueous two-phase systems strategy for the potential recovery of a recombinant protein from alfalfa (*Medicago sativa*). Sep Purif Technol 77:94–98
21. Zaslavsky A (1995) Aqueous two-phase partitioning. Physical chemistry and bioanalytical applications. Marcel Dekker Inc., New York, NY
22. Ooi CW, Tey BT, Hii SL, Kamal SMM, Lan JCW, Ariff A, Ling TC (2009) Purification of lipase derived from *Burkholderia pseudomallei* with alcohol/salt-based aqueous two-phase systems. Process Biochem 44(10):1083–1087
23. Bradford M (1976) A rapid and sensitive method for the quantification of microgram quantities of protein utilizing the principle of protein–dye binding. Anal Biochem 72:248–254
24. Laemmli UK (1970) Cleavage of structural proteins during the assembly of the head of bacteriophage T4. Nature 227:680–685
25. AOAC International (2016) Official methods of analysis of AOAC international, 19th edn. AOAC International, Rockville, MD

Chapter 8

Aqueous Two-Phase-Assisted Precipitation of Proteins: A Platform for Isolation of Process-Related Impurities from Therapeutic Proteins

Anurag S. Rathore and R. Bhambure

Abstract

Aqueous two-phase systems (ATPS) have been widely and successfully used in the purification of various biological macromolecules such as proteins, nucleic acids, antibiotics, and cell components. Interfacial precipitation of the product often results in lower recovery and selectivity of ATPS. Efficient resolubilization of the interfacial precipitate offers a way to improve the recovery as well as selectivity of ATPS systems.

In this protocol, we describe a method for aqueous two-phase-assisted precipitation and resolubilization of the recombinant human Granulocyte Colony Stimulating Factor (GCSF) for its selective isolation from *E. coli* host cell proteins as well as nucleic acids. This platform purification can be applied to other cytokines as well as most of the hydrophobic proteins that partition into the hydrophobic PEG-rich top phase. Recoveries of up to 100% of the product along with reduction of levels of *E. coli* host cell proteins (from 250–500 to 10–15 ppm) and of nucleic acids (from 15–20 to 5–15 ng/mL) were observed.

Key words Aqueous two-phase systems (ATPS), Interfacial precipitation, Host cell proteins (HCPs), Deoxyribonucleic acid (DNA), Granulocyte colony stimulating factor (GCSF)

1 Introduction

Aqueous two-phase systems (ATPS) offer efficient alternatives to chromatography for downstream processing of biomolecules with respect to various aspects such as yield, productivity, ease of scalability, and eco-friendliness. ATPS are formed spontaneously due to the mutual incompatibility between two aqueous solutions of structurally different components such as two polymers (e.g., polyethylene glycol and dextran) or a polymer and a salt (e.g., phosphate), above a certain critical concentration [1]. This phenomenon was first reported by Beijerinck in the nineteenth century [2] and was demonstrated as an effective tool for separation of biologicals by Albertson [1]. Since then, various successful efforts concerning the partitioning of biomolecules in different

Nikolaos E. Labrou (ed.), *Protein Downstream Processing: Design, Development, and Application of High and Low-Resolution Methods*, Methods in Molecular Biology, vol. 2178, https://doi.org/10.1007/978-1-0716-0775-6_8,

biphasic systems have been reported in the literature [3–12]. Precipitation-enhanced ATPS, in which the product of interest selectively accumulates at the interface while the impurities remain suspended in one of the phases, are being explored rigorously due to their higher recovery and selectivity [13, 14]. In the US patent application number 20110257378, the authors describe ATPS-augmented precipitation of monoclonal antibodies from the multicomponent mixture [15]. Recently, Rathore et al. reported the selective precipitation of target proteins at the interface of the two aqueous phases of an ATPS, resulting in higher levels of purity and yield of the target protein [16, 17]. The inherent complexity of such systems demands inclusion of the various extra steps into the standard ATPS protocol such as the separation of the interface and back extraction into a suitable buffer. A comprehensive understanding of the behavior of the product in various environments is necessary to achieve optimal recovery and product. The precipitate recovered, with or without one of the phases of an ATPS, can be later resolubilized using a suitable resolubilization buffer depending upon the properties of the specific target protein as well as the specific requirements of the follow-up step in the integrated biopurification process. Here, we describe the extraction of a 19.1 kDa cytokine that exists in two forms when introduced into the biphasic system: soluble form in the PEG-rich top phase and in solid form as a precipitate on the interface. Both of these phases are separated from the impurity-rich bottom phase and back-extracted into a suitable formulation buffer to solubilize the solid precipitate without bringing any conformational changes.

2 Materials

2.1 Equipment

15 mL falcon tubes (well graduated)

5 mL syringe with a long thin needle

Rocker shaker.

Test tube vortex mixer.

Centrifuge.

Incubator for maintaining the temperature of ATPS.

Filtration assembly with 0.2 μm filter papers.

2.2 Chemicals

Polyethylene glycol 6000, sodium sulfate anhydrous, sodium acetate anhydrous, glacial acetic acid, D-sorbitol, L-arginine, urea.

2.3 Buffers

Formulation buffer.

10 mM acetate buffer of pH 4 containing 5% (w/w) sorbitol.

Prepare 10 mM acetate pH 4.00 buffer. Weigh and add 50 g of purified D-sorbitol to the buffer (*see* **Note 1**).

Resolubilization buffer.

Formulation buffer with 1 M urea, 0.5 M arginine at pH 5.7. Take 100 mL of formulation buffer made before in a 250 mL glass bottle. Weigh and add 6 g of urea and 8.71 g of purified L-arginine powder to the bottle. Adjust the pH of the solution to 5.7 using glacial acetic acid (*see* **Note 2**).

Clarified protein solution.

The sample has to be clarified before introduction to ATPS. Take 20 mL of clarified protein solution (approximately 1 mg/mL) in a 50 mL falcon. Adjust the pH of the solution to 4 using 1:1 diluted glacial acetic acid (8.7 M). Centrifuge the solution at 4 °C for 15 min at 7000 rpm (6300 × *g*). Filter the protein solution using 0.2 μm filter paper (*see* **Note 3**).

3 Methods

3.1 Construction of the Phase Diagram

1. Select a desired temperature to make ATPS. Do all the further experimentation at this chosen temperature, unless specifically indicated. In this case, we have chosen 20 °C as our working temperature (*see* **Notes 4** and **5**).
2. Choose the two phase-forming components of ATPS, i.e., two polymers, or a salt and a polymer. In this case, ATPS involving PEG 6000 and sodium sulfate has been selected for the study (*see* **Note 6**).
3. Take a graduated 15 mL falcon. Calculate the amounts of solid salt and polymer to be added to make, say 20% w/w polymer and 15% w/w salt of the ATPS. Make the calculations as follows:
   (a) Choose the total weight of the system: say 6 g.
   (b) Amount of polymer required for 20% w/w = (20/100) × 6 = 1.2 g.
   (c) Amount of salt required for 15% w/w = (15/100) × 6 = 0.9 g.
   (d) Amount of water required for the system = total weight of the system − weight of the polymer − weight of salt = 6–1.2 − 0.9 = 3.9 g.
4. Add the calculated amount of water to a 15 mL falcon. Then add the calculated amount of salt to the falcon. Vortex the mixture. Add the calculated amount of polymer to the salt solution and vortex to dissolve the entire polymer flakes. Centrifuge the system at 20 °C for 3 min at 4000 rpm (2057 × *g*) to make the system "clear" with a sharp observable interface.

5. Add some water to the system; say 100 μL and vortex the solution. Observe the solution to be turbid on vortexing. The solution will soon form a biphasic system of different compositions than the one started with, i.e., 20% w/w REG, 15% w/w salt. Keep on diluting the solution with 100 μL of water until the solution becomes "clear", i.e., one phase is formed. This can be carried out while the system is continuously being mixed or by adding a drop, mixing, adding another drop and so on. To ensure the existence of a single phase, centrifugation, as mentioned above, can be used (*see* **Note 7**).
6. Note down the amount of water added while performing dilution to obtain a clear solution, in this case being 4.8 mL. Calculate the new total weight of the clear solution by adding the weight of water added during dilution and the initial weight of the system, i.e., 6 g. In this case, it comes out to be 10.8 g. Calculate the concentration of polymer and salt in the current system as follows:

   Final concentration of salt = amount of salt added initially/total weight of new system×100 = 0.9/10.8 × 100 = 8.33% w/w.

   Similarly, final concentration of PEG = 1.2/10.8 × 100 = 11.11% w/w. This gives us the first point on the binodal curve.
7. Repeat **steps 3–6**, taking different compositions of PEG and salt in **step 3**, to obtain more points on the binodal curve. The more the number of points, the more accurate is the binodal curve (*see* **Note 8**).

3.2 Preparation of the Aqueous Two/Three Phase System

1. After preparing the binodal curve, select the ATPS system composition. In this case, we are making 12% w/w PEG 6000, 8% w/w sodium sulfate ATPS (total system weight 12 g). Also, select a desired pH for the system (*see* **Note 9**).
2. Calculate the amount of water, polymer, and salt required for the ATPS. For example, for a 12 g total system, amount of polymer required = 12/100 × 12 = 1.44 g, salt required = 8/100 × 12 = 0.96 g, buffer required = 80/100 × 12 = 9.6 g (*see* **Notes 10** and **11**).
3. Add the required amount of salt, polymer, and water to a properly graduated falcon (*see* **Note 12**).
4. Add the calculated amount of salt to the falcon and vortex to get a clear salt solution (*see* **Note 13**).
5. Add the calculated amount of polymer to the falcon and vortex the whole solution to dissolve the polymer completely (*see* **Note 14**).

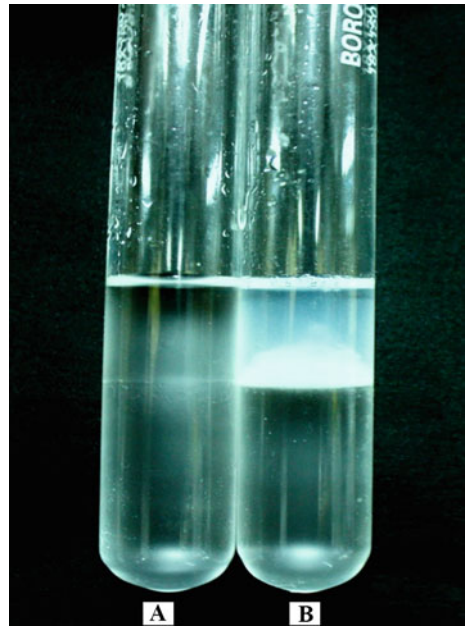

Fig. 1 Aqueous two-phase-assisted precipitation of the GCSF. Blank: (A) ATPS system containing PEG 6000 and sodium sulfate salt. (B) Sample: ATPS system containing PEG 6000, sodium sulfate salt, and protein solution (Adapted from Ref. 17)

6. Centrifuge the system at 20 °C at 4000 rpm (2057 × *g*) for 3 min.
7. Add the protein solution at the top of the polymer phase with the help of a pipette. Put the falcon on a rocker shaker for proper mixing of the system components for 10 min. Do not vortex the mixture (*see* **Note 15**).
8. Remove the falcon from the rocker shaker and leave it undisturbed in a vertical position for 3 hours, preferably in an incubator at 25 °C (*see* **Note 16**). Figure 1 shows the formation of a precipitate in an aqueous two-phase system.

3.3 Protein Recovery and Resolubilization

1. Take out the falcon from the incubator. Take proper care to keep the falcon vertical and ensure no mixing before the separation of the two phases and the formation of an interfacial precipitate in the falcon is performed (*see* **Note 17**).
2. Take a sterilized syringe fitted with a long thin needle. Very gently, open the cap of the falcon and insert the needle from the top of the polymer phase, piercing first the polymer phase and then the interfacial precipitate into the salt phase (*see* **Note 18**).
3. Gently suck the salt phase out of the falcon into the syringe. Take proper care not to suck any precipitate out with the salt phase. Drain the salt phase in another falcon for storage and analysis (*see* **Note 19**).

4. Add 6 mL of resolubilizing buffer with the help of a pipette to the falcon now having the precipitate and the polymer phase. Put the falcon on the rocker shaker for 10 min for proper dissolving of the precipitate. Do not vortex the mixture (*see* **Notes 20–22**).
5. Remove the falcon from the rocker shaker and centrifuge the solution at 4 °C at 8000 rpm (8228 × *g*) for 10 min. Collect the supernatant in a new falcon and store it at low temperature for further analysis (*see* **Note 23**).

3.4 Case Study Illustrating the Application of the ATPS Platform

Aqueous two-phase extraction incorporated precipitation was examined as a tool for selective isolation of process-related impurities from a biotherapeutic protein. An ATPS system consisting of 12% PEG 6000 and 8% sodium sulfate was selected for the study. Partition assay was set up in 15-mL graduated centrifuge tubes, which contained 3 mg of refolded GCSF. Figure 1 shows the formation of a two-phase system along with the precipitate. Top-phase and interfacial GCSF were resolubilized into the formulation buffer. Subsequently, top and bottom phases were analyzed for process-related impurities, which mainly involved host cell proteins and nucleic acids. The resolubilized GCSF contained 10–15 ppm HCPs and 5–15 ng/mL of HCDNA, which are acceptable as per the regulatory guidelines.

4 Notes

1. The choice of formulation buffer will depend upon the stability of the target protein to be purified using ATPS. The composition of the formulation buffer mentioned in the text is specific to GCSF.
2. The choice of resolubilization buffer will depend upon the stability of the target protein. Most importantly, it depends upon the dissolution efficiency of the resolubilizing buffer toward the precipitate of the protein formed and also the next purification step in the integrated purification process. It could also be the formulation buffer if ATPS is used as the final step and the formulation buffer sufficiently dissolves the precipitate.
3. The protein solution used as an input for the ATPS should be clarified of any cell debris. It has been reported in the literature [18] that cell mass gets accumulated at the interface of an ATPS, thus contaminating the probable target protein precipitate at the interface. It is essential to adjust the pH of the input protein solution to the working pH of the ATPS system in order to avoid isoelectric-point-based precipitation of host cell proteins. After pH adjustment, clarify the protein solution using centrifugation to remove any precipitated host cell proteins.

4. The binodal curve is a hyperbolic 2D phase diagram with main component 1(say peg) concentration on one axis (say Y axis) and main component 2 (say sodium sulfate) concentration on the second axis (say X axis), along with its tie lines. The binodal curve divides the component concentration where two phases are formed from the concentration region where a single homogeneous phase exists, thus delineating the potential working area. The tie lines end at the binodal curve and give the final composition of the upper and lower phases of an ATPS formed while working on a system with a composition to the right of the binodal. We get the same equilibrium composition of upper and lower phases of an ATPS when we work on points on the same tie line, but different volume ratios of the top phase to the bottom phase. The upper phase volume decreases as we go to the right or bottom of a particular tie line.
5. The phase diagrams in theory are temperature sensitive, which necessitates the fixing of a temperature during experimentation [19]. The choice of operating temperature in general is based upon the stability of your target protein at that temperature. Since gravity settling and equilibrium of an ATPS usually takes several hours, so the protein of interest should remain stable at that temperature. The range of temperature is limited by factors like solubility saturation of salts and industrial viability of the process conditions.
6. A wide list of phase-forming polymers and salts, as well s their phase diagram is readily available in the literature [20]. Furthermore, there is a choice between polymer-polymer ATPS or a polymer-salt ATPS. The choice should be made keeping in mind factors such as selectivity offered, cost, feasibility at the required temperature and pH regarding solubility and stability, back-extraction strategy, and biodegradability.
7. It is better to centrifuge the solution to check whether the solution is homogenous or an ATPS is formed. Formation of bubbles can sometimes make this observation tricky without centrifugation. If we are forming the phase diagram for a system with added neutral salts or ligands or systems with constant pH, the dilution should be performed with a suitable solution (such as water) with the same concentration of neutral salt as in the final system or constant pH buffer instead of water.
8. Similar to the initial concentration of PEG and salt used for finding the binodal point, other combinations of polymer and salt concentration are to be used (say 15% w/w polymer and 15% w/w salt). Generally, it is enough to gather 10–15 data points on the binodal for satisfactory accuracy. The current method of forming the phase diagram is called turbidometric titration. The cloud point method is also commonly used for construction of the binodal curve [21].

9. A number of system compositions can be examined in parallel to improve project efficiency. It has been observed that the phase diagram is insensitive to changes in pH [22]. Hence, pH, in general, should be chosen keeping in mind the stability of the target protein at that pH, the partition behavior of different proteins at that pH, and the feasibility of the pH for the particular components of the ATPS. For example, the ATPS systems of phosphate salt are unstable at low pH and temperatures.
10. For a constant pH biphasic system, the salt and its complementary acid/base should be added in a specific proportion so as to simultaneously achieve the total salt mass percentage as well as the desired pH, e.g., usage of K_2HPO_4/KH_2PO_4 for the phosphate system. To make small adjustments in pH, acid/base solutions can also be directly used. In our case, H_2SO_4 was used to adjust the pH of the sulfate-based ATPS.
11. It is better to add solid constituents directly to the solution rather than making stock solutions. One can work with stock solutions, instead of using dry salts and polymers, but it may result in inaccurate pipetting of highly viscous stock solutions.
12. Since the protein solution is almost an aqueous solution, it rarely affects the phase diagram and the amount of protein solution added to the system should be compensated with the amount of water to be added to the system. For example, if total of 10 mL water is needed for a particular ATPS and 2 mL of protein solution is to be added to the system, the actual amount of water that will be added to the system will be $10 - 2 = 8$ mL. It is best to use a concentrated protein solution as an input for ATPS so as to minimize any problems related to the solubility of the salt or polymer before the addition of the protein solution.
13. While dissolving the salt to the water, it is always helpful to add the salt in discreet steps and vortex immediately to make a clear solution.
14. While dissolving PEG, intense vortexing or usage of the rocker shaker may be required, if polymer flakes settle at the bottom. Numerous bubbles may be observed while vortexing the PEG solution. The centrifugation step is optional and is done to settle out all the bubbles and obtain a clear ATPS before adding any protein solution.
15. Vortexing of protein leads to excessive stress and hence subsequent denaturation. It also leads to frothing of solution incurring protein losses. Sufficient time for mixing should be given for reaching mass transfer equilibrium of various protein and nonprotein components in the ATPS. A rocker shaker is suitable for such operations.

16. An alternative to gravity settling of an ATPS is centrifugation for speedy-phase separation. However, gravity settling is likely to be the method of choice at scale and it is recommended to use the same at the lab scale as well to avoid any scale-up issues. A constant temperature should be maintained during settling. The time of incubation for gravity settling should be optimized for the selected ATPS system containing a target protein. A longer incubation time may lead to the formation of insoluble protein aggregates, whereas a shorter incubation time may lead to a nonequilibrium stage in partitioning.
17. The separation and interface between the phases of an ATPS is generally quite stable and does not get affected by minor movements. Still, proper care should be taken to avoid any mixing between the phases by keeping the falcon in a vertical position.
18. A sufficiently long needle should be used, such that the needle length alone transverses the polymer phase as well as the interfacial precipitate. It is better to insert the needle with its tip moving along the edge of the falcon for minimum disturbance at the interface.
19. One can also remove any precipitate stuck to the walls of the needle on the outside, by gently pressing the needle tip at the bottom of the falcon and moving it sideward to create minor vibrations in the needle, sufficient to remove the precipitate.
20. All the phases should be separated very neatly as the partition behavior of proteins may not be known beforehand. In our case, only the host cell proteins of *E.coli* partition to the bottom salt phase. At a large scale, an opening could be provided at the bottom of the vessel to drain the bottom phase.
21. In case one has to separate the top phase too from the interfacial precipitate, one could remove the top polymer phase after removing the bottom phase. This should be done gently with the help of a needle with its tip near the top of the polymer phase at all times to avoid sucking out the precipitate with the polymer phase. One could also use a pipette to remove the top phase instead of a syringe needle as the polymer phase is sometimes very viscous, but it should not be used to remove the bottom phase, as the large cross section of the pipette tip would disturb the interface of the ATPS.
22. An alternative to the above-mentioned step can be retrieving the precipitate on a filter membrane. The whole of ATPS could be filtered without disturbing the separation, by providing an opening at the bottom, where an appropriate filter membrane could be fitted. The precipitate would be retained at the membrane and later recovered as a filtrate by passing the resolubilizing buffer through the membrane.

23. The insoluble aggregates settle down as a precipitate at this step, and hence, centrifugation and subsequent collection of the supernatant as the final process output is a must. The parameter specifications concerning the mixing on the rocker shaker and centrifugation could again be optimized according to the protein. The final process output may now be analyzed or buffer exchanged in the formulation buffer and stored or further processed according to the integrated purification process. In this case, the output would be used as an input for the next purification step for removing product-related impurities.

References

1. Albertsson PA (1986) Partition of cell particles and macromolecules. Wiley, New York, NY
2. Diamond AD, Hsu JT (1992) Aqueous two-phase systems for biomolecule separation. Adv Biochem Eng Biotechnol 47:89–135
3. Haraguchi LH, Mohamed RS, Loh W et al (2004) Phase equilibrium and insulin partitioning in aqueous two-phase systems containing block copolymers and potassium phosphate. Fluid Phase Equilibr 215:1–15
4. Reh G, Nerli B, Pico G (2002) Isolation of alpha-1 antitrypsin from human plasma by partitioning in aqueous biphasic systems of polyethyleneglycol-phosphate. J Chromatogr B 780:389–396
5. Cavalcanti MTH, Porto TS, Neto BB et al (2006) Aqueous two-phase systems extraction of α-toxin from *Clostridium perfigens* type A. J Chromatogr B 833:135–140
6. Rosa PAJ, Azevedo AM, Ferreira IF et al (2007) Affinity partitioning of human antibodies in aqueous two-phase systems. J Chromatogr A 1162:103–113
7. Chethana S, Nayak CA, Raghavarao KSMS (2007) Aqueous two-phase extraction for purification and concentration of betalains. J Food Eng 81:679–687
8. Patil G, Raghavarao KSMS (2007) Aqueous two-phase extraction for purification of C-phycocyanin. Biochem Eng J 34:156–164
9. Johansson H, Ishii M, Minaguti M et al (2008) Separation and partitioning of green fluorescent protein from *Escherichia coli* homogenate in poly(ethylene glycol)/sodium-poly (acrylate) aqueous two-phase systems. Sep Purif Technol 62:166–174
10. Soares RR, Azevedo AM, Van Alstine JM, Aires-Barros MR (2015) Partitioning in aqueous two-phase systems: analysis of strengths, weaknesses, opportunities and threats. Biotechnol J 10:1158–1169
11. Phong WN, Le CF, Show PL, Chang JS, Ling TC (2017) Extractive disruption process integration using ultrasonication and an aqueous two-phase system for protein recovery from *Chlorella sorokiniana*. Eng Life Sci 17:357–369
12. Iqbal M et al (2016) Aqueous two-phase system (ATPS): an overview and advances in its applications. Biol Proced Online 18:18
13. Lee JW, Forciniti D (2010) Purification of human antibodies from transgenic corn using aqueous two-phase systems. Biotechnol Prog 26:159–167
14. Singh N, Sibylle H (2017) Downstream processing technologies/capturing and final purification. In: Ghose TK, Fiechter A, Blakebrough N (eds) Advances in biochemical engineering. Springer, Berlin, pp 1–64
15. Tran R, Titchener-Hooker NJ, Lacki K (2011) Aqueous two phase extraction augmented precipitation process for purification of therapeutic proteins Patent application number: 20110257378
16. Bhambure R, Sharma R, Gupta D et al (2013) A novel aqueous two phase assisted platform for efficient removal of process related impurities associated with *E. coli* based biotherapeutic protein products. J Chromatogr A 1307:49–57
17. Rathore A (2012) A process for purification of Recombinant granulocyte colony stimulating factor. Patent application number: 1880/DEL 2012
18. GuanY LTH, Garcia-Lisbona MN et al (1995) New approaches to aqueous polymer systems: theory, thermodynamics and applications to biomolecular separations. Pure Appl Chem 67:955–962
19. Mokhtarani B, Karimzadeh R, Amini MH et al (2008) Partitioning of Ciprofloxacin in aqueous two-phase system of poly(ethylene glycol)

and sodium sulphate. Biochem Eng J 38:241–247

20. Zaslavsky BS (1995) Aqueous two-phase partitioning: physical chemistry and bioanalytical applications. Marcel Dekker Inc., New York, NY
21. Kaul A (2000) Phase diagram. In: Kaul A (ed) Methods in biotechnology, vol. 11: aqueous two-phase systems: methods and protocols. Humana, Totowa, NJ
22. Ferreira GB, Evangelista AF, Junio JBS et al (2007) Partitioning optimization of proteins from *Zea mays* malt in ATPS PEG 6000/CaCl2. Braz Arch Biol Technol 50:557–564

Chapter 9

Recombinant Proteins Co-Expressed and Co-Purified in the Presence of Antibody Fragments

Ario de Marco

Abstract

Recombinant antibodies in single-domain format (VHHs) have been recently used for stabilizing antigens during their purification and crystallization. VHHs are also known for their structural stability and a significant part of them share the characteristic of remaining functionally folded also in the absence of the internal disulfide bond. Therefore, they can be expressed as intrabodies in the cell cytoplasm as well as in the bacterial periplasm. This evidence means that, in theory, VHHs can be co-expressed with their antigens independently on the redox constrains. It has also suggested the idea of using co-expression and co-purification of antigen–antibody complexes for maximizing the stabilizing effect of the antibody on its antigen during all the production steps for both cytoplasmic and periplasmic expression strategies.

Key words Single-domain antibodies, Protein crystallization, Protein complexes, Immunoaffinity purification, Intrabodies

1 Introduction

Antibody binding stabilizes the antigen structure and this characteristic has been used for improving the efficacy of crystallization trials [1]. Lately, single-domain antibodies have emerged as the most suitable format of crystallization chaperones [2, 3] and their capacity of forming stable complexes with their antigen has been exploited for immunocopurifying and solving the structure of membrane proteins [4]. This success suggested that it could be convenient trying to co-express the antigen together with its binder. The resulting complex should be stable, preventing the antigen aggregation. This strategy also allows for the recovery of untagged target proteins by means of the affinity purification of the tagged binding partner (Fig. 1) and it was successfully demonstrated with both affibodies [5] and VHH antibodies expressed in different hosts [6, 7].

Nikolaos E. Labrou (ed.), *Protein Downstream Processing: Design, Development, and Application of High and Low-Resolution Methods*, Methods in Molecular Biology, vol. 2178, https://doi.org/10.1007/978-1-0716-0775-6_9,

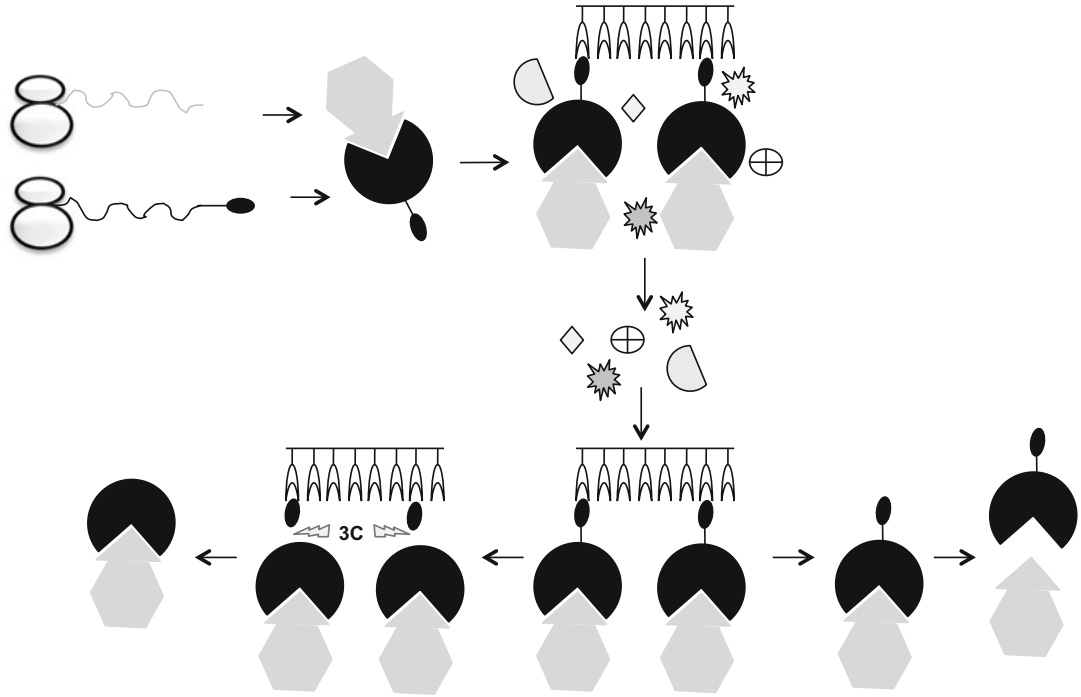

Fig. 1 Schematic representation of the antigen–recombinant antibody pairing and purification as a unique complex. Polypeptides corresponding to antigen and antibody form stabilizing antigen–antibody complexes. The tag fused to the antibody is used for affinity binding of the complex followed by contaminant removal. The components can be separated and the antigen recovered for biochemical characterization after a second affinity purification step (antibody removal) or the tag can be removed by protease digestion and the complex used as it is (structural studies)

The main shortcoming of this approach is due to the redox requirements for antibody folding. Their native structure is usually dependent on the formation of disulfide bonds and, therefore, they are commonly expressed as secreted proteins or in the bacterial periplasm. However, several cytoplasmic proteins are not correctly folded in the oxidizing milieu [8] (*see* **Note 1**) and this condition would limit the application potential of the technology. Nevertheless, a consistent amount of VHHs remains functional in the absence of disulfide-bond formation [9]; namely, they can be expressed as intrabodies. Consequently, it could be shown that antigen–VHH complexes were formed in, and purified from, both cytoplasm and periplasm [7]. The recent discovery that any VHH reaches its native folding when co-expressed in the bacterial cytoplasm in the presence of sulfhydryl oxidase [10] can further widen the above-described opportunities.

These examples indicate the feasibility of the method and its general application potential for stabilizing and co-purifying antigens from soluble cell compartments as well as from membranes. Even though the main interest for antigen–antibody co-purification

will remain the structure elucidation of the complex, the method should also be considered as an immunopurification protocol suitable for recovering untagged metastable proteins.

2 Materials

2.1 Vectors and Antigen/Antibody Pairs

1. A couple of vectors selectable using two independent resistances and having different tags for the cytoplasmic expression of polypeptides (*see* **Note 2**).
2. A couple of vectors selectable using two independent resistances and having different tags for the periplasmic expression of polypeptides.
3. One recombinant antibody specific for each of the expressed antigen (*see* **Notes 3–5**).

2.2 Small-Scale Protein Production

1. Culture medium (Lauria Bertani—LB or Terrific Broth—TB).
2. 1 M IPTG dissolved in H_2O.
3. 40% Glucose.
4. BL21 (DE3) bacteria transformed with suitable constructs.
5. 1 mg/mL DNase I.
6. 100 mg/mL Lysozyme.
7. Ni-NTA magnetic beads.
8. Lysis buffer: 50 mM Tris–HCl, pH 8.0, 500 mM NaCl, 5 mM $MgCl_2$.
9. Washing buffer: 50 mM Tris–HCl, pH 8.0, 500 mM NaCl, 15 mM imidazole, 0.02% Triton.
10. PBST.
11. Water bath sonicator.
12. Tubes for microbiology (12–15 mL).
13. 100 mg/mL Ampicillin stock solution dissolved in H_2O.
14. 50 mg/mL Kanamycin stock solution dissolved in H_2O.

2.3 Analytical Size-Exclusion Chromatography (SEC)

1. Superdex 75 5/150 GL (GE Healthcare).
2. ÄKTA-FPLC (GE Healthcare).
3. SEC buffer: 25 mM Tris–HCl, pH 7.8, 150 mM NaCl or PBS.

2.4 Periplasmic Large-Scale Protein Production

1. Culture medium (Lauria Bertani—LB or Terrific Broth—TB).
2. 1 M IPTG dissolved in H_2O.
3. 40% Glucose.
4. BL21 (DE3) bacteria transformed with suitable constructs.
5. 1 mg/mL DNase I.

6. 100 mg/mL Lysozyme.
7. Ni-NTA chromatographic column.
8. Resuspension sucrose buffer: 50 mM Tris–HCl, pH 8.0, 20% sucrose (w/v), 0.5 mM Na_2EDTA.
9. Osmotic shock buffer: 50 mM Tris–HCl, pH 8.0.
10. Washing buffer: 50 mM Tris–HCl, pH 8.0, 500 mM NaCl, 15 mM imidazole.
11. Elution buffer: 50 mM Tris–HCl, pH 8.0, 150 mM NaCl, 200 mM imidazole.
12. Centrifuge with a rotor suitable for 50 mL tubes.
13. Tubes (12–15 mL).
14. FPLC equipment.
15. 100 mg/mL Ampicillin stock solution dissolved in H_2O.
16. 50 mg/mL Kanamycin stock solution dissolved in H_2O.
17. Column for size-exclusion chromatography (SEC).
18. SEC buffer: 50 mM Tris–HCl, pH 8.0, 150 mM NaCl.

2.5 Cytoplasmic Large-Scale Protein Production

1. Culture medium (Lauria Bertani—LB or Terrific Broth—TB).
2. 1 M IPTG dissolved in H_2O.
3. 40% Glucose.
4. BL21 (DE3) bacteria transformed with suitable constructs.
5. 1 mg/mL DNase I.
6. 100 mg/mL Lysozyme.
7. Ni-NTA chromatographic column.
8. Lysis buffer: 50 mM Tris–HCl, pH 8.0, 500 mM NaCl, 5 mM $MgCl_2$.
9. Washing buffer: 50 mM Tris–HCl, pH 8.0, 500 mM NaCl, 15 mM imidazole.
10. Elution buffer: 50 mM Tris–HCl, pH 8.0, 150 mM NaCl, 200 mM imidazole.
11. Centrifuge with a rotor suitable for 50 mL tubes.
12. Tubes (12–15 mL).
13. FPLC equipment.
14. 100 mg/mL Ampicillin stock solution dissolved in H_2O.
15. 50 mg/mL Kanamycin stock solution dissolved in H_2O.
16. Column for size-exclusion chromatography (SEC).
17. SEC buffer: 50 mM Tris–HCl, pH 8.0, 150 mM NaCl.

2.6 Antigen–Antibody Complex Characterization (AI)

1. Spectrofluorimeter.
2. Spectrofluorimeter cuvette.

3 Methods

3.1 Vector Preparation

1. Standard cloning techniques are used for preparing the vectors for the expression of the antigen–antibody pairs. In this example, it is considered that the antibodies are His-tagged.

3.2 Small-Scale Protein Production

1. Inoculate the BL21(DE3) cells transformed with the two plasmids in a microbiology (12–15 mL) tube containing 2 mL of LB medium, 1% glucose, 2 μL ampicillin stock solution, and 2 μL kanamycin stock solution (*see* **Note 6**).
2. Grow overnight at 30 °C in an inclined rack (30°) inside a shaker (180 rpm).
3. The day after, add 100 μL of the pre-cultures to a 50 mL Erlenmeyer flask filled with 15 mL of LB (or TB), 15 μL ampicillin stock solution, and 15 μL kanamycin stock solution.
4. Let the bacteria grow at 37 °C in an orbital shaker (210 rpm) until the OD_{600} reaches 0.4, switch the temperature to 20 °C, and induce the protein expression after 30 min (the OD_{600} of the culture will have reached approximately the value of 0.6) by adding 0.2 mM IPTG.
5. Let the culture grow 18 h at 20 °C and then harvest the pellet by centrifuging (15 min × 11,000 × *g* at 4 °C).
6. Remove the medium and store the pellet at −20 °C.
7. Add 35 μL of magnetic bead slurry to a 2-mL Eppendorf tube.
8. Set the tube into a magnetic rack and carefully remove the solution.
9. Transfer the tube into a standard rack and resuspend the beads in 400 μL of PBST.
10. Set the tube to the magnetic rack and remove the buffer.
11. Transfer the tube in a standard rack and collect the beads in 50 μL of lysis buffer.
12. Resuspend the bacteria pellet in 500 μL of lysis buffer (*see* **Note 7**).
13. Sonicate for 5 min in a water bath at room temperature.
14. Add lysozyme to a final concentration of 1 mg/mL and DNase I to a final concentration of 50 μg/mL and incubate for 30 min at room temperature by continuous rocking. No viscous material indicating the presence of indigested nucleic acids should be detectable at the end of this step.

15. Separate the supernatant fractions by centrifugation (5 min at 16,100 × *g*) (*see* **Note 8**) and add them to the tubes with the pretreated beads.
16. Incubate the tubes 30 min under constant rotation.
17. Separate the beads from the supernatant by means of the magnetic rack and discard the supernatant.
18. Remove the magnet, resuspend the beads in 400 μL of washing buffer, and incubate 30 min under constant rotation.
19. Repeat **steps 17** and **18**.
20. Separate the beads from the supernatant by means of the magnetic rack and carefully discard the buffer (*see* **Note 9**).
21. Remove the magnet and incubate the beads 10 min in the presence of 40 μL of 50 mM Tris–HCl, pH 8.0, 250 mM NaCl, and 250 mM imidazole to elute the antigen–antibody complex.
22. Separate the beads by means of the magnet and recover the elution fraction.
23. Load 20 μL of the affinity-purified protein fractions on the pre-equilibrated SEC column.
24. Use the remaining material for running in parallel a native and a denaturing polyacrylamide gel (*see* **Note 10**).

3.3 Analytical Size-Exclusion Chromatography (SEC)

1. Pre-equilibrate the SEC column in 5 volumes of the appropriate buffer.
2. Load the sample in a mini-loop of 15 μL of volume.
3. Run the gel filtration at a flow rate of 0.2 mL/min and collect the absorbance signal at 280 nm.
4. Analyze the peak distribution (*see* **Note 11**).

3.4 Periplasmic Large-Scale Protein Production (See Note 12)

1. Inoculate the BL21(DE3) cells transformed with the two plasmids in a 200 mL Erlenmeyer flask containing 25 mL of LB medium, 1% glucose, 25 μL ampicillin stock solution, and 25 μL kanamycin stock solution.
2. Grow overnight at 30 °C inside a shaker (180 rpm).
3. The day after, add 2.5 mL of the pre-cultures to each 2000 mL Erlenmeyer flask filled with 500 mL of LB (or TB), 500 μL ampicillin stock solution, and 500 μL kanamycin stock solution.
4. Let the bacteria grow at 37 °C in an orbital shaker (210 rpm) until the OD_{600} reaches 0.4, switch the temperature to 20 °C, and induce the protein expression after 30 min (the OD_{600} of the culture will have reached approximately the value of 0.6) by adding 0.2 mM IPTG.

5. Let the culture grow 18 h at 20 °C and then harvest the pellet by centrifuging (15 min × 15,000 × *g* at 4 °C).
6. Remove the medium and store the pellet at −20 °C.
7. Resuspend the pellet corresponding to 1 L overnight culture (4–5 mL) into 20 mL of sucrose buffer (*see* **Note 13**).
8. Rock the sample 10 min and pellet the cells by centrifugation (15 min × 10,000 × *g* at 4 °C).
9. Remove the supernatant.
10. Resuspend the pellet in 20 mL of ice-cold osmotic shock buffer and incubate 10 min at 4 °C under constant rocking.
11. Pellet the cells by centrifugation (15 min × 10,000 × *g* at 4 °C) and recover the supernatant.
12. Load the supernatant onto an IMAC affinity column pre-equilibrated in washing buffer and connected to a FPLC system.
13. Wash the column until the OD_{280} reaches the baseline and then elute the protein complex in the presence of the elution buffer.
14. Load the elution fraction onto a SEC column equilibrated with SEC buffer and record the elution profile at OD_{280}.

3.5 Cytoplasmic Large-Scale Protein Production

Steps 1–4 are the same as in Subheading 3.3.

5. Resuspend the bacteria pellet from 1 L culture (4–5 mL) in 20 mL of lysis buffer.
6. Sonicate for 5 min in a water bath at room temperature (*see* **Note 14**).
7. Add lysozyme to a final concentration of 1 mg/mL and DNase I to a final concentration of 50 μg/mL and incubate for 30 min at room temperature by continuous rocking.
8. Separate the supernatant fraction by centrifugation (15 min at 10,000 × *g*). No viscous material indicating the presence of indigested nucleic acids should be detectable at the end of this step (*see* **Note 15**).

Steps 9–11 are the same as **steps 12–14** in Subheading 3.4.

3.6 Antigen–Antibody Complex Characterization

1. The aggregation index (AI) is a value that allows estimating the monodispersity of protein fractions in short time, without material consumption and it is suitable for material present at any concentration and stored in any buffer. Low AI values indicate monodispersity, high AI values aggregation; in general, AI values below 0.2 indicate monodispersity, as confirmed by other biophysical analyses (DLS, turbidity) (*see* **Note 16**).

2. Spectrofluorimeter setting. Excitation at 280 nm and emission at 340 nm, scan rate 5 and emission recovery between 260 and 400 nm.
3. Insert the cuvette with the sample (140 μL of volume).
4. Sensitivity: 600 V is used as a default, but it can be changed according to the saturating signal.
5. Run, select the peaks at 280 and 340 nm, and record the values.
6. Calculate the ratio between the values obtained for the peaks at 280 and 340 nm.

4 Notes

1. The attention of the research community has been mostly focused on the possibility to express disulfide-bond-dependent proteins in the cell cytoplasm. This is due to the practical reason of identifying reliable strategies for producing in bacteria valuable secreted proteins such as eukaryotic receptors or antibodies. In contrast, there are no many reasons for expressing in the periplasm cytosolic proteins. The available reports dealing with the limiting effect of oxidizing conditions usually refer to the deleterious effect of oxygen excess during purification of cytoplasmic expressed proteins. However, there is at least one relevant cytoplasmic protein—GFP—whose periplasmic expression has been studied. The interest comes mainly because it could be fused to recombinant antibodies, providing a convenient way for their labeling. Despite many efforts and some contrasting reports, it seems that no significant amount of functional GFP-linked recombinant antibody can be produced in the bacterial periplasm [11–13].
2. It is preferable using an expression vector that allows the tagging of the recombinant antibody and another vector for the production of the untagged antigen. This combination is compatible with the purification of the untagged antigen alone after one first affinity step leading to the isolation of the complex. The tag sequence should be separated from the recombinant antibody by means of a region cleavable using a specific protease for obtaining the untagged complex.
3. In principle, any recombinant antibody format could be used for co-expression. In the praxis, the folding constraints may limit the application of this protocol, especially when the antigen–antibody pair must be co-expressed in the cytoplasm. However, there are several reports of scFvs and VHHs that reach a functional conformation also when expressed in reducing environments [7, 14].

4. Recombinant antibodies can be isolated from immune or pre-immune libraries using purified antigens as well as peptides or cells. Generally, library panning results in the isolation of several different clones with different binding and stability features. Antibodies characterized by slow dissociation kinetic and limited aggregation are optimal for producing stable and monodispersed complexes with the corresponding antigens.
5. Optimally, an equal level of expression of both antigen and antibody should be reached. Protein co-expression using plasmids with the same origin of replication is possible whether they are selected by means of resistance to different antibiotics [15]. Different strategies should consider the use of bicistronic vectors or plasmids present in the cell at different copy number, but compensating the overall expression rate by exploiting promoters characterized by different efficiency. In our model, the expression of the constructs present in both plasmids is T7 polymerase-dependent, but other promoters can be envisaged. As an alternative, recombinant antibodies with stabilizing effect on the antigen could be expressed before their antigens using independent induction systems (for instance, arabinose and IPTG in combination with their corresponding promoters, [16]).
6. It is possible to express functional recombinant antibodies in the reducing cytoplasmic environment of *E. coli* whether the bacteria are co-transformed with a plasmid that enables the independent expression of sulfhydryl oxidase (SOX) and an isomerase [10]. The protocol foresees the preliminary accumulation of SOX (arabinose-induced) and successively the expression of the recombinant antibody. The approach allows not only the production of nanobodies (one single disulfide bond) but also the production of IgG-like macromolecules with four disulfide bonds or of nanobody fusions with large passenger proteins, including GFP [17]. Since this system has been applied to other proteins rich in disulfide bonds as well [18], it could be considered as an alternative to periplasm for producing antibody–antigen complexes involving secreted proteins.
7. The BL21(DE3) strain is mutant for Lon and Omp proteases and, therefore, the use of protease inhibitors is not usually necessary. However, they should be present at least in the lysis buffer to avoid proteolytic activity when other strains are used.
8. According to the protein stability features, the purification **steps 15–22** should be performed either at room temperature or at 4 °C.
9. Large tips for P1000 micropipettes can be used for removing most of the washing buffer, but smaller tips for P200 are advised for sucking the residual buffer. This procedure is

necessary to avoid that buffer droplets remain in the tube and dilute the sample of purified protein that will be collected after elution from the beads.

10. Ideally, the two gels should show one single and two bands, respectively, corresponding to the antigen–antibody complex and to the two separate proteins. However, since their expression will probably not be exactly the same, a second band (his-tagged polypeptide) could be present in the native gel whether it accumulates at higher rate with respect to its partner. This contamination is not relevant and will be easily removed by the SEC step. In contrast, the presence of both separated antigen and antibody would indicate that the complex is not very stable at the conditions used for the elution and that a more stabilizing buffer should be considered.
11. Small-scale analytical SEC has been described in detail previously [19, 20]. The presence of a symmetric and unique peak will confirm the presence of a homogeneous preparation. Calibration curves will help in determining the mass corresponding to peak maximum. However, this value could differ significantly from the expected, due to migration conditions that do not resemble the theoretic and only the data recovered with an in-line refractometer/multi-angle light scattering device could clearly establish the actual mass of the particles. The presence and intensity of further peaks (aggregates and monomers) will be useful to evaluate the complex stability and should be easily separated by the material of interest. Further suggestions for protein quality analysis can be found in: https://p4eu.org/protein-quality-standard-pqs.
12. Periplasmic lysis allows recovering for the target proteins in a buffer with a relatively low amount of contaminants and this should improve the efficiency of chromatographic separation. However, purification after bacterial total lysis yields similar results in terms of recovered protein and homogeneity when IMAC is used as a purification method.
13. The EDTA-dependent outer membrane destabilization effect can be increased by preincubation in the presence of bivalent cations such as Ca++ and Mg++ [21]. However, the yield improvement is limited and maybe not sufficient to justify the introduction of a further step in the purification protocol.
14. Sonication by means of tip immersion can lead to higher yields, but the sample often heats during the process and, therefore, this procedure is not suitable for sensitive proteins. Keep always the tubes on ice during tip sonication!
15. Supernatant filtration is recommended before the FPLC chromatography step when small-diameter resins are used.

16. A multi-angle light scattering equipment mounted in-line for contemporary analysis during the gel filtration chromatographic step would represent the optimal configuration for a precise biophysical characterization of the complex. However, AI is a convenient, although approximate, method for fast aggregation evaluation during protocol optimization.

References

1. Hunte C, Michel H (2002) Crystallization of membrane proteins mediated by antibody fragments. Curr Opin Struct Biol 12:503–508
2. Steyaert J, Kobilka BK (2011) Nanobody stabilization of G protein-coupled receptor conformational states. Curr Opin Struct Biol 21:567–572
3. de Marco A (2011) Biotechnological applications of recombinant single-domain antibody fragments. Microb Cell Factories 10:44
4. Conrath K, Pereira AS, Martins CE et al (2009) Camelid nanobodies raised against an integral membrane enzyme, nitric oxide reductase. Protein Sci 18:619–628
5. Macao B, Hoyer W, Sandberg A et al (2008) Recombinant amyloid beta-peptide production by co-expression with an affibody ligand. BMC Biotechnol 8:82
6. Harmsen MM, Smits CB, de Geus B (2002) Stimulation of chymosin secretion by simultaneous expression with chymosin-binding llama single-domain antibody fragments in yeast. Appl Microbiol Biotechnol 60:449–454
7. Bossi S, Ferranti B, Martinelli C et al (2010) Antibody-mediated purification of co-expressed antigen-antibody complexes. Protein Expr Purif 72:55–58
8. Siurkus J, Neubauer P (2011) Reducing conditions are the key for efficient production of active ribonuclease inhibitor in *Escherichia coli*. Microb Cell Factories 10:31
9. Monegal A, Olichon A, Bery N et al (2012) Single heavy chain antibodies with VH hallmarks are positively selected during panning of llama (*Lama glama*) naïve libraries. Dev Comp Immunol 36:150–156
10. de Marco A (2015) Recombinant antibody production evolves into multiple options aimed at yielding reagents suitable for application-specific needs. Microb Cell Factories 14:125
11. Casey JL, Coley AM, Tilley LM, Foley M (2000) Green fluorescent antibodies: novel in vitro tools. Protein Eng 13:445–452
12. Thomas JD, Daniel RA, Errington J, Robinson C (2001) Export of active green fluorescent protein to the periplasm by the twin-arginine translocase (Tat) pathway in *Escherichia coli*. Mol Microbiol 39:47–53
13. Linton E, Walsh MK, Sims RC, Miller CD (2012) Translocation of green fluorescent protein by comparative analysis with multiple signal peptides. Biotechnol J 7:667–676
14. Nizak C, Monier S, del Nery E et al (2003) Recombinant antibodies to the small GTPase Rab6 as conformation sensors. Science 300:984–987
15. de Marco A, Deuerling E, Mogk A et al (2007) Chaperone-based procedure to increase yields of soluble recombinant proteins produced in *E. coli*. BMC Biotechnol 7:32
16. de Marco A, De Marco V (2004) Bacteria co-transformed with recombinant proteins and chaperones cloned in independent plasmids are suitable for expression tuning. J Biotechnol 109:45–42
17. Djender S, Schneider A, Beugnet A et al (2014) Bacterial cytoplasm as an effective cell compartment for producing functional IgG-like recombinant antibodies. Microb Cell Factories 13:140
18. Nguyen VD, Hatahet F, Salo KE et al (2011) Pre-expression of sulfhydryl oxidase significantly increases the yields of eukaryotic disulfide bond containing proteins expressed in the cytoplasm of *E. coli*. Microb Cell Factories 10:1–13
19. Sala E, de Marco A (2010) Screening optimized protein purification protocols by coupling small-scale expression and mini-size exclusion chromatography. Protein Expr Purif 74:231–235
20. de Marco A (2012) Optimization of purification protocols based on the step-by-step monitoring of the protein aggregates in the soluble fractions. Meth Mol Biol 824:145–154
21. Chen YC, Chen LA, Chen SJ et al (2004) A modified osmotic shock for periplasmic release of a recombinant creatinase from *Escherichia coli*. Biochem Eng J 19:211–215

Part III

High-Resolution Protein Purification Methods

Chapter 10

Affinity Tags in Protein Purification and Peptide Enrichment: An Overview

Ana Sofia Pina, Íris L. Batalha, Ana M. G. C. Dias, and Ana Cecília A. Roque

Abstract

The reversible interaction between an affinity ligand and a complementary receptor has been widely explored in purification systems for several biomolecules. The development of tailored affinity ligands highly specific toward particular target biomolecules is one of the options in affinity purification systems. However, both genetic and chemical modifications in proteins and peptides widen the application of affinity ligand-tag receptors pairs toward universal capture and purification strategies. In particular, this chapter will focus on two case studies highly relevant for biotechnology and biomedical areas, namely the affinity tags and receptors employed on the production of recombinant fusion proteins, and the chemical modification of phosphate groups on proteins and peptides and the subsequent specific capture and enrichment, a mandatory step before further proteomic analysis.

Key words Recombinant proteins, Fusion proteins, Affinity tags, Affinity purification, Phosphoproteomics

1 Introduction

The production of recombinant proteins became possible with the emergency of DNA technology in the 1970s [1], which contributed for the facile manipulation of DNA sequences and consequently for the production of encoded proteins in different hosts (e.g., prokaryotic and eukaryotic host cells) [2]. Bacterial hosts are usually more attractive due to their simplicity, well-established methods for genetic manipulation, high product yields, rapid expression, and cost-effectiveness [3]. However, a major drawback is that protein expression can lead to the formation of insoluble aggregates. These aggregates, termed inclusion bodies (IBs), are formed by unfolded or highly misfolded polypeptides [3]. In order to

Ana Sofia Pina and Íris L. Batalha contributed equally to this work. Ana M. G. C. Dias reviewed and updated the chapter.

Nikolaos E. Labrou (ed.), *Protein Downstream Processing: Design, Development, and Application of High and Low-Resolution Methods*, Methods in Molecular Biology, vol. 2178, https://doi.org/10.1007/978-1-0716-0775-6_10,

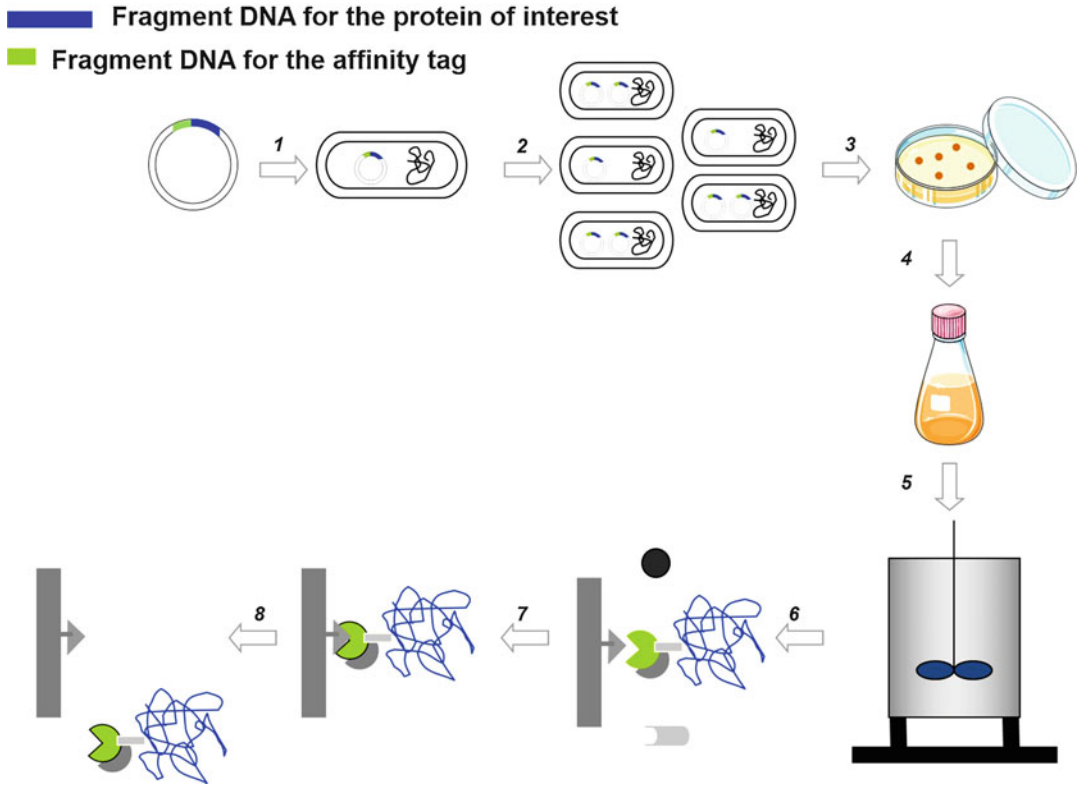

Fig. 1 Production and purification of recombinant proteins scheme, involving (1) insertion of recombinant DNA in host cells and the transformation process, (2) cloning process, (3) selection of the host cells containing recombinant DNA, (4) growth of the host cells, (5) upscalling, (6) fusion protein purification through affinity chromatography, (7) recognition of fused protein by the affinity ligand through affinity tag, and (8) elution of the purified fusion protein

address these challenges, target proteins can be fused to affinity tags to enhance the fusion partner solubility and proper folding and also overcome problems such as protein instability and host cell toxicity [4–6]. However, the main purpose of introducing affinity tags is to facilitate the purification of recombinant proteins (Fig. 1). The tag usually presents high affinity for a specific biological or chemical ligand immobilized onto a chromatographic matrix. Besides their employment in purification and as solubility enhancers, affinity tags may be used in many other applications, including labelling for imaging and localization studies, protein-protein interactions, and subcellular localization or transduction [4, 7, 8].

1.1 Affinity Tags in the Purification of Recombinant Proteins

Affinity tags vary in size, ranging from a single amino acid to whole proteins [9, 10]. The affinity tag can be introduced at both ends of the protein of interest, with the majority being placed at the C-terminal [10]. These tags must exhibit some characteristics, such as stability, selectivity, and reversible binding to their binding

Table 1
Examples of short peptides used as affinity tags

Type of affinity tag	Size (kDa)	Ligand	Reference
Enzymes			
β-Galactosidase	116	Thiogalactosidyl-sepharose	[146]
Glutathione-S-transferase	26	Glutathione-sepharose	[15]
Cloramphenicol acetyl transferase	24	Cloramphenicol-sepharose	[147]
Thierodoxin	12	Require a puritfication tag	[25]
Polypeptide-binding proteins			
Staphylococcal protein A	14–31	IgG	[36]
ZZ domains	7	Protein A	[37]
Albumin binding domain	75–25	I-Albumin	[148]
Phosphate- binding domain	34	Hydroxypatite	[149]
Carbohydrate-binding domains			
Maltose-binding domain 40		Cross-linked amylose	[22]
Cellulose binding domain	~100	Cellulose	[150]
Starch binding domain	133 aa	Starch	[151]
Exoglucanase CBD	128 aa	Cellulose	[152]
Other protein tags			
N-utilization substance (NusA)	55	Require a purification tag	[32]
Small ubiquitins modifier (SUMO)	11	Require a purification tag	[27]

partners [10, 11]. Ideally, the dissociation of the tag-receptor system should be performed under mild conditions to facilitate the recovery of the fusion protein [11].

There are a wide range of developed affinity tags to be used in the production and purification of recombinant proteins, which can be grouped into two main categories: protein affinity tags and peptide affinity tags. Protein affinity tags include enzymes (e.g., GST), polypeptide-binding proteins (e.g., SpA), and carbohydrate-binding domains (e.g., MBP, CBD) (Table 1). The use of small peptide tags presents some advantages over larger tags, for example, in terms of host cell metabolism, as less energy is consumed during fusion protein production [11]. Also, short tags are less likely to interfere with the structure and function of the target protein; therefore, they may not need to be subsequently removed [11]. The small peptides used as affinity tags fall into two categories: the peptides that bind to small ligands (e.g., poly-arginine and poly-histidine) and the peptide tags that are recognized by

Table 2
Examples of protein native domains as affinity tags

Type of affinity tag	Tag sequence	Ligand	Reference
Metal affinity tags			
Poly-His	HHHHHH	Ni^{2+}NTA, CO^{2+}CMA	[52, 54]
FlAsH tag	CCXXCC	Bis-arsenical fluorescein dye FlAsH	[153]
HAT	KDHLIHVHLEEHAHAHNK	CO^{2+} CMA	[154]
Charged peptides			
Poly-Arg	5–15 aa (R)	Anionic resins	[155]
Poly-Asp	5–16 aa (D)	Cationic resins	[156]
Poly-Cys	4 aa (C)	Tiopropyl sepharose	[157]
Glu	1 aa (E)	Cationic resins	[158]
Poly-Phe	11aa (E)	IEC	[159]
Epitope peptides			
FLAG™	DYKDDDDK	mAb M1, M2	[64, 69]
c-myc	EQKLISEEDL	mAb 9E10	[65]
T7	MASMTGGQQMG	Anti-T7 9E10	[66, 67]
Protein binding peptides			
S-tag	KETAAAKFERGHMDS	S-protein	[82]
Calmodulin bindindg protein	KRRWKKNFIAVSAANRFKKI SSSGAL	Calmodulin	[84, 87, 88]
Streptadividin binding proteins			
Bio tag	LGIFEAMKMEWR	Streptadivin/avidin	[160]
Strep-tag	SAWRHPQFGG	Streptadivin	[89, 90]
Strep-tag II	WHPQFEK	Streptactin	[94]
Avi tag	GLNDIFEAQKIEWHE	Streptadivin/avidin	[160]
Nanotag	DVEAWLGAR	Streptadivin/avidin	[161]

proteins (e.g., FLAG) (Table 2). The affinity tags based on small peptides can also be categorized into: (a) metal affinity tags; (b) charged peptides; (c) epitope peptides; (d) protein-binding peptides; and (e) streptadividin-binding proteins [4, 9–11].

The presence of the affinity tag may affect the characteristics or functions of the target protein and, depending on its final application, it might be necessary to remove the tag (Table 3) [11]. Specifically, in the case of therapeutic proteins, there is a demand for tag cleavage, as protein function can be lost and its integrity and

Table 3
Summary of enzymatic and chemical methods for tag removal

Cleavage agent	Cleavage specificity	Reference
Enzymes		
Exopeptidases		
Carboxypeptidase A	Poly H—↓—X	[54]
Carboxypeptidase B	Poly R—↓—X	[162]
Aminopeptidase I	EAE—↓—X	[158]
Endopeptidases		
Enterokinase	DDDDK—↓—X	[98]
Factor Xa	IEGR—↓—X	[100]
Thrombin	LVPR—↓—X	[101]
TEV protease	EQLYFQ—↓—X	[99]
SUMO	Sumo tertiary structure	[28]
Chemical		
Cyanogen bromide	XM—↓—X	[163]
Hydroxylamine	XN—↓—G	[164]
Acetic acid	XN—↓—P	[165]

↓ = indicated chemical cleavage site; X = unspecific amino acid

biological activity compromised due to the presence of the tag [5]. A variety of peptidases and other chemical methods are available for tag cleavage [12]. However, enzymatic methods may lead to undesired and/or suboptimal effects, such as the incomplete cleavage by the protease or the retention of additional amino acids in the fusion protein sequence from the cleavage site resulting from unspecific cleavage. Also, enzymatic methods are generally expensive and increase the costs of the manufacturing process. Self-cleaving tags have emerged to overcome some of these issues [13, 14].

1.2 Proteins as Affinity Tags

Protein affinity tags can be divided into solubility-enhancing tags and purification tags. The solubility of proteins is the bottleneck of the production of recombinant proteins in bacterial hosts. Therefore, a few protein tags are already used to enhance fusion protein expression and solubility. Examples of these tags include gluthathione-S-transferase (GST), maltose-binding protein (MBP), staphylococcal protein A (SpA), thioredoxin A (Trx), small ubiquitin-related modifier (SUMO), and N-utilization substance A (NusA) [5]. GST and MBP tags not only improve the solubility of their fusion partners but also increase the efficiency of

protein purification. The GST tag is a 26 kDa protein derived from *Schistosoma japonicum* and belongs to a family of enzymes that can modify toxic substances by transferring sulfur from glutathione [15]. The proteins fused to the GST tag can be purified from crude extracts by using affinity chromatography through the glutathione immobilized on the solid support [15]. The bound fusion proteins can be eluted under mild conditions by competitive elution with reduced glutathione [15, 16]. Other main advantages of this tag include the protection and stabilization of the recombinant protein against intracellular protease cleavage in the expression host, the cost-effectiveness of the affinity resins, and the use of mild conditions for the elution step [17]. Despite being considered a solubility-enhancing tag, this is not the case when the GST tag is fused to oligomeric proteins, hydrophobic regions enriched proteins, or with proteins larger than 100 kDa, as the expression of the fusion proteins represents a high metabolic burden for the host cell, contributing for an insoluble form expression [18]. The GST tag has been successfully used on protein-DNA binding studies and protein-protein interactions [19]. MBP is a 42 kDa periplasmic protein involved in the maltose transport system of *E. coli*, being responsible to transport maltose and maltodextrins across the cytoplasmic membrane [20]. The one-step purification is based on the strong affinity of MBP with cross-linked amylose—a low-cost matrix. Also, the bound tag can be removed by using nondenaturing conditions (e.g., competitive elution with maltose) [21, 22]. MBP is a powerful solubilising agent and can act as a general molecular chaperone preventing the self-aggregation of the fusion partner [23, 24].

Despite solubility-enhancing tags having a higher impact on the solubility of the fusion partner, often they lack an affinity ligand, hindering the purification process. Consequently, fusion proteins with a solubility tag require an additional affinity tag for protein purification. TrxA is a small protein with 11.675 kDa, belongs to a family of oxido-reductases, and presents in its active site a redox couple for a number of biological reactions [25]. This tag allows a high overall gene expression without the formation of inclusion bodies. In particular, the production of a wide variety of secreted mammalian cytokines and growth factors fused to the tag C-terminal was possible in a soluble form using *E. coli* as a host [16, 26]. Overall, Trx A presents robust folding properties that contribute to this tag to be a covalently fused molecular chaperone [16]. Also, TrxA is a cytoplasmic protein and presents inherent thermal stability, and these characteristics become helpful purification tools, facilitating the recovery of the fusion partner of the cell by osmotic–shock, and enabling heat treatments [26]. However, the purification can be facilitated by using an extra affinity purification tag.

The SUMO protein is involved in post-translational modifications in eukaryotic cells through the covalent binding to lysine side chains of the target protein, and this presents high relevance on various cellular processes (e.g., nuclear-cytosolic transport, apoptosis, and stability) [27, 28]. Once fused to the N-terminal of the partner, it greatly promotes the target protein correct folding and solubility when compared to untagged version [29]. Despite the fact that it requires an additional tag for purification, it presents an attractive feature that is the recognition by a sumo protease (*S. cerevisae* Ulp1). This SUMO protease recognizes SUMO conformation, more specifically the conserved Gly-Gly motif [28]. This technology is an effective tool for prokaryotic hosts; however, in eukaryotic hosts, there is the drawback of the natural occurrence of SUMO-tag cleavage by the SUMO proteases in vivo [29, 30]. NusA is a 55 kDa transcription elongation and termination factor that modulates transcription by enhancing and pausing at some sites [31, 32]. Recently, it was reported that NusA is also involved in the coordination of cellular responses to DNA damage [33]. NusA is one of the largest proteins being used as a carrier protein; however, it presents good solubilizing characteristics and high expression levels [34]. Moreover, this tag increases the solubility of proteins (e.g., human interleukin-3) that were being produced as IBs by themselves or when fused to other tags (TrxA) [34]. This might be related to NusA biological activity. Once again, this tag is a solubility tag and cannot be purified with a specific affinity matrix, requiring a purification affinity tag [34, 35].

Other protein tags used to increase solubility or to facilitate purification include SpA and its derivatives (Z domain or Z tag) [5]. The SpA protein is present on the surface of the gram-positive bacterium *Staphylococcus aureus* and mainly interacts with the constant region (Fc) of most mammalian class G immunoglobulins (IgG) [36]. This protein tag has been used for the purification of a variety of fusion proteins produced in different hosts, such as *E. coli*, yeast, CHO cells, baculovirus-infected insect cells, and plant cells, by using IgG affinity chromatography [37, 38]. The use of this tag presents several advantages, namely proteolytic stability, the absence of disulfide bonds, and the presence of inherent high solubility [37]. The major drawback is related to the fragility of IgG as a ligand, contributing for ligand leakage and consequently end product contamination [37]. The Z domain tag emerged as a mutated version of the B domain, which is a homologous domain of SpA with a high affinity for IgG. This affinity tag has been developed to improve the resistance of undesirable cleavage of the purified fusion protein when using a chemical tag removal strategy [39]. The main disadvantages associated with this technology are

the high costs of production and purification of the immobilized binding partner (e.g., IgG), poor stabilization under sterilization and cleaning-in-place conditions, as well as potential leakage and end-product contamination.

The Z domain was also engineered to create the Z tag (basic or acidic), a highly charged domain to be used in the purification of recombinant protein through ion-exchange chromatography [40, 41].

The Z_{basic} tag has been employed on matrix-assisted refolding strategies of proteins that were solubilized with chaotropic agents after being produced as IBs [40].

More recently, the Z domain was engineered to produce a calcium-dependent binding to antibodies. To achieve that, researchers have included a sequence from Calmodulin that binds Ca^{2+} ions in one loop. A phage display library was built and selected to improve the stability of the structure, as well as binding to IgG in a calcium-dependent manner. This strategy allowed identifying one clone that was stable, forming a new structure coined Z_{Ca}. This clone was characterized and immobilized in a solid support for the capture and purification of IgG from crude cellular extracts. High purity was achieved under mild elution conditions by using calcium-containing buffers [42].

In recent years, other protein affinity tags have been explored for applications both in academia and industry, namely: Green fluorescent Protein (GFP) as a widely used expression reporter of recombinant proteins in eukaryotic and prokaryotic cells, this protein was exploited for the development of a tag-receptor purification system with small synthetic affinity ligands immobilized in different solid supports [43–46]; Halo-tag (Promega) used as a purification, detection and immobilization partner for different proteins [47, 48]; Profinity eXact ™ (BioRad); the PDZ domain used mainly for affinity purification of other porteins [49]; ABTAG camelid single domain antibody protein that binds with high affinity to bovine serum albumin (picomolar affinity). This tag was fused with selection outputs from phage display libraries and allowed the development of a novel screening strategy [50]; and finally, the SpyTag/SpyCatcher, which allows covalently binding two proteins expressed recombinantly with a spyTag sequence and a Spy catcher, respectively. Furthermore, this strategy has been explored as a conjugation strategy between two proteins without the need for external enzymes, and can be used as an immobilization mechanism into different supports or, more recently, as a purification strategy [51].

1.3 Peptides as Affinity Tags

1.3.1 Metal Affinity Peptides

Immobilized metal affinity chromatography (IMAC) was introduced in 1975 by Porath and coworkers and is based on the affinity between proteins and heavy metal ions (Zn^{2+}, Cu^{2+}, and Ni^{2+}) [52]. This type of chromatography exploited the formation of stable complexes in an aqueous solution between histidine (His) and cysteine (Cys) residues and zinc and copper [52]. After this, Hochuli *et al.* developed a new metal chelate affinity resin, which once charged with nickel ions (Ni^{2+}-NTA) presents selectivity for neighbouring His of proteins or peptides [53].

Subsequently, Hochuli et al. were also the pioneers on using a poly-histidine peptide (His-tag) genetically fused to the mouse dihydrofolate reductase protein and produced in *E. coli* to purify the fusion protein using the Ni^{2+}-NTA adsorbent. His-tag was subsequently removed by using carboxypeptidase A [54]. Nowadays, the purification by using His-tag is one of the most used methodologies for protein purification and has been extensively described (Fig. 2) [55–57]. The main advantages of IMAC technology are related to the high protein loading capacity, ligand stability, and lower costs. Also, this technology can be easily scaled up with reproducibility and affordable costs [55]. Another advantage of using IMAC for the purification of recombinant proteins is

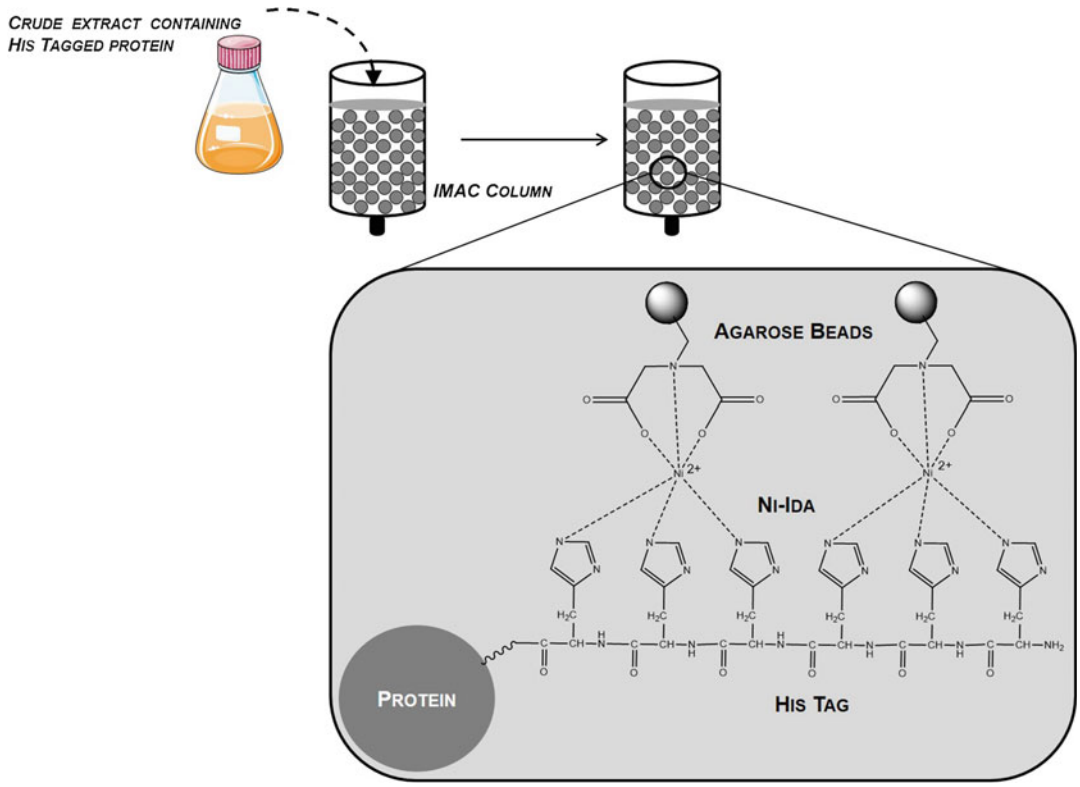

Fig. 2 Principle of protein purification through histidine affinity tag

the compatibility with denaturant agents for the solubilization and refolding of insoluble protein aggregates produced in the *E. coli* host. IMAC technology has been described as a successful strategy for the one-step refolding of His-tagged proteins [58]. The major drawbacks of using a metal affinity tag are the metal ion leakage that leads to metal contamination of the end-product. These metal ions are toxic and therefore additional steps of purification are required, especially for therapeutic proteins. Moreover, the metal resin disposal constitutes an environmental problem [55].

Although IMAC has been used mainly for protein purification, different applications have been explored such as protein refolding and solubilization [58], protein microarrays [59–61], and phage display [62]. Recently, Cysta-tag was developed for enhanced solubilization and expression. This tag includes a fusion partner, SICYS8, which is a protein that enhances protein expression in plants, and a poly-His tag. Therefore, Cysta-tag simultaneously enhances protein expression and facilitates purification using an IMAC system with the Ni^{2+} matrix [63]. In a different example, phage display-derived peptide sequences were developed to bind to a novel class of chelating ligands complexed with Ni^{2+} [62]. These chelating agents are based on the 1,4,7-triazacyclononane (TACN) structure and have been chosen to overcome ligand leaching in IMAC purification.

1.3.2 Epitope Peptides

Epitope peptides are used often as protein detection and characterization tags. These tags to a lesser extent are used for purification purposes, because the affinity matrices used are antibody-based, which accounts for higher purification costs [4]. The most frequently antigenic peptides used are Flag-tag [64], c-myc [65], T7 epitope tag [66, 67], Softags, [68] and HA tag [69].

The Flag-tag is an eight amino acid peptide with a hydrophobic sequence consisting of DYKDDDDK [64]. The Flag technology allows a rapid purification of fusion proteins in a mild, highly specific and calcium-dependent affinity chromatography procedure with an Anti-Flag M1 monoclonal antibody immobilized on the affinity support [64]. One of the features of this tag is the recognition of the five C-terminal amino acids of the peptide sequence by the protease enterokinase, facilitating tag removal [64]. Main drawbacks of this system are related to ligand leakage and stability due to their own natural character and low scalability. Also, this system cannot be used for the purification of fusion proteins produced as IBs because denaturing agents are required. Although this tag presents a highly specific sequence for enterokinase recognition, unwanted cleavage may occur in the presence of contaminant proteases [64].

Softags are epitope tags used for immunoaffinity chromatography and present high affinity for "polyol-responsive" monoclonal antibodies (mABs) [68]. These mAbs present a particular feature

regarding the elution conditions, being possible to use mild conditions supplemented with a low molecular weight polyol (e.g., ethylene glycol) and a non-chaotropic salt [5, 68]. Softag 1 is a thirteen amino acid sequence near the C-terminal of the β' subunit of *E.coli* RNA polymerase [70]; Softag 2 is a repeat heptapeptide found on the C-terminal of RNA polymerase I [71]; and Softag3 is an epitope near the N-terminal of human transcription factor [72]. The HA tag is derived from Human Influenza Hemagglutinin protein present in the virus capsid. This is a very common tag (31 amino acids) used in protein expression in eukaryotic hosts allowing purification, identification in different immunoassays, and detection in different cellular assays, as this tag has no interference in protein biological activity [69]. Furthermore, it has been used as a tag for detection of antibody fragments in phage display libraries [73]. One major advantage of this tag is the fact that antibodies that recognize the tag are highly specific and for that reason it is used frequently in the biopharmaceutical industry [7].

The major drawbacks of some of the previous tags are the high production costs and lack of specificity of some antibodies, as well as the limited life-time of resins. To overcome these limitations and expand the tag repertoire, several examples can be found in the literature, such as: PA tag (ten residues) derived from human poloplanin PLAG domain [74]; MAP tag (eight residues) derived from the platelet aggregation-stimulation domain of mouse podoplanin [75]; Target tag (21 residues) uses a highly specific antibody that can be reused several times without loss of binding capacity [76]; AGIA tag (four residues) derived from the dopamine receptor D1 C-terminal region, this tag lacks amino acids prone to post-translational modifications and that is an advantage for the recognition by the specific antibody [77]; RAP tag (12 residues) derived from rat podoplanin [78]; CP5 tag (five residues) from Dopamine receptor D1 [79]; finally, HBP tag (Heparin-binding peptide with 34 residues) has been used for affinity purification of recombinant proteins, using cross-linked agarose resin coated with heparin (a glycosaminoglycan) [80, 81].

1.3.3 Protein-Binding Peptides

S-peptide tag is a fifteen amino acid sequence polypeptide resultant fragment from the cleavage of ribonuclease A by the protease subtilisin. The other remaining product is S-protein [82]. S-peptide binds to S-protein with high affinity and this interaction allows the efficient affinity purification of recombinant proteins [82, 83].

Calmodulin binding protein (CBP) is a calcium-binding protein that plays a key role as a regulator in a wide range of calcium-dependent intracellular processes [84, 85]. Calmodulin-binding unit is a 26 amino acid peptide derived from the carboxyl-terminal of rabbit skeletal muscle myosin light chain kinase [86, 87]. This peptide binds to calmodulin with a nanomolar affinity and is also

calcium dependent [84–87]. The elution can be carried out under milder conditions and requires a calcium-chelating agent such as ethylene glycol tetraacetic acid (EGTA) [84, 87]. This tag was found out to be a versatile tag for antibody fragments [88]. However, its use in eukaryotic cells is hampered by its interference in calcium signalling pathways [5].

1.3.4 Streptadividin-Binding Peptides

The Strep-tag is a nine peptide sequence (AWRHPQFGG) and was originally developed by selection from a genetic peptide library for its capability to bind to streptavidin protein in a highly specific and reversible manner [89, 90]. Strep-tag recognizes the same pocket of streptavidin as biotin, the natural ligand, allowing one-step purification on immobilized streptavidin columns. However, the original Strep-tag needed to be fused only to the C-terminal of the recombinant protein [91, 92]. A new improved version - Strep-tag II, an eight residue peptide sequence (WSHPQFEK), was developed and optimized to overcome this constraint, and also presents affinity for streptavidin [91, 93]. Simultaneously, progress has been made to optimize the respective chromatographic matrices and an engineered streptavidin support with improved binding capacity (Strep-Tactin) has been developed [94]. The main advantages of these systems are the resistance to host cell proteases, the fact that the binding is not dependent on metal ions, the elution can be carried out at mild conditions, and the biological inertness of this tag [94].

A new streptadividin-binding protein (SBP) was also developed for the purification of recombinant proteins [95, 96]. This SBP tag presents a sequence of 38 amino acids long with a nanomolar affinity for streptadividin. The main applications of this tag are in high-throughput protein expression and purification procedures, existing already as several streptavidin-derivatized materials such as plates, beads, enzymes, fluorophores, etc. and commercially available [95].

1.3.5 Small-Synthetic Ligand Binding Peptides

In recent years, new affinity tags have been developed based on hexapeptides rich in tryptophan that are recognized through synthetic affinity ligands [45, 97]. In more detail, three major tags were developed for purification of fusion proteins—RKRKRK, NWNWNW, and WFWFWF. These tags were rationally designed to display affinity against small synthetic ligands that were produced through combinatorial chemistry using the Ugi reaction. This system allows producing a tag-receptor pair that can be used for recombinant protein expression and purification using affinity chromatography. Due to chemical synthesis these ligands are inexpensive to produce and allow obtaining purification matrixes that are selective and robust. In addition, these tags have different characteristics—charged (RKRKRK), neutral (NWNWNW), and

hydrophobic (WFWFWF). Moreover, despite these tags leading to protein expression as IBs, these proteins are recognized by the ligands immobilized in the matrixes, which allows protein refolding on-column. Nowadays, this is actually a very sought-after property, as some recombinant proteins can be extracted in higher purity with this strategy [45, 97].

1.4 Tag Removal

The removal of the affinity tag can be carried out by harsh chemical treatments (e.g., cyanogen bromide or hydroxylamine) or by enzymatic cleavage, with the latter being preferred since it can be performed under physiological conditions [9]. The chemical treatment presents significant drawbacks such as protein denaturation and side-chain modification of amino acids in the target protein [9]. Several endoproteases have been utilized for tag removal [12], such as enterokinase [98], tobacco etch virus (TEV) [99], Factor Xa [100], thrombin [100, 101], and SUMO protease [28]. Enterokinase (EK) is a serine proteinase constituted by a high chain and a light chain linked by a disulfide bond. This enzyme presents high specificity for the $(Asp)_4$-Lys sequence, which contributes for a useful tool for fusion protein cleavage [98, 102]. Factor Xa and thrombin are trypsin-like serine proteases and both recognize specific amino acid sequences (Table 3) [100]. TEV is a 49 kDa proteinase of tobacco etch virus (TEV) that cleaves the polyprotein derived from the TEV genomic RNA at five locations [99]. Most of these enzymes are able to cleave without requiring a specific sequence at the C-terminal, allowing for the complete removal of the tag [9, 12]. The major drawback associated with these enzymes is related to the high enzyme/protein ratios and the long incubation times required. Moreover, for an efficient tag removal, it is also necessary to take into account the absence of cryptic sites recognized by endoproteases in the native protein sequence [12].

Tag cleavage by using enzymatic or chemical methods always requires additional purification steps that contribute for the higher costs. In this way, other emerging technologies have been developed, namely self-cleaving tags. There are different types of self-cleaving tags, such as inteins, Sortase A, N-terminal protease, and FrpC module [13, 14]. In this particular case, these tags present inducible proteolytic activity under certain conditions such as pH or/and temperature shift and addition of specific reagents (e.g., Dithiothreitol (DTT), Ethylenediaminetetraacetic acid (EDTA), and Ca^{2+}) [14]. Although these self-cleaving tags seem to be attractive from the economic point of view, there are still a few drawbacks associated with premature cleaving and consequently target-protein losses and minor product compatibility with cleaving conditions [13, 103].

1.5 Affinity Tags for the Enrichment of Phosphorylated Proteins and Peptides

Post-translational modifications (PTMs) are involved in the regulation of several cellular processes, such as gene expression, signal transduction, metabolism, homeostasis, cell division, and apoptosis, by modulating protein folding and function [104, 105]. Over 300 types of PTMs are known, but only a few play determinant roles in biological processes [106, 107]. Protein phosphorylation is one of the most common PTMs and exhibits a transient and reversible character, being regulated by the dynamic action of kinases and phosphatases. There are more than hundred thousand potential phosphorylation sites in the human proteome, being estimated that 30–50% of all proteins are phosphorylated at some point during their lifetime. In eukaryotic systems, phosphorylation occurs essentially in serine and threonine residues, followed by tyrosine, with a ratio of 1800:200:1 [105, 108, 109]. Phosphorylation events have been associated with a variety of diseases, such as cancer [110], type II diabetes [111], cystic fibrosis [112, 113], neurological diseases including Parkinson's [114] and Alzheimer's [115], and neuropsychiatric disorders (e.g., schizophrenia) [116]. The degree of phosphorylation and the localization of specific phosphosites provide meaningful insights to better understand disease-associated signalling pathways, contributing to the development of novel biomarkers and drug targets.

Currently, the characterization of phosphoproteins and correspondent chemical or proteolytic digests is generally performed using Mass Spectrometry (MS) techniques. However, this analysis is not always straightforward since phosphopeptides present lower ionization efficiency than their non-phosphorylated counterparts, which results in lower signal intensities in positive ion mode. Moreover, phosphorylated species are usually present at sub-stoichiometric levels and are easily adsorbed by plastics and metals during sample handling [106, 117]. These problems can be partially overcome by using materials with low protein-binding properties and efficient enrichment methods before MS analysis.

Enrichment methods are generally based on the affinity capture of the phosphate groups, either by charge interactions (e.g., chromatofocusing, ion exchange chromatography), chelation (e.g., IMAC, metal oxide affinity chromatography (MOAC), hydroxyapatite, phosphate-binding ligands) or molecular recognition (e.g., immunoaffinity chromatography and affinity chromatography based on phosphoprotein-binding domains) (Fig. 3). Particularly, our group has put significant efforts toward the development of both chemical and peptide affinity ligand libraries for phosphopeptide enrichment [118, 119]. For further details on affinity capture of phosphorylated targets, the authors recommend the following reviews [105, 120–123]. However, strategies consisting of the chemical modification or replacement of the phosphate moieties by affinity tags are also viable alternatives (Fig. 4). Table 4 summarizes the chemical tags used for phosphoprotein and phosphopeptide enrichment.

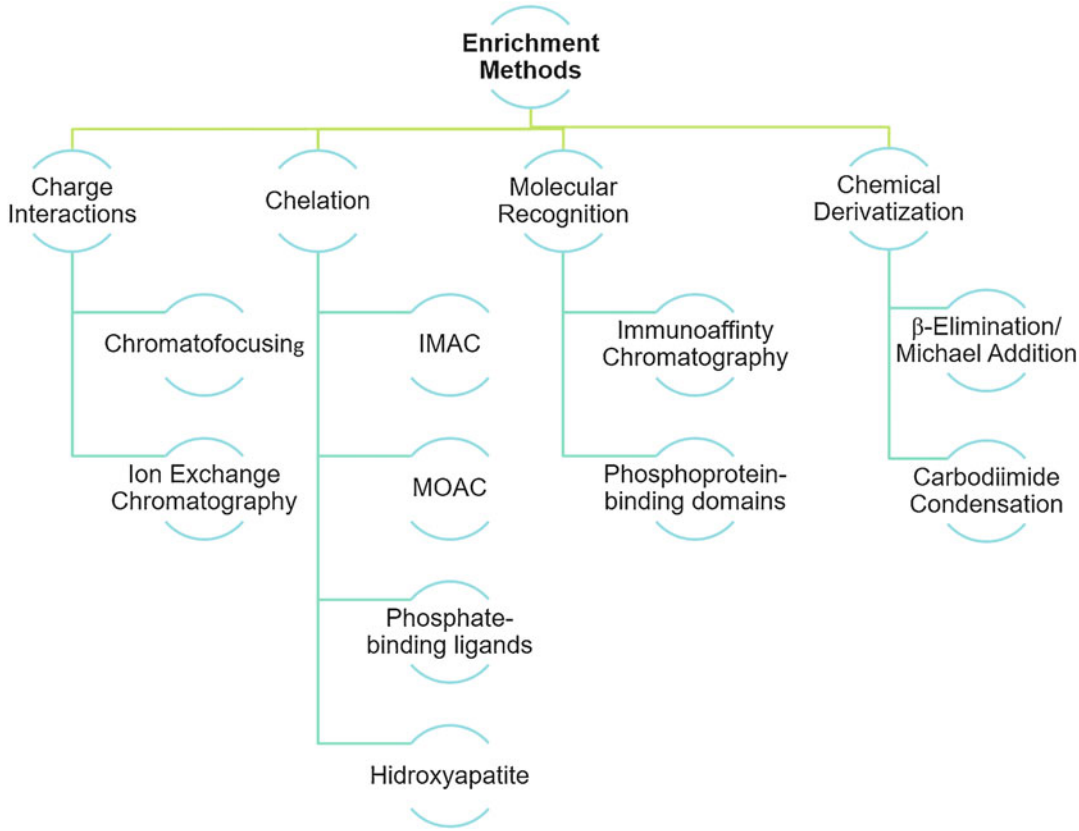

Fig. 3 Phosphoprotein and phosphopeptide enrichment methods. The most common methods are based on charge interactions, chelation, molecular recognition, and chemical derivatization

Both phosphoserine (p-Ser) and phosphothreonine (p-Thr) residues undergo β-elimination of phosphoric acid under strong alkaline conditions, yielding dehydroalanine and β-methyldehydroalanine, respectively [124]. These analogs are susceptible to Michael addition by several nucleophiles, such as amine, alcohol, and thiol groups [125]. Oda et al. replaced phosphate moieties of p-Ser and p-Thr by a biotin affinity tag via a maleimide group, using ethanedithiol (EDT) as a Michael donor and cross-linker. These biotin-labeled peptides were then enriched using avidin chromatography [126]. A similar approach using a phosphoprotein isotope-coded affinity tag (PhIAT) allows the determination and comparative quantification of the phosphorylation sites of proteins, by using either EDT or its deuterated version, and a biotinylation reagent—(+)-biotinyliodoacetamidyl-3,6-dioxaoctanediamine. One of the advantages of the latter method is that it does not use the maleimide group, which undergoes partial hydrolysis [127]. Biotin-avidin chromatography presents some drawbacks associated with the nonspecific binding of samples containing endogenous biotin and biotin-binding proteins and

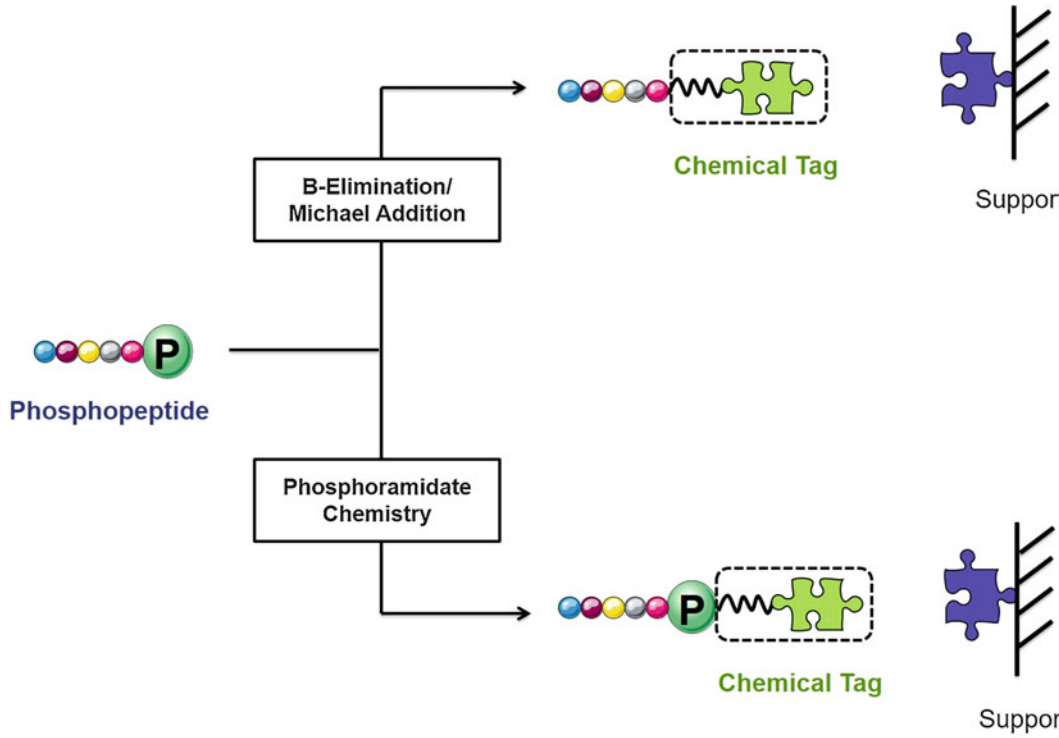

Fig. 4 Phosphopeptide enrichment using chemical tags. B-elimination/Michael addition and phosphoramidate chemistry are the most common chemical derivatization strategies

the harsh conditions used during elution that might induce denaturation of target proteins. The utilization of monomeric avidin, which has a lower affinity toward biotin, allows the employment of milder elution conditions. Yet, a weaker biotin-avidin interaction may lead to an inefficient capture of biotinylated molecules in the presence of strong detergents, which are often used to solubilize hydrophobic molecules, such as membrane proteins [128]. Adamczyk et al. used a pyridyldithiol-activated biotinylation reagent—biotin-HPDP (N-[6-(biotinamido)hexyl]-3′-(2′-pyridyldithio) propionamide), which conjugates via a cleavable disulfide bond, allowing the reversible biotinylation of the phosphopeptides [129]. However, these types of reagents may be unstable under some biological conditions. Van der Veken et al. developed an alternative approach by introducing an acid-labile linker within a biotin-based tag, allowing full recovery of affinity-purified material and elimination of affinity tag prior to MS analysis [130]. Several other tags were developed as alternatives to the biotin-based ones, but still using β-elimination/Michael addition protocols. Biotin-HPDP can be substituted by different pyridyldithiol-activated resins, presenting similar reaction mechanisms. Thiol-activated peptides displace the thiopyridyl group by disulfide exchange,

Table 4
List of chemical tags used in phosphoproteomics and their correspondent solid supports

Chemistry	Chemical tag	Solid support	Elution	Reference
B-elimination/ Michael addition	Ethanedithiol (EDT) coupled to biotin	Avidin resin	Trifluoroacetic acid (TFA)	[126, 127, 130]
			Dithiothreitol (DTT)	[129]
	Engineered biotin tag		Triethylamine (TEA)	[139]
	EDT	Thiol-activated resins	DTT	[131]
	Propanedithiol			[132]
	EDT	PhIST[a]	UV light	[133]
	Cysteamine	PEG-PS resin[b]	TFA	[134]
	Guanidinoethanethiol (GET)	–	–	[135, 136]
	Fluorescent affinity tag (FAT)	Anti-rhodamine antibodies	TFA	[137]
	Engineered His-tag	Ni^{2+}-IMAC	Factor Xa	[138]
Carbodiimide condensation	Cystamine	Glass beads wih iodoacetyl groups	TFA	[141]
	Cystamine	Glass beads wih maleimide groups		[142]
	Dendrimer	–		[143]

[a]PhIST—aminopropyl beads with a photosensitive linker, a stable isotope-coded leucine moiety and a thiolate-reactive group
[b]PEG-PS resin—polyethyleneglycol-polystyrene copolymer base resin with cystamine as the benzyl carbamate

which rearranges to form a thione [131, 132]. Thaler et al. used propanedithiol as a Michael donor, possessing six hydrogen atoms instead of the four of EDT, which when replaced by deuteriums provide a higher difference in mass [132]. Using a similar protocol, McLachlin and Chait observed a problematic side reaction in which 1–2% of the thiol tag was incorporated into nonmodified serine residues, since some of these residues undergo β-elimination of water to form dehydroalanine. This will lead to sample enrichment in both phosphorylated and nonphosphorylated species [131].

A phosphoprotein isotope-coded solid-phase tag (PhIST) was introduced as an improvement of the PhIAT. The biotin tag was replaced by a photosensitive linker covalently bound to aminopropyl glass beads, a leucine isotope-coded linker containing six ^{12}C and one ^{14}N (light) or six ^{13}C and one ^{15}N (heavy), and a thiolate-reactive group. B-elimination, Michael addition, trypic digestion, and solid-phase labelling may be all performed in the same vial. Moreover, the reaction is not affected by the presence of denaturants or detergents, and the beads can be thoroughly washed without the risk of sample losses, leading to high reaction yields. The bound peptides are simply released by UV photocleavage of the photosensitive linker [133].

Knight et al. converted p-Ser and p-Thr residues into lysine analogs, aminoethylcysteine, and β-methylaminoethylcysteine, respectively. As aminoethylcysteine and lysine are isosteres, the modified peptides are then easily cleaved using a LysC endoprotease. They successfully enriched the samples in p-Ser by using a polyethyleneglycol-polystyrene (PEG-PS) resin functionalized with a methoxybenzyl carbamate spacer and cystamine. The methoxybenzyl carbamate linkage is stable under the alkaline conditions used during the β-elimination reaction, but is highly acid-labile, allowing peptide release at acidic pH. This methodology allows direct enzymatic cleavage of the peptides at the site of phosphorylation, which facilitates phosphorylation site mapping [134].

In a different work, p-Ser residues were converted into guanidinoethylcysteine (Gec), by adding a guanidinoethanethiol (GET) tag to β-eliminated peptides. Gec is recognized as a trypsin cleavage site, providing selective enzymatic digestion and thus facilitating the assignment of phosphorylation sites. Also, the basic guanidine moiety of the tag possesses superior proton affinity, increasing peak intensities in MS [135, 136].

In a one-step reaction, a fluorescent affinity tag (FAT) consisting of rhodamine conjugated to a cysteamine moiety selectively modifies p-Ser and p-Thr through a β-elimination/Michael addition strategy. FAT-labeled peptides may then be enriched simply by using commercially available antirhodamine affinity columns [137].

His-tag may also be used to chemically derivatize p-Ser and p-Thr containing peptides. An engineered His-tag possessing six histidines, a specific recognition site of protease Factor Xa (IEGR), a glycine spacer, and a sulfhydryl-containing cysteine residue was used to enrich phosphopeptides by Ni^{2+}-IMAC. The thiol group of the side chain of cysteine functioned as a nucleophile in the Michael addition reaction. His-tag peptides were then cleaved at the C-terminal side of arginine of the recognition sequence [138].

A chemically engineered biotinylated tag, consisting of a biotin group, a base-labile 4-carboxy fluorenyl methoxycarbonyl group and a sulfhydryl moiety, was developed as a refinement of the previously described His-tag. This engineered biotin-tag is smaller and easier to couple and requires mild alkaline conditions instead of the expensive Factor Xa upon release of the peptides [139].

Although β-elimination/Michael addition reactions are very well established and straightforward procedures, there are some drawbacks related to their application in phosphoproteomics. First, tyrosine residues are not able to undergo β-elimination. Second, cysteine residues need to be protected by oxidation or alkylation to prevent side reactions. Third, O-glycosylated residues also undergo β-elimination to form dehydroanalanyl residues, and therefore enzymatic deglycosylation is recommended to reduce nonspecific labeling. Forth, deamidation of asparagine may occur, especially under strong alkaline conditions. Finally, Michael

addition might occur at both Cα and Cβ, leading to the formation of epimers [106, 126].

Combining both IMAC and β-elimination methods minimizes their individual limitations. Phosphopeptides can be captured using an IMAC resin, which discriminates them from O-glycosylated residues, and then directly eluted by β-elimination. Several chemical tags can be reacted with the β-eliminated peptides, making them easily distinguishable from nonmodified peptides that were also bound to the resin [140].

Phosphoramidate chemistry is a standard alternative to β-elimination/Michael addition procedures. Zhou et al. used a series of six chemical reactions, involving two carbodiimide-catalyzed condensations. Phosphate groups of the peptides were derivatized with sulfhydryl groups, and then captured using iodoacetyl groups immobilized on glass beads. This method is highly selective and allows the identification of p-Ser, p-Thr, and p-Tyr residues. However, it presents a low recovery yield of approximately 20% [141].

Using a different approach, phosphate groups can be activated using carbodiimide and imidazole and reacted with cystamine to form phosphoramidate bonds in a single-step, eliminating the need to protect amine groups on the peptides. After the generation of free thiol groups by reduction, the peptides can be captured using maleimide groups immobilized on glass beads [142]. Using the same chemistry and as an alternative to the solid-phase strategies, phosphorylated peptides can be coupled to a soluble synthetic polyamine (dendrimer), allowing for a homogenous reaction [143].

2 Future Perspectives

In this chapter, several affinity tags are described with different properties and a major trend is always exploring tags that can be detected specifically by their ligands — small synthetic affinity ligands, other proteins, or antibodies. In particular, for affinity purification purpose, the price of the matrices, their reusability, or the fact that they ensure reliable purifications will continue to drive future research. To some extent, novel supports that can allow one-use purifications and that are environmentally friendly and sustainable to produce, as well as biodegradable, are currently the focus of many researchers. Furthermore, alternatives to affinity purification are expanding, such as peptides based on elastin sequences that are fused with proteins of interest. Elastin peptides self-assemble in a supramolecular structure, which allows selectively purifying proteins using cycles of temperature and centrifugation [144, 145]. This is an exciting field of research as new methods of purification are required in different fields of biotechnology to decrease costs and also streamline workflows.

In the phosphopeptide enrichment field, research efforts have mainly been focused on the development of novel affinity ligands that recognise phosphorylated sequences, and on the improvement of MS methods and instrumentation to allow more sensitive detection, rather than the chemical modification of phosphate groups with tags. This likely reflects the challenging process of site-specific modification of phosphate groups in the chemically complex and diverse environment of biological samples. Nevertheless, this is an exciting field with possibilities in diagnostics that will certainly impact positively healthcare research.

Acknowledgments

This work was financed by FCT/MEC (UID/Multi/04378/2019) and co-financed by the ERDF under the PT2020 Partnership Agreement (POCI-01-0145-FEDER-007728). The authors thank FCT/MEC for the research fellowship SFRH/BPD/97585/2013 for A.S.P, SFRH/BD/64427/2009 for I.L.B. and A.M.G.C.D. for Junior Research contract under Sea2See project financed by FCT (PTDC/BII-BIO/28878/2017) and co-financed by ERDF under the PT2020 Partnership Agreement (LISBOA-01-0145-FEDER-028878).

References

1. Woodbury C (2006) Recombinant DNA basics. In: Groves M (ed) Pharmaceutical biotechnology. Taylor & Francis Group, Abingdon, pp 31–60
2. Young CL, Britton ZT, Robinson AS (2012) Recombinant protein expression and purification: a comprehensive review of affinity tags and microbial applications. Biotechnol J 7:620–634
3. Demain AL, Vaishnav P (2009) Production of recombinant proteins by microbes and higher organisms. Biotechnol Adv 27:297–306
4. Malhotra A (2009) Tagging for protein expression. In: Richard R, Murray P (eds) Methods in enzymology: guide to protein purification. Academic, Cambridge, MA, pp 239–258
5. Walls D, Loughran S (2011) Tagging recombinant proteins to enhance solubility and aid purification. In: Walls D, Loughran S (eds) Protein chromatography: methods and protocols. Humana, Totowa, NJ, pp 151–175
6. Loughran ST, Walls D (2017) Tagging recombinant proteins to enhance solubility and aid purification. Methods Mol Biol 1485:131–156
7. Kimple ME, Brill AL, Pasker RL (2013) Overview of affinity tags for protein purification. Curr Protoc Protein Sci 9(9):1–23
8. Pina AS, Lowe CR, Roque ACA (2014) Challenges and opportunities in the purification of recombinant tagged proteins. Biotechnol Adv 32:366–381
9. Arnau J, Lauritzen C, Petersen GE, Pedersen J (2006) Current strategies for the use of affinity tags and tag removal for the purification of recombinant proteins. Protein Expr Purif 48:1–13
10. Nilsson J, Ståhl S, Lundeberg J, Uhlén M, Nygren PÅ (1997) Affinity fusion strategies for detection, purification, and immobilization of recombinant proteins. Protein Expr Purif 11:1–16
11. Terpe K (2003) Overview of tag protein fusions: from molecular and biochemical fundamentals to commercial systems. Appl Microbiol Biotechnol 60:523–533
12. Waugh DS (2011) An overview of enzymatic reagents for the removal of affinity tags. Protein Expr Purif 80:283–293
13. Fong BA, Wu W-Y, Wood DW (2010) The potential role of self-cleaving purification tags

in commercial-scale processes. Trends Biotechnol 28:272–279
14. Li Y (2011) Self-cleaving fusion tags for recombinant protein production. Biotechnol Lett 33:869–881
15. Smith DB, Johnson KS (1988) Single-step purification of polypeptides expressed in *Escherichia coli* as fusions with glutathione S-transferase. Gene 67:31–40
16. LaVallie E, Lu Z (2000) Thioredoxin as a fusion partner for production of soluble recombinant proteins in *Escherichia coli*. In: Thorner J, Emr S, Abelson J (eds) Applications of chimeric genes and hybrid proteins: gene expression and protein purification. Elsevier, Amsterdam, pp 322–340
17. Kaplan W et al (1997) Conformational stability of pGEX-expressed Schistosoma japonicum glutathione S-transferase: a detoxification enzyme and fusion-protein affinity tag. Protein Sci 6:399–406
18. Frangioni JV, Neel BG (1993) Solubilization and purification of enzymatically active glutathione S-transferase (pGEX) fusion proteins. Anal Biochem 210:179–187
19. Singh C, Asano K (2007) Localization and characterization of protein-protein interactions sites. In: Jon L (ed) Methods in enzymology: translation initiation: extract systems and molecular genetics. Academic, Cambridge, MA, pp 139–161
20. Nikaido H (1994) Maltose transport system of *Escherichia coli*: an ABC-type transporter. FEBS Lett 346:55–58
21. Kellerman O, Ferenci T (1982) Maltose-binding protein from *Escherichia coli*. In: Wills AW (ed) Methods in enzymology: carbohydrate metabolism – parte E. Academic, Cambridge, MA, pp 459–463
22. di Guana C, Lib P, Riggsa PD, Inouyeb H (1988) Vectors that facilitate the expression and purification of foreign peptides in *Escherichia coli* by fusion to maltose-binding protein. Gene 67:21–30
23. Fox JD, Waugh DS (2003) Maltose-binding protein as a solubility enhancer. In: Vaillancourt P (ed) Methods in molecular biology – *E. coli* gene expression protocols. Humana, Totowa, NJ, pp 99–118. https://doi.org/10.1385/1-59259-301-1:99
24. Kapust RB, Waugh DS (1999) *Escherichia coli* maltose-binding protein is uncommonly effective at promoting the solubility of polypeptides to which it is fused. Protein Sci 8:1668–1674
25. Katti SK, LeMaster DM, Eklund H (1990) Crystal structure of thioredoxin from *Escherichia coli* at 1.68 A resolution. J Mol Biol 212:167–184
26. LaVallie ER et al (1993) A thioredoxin gene fusion expression system that circumvents inclusion body formation in the E coli cytoplasm. Nat Biotechnol 11:187–193
27. Marblestone JG et al (2006) Comparison of SUMO fusion technology with traditional gene fusion systems: enhanced expression and solubility with SUMO. Protein Sci 15:182–189
28. Li SJ, Hochstrasser M (1999) A new protease required for cell-cycle progression in yeast. Nature 398:246–251
29. Panavas T, Sanders C, Butt TR (2009) SUMO fusion technology for enhanced protein production in prokaryotic and eukaryotic expression systems. Methods Mol Biol 497:303–317
30. Malakhov MP et al (2004) SUMO fusions and SUMO-specific protease for efficient expression and purification of proteins. J Struct Funct Genom 5:75–86
31. Gusarov I, Nudler E (2001) Control of intrinsic transcription termination by N and NusA: the basic mechanisms. Cell 107:437–449
32. Liu K, Hanna MM (1995) NusA contacts nascent RNA in *Escherichia coli* transcription complexes. J Mol Biol 247:547–558
33. Cohen SE et al (2010) Roles for the transcription elongation factor NusA in both DNA repair and damage tolerance pathways in *Escherichia coli*. Proc Natl Acad Sci U S A 107:15517–15522
34. Harrison R (2000) Expression of soluble heterologous proteins via fusion with NusA protein. Innovations 11:4–7
35. Davis GD, Elisee C, Newham DM, Harrison RG (1999) New fusion protein systems designed to give soluble expression in *Escherichia coli*. Biotechnol Bioeng 65:382–388
36. Nilsson B, Abrahmsén L (1990) Fusions to staphylococcal protein A. Methods Enzymol 185:144–161
37. Eklund M, Axelsson L, Uhlén M, Nygren P-A (2002) Anti-idiotypic protein domains selected from protein A-based affibody libraries. Proteins 48:454–462
38. Nilsson B, Abrahmsén L, Uhlén M (1985) Immobilization and purification of enzymes with staphylococcal protein A gene fusion vectors. EMBO J 4:1075–1080

39. Nilsson B et al (1987) A synthetic IgG-binding domain based on staphylococcal protein A. Protein Eng 1:107–113
40. Hedhammar M, Alm T, Gräslund T, Hober S (2006) Single-step recovery and solid-phase refolding of inclusion body proteins using a polycationic purification tag. Biotechnol J 1:187–196
41. Hedhammar M, Gräslund T, Uhlén M, Hober S (2004) Negatively charged purification tags for selective anion-exchange recovery. Protein Eng Des Sel PEDS 17:779–786
42. Kanje S et al (2018) Protein engineering allows for mild affinity-based elution of therapeutic antibodies. J Mol Biol 430:3427–3438
43. Fernandes CSM, Pina AS, Dias AMGC, Branco RJF, Roque ACA (2014) A theoretical and experimental approach toward the development of affinity adsorbents for GFP and GFP-fusion proteins purification. J Biotechnol 186:13–20
44. Pina AS et al (2015) Mild and cost-effective green fluorescent protein purification employing small synthetic ligands. J Chromatogr A 1418:83–93
45. Pina AS et al (2016) Tryptophan tags and de novo designed complementary affinity ligands for the expression and purification of recombinant proteins. J Chromatogr A 1472:55–65
46. Fernandes CSM, Pina AS, Batalha ÍL, Roque ACA (2017) Magnetic fishing of recombinant green fluorescent proteins and tagged proteins with designed synthetic ligands. Sep Sci Technol 52:2907–2915
47. Locatelli-Hoops S, Sheen FC, Zoubak L, Gawrisch K, Yeliseev AA (2013) Application of HaloTag technology to expression and purification of cannabinoid receptor CB2. Protein Expr Purif 89:62–72
48. England CG, Luo H, Cai W (2015) HaloTag technology: a versatile platform for biomedical applications. Bioconjug Chem 26:975–986
49. Walkup WG, Kennedy MB (2015) Protein purification using PDZ affinity chromatography. Curr Protoc Protein Sci 80:9.10.1–9.10.37
50. Hussack G et al (2017) A novel affinity tag, ABTAG, and its application to the affinity screening of single-domain antibodies selected by phage display. Front Immunol 8:1406
51. Khairil Anuar INA et al (2019) Spy&Go purification of SpyTag-proteins using pseudo-SpyCatcher to access an oligomerization toolbox. Nat Commun 10:1–13
52. Porath J, Carlsson J, Olsson I, Belfrage G (1975) Metal chelate affinity chromatography, a new approach to protein fractionation. Nature 258:598–599
53. Hochuli E, Döbeli H, Schacher A (1987) New metal chelate adsorbent selective for proteins and peptides containing neighbouring histidine residues. J Chromatogr A 411:177–184
54. Hochuli E, Bannwarth W, Dobeli H, Gentzi R, Stuber D (1988) Genetic approach to facilitate purification of recombinant proteins with a novel metal chelate adsorbent. Nat Biotechnol 6:1321–1325
55. Block H et al (2009) Immobilized-metal affinity chromatography (IMAC): a review. Methods Enzymol 463:439–473
56. Gaberc-Porekar V, Menart V (2001) Perspectives of immobilized-metal affinity chromatography. J Biochem Biophys Methods 49:335–360
57. Gutiérrez R, Martín Del Valle EM, Galán MA (2007) Immobilized metal-ion affinity chromatography: status and trends. Sep Purif Rev 36:71–111
58. Dashivets T, Wood N, Hergersberg C, Buchner J, Haslbeck M (2009) Rapid matrix-assisted refolding of histidine-tagged proteins. Chembiochem 10:869–876
59. Kato K, Sato H, Iwata H (2005) Immobilization of histidine-tagged recombinant proteins onto micropatterned surfaces for cell-based functional assays. Langmuir ACS J Surf Colloids 21:7071–7075
60. Wegner GJ, Lee HJ, Marriott G, Corn RM (2003) Fabrication of histidine-tagged fusion protein arrays for surface plasmon resonance imaging studies of protein-protein and protein-DNA interactions. Anal Chem 75:4740–4746
61. Wilson DS, Nock S (2002) Functional protein microarrays. Curr Opin Chem Biol 6:81–85
62. Mooney JT, Fredericks D, Hearn MTW (2011) Use of phage display methods to identify heptapeptide sequences for use as affinity purification 'tags' with novel chelating ligands in immobilized metal ion affinity chromatography. J Chromatogr A 1218:92–99
63. Sainsbury F, Jutras PV, Vorster J, Goulet M-C, Michaud D (2016) A chimeric affinity tag for efficient expression and chromatographic purification of heterologous proteins from plants. Front Plant Sci 7:1–11
64. Einhauer A, Jungbauer A (2001) The FLAG peptide, a versatile fusion tag for the purification of recombinant proteins. J Biochem Biophys Methods 49:455–465
65. Evan GI, Lewis GK, Ramsay G, Bishop JM (1985) Isolation of monoclonal antibodies

specific for human c-myc proto-oncogene product. Mol Cell Biol 5:3610–3616
66. Chatterjee DK, Esposito D (2006) Enhanced soluble protein expression using two new fusion tags. Protein Expr Purif 46:122–129
67. Studier FW, Moffatt BA (1986) Use of bacteriophage T7 RNA polymerase to direct selective high-level expression of cloned genes. J Mol Biol 189:113–130
68. Burgess RR, Thompson NE (2002) Advances in gentle immunoaffinity chromatography. Curr Opin Biotechnol 13:304–308
69. Hopp TP et al (1988) A short polypeptide marker sequence useful for recombinant protein identification and purification. Nat Biotechnol 6:1204–1210
70. Thompson NE, Arthur TM, Burgess RR (2003) Development of an epitope tag for the gentle purification of proteins by immunoaffinity chromatography: application to epitope-tagged green fluorescent protein. Anal Biochem 323:171–179
71. Edwards AM et al (1990) Purification and lipid-layer crystallization of yeast RNA polymerase II. Proc Natl Acad Sci U S A 87:2122–2126
72. Duellman SJ, Thompson NE, Burgess RR (2004) An epitope tag derived from human transcription factor IIB that reacts with a polyol-responsive monoclonal antibody. Protein Expr Purif 35:147–155
73. Barbas CF III, Burton DR, Scott JK, Silverman GJ (2001) Phage display: a laboratory manual. Cold Spring Harbor Laboratory Press, Cold Spring Harbor, NY
74. Fujii Y et al (2014) PA tag: a versatile protein tagging system using a super high affinity antibody against a dodecapeptide derived from human podoplanin. Protein Expr Purif 95:240–247
75. Fujii Y, Kaneko MK, Kato Y (2016) MAP Tag: a novel tagging system for protein purification and detection. Monoclon Antib Immunodiagn Immunother 35:293–299
76. Tabata S et al (2010) A rapid screening method for cell lines producing singly-tagged recombinant proteins using the 'TARGET tag' system. J Proteome 73:1777–1785
77. Yano T et al (2016) AGIA tag system based on a high affinity rabbit monoclonal antibody against human dopamine receptor D1 for protein analysis. PLoS One 11:1–20
78. Fujii Y et al (2017) Development of RAP tag, a novel tagging system for protein detection and purification. Monoclon Antib Immunodiagn Immunother 36:68–71
79. Takeda H et al (2017) CP5 system, for simple and highly efficient protein purification with a C-terminal designed mini tag. PLoS One 12:1–18
80. Morris J et al (2016) Heparin-binding peptide as a novel affinity tag for purification of recombinant proteins. Protein Expr Purif 126:93–103
81. Jayanthi S, Gundampati RK, Kumar TKS (2017) Simple and efficient purification of recombinant proteins using the heparin-binding affinity tag. Curr Protoc Protein Sci 90:6.16.1–6.16.13
82. Kim JS, Raines RT (1993) Ribonuclease S-peptide as a carrier in fusion proteins. Protein Sci 2:348–356
83. Karpeisky MY, Senchenko VN, Dianova MV, Kanevsky VY (1994) Formation and properties of S-protein complex with S-peptide-containing fusion protein. FEBS Lett 339:209–212
84. Vaillancourt P, Zheng C-F, Hoang DQ, Breister L (2000) Affinity purification of recombinant proteins fused to calmodulin or to calmodulin-binding peptides. In: Thorner J, Emr S, Abelson J (eds) Methods in enzymology. Academic, Cambridge, MA, pp 340–362. https://doi.org/10.1016/S0076-6879(00)26064-3
85. Melkko S, Neri D (2003) Calmodulin as an affinity purification tag. In: Vaillancourt P (ed) *E. coli* gene expression protocols. Humana, Totowa, NJ, pp 69–78. https://doi.org/10.1385/1-59259-301-1:69
86. Stofko-Hahn RE, Carr DW, Scott JD (1992) A single step purification for recombinant proteins. Characterization of a microtubule associated protein (MAP2) fragment which associates with the type II cAMP-dependent protein kinase. FEBS Lett 302:274–278
87. Zheng CF, Simcox T, Xu L, Vaillancourt P (1997) A new expression vector for high level protein production, one step purification and direct isotopic labeling of calmodulin-binding peptide fusion proteins. Gene 186:55–60
88. Neri D, De Lalla C, Petrul H, Neri P, Winter G (1995) Calmodulin as a versatile tag for antibody fragments. Nat Biotechnol 13:373–377
89. Schmidt TG, Skerra A (1993) The random peptide library-assisted engineering of a C-terminal affinity peptide, useful for the detection and purification of a functional Ig Fv fragment. Protein Eng 6:109–122
90. Skerra A, Schmidt TGM (2000) Use of the Strep-tag and streptavidin for detection and purification of recombinant proteins. In: Sdejna JT (ed) Methods in enzymology: applications of chimeric genes and hybrid proteins part a: gene expression and protein

purification. Academic, New York, NY, pp 271–304. https://doi.org/10.1016/S0076-6879(00)26060-6

91. Schmidt TG, Koepke J, Frank R, Skerra A (1996) Molecular interaction between the Strep-tag affinity peptide and its cognate target, streptavidin. J Mol Biol 255:753–766
92. Korndörfer IP, Skerra A (2002) Improved affinity of engineered streptavidin for the Strep-tag II peptide is due to a fixed open conformation of the lid-like loop at the binding site. Protein Sci 11:883–893
93. Voss S, Skerra A (1997) Mutagenesis of a flexible loop in streptavidin leads to higher affinity for the Strep-tag II peptide and improved performance in recombinant protein purification. Protein Eng 10:975–982
94. Schmidt TGM, Skerra A (2007) The Strep-tag system for one-step purification and high-affinity detection or capturing of proteins. Nat Protoc 2:1528–1535
95. Keefe AD, Wilson DS, Seelig B, Szostak JW (2001) One-step purification of recombinant proteins using a nanomolar-affinity streptavidin-binding peptide, the SBP-Tag. Protein Expr Purif 23:440–446
96. Wilson DS, Keefe AD, Szostak JW (2001) The use of mRNA display to select high-affinity protein-binding peptides. Proc Natl Acad Sci U S A 98:3750–3755
97. Pina AS, Pereira AS, Branco RJF, El Khoury G, Lowe CR (2014) A tailor-made "tag–receptor" affinity pair for the purification of fusion proteins. Chembiochem 15:1423–1435
98. Choi SI, Song HW, Moon JW, Seong BL (2001) Recombinant enterokinase light chain with affinity tag: expression from *Saccharomyces cerevisiae* and its utilities in fusion protein technology. Biotechnol Bioeng 75:718–724
99. Dougherty WG, Carrington JC, Cary SM, Parks TD (1988) Biochemical and mutational analysis of a plant virus polyprotein cleavage site. EMBO J 7:1281–1287
100. Jenny RJ, Mann KG, Lundblad RL (2003) A critical review of the methods for cleavage of fusion proteins with thrombin and factor Xa. Protein Expr Purif 31:1–11
101. Chang J-Y (1985) Thrombin specificity: requirement for apolar amino acids adjacent to the thrombin cleavage site of polypeptide substrate. Eur J Biochem 151:217–224
102. Yuan L-D, Hua Z-C (2002) Expression, purification, and characterization of a biologically active bovine enterokinase catalytic subunit in *Escherichia coli*. Protein Expr Purif 25:300–304
103. Goh HC, Sobota RM, Ghadessy FJ, Nirantar S (2017) Going native: complete removal of protein purification affinity tags by simple modification of existing tags and proteases. Protein Expr Purif 129:18–24
104. Tichy A et al (2011) Phosphoproteomics: searching for a needle in a haystack. J Proteome 74:2786–2797
105. Thingholm TE, Jensen ON, Larsen MR (2009) Analytical strategies for phosphoproteomics. Proteomics 9:1451–1468
106. Witze ES, Old WM, Resing KA, Ahn NG (2007) Mapping protein post-translational modifications with mass spectrometry. Nat Methods 4:798–806
107. Jensen ON (2006) Interpreting the protein language using proteomics. Nat Rev Mol Cell Biol 7:391–403
108. Reinders J, Sickmann A (2005) State-of-the-art in phosphoproteomics. Proteomics 5:4052–4061
109. Paradela A, Albar JP (2008) Advances in the analysis of protein phosphorylation. J Proteome Res 7:1809–1818
110. Harsha HC, Pandey A (2010) Phosphoproteomics in cancer. Mol Oncol 4:482–495
111. Højlund K et al (2003) Proteome analysis reveals phosphorylation of ATP synthase beta -subunit in human skeletal muscle and proteins with potential roles in type 2 diabetes. J Biol Chem 278:10436–10442
112. Levitan IB (1994) Modulation of ion channels by protein phosphorylation and dephosphorylation. Annu Rev Physiol 56:193–212
113. Davis MJ et al (2001) Regulation of ion channels by protein tyrosine phosphorylation. Am J Physiol Heart Circ Physiol 281: H1835–H1862
114. Gloeckner CJ et al (2010) Phosphopeptide analysis reveals two discrete clusters of phosphorylation in the N-terminus and the Roc domain of the Parkinson-disease associated protein kinase LRRK2. J Proteome Res 9:1738–1745
115. Hanger DP, Anderton BH, Noble W (2009) Tau phosphorylation: the therapeutic challenge for neurodegenerative disease. Trends Mol Med 15:112–119
116. Schwarz E, Bahn S (2008) Biomarker discovery in psychiatric disorders. Electrophoresis 29:2884–2890
117. Mann M et al (2002) Analysis of protein phosphorylation using mass spectrometry: deciphering the phosphoproteome. Trends Biotechnol 20:261–268
118. Batalha I, Zhou H, Lilley K, Lowe C (2016) Mimicking nature: phosphopeptide

enrichment using combinatorial libraries of affinity ligands. J Chromatogr A 1457:76–87

119. Batalha IL, Lychko I, Branco RJF, Iranzo O, Roque AC (2019) A β-Hairpins as peptidomimetics of human phosphoprotein-binding domains. Org Biomol Chem 17:3996–4004
120. Schmidt SR, Andersson ME, Schweikart F, Andersson ME (2007) Current methods for phosphoprotein isolation and enrichment Split Inteins technology development View project single-use and disposables in bioprocessing View project current methods for phosphoprotein isolation and enrichment. J Chromatogr B 849:154–162
121. Batalha IL, Lowe CR, Roque ACA (2012) Platforms for enrichment of phosphorylated proteins and peptides in proteomics. Trends Biotechnol 30:100–110
122. Batalha I, Roque A (2016) Phosphopeptide enrichment using various magnetic nanocomposites: an overview. In: von Stechow L (ed) Phospho-proteomics. Methods in molecular biology, vol 1355. Springer, New York, NY, pp 193–209
123. Arrington JV, Hsu CC, Elder SG, Andy Tao W (2017) Recent advances in phosphoproteomics and application to neurological diseases. Analyst 142:4373–4387
124. Byford MF (1991) Rapid and selective modification of phosphoserine residues catalysed by Ba2+ ions for their detection during peptide microsequencing. Biochem J 280 (Pt 1):261–265
125. Meyer HE, Hoffmann-Posorske E, Korte H, Heilmeyer LM (1986) Sequence analysis of phosphoserine-containing peptides. Modification for picomolar sensitivity. FEBS Lett 204:61–66
126. Oda Y, Nagasu T, Chait BT (2001) Enrichment analysis of phosphorylated proteins as a tool for probing the phosphoproteome. Nat Biotechnol 19:379–382
127. Goshe MB et al (2001) Phosphoprotein isotope-coded affinity tag approach for isolating and quantitating phosphopeptides in proteome-wide analyses. Anal Chem 73:2578–2586
128. Rybak J-N, Scheurer SB, Neri D, Elia G (2004) Purification of biotinylated proteins on streptavidin resin: a protocol for quantitative elution. Proteomics 4:2296–2299
129. Adamczyk M, Gebler JC, Wu J (2001) Selective analysis of phosphopeptides within a protein mixture by chemical modification, reversible biotinylation and mass spectrometry. Rapid Commun Mass Spectrom 15:1481–1488
130. van der Veken P et al (2005) Development of a novel chemical probe for the selective enrichment of phosphorylated serine- and threonine-containing peptides. Chembiochem 6:2271–2280
131. McLachlin DT, Chait BT (2003) Improved beta-elimination-based affinity purification strategy for enrichment of phosphopeptides. Anal Chem 75:6826–6836
132. Thaler F et al (2003) A new approach to phosphoserine and phosphothreonine analysis in peptides and proteins: chemical modification, enrichment via solid-phase reversible binding, and analysis by mass spectrometry. Anal Bioanal Chem 376:366–373
133. Qian WJ et al (2003) Phosphoprotein isotope-coded solid-phase tag approach for enrichment and quantitative analysis of phosphopeptides from complex mixtures. Anal Chem 75:5441–5450
134. Knight ZA et al (2003) Phosphospecific proteolysis for mapping sites of protein phosphorylation. Nat Biotechnol 21:1047–1054
135. Ahn YH, Ji ES, Lee JY, Cho K, Yoo JS (2007) Coupling of TiO(2)-mediated enrichment and on-bead guanidinoethanethiol labeling for effective phosphopeptide analysis by matrix-assisted laser desorption/ionization mass spectrometry. Rapid Commun Mass Spectrom 21:3987–3994
136. Ahn YH et al (2007) Protein phosphorylation analysis by site-specific arginine-mimic labeling in gel electrophoresis and matrix-assisted laser desorption/ionization time-of-flight mass spectrometry. Anal Biochem 370:77–86
137. Stevens SM et al (2005) Enhancement of phosphoprotein analysis using a fluorescent affinity tag and mass spectrometry. Rapid Commun Mass Spectrom 19:2157–2162
138. Jalili PR, Sharma D, Ball HL (2007) Enhancement of ionization efficiency and selective enrichment of phosphorylated peptides from complex protein mixtures using a reversible poly-histidine tag. J Am Soc Mass Spectrom 18:1007–1017
139. Jalili PR, Ball HL (2008) Novel reversible biotinylated probe for the selective enrichment of phosphorylated peptides from complex mixtures. J Am Soc Mass Spectrom 19:741–750
140. Thompson AJ et al (2003) Characterization of protein phosphorylation by mass spectrometry using immobilized metal ion affinity chromatography with on-resin beta-elimination and Michael addition. Anal Chem 75:3232–3243

141. Zhou H, Watts JD, Aebersold R (2001) A systematic approach to the analysis of protein phosphorylation. Nat Biotechnol 19:375–378
142. Bodenmiller B et al (2007) An integrated chemical, mass spectrometric and computational strategy for (quantitative) phosphoproteomics: application to *Drosophila melanogaster* Kc167 cells. Mol BioSyst 3:275–286
143. Tao WA et al (2005) Quantitative phosphoproteome analysis using a dendrimer conjugation chemistry and tandem mass spectrometry. Nat Methods 2:591–598
144. Hu F et al (2010) Expression and purification of an antimicrobial peptide by fusion with elastin-like polypeptides in *Escherichia coli*. Appl Biochem Biotechnol 160:2377–2387
145. Yeboah A, Cohen RI, Rabolli C, Yarmush ML, Berthiaume F (2016) Elastin-like polypeptides: a strategic fusion partner for biologics. Biotechnol Bioeng 113:1617–1627
146. Ullmann A (1984) One-step purification of hybrid proteins which have beta-galactosidase activity. Gene 29:27–31
147. Dykes CW et al (1988) Expression of atrial natriuretic factor as a cleavable fusion protein with chloramphenicol acetyltransferase in *Escherichia coli*. Eur J Biochem 174:411–416
148. Sjölander A et al (1997) The serum albumin-binding region of streptococcal protein G: a bacterial fusion partner with carrier-related properties. J Immunol Methods 201:115–123
149. Anba J et al (1987) Expression vector promoting the synthesis and export of the human growth-hormone-releasing factor in *Escherichia coli*. Gene 53:219–226
150. Tomme P et al (1998) Characterization and affinity applications of cellulose-binding domains. J Chromatogr B Biomed Sci Appl 715:283–296
151. Luojing C, Ford C, Nikolov Z (1991) Adsorption to starch of a β-galactosidase fusion protein containing the starch-binding region of *Aspergillus glucoamylase*. Gene 99:121–126
152. Ong E et al (1989) The cellulose-binding domains of cellulases: tools for biotechnology. Trends Biotechnol 7:239–243
153. Thorn KS, Naber N, Matuska M, Vale RD, Cooke R (2000) A novel method of affinity-purifying proteins using a bis-arsenical fluorescein. Protein Sci 9:213–217
154. Chaga G, Bochkariov DE, Jokhadze GG, Hopp J, Nelson P (1999) Natural polyhistidine affinity tag for purification of recombinant proteins on cobalt(II)-carboxymethylaspartate crosslinked agarose. J Chromatogr A 864:247–256
155. Sassenfeld HM, Brewer SJ (1984) A polypeptide fusion designed por the purification of recombinant proteins. Nat Biotechnol 2:76–81
156. Stubenrauch K, Bachmann A, Rudolph R, Lilie H (2000) Purification of a viral coat protein by an engineered polyionic sequence. J Chromatogr B Biomed Sci Appl 737:77–84
157. Zhao JY, Ford CF, Glatz CE, Rougvie MA, Gendel SM (1990) Polyelectrolyte precipitation of beta-galactosidase fusions containing poly-aspartic acid tails. J Biotechnol 14:273–283
158. Dalboge H, Dahl HHM, Pedersen J, Hansen JW, Christensen T (1987) A novel enzymatic method for production of authentic hgh from an escherichia coll produced hGH-precursor. Nat Biotechnol 5:161–164
159. Persson M, Bergstrand MG, Bülow L, Mosbach K (1988) Enzyme purification by genetically attached polycysteine and polyphenylalanine affinity tails. Anal Biochem 172:330–337
160. Schatz PJ (1993) Use of peptide libraries to map the substrate specificity of a peptide-modifying enzyme: a 13 residue consensus peptide specifies biotinylation in *Escherichia coli*. Nat Biotechnol 11:1138–1143
161. Lamla T, Stiege W, Erdmann VA (2002) An improved protein bioreactor: efficient product isolation during in vitro protein biosynthesis via affinity tag. Mol Cell Proteomics 1:466–471
162. Smith JC et al (1984) Chemical synthesis and cloning of a poly(arginine)-coding gene fragment designed to aid polypeptide purification. Gene 32:321–327
163. Goeddel DV et al (1979) Expression in Escherichia coli of chemically synthesized genes for human insulin. Proc Natl Acad Sci U S A 76:106–110
164. Moks T et al (1987) Expression of human insulin-like growth factor I in bacteria: use of optimized gene fusion vectors to facilitate protein purification. Biochemistry 26:5239–5244
165. Huston JS et al (1988) Protein engineering of antibody binding sites: recovery of specific activity in an anti-digoxin single-chain Fv analogue produced in *Escherichia coli*. Proc Natl Acad Sci U S A 85:5879–5883

Chapter 11

Synthetic Ligand Affinity Chromatography Purification of Human Serum Albumin and Related Fusion Proteins

Sharon Williams, Phil Morton, and Dev Baines

Abstract

Synthetic ligand affinity adsorbents offer an efficient means for purification of biopharmaceuticals. Single-isomer textile dye C.I. Reactive Blue and newer ligands developed by rational design and screening of chemical combinatorial libraries based on a triazine scaffold are routinely used for the capture and purification of these proteins from engineered recombinant expression systems. Here, we describe methods for the purification of recombinant human serum albumin and related fusion proteins using synthetic ligand affinity adsorbents.

Key words Human serum albumin, Albumin fusion proteins, Affinity chromatography, Synthetic affinity adsorbents

1 Introduction

Human serum albumin isolated by the traditional cold ethanol plasma protein fractionation process is by far the largest volume of a therapeutic protein produced, and annual consumption is estimated to be around 200–400 kg per million population [1, 2]. Alternative purification methods based on gel filtration and subsequent ion-exchange chromatography were developed in the 1980s for the purification of albumin from plasma [3–5].

The use of immobilized Cibacron Blue F3G-A, a sulfonated triazine dye for isolation and purification of albumin from serum, is one of the earliest examples of the use of synthetic ligands in affinity chromatography [6, 7]. Dye affinity chromatography for protein purification is widely used since the immobilized reactive dyes bind to a wide variety of proteins in a selective and reversible manner [8–10]. Although it has been reported that the dye binds to the bilirubin binding site on human serum albumin (HSA) [11], the fact that the bound albumin can be eluted using fatty acids suggests that there are likely to be overlaps with the fatty acid biding site.

Nikolaos E. Labrou (ed.), *Protein Downstream Processing: Design, Development, and Application of High and Low-Resolution Methods*, Methods in Molecular Biology, vol. 2178, https://doi.org/10.1007/978-1-0716-0775-6_11,

Original textile dyes were produced as bulk chemicals for the textile industry, and it was noted that they contain different isomers of the main product and many impurities. Consequently, they did not meet the rigorous requirements for the purification of biopharmaceuticals [12]. Synthesis of a single isomer of C.I. Reactive Blue 2 led to the development of well-defined synthetic ligand adsorbents for purification of proteins [13, 14].

The use of synthetic, single-isomer analogue adsorbents of the blue textile dye for the capture and purification of albumin is being driven by the growing interest in the expression and production of recombinant albumin. Albumin is the most abundant protein in plasma and functions as a carrier protein with a long circulatory half-life. This makes albumin an ideal carrier for therapeutic peptides and proteins, either in the form of an albumin fusion protein or by encapsulation in albumin nanoparticles or microencapsulated vesicles.

Albumin fusion protein technology is becoming an important tool for the delivery of therapeutic peptides and proteins. Albumin is genetically fused with the therapeutic partner resulting in a contiguous protein that has an extended circulatory half-life while retaining therapeutic activity [18, 19].

There are a number of therapeutic molecules that have been fused to albumin, including cytokines such as interferon [20] and interleukin-2 [21], growth factor and insulin [22], and smaller bioactive peptide hormones such as glucagon-like peptide-1 [23].

The application of rational design and combinatorial chemistry has enabled the development of next-generation affinity ligands based on a central triazine scaffold [15–17], which are ideally suited to the purification of albumin fusion proteins. Such an adsorbent is AlbuPure® (*see* **Note 1**). This is a colorless, synthetic ligand affinity adsorbent that was designed to specifically target the albumin portion of an albumin fusion protein.

Procedures are described here for the capture and high-level purification of human serum albumin from plasma/serum and recombinant-derived or chemical conjugates of human serum albumin proteins using synthetic ligand affinity adsorbents (*see* **Note 2**).

2 Materials

All buffers and solutions should be freshly prepared from analytical-grade reagents and filtered through a 0.45 μm filter before use. All buffers and solutions should be prepared at room temperature (unless otherwise indicated) and prepared using reverse osmosis water.

2.1 Bromocresol Purple Assay Components

1. Stock solutions of 15% v/v acetic acid (15 mL of glacial acetic acid added to 85 mL of water) and 40 mM bromocresol purple (BCP; 21.6 g BCP made up to 1 L with water; sulfone form; Sigma Aldrich) can be prepared and stored until required (*see* **Note 3**).
2. BCP working reagent is prepared by dissolving 8.2 g of sodium acetate (final concentration 100 mM; *see* **Note 4**) in 800 mL of water. 10.0 mL of 15% acetic acid, 1.0 mL 30% of Brij-35 (v/v; 0.3 mL Brij-35 added to 0.7 mL of water; Sigma Aldrich), and 3.0 mL of BCP stock solution are added together and mixed using a vortex mixer. The pH of the solution is adjusted to pH 5.2 using glacial acetic acid or 1 M NaOH and the volume is adjusted to 1.0 L.

2.2 Mimetic Blue® SA HL P6HL Chromatography Components: Purification of Human Serum Albumin from Plasma (See Note 5)

1. Chromatography workstation.
2. C10 (1 cm i.d. and up to 40 cm bed height) and XK columns (1.6, 2.6, and 5 cm i.d. and up to 100 cm bed height; GE Healthcare).
3. 0.45 μm cellulose acetate syringe filter (Fisher Scientific).
4. 0.1 M NaCl solution (*see* **Note 6**).
5. 50 mM sodium phosphate buffer, pH 6.0 (*see* **Note 7**).
6. 25 mM sodium phosphate buffer, 150 mM NaCl with 30 mM sodium caprylate, pH 6.0 (*see* **Note 8**).
7. 2 M NaCl (*see* **Note 9**).
8. 0.5 M NaOH (*see* **Note 10**).
9. 20% ethanol/80% 0.1 M NaCl (*see* **Note 11**).

2.3 Mimetic Blue® SA HL P6HL Chromatography Components: Purification of Albumin Fusion Protein

1. Automated chromatography workstation.
2. C10 (1 cm i.d. and up to 40 cm bed height) and XK columns (1.6, 2.6, and 5 cm i.d. and up to 100 cm bed height; GE Healthcare).
3. 0.45 μm cellulose acetate syringe filter (Fisher Scientific).
4. 50 mM sodium phosphate buffer, 25 mM NaCl, pH 7.0 (*see* **Note 12**).
5. 50 mM sodium phosphate buffer, 25 mM NaCl, 30 mM sodium caprylate, pH 7.0 (*see* **Note 13**).
6. 0.5 M NaOH (*see* **Note 10**).
7. 20% ethanol/80% 0.1 M NaCl (*see* **Note 11**).

2.4 AlbuPure® Chromatography Components

1. Automated chromatography workstation.
2. C10 (1 cm i.d. and up to 40 cm bed height) and XK columns (1.6, 2.6, and 5 cm i.d. and up to 100 cm bed height; GE Healthcare).
3. 0.45 μm cellulose acetate syringe filter (Fisher Scientific).

4. 0.1 M NaCl solution (*see* **Note 6**).
5. 50 mM sodium citrate buffer, pH 5.4 (*see* **Note 14**).
6. 50 mM sodium phosphate buffer, pH 6.0 (*see* **Note 7**).
7. 50 mM sodium phosphate buffer, pH 7.0 (*see* **Note 15**).
8. 50 mM ammonium acetate buffer, pH 8.0 (*see* **Note 16**).
9. 50 mM sodium carbonate buffer, pH 10 (*see* **Note 17**).
10. 0.5 M NaOH (*see* **Note 10**).
11. 20% ethanol/80% 0.1 M NaCl (*see* **Note 11**).

3 Methods

Availability of a specific assay for albumin or albumin-related proteins such as an ELISA is useful for determining the concentration and purity of the target protein during the purification. In the absence of a specific assay, alternative general assays and SDS-polyacrylamide gel electrophoresis (SDS-PAGE) may be used to analyze column fractions.

3.1 General Assay Human for Serum Albumin Determination

Bromocresol purple (BCP) provides a simple and direct procedure for measuring human serum albumin in biological samples derived either from human plasma or from recombinant sources without any pretreatment of the sample [24]. The assay can be used either in a high-throughput 96-well plate format or in a cuvette format.

3.1.1 96-Well Plate BCP Assay for Human Serum Albumin

1. Prepare a standard curve of HSA in the range of 0–1 mg/mL. Suggested concentration range is 0, 0.063, 0.125, 0.25, 0.5, and 1.0 mg/mL, diluting the stock HSA with the same buffer present in the test sample.
2. Add 150 μL of calibration standards and sample solutions to microplate wells, in duplicate or triplicate.
3. Add 200 μL of BCP using a multichannel pipette and mix it thoroughly.
4. Measure the absorbance at 600 nm.
5. Plot the concentration of HSA standards against the corresponding absorbance.
6. Determine the concentration of the unknown sample from the calibration plot (linear) and correct for any dilution factors.

3.1.2 Cuvette BCP Assay for Human Serum Albumin

1. Prepare a standard curve of HSA in the range of 0–3 mg/mL. A suggested concentration range is 0, 0.5, 1.0, 1.5, 2.0, 2.5, and 3.0 mg/mL, diluting the stock HSA with the same buffer present in the test sample after neutralization. If concentrations >2.5 mg/mL are expected, dilute samples in the same buffer as the calibrants. For added confidence in the results, samples may be assayed at more than one dilution.

2. Add 100 μL of calibration standards and sample solutions to 1.5 mL polystyrene cuvette.
3. Add 1 mL of BCP to the cuvette and mix it thoroughly.
4. Measure the absorbance at 603 nm using BCP reagent blank in the reference cell.
5. Plot the concentration of HSA standards against the corresponding absorbance.
6. Determine the concentration of the unknown sample from the calibration plot and correct for any dilution factors.

3.2 Purification of Human Serum Albumin Using Mimetic Blue® SA HL P6XL

3.2.1 Preparation of Plasma Load

1. Rapidly thaw human plasma at 37 °C in a recirculating water bath.
2. Filter the plasma through a 0.45 μm filter.

3.2.2 Column Packing (for Laboratory-Scale Axial Flow Columns)

1. Decant off the shipping preservative and prepare a 50% slurry of the adsorbent in 0.1 M NaCl solution (*see* **Note 18**). Before commencing the column pack, consult the relevant manufacturer's instructions for the selected column (*see* **Notes 19**, **20**, and **28**).
2. Assemble the column and remove air from the dead spaces by flushing the end piece and adaptor with packing solution and then close the column outlet.
3. Allow all materials to equilibrate to the temperature at which the chromatography process is to be performed.
4. Pour the 50% adsorbent slurry into the column in a single continuous step. Pouring the adsorbent down the side of the column helps to prevent air becoming trapped within the adsorbent bed.
5. Ensure the top adaptor is free from air by pumping the packing solution through it and then attach to the top of the column. Open the column outlet and apply the desired flow to the bed. Ideally, the adsorbent should be packed at a constant pressure not exceeding 3 bar (45 psi).
6. Once the bed has settled, close the column outlet and stop the liquid flow through the bed.
7. If a space between the top adaptor and the adsorbent bed has been created during packing, drop the top adaptor down to the top of the bed so that the adsorbent surface is in contact with the adaptor. Do not push the top adaptor into the adsorbent bed.

8. Open the column outlet and apply flow to the column again. If a space is formed between the top of the bed and the adaptor, repeat the step above. If no space forms, the column is packed and ready to use.

3.2.3 Sample Loading

1. Equilibrate the packed column with 50 mM sodium phosphate buffer, pH 6.0 (equilibration buffer), for 5 column volumes (CV) or until the conductivity and pH are steady (*see* **Note 21**).
2. Apply the prepared plasma (*see* Subheading 3.2.1) at a suitable flow rate to achieve a residence time of 6 min (e.g., for a 15 cm bed height column with a 1 cm internal diameter, the linear flow rate will be 150 cm/h).
3. Collect the flow-through from the column outlet either in 0.5 CV fractions or as a single-process fraction. If 0.5 CV fractions are collected, a breakthrough profile of the target protein can be determined by plotting the target protein concentration versus the volume of feed loaded onto the column.
4. After the plasma has been loaded, remove the non-bound and loosely bound protein by washing with the equilibration buffer for 5 CV or until the measured UV absorption is either zero or has achieved a steady baseline.

3.2.4 Elution

1. The bound albumin can be eluted with a specific elution condition such as sodium caprylate (25–100 mM), which displaces the ligand by interacting with the binding site on the albumin molecule. The albumin can also be eluted nonspecifically with up to 2 M sodium chloride, which is often more effective when combined with an increase in pH to 8.0 or above.
2. It is recommended that the bound albumin is eluted with 2–4 CV of 25 mM sodium phosphate buffer, 150 mM NaCl with 30 mM sodium caprylate at pH 6.0.
3. The absorbance peak from the eluted protein is collected until a steady baseline is achieved and then stored at 4 °C until analyzed.

3.2.5 Clean in Place and Sanitization

1. Removal of any residual absorbed material, including microorganisms, viruses, and endotoxin, can be achieved by washing the column with sodium hydroxide (NaOH).
2. The adsorbent is cleaned by washing with 5 CV of 0.5 M NaOH at a flow rate of $\leq$100 cm/h.
3. A contact time of 1 h will normally be sufficient to ensure destruction of viable organisms, but for endotoxin, inactivation requires contact time of up to 5 h with 0.5 M NaOH.

4. Once the column has been cleaned, re-equilibrate the column with at least 5 CV of equilibration buffer until the pH and conductivity of the column eluate are equal to that of the equilibration buffer.
5. To store the column, equilibrate the column with 20% ethanol/80% 0.1 M NaCl (v/v) and store at 2–30 °C.

3.3 Purification of Albumin Fusion Proteins Using Mimetic Blue® SA HL P6XL

1. Cell culture supernatant containing albumin fusion protein was supplied and was filtered using a 0.45 μm filter before application to the packed adsorbent.

3.3.1 Preparation of Load

3.3.2 Column Packing

1. As described in Subheading. 3.2.2.

3.3.3 Sample Loading

1. Equilibrate the packed column with 50 mM sodium phosphate buffer, 25 mM NaCl, pH 7.0 (equilibration buffer), for 5 column volumes (CV) or until the conductivity and pH are steady (*see* **Note 22**).
2. Apply the prepared cell culture supernatant containing the albumin fusion protein (*see* Subheading 3.3.1) at a suitable flow rate to achieve a residence time of 6 min (e.g., for a 15 cm column with a 1 cm internal diameter, the linear flow rate will be 150 cm/h).
3. Collect the flow-through from the column outlet either in 0.5 CV fractions or as a single-process fraction.
4. After the cell culture supernatant has been loaded, remove the non-bound and loosely bound protein by washing with the equilibration buffer for 5 CV or until the measured UV absorption is either zero or has achieved a steady baseline.

3.3.4 Elution

1. The bound albumin fusion protein is eluted with 2–4 CV of 50 mM sodium phosphate buffer, 25 mM NaCl with 30 mM sodium caprylate at pH 7.0.
2. The absorbance peak from the eluted protein is collected until a steady baseline is achieved and then stored at 4 °C until analyzed.

3.3.5 Clean in Place and Sanitization

1. As described in Subheading 3.2.5.

3.4 Purification of Albumin Fusion Proteins Using AlbuPure®

1. The albumin fusion protein was produced using the Albufuse® technology developed by Albumedix (previously, Novozymes Biopharma) and consists of a yeast cell culture supernatant containing an expressed albumin fusion protein.

3.4.1 Preparation of Cell Culture Supernatant Load

3.4.2 Column Packing (for Laboratory-Scale Axial Flow Columns)

1. There is no requirement to remove the 20% ethanol/80% 0.1 M NaCl (v/v) preservative solution prior to packing.
2. Before commencing the column pack, consult the relevant manufacturer's instructions for the selected column (*see* **Notes 23** and **24**).
3. Degassing of the adsorbent slurry before packing is recommended (*see* **Note 25**).
4. Assemble the column and remove the air from the dead spaces by flushing the end piece and adaptor with 0.1 M NaCl (packing solution) and then close the column outlet.
5. Allow all materials to equilibrate to the temperature at which the chromatography process is to be performed.
6. Pour the 50% adsorbent slurry into the column in a single continuous step. Pouring the adsorbent down the side of the column helps to prevent air becoming trapped within the adsorbent bed.
7. Attach the (open) top adaptor to the top of the column and adjust the adaptor to ~1 cm above the bed, tighten the adaptor, and attach to the work station. Open the column outlet and apply the desired flow to the bed. The recommended packing condition to obtain a uniform pack is at a constant pressure of 1.5 bar (22 psi).
8. Once the bed has settled, close the column outlet and stop the liquid flow through the bed.
9. If a space between the top adaptor and the adsorbent bed has been created during packing, drop the top adaptor down to the top of the bed so that the adsorbent is in contact with the adaptor. Do not push the top adaptor into the adsorbent bed.
9. Open the column outlet and apply flow to the column again. If a space is formed between the top of the bed and the adaptor, repeat the step above. If no space forms, the column is packed and ready to use.

3.4.3 Sample Loading

1. Equilibrate the packed column with 2–5 CV of 50 mM sodium citrate buffer, pH 5.4.
2. Apply the cell culture supernatant, pH adjusted to match the pH of the equilibration buffer (*see* **Note 26**) at a suitable flow rate to achieve a residence time of 3 min.

3. Collect the flow-through from the column outlet either in 0.5 CV fractions or as a single-process fraction.
4. After the cell culture supernatant has been loaded, remove the non-bound and loosely bound protein by washing with the equilibration buffer for 5 CV or until the measured UV absorption is either zero or has achieved a steady baseline (*see* **Note 27**).

3.4.4 Intermediate Wash Steps

1. Nonspecifically bound protein can be removed using a series of buffers with increasing pH steps.
2. Wash 1—Apply 3–5 CV of 50 mM sodium phosphate, pH 6.0, to the column.
3. Wash 2—Apply 3–5 CV of 50 mM sodium phosphate, pH 7.0, to the column.
4. Wash 3—Apply 3–5 CV of 50 mM ammonium acetate, pH 8.0, to the column.

3.4.5 Elution

1. The bound albumin fusion protein can be removed using 50 mM ammonium acetate buffer, 10 mM sodium caprylate, pH 8.0. Up to 100 mM sodium caprylate can be used to achieve complete elution of the albumin fusion protein.
2. An alternative elution buffer is 50 mM sodium carbonate buffer, pH 10.0.

3.4.6 Clean in Place

1. As described in Subheading 3.2.5.

3.5 Analysis of Results

1. The automated chromatography system uses a UV detector with a wavelength of 280 nm to monitor the protein during the chromatographic separation. Figure 1 shows a typical chromatogram for the capture and recovery of albumin using affinity chromatography.
2. The albumin concentration of each of the process fractions is determined by BCP, and SDS-PAGE analysis is used both for determining the purity of the elution fraction and for identifying the presence or absence of the target protein in each of the process fractions. Figure 2 shows the SDS-PAGE of process fractions for a typical albumin purification from human plasma, and Fig. 3 shows a chromatogram for the purification of albumin fusion protein using AlbuPure®. Figure 4 shows the SDS-PAGE of process samples for an albumin fusion protein purification using AlbuPure®.

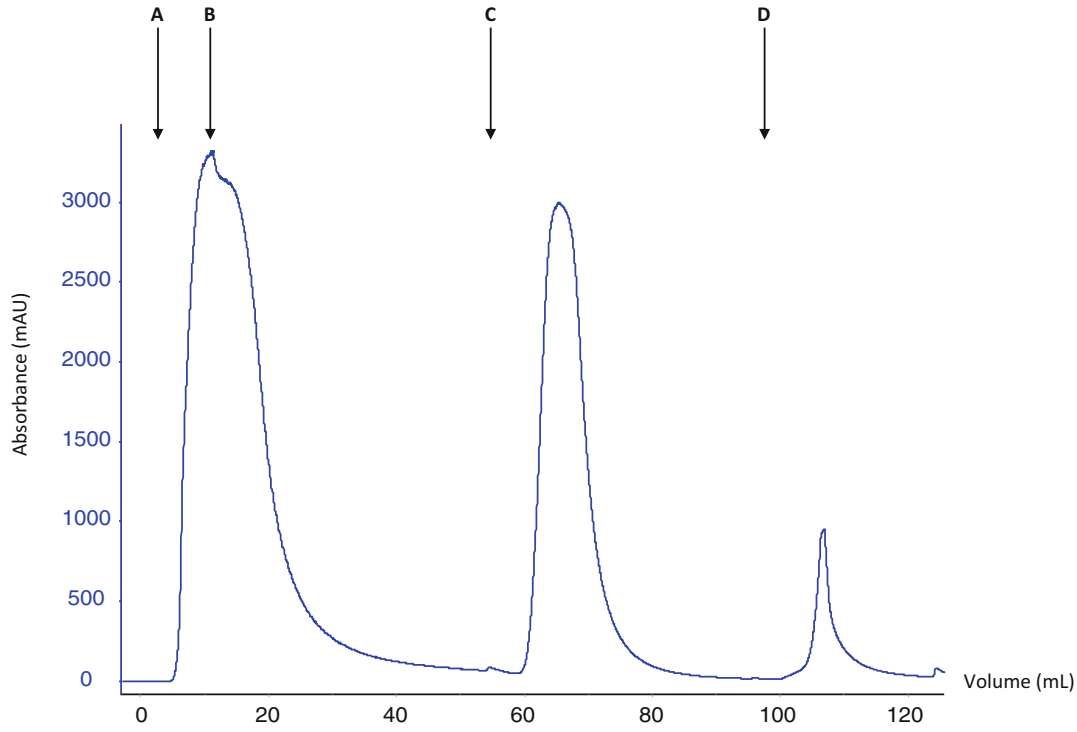

Fig. 1 Purification of human serum albumin from plasma using Mimetic Blue® SA HL P6XL. Column: 1 cm i.d. × 15 cm bed height (12 mL column volume). Process solutions: (A) 7 mL filtered human plasma buffered to pH 7.5; (B) 50 mM sodium phosphate buffer, 150 mM NaCl, pH 7.5; (C) 25 mM sodium phosphate buffer, 150 mM NaCl, 30 mM sodium caprylate, pH 6.0; (D) 0.5 M NaOH

4 Notes

1. AlbuPure® is a selective affinity chromatography adsorbent developed by ProMetic BioSciences Ltd. (PBL) in collaboration with Novozymes Biopharma UK Ltd. for the purification of albumin fusion proteins.
2. Synthetic adsorbents are stable in the pH range 3.0–13.0 in column chromatography operations. For clean in place, washing the column with 0.5 M NaOH (the standard industry practice) is the recommended procedure, although concentrations up to 1.0 M NaOH can be used for heavily fouled columns. Storage of the adsorbents for prolonged periods at extremes of pH is not advised (particularly storage at low pH) due to possible degradation of the base matrix. Consequently, after the CIP step, the columns should be flushed with water or an appropriate buffer to reduce the effluent pH to near-neutral pH before transferring the column into 20% ethanol/80% 0.1 M NaCl as an antibacterial preservative.

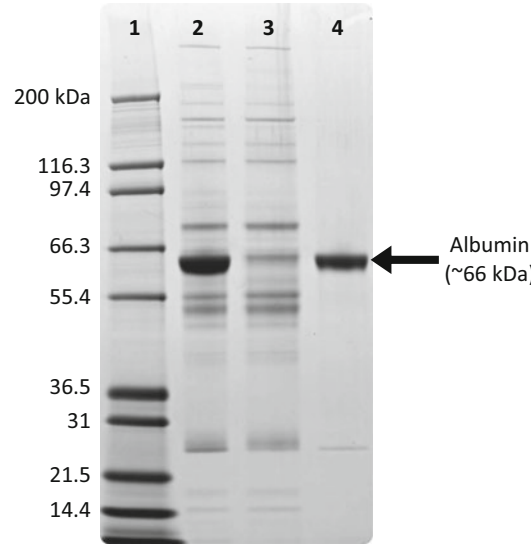

Fig. 2 Reduced SDS-PAGE of the chromatography fractions for the capture and purification of human serum albumin from human plasma using Mimetic Blue® SA HL P6XL; *Lane 1*: molecular weight marker; *Lane 2:* load; *Lane 3:* flow-through; *Lane 4*: elution

3. BCP stock solution should be used at ambient room temperature.
4. The sodium acetate concentration should be 100 mM, and so adjust the weight of sodium acetate added if using a hydrate form of the chemical.
5. Commercial immobilized Cibacron Blue F3G-A adsorbents are available from a number of suppliers including Bio-Rad (Affi-Gel®), Pall Life Sciences (Blue Trisacryl® M Resin), and GE Healthcare (Blue Sepharose® 6B CL). However, the origin, purity, and isomeric composition of the textile dyes used in the construction of these materials are obscure since Cibacron Blue F3G-A has not been produced by the original manufacturer for many years. A range of Mimetic Blue® adsorbents with single-isomer ligands and the synthetic ligand adsorbent AlbuPure® specifically developed for the purification of albumin and albumin fusion proteins are now available. It is important to carry out small scouting experiments to determine whether these adsorbents provide the required binding capacity and purity of the product before carrying out preparative purification.
6. 0.1 M NaCl solution; 5.84 g of NaCl made up to 1 L in water.
7. 50 mM sodium phosphate buffer, pH 6.0; 6.84 g of sodium dihydrogen phosphate (dihydrate) and 1.09 g of disodium hydrogen phosphate (dihydrate) made up to 1 L with water.

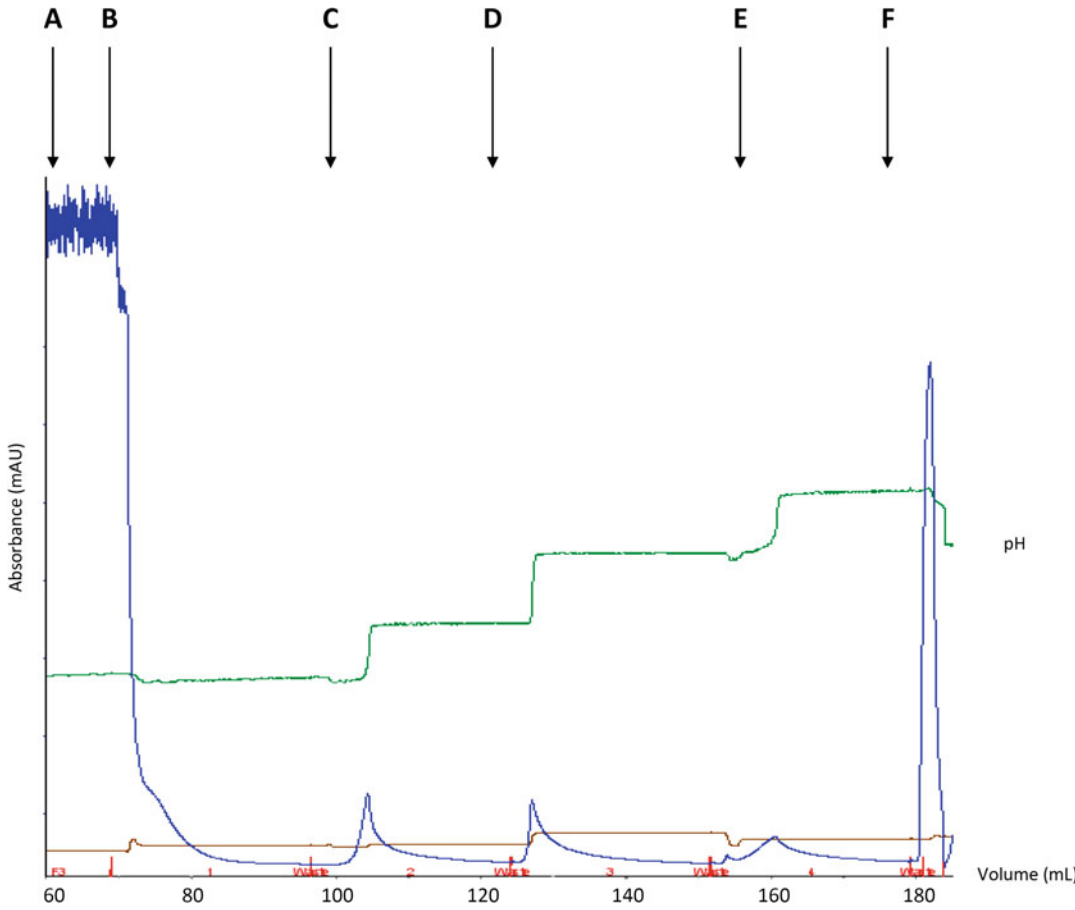

Fig. 3 Purification of albumin fusion protein from cell culture supernatant using AlbuPure®. Column: 1.6 cm i.d. × 11 cm bed height (22 mL column volume). Process solutions: (A) cell culture supernatant load containing albumin fusion protein (up to 20 mg/mL of adsorbent); (B) 50 mM sodium acetate buffer, pH 5.3; (C) 50 mM sodium phosphate buffer, pH 6.0; (D) 50 mM sodium phosphate buffer, pH 7.0; (E) 50 mM ammonium acetate buffer, pH 8.0; (F) 50 mM ammonium acetate, 10 mM sodium caprylate, pH 8.0

8. 25 mM sodium phosphate buffer, 150 mM NaCl with 30 mM sodium caprylate; 6.84 g of sodium dihydrogen phosphate (dihydrate), 1.09 g of disodium hydrogen phosphate (dehydrate), and 8.77 g NaCl with 4.99 g sodium caprylate made up to 1 L with water.
9. 2 M NaCl; 116.9 g of NaCl made up to 1 L with water.
10. 0.5 M NaOH; add 50 mL of 10 M NaOH to 950 mL of water.
11. 20% ethanol/80% 0.1 M NaCl; 5.84 g of NaCl with 200 mL absolute ethanol made up to 1 L with water.
12. 50 mM sodium phosphate buffer, 25 mM NaCl, pH 7.0; 3.04 g of sodium dihydrogen phosphate (dihydrate), 5.43 g of disodium hydrogen phosphate (dihydrate) with 1.46 g of NaCl made up to 1 L with water.

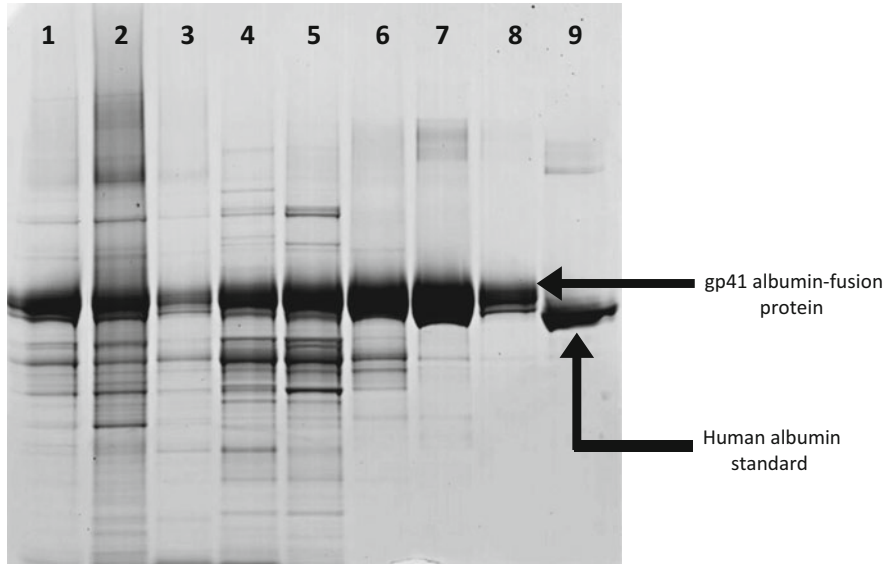

Fig. 4 Nonreduced SDS-PAGE of the process fractions for the capture and recovery of albumin fusion protein from cell culture supernatant using AlbuPure®; *Lane 1*: load (sample diluted); *Lane 2*: flow-through (no sample dilution); *Lane 3*: post load wash (no sample dilution); *Lane 4*: 50 mM sodium phosphate buffer, pH 6.0 wash (no sample dilution); *Lane 5*: 50 mM sodium phosphate buffer, pH 7.0 wash (no sample dilution); *Lane 6*: 50 mM ammonium acetate buffer, pH 8.0 wash (no sample dilution); *Lane 7*: elution (sample diluted); *Lane 8*: elution fraction with a ten-fold dilution cf. to *lane 7*; *Lane 9*: Human albumin standard (1 μg)

13. 50 mM sodium phosphate buffer, 25 mM NaCl, 30 mM sodium caprylate, pH 7.0; 3.04 g of sodium dihydrogen phosphate (dihydrate), 5.43 g of disodium hydrogen phosphate (dihydrate), and 4.99 g of sodium caprylate with 1.46 g of NaCl made up to 1 L with water.
14. 50 mM sodium citrate buffer, pH 5.4; 2.68 g citric acid (monohydrate) and 7.83 g of trisodium citrate (dihydrate) made up to 1 L with water.
15. 50 mM sodium phosphate buffer, pH 7.0; 3.04 g of sodium dihydrogen phosphate (dihydrate) with 5.43 g of disodium hydrogen phosphate (dihydrate) l made up to 1 L with water.
16. 50 mM ammonium acetate buffer, pH 8.0; 3.85 g of ammonium acetate made up to 1 L with water and pH adjusted with glacial acetic acid to pH 8.0.
17. 50 mM sodium carbonate buffer, pH 10; 4.2 g of sodium hydrogen carbonate and pH adjusted with 1 M NaOH to pH 10, then made up to 1 L with water.
18. It is important that column packing is carried out using solutions or buffers containing 0.1 M NaCl to provide counterions for the charged groups present on synthetic ligand.

19. The recommended maximum operational flow rate for Mimetic Blue® SA HL P6XL is up to 500 cm/h (<3 cm diameter columns) and up to 200 cm/h (>5 cm diameter columns).
20. Mimetic Blue® SA HL P6XL should be packed at a constant pressure not exceeding 3 bar.
21. The binding capacity of the adsorbent is dependent on pH and conductivity. The adsorbent binds albumin across a broad pH range (pH 5.0–8.0). The maximum binding capacity is achieved by loading the plasma at pH 6.0 and the maximum purity is achieved by loading the plasma at pH 8.0.
22. The binding capacity of the adsorbent is dependent on pH. The adsorbent binds albumin fusion proteins across a broad pH range (pH 4.5–8.0). Between pH 4.5 and pH 5.5, a 50 mM sodium citrate buffer is recommended and between pH 6.0 and 8.0, 50 mM sodium phosphate buffer. Higher binding capacities will be achieved using a lower pH equilibration buffer and load.
23. The recommended maximum operational flow rate for AlbuPure® is up to 500 cm/h.
24. AlbuPure® should be packed at a constant pressure of 1.5 bar.
25. Dissolved gases in buffers and solutions that are used to slurry the adsorbent may come out of solution (termed degassing) during the column packing. This can cause air bubbles to become trapped within the column bed affecting the integrity of the packed column. To degas, place the adsorbent slurry into a Büchner flask and attach a hose to the side arm. Attach the hose to a vacuum and place a rubber stopper on the top of the flask and turn on the vacuum. During the degassing process, bubbles will rise out of the slurry. Agitate the slurry until no further bubbles are seen. The slurry will now be degassed.
26. If the pH of the feedstream is different to the pH of the equilibration buffer, the feed can be adjusted using either 1.0 M NaOH or 1.0 M HCl. Take care and mix well when adding acid or alkali to avoid creating microenvironments where the pH is very high or very low, which can cause protein denaturation and precipitation.
27. The binding capacity of a given albumin-related protein will be dependent on the nature of the protein as well as the feedstock. Consequently, it is important to determine the dynamic binding capacity by frontal analysis. In frontal analysis, the column is loaded continuously until the target protein appears in the outlet of the column. Typically, the columns are loaded to 10% breakthrough.

28. For scaling up the purification, it is important to maintain the ratio of column volume to sample load and the column residence time; scale-up is carried by maintaining a constant bed height and increasing the column diameter.

Acknowledgments

Bastiaan Lobbezoo and Steve Burton for valuable discussions.
Prometic Bioseparations Ltd. is a trademark of Prometic Bioseparations Ltd. Mimetic Blue® is registered with the US Patent and Trademark Office. AlbuPure® and Albufuse® are registered trademarks of Albumedix Ltd. AlbuPure® is sold under license for the use in the purification of albumin fusion proteins with no warranty of merchantability or fitness for a particular purpose.

References

1. Cohn EJ, Strong LE, Hughes WL Jr et al (1946) Preparation and properties of serum and plasma proteins. IV. A system for the separation into fractions of the protein and lipoprotein components of biological tissues and fluids. J Am Chem Soc 68:459–475
2. Burnouf T (2000) Plasma protein technologies; what next? Transfus Today 14:11–13
3. Bergloff JH, Eriksson S, Suomela H et al (1983) Albumin from human plasma, preparation and *in vitro* properties. In: Curling JM (ed) Separation of plasma proteins. Pharmacia, Uppsala, pp 51–58
4. Curling JM (1980) Albumin purification by ion-exchange chromatography. In: Curling JM (ed) Methods in plasma fractionation. Academic Press, London, pp 77–92
5. Stoltz JF, Rivat C, Gescheir C et al (1991) Chromatographic purification of human albumin for clinical use. Pharm Tech Int 3:60–65
6. Travis J, Bowen J, Tewkesbury D et al (1976) Isolation of albumin from human plasma and fractionation of albumin-depleted plasma. Biochem J 157:301–306
7. Ghoggeri GM, Candidiano G, Delfino G et al (1985) Highly selective one-step chromatography of serum and urinary albumin on immobilized Cibacron Blue F3G-A: studies on normal and glycosylated albumin. Clin Chem Acta 145:205–211
8. Subramanian S (1984) Dye-ligand affinity chromatography; the interaction of Cibacron Blue F3GA with proteins and enzymes. CRC Crit Rev Biochem 16(2):169–205
9. Burton SJ (1992) Dye-ligand affinity chromatography. Methods Mol Biol 11:91–103
10. Dean PD, Watson DH (1979) Protein purification using immobilised triazine dyes. J Chromatogr 165(3):301–319
11. Leatherbarrow RJ, Dean PD (1980) Studies on the mechanism serum albumins binding to immobilized Cibacron Blue F3G A. Biochem J 189:27–34
12. Metcalf EC, Crow B, Dean PD (1981) The effect of ligand pre-saturation on the interaction of serum albumins with immobilized Cibacron Blue 3G-A studied by affinity gel electrophoresis. Biochem J 199:465–472
13. Hanggi D, Carr P (1985) Analytical evaluation of the purity of commercial preparations of Cibacron Blue F3GA and related dyes. Anal Biochem 149(1):91–104
14. Burton SJ, McLoughlin SB, Stead CV et al (1988) Design and applications of biomimetic anthraquinone dyes. I. Synthesis and characterization of terminal ring isomers of C.I. Reactive Blue 2. J Chromatogr A 435:127–137
15. Scoble J, Scopes R (1996) Well Defined dye adsorbents for protein purification. J Mol Recognit 9:728–732
16. Lowe CR (2001) Combinatorial approaches to affinity chromatography. Curr Opin Chem Biol 5(3):248–256
17. Curling J (2004) Affinity chromatography – from textile dyes to synthetic ligands by design. BioPharm Int 17(7):34–42

18. Subramanian GM, Fiscella M, Lamouse-Smith A et al (2007) Albinterferon alpha-2b: a genetic fusion protein for the treatment of chronic hepatitis C. Nat Biotechnol 25:1411–1419
19. Sheffield WP, Eltringham-Smith LJ (2011) Incorporation of albumin fusion proteins into fibrin clots *in vitro* and *in vivo*: comparison of difference fusion motifs recognized by factor XIIIa. BMC Biotechnol 11:127
20. Melder RJ, Osborn BL, Riccobone T et al (2004) Pharmacokinetics and in vitro and in vivo anti-tumor response of an interleukin-2-human serum albumin fusion protein in mice. Cancer Immunol Immunother 54 (6):535–547
21. Osborn BL, Sekut L, Corcoran M et al (2002) Albutropin: a growth hormone-albumin fusion with improved pharmacokinetics and pharmacodynamics in rats and monkeys. Eur J Pharmacol 456:149–148
22. Duttaroy A, Kanakaraj P, Osborn BL et al (2005) Development of a long-acting insulin analog using albumin fusion technology. Diabetes 54:251–258
23. Gao Z, Bai G, Chen J et al (2009) Development, characterization, and evaluation of a fusion protein of a novel glucagon-like peptide-1 (GLP-1) analog and human serum albumin in *Pichia pastoris*. Biosci Biotechnol Biochem 73(3):688–694
24. Parviainen MT, Harmoinen A, Jokela H (1985) Serum albumin assay with bromocresol purple dye. Scand J Clin Lab Invest 45:561–564

Chapter 12

Z_{basic}: A Purification Tag for Selective Ion-Exchange Recovery

My Hedhammar, Johan Nilvebrant, and Sophia Hober

Abstract

A positively charged protein domain, denoted Z_{basic}, can be used as a general purification tag for purification of recombinantly produced target proteins by cation-exchange chromatography. The Z_{basic} domain is constructed from the Protein A-derived Z-domain, and engineered to be highly charged, which allows selective capture on a cation exchanger at physiological pH values. Moreover, Z_{basic} is selective also under denaturing conditions and can be used for purification of proteins solubilized from inclusion bodies. Z_{basic} can then be used as a flexible linker to the cation-exchanger resin, and thereby allows solid-phase refolding of the target protein.

Herein, protocols for purification of soluble Z_{basic}-tagged fusion proteins, as well as for integrated purification and solid-phase refolding of insoluble fusion proteins, are described. In addition, a procedure for enzymatic tag removal and recovery of native target protein is outlined.

Key words Ion-exchange chromatography, Protein A, Fusion tag, Z_{basic}, Solid-phase refolding, Proteolytic cleavage

1 Introduction

As a result of the rapid development of recombinant DNA technology and proteomics, there is a need for effective and general strategies for protein purification. A key challenge is to increase the selectivity to reduce the number of unit operations required to obtain a highly pure target protein. Ion exchange chromatography (IEXC) is, for many reasons, a widely used protein purification technique; the resins are common, relatively cheap, tolerate harsh conditions used for sanitization, and can withstand repeated cycles [1, 2]. IEXC also offers high-resolution separation and high capacity. For protein purification, cation exchange is generally more suitable than anion exchange since nucleic acids, endotoxins, and

My Hedhammar and Johan Nilvebrant contributed equally to this work.

Nikolaos E. Labrou (ed.), *Protein Downstream Processing: Design, Development, and Application of High and Low-Resolution Methods*, Methods in Molecular Biology, vol. 2178, https://doi.org/10.1007/978-1-0716-0775-6_12,

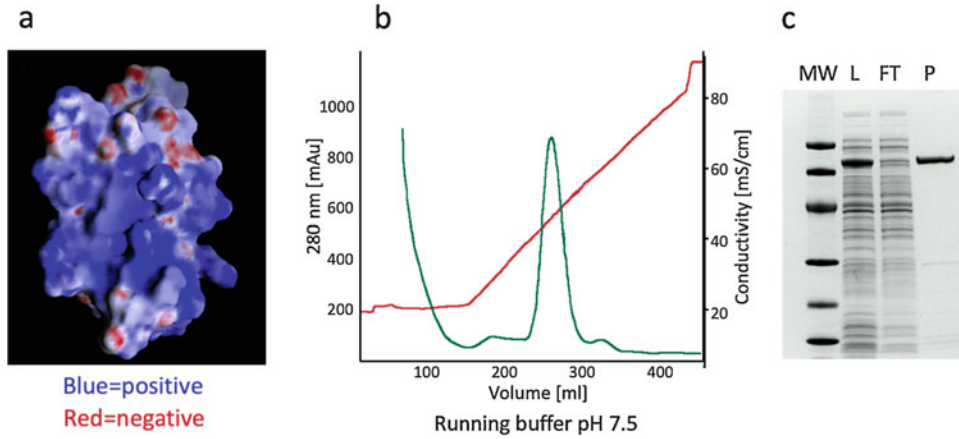

Fig. 1 Z_{basic} – a positively charged purification tag for selective capture on a cation exchanger. (**a**) Model of the electrostatic potential of Z_{basic} at pH 7. (**b**) Representative chromatogram from a purification of a Z_{basic} fusion protein at pH 7.5. Red = salt gradient, green = A_{280}. (**c**) Representative SDS-PAGE analysis of the purification of a Z_{basic} fusion protein. *L* loaded sample, *FT* collected flow-through, *E* eluted target protein

cell surfaces carry negative charge [3, 4]. However, time-consuming and protein-specific optimization is normally required to find suitable conditions for purification of each target protein [5].

To provide a general gene fusion system for selective ion-exchange recovery, a positively charged purification handle (Z_{basic}) was designed to have unique adsorption characteristics for capture on a cation exchange resin at conditions when most host-cell proteins do not bind. Z_{basic} was constructed from a 58 amino acid (7 kDa) Z-domain derived from one of the domains of Staphylococcal protein A [6]. This scaffold is stable, highly soluble, and devoid of cysteines [6]. Through protein engineering, ten arginine residues were introduced at surface-exposed positions to provide a basic domain with very high local concentration of positive charges [7] (Fig. 1a). The calculated isoelectric point (p*I*) of Z_{basic} (10.5) is much higher than for the majority of bacterial host proteins, which have neutral or low p*I* [8]. This property allows selective capture of tagged proteins on a cationic resin followed by elution by increased salt concentration (Fig. 1b, c) or low pH.

Z_{basic} has been shown to work as a general purification handle under both native [9] and denaturing conditions [10] and the whole procedure can be performed at a neutral pH. This method facilitates high-throughput purification of proteins solubilized from inclusion bodies. For refolding of denatured proteins, spatial separation is required to prevent aggregation. This can be achieved by reversible binding and refolding on a solid support or by dilution techniques. The Z_{basic} tag provides an integrated strategy for purification and solid-phase refolding on a column with cationic ion exchange resin [10] (Fig. 2). The fusion protein is captured on the

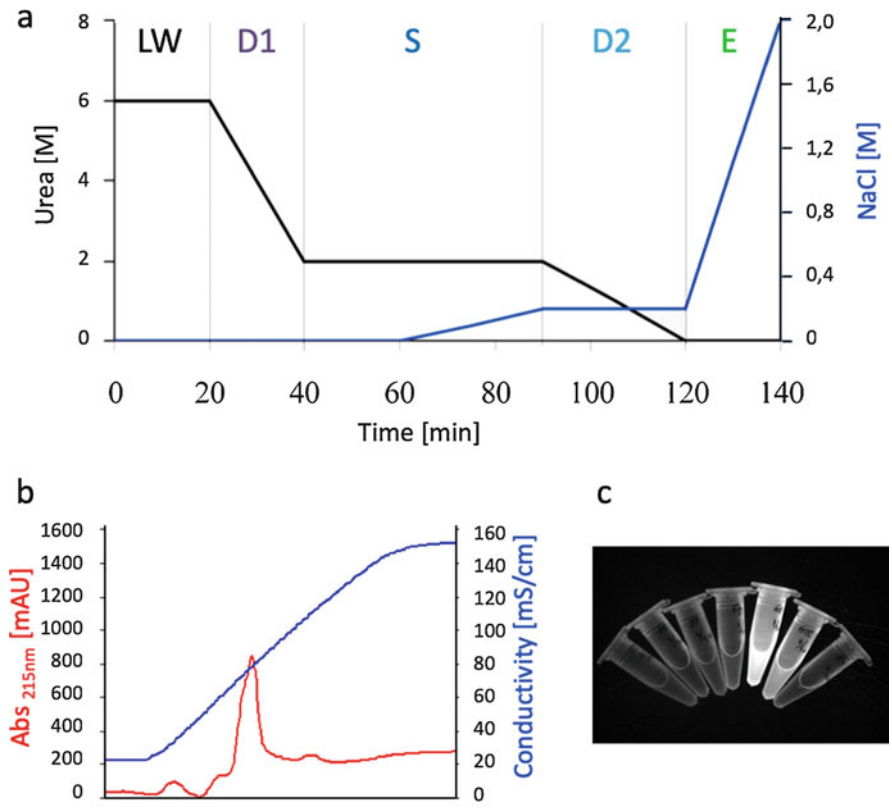

Fig. 2 Schematic description of the program used for solid-phase refolding of a Z_{basic} tagged protein. (**a**) The fusion protein is dissolved in urea and selectively loaded on a cation exchanger (LW). Nonbound proteins are washed away before the urea concentration is gradually decreased to 2 M (D1). Then the conductivity is increased using 200 mM NaCl (S) before the remaining urea is removed (D2). The renatured fusion protein can be eluted (E) using a salt gradient. (**b**) Elution profile of Z_{basic} GFP. (**c**) Successful renaturation is confirmed by the UV-transilluminated GFP

matrix to allow refolding, e.g., by gradual removal of denaturant from the running buffer prior to elution (Fig. 2b). The Z_{basic} tag has also been used for oriented immobilization of enzymes [11–14].

Systems have also been devised for subsequent proteolytic removal of the Z_{basic} tag. The viral protease 3C, which specifically cleaves a heptapeptide motif introduced between the tag and the target protein, allows recovery of concentrated native target in a suitable buffer [15]. To efficiently remove the protease and cleaved-off tag, the use of a protease expressed and purified with the same tag facilitates capture in an additional IEXC step [15] (Fig. 3). Alternatively, the Z_{basic} tag can be used in combination with a self-cleavable intein [16].

The Z_{basic} tag has been used both N- and C-terminally of the target protein, for both intracellular and periplasmic expression [9, 10]. Due to the high local concentration of positive charge on the surface of Z_{basic}, efficient capture can be achieved even at pH

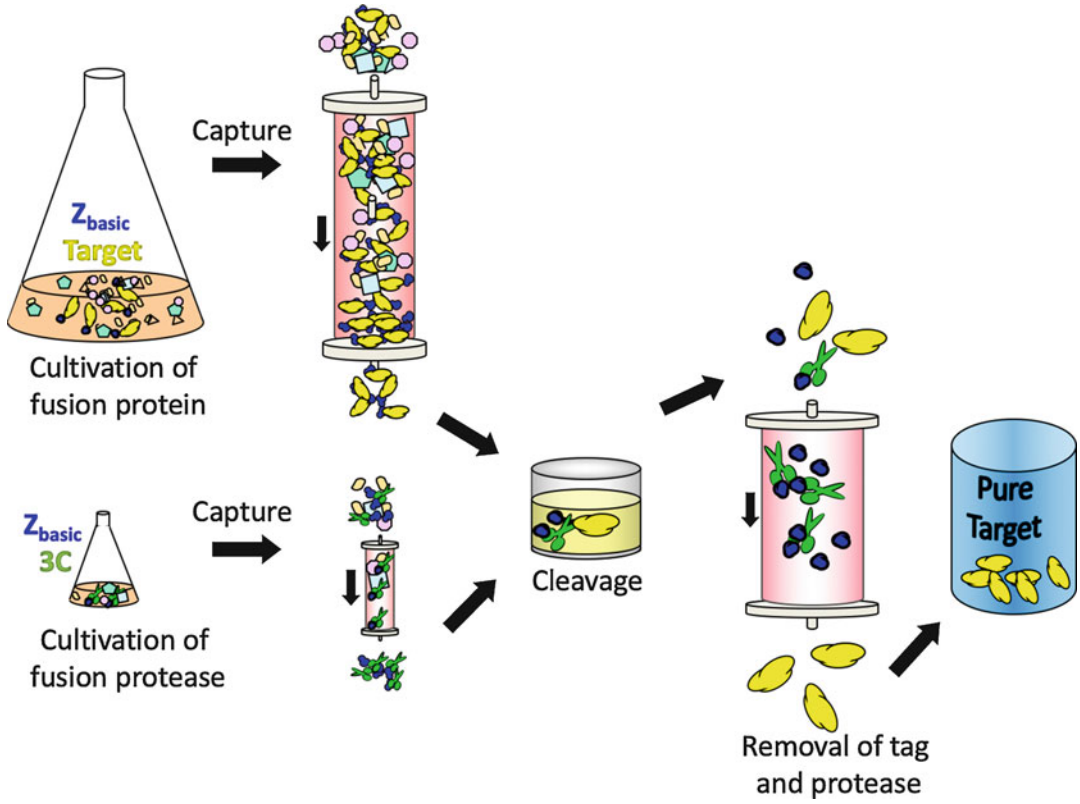

Fig. 3 Strategy for an integrated production and purification procedure of Z_{basic}-tagged fusion proteins. Both the target protein and a site-specific protease are produced in fusion with Z_{basic} and can thus be selectively captured using a cation exchanger. The Z_{basic} tag is proteolytically removed from the target protein using Z_{basic}3C. Both the released tag and the protease can next be captured in a second cation exchange step, which allows collection of pure target protein in the flow-through fraction

values higher than the pI of the fusion protein [9]. This system offers a competitive alternative to the widely used His_6-tag under both native and denaturing conditions and yields purity comparable to affinity chromatography in a single step. The main advantages are that all steps can be carried out in a general fashion at neutral pH on an inexpensive and robust resin. As compared to immobilized metal ion affinity chromatography (IMAC) resins, risk of metal leakage, unwanted reactions catalyzed by metal ions, and limitations related to the usage of reducing agents can be avoided [17].

2 Materials

Prepare all buffers using deionized water and degas buffers to avoid air bubbles on the columns. All buffers are insensitive to light and can be stored at 4 °C.

2.1 Buffers for Purification of Soluble Protein (Denoted with a Subscript s)

1. Buffer A_s (loading): 50 mM sodium phosphate, pH 7.5.
2. Buffer B (elution): 50 mM sodium phosphate, 1 M NaCl, pH 7.5.

2.2 Buffers for Purification of Insoluble Protein (Denoted with a Subscript i)

All buffers containing urea should be freshly prepared, and they can be stored at 4 °C prior to use.

1. Buffer A_i1 (dissolving): 50 mM sodium phosphate, 8 M urea, pH 7.5.
2. Buffer A_i2 (loading): 50 mM sodium phosphate, 6 M urea, pH 7.5.
3. Buffer B1 (refolding): 50 mM sodium phosphate, pH 7.5.
4. Buffer B2 (elution): 50 mM sodium phosphate, 1 M NaCl, pH 7.5.

2.3 Chromatography Media and System

Different cation-exchange media and purification systems can be used, from small gravity or HiTrap columns to large-scale columns for purification in expanded bed adsorption (EBA) format. Below is stated what is used in the following protocol:

1. 1 mL HiTrap S HP column (GE Healthcare).
2. ÄKTA explorer system (GE Healthcare). Typical flow rates of 1 mL/min.

2.4 Proteolytic Cleavage

1. Protease 3C fused to Z_{basic}, purified as described under Subheading 3.3.
2. β-Mercaptoethanol.

3 Methods

See Table 1 and **Notes 1** and **2** for comments on the construction of an expression vector and protein expression.

3.1 Purification of Soluble Z_{basic} Fusion Proteins

Use the following protocol if your target protein is found in the soluble fraction when expressed as a Z_{basic} fusion protein (*see* **Note 3**). The protocol is based on a 100 mL shake flask cultivation (*see* **Note 4**).

1. Resuspend the cell pellet in 30 mL Buffer A_s.
2. Disrupt the cells by sonication in an ice bath (*see* **Note 5**).
3. Remove insoluble material by centrifugation at 10,000 × *g* for 10 min at 4 °C (*see* **Note 6**). If inclusion bodies have been formed, save the pellet for purification from the insoluble fraction (*see* Subheading 3.4).

Table 1
Nucleotide- and amino acid-sequence of Z_{basic}, including an N-terminal leader sequence used to enhance the production

```
ATGAAAGCAATTTTCGTACTGAATGCGCAACACGATGAAGCCGTAGACAACAAA
  TTCAACAAAGAACGTCGCCGTGCTCGCCGTGAAATCCGTCACTTACCTAACTTAAACCG
  TGAACAACGCCGTGCTTTCATTCGTTCCCTGCGTGATGACCCAAGCCAAAGCGCTAACTTGC
  TAGCAGAAGCTAAAAAGCTAAATGATGCTCAGGCGCCGAAA

M K A I F V L N A Q H D E A V D N K F N K E R R R A R R E I R H L P N L N R E Q R R A F I R S L R D D P
  S Q S A N L L A E A K K L N D A Q A P K
```

4. Filtrate the protein sample through a 0.45 μm filter (Acrodisc® 32 mm Syringe Filter, Pall Corporation, Port Washington, NY, USA).
5. Load the clarified lysate to a 1 mL HiTrap S column previously equilibrated with 5 CV of Buffer A_s (*see* **Note 7**).
6. Wash away unbound material using 10 CV of Buffer A_s.
7. Wash away weakly bound material using 10 CV of Buffer A_s with 120 mM NaCl (12% Buffer B).
8. Elute the fusion protein using a linear gradient from 120 mM to 1 M NaCl (12–100% Buffer B), typically during 15 CV (*see* **Note 8**).
9. Collect 1 mL fractions and monitor A_{280} during elution.
10. Measure protein concentration on selected fractions using A_{280} and check the purity using sodium dodecyl sulfate-polyacrylamide gel electrophoresis (SDS-PAGE). A representative chromatogram and SDS-PAGE results are shown in Fig. 1b, c.

3.2 Purification and Solid-Phase Refolding of Insoluble Z_{basic} Fusion Proteins

Use the following protocol if your target protein is found in the insoluble fraction when expressed as a Z_{basic} fusion protein. The protocol is based on a 100 mL shake flask cultivation. The program used for solid-phase refolding is schematically described in Fig. 2.

1. Dissolve the insoluble pellet (from Subheading 3.3, **step 3**) in 30 mL Buffer A_i1 (with 8 M urea) (*see* **Note 9**).
2. Remove undissolved material by centrifugation at 10,000 × *g* for 10 min at 4 °C, followed by filtration through a 0.45 μm filter.
3. Load the dissolved protein sample to a 1 mL HiTrap S column previously equilibrated with 5 CV of Buffer A_i2 (with 6 M urea).
4. Wash away unbound material using 10 CV of Buffer A_i2 (with 6 M urea).

5. Decrease the urea concentration from 6 to 2 M using a linear gradient over 20 min (100–33% Buffer A_i2 to B1).
6. Increase the conductivity from 0 to 200 mM NaCl using a linear gradient over 30 min (while keeping the pH and the urea concentration constant, *see* **Note 10**).
7. Remove the remaining urea, from 2 to 0 M using a linear gradient over 30 min. (*see* **Note 11**).
8. Elute the refolded fusion protein using a linear gradient from 200 mM to 1 M NaCl (Buffer B2).
9. Measure protein concentration using A_{280} and check the purity by SDS-PAGE.

3.3 Cleavage Using Z_{basic} Tagged Protease

The target protein can be released by proteolytic cleavage either in solution or using an immobilized protease (further described in [15]). Herein, cleavage using protease 3C in solution is described.

1. Perform dialysis to lower the salt concentration in the eluted protein fractions using a dialysis cassette (e.g., Slide-A-Lyzer, Thermo Fisher Scientific Inc., Rockford, IL, USA) or equivalent, or dilute the sample to a final conductivity of 20 mS/cm or less (*see* **Note 12**).
2. Add 5 mM β-mercaptoethanol (required for protease 3C activity) and 1:50 molar ratio of Z_{basic}-3C (*see* **Note 13**).
3. Incubate the cleavage mixture for 90 min at room temperature (or 2 h, at 4 °C if your target protein is temperature sensitive).

3.4 Isolation of Target Protein

If a Z_{basic} tagged protease is used, both the released tag and the protease can be removed in a single step. The outline of this strategy is described in Fig. 3.

1. Load the cleavage mixture onto a 1 mL HiTrap S column previously equilibrated with 5 CV of Buffer A_s.
2. Collect the flow-through, which should contain your pure target protein.
3. Measure protein concentration using A_{280} and check the purity by SDS-PAGE.

4 Notes

1. Construction of expression vector: Construct your expression vector as most suitable for your target protein. Z_{basic} can be used as either an N-terminal or C-terminal purification tag, although most of our studies have been done with Z_{basic} at the N-terminus. We typically use a low copy number plasmid with the T7 promoter and a gene for kanamycin resistance. In

order to be able to proteolytically release the target protein, a site-specific cleavage site should be included between Z_{basic} and the target protein. A pET24a-based plasmid denoted pT7ZbQG [15], containing Z_{basic} followed by a viral protease 3C recognition sequence, can be used for insertion of a gene with flanking *Eco*RI and *Hin*dIII sites. The target protein is then expressed as a Z_{basic} fusion protein that can be subsequently cleaved by protease 3C.

2. Expression of Z_{basic} fusion proteins: Express the Z_{basic} fusion protein in your preferred host organism under conditions suitable for your target protein. Z_{basic} has been shown to increase the fraction of soluble protein in several cases [16, 18]. We typically use the *Escherichia coli* (*E. coli*) strain BL21 (DE3) (Novagen) for production. 1% of overnight culture is used for inoculation of fresh Tryptic soy broth (TSB) media (supplemented with 5 g/L yeast extract and 50 μg/mL kanamycin) and further cultured at 25–37 °C until an $OD_{600\ nm}$ of 1 is reached. Protein expression is induced by addition of isopropyl-β-D-thiogalactoside (IPTG) to a final concentration of 0.3–1 mM followed by up to 18 h of further cultivation. The cell suspension is gently harvested (4000 × *g*, 8 min, 4 °C), resuspended, and lysed in suitable loading Buffer A (see below). The resuspended cells can be frozen and thawed for later use, if desired.
3. In order to find out if your target protein is mainly in the soluble or insoluble fraction, take out a small sample after cultivation, disrupt the cells by sonication, centrifuge, and run SDS-PAGE. Alternatively, analyze your cell sample using a flow cytometry-based method as described in [18].
4. To process many proteins in parallel, an automated protocol for purification on a laboratory robot can be used, as described in [19].
5. Suggestion of sonication protocol: 60% duty cycle for 3 min with 1.0 s pulses. Alternatively, cell lysis can be done by the addition of lysozyme. However, note that lysozyme is also basic and will bind to a cation exchanger.
6. If the Z_{basic} fusion protein does not bind, check the conductivity of the load and dilute if too high. The Z_{basic} fusion elutes at conductivity around 40 mS/cm.
7. The utility of this purification strategy for expanded bed adsorption (EBA), which allows purification from unclarified *E. coli* homogenates in a single step, has been described [20].
8. If performing manual purification using gravity columns, use a stepwise elution. The Z_{basic} fusion protein will elute at conductivity around 40 mS/cm.

9. If your target protein contains cysteines, add 10 mM DTT to the refolding buffers.
10. Strict adjustments of the conductivity are important for successful renaturation of the protein on the column, unless the target protein is easily folded [10].
11. Omit DTT in this and following buffers.
12. Corresponding to approximately 150 mM NaCl.
13. Z_{basic}3C can be produced using the vector pT7Zb3C and purified as described under Subheading 3.3.

References

1. Asplund M, Ramberg M, Johansson B-L (2000) Development of a cleaning in place protocol and repetitive application of *Escherichia coli* homogenate on STREAMLINE™ Q XL. Process Biochem 35:1111–1118
2. Hale G, Drumm A, Harrison P et al (1994) Repeated cleaning of protein A affinity column with sodium hydroxide. J Immunol Methods 171:15–21
3. Anspach FB, Curbelo D, Hartmann R et al (1999) Expanded-bed chromatography in primary protein purification. J Chromatogr A 865:129–144
4. Feuser J, Walter J, Kula MR et al (1999) Cell/adsorbent interactions in expanded bed adsorption of proteins. Bioseparation 8:99–109
5. Hedhammar M, Gräslund T, Hober S (2005) Protein engineering strategies for selective protein purification. Chem Eng Technol 28:1315–1325
6. Nilsson B, Moks T, Jansson B et al (1987) A synthetic IgG-binding domain based on staphylococcal protein A. Protein Eng 1:107–113
7. Graslund T, Lundin G, Uhlen M et al (2000) Charge engineering of a protein domain to allow efficient ion-exchange recovery. Protein Eng 13:703–709
8. Link AJ, Robison K, Church GM (1997) Comparing the predicted and observed properties of proteins encoded in the genome of *Escherichia coli* K-12. Electrophoresis 18:1259–1313
9. Graslund T, Ehn M, Lundin G et al (2002) Strategy for highly selective ion-exchange capture using a charge-polarizing fusion partner. J Chromatogr A 942:157–166
10. Hedhammar M, Alm T, Graslund T et al (2006) Single-step recovery and solid-phase refolding of inclusion body proteins using a polycationic purification tag. Biotechnol J 1:187–196
11. Wiesbauer J, Bolivar JM, Mueller M et al (2011) Oriented immobilization of enzymes made fit for applied biocatalysis: non-covalent attachment to anionic supports using Zbasic2 module. ChemCatChem 3:1299–1303
12. Bolivar JM, Nidetzky B (2012) Oriented and selective enzyme immobilization on functionalized silica carrier using the cationic binding module Z basic2: design of a heterogeneous D-amino acid oxidase catalyst on porous glass. Biotechnol Bioeng 109:1490–1498
13. Bolivar JM, Nidetzky B (2012) Positively charged mini-protein Z basic2 as a highly efficient silica binding module: opportunities for enzyme immobilization on unmodified silica supports. Langmuir 28:10040–10049
14. Bolivar JM, Luley-Goedl C, Leitner E et al (2017) Production of glucosyl glycerol by immobilized sucrose phosphorylase: options for enzyme fixation on a solid support and application in microscale flow format. J Biotechnol 257:131–138
15. Hedhammar M, Jung HR, Hober S (2006) Enzymatic cleavage of fusion proteins using immobilised protease 3C. Protein Expr Purif 47:422–426
16. Shi S, Chen H, Jiang H et al (2017) A novel self-cleavable tag Zbasic–ΔI-CM and its application in the soluble expression of recombinant human interleukin-15 in *Escherichia coli*. Appl Microbiol Biotechnol 101:1133–1142
17. Yip TT, Nakagawa Y, Porath J (1989) Evaluation of the interaction of peptides with Cu(II), Ni(II), and Zn(II) by high-performance immobilized metal ion affinity chromatography. Anal Biochem 183:159–171

18. Hedhammar M, Stenvall M, Lonneborg R et al (2005) A novel flow cytometry-based method for analysis of expression levels in *Escherichia coli*, giving information about precipitated and soluble protein. J Biotechnol 119:133–146
19. Alm T, Steen J, Ottosson J et al (2007) High-throughput protein purification under denaturating conditions by the use of cation exchange chromatography. Biotechnol J 2:709–716
20. Graslund T, Hedhammar M, Uhlen M et al (2002) Integrated strategy for selective expanded bed ion-exchange adsorption and site-specific protein processing using gene fusion technology. J Biotechnol 96:93–102

Chapter 13

An Orthogonal Fusion Tag for Efficient Protein Purification

Johan Nilvebrant, Mikael Åstrand, and Sophia Hober

Abstract

In this chapter, we present an efficient method for stringent protein purification facilitated by a dual affinity tag referred to as ABDz1, which is based on a 5 kDa albumin-binding domain from *Streptococcal* Protein G. The small fusion tag enables an orthogonal affinity purification approach based on two successive and highly specific affinity purification steps. This approach is enabled by native binding of ABDz1 to human serum albumin and engineered binding to Staphylococcal Protein A, respectively. The ABDz1-tag can be fused to either terminus of a protein of interest and the purification steps can be carried out using standard laboratory equipment.

Key words Orthogonal affinity purification, ABDz1, Protein G, Human serum albumin, Protein A, Albumin binding, Fusion tag

1 Introduction

Genetically encoded affinity or epitope tags are widely used to facilitate the purification and detection of recombinant proteins via generic strategies [1]. Given the different biophysical properties and sensitivities to environmental conditions of diverse target proteins and a large number of available tags and affinity resins, it is not always straightforward to devise a protocol to purify a protein of interest [2]. Peptide tags such as the ubiquitous hexahistidine tag are popular due to the small size and ease of protein purification. In addition to its small size, the hexahistidine tag can be used under both denaturing and nondenaturing buffer conditions [3]. However, the use of, e.g., immobilized metal affinity chromatography has been linked to unwanted co-purification of host proteins binding to metal-chelating resins [4] and, thus, led to efforts to overcome such issues [5, 6]. A limitation with all single-tag systems is that they are specifically designed for one particular unit operation, which is commonly linked to certain contaminant proteins that might be co-purified via nonspecific binding to the resin. Several dual tagging systems have been developed to reduce nonspecific

Nikolaos E. Labrou (ed.), *Protein Downstream Processing: Design, Development, and Application of High and Low-Resolution Methods*, Methods in Molecular Biology, vol. 2178, https://doi.org/10.1007/978-1-0716-0775-6_13,

Table 1
Nucleotide- and amino acid-sequence of ABDz1

GATGAAGCCGTCGACGCGAATTCATTAGCTCTTGCTAAATGTCGTGCTCTGCGTGGTCTTGACCA TTATGGAGTAAGTGACTATTACAAGGACCTAATCGATAAAGCCAAAACTGTTGAAGGTGTACA TGCACTGTGGTTTGAAATTTTACAGGCATTACCT
*DEAVDANS***LALAKCRALRGLDHYGVSDYYKDLIDKAKTVEGVHALWFEILQALP**

Apart from the 46-residue ABDz1 tag (bold), an N-terminal leader sequence, which is commonly included when the ABDz1-tag is positioned at the N-terminus of a fusion construct, is included

background via two successive purification steps while also fulfilling accessory functions such as enhancing solubility or enabling detection of the protein of interest [7–10]. Our method provides an alternative and complementary strategy based on a single, bifunctional affinity tag, ABDz1, which can be combined with two different affinity resins used either alone or in tandem.

ABDz1 is a 46-residue (5 kDa) tag (Table 1) that is based on one of the three-helix bundle albumin-binding domains (ABD) of Streptococcal Protein G [11]. In addition to binding human serum albumin (HSA), ABDz1 has been adapted to bind Staphylococcal Protein A via a new binding interface engineered onto the opposite side of the protein [12] (Fig. 1). For one of the purification steps, an ordinary Protein A matrix (e.g., MabSelect SuRe) can be used, and for the second step, human serum albumin can be easily conjugated to a resin. A main advantage of the method is the high purity that is achieved after two successive affinity purification steps. The ABDz1 tag has been used for recombinant protein expression in *Escherischia coli* but due to its stability, ease of expression, and small size, it should in principle also be compatible with other host organisms. Orthogonal purification through ABDz1 has been evaluated for several target proteins of different molecular weight, isoelectric point, and solubility [12]. The tag has been primarily evaluated as an N-terminal fusion but is expected to also work as a C-terminal tag or in combination with proteolytic tag removal. Since the function of the ABDz1 tag depends on correct folding of the domain to efficiently expose its two binding surfaces, the method is limited to proteins expressed in soluble form and not suited for purification under denaturing conditions. Moreover, reducing agents should be avoided since they interfere with the binding of ABDz1 to the Protein A matrix, which is dependent on a nonreduced cysteine residue in the ABDz1 domain [12].

The engineering approach used to develop the bispecific ABDz1 domain has been further validated by generating bispecific ABD-based domains binding to tumor necrosis factor alpha [13], human epidermal growth factor receptor 2 [14], and human epidermal growth factor receptor 3 [15], respectively. The versatility of using similar combinatorial protein engineering approaches to develop custom-made protein domains for affinity purification is

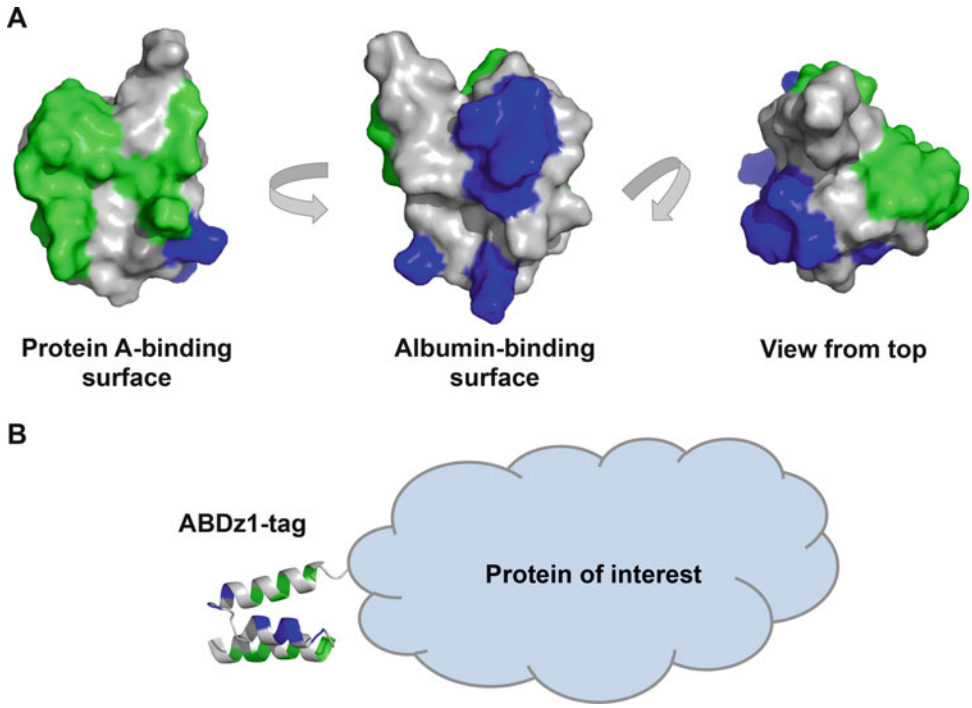

Fig. 1 Binding interfaces of ABDz1. (**a**) The ABDz1 tag contains two nonoverlapping binding surfaces for Protein A (shown in green) and albumin (shown in blue), respectively. The albumin-binding site is inherent in the wild-type domain, whereas the second interface was created using combinatorial mutagenesis of 11 surface-exposed residues and phage display selection. (**b**) Schematic genetic fusion of an N-terminal ABDz1-tag to a protein of interest. The unstructured leader sequence included in Table 1 is not shown. The pictures were generated in PyMOL using PDB 1GJT

also reflected in the use of such moieties as tailored capture ligands on affinity resins for, e.g., mild antibody purification [16] or highly specific purification of GFP-tagged proteins [17].

2 Materials

2.1 Buffers

All buffers are insensitive to light and can be stored at room temperature.

1. Running buffer: 25 mM Tris–HCl, 200 mM NaCl, 1 mM EDTA, 0.05% (v/v) Tween 20, pH 8.0.
2. Washing buffer: 5 mM NH_4Ac, pH 5.5.
3. Elution buffer: 0.5 M HAc, pH 2.5.
4. Protein A running buffer: 20 mM phosphate, 150 mM NaCl, pH 7.2.
5. Protein A elution buffer: 0.2 M HAc, pH 2.7.
6. pH-adjustment buffer: 1 M Tris–HCl, pH 8.0.

2.2 Chromatography Media and System

1. 1 mL HSA-Sepharose column or NHS-activated column coupled with human serum albumin according to the supplier's recommendations.
2. 1 mL Protein A column (GE Healthcare) or equivalent.
3. ÄKTA Explorer system (GE Healthcare) or equivalent; flow rates of 1 mL/min are used throughout the protocol except during sample loading (0.5 mL/min).

3 Methods

A schematic flow chart of the purification strategy is shown in Fig. 2. For further reference, a video protocol outlining the experimental procedures of this method is available [18].

3.1 Orthogonal Affinity Purification of ABDz1 Fusion Proteins

This protocol is based on purification from a 100-mL shake flask cultivation. It is very important that no reducing agents are added to any of the buffers because this will prevent ABDz1 from interacting with the Protein A column [12]. *See* Table 1 and **Notes 1** and **2** for construction of the ABDz1 expression vector and **Note 3** for protein expression.

1. Resuspend the bacterial pellet in 25 mL running buffer.
2. Disrupt the bacterial cells by sonication (Vibra Cell, Sonics and Materials Inc., Danbury, CT, USA) (*see* **Note 4**).
3. Centrifuge at 10,000 × *g* for 10 min at 4 °C to remove cell debris.
4. Filtrate the supernatant through a 0.45 μm syringe filter (Acrodisc® 32 mm Syringe Filter, Pall Corporation, Port Washington, NY, USA) (*see* **Note 5**) and store on ice until loading (**step 6**).
5. Equilibrate a 1 mL HSA-Sepharose column with 10 column volumes (CV) of running buffer (1 mL/min). The two affinity purification steps (purification on HSA-Sepharose and Protein A matrix) may also be used in the reverse order (*see* **Note 6**).
6. Load the sample at 0.5 mL/min.
7. Wash the column with 5 CV of running buffer followed by 5 CV of washing buffer (1 mL/min).
8. Elute the fusion proteins with elution buffer (1 mL/min), collect 1 mL fractions, and monitor A_{280} during elution. Representative chromatograms are shown in Fig. 2.
9. Select fractions that contain the protein of interest for further purification on a Protein A matrix (*see* **Note 7**).

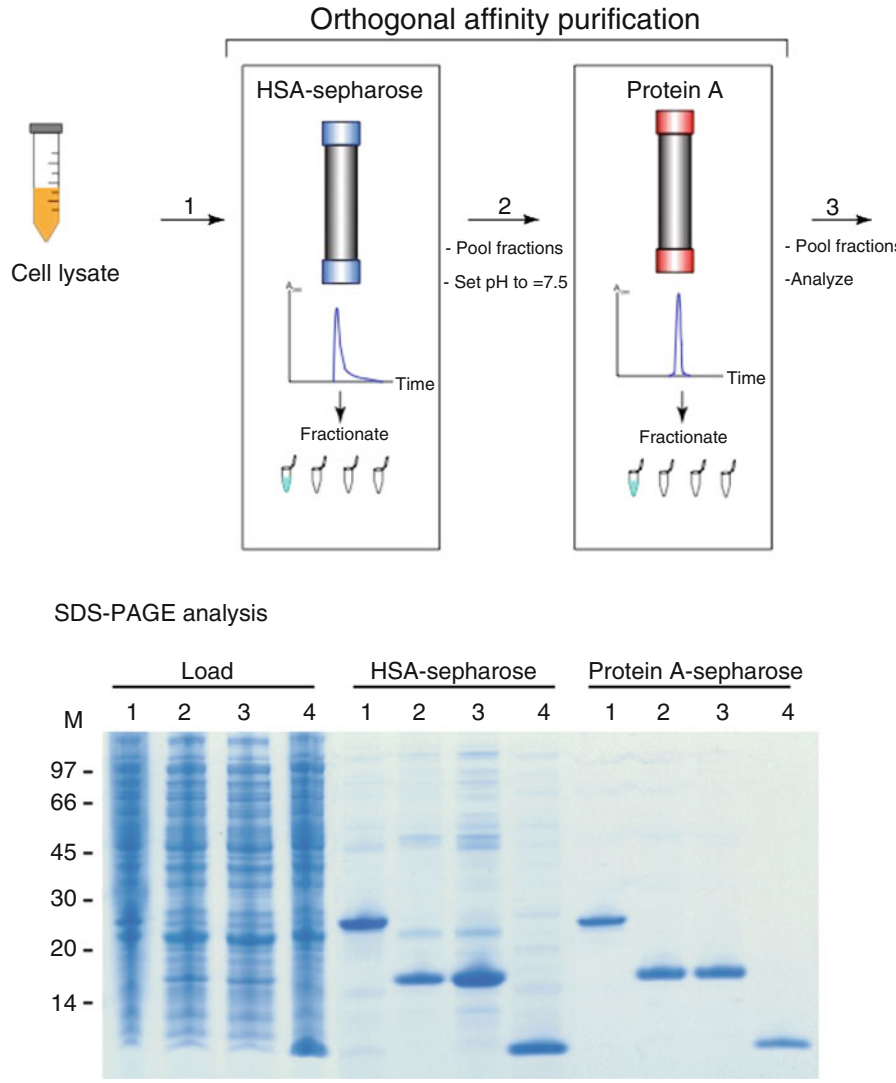

Fig. 2 Method workflow. The target protein fused to ABDz1 is expressed in *E. coli*, harvested, and lysed. The clarified cell lysate is loaded onto a HSA-Sepharose column, washed, and eluted by decreased pH. After pooling of selected fractions and adjustment to pH 7.5, the sample is purified on a Protein A column. The purity of the protein is subsequently assessed by SDS-PAGE analysis, as exemplified by four different ABDz1-fusion proteins before purification, after HSA-purification, and after the full orthogonal purification procedure

10. Pool the most highly concentrated fractions and dilute in an equal amount of Protein A running buffer. Measure pH and make sure it is between 7 and 8, and add 1 M Tris–HCl to increase pH if necessary.
11. Load the sample (0.5 mL/min) on a 1 mL Protein A column, previously equilibrated (1 mL/min) with 10 CV of Protein A running buffer.
12. Wash the column with 5 CV of Protein A running buffer.

13. Elute bound fusion proteins with Protein A elution buffer, collect 1 mL fractions, and monitor A_{280} during elution (*see* **Note 8**). A representative chromatogram is shown in Fig. 2.
14. Measure protein concentration on selected fractions using A_{280} or a comparable method and check the purity by sodium dodecyl sulphate-polyacrylamide gel electrophoresis (SDS-PAGE) (*see* **Note 9**). A typical SDS-PAGE result is shown in Fig. 2.

4 Notes

1. Construction of ABDz1 expression vector: Clone the ABDz1-tag as an N-terminal fusion to your protein of interest. The ABDz1-tag itself consists of 46 amino acids and contributes a mass of 5.2 kDa to the fusion protein. We typically use the TOP10 *E. coli* strain for cloning steps and a medium copy number plasmid with kanamycin resistance and expression controlled by a T7 promoter induced by isopropyl-β-D-thiogalactopyranoside (IPTG).
2. A plasmid containing ABDz1 for PCR-amplification or direct cloning of fusion proteins is freely available through a material transfer agreement. For enhanced expression, it is recommended to include a short leader sequence at the N-terminus of the construct (*see* Table 1).
3. Expression of ABDz1 fusion proteins: Transform the expression vector containing the DNA-sequence-verified ABDz1-target protein gene fusion to your preferred expression host. We typically use *E. coli* Rosetta (DE3) or BL21(DE3) for protein expression. Inoculate a single bacterial colony to 10 mL of tryptic soy broth (TSB) supplemented with appropriate antibiotics and incubate at 150 rpm at 37 °C overnight. Inoculate 100 mL fresh medium supplemented with 5 g/L yeast extract and antibiotics with 1 mL of overnight culture and incubate (150 rpm at 37 °C) until OD_{600nm} reaches 0.5–1. Induce protein expression by addition of IPTG to a final concentration of 1 mM (if a lac operon is used). Incubate at 150 rpm at 25 °C overnight. Harvest the cells by centrifugation (2700 × *g* for 15 min at 4 °C).
4. It is recommended to use a 60% duty cycle for 3 min with 1 s pulses, keep samples on ice during sonication to prevent heating.
5. If desired, collect a sample of the lysate before purification and analyze by SDS-PAGE to check for the presence of the ABDz1-fusion protein.

6. The two purification steps can be used in the reverse order if desired. If the Protein A column is used first, the chosen fractions can be diluted in running buffer and the pH adjusted to 8 by addition of 1 M Tris–HCl. Narrower elution peaks are generally observed when the Protein A matrix is employed in the last purification step.
7. Eluted fractions from **step 8** can be neutralized by addition of 1 M Tris–HCl and analyzed by SDS-PAGE if desired. The initial HSA affinity purification step itself generally results in a reasonably or even highly pure fusion protein.
8. For sensitive target proteins, the eluate can be neutralized directly upon collection by addition of 1 M Tris–HCl to the bottom of the wells of the fraction collection plate. The pH of the Protein A elution buffer can also be increased to pH 4 in this step [12].
9. It is important to fully reduce the sample prior to SDS-PAGE since the free cysteine in ABDz1 may form dimeric products.

References

1. Wingfield PT (2015) Overview of the purification of recombinant proteins. Curr Protoc Protein Sci 80(6):1–35. https://doi.org/10.1002/0471140864.ps0601s80
2. Kimple ME, Brill AL, Pasker RL (2013) Overview of affinity tags for protein purification. Curr Protoc Protein Sci 73:Unit 9 9. https://doi.org/10.1002/0471140864.ps0909s73
3. Porath J (1992) Immobilized metal ion affinity chromatography. Protein Expr Purif 3 (4):263–281
4. Bolanos-Garcia VM, Davies OR (2006) Structural analysis and classification of native proteins from *E. coli* commonly co-purified by immobilised metal affinity chromatography. Biochim Biophys Acta 1760(9):1304–1313. https://doi.org/10.1016/j.bbagen.2006.03.027
5. Hu Y, Romao E, Vertommen D, Vincke C, Morales-Yanez F, Gutierrez C, Liu C, Muyldermans S (2017) Generation of nanobodies against SlyD and development of tools to eliminate this bacterial contaminant from recombinant proteins. Protein Expr Purif 137:64–76. https://doi.org/10.1016/j.pep.2017.06.016
6. Parsy CB, Chapman CJ, Barnes AC, Robertson JF, Murray A (2007) Two-step method to isolate target recombinant protein from co-purified bacterial contaminant SlyD after immobilised metal affinity chromatography. J Chromatogr B Analyt Technol Biomed Life Sci 853(1–2):314–319. https://doi.org/10.1016/j.jchromb.2007.03.046
7. Li Y (2010) Commonly used tag combinations for tandem affinity purification. Biotechnol Appl Biochem 55(2):73–83. https://doi.org/10.1042/BA20090273
8. Miladi B, Dridi C, El Marjou A, Boeuf G, Bouallagui H, Dufour F, Di Martino P, Elm'-selmi A (2013) An improved strategy for easy process monitoring and advanced purification of recombinant proteins. Mol Biotechnol 55 (3):227–235. https://doi.org/10.1007/s12033-013-9673-5
9. Waugh DS (2011) Reprint of: making the most of affinity tags. Protein Expr Purif. https://doi.org/10.1016/j.pep.2011.08.019
10. Wood DW (2014) New trends and affinity tag designs for recombinant protein purification. Curr Opin Struct Biol 26:54–61. https://doi.org/10.1016/j.sbi.2014.04.006
11. Nilvebrant J, Hober S (2013) The albumin-binding domain as a scaffold for protein engineering. Comput Struct Biotechnol J 6: e201303009. https://doi.org/10.5936/csbj.201303009
12. Alm T, Yderland L, Nilvebrant J, Halldin A, Hober S (2010) A small bispecific protein selected for orthogonal affinity purification. Biotechnol J 5(6):605–617. https://doi.org/10.1002/biot.201000041

13. Nilvebrant J, Alm T, Hober S, Lofblom J (2011) Engineering bispecificity into a single albumin-binding domain. PLoS One 6(10): e25791. https://doi.org/10.1371/journal.pone.0025791
14. Nilvebrant J, Astrand M, Georgieva-Kotseva M, Bjornmalm M, Lofblom J, Hober S (2014) Engineering of bispecific affinity proteins with high affinity for ERBB2 and adaptable binding to albumin. PLoS One 9(8):e103094. https://doi.org/10.1371/journal.pone.0103094
15. Nilvebrant J, Astrand M, Lofblom J, Hober S (2013) Development and characterization of small bispecific albumin-binding domains with high affinity for ErbB3. Cell Mol Life Sci 70 (20):3973–3985. https://doi.org/10.1007/s00018-013-1370-9
16. Kanje S, Venskutonyte R, Scheffel J, Nilvebrant J, Lindkvist-Petersson K, Hober S (2018) Protein engineering allows for mild affinity-based elution of therapeutic antibodies. J Mol Biol 430(18 Pt B):3427–3438. https://doi.org/10.1016/j.jmb.2018.06.004
17. Hansen S, Stuber JC, Ernst P, Koch A, Bojar D, Batyuk A, Pluckthun A (2017) Design and applications of a clamp for green fluorescent protein with picomolar affinity. Sci Rep 7 (1):16292. https://doi.org/10.1038/s41598-017-15711-z
18. Nilvebrant J, Alm T, Hober S (2012) Orthogonal protein purification facilitated by a small bispecific affinity tag. J Vis Exp 59. https://doi.org/10.3791/3370

Chapter 14

Biomimetic Affinity Ligands for Protein Purification

Isabel T. Sousa and M. Ângela Taipa

Abstract

The development of sophisticated molecular modeling software and new bioinformatic tools, as well as the emergence of data banks containing detailed information about a huge number of proteins, enabled the de novo intelligent design of synthetic affinity ligands. Such synthetic compounds can be tailored to mimic natural biological recognition motifs or to interact with key surface-exposed residues on target proteins, and are designated as "biomimetic ligands". A well-established methodology for generating biomimetic or synthetic affinity ligands integrates rational design with combinatorial solid-phase synthesis and screening, using the triazine scaffold and analogs of amino acid side chains to create molecular diversity.

Triazine-based synthetic ligands are nontoxic, low-cost, and highly stable compounds that can replace advantageously natural biological ligands in the purification of proteins by affinity-based methodologies.

Key words Affinity, Biomimetic, Triazine-scaffolded ligands, Design, Combinatorial synthesis, Screening, Protein purification

1 Introduction

1.1 Affinity Ligands

Affinity techniques are based on the molecular recognition between biological macromolecules (of which proteins are important representatives) and complementary ligands. Hence, they have the advantage of being highly selective. Affinity is a fundamental aspect of biological systems and how they function. Biorecognition is what allows, for example, antigen/antibody, hormone/receptor, and enzyme/substrate interactions. Biotechnology takes advantage of this natural ability of biomolecules to selectively bind other molecules, to devise useful applications, namely for their purification but also in other important areas such as drug design and development of biosensors.

Affinity ligands for protein purification (as well as for other purposes that take advantage of affinity interactions) can be natural molecules such as enzyme substrates and inhibitors, effectors, coenzymes, hormones, antigens, nucleic acids, and sugars, for example [1]. However, the increasing demands of worldwide markets for

Nikolaos E. Labrou (ed.), *Protein Downstream Processing: Design, Development, and Application of High and Low-Resolution Methods*, Methods in Molecular Biology, vol. 2178, https://doi.org/10.1007/978-1-0716-0775-6_14,

highly purified proteins favored the development of synthetic affinity ligands, generally regarded as safe and more economic alternatives to natural ligands. The latter are usually labile, expensive, and often immunogenic, which is problematic in the case of leakage when purifying proteins for use as therapeutics [2].

Synthetic ligands may show moderate affinity for the protein of interest, which can be advantageous since, in those cases, mild elution conditions can be used. The main advantages of the use of synthetic ligands for affinity processes arise from the fact that they are inexpensive, scalable, durable, and reusable over multiple cycles. They are also generally not toxic per se nor are the respective column leachates and, furthermore, their exceptional stability allows harsh elution as well as in-place cleaning and sterilization procedures [3, 4].

1.2 Triazine-Scaffolded Ligands

Reactive textile dyes are a type of synthetic ligands originating from the serendipitous observation of the dye component of blue dextran—Cibacron Blue F3G-A—bound to pyruvate kinase during gel filtration [5]. This dye was only one of a large family of triazine dyes with the ability to bind proteins [6]. The structure of such dyes consists of a triazine ring substituted at two positions, with the third position allowing the coupling to a matrix.

Although traditional textile dyes showed remarkable selectivity in some cases, most usually they interacted with a large number of quite dissimilar proteins. This fact often compromised protein binding specificity and was a major drawback to their use. The use of buffers/compounds, which eluted specifically the target protein (affinity elution) was one way to deal with this problem [7]. It became apparent, however, that ligand engineering or design was an effective way of tailoring specific binding. New dye-ligands with improved affinity and selectivity for target proteins began then to be designed.

1.2.1 Design of Synthetic Affinity Ligands

Synthetic ligands that mimic the structure and binding of natural biological ligands were termed "biomimetic ligands" [7]. It was only many years after the first uses of textile dyes as "pseudo-affinity" ligands that this technology could start to be based on de novo synthesis and rational ligand design concepts [1]. The first generation of biomimetic ligands was developed in the early 1980s, a time when sophisticated molecular modeling software, needed for the study of ligand-protein interactions, was not available. Hence, biomimetic ligand design relied only on known binding preferences of the target protein for natural ligands, X-ray crystallography, and other available biochemical information [7]. Over the 1990s, the development of sophisticated computer-based molecular modeling software and new bioinformatic tools, as well as of data banks containing extensive and detailed information about a huge number of proteins, enabled the in silico exploitation of virtual ligand-

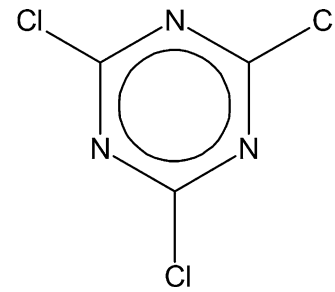

Fig. 1 Structure of 2,4,6-trichloro-*s*-trazine with its three reactive chlorines

protein complexes and the emergence of a convenient and well-succeeded approach for the de novo intelligent design of synthetic affinity ligands [7]. Simultaneously, the ease of manipulation of the triazine scaffold has attracted large interest in exploring its combinatorial derivatization for biological applications. As a result, over the last few decades, a number of synthetic approaches, adapted to solid-phase methodologies to facilitate the construction of large libraries, have converted the triazine structure (Fig. 1) into a key scaffold for the discovery of novel bioactive compunds [8, 9].

Namely, the reactivity of cyanuric chloride (2,4,6-trichloro-*s*-trazine) toward amines together with its structural rigidity, the ease in generating molecular diversity, and the formation of nonfissile bonds with the substituents have prompted its extensive use for the generation of synthetic mimic bifunctional protein ligands [3, 4, 10]. Several biomimetic triazine-based ligands have been thereof successfully designed as stable synthetic analogs that replace natural biological ligands. Table 1, without being exhaustive, is representative of a variety of target proteins and different types of natural ligands mimicked by de novo designed triazine-based compounds.

Among the examples given, synthetic affinity ligands mimicking the interaction of immunoglobulins with bacterial IgG-binding receptors have attracted renewed attention due to the increased demand for antibody therapeutics. These synthetic ligands, named as "artificial proteins", can surmount problems associated with their natural biological templates, such as high-production costs, toxicity, and low-stability [2], while preserving affinity and specificity to target antibodies. "Ligand 22/8" (4-[4-Chloro-6-(3-hydroxy-phenylamino)-[1,3,5]triazin-2-ylamino]-naphthalen-1-ol), named as "artificial Protein A", mimics the natural *Staphylococcus aureus* Protein A receptor in binding IgG from various sources, separating IgG from human plasma to purities of 98–99% [14, 16]. "Ligand 8/7" (4-4-(4-carbamoyl-phenylamino)-6-chloro-[1,3,5]triazin-2-ylamino]-butyric acid) or "artificial Protein L" has been shown to mimic Protein L (a bacterial receptor from *Peptostreptococcus magnus* strains, which binds to the Fab portion of immunoglobulins) in terms of human IgG binding/elution

Table 1
Examples of successful design of triazine-based ligands for specific target proteins

Target protein	Mimicked natural ligand	Type of natural ligand	Function of natural ligand	References
Porcine pancreatic kallikrein	Arginyl dipeptides (molecular modeling based on the X-ray crystallographic structure of the complex with bovine pancreatic trypsin inhibitor)	Peptidic	Substrate/ inhibitor	[11]
L-Lactate dehydrogenase	Pyruvate and oxamate	Organic acids	Substrate and inhibitor respectively	[12]
	Lactate and NAD^+	Organic acid and dinucleotide	Substrate and cofactor respectively	[13]
IgG	Staphylococcus aureus Protein A (more specifically dipeptide Phe132-Tyr133)	Proteic	Virulence factor	[14]
	Staphylococcus aureus Protein A (more specifically dipeptide Phe132-Tyr133)[a]	Proteic	Virulence factor	[15, 16]
	Peptostreptococcus magnus Protein L	Proteic	Virulence factor	[17, 18]
Glycoproteins (e.g., glucose oxidase)	Proteins that bind to the sugar moiety of glycoproteins (e.g., lectins)	Proteic	Sugar-binding proteins	[19, 20]
Elastase	Turkey ovomucoid inhibitor third domain (OMTKY3)	Proteic	Inhibitor	[21]
Glutathione-recognising enzymes	Glutathione	Peptidic	Substrate/ cofactor	[22]
DNA-polymerase	Deoxyribonucleotides-triphosphate (dNTPs)	Nucleotidic	Substrate	[23]
Phosphorylated proteins	Phosphorylated peptides	Peptidic	Physiological functions	[24]
Human serum albumin (HSA)	HSA Domain II	Proteic	Natural binders	[25]
Recombinant human insulin precursor MI3	–	–	–	[26]
Human recombinant clotting factor VIIa	–	–	–	[27]
Cutinase	–	–	–	[28–31]

(continued)

Table 1
(continued)

Target protein	Mimicked natural ligand	Type of natural ligand	Function of natural ligand	References
Anti-human immunodeficiency virus (anti-HIV) 2F5 monoclonal antibody (mAb)	–	b	–	[32]
Human (anti-HIV) mAb 4E10	–	c	–	[33]

Different natural ligands, with various functions, are mimicked in some cases and, in other cases, the design was performed without the aid of templates (natural protein/ligand complexes) or with the aid of a non-natural-ligand template

[a]Lead optimization by construction of a focused biased library of near-neighbor analogs of the dipeptide (Phe-Tyr) mimic ligand found by [14]

[b]A lock-and-key motif found in glutathione S-transferases was used as a concept for the design of the ligands, rather than a natural ligand/protein complex

[c]Peptides selected from a peptide display library with affinity for the target were mimicked rather than a natural ligand

performance and specificity toward the Fab moiety (Fig. 2). The "artificial Protein L" (with an affinity constant (K_a) estimated for hIgG of ~10^4 M^{-1}) has also shown to compare well with the natural receptor (K_a ~ $10^{7–9}$ M^{-1}) in the isolation of immunoglobulins from different classes (human IgG, IgA, and IgM) and species (rabbit and goat), and of a recombinant scFv-based protein from crude extracts [17, 34].

However, the approach exemplified above for synthetic mimics of immunoglobulin-binding receptors is restricted to target proteins for which a suitable template structure, derived from known complementary binding molecules, is available. Sproule et al. and Morril et al. have extended the concept of "biomimetic ligand" and presented a more general approach, which exploited the knowledge of the target protein per se, combined with rational design and synthesis of combinatorial libraries of complementary ligands (able to bind target key surface residues) and appropriate screening methodologies [27]. Platis and coworkers also found that a lock-and-key (LAK) motif, which is a common structural feature found in subunit interfaces of glutathione S-transferases (GSTs), formed an adequate model for a templateless design of synthetic affinity ligands. This motif, found in GST, bears a phenylalanine and a glutamine residue and is crucial for the quaternary structure and integrity as well as for the thermal stability of the enzyme, as demonstrated by mutation of these residues [32]. The authors reasoned that such a LAK motif could serve as a concept for the generation of affinity adsorbents for different target proteins.

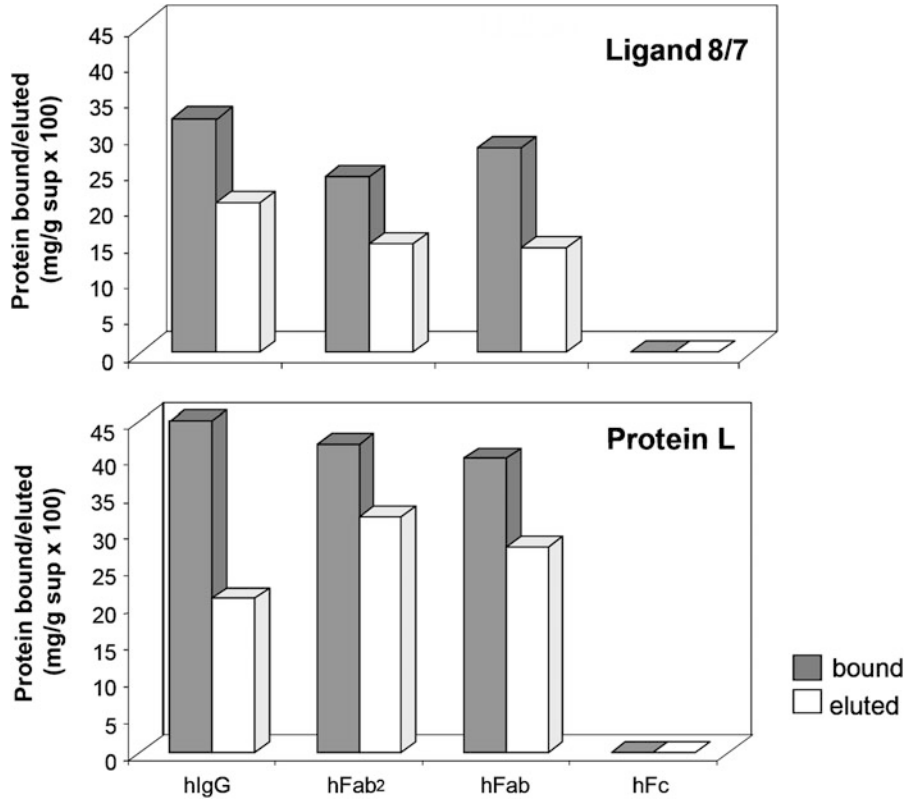

Fig. 2 Binding properties of "artificial" Protein L (ligand 8/7) and a commercial Protein L toward human IgG, F $(ab)_2$, Fab, and Fc. Comparison of the amount of target proteins bound and eluted (in mg protein/g support) (Adapted with permission from Refs. 18, 34)

Hence, they followed a "structure-guided" or "directed combinatorial method" in which the ligand was selected from an intentionally biased combinatorial library, based on a rationally designed lead ligand. The lead was predicted to bind to the target using a computational model. In this approach, the triazine-ligand bore a LAK motif combining a phenylalanine (the "key") and another hydrophobic, polar, or charged residue. A LAK-mimetic ligand (Phe--triazine-Asp) was exploited as an affinity ligand for the purification of an anti-human immunodeficiency virus (anti-HIV) 2F5 monoclonal antibody (mAb 2F5). The mAb was purified in a single-step from an impure corn extract, with 70–80% recovery and purity up to 95% [32].

The design of ligands directed toward the surface of cutinase is another example mentioned in Table 1, where there was also no structural template from which specific interactions could be mimicked [28]. The rationale of this work was finding stabilizing ligands, which were able to bind cutinase with high affinity while retaining enzymatic activity [28]. Therefore, it was not convenient to mimic interactions with substrates or inhibitors since binding to

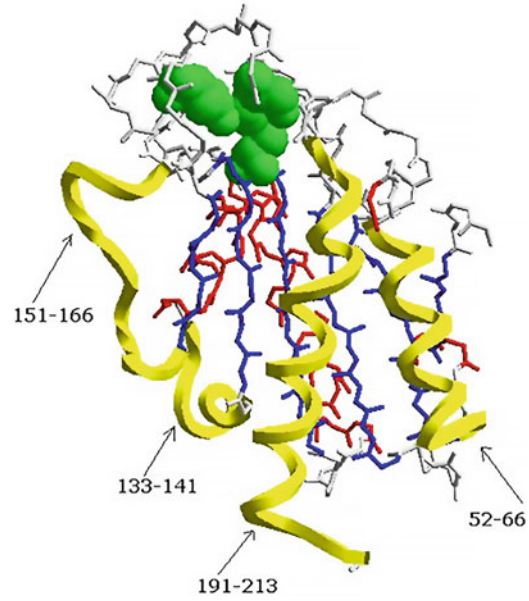

Fig. 3 Representation of Fusarium solani *pisi* cutinase showing its "weak regions", recognized to be involved in the initiation of the unfolding. The "weak regions" comprising residues 52–66, 133–141, 151–166, and 191–213 are shown in ribbon representation (yellow); the active site residues Ser120, Asp175, and His188 are shown in green and the remaining backbone (with side-chains omitted) is colored according to the secondary structure, with β-strands in blue, α-helices in red, and the remaining portions in grey. Representation obtained with Swiss-PdbViewer 3.7 software (pdb file: 1CUS)

the functional regions of the protein would, most likely, eliminate or greatly reduce its activity. The target surface regions (named as "weak regions") considered suitable for the design of complementary ligands were the ones previously found to be involved in the early unfolding events of cutinase [35] and do not include the active site (Fig. 3).

From the surface regions studied in silico, five amino acid residues, included in the "weak region", were identified as key residues that are exposed to the surface and are amenable for the establishment of intermolecular interactions, including hydrophobic and hydrogen bonds [28, 36]. These amino acids served as targets for the rational design of complementary bifunctional triazine-based synthetic affinity ligands. Two examples of designed ligand-cutinase complexes after energy minimization are represented in Fig. 4.

The approach followed by Ruiu et al. was extended in the work of Sousa et al., which was based on the selection of ligands for cutinase with moieties bearing resemblance with a variety of amino acid side chains from a larger random combinatorial ligand library and the synthesis of a semi-rational ligand library. This was found to

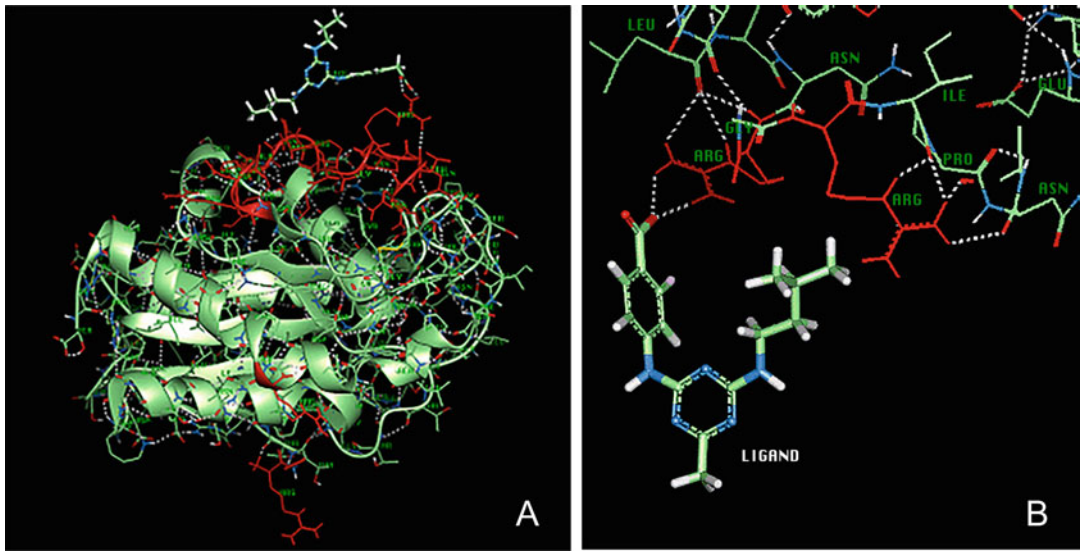

Fig. 4 Molecular models showing triazine-based ligands docked on the surface of cutinase. (**a**) ligand 4/5 docked on the surface of cutinase (interacting with Arg 156) showing also the relative size of both molecules; (**b**) ligand 3/5 docked on the surface of cutinase (interacting with Arg 158). Hydrogen bonds are shown as dashed lines (Adapted with permission from Refs. 28, 36)

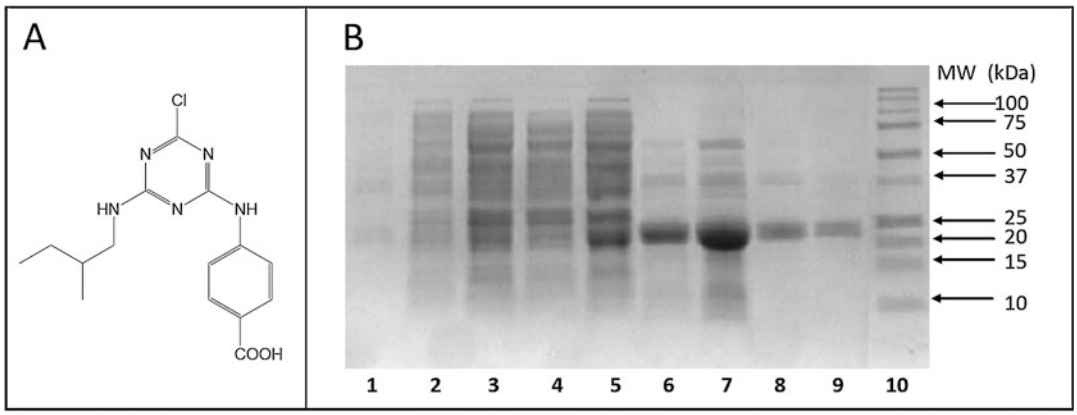

Fig. 5 (**a**) Structural formula of ligand 11/3′ (4-({4-chloro-6-[(2-methylbutyl)amino]-1,3,5-triazin-2-yl}amino) benzoic acid); (**b**) SDS-PAGE analysis of the fractions resulting from the partial purification of a cutinase extract using a 11/3′ solid-phase ligand-derivatized adsorbent. Lane 1: fraction 2 of the washing step; lane 2: fraction 1 of the washing step; lane 3: fraction 2 of flow-through; lane 4: fraction 1 of flow-through; lane 5: impure extract containing cutinase; lane 6: fraction 3 of elution; lane 7: fraction 2 of elution; lane 8: fraction 4 of elution; lane 9: fraction 1 of elution; and lane 10: molecular weight markers (Adapted from [31])

be a suitable strategy to find a number of triazine-scaffolded synthetic compounds binding cutinase with high affinity and selectivity while stabilizing its biological activity [29, 30]. Figure 5 shows the structure of a lead stabilizing ligand and the analysis by SDS-PAGE of the purification of a recombinant *E. coli* extract of cutinase from

Fusarium solani pisi with a ligand-derivatized adsorbent. Under nonoptimized conditions, lead ligand 11/3′ showed high selectivity toward cutinase (MW ≈ 22 kDa), with low nonspecific adsorption of other contaminant proteins, indicating the potential of stabilizing ligand-derivatized resins as affinity adsorbents for cutinase purification [31].

1.2.2 Combinatorial Approach in Ligand Synthesis and Selection

Although the de novo ligand design strategies endow the selection of leads with a more rational character, the whole process, including selection of an appropriate target site and the design, synthesis, and evaluation of a synthetic ligand, is still, at best, considered a semi-rational one [3]. Numerous unknown factors and uncertainties may affect the ultimate outcome of the design strategy, namely due to the immobilization of the ligand in a solid phase, since the affinity of the coupled ligand can depend on the ligand itself, the matrix, the activation, and the coupling chemistry [3, 4]. The use of a solid-phase combinatorial strategy, usually after the molecular design step, is a way to obviate this problem by creating molecular diversity from which it is more likely to select a suitable ligand. Solid-phase synthesis allows the production of a large number of different ligands for random screening, in a time- and resource-effective manner, and may eventually offer synthetic transformations that would be very difficult to achieve in solution [19].

A well-established and most effective methodology for obtaining triazine-based biomimetic ligands, integrating rational design with combinatorial synthesis and screening on the same support, was pioneered and established by Lowe and coworkers [4]. The solid support utilized, agarose, has proven to satisfy both the exigencies for solid-phase synthesis and the properties required for ligand screening and application in affinity chromatography [3]. The general strategy for the generation of such effective de novo designed triazine-based synthetic mimic ligands is represented in Fig. 6.

The main steps of this strategy are (1) molecular modeling based on structural information available (NMR, X-ray Crystallography) on the target biomolecules or their complexes with natural ligands; (2) in silico design of n chemical analogs that mimic the key residues involved in a specific (bio)molecular recognition (template approach) or that can interact in a complementary affinity-like mode with surface-exposed key residues (templateless approach); (3) synthesis of an $n \times n$ member solid-phase combinatorial library of triazine-based ligands in agarose; (4) development of effective/high-throughput assays for ligand screening; (5) solution-phase synthesis and further characterization/optimization of lead ligands and of affinity chromatographic conditions. In some cases, a second-generation library may be designed to improve the affinity/selectivity of selected putative lead ligands, allowing the

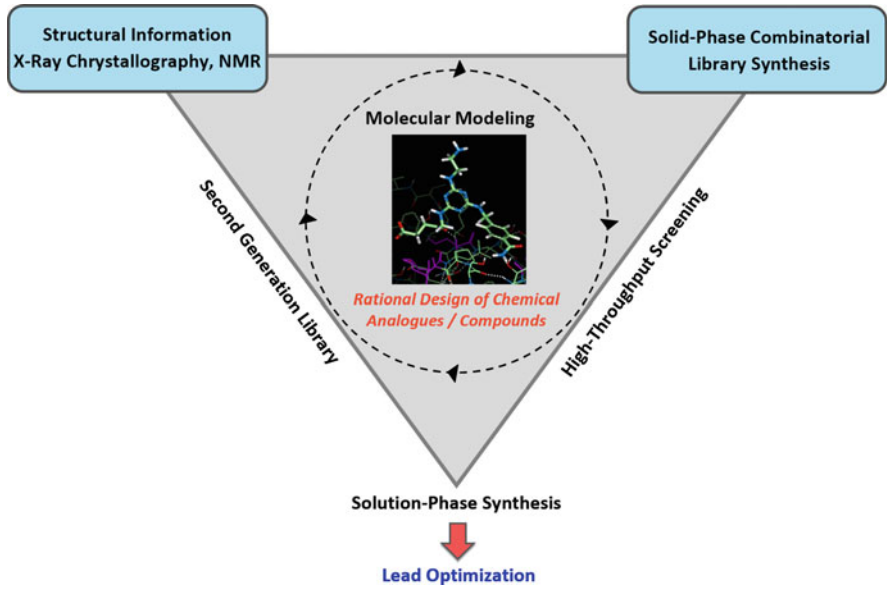

Fig. 6 General research strategy for the generation of effective de novo designed triazine-based synthetic affinity ligands

synthesis of better mimics. Solid-phase combinatorial generation of disubstituted triazine-ligand libraries is achieved by a "split synthesis"method [37] in which the first chlorine of the triazine ring is substituted by all different *n* amines, and then each of these monosubstituted derivatives is split into *n* portions for the substitution of the second chlorine with each amine (Fig. 7).

An alternative to the well-established triazine chemistry for the generation of synthetic mimic affinity ligands is based on the Ugi scaffold [38–42]. The multicomponent Ugi reaction allows the generation of a greater diversity of affinity ligands via a diamide peptoidal scaffold in a one-pot reaction at constant temperature (50 °C), and offers an advantage to the triazine route that requires temperature changes between 0 and 90 °C. Both synthetic approaches allow the generation of branched, cyclized, and 3D affinity ligands, [39] although the Ugi scaffold can likely adopt more structural flexibility by possessing a less planar structure than the triazine scaffold [38].

1.2.3 Screening and Selection of Lead Ligands

Once a set of mimic ligands has been synthesized, an effective screening strategy has to be outlined and applied for the selection of lead compounds. The screening process assesses molecular binding interactions between the synthesized ligands and the target protein and aims at selecting the most potent and selective binders for further optimization. In silico screening is a widely used methodology for the fast assessment of a large number of ligands against a target and the identification of the main lead candidates [43]. However, in the case of triazine-based ligands, several

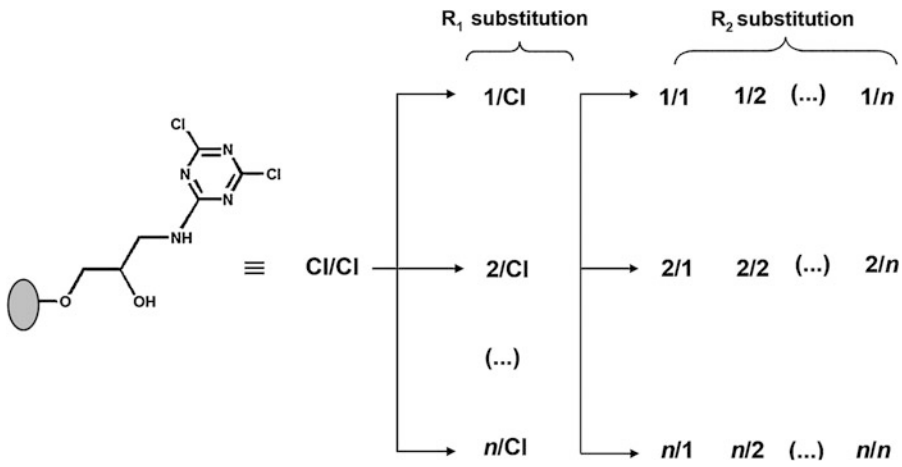

Fig. 7 Combinatorial synthesis of a library of triazine-based bifunctional ligands, containing *n* different R_1 or R_2 substituents. Dichlorotriazinyl agarose is divided into aliquots and each reacts with one of the *n* chosen amino acid analog compounds at 30 °C (R_1 substitution). Each of the R_1 substituted gels is again divided into *n* portions and reacted with each of the *n* amines at 85 °C (R_2 substitution). This procedure results in a library composed of n^2 elements, which corresponds to all possible arrangements (with repetition) of any two of the *n* aminated compounds. Cl/Cl corresponds to the dichlorotriazinyl agarose, R_1/Cl corresponds to the mono-substituted ligand, and R_1/R_2 is the final bisubstituted ligand, with R_1 and R_2 being the amines 1–*n*

important factors that derive from ligand synthesis/immobilization on a solid support need to be taken into account when delineating the screening process. Previous studies have confirmed that the strength of binding between immobilized ligands and proteins can be indirectly affected by interactions with the support material [44] thus reinforcing the advantages of carrying out synthesis and screening on the same support. As so, on-bead fluorescence-based binding assessment [45, 46] and affinity chromatography, alone or combined with an immunoassay, are the most common and effective strategies to screen large solid-phase combinatorial libraries of triazine-based synthetic affinity ligands [15, 18, 19, 28, 29].

Fluorescence microscopy has been shown to be a reliable, versatile, and accurate technique for on-bead assessment of large combinatorial ligand libraries using fluorescein isothiocyanate (FITC) as the target-protein label. This rapid qualitative screening methodology, which requires very low amounts of both reactants (conjugated protein and immobilized ligand) and facile instrumentation, was proved successful as a first approach to reduce the number of potential lead candidates of a combinatorial library designed to bind human IgG [45] and in the search for cutinase strong binders in a random evaluation of the same library [29]. The method tends to give false positives but not false negatives [45, 46]. False positives may increase slightly the number of ligands selected to proceed for further assessment. Oppositely, false-negative results are undesirable as potential lead ligands may not proceed to ligand optimization.

The second stage of screening involves generally a more detailed and quantitative assessment of binding between ligands and the target biomolecule by label-free techniques, such as affinity chromatography and affinity partition. Affinity chromatography screening represents the best practice to calculate a precise value for the percentage of target protein bound and eluted by a ligand-adsorbent under specific conditions, whereas affinity partitioning is commonly utilized to determine affinity constants, maximum binding capacity, and molar ligand occupation for lead compounds.

Immunoassays such as ELISA (enzyme-linked immunosorbent assay) are known for their versatility, sensitivity, and high throughput, thus being a valuable tool to combine with affinity chromatography for the iterative screening of combinatorial ligand libraries for tailored specificities and improved affinities.

An example of application of a multifaceted screening strategy, involving the methodologies described above, was in the discovery of an artificial Protein L binding specifically to the Fab domain of human IgG [18]. A 169-membered solid-phase combinatorial library of triazine-scaffolded ligands was firstly assessed for binding to human IgG by the on-bead FITC-based method [45]. The results were validated by screening with a standard affinity chromatographic method. However, "scale-down" and high-throughput analysis for selectivity against Fab and Fc moieties of immunoglobulin molecules was imposed by the high cost and limited supply of human IgG fragments. Therefore, positive ligands for human IgG were assessed for binding to human Fab by a quantitative ELISA, combined with a microscale affinity chromatography. Putative leads binding to Fab were screened against human Fc using a similar methodology. A limited number of ligands emerging from this strategy were then rescreened, by a standard affinity chromatographic assay, for their selectivity toward human Fab [18].

Biological activity assessment is also of crucial importance in the selection of leads for further optimization. Although often neglected in the screening process, a high activity recovery of the target protein should be obtained after the elution step in order to validate large-scale applications. Recently, triazine-scaffolded biomimetic ligands were assessed for their ability to bind a protein while, simultaneously, preserving its biological activity and enhancing its stability [29, 30]. In this study, a small lipolytic enzyme (cutinase) was used as a model protein. A dual screening of a biased solid-phase library enabled the selection of ligands binding cutinase with high affinity while retaining its functionality. When bound to different types of ligands, the enzyme showed markedly distinct activity retention profiles, with some synthetic ligands displaying a stabilizing effect on cutinase and others a clearly destabilizing effect, when compared with the free protein [29]. Thermostability

assessment with cutinase adsorbed to a lead compound at elevated temperatures highlighted the potential of biomimetic affinity ligands as a novel protein-stabilizing tool [30]. As a general strategy, designing and screening selective biomimetic affinity ligands that simultaneously have a stabilizing effect, may be useful either for the purification of proteins or the utilization of the macromolecular ligand-protein supports (e.g., as biocatalysts) under extreme and unfavorable conditions. Additionally, integration of purification and immobilization of proteins in a single step can bring an important advantage to some specific applications.

2 Materials

2.1 Design

1. Molecular modeling. Appropriate molecular modeling software is required. There is a wide range of commercially available software packages to perform molecular modeling studies that can be utilized [47]. An example is QUANTA2000 from Molecular Simulation Inc., which can run on a Silicon Graphics Octane MIPS RISC R12000 300 MHz workstation (e.g., used in the modeling of triazine-based ligands directed toward key surface residues in cutinase from Fusarium solani *pisi*. Some molecular modeling studies can also be complemented on standard desktop computers using Web LabViewerLite (www.msi.com), Swiss PDB Viewer 3.7 (http://www.expasy.ch/spdbv), and RasMol V2.7.1.1(www.umass.edu/microbio/rasmol/).

2.2 Syntheses

1. Cyanuric chloride (2,4,6-trichloro-1,3,5-triazine) with high-purity (99%) (*see* **Note 1**).
2. Epichlorohydrin (1-chloro-2,3-epoxypropane) with high purity (99%) (*see* **Note 2**).
3. Ammonium hydroxide 35% (v/v) (*see* **Note 3**).
4. 2,4,6-Trinitrobenzenesulfonic acid (TNBS) (*see* **Note 4**).
5. Ninhydrin (2,2-Dihydroxy-1,3-indanedione) (*see* **Note 5**).
6. Amines. The amines selected for the nucleophilic substitution of the chlorine atoms of cyanuric chloride should be handled according to their specific characteristics (*see* **Note 6**).
7. Chromatographic supports. Sepharose CL-6B is available from Sigma-Aldrich as a suspension in 20% (v/v) ethanol aqueous solution (*see* **Note 7**). Silica gel $60F_{254}$ thin layer chromatography (TLC) plates are available from Merck.
8. Instrumentation. For the synthesis of ligands, an incubator/shaker is necessary for the steps performed at 85 °C. A hybridization oven/shaker, for example, can be used for this

purpose. A rotary evaporator and respective pump are needed to dry the compounds synthesized by conventional organic synthesis. UV fluorescence from TLC plates should be observed in a TLC cabinet. A NMR spectrometer is needed to acquire the ^{1}H- and ^{13}C-NMR spectra. When possible, a melting point apparatus is used to determine the melting points of the synthesized compounds.

2.3 Screening and Characterization

2.3.1 Fluorescein-5-Isothiocyanate-Based Ligand Screening

1. Fluorescein-5-Isothiocyanate (FITC) isomer I conjugated target protein (*see* **Note 8**). Pre-conjugated protein may either be bought or must be conjugated using, for instance, the FluoroTag™ FITC conjugation kit from Sigma-Aldrich, following the instructions from the supplier. The conjugate is then separated from free FITC by fast gel filtration and fractions containing the conjugate are pooled. The fluorophore/protein (F/P) ratio is determined spectrophotometrically.
2. Sephadex G-25 column.
3. Glass slides.
4. Fluorescence microscope with a camera, an appropriate filter, and software to acquire fluorescence images.

2.3.2 Screening of Ligands by Affinity Chromatography

1. Binding and elution buffers. Appropriate buffers should be chosen according to the target protein (composition and pH should be adequate to retain its activity) and the type of affinity interaction with the ligands. For cutinase, for instance, 20 mM Tris–HCl pH 8.0 is used for binding and washing. Elution is performed by lowering the pH, using 0.1 M Glycine-HCl pH 2.5. Buffer 1 M Tris–HCl pH 9.0 is used to neutralize the elution fractions (*see* **Note 9**). For other target proteins and different types of affinity interactions, various elution strategies may be used such as by changing the pH, ionic strength, temperature, or adding a competitive molecule, for example, with the objective of disrupting the ligand-protein interactions releasing the protein to the mobile form while retaining its biological activity. Conditions must therefore be chosen on a case-by-case basis.
2. Regeneration solution. An aqueous solution containing 0.1 M NaOH in 30% (v/v) isopropanol is usually adequate to remove noncovalently attached ligands and proteins from the affinity matrix. It should be used before and after the screening procedure (*see* **Note 10**).
3. Chromatography columns. Disposable polypropylene 4 mL columns (e.g., Bond Elut TCA® with 20-μm frits from Varian, Inc) are suitable for the matrix volumes usually used for screening and for testing protein affinity purification from crude

extacts. If an automated chromatograph is used, the matrixes should be packed onto columns recommended by the supplier of the equipment.

4. Sodium dodecyl sulfate polyacrylamide gel electrophoresis (SDS-PAGE) for purity assessment. For the preparation of the stacking and resolving SDS-PAGE gels the following reagents/solutions are needed: stock solutions of Tris–HCl (1.0 M, pH 6.8 and 1.5 M, pH 8.8 respectively) (*see* **Note 11**), acrylamide/bis-acrylamide 40% (w/v) solution (*see* **Note 12**), sodium dodecyl sulfate (SDS) 10% (w/v) stock solution (*see* **Note 13**), *N,N,N′,N′*-Tetramethylethylenediamine (TEMED) (*see* **Note 14**), and ammonium persulfate (APS) 10% (w/v) solution (*see* **Note 15**).

Stacking and resolving gels are prepared in 5% and 15% (w/v) concentrations, respectively (*see* **Note 16**). Gels are polymerized in properly assembled cassettes [48]. For the preparation of the loading buffer, bromophenol blue, glycerol, SDS, 2 M Tris–HCl pH 6.8, and β-mercaptoethanol are used (*see* **Notes 16** and **17**).

SDS-PAGE molecular weight markers must be chosen with a range including the molecular weight of the target protein (e.g., Precision Plus Protein™ all blue (10–250 kDa) and the SDS-PAGE standard low range (14.4–97 kDa) from Bio-Rad).

SDS-PAGE and power supply apparatuses are available from Bio-Rad. An electrophoresis/gel imaging video capture system, including image analysis software, is also required (e.g., Stratagene Eagle Eye II Gel Imaging Still Video).

2.3.3 Enzyme-Linked Immunosorbent Assay

1. 96-well microplates for ELISA, e.g., from Nunc™.
2. Coating buffer (0.05 M Carbonate-Bicarbonate, pH 9.6) and blocking buffer (PBS with 0.05% (v/v) Tween 20) (*see* **Note 18**).
3. Antibody against the target protein (unlabeled or labeled with an enzyme) and an enzyme-conjugate secondary anti-antibody (in the case where an unlabeled primary antibody is used). The ELISA system has to be designed according to each situation.
4. Solution of the appropriate substrate for the enzyme chosen (e.g., 1 mg/mL *para*-nitrophenyl phosphate (*p*-NPP) in 0.1 M diethanolamine-HCl, pH 9.8, for alkaline phosphatase conjugates; 5 mM Na_2HPO_4, 2 mM citric acid, 1.85 mM *ortho*-phenylenediamine (oPD), and 0.04% (v/v) H_2O_2 for horseradish peroxidase conjugates—*see* **Note 19**).
5. ELISA microplate reader equipment.

2.3.4 Biological Activity Screening

The materials used will depend on the target protein and on the type of biological screening. We present the materials used for the biological activity screening of ligands targeted at an enzyme, cutinase, with the aim of binding the protein while preserving its

enzymatic activity [29, 30]. Such screening includes standard adsorption and activity assays performed with the enzyme bound to the ligand support. A similar activity screening assay with free enzyme can be used to monitor the biological activity recovered after the elution step on affinity chromatography.

1. Buffers. An appropriate buffer is needed to solubilize the enzyme during the several steps of the biological activity screening. Depending on the enzyme, buffers should be chosen in order to favor the binding to the ligand (note that pH is usually a critical parameter for ligand affinity). For cutinase, 20 mM Tris–HCl pH 8.0 (*see* **Note 20**) is a suitable buffer for adsorption and activity studies.
2. Enzyme substrate. An appropriate substrate must be chosen for the enzyme assay. Note that emulsifiers/detergents/solvents eventually required for the solubilization of substrates may desorb the enzyme from the ligand-derivatized support. Hence, their effect on the protein/ligand affinity should be tested on a case-by-case basis. For cutinase, *p*-nitrophenylacetate (*p*-NPA), solubilized in acetonitrile, is an adequate substrate.
3. Bicinchoninic acid (BCA) method for protein quantification. Depending on the protein concentration range, either the BCA™ Protein Assay kit (suitable for concentrations ranging from 20 to 2000 μg/mL) or the Micro BCA™ Protein Assay kit can be used (for concentrations between 2 and 40 μg/mL). The kits contain the necessary reagent solutions and are available from Thermo Scientific. Bovine serum albumin (BSA) standard solutions are also available from the same supplier. However, we recommend using the target protein itself (if available in a purified form) as a standard for its quantification to avoid errors due to protein-to-protein response variations. Nontreated 96-well clear microplates are necessary and are available from several suppliers such as Nunc™ plates from Thermo Scientific or BRANDplates® from Brandtech Scientific.
4. Instrumentation. Equipment for orbital agitation (e.g., a carousel-type rotating agitator) for the adsorption assay, and equipment for activity measurement (e.g., a spectrophotometer with stirring, temperature control and suitable cuvettes for colorimetric activity assays, and an automatic titrator for titrimetric assays). Microplate mixer/incubator and a microplate reader (absorbance) for the BCA protein quantification.

3 Methods

3.1 Library Design

Triazine-based ligands for specific proteins may be screened from rationally designed libraries or from random libraries.

Rational approaches make use of the knowledge derived from studies performed in silico. The de novo design of affinity ligands can be accomplished by studying the structure of the protein by accessing its 3D structure (X-ray crystallography, NMR, or homology structural data) or of a protein complex with a natural ligand (to be mimicked), available at the protein data banks, followed by choosing surface target regions, analysis of binding sites/potential interactions and designing complementary synthetic affinity ligands (mimicking the natural template or, in templateless approaches, interacting by affinity-like interactions with target exposed amino acids).

Key amino acid residues involved in the molecular recognition are used as the basis for the selection of analog compounds, which are commonly commercially available amines. The de novo designed triazine-based ligands are then docked to the putative binding sites containing the selected surface-exposed residues. Manual docking can be performed, for example, with Quanta 2000 software. This is done by placing the ligand in the vicinity of the binding site, adjusting its functional groups by turning and translational movements, in order to obtain the most convenient orientation to form hydrogen bonds. After energy minimization of the ligand-protein complex, the presence of hydrogen bonds is recorded and ligand structures, which were not able to maintain hydrogen bonds, are rejected.

Using random libraries for ligand screening can also lead to positive results. Mixed approaches, where the results from a rational library are combined with the results from a random screening to form a second-generation library, may also be used. For instance, by screening a library that had been designed to select leads for the purification of antibodies and related fragments [18], several ligands with high affinity for cutinase were found. This library is said to be random for cutinase, given that its construction did not have the interaction with this enzyme as a goal. The amines from the best binders of this library were combined with the amines of a rationally designed library for cutinase [28] to synthesize a second-generation combinatorial library from which several lead ligands could be selected [29].

3.2 Synthesis of a Solid-Phase Combinatorial Library of Ligands

1. Epoxy activation of Sepharose CL-6B. This procedure can be performed according to a protocol described in [21]. Sepharose CL-6B is washed thoroughly with distilled water on a sinter funnel to remove the storage ethanol solution. The gel is suspended in 0.8 mL of 1 M NaOH per gram of moist gel.

Epichlorohydrin is added in a proportion of 0.1 mL/g of gel and the mixture is incubated overnight with gentle agitation in a rotary shaker at 30 °C. Lower epoxy group densities can be obtained by stopping the reaction at different times, instead of letting the reaction proceed overnight to completeness. The activated gel is washed thoroughly with distilled water and used for the amination step. The epoxy content is determined according to **Note 21**.

2. Amination of epoxy-activated Sepharose CL-6B. This protocol is an adaptation of the procedure described in [18]. The washed epoxy-activated gel is suspended in 1.5 mL of ammonia per gram of moist gel. The slurry is incubated overnight at 30 °C with gentle agitation in a rotary shaker. The aminated support is washed thoroughly in a sinter funnel with distilled water to remove any traces of ammonia. Washing is performed until the pH in the washing solution is lowered to the pH of distilled water and no ammoniac odor can be detected. Aminated supports are either used immediately for activation with cyanuric chloride or stored in 20% (v/v) ethanol at 2–8 °C. The extent of amination is determined according to **Note 22**. To add a spacer arm between the ligand and the solid support, diamines with variable lengths may be used instead of ammonia in this step.
3. Activation of aminated Sepharose with cyanuric chloride. This methodology is an adaptation of various protocols described in the literature [15, 18, 19]. Aminated agarose is suspended in acetone/water 50% (v/v) (1 mL/g of gel). The slurry is maintained at 0 °C in an ice bath on a shaker. An amount corresponding to 5 molar equivalent of cyanuric chloride (relative to the extent of amination) is dissolved in acetone (8.6 mL/g of cyanuric chloride) and divided into four aliquots. Each aliquot is added to the aminated gel slurry with intervals of about 30 min, maintaining the mixture at 0 °C with constant shaking. The pH is monitored and maintained neutral by addition of a NaOH solution (1 M). The ninhydrin test (*see* **Note 23**) is used to confirm that the activation is complete. The gel is then washed with 2 × 10 gel volumes of each acetone/distilled water mixture (v/v)—1:1, 1:3, 0:1, 1:1, 3:1, 1:0—and then with abundant water to remove unreacted cyanuric chloride [34]. The cyanuric chloride activated gel is not stored but immediately used for the substitution of R_1.
4. Nucleophilic substitution of the second and third chlorine atoms of dichlorotriazinyl Sepharose. After the activation of aminated sepharose with cyanuric chloride, the second and third chlorines (in the R_1 and R_2 positions respectively) of the dichlorotriazinyl agarose are sequentially substituted with selected amines [28, 34]—*see* Fig. 7.

For the substitution with aminated compound R_1, the cyanuric chloride activated gel is divided into aliquots. Each aliquot is used for the substitution of the second available chlorine in the triazine ring with a different aminated compound. An amount corresponding to 2 molar equivalent of each amine (relative to the determined density of amine groups in the support) is dissolved in an appropriate solvent. The volume of the solvent used is 1 mL/g of gel. Each aliquot of dichlorotriazinyl agarose with the respective amine solution is then incubated at 30 °C for 24 h in a rotary shaker. After this period, each gel is thoroughly washed with an appropriate solvent on a sinter funnel. The R_1 monosubstituted gels are either stored in 20% (v/v) ethanol at 2–8 °C or used immediately for the substitution with amino compounds R_2.

The subsequent R_2 substitution is performed using the same amines (and respective solvents) as in the R_1 substitution, in a combinatorial way. For this step, a fivefold molar equivalent (relative to the determined density of amine groups in the support) of aminated compounds is used and the volume of the solvent is 3 mL/g of gel. The substitution is carried out in a rotary oven at 85 °C for 72 h. The gels are thoroughly washed with appropriate solvents and stored in 20% (v/v) ethanol at 2–8 °C.

3.3 Fluorescence-Based Screening of Ligand Libraries with FITC-Protein Conjugates

One possible method of ligand screening involves labeling the protein, for which we wish to select ligands for, with fluorescein isothiocyanate (FITC) and, after adsorption, imaging of the agarose ligand-derivatized beads by fluorescence microscopy (*see* **Note 24**).

1. FITC-labeling of protein. FITC of isomer I is among the most widely used fluorescent labeling reagents, and has a maximum absorption at 495 nm while proteins absorb mostly at 280 nm. FITC reacts with free protein amino groups to form stable conjugates. Conjugation kits (e.g., FluoroTag™ FITC Conjugation Kit from Sigma) are commercially available. The labeling with FITC is performed, by adding a solution containing FITC to a solution of protein, according to the instructions provided by the supplier. The mixture is then incubated for 2 h in the absence of light and with gentle stirring (orbital agitation).
2. Purification of the labeled protein. The labeled protein is purified from the unconjugated fluorescein by gel filtration using a quick Sephadex G-25 M column, according to the instructions provided with the conjugation kit. The mixture is loaded onto the column previously equilibrated with appropriate buffer. The column is then eluted with the buffer and 1 mL eluent fractions are collected. Absorbances at 280 and 495 nm are read. Fractions where curves of Abs 280 and 495 nm overlap are collected and the absorbances read again. The F/P molar ratio of a generic-labeled target protein is determined according to the following equation:

$$\text{Molar}\frac{F}{P} = \frac{\text{MW}_{\text{protein}}}{389} \times \frac{A_{495}/195}{A_{280} - [(0.35 \times A_{495})]/\varepsilon_{280}^{0.1\%}}.$$

where MW is the molecular weight of the protein, A is the absorbance of the conjugate (which must be measured at both 280 and 495 nm), and $\varepsilon_{280}^{0.1\%}$ is the absorption at 280 nm of the protein with a concentration of 1 mg/mL.

The FITC–protein conjugate can be stored at 4 °C in the absence of light for further use.

3. Fluorescence-based screening. The resins (including, as controls, Sepharose CL-6B, aminated agarose, and agarose derivatized with triazine ligand bis-substituted with ammonia) are washed with regeneration solution (0.1 M NaOH in 30% (v/v) isopropanol) and then with distilled water to neutralize the pH. After neutralization, resins are equilibrated in an adequate buffer (e.g., 20 mM Tris–HCl, pH 8.0, is used for cutinase [28] but according to the target protein, the most suitable buffer should be chosen). FITC conjugated protein (50 μL; 1 mg/mL in suitable buffer) is added to 50 μL of each resin and the mixtures are incubated in the absence of light for 15 min with orbital agitation. The resins are then washed with 3 × 1 mL of buffer (centrifuging and discarding the supernatant between each washing step) and each matrix is placed on a microscope slide and observed under a fluorescence microscope (FITC-λ_{exc} = 495 nm; λ_{em} = 525 nm). Fluorescence imaging is carried out for the labeled beads to be scored according to their fluorescence intensity.

3.4 Screening of Ligands by Affinity Chromatography

Affinity chromatographic assays are performed at room temperature.

1. The ligand-derivatized agarose gels are packed into 4 mL columns (0.5 mL of packed gel) and are washed with 3 × 2 mL regeneration solution (0.1 M NaOH in 30% (v/v) isopropanol), then with water to bring the pH to neutral and finally equilibrated with equilibration buffer.
2. For each matrix, 1 mL of the protein solution (0.5–1.0 mg/mL in binding buffer) is loaded to the column. Washing with equilibration buffer proceeds and 1 mL fractions are collected until the absorbance at 280 nm becomes $\leq$0.005.
3. Bound protein is eluted with a suitable buffer (0.1 M Glycine–HCl pH 2.5 is commonly used) until the absorbance at 280 nm becomes $\leq$0.005. Fractions of 1 mL are collected and, when a low pH elution buffer is used, the pH is immediately neutralized (100 μL of 1 M Tris–HCl pH 9.0 is adequate for the referred elution buffer). Percentages of bound and eluted protein are calculated by difference from the initially loaded amount.

4. After elution, the columns are regenerated with regeneration solution, followed by distilled water, and stored at 2–8 °C in 20% (v/v) ethanol.

Affinity chromatography can also be used to test a lead ligand for its selectivity for the target protein and its ability to purify the protein from crude extracts (*see* **Note 25** for an example regarding a lead ligand for cutinase).

3.5 Screening by a Quantitative Direct ELISA Assay Combined with a Microscale Affinity Chromatography

When an antibody that recognizes the target protein is available, an ELISA-based screening assay, combined with microscale affinity chromatography, can be performed (Fig. 8).

The procedure described was used in the screening of a combinatorial library of ligands mimicking Protein L-Ig interaction [18]. Affinity ligands showing more than 20% binding of loaded human IgG (by the standard chromatographic assay) were also screened for binding to human Fab. From those ligands binding more than 20% loaded human Fab, the affinity for human Fc was also assessed. Due to the high cost and limited availability of human IgG fragments, for the screening with Fab and Fc the chromatographic process was scaled-down by reducing the amount of

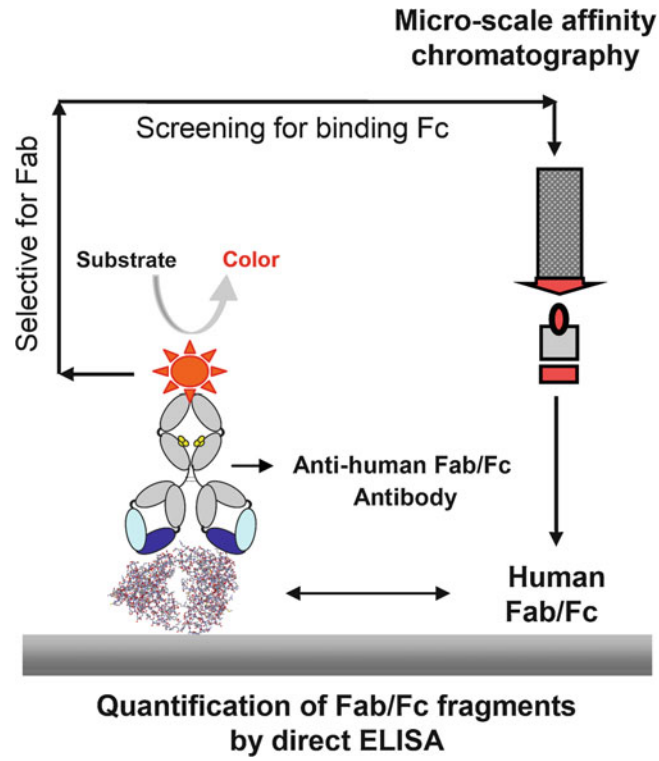

Fig. 8 Schematic representation of a screening strategy used in the assessment of a combinatorial library of ligands mimicking Protein L-Ig interaction to bind human IgG fragments (Fab and Fc)

resin (0.2 g rather than 1 g) and the amount of protein loaded (40 μg instead of 0.5 mg). Fractions of 250–500 μL were collected and neutralized with 25–50 μL of 1 M Tris–HCl pH 9.0. Since values of absorbance at 280 nm (A_{280}) measured on the spectrophotometer are not reliable if values inferior to 0.01 are obtained, in the microscale affinity chromatographic assay it is not possible to quantify protein bound and eluted by measuring A_{280}. A quantitative ELISA, using antibodies recognizing the target protein may be used instead. ELISA methods present several advantages when testing large numbers of samples due to high sensitivity and the possibility to use standard 96 microwell plates (*see* **Note 26**).

1. Samples collected from a microscale affinity chromatography assay are diluted 1:10 (*see* **Note 27**) in coating buffer (0.05 M Carbonate-Bicarbonate, pH 9.6) and 100 μL of each added to different wells of a 96 well ELISA plate. In the negative control, 100 μL of coating buffer is dispensed. Plates are incubated for 1 h at 37 °C or at 2–8 °C for 12 h.
2. After the incubation period, wells are washed 3× with PBS-Tween 20 (0.05% (v/v)) and PBS-Tween (200 μL) is added to each well as a blocking solution. The plates are kept for 1 h at room temperature and are washed again with 3× with PBS-Tween.
3. For colorimetric detection, 100 μL of a commercial enzyme-conjugated antibody specific for the target protein (*see* **Note 28**), diluted according to the instructions from the supplier, is added to each well. The plates are incubated for 1–2 h at room temperature, washed again 3× with PBS-Tween, and 100 μL of the appropriate substrate solution (to the enzyme conjugated with the antibody) is added to each well. The plates are incubated at room temperature in the dark until appropriate color intensity is developed (depending on the antibody and substrate utilized). For the HRP-conjugate assays, 50 μL of 2 M H_2SO_4 is added to each well after the incubation period, to stop the reaction. The absorbance in each well is then read at the specific wavelengths (405 nm for alkaline phosphatase conjugates and 490 nm for horseradish peroxidase conjugates). Calibration curves, to correlate the target protein and the absorbance at the specific wavelength, have to be constructed for each specific assay. The concentration range where a linear trend is observed depends on the commercial antibody used and has to be optimized on a case-to-case basis.

3.6 Biological Activity Screening

Besides showing affinity for a given target, ligands may be screened for retaining biological activity, under different conditions. If the target is an antibody to be purified with the aid of the synthetic ligand, the ability to recognize the antigen must be retained after

purification. Ligands may also be screened for binding and stabilizing an enzyme, such as cutinase, while retaining high enzymatic activity. In that case, a standard adsorption assay may be performed followed by an appropriate enzymatic activity assay [29].

1. Standard adsorption assay. An amount of 0.5 mL (moist gel) of each resin is washed with 3 × 2 mL of the regeneration solution (0.1 M NaOH in 30% (v/v) isopropanol), then with distilled water to bring the pH to neutral, and finally with 5 × 2 mL equilibration buffer (20 mM Tris–HCl, pH 8.0 for cutinase). A solution of protein (e.g., 1 mL of 0.5 mg/mL or 22 μM in equilibration buffer for cutinase) is added to each resin and the mixture is incubated for 15 min in a carousel-type rotating agitator. The liquid phase is separated and collected for protein determination. The resins are then washed (until no protein can be detected) with 1 mL fractions of buffer and the protein released is determined. Protein is measured by the absorbance of the different fractions at 280 nm or by another protein quantification method such as the bicinchoninic acid (BCA) method as described in **Note 29**. The percentage of adsorbed protein is calculated from the difference of the amount present in the initial stock solution and the amount released after adsorption/washing.
2. Activity assessment after ligand binding. Affinity synthetic ligands were shown to be potentially useful for enzyme immobilization and stabilization purposes [29, 30]. When that is the aim of a ligand screening, it is necessary to verify whether enzymatic activity is retained upon binding. A useful activity assay for cutinase, for example, is a spectrophotometric assay using *p*-nitrophenylacetate (*p*-NPA) as the substrate (*see* **Note 30**). A stock solution *p*-NPA is prepared in pure acetonitrile with a concentration of 150 mM. Activity assays are performed in 20 mM Tris–HCl pH 8.0, at 30 °C in a stirred cuvette, with a total reaction volume of 1.5 mL. The cutinase sample (a suspension of derivatized resin with adsorbed enzyme) is added to a final concentration of 16 nM. The reaction is initiated by the addition of 15 μL of the stock substrate solution. Release of *p*-nitrophenol is monitored by reading the absorbance at 400 nm ($\varepsilon = 15{,}400\ M^{-1}\ cm^{-1}$) [49], every 6 s, during one minute. The enzyme concentration falls on the range where the absorbance varies linearly in the time of the assay, and the enzyme activity is proportional to the amount of enzyme. One enzyme activity unit (U) under standard assay conditions is defined as the quantity of enzyme that catalyzes the formation of 1 μmol of *p*-nitrophenol per minute. The percentage of activity retention is measured by comparing the enzymatic activity before (a similar assay with free enzyme) and after binding.

3.7 Synthesis and Characterization of Lead Ligands: Solution-Phase Synthesis of Triazine-Based Ligands

After ligand screening, ligand leads are synthesized in the liquid phase and directly coupled to aminated sepharose for further studies.

The conditions for the solution synthesis of triazine-scaffolded ligands vary according to the ligand in question. We describe the synthesis of 4-({4-chloro-6-[(2-methylbutyl)amino]-1,3,5-triazin-2-yl}amino)benzoic acid (ligand 3′/11) as an example [30]. This ligand was selected to bind and simultaneously stabilize cutinase by affinity interactions. Characterization of the solution synthesized ligands can be performed by ^{1}H-NMR, ^{13}C-NMR, mass spectroscopy, and elemental analysis. The synthesis is performed using two sequential nucleophilic substitutions. The intermediate monosubstituted compounds (2-amino-4,6-dichloro-*s*-triazines) are often susceptible to hydrolysis [50], so care should be taken during handling and eventual storage. Particularly labile intermediate compounds should be immediately used in a subsequent reactional step. Regarding the reaction temperature of the second nucleophilic substitution (*see* **Note 31**).

1. Substitution with the least nucleophilic amine, 4-amino benzoic acid, to yield 4-[(4,6-dichloro-1,3,5-triazin-2-yl)amino] benzoic acid. A solution of 4-aminobenzoic acid (0.7442 g, 5.4 mmol) in 11 mL of cold acetone/water (1:1, (v/v)) is mixed with a solution of $NaHCO_3$ (0.4556 g, 5.4 mmol) in 11 mL of cold distilled water and kept in a flask in an ice bath. Cyanuric chloride (1 g, 5.4 mmol) is suspended in 13 mL of cold acetone and kept in the reaction vessel in an ice bath. The solution of 4-aminobenzoic acid and $NaHCO_3$ is added dropwise to the stirred suspension of cyanuric chloride. The reaction proceeds for 2 h and is followed by TLC using ethyl acetate/methanol (95:5, (v/v)) as the solvent system, until no cyanuric chloride is detected. The product is then filtered and washed. For labile intermediate products, which are not stored but rather used immediately for the subsequent reactional step, filtration/washing may be performed via a cannula with a paper filter fitted into the tip. This is done with no need to remove the product from the reaction flask and thus keeping it at 0 °C during these steps. A low temperature minimizes the possibility of hydrolysis of the remaining chlorines in the triazine ring, which can eventually happen at room temperature due to the aqueous reaction medium. The fact that the product is not removed from the reaction flask also helps to minimize product losses. In the case of 4-[(4,6-dichloro-1,3,5-triazin-2-yl)amino]benzoic acid, two washing steps are performed using a total amount of about 80 mL of a mixture acetone/water in the same proportions present in the reaction medium. After washing, the purity of the compound is verified by TLC to confirm that no free amine or cyanuric chloride is present.

2. Substitution with the most nucleophilic amine, 2-methylbutylamine, to yield 4-({4-chloro-6-[(2-methylbutyl)amino]-1,3,5-triazin-2-yl}amino)benzoic acid. A solution of 4-[(4,6-dichloro-1,3,5-triazin-2-yl)amino]benzoic acid (1.431 g, 5 mmol) in 21 mL of DMF is prepared in the reaction vessel. To this solution, an aqueous solution containing $NaHCO_3$ (0.4220 g, 5 mmol) and 2-methylbutylamine in slight excess (0.4848 g, 5.5 mmol) is added. The reaction proceeds at 30 °C and is stopped when no 4-[(4,6-dichloro-1,3,5-triazin-2-yl)amino]benzoic acid is detected in the mixture by TLC analysis using ethyl acetate/methanol (95:5, (v/v)) as the solvent system. The product is filtered with a Büchner funnel, washed thoroughly with distilled water, and dried under vacuum.

3.8 Direct Coupling of Solution-Phase Synthesized Ligands to Aminated Agarose

1. Aminated agarose (containing about 23 μmol amine groups/g moist weight gel) is added to a solution containing the ligand to be coupled (5 molar equivalent) and $NaHCO_3$ in an appropriate solvent, such as 50% (v/v) of DMF:H_2O. The number of equivalents of $NaHCO_3$ depends on the chemical nature of the substituents on the triazine ring (if there are acidic groups, for instance) and the objective is to favor the coupling by neutralizing the hydrochloric acid formed due to the substitution of a chlorine atom on the triazine ring. We found that an excess of $NaHCO_3$ (up to 10 molar equivalent) did not show any effect on the degree of substitution of the support with the ligand, however.
2. The reaction usually proceeds for 72 h at 85 °C in a rotary oven. Increasing the coupling time, however, may increase the degree of ligand coupling. After the reaction, the gel is sequentially washed with DMF:water (1:1; 1:0; 1:1, v/v) and then with abundant distilled water.
3. The resulting support is tested for free primary amino groups (*see* **Note 22**) and the ligand density is calculated (*see* **Note 32**). The resin is stored in ethanol 20% (v/v) at 2-8 °C.

3.9 Characterization of Affinity Interactions by Partition-Equilibrium Analysis

The affinity constants between the target protein and ligand-derivatized supports can be calculated using Scatchard plot analysis of the Langmuir type isotherms (obtained by partition assays). We present the partition of cutinase as an example [30]. For other target proteins, an appropriate buffer should be used and the concentration range may need to be adjusted.

1. Ligand-derivatized agarose gels are washed with regeneration solution (0.1 M NaOH in 30% (v/v) isopropanol), then with distilled water, and finally equilibrated with equilibration buffer (20 mM Tris–HCl, pH 8.0).

2. To an amount of 50 mg of each resin, 250 μL of the protein solution with concentrations in the range 1–25 mg/mL in (20 mM Tris–HCl, pH 8.0) is added. The suspensions are incubated at room temperature for 2 h in a carousel-type rotating agitator. The resins are then centrifuged at ca. 18,500 × *g* for 5 min and allowed do completely settle before the supernatant is carefully removed for protein determination. Protein can be determined by the BCA method (*see* **Note 29**). Adsorbed protein is calculated by difference between the initially added and the final measured amount.

4 Notes

1. Strongly reactive substance (including with water) should be stored in a dry environment between 2 and 8 °C. Hazards: very toxic/harmful by ingestion and inhalation. May cause severe burns when in contact with skin and eyes. Toxicity data: LD50 315 mg/kg oral, rat. Use protective clothes, gloves, facial/eye protection, and handle in a fume hood. Do not breathe fumes/dust.
2. Unstable compound. Store in a cool, dry, and well-ventilated environment. Hazards: Toxic by ingestion, inhalation, and skin contact. Carcinogen. Flammable. Toxicity data: LD50 90 mg/kg oral, rat. Use protective clothes, gloves, facial/eye protection, and handle in a fume hood.
3. Store in a cool, dry, and well-ventilated environment. Hazards: corrosive, can cause severe burns when in contact with skin and eyes. Toxicity data: LD50 350 mg/kg oral, rat. Use protective clothes, gloves, facial/eye protection, and handle in a fume hood. Do not breathe fumes.
4. Available from Sigma-Aldrich as a 5% (w/v) aqueous solution. Store at 2–8 °C. Harmful by ingestion. Corrosive. May cause burns when in contact with skin and eyes. Explosive when dry. Use protective clothes, gloves, and facial/eye protection avoiding contact with the skin.
5. Store in a cool and well-ventilated area protected from light (photosensitive compound). Harmful by ingestion. Irritant for the skin, eyes, and respiratory system. Toxicity data: LD50 600 mg/kg oral, rat. Use protection equipment including gloves.
6. Safety procedures must be followed according to the hazard and toxicity data for each compound. It should be noted that many amines are commercially available. If the amine needs to be synthesized, the synthetic strategy should take in consideration the need to protect reactive groups, if necessary.

7. Store at 2–8 °C. In order to maintain the integrity of the agarose beads, avoid handling procedures that involve mechanical shear forces such as magnetic stirring. Also, avoid prolonged dryness.
8. FITC and FITC-labeled protein should be kept and handled in the dark (aluminum foil may be used to protect these components from intense light).
9. Buffers are preferably freshly prepared. However, storage for a few days is possible at 2–8 °C to prevent microbial contamination.
10. Store regeneration solution at 2–8 °C. Hazards regarding the handling of isopropanol (2-propanol): flammable, irritant to the eyes, skin, and respiratory system. Do not inhale vapors. Toxicity data: LD50 5045 mg/kg oral, rat.
11. Store stock solutions at 2–8 °C.
12. Acrylamide/bis-acrylamide is sensitive to light and should be stored at 2–8 °C. Hazards regarding the handling of Acrylamide/bis-acrylamide: toxic, cancerigenous and teratogenic product, harmful if ingested, inhaled, and in contact with skin and eyes. It affects specific target-organs as a result of prolonged or repeated exposure. Toxicity data for acrylamide: LD50 124 mg/kg oral, rat.
13. Consider the following hazards when handling SDS: irritant to the eyes, skin, and respiratory tract. Do not inhale the dust. Toxicity data for SDS: LD50 1288 mg/kg oral, rat.
14. *N,N,N′,N′*-Tetramethylethylenediamine (TEMED) causes eye and skin burns, as well as severe digestive and respiratory tract burns. Flammable liquid and vapor. Harmful if inhaled or swallowed. May be absorbed through intact skin. Toxicity data for TEMED: LD50 268 mg/kg oral, rat.
15. Ammonium persulfate (APS) is hazardous in the case of skin contact (irritant, sensitizer), of eye contact (irritant), of ingestion, and of inhalation (lung irritant and sensitizer). Prolonged exposure may result in skin burns and ulcerations. Toxicity data for APS: LD50 689 mg/kg oral, rat.
16. For a stacking acrylamide gel with 5% (w/v) concentration use: 0.51 mL of stock acrylamide/bis-acrylamide (40% (w/v)), 0.5 mL of 1.0 M Tris–HCl, pH 6.8, 40 μL of SDS stock solution (10% (w/v)), 2.87 mL of distilled water, 5 μL of TEMED, and 40 μL of APS (10% (w/v)). For a resolving acrylamide gel with 15% (w/v) concentration use: 3.75 mL of stock acrylamide/bis-acrylamide (40% (w/v)), 2.5 mL of 1.5 M Tris–HCl, pH 8.8, 100 μL of SDS stock solution (10% (w/v)), 3.55 mL of distilled water, 4 μL of TEMED, and 100 μL of APS (10% (w/v)).

Loading buffer (12.5 mL of Tris–HCl, 2 M, pH 6.8, 2.2 g SDS, 11.5 mL glycerol, 0.01 g bromophenol blue, and 1 mL β-mercaptoethanol, for a 25 mL solution of a 4× concentrated buffer) is added to the samples (5 μL of loading buffer to 15 μL of sample), and the samples are boiled for 5 min. Samples are loaded onto each well of the gel and run at 90–120 V (electrophoresis buffer (2 L): 12 g Tris, 57.6 g glycine, and 2 g SDS). Once the run ends, the resolving gel is stained (0.1% (w/v) Coomassie brilliant blue in a 40% (v/v) ethanol and 10% (v/v) acetic acid solution) and then destained (10% (v/v) acetic acid and 30% (v/v) ethanol) until all bands are clearly visible on the gel.

17. β-mercaptoethanol is very hazardous in the case of skin contact (permeator), ingestion, and inhalation. Combustible substance. Toxicity data for β-mercaptoethanol: LD50 244 mg/kg oral, rat. Use protective clothes and gloves.
18. Store buffers at 2–8 °C.
19. Substrate solutions are light sensitive and should always be freshly prepared. In the case of oPD, H_2O_2 should be added right before use. Reactions for color development have to be undertaken in the dark.
20. Buffer solution (20 mM Tris–HCl pH 8.0) should be freshly prepared or stored at 4 °C for a few days.
21. The extent of epoxy activation is evaluated by estimation of the density of epoxy groups on the activated agarose support as described in [21]: 1 g of thoroughly washed and drained epoxy-activated gel is suspended in 3 mL of 1.3 M sodium thiosulfate solution and the mixture is incubated at room temperature for 20 min. The suspension is then titrated to pH 7.0 with 0.1 M HCl. The epoxy group density is calculated from the amount of titrant needed for the neutralization. Maximum epoxy contents of about 27 μmol/g moist weight gel are usually obtained, except when the ligand density is varied by controlling the time of epoxidation.
22. The extent of amination on Sepharose beads is determined by the density of primary amine groups on the aminated support, measured with a 2,4,6-trinitrobenzenesulfonic acid (TNBS)-based method. This method is based on the reaction of the matrix with excess of TNBS and, after removal of the solid phase, the spectrophotometric analysis of the remaining TNBS by reaction with glycine. The protocol is an adaptation of the one published by Antoni et al., which is suitable for the determination of free amino groups on solid insoluble supports [51]. To an amount of aminated gel containing not more than a total of 2–2.5 μmol of amino groups, 4.5 mL of 0.1 M sodium tetraborate ($Na_2B_4O_7$) and 0.5 mL of 0.01 M TNBS

are added. A reference sample, without the gel, is also prepared. After incubating for 2 h at 37 °C with agitation in a rotary shaker, the gel is centrifuged (5 min at ca. 4000 × *g*) and 0.5 mL of the supernatant solution is diluted with 2.5 mL of 0.1 M tetraborate, and 0.25 mL of 0.03 M glycine is added. For each sample (and each replicate), a blank is prepared composed of 0.5 mL of the supernatant and 2.5 mL of 0.1 M tetraborate, with 0.25 mL of water used instead of glycine. After 25 min at room temperature, 5 mL of cold methanol is added and the absorbance of each sample is determined against its own blank at 340 nm. The concentration of amino groups on the support is determined from the difference between the absorbances of each sample and the reference sample, using a molar absorption coefficient $\varepsilon = 1.24 \times 10^4\ M^{-1}\ cm^{-1}$ (for the trinitrophenyl derivative of glycine) [51]. For a gel epoxy activated overnight to the maximum extent, a value of about 23 μmol amine groups/gmoist weight gel is obtained.

23. A qualitative test can be used to detect the presence of primary amines in Sepharose beads. This test is useful to assess the extent of activation with cyanuric chloride or the presence of remaining free amine groups after the coupling of ligands. A small sample of gel is placed in a test tube and a few drops of a ninhydrin solution (0.2% (w/v) in ethanol) are added. The mixture is heated with hot air from a hairdryer. The development of purple color indicates the presence of free aliphatic amines since ninhydrin reacts with these groups originating a purple product (Ruhemann's purple) [52].
24. This qualitative screening methodology is reliable for the selection of strongly binding ligands, when compared with the quantitative methods, but tends to give false-positive results, thus increasing slightly the number of ligands selected to proceed for further assessment. However, false negatives are not observed. The occurrence of false positives does not appear to be related to the chemical structure of the tested compounds; this means that the method can be used to screen any bifunctional triazine-based solid-phase combinatorial library. Low F/P ratios are advisable, since this was shown to reduce the number of false positives detected. An optimal F/P ratio of 2 is recommended for distinguishing binding and nonbinding ligands with reproducible results [45].
25. Purification of cutinase from an impure extract by chromatography using a ligand-derivatized support was assessed with a ligand 11/3′ (symmetric of 3′/11) derivatized affinity adsorbent. The protocol used is similar to the one described for a standard affinity chromatographic assay. The column was connected to a peristaltic pump in order to maintain a constant flow rate (0.5 mL/min) and loaded with 15 mL of the cutinase

extract, which was obtained after osmotic shock of recombinant cutinase producing *E.coli* cells and partial purification by acid precipitation and dialysis. Impure extract, flow-through, washing, and elution fractions were subjected to sodium dodecyl sulfate polyacrylamide gel electrophoresis (SDS-PAGE) analysis in order to evaluate the selectivity of the ligand toward cutinase (*see* Fig. 5 and **Note 16**).

26. If desirable, some of the ligands showing high affinities to the target protein can be rescreened by scaling-up the process with the use of standard affinity chromatography, in order to validate the results from the microscale assay.
27. When necessary, some samples can be further diluted (1:20, 1:100, 1:400).
28. The procedure described is for a direct ELISA assay, which requires a specific antibody to the target protein labeled with an enzyme. This procedure can, however, be designed as an indirect ELISA assay. In such a case, the first incubation is performed with an unlabeled specific antibody (primary antibody) followed by the addition of a secondary enzyme-conjugated anti-antibody.
29. Protein concentrations can be determined in a microplate assay by the bicinchoninic acid (BCA) method patented by Pierce [53]. According to the range of concentrations required, either the BCA™ Protein Assay kit (suitable for concentrations ranging from 20 to 2000 μg/mL) or the Micro BCA™ Protein Assay kit can be used (for concentrations between 2 and 40 μg/mL). The detection reagents are prepared according to the instructions included in each kit: 50 parts of reagent A and 1 part of reagent B (for the standard BCA assay) or 25 parts of reagent A plus 24 parts of reagent B and 1 part of reagent C (for the Micro BCA assay). For protein determination using the BCA™ Protein Assay, sample volumes are usually either 25 or 50 μL, and the detection reagent volume is 200 μL. When using the Micro BCA™ Protein Assay, the sample volume is commonly 150 μL and the detection reagent volume is 150 μL. However, the volume ratio of the sample/detection reagent, as well as the incubation temperature and time, may be adjusted in order to shift the working concentration range.

    After adding both the sample and the detection reagent to each microplate well, the plate is thoroughly mixed for some seconds and then incubated for 30 min at 37 °C (in the case of the standard BCA assay) or 2 h at 37 °C (for the Micro BCA assay) in a plate mixer/incubator. After cooling to room temperature, absorbance is read at 562 nm in a microplate reader. Appropriate standard curves with bovine serum albumin (BSA)

or the pure target protein (when available) have to be constructed for each assay. Standards must always be prepared in the same buffer as the samples since the buffer strongly affects the results of BCA-based assays.

30. When choosing a suitable activity assay for a given enzyme, one should bear in mind that set-up conditions must guarantee the preservation of activity and prevent desorption of the protein from the support. Substrates toward which the enzyme/protein have high activity may not be the most suitable since very little amounts of adsorbed enzyme protein are needed and that may lead to measurement errors. That is the case with cutinase, which shows very high activity toward *p*-nitrophenylbutyrate (*p*-NPB). Hydrolysis of *p*-nitrophenylacetate (*p*-NPA), yielding *p*-nitrophenol and acetic acid, has been found to be a more suitable and still rapid activity assay, which does not require the use of emulsifiers/detergents (that may potentially desorb the enzyme from the ligand-derivatized support). Note that both *p*-NPB and *p*-NPA stock solutions should be stored at −20 °C and in the absence of light.
31. The substitution of the second chlorine atom in the triazine ring is reported at relatively high temperatures such as 50 °C [18, 36]. We found that for a highly nucleophilic amine such as 2-methylbutylamine, lower temperatures were adequate in order to prevent the substitution of the third available chlorine. For the synthesis of 6-chloro-*N*,*N*′-bis(2-methylbutyl)-1,3,5-triazine-2,4-diamine, the second substitution with 2-methylbutylamine was performed at a temperature as low as 4 °C, for instance. Therefore, the adequate temperature should be selected on a case-by-case basis.
32. Determination of ligand density in agarose beads. Ligand density in agarose derivatized beads can be determined by quantifying the remaining amine groups (*see* **Note 21**) and calculating the ligand density by difference (between the initial and final amounts of amine groups in the support).

References

1. Lowe CR, Burton SJ, Burton NP et al (1992) Designer dyes—biomimetic ligands for the purification of pharmaceutical proteins by affinity-chromatography. Trends Biotechnol 10:442–448
2. Roque ACA, Silva CSO, Taipa MA (2007) Affinity-based methodologies and ligands for antibody purification: advances and perspectives. J Chromatogr A 1160:44–55
3. Lowe CR, Lowe AR, Gupta G (2001) New developments in affinity chromatography with potential application in the production of biopharmaceuticals. J Biochem Bioph Meth 49:561–574
4. Lowe CR (2001) Combinatorial approaches to affinity chromatography. Curr Opin Chem Biol 5:248–256
5. Haeckel R, Hess B, Lauterbo W et al (1968) Purification and allosteric properities of yeast pyruvate kinase. H-S Z Physiol Chem 349:699–714
6. Garg N, Galaev IY, Mattiasson B (1996) Dye-affinity techniques for bioprocessing:

recent developments. J Mol Recognit 9:259–274
7. Clonis YD, Labrou NE, Kotsira VP et al (2000) Biomimetic dyes as affinity chromatography tools in enzyme purification. J Chromatogr A 891:33–44
8. Lowik DWPM, Lowe CR (2000) A stepwise synthesis of triazine-based macrocyclic scaffolds. Tetrahedron Lett 41:1837–1840
9. Kim JYH, Lee JW, Lee WS et al (2012) Combinatorial solid-phase synthesis of 4,6-diaryl and 4-aryl, 6-alkyl-1,3,5-triazines and their application to efficient biofuel production. ACS Comb Sci 14:395–398
10. Ye L, Xu AZ, Cheng C et al (2011) Design and synthesis of affinity ligands and relation of their structure with adsorption of proteins. J Sep Sci 34:3145–3150
11. Burton NP, Lowe CR (1992) Design of novel affinity adsorbents for the purification of trypsin-like proteases. J Mol Recognit 5:55–68
12. Labrou NE, Clonis YD (1995) Biomimetic dye affinity chromatography for the purification of bovine heart lactate dehydrogenase. J Chromatogr A 718:35–44
13. Labrou NE, Eliopoulos E, Clonis YD (1999) Molecular modeling for the design of a biomimetic chimeric ligand. Application to the purification of bovine heart L-lactate dehydrogenase. Biotechnol Bioeng 63:322–332
14. Li R, Dowd V, Stewart DJ et al (1998) Design, synthesis, and application of a protein A mimetic. Nat Biotechnol 16:190–195
15. Teng SF, Sproule K, Hussain A et al (1999) A strategy for the generation of biomimetic ligands for affinity chromatography. Combinatorial synthesis and biological evaluation of an IgG binding ligand. J Mol Recognit 12:67–75
16. Teng SF, Sproule K, Husain A et al (2000) Affinity chromatography on immobilized "biomimetic" ligands synthesis, immobilization and chromatographic assessment of an immunoglobulin G-binding ligand. J Chromatogr B 740:1–15
17. Roque ACA, Taipa MA, Lowe CR (2005) An artificial protein L for the purification of immunoglobulins and Fab fragments by affinity chromatography. J Chromatogr A 1064:157–167
18. Roque ACA, Taipa MA, Lowe CR (2005) Synthesis and screening of a rationally designed combinatorial library of affinity ligands mimicking protein L from *Pentostreptococcus magnus*. J Mol Recognit 18:213–224
19. Palanisamy UD, Hussain A, Iqbal S et al (1999) Design, synthesis and characterisation of affinity ligands for glycoproteins. J Mol Recognit 12:57–66
20. Palanisamy UD, Winzor DJ, Lowe CR (2000) Synthesis and evaluation of affinity adsorbents for glycoproteins: an artificial lectin. J Chromatogr B 746:265–281
21. Filippusson H, Erlendsson LS, Lowe CR (2000) Design, synthesis and evaluation of biomimetic affinity ligands for elastases. J Mol Recognit 13:370–381
22. Melissis SC, Rigden DJ, Clonis YD (2001) New family of glutathionyl-biomimetic ligands for affinity chromatography of glutathione-recognising enzymes. J Chromatogr A 917:29–42
23. Melissis S, Labrou NE, Clonis YD (2006) Nucleotide-mimetic synthetic ligands for DNA-recognizing enzymes—one-step purification of Pfu DNA polymerase. J Chromatogr A 1122:63–75
24. Batalha IL, Zhou H, Lilley K et al (2016) Mimicking nature: phosphopeptide enrichment using combinatorial libraries of affinity ligands. J Chromatogr A 1457:76–87
25. Santos R, Figueiredo C, Viecinski AC et al (2019) Designed affinity ligands to capture human serum albumin. J Chromatogr A 1583:88–97
26. Sproule K, Morrill P, Pearson JC et al (2000) New strategy for the design of ligands for the purification of pharmaceutical proteins by affinity chromatography. J Chromatogr B 740:17–33
27. Morrill PR, Gupta G, Sproule K et al (2002) Rational combinatorial chemistry-based selection, synthesis and evaluation of an affinity adsorbent for recombinant human clotting factor VII. J Chromatogr B 774:1–15
28. Ruiu L, Roque ACA, Taipa MA et al (2006) De novo design, synthesis and screening of a combinatorial library of complementary ligands directed towards the surface of cutinase from *Fusarium solani* pisi. J Mol Recognit 19:372–378
29. Sousa IT, Ruiu L, Lowe CR et al (2009) Synthetic affinity ligands as a novel tool to improve protein stability. J Mol Recognit 22:83–90
30. Sousa IT, Lourenco NMT, Afonso CAM et al (2013) Protein stabilization with a dipeptide-mimic triazine-scaffolded synthetic affinity ligand. J Mol Recognit 26:104–112
31. Sousa IT (2011) A novel tool to improve protein stability: synthesis and screening of triazine-scaffolded affinity ligands to bind and stabilise cutinase. Doctoral thesis. Universidade Técnica de Lisboa, Lisbon

32. Platis D, Sotriffer CA, Clonis Y et al (2006) Lock-and-key motif as a concept for designing affinity adsorbents for protein purification. J Chromatogr A 1128:138–151
33. Platis D, Maltezos A, Ma JKC et al (2009) Combinatorial de novo design and application of a biomimetic affinity ligand for the purification of human anti-HIV mAb 4E10 from transgenic tobacco. J Mol Recognit 22:415–424
34. Roque ACA (2004) Design, synthesis and evaluation of immunoglobulin binding ligands: an artificial protein L. Doctoral thesis. Universidade Técnica de Lisboa, Lisbon
35. Creveld LD, Amadei A, van Schaik RC et al (1998) Identification of functional and unfolding motions of cutinase as obtained from molecular dynamics computer simulations. Proteins 33:253–264
36. Ruiu L (2008) *De novo* design, synthesis and screening of combinatorial libraries of affinity ligands directed towards the surface of cutinase from *Fusarium solani pisi*. Doctoral thesis. Universidade Técnica de Lisboa, Lisbon
37. Lam KS, Salmon SE, Hersh EM et al (1991) A new type of synthetic peptide library for identifying ligand-binding activity. Nature 354:82–84
38. Qian J, El Khoury G, Issa H et al (2012) A synthetic Protein G adsorbent based on the multi-component Ugi reaction for the purification of mammalian immunoglobulins. J Chromatogr B 898:15–23
39. El Khoury G, Lowe CR (2013) A biomimetic protein G adsorbent : an Ugi ligand for immunoglobulins and Fab fragments based on the third IgG-binding domain of Protein G. J Mol Recognit 26:190–200
40. Chen C, El Khoury G, Lowe CR (2014) Affinity ligands for glycoprotein purification based on the multi-component Ugi reaction. J Chromatogr A 969:171–180
41. Pina AS, Dias AMGC, Ustok FI et al (2015) Mild and cost-effective green fluorescent protein purification employing small synthetic ligands. J Chromatogr A 1418:83–93
42. Pina AS, Carvalho S, Dias AMGC et al (2016) Tryptophan tags and *de novo* designed complementary affinity ligands for the expression and purification of recombinant proteins. J Chromatogr A 1472:55–65
43. Langer T, Wolber G (2004) Virtual combinatorial chemistry and in silico screening: efficient tools for lead structure discovery? Pure Appl Chem 76:991–996
44. Zamolo L, Busini V, Moiani D et al (2008) Molecular dynamic investigation of the interaction of supported affinity ligands with monoclonal antibodies. Biotechnol Prog 24:527–539
45. Roque ACA, Taipa MA, Lowe CR (2004) A new method for the screening of solid-phase combinatorial libraries for affinity chromatography. J Mol Recognit 17:262–267
46. Pina AS, Lowe CR, Roque ACA (2010) Comparison of fluorescence labelling techniques for the selection of affinity ligands from solid-phase combinatorial libraries. Sep Sci Technol 45:2187–2193
47. Taipa MA (2014) Affinity separations. rational design, synthesis and evaluation: affinity ligands. In: Reedijk J (ed) Elsevier reference module in chemistry, molecular sciences and chemical engineering. Elsevier, Waltham, MA. https://doi.org/10.1016/B978-0-12-409547-2.10738-3
48. Walker JM (1996) SDS polyacrylamide gel electrophoresis of proteins. In: Walker JM (ed) The protein protocols handbook. Humana, Totowa, NJ, pp 55–62
49. Goncalves AM, Serro AP, Aires-Barros MR et al (2000) Effects of ionic surfactants used in reversed micelles on cutinase activity and stability. BBA-Protein Struct M 1480:92–106
50. Thurston JT, Dudley JR, Kaiser DW et al (1951) Cyanuric chloride derivatives. 1. Aminochloro-S-triazines. J Am Chem Soc 73:2981–2983
51. Antoni G, Presentini R, Neri P (1983) A simple method for the estimation of amino groups on insoluble matrix beads. Anal Biochem 129:60–63
52. West R (1965) Siegfried ruhemann and discovery of ninhydrin. J Chem Educ 42:386–387
53. Smith PK, Krohn RI, Hermanson GT et al (1985) Measurement of protein using bicinchoninic acid. Anal Biochem 150:76–85

Chapter 15

Synthesis and Evaluation of Dye-Ligand Affinity Adsorbents for Protein Purification

Evangelia G. Chronopoulou, Georgios Premetis, Christina Varotsou, Nikolaos Georgakis, Elisavet Ioannou, and Nikolaos E. Labrou

Abstract

Dye-ligand affinity chromatography is a widely used technique in protein purification. The utility of the reactive dyes as affinity ligands results from their unique chemistry, which confers wide specificity toward a large number of proteins. They are commercially available, inexpensive, stable and can easily be immobilized. Significant factors that contribute to the successful operation of a dye-ligand chromatography include matrix type, dye-ligand density, adsorption along with elution conditions and flow rate. The present chapter provides protocols for the synthesis of dye-ligand affinity adsorbents as well as protocols for screening, selection, and optimization of a given dye-ligand purification step. The purification of the glutathione transferases from *Phaseolus vulgaris* on Cibacron Blue 3GA-Sepharose affinity adsorbent is given as an example.

Key words Affinity chromatography, Cibacron Blue 3GA, Dye-ligand chromatography, Glutathione transferase, Triazine dyes

1 Introduction

Dye-ligand chromatography is a convenient affinity chromatography able to address different needs of protein purification [1–6]. Specifically, this type of chromatography is based on the pseudoaffinity between protein and synthetic dyes that mimic the structural features of natural ligands (substrates, cofactors, vitamins, etc.) [6–10].

Complex combination of electrostatic, hydrophobic and hydrogen-bonding interactions can manipulate dye-ligand binding on proteins either specifically at the protein's binding site or nonspecifically at the cavities or patches on the protein surface [5, 7, 11–13]. Recently, molecular dynamic (MD) simulations have been used to study the interaction between human and bovine serum albumins with Cibacron Blue dye and the mechanism of molecular

Nikolaos E. Labrou (ed.), *Protein Downstream Processing: Design, Development, and Application of High and Low-Resolution Methods*, Methods in Molecular Biology, vol. 2178, https://doi.org/10.1007/978-1-0716-0775-6_15,

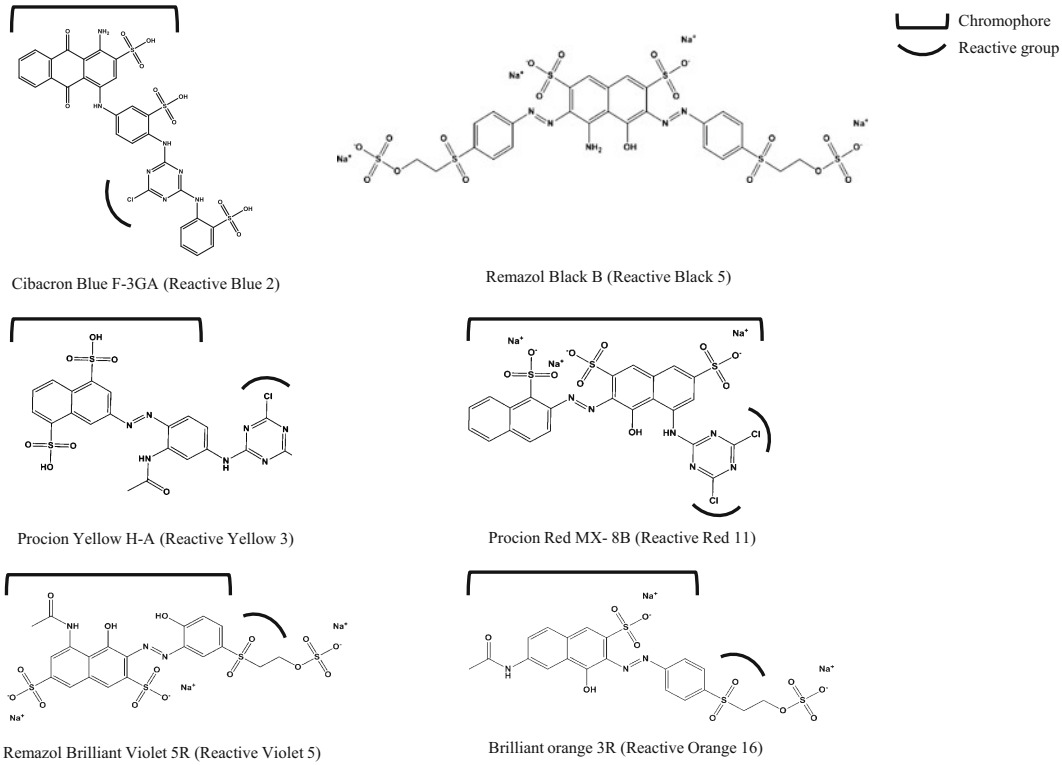

Fig. 1 Structure of some dye ligands

recognition under different pH and salt conditions [11]. Several dye-ligand affinity adsorbents have been used for the isolation of a variety of proteins, including dehydrogenases, kinases, phosphotransferases, plasma or serum proteins, and several others [3, 7, 10, 12, 14]. Some of these, such as Cibacron Blue 3GA or Procion Blue, have been shown to display high affinity for enzymes requiring adenylyl-containing cofactors [e.g., NAD(H), NADP(H)] [13, 15–23]. Most of these reactive dyes consist of the chromophore and the reactive group; the chromophore can be azo dye, anthraquinone or phathalocyanine that is joined via an amino bridge with a reactive group like a mono- or dichlorotriazine ring, vinylsulfone or trichloropyrimidine (example structures are shown in Fig. 1) [24, 25]. The reactive unit provides the site for covalent attachment to the insoluble support. The first and most successful reactive group that was explored in dye chemistry was cyanuric chloride (1,3,5-sym-trichlorotriazine) [13, 16, 17].

Dye ligands display several advantages compared to specific biological ligands due to their easy immobilization, high chemical and biological stability, high binding capacity and low cost (Table 1) [11]. Factors such as adsorbent properties, immobilized ligand density, adsorption and elution conditions, steric hindrance, temperature, flow rate, and column geometry [3, 11, 12, 18, 22]

Table 1
Advantages of dye-ligand affinity adsorbents

Advantages
Low cost
Readily available in bulk quantities
High chemical stability over a range of pH conditions
Resistant to biological degradation
Easily coupled to matrices via reactive groups
Display high binding capacity for a wide range of proteins
Wide structural diversity can offer a library of different matrices

contribute to the successful operation of a dye-ligand chromatographic step. Specific eluents and structural-based designs of new dye ligands can address the need for improved affinity and specificity [10, 11, 23, 26–30]. Additionally, nanomaterials or magnetic microspheres can be used in dye affinity chromatography for less time-consuming protein purification procedures [12, 31, 32].

The present chapter describes protocols for the synthesis of dye-ligand affinity adsorbents using as a model the widely used triazine dye Cibacron blue 3GA as well as protocols for screening, selection, and optimization of a dye-ligand purification step.

2 Materials

2.1 Dye Purification and Characterization

1. Cibacron blue 3GA (Sigma-Aldrich).
2. Diethyl ether.
3. Acetone.
4. Analytical TLC plates (e.g., 0.2 mm silica gel-60, Merck).
5. Sephadex LH-20 column (2.5 cm × 30 cm). Sephadex LH-20 is available from Sigma-Aldrich.
6. Whatman filter paper, hardened ashless, Grade 542, diameter: 70 mm.
7. Methanol/H_2O (50/50, v/v).
8. Solvent system for TLC: butan-1-ol/propan-2-ol/ethyl acetate/H_2O (2/4/1/3, v/v/v/v).
9. Reverse-phase HPLC column (e.g., C18 S5 ODS2 Spherisorb silica column, 250 mm × 4.6 mm, Gilson, USA).
10. *N*-Cetyltrimethylammonium bromide, (CTMB, HPLC grade, Sigma-Aldrich).

11. Solvent A: methanol/0.1% (w/v) aqueous CTMB (80/20, v/v), solvent B: methanol/0.1% (w/v) aqueous CTMB (95/5, v/v).
12. 0.45-μm cellulose membrane filter (e.g., Millipore).

2.2 Direct Dye Immobilization

1. Agarose-based support (e.g., Sepharose CL6B, Sigma-Aldrich).
2. Solid Na_2CO_3.
3. 22% (w/v) NaCl solution.
4. 1 M NaCl solution.
5. DMSO/H_2O 50% (v/v) solution.

2.3 Synthesis of 6-Aminohexyl Derivative of Cibacron Blue 3GA

1. Cibacron blue 3GA (Sigma-Aldrich).
2. 1,6-Diaminohexane.
3. Solid NaCl.
4. Concentrated HCl.
5. 1 M HCl solution.
6. Acetone.

2.4 Immobilization of 6-Aminohexyl-Cibacron Blue 3GA to Sepharose

1. Sepharose CL6B (Sigma-Aldrich).
2. Water/acetone (2:1, v/v), water/acetone (1:2, v/v).
3. Dried acetone.
4. 1,1-Carbonyldiimidazole.
5. DMSO/water (50/50, v/v).
6. 2 M Na_2CO_3 solution.

2.5 Determination of Immobilized Dye Concentration

1. 5 M HCl.
2. 10 M NaOH.
3. 1 M Potassium phosphate buffer, pH 7.6.

2.6 Dye Screening: Selection of Dyes as Ligands for Affinity Chromatography

1. Dye-ligand affinity adsorbents: a selection of immobilized dye adsorbents (0.5–1 mL) with different immobilized dye, packed in small chromatographic columns (0.5 cm × 5 cm). Adsorbent screening kits with prepacked columns are available commercially (e.g., Sigma-Aldrich).

2.7 Regeneration and Storage of Dye-Ligand Adsorbents

1. Sodium thiocyanate solution (3 M).
2. Aqueous ethanol solution, 20% (v/v).

2.8 Purification of Phaseolus vulgaris Glutathione Transferases on Cibacron Blue 3GA-Sepharose Affinity Adsorbent

1. *Phaseolus vulgaris* seeds (the common bean).
2. Mortar (diameter: 10 cm) and pestle.
3. Potassium phosphate buffer, 20 mM, pH 6.0.
4. Cibacron Blue 3GA-Sepharose column (1 mL).
5. Cheesecloth.
6. Cellulose filter (0.45-μm pore size).
7. Glutathione solution (10 mM) in 20 mM potassium phosphate buffer, pH 6.0.
8. Sodium thiocyanate (3 M) solution.

3 Methods

Analytical-grade chemicals and double-distilled water were used to prepare the buffers for ligand immobilization and affinity chromatography. All buffers were stored at 4 °C.

3.1 Dye Purification and Characterization

Commercial dye preparations are highly heterogeneous mixtures and are known to contain added buffers, stabilizers, and organic by-products [20, 21]. The following purification protocol, based on Sephadex LH-20 column chromatography, usually gives satisfactory purification (>95%) (*see* **Note 1**):

1. Dissolve 500 mg of crude dye (e.g., Cibacron blue 3GA, purity ~60%) in 40 mL deionized water.
2. Extract the solution twice with diethyl ether (2 × 50 mL) and concentrate the aqueous phase approximately three fold using a rotary evaporator.
3. To the aqueous phase, add 100 mL of cold acetone (−20 °C) to precipitate the dye.
4. Filter the precipitate through Whatman filter paper and dry it under reduced pressure.
5. Dissolve 100 mg dried dye in water/methanol (5 mL, 50/50, v/v) and filter the solution through a 0.45-μm cellulose membrane filter.
6. Load the dye solution on a Sephadex LH-20 column (2.5 cm × 30 cm), which has been previously equilibrated in water/MeOH (50/50, v/v). Develop the column isocratically at a flow rate of 0.1 mL/min/cm.
7. Collect fractions (5 mL) and analyze by TLC using the solvent system: butan-1-ol/propan-2-ol/ethyl acetate/H_2O (2/4/1/3, v/v/v/v). Pool the pure fractions containing the desired dye and concentrate the solution by 60% using a rotary evaporator under reduced pressure (50 °C). Lyophilize and store the pure dye powder desiccated at 4 °C.

Analysis of dye preparations may be achieved by HPLC on a C18 reverse-phase column (e.g., C18 ODS2 Spherisorb, Gilson, USA) using the ion-pair reagent *N*-cetyltrimethylammonium bromide (CTMB) [21].

1. Equilibrate the column using the solvent system methanol/0.1% (w/v) aqueous CTMB (80/20, v/v) at a flow rate of 0.5 mL/min.
2. Prepare dye sample as 0.5 mM solution in the above system. Inject sample (10–20 μmol).
3. Develop the column at a flow rate of 0.5 mL/min using the following gradient: 0–4 min 80% B, 4–5 min 85% B, 5–16 min 90% B, 16–18 min 95% B, 18–30 min 95% B. Elution may be monitored at both 220 and 620 nm.

3.2 Direct Dye Immobilization

Two different procedures have been used for dye immobilization to polyhydroxyl matrices: direct coupling of dyes via the chlorotriazine ring and coupling via a spacer molecule (Fig. 2) [15, 18, 19]. A hexamethyldiamine spacer molecule may be inserted between the ligand and the matrix. This leads to an increase in dye selectivity by reducing steric interference from the matrix backbone [15]. A hexyl spacer may be inserted by substitution of 1,6-diaminohexane at one of the chlorine atoms of the triazinyl group and the dye-spacer conjugate may be immobilized to 1,1-carbonyldiimidazole-activated agarose (*see* **Note 2**).

1. To prewashed agarose gel (1 g), add a solution of purified dye (1 mL, 4–30 mg dye/g gel, *see* **Note 3**) and 0.2 mL of NaCl solution (22% w/v).
2. Leave the suspension shaking for 30 min at room temperature (*see* **Note 4**).

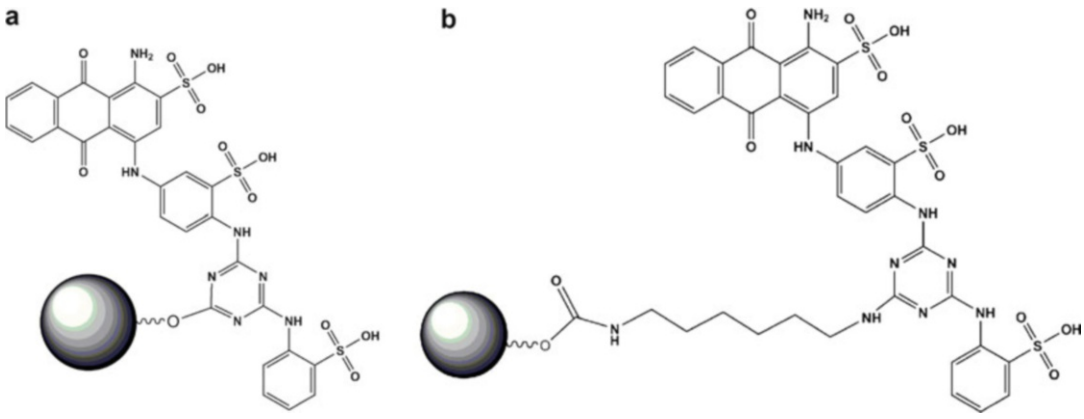

Fig. 2 Immobilization of chlorotriazine anthraquinone dyes. (**a**) Direct coupling via the chlorotriazine ring, (**b**) coupled to 1,1-carbonyldiimidazole-activated agarose by a triazine ring-coupled 6-aminohexyl spacer arm

3. Add solid sodium carbonate at a final concentration of 1% (w/v) (*see* **Note 4**).
4. Leave the suspension shaking at 60 °C for 4–8 h for monochlorotriazine dyes, and at room temperature for 5–20 min for dichlorotriazine dyes.
5. After completion of the reaction (*see* **Note 5**), wash the dyed gel to remove unreacted dye sequentially with water (100 mL), 1 M NaCl (50 mL), 50% (v/v) DMSO (10 mL), 1 M NaCl (50 mL), and finally water (100 mL).

3.3 Synthesis of 6-Aminohexyl Derivative of Cibacron Blue 3GA

1. To a stirred solution of 1,6-diaminohexane in water (6 mmol, 10 mL), add a solution of purified dye (0.6 mmol, 25 mL) in water and increase temperature to 60 °C.
2. Leave the mixture stirring for 3 h at 60 °C.
3. Add solid sodium chloride to a final concentration of 3% (w/v) and allow the solution to cool at 4 °C.
4. Add concentrated HCl to reduce the pH to 2.0. Filter off the precipitated product and wash it with hydrochloric acid solution (1 M, 50 mL), acetone (50 mL), and dry under vacuum.

3.4 Immobilization of 6-Aminohexyl-Cibacron Blue 3GA to Sepharose

Sepharose CL6B first is activated with 1,1-carbonyldiimidazole to facilitate the immobilization of 6-aminohexyl dye analog.

1. Wash agarose (1 g) sequentially with water/acetone (2:1, v/v; 10 mL), water/acetone (1:2, v/v; 10 mL), acetone (10 mL), and dried acetone (20 mL).
2. Resuspend the gel in dried acetone (5 mL) and add 0.1 g of 1,1-carbonyldiimidazole. Agitate the mixture for 15–20 min at 20–25 °C.
3. Wash the gel with dried acetone (50 mL). Add a solution of 6-aminohexyl Cibacron Blue 3GA (0.1 mmol) in DMSO/water (50/50, v/v, 4 mL), the pH of which has been previously adjusted to 10.0 with 2 M Na_2CO_3.
4. Shake the mixture overnight at 4 °C. After completion of the reaction, wash the gel as in Subheading 3.2, **item 1**.

3.5 Determination of Immobilized Dye Concentration

Determination of immobilized dye concentration may be achieved by spectrophotometric measurement of the dye released after acid hydrolysis of the gel.

1. Suspend 30 mg of dyed gel in hydrochloric acid solution (5 M, 0.6 mL) and incubate at 70 °C for 3–5 min.
2. To the hydrolysate, add NaOH (10 M, 0.3 mL) and potassium phosphate buffer (1 M, pH 7.6, 2.1 mL).
3. Read the absorbance of the hydrolysate at 620 nm against an equal amount of hydrolyzed unsubstituted gel. Calculate the

concentration of the immobilized dye as micromoles of dye/g wet gel.

3.6 Dye Screening: Selection of Dyes as Ligands for Affinity Chromatography

Dye-ligand affinity chromatography is an empirical approach to protein purification, and one cannot easily predict whether a specific protein will bind or not to a certain dye column. Thus, for efficient use of this technique, a large number of different dye adsorbents need to be screened to evaluate their ability to bind and purify a particular protein [15, 16, 18, 19].

1. Degas the adsorbents to prevent air bubble formation, and pack them into individual columns of 0.5–1 mL bed vol.
2. Dialyze the protein sample against 50 vol. of equilibration buffer. Alternatively, this can be achieved using a desalting Sephadex G-25 gel-filtration column.
3. Filter the protein sample through 0.4-μm pore-sized filter or centrifuge to remove any insoluble material.
4. Wash the dye adsorbents with 10 bed vol. of equilibration buffer. Load 0.5–5 mL of the protein sample (*see* **Note 6**) to the columns at a linear flow rate of 10–20 cm/mL.
5. Wash nonbound proteins from the columns with 10 bed vol. of equilibration buffer. Collect nonbound proteins in one fraction.
6. Elute the bound proteins with 5 bed vol. of elution buffer (*see* **Note 7**) and collect the eluted protein in a fresh new tube as one fraction.
7. Assay both fractions for enzyme activity and for total protein.
8. Determine the capacity, purification factor, and recovery achieved with each column. The best dye adsorbent is the one that combines highest capacity, purification, and recovery (*see* **Note 8**).

3.7 Optimization of a Dye-Ligand Purification Step

After a dye-ligand adsorbent has been selected from a dye-screening procedure (Subheading 3.6), optimization of the chromatographic step can be achieved by improving the loading and elution conditions using a small-scale column (1 mL).

The capacity of the dye-adsorbent (optimal column loading) for the target protein can be determined by frontal analysis [16, 18, 19]. This is achieved by continuous loading of the sample solution onto the column until the desired protein is detected in the eluate. The optimal loading is equivalent to 85–90% of the sample volume required for frontal detection of the desired protein.

Attention should be paid to variables such as pH, buffer composition and ionic strength of the equilibration buffer in order to maximize protein binding. In general, low pH (pH < 8.0) and ionic strength (10–50 mM), absence of phosphate ions, and the

presence of divalent metal ions such as Mg^{+2}, Mn^{+2}, Ca^{+2} may increase binding (*see* **Note 9**) [22].

A simple test-tube method can be performed to determine the optimal starting pH and ionic strength of the equilibration buffer.

1. Set up five 1-mL columns. Equilibrate each adsorbent with a different pH buffer of the same ionic strength (e.g., 20 mM). Use a range from pH 6–8 in 0.5 pH unit intervals.
2. Load each column with sample and wash them with 5–10 bed vol. of equilibration buffer.
3. Elute the protein with 5 bed vol. of 1 M KCl and collect the eluted protein as one fraction.
4. Assay for protein and enzyme activity.
5. Determine the capacity of each column and the purification achieved.

When the optimum pH has been established, the same experimental approach may be followed to determine which ionic strength buffer can be used to achieve optimal purification and capacity. Use a range of ionic strength buffers with 10-mM intervals.

Special consideration should be given to the elution step in dye-ligand affinity chromatography. Selective or nonselective techniques may be exploited to elute the target protein [22]. Nonselective techniques (increase salt concentration, pH or reduce the polarity of the elution buffer by adding ethyleneglycol or glycerol at concentrations of 10–50%, v/v) normally give moderate purification (*see* **Note 10**). Selective elution is achieved by using a soluble ligand (e.g., substrate, product, cofactor, inhibitor, allosteric effector), which competes with the dye for the same binding site on the protein. This technique, although more expensive than nonselective methods, in general, provides a more powerful purification.

The selection of a suitable competing ligand is critical and often must be done empirically in small test columns using a number of substrates, cofactors, inhibitors or in some instances a suitable combination of these [5]:

1. Load a 1-mL column with sample and wash with 5–10 bed vol. of equilibration buffer.
2. Wash the column with a buffer of an ionic strength just below that required to elute the protein of interest to remove undesired proteins.
3. Elute the desired protein with 3 bed vol. of equilibration buffer containing appropriate concentration of a specific ligand (*see* **Note 11**).
4. Collect fractions and assay for protein and enzyme activity.

5. Evaluate the effectiveness of each specific ligand by determining the purification and recovery achieved.

3.8 Regeneration and Storage of Dye-Ligand Adsorbents

Dye-ligand adsorbents may be effectively regenerated by applying 3 column volumes of chaotropic solutions of urea or guanidine hydrochloride (6–8 M) or sodium thiocyanate (3 M). In some instances, where sterilizing and removing of pyrogens from the chromatographic columns is desired, regeneration with 1 M NaOH may be achieved. After regeneration, wash the column with 10 bed vol. water and finally with 20% (v/v) aqueous ethanol solution and store at 4 °C.

3.9 Purification of Phaseolus vulgaris Glutathione Transferases on Cibacron Blue 3GA-Sepharose Affinity Adsorbent

Using this protocol, the isoenzymes of glutathione transferase (GST, EC 2.5.1.18) from *Phaseolus vulgaris* can be purified. The optimum buffers for GSTs binding and elution on Cibacron Blue 3GA-Sepharose were established according to Protocol in Subheading 3.7. All procedures were performed at 4 °C.

1. Soak *Phaseolus vulgaris* seeds (5 g) overnight in water.
2. Decant the water and transfer the seeds to the mortar with 15 mL of potassium phosphate buffer, pH 6.0 (20 mM). Crush the plant seeds in the mortar with the pestle. Squeeze the homogenate through cheesecloth and collect the extract in a beaker.
3. Clarify the extract by centrifugation (14,000 × *g*, 15 min). Collect the supernatant and clarify by filtration through a cellulose filter (0.45-μm pore size).
4. Equilibrate the adsorbent (Cibacron Blue 3GA-Sepharose, 1 mL) with 10 bed vol. of 20 mM potassium phosphate buffer, pH 6.0.
5. Apply the extract (~4 mL) to the affinity adsorbent (1 mL, 5 μmol immobilized dye/g wet gel).
6. Wash off nonadsorbed protein with equilibration buffer (~10 mL). This washing step removes unbound and weakly bound soluble contaminants from the chromatographic bed. Washing of the adsorbent is performed by pumping starting buffer through the bed until the UV signal from the column effluent returns close to the baseline. This requires approximately 7-bed vol. of buffer.
7. Elute the bound GSTs with the equilibration buffer (20 mM potassium phosphate buffer, pH 6.0) containing 10 mM reduced glutathione (10 mL). Collect 1 mL fractions.
8. Assay for GST activity and protein. The protein content of each fraction may be estimated by the Bradford method [33]. Assay of enzyme activity may be achieved according to [34].
9. Regenerate the adsorbent by applying 3 bed vol of sodium thiocyanate (3 M).

4 Notes

1. Alternatively, purification may be accomplished by preparative TLC on Kieselgel 60 glass plates (Merck) using a solvent system comprising butan-1-ol/propan-1-ol/ethyl acetate/water 2/4/1/3 [23]. A typical protocol is as follows: Dissolve crude dye (approx. 50 mg) in water (0.5 mL). Apply the solution as a narrow strip onto the TLC plate and chromatograph at room temperature. Dry the plate and scrape off the band of interest. Elute the dye from the silica with distilled water, filter through 0.45-μm cellulose membrane filter and lyophilize.
2. Immobilized ligand concentration plays an important role in dye-ligand affinity chromatography. This should be rigorously defined since this parameter determines the strength of the interaction between the macromolecule and immobilized dye as well as the capacity of the adsorbent for the target protein [19, 26]. High ligand concentrations do not necessarily translate into equally high capacity for the target protein, since extreme levels of ligand substitution may lead to no binding due to the steric effect caused by a large number of dye molecules or even to nonspecific protein binding [19, 26]. On the other hand, low levels of ligand substitution reduce the capacity of the absorbent. An optimum ligand concentration, which combines both specific protein binding and high capacity, falls in the range of 2.0–3.0 μmol dye/g wet gel [15, 16, 18, 19, 27].
3. The amount of dye and the reaction time required to effect immobilized dye concentration in the range of 2.0–3.0 μmol dye/g gel depend on the chemical nature of the dye (e.g., dichlorotriazine dyes in general are more reactive than monochlorotriazines; thus, less dye and shorter reaction times are required). In the case of biomimetic dyes, the nature of terminal biomimetic moiety (aliphatic or aromatic substituent) influences the electrophilicity of the triazine chloride and thus the reaction time [18].
4. This short incubation and the presence of electrolyte (e.g., NaCl) during the immobilization reaction are used in order to "salt out" the dye molecules onto the matrix and to reduce hydrolysis of the triazine chloride by the solvent. The presence of sodium carbonate provides the alkaline pH (pH 10–11) necessary during the immobilization reaction in order to activate the hydroxyl group of the matrix to act as a nucleophile. The dye can be attached either by hydroxyl ions leading to favorable dye hydrolysis or by carboxydrate-O^- ions resulting in dye immobilization.

5. In the case of dichlorotriazine dye immobilization, residual unreacted chlorines in the coupled dye may be converted to hydroxyl groups by incubating the matrix at pH 8.5 at room temperature for 2–3 days or to amino groups by reaction with 2 M NH_4Cl at pH 8.5 for 8 h at room temperature [15, 18].
6. The total protein concentration of the applied sample may vary enormously. Ideally, 20–30 mg total protein/mL of absorbent in a volume of 1–5 mL should be applied to each column, assuming that the target protein constitutes 1–5 mg of the total protein. Column overloading should be avoided since it reduces the purifying ability of the absorbent, unless protein-protein displacement phenomena occur in the adsorption step. Such phenomena have been demonstrated, for example, during the purification of formate, lactate, and malate dehydrogenase on immobilized biomimetic dyes [18, 19, 27].
7. Elute binds protein either nonspecifically with high salt concentration (e.g., 1 M KCl) or specifically by inclusion in the buffer of a soluble ligand that competes with dye for the same binding site of the protein (e.g., 5 mM NAD^+, NADH, ATP, an inhibitor, a substrate). Salt elution leads to practically total protein desorption; therefore, the technique reveals the adsorbent's affinity during the binding process. According to the type of interaction between protein and dye, the elution conditions can be modified by varying pH and ionic strength or by adding nondenaturing solvents (e.g., ethylene glycol, glycerol) or chaotropic agents (urea, guanidine) [4, 7]. Specific elution of the protein provides information on the ability of the bound enzyme to elute biospecifically, leaving unwanted protein bound [18, 19, 27, 29].
8. Another procedure for screening dye-ligand adsorbents is dye-ligand centrifugal affinity chromatography [28]. This method is based on centrifugal column chromatography and uses centrifugal force rather than gravity to pass solutions through a column. Using this technique, a large number of dye columns can be screened simultaneously and has been shown to be both satisfactory and faster compared with conventional gravity flow dye-ligand chromatography.
9. Normally raising the pH of the starting or eluting buffer will weaken the binding of proteins to dye-ligand adsorbents [22]. Below pH 6.0, many proteins will begin to bind nonspecifically due to ionic effects. Metal cations often promote binding of proteins to triazine dyes, and may be added at concentrations in the range of 0.1–10 mM [22]. Metal ion precipitation can be a problem; therefore, the appropriate conditions should be followed [25].

10. Considering the type of dye-ligand and protein interactions, nonselective elution can be performed by modifying the elution buffer in each case. Electrostatic interactions can be distorted by increasing the pH, while hydrophobic interactions can be perturbed by using ethylene glycol or glycerol (about 10–50% v/v) in the elution buffer [25]. Elution by reducing the polarity of eluent often gives broad peak profiles compared to salt or pH elution.
11. The required concentration of competing ligand may vary from 1 μM to 25 mM, but most have been found to be in the range of 1–5 mM [3, 15, 16, 18, 19, 27]. Gradient elution is not usually as effective as stepwise elution because it broadens the elution peaks. However, such gradients can be used to determine the lowest required soluble ligand concentration for effective elution of the protein of interest.

Acknowledgments

EI acknowledges the State Scholarships Foundation (IKY) for financial support. This research is co-financed by Greece and the European Union (European Social Fund- ESF) through the Operational Programme "Human Resources Development, Education and Lifelong Learning" in the context of the project "Strengthening Human Resources Research Potential via Doctorate Research" (MIS-5000432), implemented by the State Scholarships Foundation (IKY).

References

1. Eisele T, Stressler T, Kranz B, Fischer L (2012) Automated multi-step purification protocol for angiotensin-I-converting-enzyme (ACE). J Chromatogr B Analyt Technol Biomed Life Sci 911:64–70
2. Clonis YD, Labrou NE, Kotsira V, Mazitsos C, Melissis S, Gogolas G (2000) Biomimetic dyes as affinity chromatography tools in enzyme purification. J Chromatogr A 891:33–44
3. Labrou NE, Mazitsos K, Clonis YD (2005) Dye-ligand and biomimetic affinity chromatography. In: Hage DS (ed) Handbook of affinity chromatography. Marcel Dekker, Inc, New York, NY, pp 231–255
4. Gallant SR, Koppaka V, Zecherle N (2008) Dye ligand chromatography. In: Zachariou M (ed) Affinity chromatography. Methods in molecular biology™. Humana, Totowa, NJ, pp 61–70
5. Chronopoulou EG (2018) Column chromatography overview: an evolving method in protein purification. In: Labrou N, Chronopoulou E, Ataya F (eds) Handbook on protein purification: industry challenges and technological developments. Nova Science Publishers, Inc., New York, NY, pp 1–17
6. Marinou M, Platis D, Ataya FS, Chronopoulou E, Vlachakis D, Labrou NE (2018) Structure-based design and application of a nucleotide coenzyme mimetic ligand: application to the affinity purification of nucleotide dependent enzymes. J Chromatogr A 1535:88–100
7. Kumar S, Punekar NS (2014) High-throughput screening of dye-ligands for chromatography. In: Labrou N (ed) Protein downstream processing. Methods in molecular

biology (methods and protocols). Humana, Totowa, NJ, pp 53–65
8. Labrou NE (2014) Protein purification: an overview. In: Labrou N (ed) Protein downstream processing, Methods in molecular biology (methods and protocols), vol 1129. Humana, Totowa, NJ, pp 3–10
9. Gianazza E, Arnaud P (1982) Chromatography of plasma proteins on immobilized Cibacron Blue F3-GA. Mechanism of the molecular interaction. Biochem J 203:637–641
10. Andac M, Galaev I, Denizli A (2012) Dye attached poly(hydroxyethyl methacrylate) cryogel for albumin depletion from human serum. J Sep Sci 35:1173–1182
11. Liang-Schenkelberg J, Fieg G, Waluga T (2017) Molecular insight into affinity interaction between cibacron blue and proteins. Ind Eng Chem Res 56:9691–9697
12. Wang SSS, Yang SM, Hsin A, Chang YK (2018) Dye-affinity nanofibrous membrane for adsorption of lysozyme: preparation and performance evaluation. Food Technol Biotechnol 56:40–50
13. Maltezos A, Platis D, Vlachakis D, Kossida S, Marinou M, Labrou NE (2014) Design, synthesis and application of benzyl-sulfonate biomimetic affinity adsorbents for monoclonal antibody purification from transgenic corn. J Mol Recogn 27:19–31
14. Jahanshahi M, Najafpour G (2007) Advanced downstream processing in biotechnology. In: Najafpour GD (ed) Biochemical engineering and biotechnology. Elsevier, Amsterdam, pp 390–415
15. Burton SJ, Stead CV, Lowe CR (1988) Design and application of biomimetic dyes II: the interaction of C.I. reactive blue 2 analogs bearing terminal ring modifications with horse liver alcohol dehydrogenase. J Chromatogr 455:201–206
16. Lindner NM, Jeffcoat R, Lowe CR (1989) Design and application of biomimetic dyes: purification of calf intestinal alkaline phosphatase with immobilized terminal ring analogs of C.I. Reactive Blue 2. J Chromatogr 473:227–240
17. Labrou NE, Eliopoulos E, Clonis YD (1996) Molecular modelling for the design of chimaeric biomimetic dye-ligands and their interaction with bovine heart mitochondrial malate dehydrogenase. Biochem J 315:695–703
18. Katsos NE, Labrou NE, Clonis YD (2004) Interaction of L-glutamate oxidase with triazine dyes: selection of ligands for affinity chromatography. J Chromatogr B Analyt Technol Biomed Life Sci 807:277–285
19. Labrou NE, Clonis YD (1995) Biomimetic-dye affinity chromatography for the purification of bovine heart lactate dehydrogenase. J Chromatogr 718:35–44
20. Labrou NE, Clonis YD (1995) The interaction of *Candida boidinii* formate dehydrogenase with a new family of chimeric biomimetic dye-ligands. Arch Biochem Biophys 316:169–178
21. Burton SJ, McLoughlin SB, Stead V, Lowe SR (1988) Design and application of biomimetic dyes I: synthesis and characterization of terminal ring isomers of C.I. reactive Blue 2. J Chromatogr 435:127–137
22. Scopes RK (1986) Strategies for enzyme isolation using dye-ligand and related adsorbents. J Chromatogr 376:131–140
23. Kuralay F, Yılmaz E, Uzun L, Denizli A (2013) Cibacron Blue F3GA modified disposable pencil graphite electrode for the investigation of affinity binding to bovine serum albumin. Colloids Surf B Biointerfaces 110C:270–274
24. Kirchberger J, Böhme HJ (2000) Dye-ligand affinity chromatography. In: Kastner M (ed) Journal of chromatography library. Elsevier, New York, NY, pp 415–448
25. Denizli A, Piskin E (2001) Dye-ligand affinity systems. J Biochem Biophys Methods 49:391–416
26. Boyer PM, Hsu JT (1992) Effects of ligand concentration on protein adsorption in dye-ligand adsorbents. Chem Eng Sci 47:241–251
27. Labrou NE, Clonis YD (1995) Biomimetic-dye affinity chromatography for the purification of L-malate dehydrogenase from bovine heart. J Biotechnol 45:185–194
28. Berg A, Scouten WH (1990) Dye-ligand centrifugal affinity chromatography. Bioseparation 1:23–31
29. Labrou NE (2003) Design and selection of affinity ligands for affinity chromatography. J Chromatogr B 790:67–78
30. Doğan A, Özkara S, Sarı MM, Uzun L, Denizli A (2012) Evaluation of human interferon adsorption performance of Cibacron Blue F3GA attached cryogels and interferon purification by using FPLC system. J Chromatogr B Analyt Technol Biomed Life Sci 893–894:69–76
31. Li Z, Cao M, Zhang W, Liu L, Wang J, Ge W, Yuan Y, Yue T, Li R, Yu WW (2014) Affinity adsorption of lysozyme with Reactive Red 120 modified magnetic chitosan microspheres. Food Chem 145:749–755
32. Ng IS, Song CP, Ooi CW, Tey BT, Lee YH, Chang YK (2019) Purification of lysozyme

from chicken egg white using nanofiber membrane immobilized with Reactive Orange 4 dye. Int J Biol Macromol 134:458–468

33. Bradford MM (1976) Rapid and sensitive method for the quantitation of microgram quantities of protein utilizing the principle of protein-dye binding. Anal Biochem 72:248–254

34. Chronopoulou E, Madesis P, Asimakopoulou B, Platis D, Tsaftaris A, Labrou NE (2012) Catalytic and structural diversity of the fluazifop-inducible glutathione transferases from *Phaseolus vulgaris*. Planta 235:1253–1269

Chapter 16

Design of Affinity Chromatography Peptide Ligands Through Combinatorial Peptide Library Screening

G. R. Barredo, S. L. Saavedra, M. C. Martínez-Ceron, S. L. Giudicessi, M. M. Marani, F. Albericio, O. Cascone, and S. A. Camperi

Abstract

In this chapter, a protocol to design affinity chromatography matrices with short peptide ligands immobilized for protein purification is described. The first step consists of the synthesis of a combinatorial peptide library on the hydroxymethylbenzoyl (HMBA)-ChemMatrix resin by the divide–couple–recombine (DCR) method using the Fmoc chemistry. Next, the library is screened with the protein of interest labeled with a fluorescent dye or biotin. Subsequently, peptides contained on positive beads are identified by tandem matrix-assisted laser desorption/ionization time-of-flight mass spectrometry (MALDI-TOF MS/MS), and those sequences showing greater consensus are synthesized in larger quantities and immobilized on chromatographic supports. Finally, target protein adsorption on peptide affinity matrices is evaluated through equilibrium adsorption isotherms and breakthrough curves.

Key words Peptide ligand, Solid-phase peptide synthesis, One-bead one-peptide, Combinatorial libraries, ChemMatrix resin, Tandem-mass spectrometry

1 Introduction

Affinity chromatography relies on the specific interactions between an immobilized ligand and a target protein [1]. The availability of a selective ligand is critical to obtain a highly pure protein from a complex mixture in a single step. Small peptides consisting of a few amino acids represent promising affinity ligand candidates for industrial separations. Peptideligands are much more physically and chemically stable than antibodyligands and are more resistant to proteolytic cleavage. They can be readily synthesized by standard chemistry, in bulk amounts, and at a lower cost under good manufacturing practices (GMPs). Furthermore, peptides allow site-directed immobilization and high ligand density, and the matrices are more robust during elution and regeneration than

Nikolaos E. Labrou (ed.), *Protein Downstream Processing: Design, Development, and Application of High and Low-Resolution Methods*, Methods in Molecular Biology, vol. 2178, https://doi.org/10.1007/978-1-0716-0775-6_16,

protein-based affinity matrices such as those with monoclonal antibodies as ligands.

The combinatorial synthesis of peptide libraries allows obtaining millions of peptides with varied chemical properties and functional groups, thus greatly facilitating the discovery of suitable affinity ligands for any given protein of interest [2].

Among the solid-phase strategies available for library preparation, the divide–couple–recombine (DCR) method, also known as the split-and-mix method, is the most advantageous [3, 4]. This approach entails the following: (1) dividing the solid support (resin beads) into equal portions, (2) coupling each portion individually with a different building block (amino acid), and (3) mixing the portions. This procedure assures a theoretically even representation of the library members and a "one-bead one-compound" distribution. The composition and final structure of the peptide library depend on the number of amino acids used in each coupling cycle and the number of coupling cycles performed. For statistical reasons, the number of beads must exceed the number of peptides that compose the library by a factor of at least 10. Therefore, the number of building blocks and the length of the peptides should be designed to obtain a one-bead-one-peptide library of a size that could be easily manipulated. Cysteine is often omitted from the synthesis of linear peptide libraries to avoid the complication of intrachain and/or interchain cross-linking.

To screen these combinatorial libraries, tens of thousands to millions of compound beads are first mixed with the probe molecule. The beads that interact with it will be identified and then isolated for compound structure determination. A reporter group such as a fluorescent dye is conjugated to probe molecules that cannot be detected directly. Finally, the sequence of peptides contained on positive beads is determined. Although peptides traditionally can be identified by Edman microsequencing, this method is time consuming and expensive. Here we describe a rapid and inexpensive strategy using matrix-assisted laser desorption/ionizationtime-of-flight mass spectrometry (MALDI-TOF MS) for identifying the peptides on positive beads. The cornerstone of this methodology is the choice of the solid support and linker to be used. Herein, a strategy based on the ChemMatrix [5] solid support together with 4-hydroxymethylbenzoic acid (HMBA) linker [6] is described. ChemMatrix resin is compatible with both organic and aqueous solvents, which are used for the peptide synthesis and for the screening step, respectively, and therefore it is highly suitable for the whole process. The bond formed between the first amino acid and the linker HMBA is stable to all synthetic elongation reactions as well as to the conditions required for the removal of the side-chain-protecting groups. The solid support is amenable to easy release of the peptide for mass spectrometry (MS) analysis [7, 8]. For peptides shorter than six amino acids, Ala

and/or Gly residues may be introduced in the C termini to increase their molecular weight in order to facilitate MS analysis. This also overcomes the poor cleavage efficiency of esters of Ile and Val [9] and behaves as a spacer arm to facilitate the effective binding between the target protein and the ligand when the binding site of the protein is within the clefts and cavities of the molecule.

Those peptides showing greater consensus are synthesized and immobilized on a chromatography matrix to optimize the purification by affinity chromatography of the target protein.

2 Materials

For all solid-phase reactions [solid-phase peptide synthesis (SPPS), combinatorial library synthesis, and peptideligand coupling on chromatographic supports], Bond Elut Empty SPE Cartridges and 20-μm polypropylene frits may be acquired from Varian Inc. or Agilent Technologies. Otherwise, chromatography tubes or polyethylene syringes fitted with polypropylene porous disk home-made with a hole puncher may be used (Fig. 1).

Vacuum manifolds to evacuate the fluids from each syringe by filtration can be obtained from different suppliers (e.g., Promega, Supelco, Phenomenex) (Fig. 2).

The reaction vessels can be gently agitated on a shaker table during the reactions.

Prepare and store all reagents at room temperature (unless indicated otherwise).

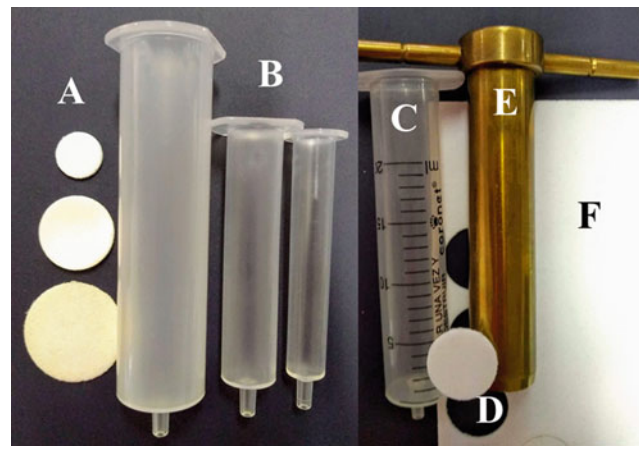

Fig. 1 Vessels and frits for solid-phase reaction: (**a**) 20-μm polypropylene frits, (**b**) Bond Elut Empty SPE Cartridges, (**c**) polyethylene syringe, (**d**) home-made frit, (**e**) hole puncher (**f**) polypropylene

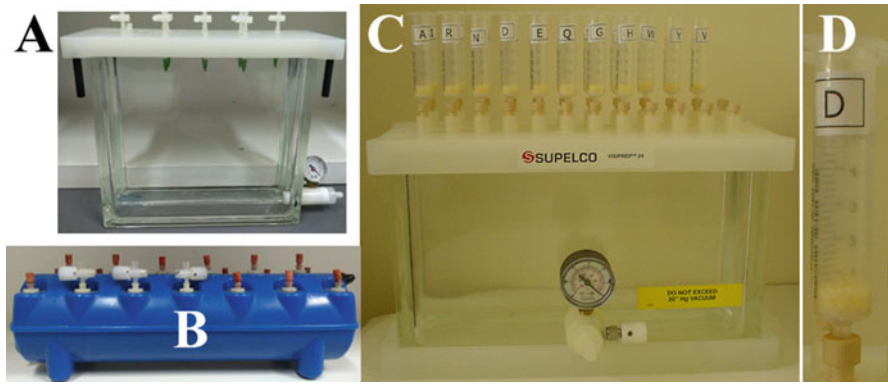

Fig. 2 Systems to evacuate the fluids from each reaction vessel by filtration (**a**) SPE Vacuum manifold (Phenomenex), (**b**) Vac-Man® Laboratory Vacuum Manifold (Promega), (**c**) SPE Vacuum manifold (Supelco), (**d**) Reaction vessel connected to the vacuum manifold

2.1 Reagents and Equipment for the Combinatorial Peptide Library Synthesis

1. 4-Hydroxymethylbenzoic acid (HMBA), aminomethyl-ChemMatrix resin (0.64 mmol/g), hydroxymethylbenzoic-ChemMatrix resin (HMBA-CM) (35–100 mesh, 0.64 mmol/g) (Merck) (*see* **Note 1**).
2. Fluorenylmethoxycarbonyl amino acids (Fmoc-amino acids) with side-chain-protecting groups, *N*-hydroxybenzotriazole (HOBt), OxymaPure (ethyl 2-cyano-2-(hydroxyimino)-acetate), 2-(1H-Benzotriazole-1-yl)-1,1,3,3-tetramethylaminium tetrafluoroborate (TBTU), and benzotriazol-1-yl-oxytripyrrolidinophosphonium hexafluorophosphate (PyBOP) may be obtained from many different suppliers, such as Peptides International, IRIS Biotech GmbH, Bachem, Merck, MatrixInnovation Inc., among others.
3. *N,N*-diisopropylethylamine (DIPEA), 4-(*N,N*-dimethylamino)pyridine (DMAP), 1,3-diisopropylcarbodiimide (DIC), dimethylformamide (DMF), dichloromethane, piperidine, trifluoroacetic acid (TFA), triisopropyl silane (TIS), acetic anhydride (Ac_2O), methanol (MeOH), and diethyl ether may be obtained from many different chemical suppliers.
4. 1 M HCl, NaOH (1 M)/DMF (1:1), DMF/H_2O (1:1). Store at room temperature.
5. Reagent for Fmoc removal: 20% (v/v) piperidine in DMF. Store at room temperature.
6. Cleavage cocktail: TFA/TIS/H_2O (95:2.5:2.5). Prepare just before use (*see* **Note 2**).

2.2 Solutions and Equipment for Ninhydrin Test or Kaiser Test [10]

1. Ninhydrin reactive solution A_1: 40 g phenol in 10 mL of ethanol.
2. Ninhydrin reactive solution A_2: 2 mL of 0.001 M KCN in 98-mL of pyridine.
3. Ninhydrin reactive solution A: A_1/A_2 (1:1). Store protected from light at room temperature.
4. Ninhydrin reactive solution B: 5% (w/v) ninhydrin in ethanol. Store protected from light at room temperature.
5. Heater.

2.3 Solutions and Reagent for Chloranil Test [11] (See Note 3)

1. Saturated chloranil solution in toluene: mix in a conical centrifuge microtube (Eppendorf) approximately 25 mg of chloranil and 1 mL of toluene. Centrifuge and recover the supernatant. Store light protected at 2–8 °C.
2. Acetone.

2.4 Protein Label with Texas Red [12, 13] (See Note 4) or Biotin [14, 15]

1. Texas Red sulfonyl chloride, EZ-Link™ Sulfo-NHS-Biotin (Thermo Fisher Scientific) (*see* **Note 5**).
2. Conjugation buffer: 0.1 M $Na_2CO_3/NaHCO_3$, pH 9.0. Store at 2–8 °C.
3. Phosphate-buffered saline (PBS): 4.4 mM KH_2PO_4, 5.5 mM Na_2HPO_4, 150 mM NaCl, pH 6.8. Store at 2–8 °C.
4. Desalting column: Column containing a size-exclusion matrix with a 5000-Da exclusion limit (PD-10 desalting columns, GE Healthcare).

2.5 Solutions and Equipment for One-Bead One-Peptide Library Screening

1. PBS 10×: 44 mM KH_2PO_4, 55 mM Na_2HPO_4, 1.5 M NaCl, pH 6.8. Store at 2–8 °C.
2. Blocking library solution: 10% (w/v) skim milk, 2% (w/v) bovine serum albumin (BSA) in PBS. Prepare just before use.
3. PBS-Tween: 0.05% (v/v) Tween 20 in PBS. Store at 2–8 °C.
4. Probe protein coupled with Texas Red or biotin.
5. Streptavidine-peroxidase conjugated (SA-POD).
6. Reactive peroxidase solutions (prepared just before use): A) 3 mg 4-chloro-1-naphthol in 1 mL CH_3OH, B) 4-mL PBS containing 20 μL of 30 vol H_2O_2 (*see* **Note 6**).
7. Fluorescent stereoscopic microscope (Leica, Zeiss).
8. COPAS BIO-BEAD flow-sorting equipment (Union Biometrica).
9. COPAS GP Sheath reagent (Union Biometrica).

2.6 Solution and Solvents for Bead Washing After Screening

1. H_2O.
2. Acetic acid (AcOH)/acetonitrile (MeCN)/H_2O (3:4:3).
3. MeCN.
4. CH_2Cl_2.

2.7 Solutions and Equipment for PeptideCleavage and Elution from the Bead

1. Drying chamber.
2. Microcentrifuge.
3. NH_4OH 30% (v/v).
4. AcOH/MeCN/H_2O (3:4:3) (v/v).

2.8 MALDI MSSequencing

1. CHCA matrix solution: α-cyano-4-hydroxycinnamic acid (CHCA) 4 mg/mL in MeCN/H_2O (1:1) with 0.1% (v/v) TFA. Prepare just before use.
2. Mass spectra are acquired in a MALDI TOF/TOF spectrometer (Bruker, Applied Biosystems).

2.9 Solid-Phase Peptide Ligand Synthesis

1. Rink Amide MBHA (e.g., Peptides International, Merck or IRIS Biotech GmbH), (*see* **Note 7**).
2. Fmoc-amino acids with side-chain-protecting groups, HOBt. TBTU, OxymaPure, and PyBOP (e.g., Peptides International, Merck-Millipore, IRIS Biotech GmbH, and Matrix Innovation Inc.).
2. DIPEA, DIC, DMF, CH_2Cl_2, piperidine, Ac_2O, TFA, TIS, MeOH, and diethylether.
3. Reagent for Fmoc removal: 20% (v/v) piperidine in DMF. Store at room temperature.
4. Cleavage cocktail for peptides without Cys: TFA/H_2O/TIS/ (95:2.5:2.5). Prepare just before use.
5. Cleavage cocktail for peptides with Cys: TFA/H_2O/Ethanedithiol (EDT)/TIS (94.5:2.5: 2.5: 1) or TFA/H_2O/TIS/3,6-dioxa-1,8-octanedithiol (DODT) (92.5:2.5:2.5:2.5). Prepare just before use.
6. 50-mL conical centrifuge tubes.
7. −20 °C freezer.
8. Refrigerated tabletop centrifuge (with the ability to cool down to ~4 °C), accommodate 50-mL conical tubes, and have a rotor speed of 10,000 × *g*.
9. Lyophilizer equipped with a noncorrosive vacuum pump.

2.10 Coupling Peptidesvia Primary Amino Groups on Agarose: Peptides with C-Terminal Lysine [16]

1. Sepharose CL-6B (GE Healthcare).
2. *N,N′*-Disuccinimidyl carbonate (DSC) (Merck).
3. DMF, DMAP, DIPEA and ethanolamine.
4. Storage solutions: 0.05% (w/v) sodium azide (NaN_3) or ethanol 20% (w/v).

2.11 Coupling Peptidesvia Sulfhydryl Groups on Agarose: Peptide with C-Terminal Cysteine [16]

1. Sepharose CL-6B (GE Healthcare).
2. Diaminodipropylamine (DADPA), 1-ethyl-3-(3-dimethylaminopropyl) carbodiimide (EDC), L-cysteine·HCl and iodoacetic acid (Merck).
3. Coupling buffer: 0.05 M Tris–HCl, 0.005 M EDTA-Na, pH 8.5. Store at 2–8 °C.
4. Capping solution: 0.05 M cysteine in coupling buffer. Prepare just before use.
5. Wash solution: 1 M sodium chloride (NaCl).
6. Storage solutions: (a) 0.01 M EDTA containing 0.02% (w/v) sodium azide (NaN_3), pH 7.2; (b) 0.05% (w/v) NaN_3; (c) ethanol 20% (v/v).
7. 50% HCl.
8. 50% NaOH.

2.12 Solutions and Reagent for Immobilized N-Hydroxysuccinimide Esters (NHS) Assay [17]

1. Ammonium hydroxide solution 28% in H_2O.
2. Polyethylene syringe fitted with polypropylene porous disk.
3. Absorption UV/VIS spectrophotometer.
4. 10-mm silica UV cell.

2.13 Isotherms

1. Pure protein stock solution of known concentration.
2. Conical centrifuge micro tubes (Eppendorf).
3. Micro centrifuge.
4. Thermomixer (Eppendorf).
5. Sigma Plot software (http://www.sgmaplot.com/products/sigmaplot/sigmaplot-details.php).

2.14 Breakthrough with Crude Samples

1. Pure protein stock solution of known concentration or the crude material protein of interest.
2. Low-pressure liquid chromatography system (Bio-Rad, GE Healthcare).
3. Chromatography columns compatible with the liquid chromatography system (GE Healthcare, Bio-Rad, Merck).

3 Methods

3.1 Ala-Gly-HMBA-ChemMatrix Resin Synthesis [18]

This process must be performed in a fume hood.

1. Place the aminomethyl-ChemMatrix resin (1 g, 0.64 mmol/g = 1 eq.) (*see* **Note 8**) in a solid-phase reactor. Wash as follows: 1 M HCl (5 × 1 min), H_2O (5 × 1 min), MeOH (5 × 1 min), CH_2Cl_2 (5 × 1 min), DMF (5 × 1 min) (*see* **Note 9**).
2. To incorporate HMBA into the aminomethyl-ChemMatrix resin, dissolve HMBA (3 eq.) and TBTU (3 eq.) in a minimum amount of DMF and transfer the solution to the amino-functionalized resin (1 eq.) contained in the solid-phase reactor.
3. Add DIPEA (6 eq.).
4. Allow the reaction to proceed overnight at room temperature.
5. Remove a small sample of resin beads (10–15 beads, approximately 0.1 mg) for analysis. Wash the sample with DMF (2 × 1 mL) and CH_2Cl_2 (2 × 1 mL) by filtration or decantation. Submit the sample to the Kaiser test. A positive result (blue coloration of the solution and/or resin beads) indicates that the reaction is not complete.
6. If the reaction is not complete, draw off the reagent mixture and replenish the reaction as described in **steps 2–4**.
7. When the reaction is complete, subject the resin to 5 × 1 min washes with one bed volume of DMF.
8. Stir the resin with an aqueous NaOH solution (1.0 M)/DMF (1:1) for 15 min at room temperature.
9. Wash the resin with 2 × 1 min washes with one bed volume of DMF/H_2O (1:1) followed by 2 × 1 min washes with one bed volume of DMF and 2 × 1 min with one bed volume of CH_2Cl_2 (2 × 1 min) (*see* **Note 10**).
10. Dissolve Fmoc-Gly-OH (3 eq.) in a minimum amount of DMF and transfer the solution to the HMBA-resin (1 eq.) contained in the solid-phase reactor.
11. Add the minimum amount of DMF to allow agitation.
12. Add DIC (4 eq.), followed by dropwise addition of a solution of DMAP dissolved in DMF (0.1 eq., ca. 50 mmol/L).
13. Allow the reaction to proceed for 1 h at room temperature, draw off the reaction solution and wash the resin with 2 × 2 min washes with one bed volume of DMF.
14. Recouple the amino acid as in **steps 10–13**.
15. Wash the resin with 5 × 2 min with one bed volume of DMF.

16. To acetylate any remaining hydroxyl groups, add Ac_2O (6 eq.), DMAP (0.1 eq.), and enough DMF to allow resin suspension agitation.
17. Stir for 1 h at room temperature.
18. Draw off the reaction solution and wash the resin with 10 bed volumes of DMF.
19. Add 20% (v/v) piperidine in DMF (v/v) (2 × 5 min) to remove Fmoc groups.
20. Wash the resin with DMF (5 × 1 min).
21. Couple Ala by adding Fmoc-Ala-OH (3 eq.) and OxymaPure (3 eq.) in a sample vial with the minimum volume of DMF for its dissolution (*see* **Note 11**).
22. Add DIC dropwise (3 eq.).
23. Stir the mixture for 1 min for chemical carboxyl activation and add the solution to the N-deblocked peptidyl resin.
24. Agitate resin gently for 45 min at room temperature on an orbital shaker.
25. Remove a small sample of resin beads (10–15 beads, approximately 0.01 mg) for analysis. Wash the sample with DMF (2 × 1 mL) and CH_2Cl_2 (2 × 1 mL) by filtration or decantation. Submit the sample to the Kaiser test. A positive result (blue coloration of the solution and/or resin beads) indicates that the reaction is not complete. If positive, wash resin with DMF (2 × 1 min) and repeat coupling reaction with fresh reagents. If negative, remove Fmoc group as indicated in **step 19**.

3.2 Combinatorial Library X-X-X-X-X-Ala-Gly synthesis: Solid-Phase Split Synthesis Method (See Notes 12 and 13)

The method for the synthesis of a linear combinatorial library containing 10^5 = 100,000 heptapeptides X-X-X-X-X-Ala-Gly, using ten different standard amino acids at each of five variable positions (X), is described here. This process must be performed in a fume hood.

1. Prepare ten polypropylene syringes fitted with a polyethylene porous disk and engraved with a letter corresponding to each specific amino acid to ensure no mix-up during the synthesis. Suspend the Ala-Gly-HMBA-ChemMatrix resin beads in 1 volume of DMF to prepare a 1:1 suspension of the resin in DMF. Distribute the suspension equally into the ten polypropylene syringes with an automatic pipette with the tip cut at the end in order to increase its diameter (Fig. 2).
2. Remove most of the DMF using vacuum filtration with a vacuum manifold.

3. Add each Fmoc-protected amino acid (3 eq.) in ten different labeled sample vials with the minimum of DMF for its dissolution.
4. Add OxymaPure (30 eq.) to a sample vial with the minimum of DMF to dissolve and add in the vials containing each of the Fmoc-protected amino acids the volume of OxymaPure solution corresponding to 3 eq. (*see* **Note 14**).
5. Add DIC dropwise in each sample vessel (3 eq.).
6. Stir the mixture for 1 min for chemical carboxyl activation and add each solution to the N-deblocked peptidyl resin portion (*see* **Note 15**).
7. Agitate gently for 45 min at room temperature.
8. To confirm the completion of the coupling reaction, withdraw a minimum amount of resin from each reaction syringe into individual small glass tubes (6 × 50 mm) and perform Kaiser or Chloranil test as described later (*see* **Note 3**). If positive, wash the resin with DMF (2 × 1 min) and repeat the coupling reaction with fresh reagents.
9. After the ten coupling reactions are completed, all the beads are transferred to the randomization vessel. Wash the beads with DMF (5 × 2 min).
10. Add 20% (v/v) piperidine in DMF (2 × 5 min) to the randomization vessel to remove the Fmoc-protecting group.
11. Wash the resin with DMF (5 × 1 min).
12. Distribute the beads into each of the reaction syringes and carry out the next coupling reaction as described earlier (**steps 2–9**).
13. After all the randomization steps are completed, remove the last Fmoc-protecting group with piperidine as described and then acetylate the N-terminus by adding Ac_2O (10 eq.), DIC (10 eq.), and enough CH_2Cl_2 to allow the swollen resin mobility to agitation. Stir 1 h at room temperature.
14. Wash the library thoroughly with DMF (5 × 1 min) followed by CH_2Cl_2 (5 × 1 min).
15. For side-chain-protecting group cleavage, add 15 mL of cocktail to the randomization vessel for 2 h at room temperature.
16. Wash the deprotected resin thoroughly with DMF (5 × 1 min) and CH_2Cl_2 (5 × 1 min).
17. Store the bead library in CH_2Cl_2 at 4 °C.

3.3 Kaiser Test (Ninhydrin Analysis)

1. Wash a minimum quantity of resin beads (10–15 beads, approximately 0.01 mg) sequentially with the following solvents: DMF (5 × 1 min), CH_2Cl_2 (5 × 1 min) and put the washed resin in a small glass tube (6 × 50 mm).

2. In a fume hood, add 60 μL ninhydrin reactive solution A and 20 μL ninhydrin reactive solution B to the tube.
3. Heat at 110 °C for 3 min.
4. Observe the beads' color intensity. Blue resin beads indicate the presence of resin-bound free amine, suggesting that the coupling reaction is incomplete (*see* **Note 16**).

3.4 Chloranil Test

1. Place a minute amount of resin beads (10–15 beads, approximately 0.01 mg) in a small test tube.
2. Add 50 μL of chloranil solution and 150 μL of acetone.
3. Mix and leave at room temperature for 5 min.
4. Watch the color of the beads. Green/blue stained resin beads indicate the presence of free amines suggesting that the coupling reaction is incomplete.

3.5 ProteinLabeling [12–15]

Perform **steps 1–4** on ice.

1. Dissolve 1–5 mg protein in 1 mL of chilled conjugation buffer.
2. Dissolve six-fold molar excess of Texas Red sulfonyl chloride in the minimum volume of DMF necessary to dissolve the label or NHS-Biotin in 224 μL of water (*see* **Note 17**).
3. Add the label solution to the protein sample and rapidly mix.
4. Incubate the reaction mixture for 4 h on ice.
5. Desalt the reaction mixture using a desalting column equilibrated with PBS or another suitable buffer to separate the conjugated protein from the reagents.

3.6 Peptide Library Screening (See Note 18)

1. Deposit aliquots of the library in syringes, each fitted with a polypropylene porous disk.
2. Exchange sequentially the combinatorial peptide library from CH_2Cl_2 into water by washing successively with CH_2Cl_2 (5 × 1 min), DMF (5 × 1 min), and DMF/H_2O (7:3), then (5:5) followed by (3:7) (5 × 1 min each one) and H_2O (5 × 1 min).
3. Block the library with 10% (w/v) skim milk, 2% (w/v) BSA in PBS, pH 6.8 for 1 h at room temperature.
4. Wash the beads 5 × 1 min with PBS-Tween.
5. Stir the library with the target protein coupled with Texas Red or biotin in PBS-Tween for 1 h at room temperature.
6. Wash the beads thoroughly with PBS-Tween (5 × 1 min).
7. When using a protein labeled with biotin, incubate the beads with 1 U/mL SA-POD in PBS-Tween for 1 h and then wash the beads thoroughly with PBS-Tween (5 × 1 min) and PBS (5 × 1 min) and reveal with a mixture of 1 mL of reactive

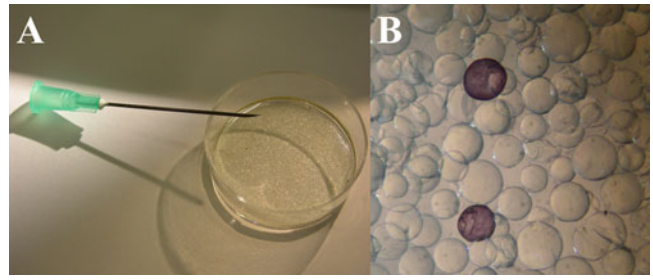

Fig. 3 (**a**) Needle and plate to manually sort beads after screening process. (**b**) Photomicrograph of positives beads surrounded by negative beads after incubation with streptavidine-peroxidase-marked protein and H_2O_2

peroxidase solution A and 4-mL reactive peroxidase solution B. After 5 min, positive beads turned in violet (*see* **Note 6**). Violet-colored beads are then isolated manually with a stereoscopic microscope and needles (Fig. 3) (*see* **Note 19**). When using proteins labeled with Texas Red, fluorescent beads are detected using a fluorescence stereoscopic microscope and isolated manually with needles (*see* **Note 20**) or using the COPAS BIO-BEAD flow-sorting equipment (Union Biometrica) [19, 20]. In the latter, the beads are suspended in a COPAS GP Sheath reagent and poured into the sample cup at a density of about 50 beads/mL. Gating and sorting regions are defined for sorting beads on COPAS based on their time-of-flight (TOF) to sort uniform-sized beads and red fluorescence intensity (RED). All sorted beads are transferred into a Petri dish and examined under a fluorescence microscope.

8. A manual inspection of the fluorescent beads sorted by the COPAS is performed to separate positive beads caused by peptide–protein interaction and false-positive beads caused by peptide–fluorescent dye interaction. False-positive beads present bright homogeneous fluorescence, while positive ones have a characteristic halo appearance, with the highest fluorescence intensity at the bead surface and the lowest in the core [21] (Fig. 4) (*see* **Note 21**). Only positive beads are isolated for MALDI-TOF MS analysis.

3.7 Bead Washing After Screening

1. Isolate positive beads and wash them with H_2O (5 × 1 μL).
2. Treat each bead with 10 μL AcOH/MeCN/H_2O (3:4:3).
3. Wash each bead sequentially with MeCN (5 × 1 μL) and CH_2Cl_2 (5 × 1 μL).
4. Air-dry the beads.

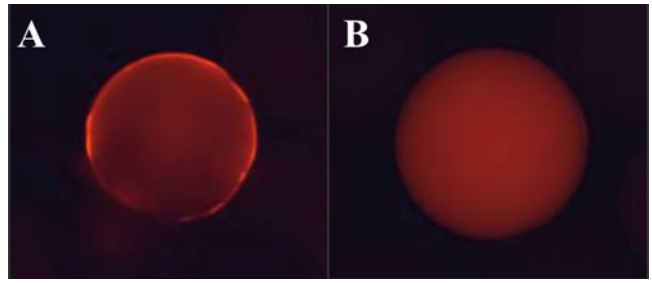

Fig. 4 Fluorescence microscope images of beads. (**a**) True-positive and (**b**) False-positive bead, after incubation with the proteins labeled with Texas Red

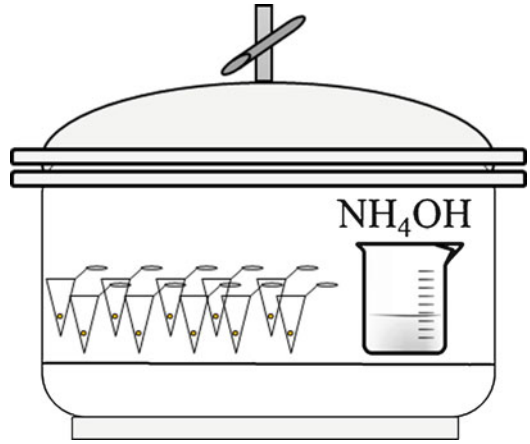

Fig. 5 Diagram of the system used for ammonia vapor peptide cleavage. Single peptide-bead samples are placed into separate microtubes in a drying chamber together with a flask containing NH_4OH 30% (v/v)

3.8 PeptideCleavage and Elution from the Bead (See Note 22)

Peptides are cleaved from the beads using ammonia vapor. This process must be performed in an efficient fume hood.

1. Place single peptide beads into separate microtubes.
2. Put the microtubes open with the beads inside in a drying chamber together with a flask containing NH_4OH 30% (v/v) (Fig. 5).
3. Clamp shut the drying chamber and leave it to stand overnight at room temperature.
4. Take out the microtubes from the drying chamber and leave them in the fume hood to let the ammonia evaporate.
5. Make a quick-spin centrifugation of each microtube to place the bead at the bottom of it.
6. Elute the released peptides from each bead with 20 μL AcOH/MeCN/H_2O (3:4:3) overnight.

3.9 MALDI-TOF/TOF MS/MS Analysis of the Eluted Peptides

1. Load 1 μL of eluted peptide solution from a single bead onto the MALDI spectrometer sample plate.
2. Air-dry at room temperature.
3. Add 1 μL CHCA matrix solution on the sample dry layer (*see* **Note 23**) (successive-dry-layer deposit method).
4. Acquire mass spectra in the MS reflector positive-ion mode and Tandem mass spectra using a MS/MS positive acquisition method.

3.10 Solid-Phase Peptide Ligand Synthesis [22]

The sequences showing greater consensus between them or repeatedly identified are synthesized to evaluate them as affinity ligands for proteinpurification (*see* **Note 24**).

This process must be performed in an efficient fume hood.

1. Place 1 g Rink Amide AM resin (*see* **Note 25**) in a solid-phase reactor.
2. Swell the resin by washing it with CH_2Cl_2 (5 × 1 min) and DMF (5 × 1 min).
3. Remove the Fmoc group by adding 20% piperidine in DMF (v/v) (2 × 5 min).
4. Wash the resin with DMF (5 × 1 min).
5. For coupling, weigh the Fmoc-amino acid (3 eq.) and OxymaPure (3 eq.) into a dry glass vial and dissolve in the minimum amount of DMF (*see* **Note 11**).
6. Add DIC dropwise (3 eq.).
7. Stir the mixture for 1 min for chemical carboxyl activation and add the solution to the resin.
8. Agitate the resin gently for 45 min at room temperature on an orbital shaker.
9. Perform Kaiser test to confirm the completion of the coupling reaction. If positive, wash the resin with DMF (5 × 1 min) and repeat the coupling reaction with fresh reagents (**steps 5**–**8**). If negative, remove Fmoc group and couple the next Fmoc–amino acid as indicated in **steps 3**–**8**.
10. After completion of the elongation, remove the last Fmoc-protecting group as indicated in **step 3** and then acetylate the N-terminus by adding Ac_2O (10 eq.), DIC (10 eq.), and enough CH_2Cl_2 to allow the swollen resin mobility to agitation. Stir 1 h at room temperature.
11. Wash thoroughly the peptidyl resin successively with DMF (5 × 1 min) followed by CH_2Cl_2 (5 × 1 min) and MeOH (5 × 1 min).
12. Air-dry the resin by application of vacuum for 10 min.

13. For peptide cleavage, add 15 mL of cleavage cocktail to the resin for 2 h at room temperature (*see* **Note 26**).
14. Remove the resin by filtration and collect the filtrate. Wash the resin twice with clean TFA and combine all the filtrates.
15. Add the filtrates directly to a ten-fold volume of cold ether (*see* **Note 27**). The peptide precipitates.
16. Centrifuge the peptide suspension at 10,000 × *g* at 4 °C for 10 min to ensure complete precipitation of the peptide.
17. Decant the ether to waste.
18. Wash the precipitate (3×) by adding more ether and shaking and repeat **steps 16–17**.
19. After the final ether extraction, allow the pellet to partially dry under a hood for 15 min.
20. Dissolve the peptide in MeCN/H_2O (1:1) and lyophilize (*see* **Note 28**).

3.11 Coupling Peptides via Primary Amine Groups: Peptide with C-Terminal Lysine Immobilization on 1-mL Sepharose [16] (See Note 29)

This process must be performed in a fume hood.

1. Wash 1-mL Sepharose CL-6B with 4–5× gel volume of deionized water to remove preservatives.
2. Sequentially exchange the Sepharose CL-6B into DMF (*see* **Note 30**). Wash thoroughly the gel successively with 4-mL quantities of DMF/water (30:70), then 50:50, followed by 70:30. Finally, filter three times with 4 mL of dry pure DMF (*see* **Note 31**).
3. Dissolve 0.080 g (300 μmol) DSC in 1-mL DMF and stir to dissolve (*see* **Note 32**).
4. Add to the DMF damp gel the DSC solution and then 0.065 g (540 μmol) of DMAP (*see* **Note 33**). Continue stirring for an additional hour at room temperature.
5. Filter and sequentially wash the activated gel with 10 × 2 mL DMF (*see* **Notes 34** and **35**).
6. To measure immobilized NHS (gel activity), withdraw 0.1 mL of resin and transfer it to an empty syringe and perform the NHS analysis as described here.
7. Add to the NHS carbonate-activated Sepharose a threefold excess, of the gel activity, of the primary amine-containing ligand dissolved in 1-mL DMF (*see* **Note 36**).
8. Add to the gel/ligand slurry a six-fold excess of DIPEA (*see* **Note 37**).
9. Stir 2 h at room temperature.
10. Filter the ligand-loaded gel and slurry.
11. Wash the gel three times with 2× gel volume quantities of fresh DMF.

12. Block any remaining unreacted groups by addition of a 4× excess of ethanolamine in 450 μL DMF.
13. Agitate for 30 min at room temperature.
14. Gradually add degassed deionized water to the matrix. Wash thoroughly the gel successively with mixtures of DMF/water (70:30), then 50:50, followed by 70:30. Finally, continue washing with degassed deionized water 3–4 times with 4× gel volume quantities.
15. Store in NaN_3 0.05% (w/v) or ethanol 20% (v/v) at 4 °C.

3.12 Coupling Peptides via Sulfhydryl Groups on 1-mL Sepharose: Peptides with C-Terminal Cysteine [16]

This process must be performed in a fume hood.

1. Synthesize NHS-Sepharose as indicated in protocol in Subheading 3.11 (**steps 1–5**).
2. Couple DADPA on NHS-Sepharose as indicated in protocol in Subheading 3.11 (**steps 7–14**).
3. Wash 1-mL DADPA-Sepharose with 10-mL water.
4. Suspend the gel in 0.5-mL water and stir the suspension.
5. Dissolve iodoacetic acid (120 mg) in 0.5-mL water, adjust the pH to 4.5 using 50% NaOH, and add the solution to the gel suspension.
6. While stirring, add EDC (100 mg) to the reaction mixture, and maintain the pH at 4.5 for 1 h by adding first 50% HCl and then 50% NaOH.
7. Continue the reaction for 2 h at room temperature.
8. Filter the reaction mixture and wash extensively with water. Iodoacetyl-agarose can be stored in 0.01 M EDTA containing 0.02% (w/v) NaN_3, pH 7.2, at 4 °C protected from light (*see* **Notes 38** and **39**).
9. Equilibrate the iodoacetyl-agarose with four resin-bed volumes of coupling buffer.
10. Dissolve three-fold excess of peptide with C-terminal Cys (*see* **Note 40**) in 1-mL coupling buffer.
11. Agitate at room temperature for 1 h.
12. Allow the solution to filtrate from the solid-phase reaction vessel.
13. Wash the matrix with three resin-bed volumes of coupling buffer.
14. Block unreacted iodoacetyl sites on the matrix by adding one resin-bed volume of 0.05 M cysteine in coupling buffer.
15. Agitate at room temperature for 1 h.
16. Wash the matrix with six resin-bed volumes of wash solution.

17. Wash the column with two resin-bed volumes of degassed 0.05% (w/v) NaN_3 or ethanol 20% (v/v) (storage solution).
18. Add one additional resin-bed volume of storage solution.
19. Store at 4 °C.

3.13 Immobilized NHS Measurement [17]

1. Transfer 0.1 mL of NHS-activated Sepharose to an empty syringe.
2. Wash the resin with DMF (5 × 1 min).
3. Add 0.1 mL of NH_4OH (28%) to the activated resin.
4. Agitate the resin suspension for 15 min at room temperature.
5. Filter and collect the 0.1 mL in a 15-mL falcon tube.
6. Wash the resin with NH_4OH (28%) (4 × 0.1 mL) and collect and combine all the filtrates in the same falcon tube.
7. After appropriate dilution with water, read the absorbance of the solution at 260 nm.
8. Calculate NHS concentration based on ε 9700 M^{-1}/cm^{-1}.

3.14 Protein Adsorption Isotherm Determination [23]

Adsorption isotherms for target protein binding to the peptide immobilized on the chromatographic support are measured in stirred-batch systems. The experiment may be performed under different buffer conditions or temperatures to assess the effect of pH, ionic strength, temperature, and other factors on the binding of the target protein to the peptideaffinity chromatography matrix.

1. Fill a chromatographic column with the peptide affinity chromatographic support and equilibrate it by pumping 20 volumes of the adsorption buffer to be assessed.
2. Add 30 μL of the chromatographic matrix to conical centrifuge microtubes. (*see* **Note 41**).
3. Add to sequential labeled microtubes increasing volumes of a pure protein stock solution of known concentration and the volume of buffer necessary to reach 1 mL of final volume.
4. Prepare another set of labeled tubes with the same volume of protein stock solution and buffer but without matrix.
5. Gently shake the tubes overnight at the desired temperature to enable the system to reach its equilibrium.
6. Centrifuge slowly to decant the resin and remove an aliquot of the protein solution from each tube. Measure protein concentration with Bradford reagent [24] or other available methods for proteins. Determine the free protein concentration at equilibrium (c^*) with the first set of tubes and the total protein concentration (c_t) with the second set of tubes.

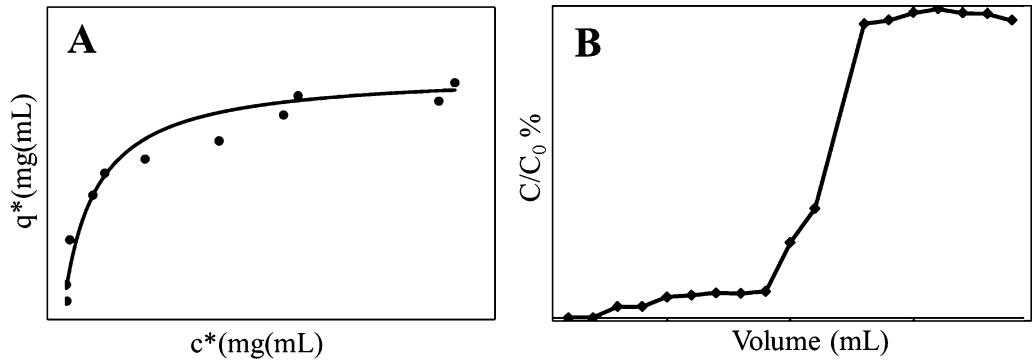

Fig. 6 (**a**) Graph of $q^* = f(c^*)$ describing the adsorption isotherms for target protein binding to peptide immobilized on the chromatographic support, c^* = free protein concentration at equilibrium, q^* = the equilibrium concentration of the target protein bound to the immobilized peptide per unit of total chromatographic matrix volume. (**b**) A breakthrough curve: variation of the concentration of target protein in the column outlet as a function of volume

7. The equilibrium concentration of the target protein bound to the immobilized peptide, per unit of total chromatographic matrix volume (q^*), is calculated as the total amount of protein present at the beginning of the experiment (c_t) less the amount present in the soluble phase at equilibrium:

$$q^* = (c_t - c^*)1000/30. \quad (1)$$

8. Make a graph of $q^* = f(c^*)$ (Fig. 6a).
9. For nonlineal curve regression use an appropriate graph software, such as *Sigma Plot*, employing a one-to-one Langmuir binding model (*see* **Note 42**):

$$q^* = q_m \cdot c^*/(K_d + c^*). \quad (2)$$

10. Calculate the maximum capacity for the protein of interest per volume of chromatographic matrix (q_m) and the dissociation constant (K_d) for each matrix (*see* **Note 43**).
11. Otherwise, rearrange Eq. 2 and determine K_d and q_m values from straight-line plots of c^*/q^* against c^*:

$$c^*/q^* = c^*/q_m + K_d/q_m \quad (3)$$

12. The interception of such plots on the c^* axis is at $-K_d$ and the slope of the line is $1/q_m$.

3.15 Breakthrough Curves

The breakthrough curves are constructed to assess the effect of changes in certain operating variables, such as flow rate (or residence time) and feed concentration on the dynamic capacity of the chromatographic system. The experiment can be performed with pure or crude samples. Breakthrough curves can be measured

in packed columns onto which the sample is fed continuously until the target protein begins to appear in the column outlet, thus indicating that the available capacity of the column is exhausted. The breakthrough curve is described by the variation of the concentration of target protein in the column outlet as a function of time or volume [23] (*see* **Note 44**).

1. Pump pure protein solution at a defined concentration, or a crude sample containing the protein of interest, through a 1-mL packed column of peptide-agarose adsorbent at the desired flow rate.
2. Monitor the outlet of the column for the level of protein of interest either by continuous measurement of the optical adsorption at 280 nm in the case of pure protein solutions, or by measuring the protein of interest with a specific method, in 0.5-mL collected fractions.
3. Dynamic capacity is calculated as the amount of protein adsorbed by the matrix before 10% of the initial protein concentration is detected at the column outlet (Fig. 6b).

4 Notes

1. HMBA linkage agent can be coupled to the aminomethyl-ChemMatrix as indicated in protocol in Subheading 3.1 (**steps 1–9**). Otherwise, HMBA-ChemMatrix resin can be purchased. Although HMBA-ChemMatrix resin is an optimized combination, other combinations of solid support and linker can be used. The solid support should be water compatible because the screening is carried out in aqueous solution. It also should be compatible with the organic solvents used for solid-phase peptide synthesis. The bond formed between the first amino acid and the linker should be stable to all synthetic elongation reactions as well as to the conditions required for the removal of the side-chain-protecting groups. Removal of protecting groups is required since screening is carried out on fully unprotected peptides bound to the resin. The linker is necessary to release the peptides from the solid support before their sequencing by tandem mass spectrometry (but it is not necessary if Edman microsequencing is used for peptideidentification). The resin must be compatible with the chemistry used to release the peptide from the linker.
2. There are many cleavage mixtures to remove all the side-chain-protecting groups of the amino acid residues after Fmoc SPPS. The resin is treated with TFA with a small quantity of nucleophilic reagents (known as scavengers) to quench highly reactive cationic species generated from the protecting groups

[25]. The HMBA inertness to TFA allows side-chain cleavage without releasing the peptide from the resin. The removal of protecting groups is required since screening is normally carried out on fully unprotected peptides bound to the resin.

3. The Kaiser test is a qualitative test for primary amines; hence, it cannot be reliably applied to the evaluation of Fmoc-AA-OH couplings next to Pro or other N-substituted amino acids. In those cases, the Chloranil test should be used.
4. Dyes with maximum emission in the red are selected because resin beads exhibit a significant intrinsic fluorescence with maximum emission in the green. This is a problem when screening against fluorescein-labeled proteins [26].
5. Other amine-reactive reagents for proteinlabeling and the corresponding protocols may be acquired from different providers.
6. Other protocols based on different peroxidase substrates such as 3,3′-diaminobenzidine can be used [27].
7. This support is ideal for the Fmoc SPPS of peptide amides.
8. Here we describe a synthesis of a one-bead-one-peptide library in which 10 amino acids are varied in five variable positions obtaining $10^5 = 100{,}000$ different peptide sequences. Considering that for statistical reasons the number of beads must exceed the number of peptides by a factor of at least 10 and that 1 g of ChemMatrix resin contains 10^6 beads [28], 1 g of resin is required to synthesize the library.
9. The washing protocol avoids bead clumping, which interferes in the synthesis and screening processes.
10. In the case of using commercial HMBA-ChemMatrix, wash it as follows: CH_2Cl_2 (2×1 min), DMF (2×1 min), CH_2Cl_2 (2×1 min), and start the synthesis from **step 10**.
11. Other coupling methods that are described in many manuals can be used [29, 30]. OxymaPure/DIC showed clear superiority to HOBt/DIC or carbodiimide alone in terms of purity and yield [31]. Precautions must be taken during the incorporation of the second, usually Ala, and third residue (Xxx-Ala-Gly-HMBA-ChemMatrix), because the presence of Gly as C-terminal can favor the formation of diketopiperazine (DKP). Thus, the Fmoc group removal from the second residue (Ala) should be carried out quickly to avoid the formation of DKP (3×1 min). Alternatively, the second residue Ala can be incorporated with Boc instead of Fmoc, whereby removal is achieved with TFA/CH_2Cl_2 (4:6). Incorporation of the third residue (Xxx) would then use Fmoc protection and an in situ neutralization/coupling protocol [32].

12. There are many published protocols describing the solid-phase split synthesis method [33, 34].
13. The present protocol describes the construction of linear peptide libraries. For cyclic peptide libraries, other protocols have been described elsewhere [35].
14. Most amino acids may be coupled using OxymaPure/DIC chemistry. In the case of Arg, stronger coupling conditions must be used such as using 3 eq. of Fmoc-Arg(Pbf)-OH, 3 eq. of PyBOP and 6 eq. of DIPEA.
15. Preactivation time should be kept to the minimum, since activated species can give rise to several side reactions, including racemization, formation of δ-lactam (Arg), cyano derivatives (Asn or Gln), or α-aminocrotonic acid (Thr) [36].
16. On some occasions, certain amino acid residues can give unusual colorations ranging from red to blue (Asn, Cys, Ser, and Thr, in particular).
17. Do not dissolve Texas Red sulfonyl chloride in dimethyl sulfoxide because it reacts with sulfonyl chlorides [37].
18. To avoid false-positive bead selection, a two-stage screening may be used in which the positive beads from the first screening are subjected to a different screening process. The drawback of this strategy is that it is time consuming and laborious to wash the beads for the second screening process and some beads can be damaged or lost. Another option is to use two different screening methods with two different library portions and after peptidesequencing of all the selected beads, choose the peptide sequences selected with both screening methods [38].
19. When screening the library with the target protein coupled with biotin and then revealing with SA-POD, false-positive peptide beads with His-Pro-Gln and His-Pro-Met motifs with high affinity for SA may be selected [39]. Those motifs should be omitted when designing the library.
20. When isolating fluorescent beads, do not let them dry. Dry beads are fluorescent and positive cannot be distinguished from negative beads.
21. The use of fluorescent dyes to conjugate the target protein allows the use of COPAS to facilitate the screening of one-bead one-compound combinatorial libraries. COPAS sorts beads based on their fluorescence intensity and two groups of beads are isolated: positive beads, as a result of the interaction of the protein with the peptides, and false-positive beads, caused by the interaction of the fluorescent dyes with the peptides. When screening the library with the target protein coupled with fluorescent dyes, peptides interacting with dyes are a drawback. A manual inspection of the fluorescent

beads sorted by the COPAS shows that false positives present bright homogeneous fluorescence, while positive ones have a characteristic halo appearance (*see* Fig. 4). ChemMatrix resin, as other polyethylenglycol (PEG) resins, is a porous gel-type matrix in the form of spherical particles. Small molecules like amino acids and peptides have full access to the pores, thus allowing peptide synthesis with high loadings. High-molecular-weight proteins do not reach the interior of the bead and, therefore, protein adsorption only takes place on the bead surface. We hypothesize that the difference between true-positive and false-positive beads is caused by the orientation of the complex on the bead surface. If the protein-dye complex binds to the peptide bead via peptide-protein interaction, there is a space between the bead and the emitter (fluorescent dye), thus resulting in beads with halo appearance. Alternatively, if the protein–dye complex binds by means of peptide–dye interaction, there is no distance between the emitter and the bead, and therefore the coat is more compact [40]. Thus, the possibility of differentiating true from false-positive beads would depend on the protein target molecular weight and the resin pore diameter. If the target has full access to the interior of the bead, true- from false-positive beads cannot be differentiated and fluorescent dyes will not be a good option for on-bead screening, especially when peptide libraries with hydrophobic amino acids are used.

22. HMBA linker is susceptible to nucleophilic attack. The ammonia vapor has the advantage over other nucleophiles such as NaOH. The first is evaporated easily and does not leave residues that could interfere with the MS analysis of the released peptides. The method here described consists of placing single beads into separate microtubes in a drying chamber together with a flask containing NH_4OH 30% (v/v). With NH_4OH, peptides are released as peptide amide with yields of 85–90%, which is similar to those yields previously obtained by Bray et al. with NH_3/THF [9], but the method using NH_4OH is easier to handle, more economical, and safer. ChemMatrix resin is a highly cross-linked, amphiphilic solid support composed entirely of PEGmonomers containing primary ether bonds exclusively. These bonds confer high chemical stability to nucleophiles. Other PEG resins based on ester bonds are less recommendable, because they are susceptible to nucleophilic attack.
23. CHCA concentration has a great influence on the final spectrum and must be optimized for each spectrometer. Low concentrations decrease peptide peak signal intensity and high concentrations not only decrease peptide peak signal intensity but also increase matrix cluster peaks [8].

24. The peptide amide is synthesized to prevent peptide polymerization during coupling to the chromatographic resin. The N-terminus is acetylated and at the C-terminal a Cys (Fmoc-Cys(Trt)-OH) or Lys (Fmoc-Lys(Boc)-OH) is incorporated to allow the peptide to be coupled only through the side-chain sulfhydryl (Cys) or amine group (Lys), thus ensuring the same peptide orientation in the agarose support as that in the library bead. The use of Lys is preferred to Cys because odorous and/or expensive scavengers are needed to cleave the Cys side-chain-protecting group. Cys is chosen when the peptide sequence has a Lys itself to ensure a site-directed immobilization and to avoid many orientations of the peptide molecule on the matrix. The peptideligands can be immobilized on commercial activated matrices that usually provide a spacer arm. Otherwise, the peptide ligand may be synthesized with a spacer arm by adding between the C-terminal amino acid and the rest of the peptide sequence Fmoc-Gly, Fmoc-Ala, or Fmoc-6-aminohexanoic acid.
25. Other resins for Fmoc SPPS of peptide amide may be used.
26. Scavengers used in the cleavage cocktail depend on the side-change-protecting groups. For peptides without Cys, TFA/H_2O/TIS/ (95:2.5:2.5) can be used. For peptides with Cys, the cleavage cocktail TFA/H_2O/EDT/TIS (94:2.5: 2.5: 1) gives good results, but EDT is too odorous. Other cocktails such as TFA/H_2O/TIS/DODT (92.5:2.5:2.5:2.5) are also efficient and avoid odorous chemicals.
27. Following the cleavage reaction, the peptide is usually isolated by precipitation adding cold diethyl ether to the peptide/TFA solution. The precipitation can be done directly from the peptide/TFA solution, or the volume can be previously reduced in a rotary evaporator before precipitation.
28. Avoid using acids to dissolve the peptides for lyophilization. The acid crystallizes together with the peptide and interferes in the subsequent peptide immobilization on the chromatographic matrix, which must be performed under basic conditions.
29. The use of *N*-hydroxy succinimide (NHS) esters as activated groups is ideal to bind ligands with primary amines by the formation of an amide bond.
30. A gradual exchange of solvent in the water-swollen matrix is necessary to avoid damage or clumping of the particles.
31. Other solvents instead of DMF may be used such as acetone, dimethyl sulfoxide, and dioxane.

32. Although some DSC can remain insoluble in the solution, it will dissolve as the reaction goes on.
33. Other base instead of DMAP can be used to catalyze the reaction such as anhydrous triethylamine (750 μl).
34. Although the NHS carbonate–activated support can be stored as a 50% slurry in dry isopropanol at 4 °C, its immediate use is highly recommended. Avoid water because it hydrolyzes the activated matrix and MeOH because it will produce a "transesterification" reaction with NHS esters, yielding methyl esters.
35. NHS-activated chromatographic matrices can be purchased from different suppliers (GE Healthcare, Thermo Fisher Scientific, Bio-Rad) or synthesized as indicated in protocol 3.11 (**steps 1–5**). Agarose activated by DSC as well as commercial NHS-activated agarose typically contains approximately 18 μmol NHS/mL.
36. Nonaqueous solvents such as DMF, dimethyl sulfoxide, acetone, and tetrahydrofuran are preferred to aqueous solutions during coupling short peptideligands to avoid the gel hydrolysis.
37. A two-times mole excess over the amount of peptide of an organic base such as DIPEA, DMAP, or triethylamine should be added to catalyze the coupling reaction.
38. Alkyl halide-containing compounds are extremely light sensitive.
39. Iodoacetyl-containing matrices are excellent activated supports for the immobilization of ligands containing sulfhydryl groups. The matrices will provide extremely stable thioether bonds between the ligand and the matrix. These matrices can be purchased (Thermo Fisher Scientific) or synthesized as indicated in protocol in Subheading 3.12 (**steps 1–8**).
40. Cys is required with its side-chain in the free thiol form for peptide immobilization, so peptide must be dissolved immediately before immobilization avoiding long exposure to air or basic conditions.
41. To facilitate the measurement, prepare a 1:1 suspension of the chromatographic matrix in adsorption buffer. While agitating, measure 60 μL of the suspension with an automatic pipette with the tip cut at the end to increase its diameter.
42. Protein adsorption on a chromatographic matrix can be described by different adsorption isotherms. Generally, the Langmuir model shows good agreement with the experimental results. The Langmuir model, described by Eq. 2, assumes that the adsorption process takes place on a surface composed of a fixed number of adsorption sites of equal energy, with one

molecule adsorbed per adsorption site until a monolayer coverage is obtained [41]. Some of the assumptions made in this model are not necessarily realistic because of the large difference between macromolecules and small molecules in the adsorption mechanism at interfaces. The differences result mainly from: multiple site binding for proteins, which often results in irreversible adsorption, heterogeneous nature of most solid surfaces, and lateral and other interactions referred to as cooperative interactions [42, 43].

43. The equilibrium nature of the interaction between protein and adsorbent results in the utilization of the maximum capacity of the adsorbent only in situations where the inlet protein concentration (c_t) is much greater than K_d ($c_t > 12\ K_d$) [23]. To adsorb a protein to an affinity gel, the binding constant K_a for the interaction needs, for most practical purposes, to exceed or be equal to 10^5–10^6 M corresponding to a K_d of 1–10 μM (the K_d is equal to the inverse of K_a). The moderate dissociation constants allow, at the same time, adsorbing the protein at a low concentration and quantitative elution under mild conditions [44].
44. Sharper breakthrough curves result in more material being retained by the column. There are many parameters influencing the shape of the breakthrough curves and hence the performance of the adsorption stage of packed column affinity processes such as flow rate, target protein concentration, dissociation constant, etc.

Acknowledgments

Work in the author's laboratories was partially supported by grants from the Universidad de Buenos Aires (UBACyT, 20020170100030BA, PIDAE28), the Agencia Nacional de Promoción Científica y Tecnológica (ANPCyT, PICT-2018-00498), and Consejo Nacional de Investigaciones Científicas y Técnicas de la República Argentina (PIP 11220130100119CO, PU-E 2018). M.C. Martínez Ceron, S.L. Giudicessi, M.M. Marani, O. Cascone, and S.A. Camperi are career researchers of the Consejo Nacional de Investigaciones Científicas y Técnicas de la República Argentina (CONICET).

References

1. Cuatrecasas P, Wilchek M, Anfinsen CB (1968) Selective enzyme purification by affinity chromatography. Proc Natl Acad Sci U S A 61:636–643
2. Saavedra SL, Barredo GR, Martínez-Ceron MC et al (2018) Design, synthesis and application of short-peptide and peptidomimetic ligands for affinity chromatography. In: Labrou

N (ed) Handbook on protein purification: industry challenges and technological developments. Nova Science Publishers, Inc., New York, NY, pp 19–50

3. Furka A, Sebestyen F, Asgedom M et al (1991) General method for rapid synthesis of multicomponent peptide mixtures. Int J Peptide Protein Res 37:487–493
4. Lam KS, Salmon SE, Hersh EM et al (1991) A new type of synthetic peptide library for identifying ligand-binding activity. Nature 354:82–84
5. García-Martin F, Quintanar-Audelo M, García-Ramos Y et al (2006) ChemMatrix, a poly (ethylene glycol)-based support for the solid-phase synthesis of complex peptides. J Comb Chem 8:213–220
6. Atherton E, Logan CJ, Sheppard RC (1981) Peptide synthesis. Part 2. Procedures for solid-phase synthesis using N-α-fluorenylmethoxycarbonylamino-acids on polyamide supports. Synthesis of substance P and of acyl carrier protein 65-74 decapeptide. J Chem Soc Perkin Trans 1:538–546
7. Camperi SA, Marani MM, Iannucci NB et al (2005) An efficient strategy for the preparation of one-bead-one-peptide libraries on a new biocompatible solid support. Tetrahedron Lett 46:1561–1564
8. Martinez-Ceron MC, Giudicessi SL, Marani MM et al (2010) Sample preparation for sequencing hits from one-bead-one-peptide combinatorial libraries by matrix-assisted laser desorption/ionization time-of-flight mass spectrometry. Anal Biochem 400:295–297
9. Bray AM, Valerio RM, Maeji NJ (1993) Cleavage of resin-bound peptide esters with ammonia vapour. Simultaneous multiple synthesis of peptide amides. Tetrahedron Lett 34:4411–4414
10. Kaiser E, Colescott RL, Bossinger CD et al (1970) Color test for detection of free terminal amino groups in the solid-phase synthesis of peptides. Anal Biochem 34:595–598
11. Christensen T (1979) A qualitative test for monitoring coupling completeness in solid phase peptide synthesis using chloranil. Acta Chem Scand 33:763–766
12. Thermo Scientific. Instructions. Texas red sulfonyl chloride. https://assets.thermofisher.com/TFS-Assets/LSG/manuals/MAN0011223_TexasRed_Sulfonyl_Chloride_UG.pdf. Accessed 23 Feb 2019
13. Hermanson GT (2013) Fluorescent probes. In: Hermanson GT (ed) Bioconjugate techniques, 3rd edn. Elsevier, New York, NY, pp 395–463
14. Instruction. EZ-Link™ Sulfo-NHS-Biotin. https://assets.thermofisher.com/TFS-Assets/LSG/manuals/MAN0016134_2161850_EZLinkSulfoNHS_Biotin_UG.pdf. Accessed 23 Feb 2019
15. Hermanson GT (2013) (Strept)avidin–biotin systems. In: Hermanson GT (ed) Bioconjugate techniques, 3rd edn. Elsevier, New York, NY, pp 465–505
16. Hermanson GT (2013) Immobilization of ligands on chromatography supports. In: Hermanson GT (ed) Bioconjugate techniques, 3rd edn. Elsevier, New York, NY, pp 588–740
17. Miron T, Wilchek MA (1982) Spectrophotometric assay for soluble and immobilized N-hydroxysuccinimide esters. Anal Biochem 126:433–435
18. Mellor SL, Welling DA, Fehrentz JA et al (2000) Synthesis of modified peptides. In: Chan WC, White PD (eds) Fmoc solid phase peptide synthesis: a practical approach. Oxford University Press, New York, NY, pp 137–181
19. Union Biometrica. http://www.unionbio.com Accessed 16 Oct 2012
20. Christensen C, Groth T, Schiødt CB et al (2003) Automated sorting of beads from a "one-bead-two-compounds" combinatorial library of metalloproteinase inhibitors. QSAR Comb Sci 22:737–744
21. Marani MM, Martínez-Ceron MC, Giudicessi SL et al (2009) Screening of one-bead-one-peptide combinatorial library using red fluorescent dyes. Presence of positive and false positive beads. J Comb Chem 11:146–150
22. Chan WC, White PD (2000) Basic procedures. In: Chan WC, White PD (eds) Fmoc solid phase peptide synthesis: a practical approach. Oxford University Press, New York, NY, pp 41–76
23. Chase HA (1984) Prediction of the performance of preparative affinity chromatography. J Chromatogr 297:179–202
24. Bradford MM (1976) A rapid and sensitive method for the quantitation of microgram quantities of protein utilizing the principle of protein-dye binding. Anal Biochem 72:248–254
25. Guy CA, Fields GB (1997) Trifluoroacetic acid cleavage and deprotection of resin-bound peptides following synthesis by Fmoc chemistry. In: Fields GB (ed) Solid phase peptide synthesis. Methods in enzymology, vol 289. Academic, New York, NY, pp 67–83
26. Kodadek T, Bachhawat-Sikder K (2006) Optimized protocols for the isolation of specific protein-binding peptides or peptoids from combinatorial libraries displayed on beads. Mol BioSyst 2:25–35

27. Messing A, Stieber A, Gonatas NK (1985) Resolution of diaminobenzidine for the detection of horseradish peroxidase on surfaces of cultured cells. J Histochem Cytochem 33:837–839
28. Marani MM, Oliveira E, Côté S et al (2007) Identification of protein-binding peptides by direct matrix-assisted laser desorption ionization time-of-flight mass spectrometry analysis of peptide beads selected from the screening of one bead-one peptide combinatorial libraries. Anal Biochem 370:215–222
29. Chan WC, White PD (2000) Fmoc solid phase peptide synthesis: a practical approach. Oxford University Press, New York, NY
30. Fields GB (1997) Solid-phase peptide synthesis. Methods in enzymology, vol 289. Academic, New York, NY
31. El-Faham A, Al Marhoon Z, Abdel-Megeed A et al (2013) OxymaPure/DIC: an efficient reagent for the synthesis of a novel series of 4-[2-(2-acetylaminophenyl)-2-oxo-acetylamino] benzoyl amino acid ester derivatives. Molecules 18:4747–4759
32. Gairí M, Lloyd-Williams P, Albericio F et al (1990) Use of BOP reagent for the suppression of diketopiperazine formation in boc/bzl solid-phase peptide synthesis. Tetrahedron Lett 31:7363–7366
33. Lam KS, Lehman AL, Song A et al (2003) Synthesis and screening of "one-bead one--compound" combinatorial peptide libraries. In: Morales GA, Bunin BA (eds) Combinatorial chemistry, Part B. Methods in enzymology, vol 369. Academic, New York, NY, pp 298–322
34. Lam KS, Lebl M (1997) Synthesis of a one-bead one-compound combinatorial peptide library. In: Cabilly S (ed) Combinatorial peptide library protocols. Methods in molecular biology, Human. Totawa, NJ 87, pp 1-6
35. Camperi SA, Giudicessi SL, Martínez-Ceron MC et al (2016) Combinatorial library screening coupled to mass spectrometry to identify valuable cyclic peptides. Curr Protoc Chem Biol 8:109–130
36. Al-Warhia TI, Al-Hazimi HMA, El-Faham A (2012) Recent development in peptide coupling reagents. J Saudi Chem Soc 16:97–116
37. Boyle R (1966) The reaction of dimethyl sulfoxide and 5-dimethylaminonapthalene-1-sulfonyl chloride. J Org Chem 31:3880–3882
38. Martínez-Ceron MC, Giudicessi SL, Kruszyn JN et al (2016) Two-stage screening of combinatorial peptide libraries. Application to bovine serum albumin ligand selection. Rev Cenic Cienc Biol 46:76–86
39. Lam KS, Lebl M (1992) Streptavidin and avidin recognize peptide ligands with different motifs. ImmunoMethods 1:11–15
40. Axelrod D, Hellen EH, Fulbright RM (1991) Total internal reflection fluorescence. In: Lakowicz JR (ed) Topics in fluorescence spectroscopy, biochemical applications, vol 3. Plenum, New York, NY, pp 289–344
41. Adamson AW, Gast AP (1997) Physical chemistry of surfaces. Wiley, New York, NY
42. Luo Q, Andrade JD (1998) Cooperative adsorption of proteins onto hydroxyapatite. J Colloid Interface Sci 200:104–113
43. Bellot JC, Condoret JS (1993) Modelling of liquid chromatography equilibria. Process Biochem 28:365–376
44. Carlsson J, Janson JC, Sparman M (1988) Affinity chromatography. In: Janson JC, Rydén L (eds) Protein purification, 2nd edn. Wiley, New York, NY, pp 375–442

Chapter 17

Z_{Ca}: A Protein A-Derived Domain with Calcium-Dependent Affinity for Mild Antibody Purification

Julia Scheffel, Sara Kanje, and Sophia Hober

Abstract

Therapeutic antibodies are at the forefront of modern medicine where high purity, which is typically obtained by Protein A-based affinity purification, is of utmost importance. In this chapter, we present a method for neutral and selective purification of antibodies by utilizing an engineered affinity ligand, Z_{Ca}, derived from Protein A. This domain displays a calcium-dependent binding of antibodies and has been multimerized and immobilized to a chromatography resin to achieve an affinity matrix with high binding capacity. IgG antibodies can be eluted from the tetrameric Z_{Ca} ligand at pH 7 with the addition of EDTA, or at pH 5.5 with EDTA for purification of monoclonal IgG1, which is significantly milder than the low pH (3–4) required in conventional Protein A affinity chromatography. Here, a protocol for selective capture of IgG with elution at neutral pH from a Z_{Ca} tetramer ligand immobilized on a chromatography resin is described.

Key words Antibody purification, Protein A, Z_{Ca}, Elution, Ligand, Calcium, pH

1 Introduction

Biopharmaceuticals are increasingly used in the treatment of various diseases, with numerous advantages over small-molecule drugs such as fewer undesirable side effects associated with a higher target specificity [1]. Antibodies make up about half of the total sales of all biopharmaceuticals, and the number of monoclonal antibodies on the market is rapidly increasing [2]. Significant effort has been put on optimizing upstream processes for antibody production, but the advances in downstream processing have been limited [3]. In most antibody purification processes, affinity chromatography based on Protein A is used due to its ability to yield a product that is highly pure and concentrated in merely one purification step [4, 5]. A major problem with Protein A chromatography concerns the conditions necessary for elution of the captured antibody from the Protein A column, which requires a low pH to break the interaction

Nikolaos E. Labrou (ed.), *Protein Downstream Processing: Design, Development, and Application of High and Low-Resolution Methods*, Methods in Molecular Biology, vol. 2178, https://doi.org/10.1007/978-1-0716-0775-6_17,

between the high-affinity Protein A ligand and the antibody [6]. There are antibodies, as well as Fc-fusion proteins, that do not tolerate acidic conditions, which can lead to aggregate formation and significantly impaired biological activity. The harsh elution conditions used to obtain the pure antibody may therefore stand in the way of the development of new antibodies that display this acid sensitivity, despite promising therapeutic potential [7–10].

To enable purification of all antibodies that bind to Protein A, regardless of their stability at low pH, a Protein A-derived domain that allows for milder elution of the captured antibody has been engineered [11]. The protein domain is based on the small and stable Z domain, consisting of 58 amino acids and no cysteines, which is derived from one of the IgG-binding domains of staphylococcal Protein A, the B domain. Z has a high affinity for the Fc region of IgG, but does not bind to the Fab fragment, and has previously been used in the purification of recombinant proteins as a fusion tag for affinity purification on IgG columns [5]. The Z domain was engineered to bind antibodies in a calcium-dependent manner with the intended use as a ligand in affinity purification. Thereby, the calcium-dependent binding could be utilized for capture and elution of the antibodies by depleting calcium instead of lowering the pH. To achieve this, a library of Z domains with randomized loops between the second and the third helices of Z was built. The variable loop library was designed, based on the naturally occurring EF-hand motif. Positions that were known to be of importance for the structural stability of the Z domain were also randomized and calcium-dependent binders to IgG were selected by phage display.

By X-ray crystallography, the developed protein, Z_{Ca}, was shown to coordinate a calcium ion in the introduced loop (Fig. 1a). Also, the domain was shown to interact with the Fc region of antibodies in a similar way as the Z domain (Fig. 1b). Furthermore, Z_{Ca} was shown to display a calcium-dependent IgG binding, and by coupling the ligand to a chromatography resin, antibodies could be captured in the presence of calcium and eluted at neutral pH by removal of the calcium ions with a chelator, such as ethylenediaminetetraacetic acid (EDTA). Antibodies of subclass IgG2 and IgG4 can be eluted at neutral pH, while antibodies of subclass IgG1 require a slight decrease in pH for complete elution, although not lower than pH 5.5. This is a large improvement over conventional Protein A processes, where pH 3.2 is usually needed. Most antibodies that are approved for clinical use today are indeed of subclass IgG1, but IgG2 and IgG4 antibody therapeutics are on the rise and most of the antibodies that have been under regulatory review recently are based on IgG2 and IgG4 [12].

For an enhanced binding capacity of the chromatography resin, the protein domain was multimerized. A tetrameric version of the ligand was coupled to a chromatography resin using a cysteine

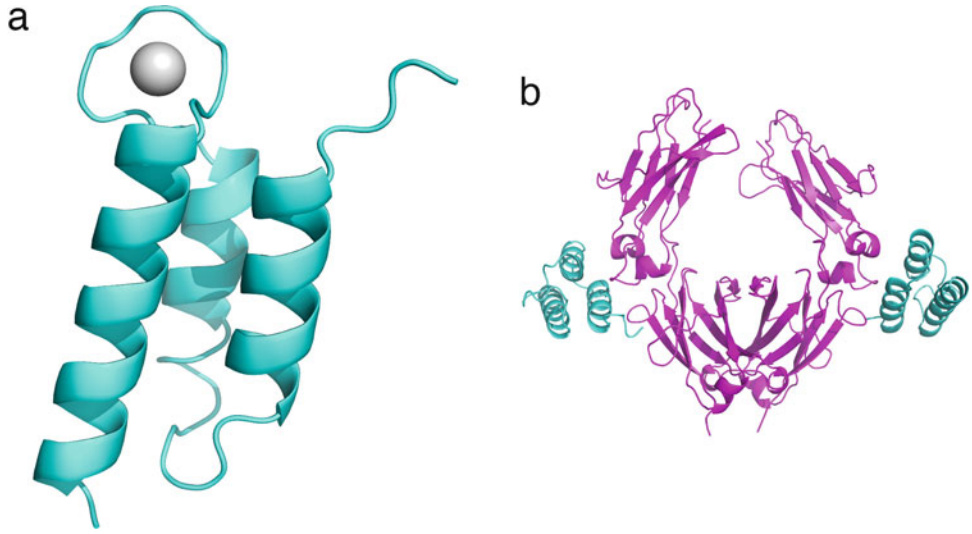

Fig. 1 X-ray structure of the monomeric Z_{Ca} and Fc presented as a ribbon diagram. (**a**) Z_{Ca} (cyan) with a calcium ion (gray) coordinated by the introduced calcium-binding loop. (**b**) Fc dimer (magenta) in complex with two Z_{Ca} (cyan)

incorporated C-terminally, reducing the risk of disrupting the binding sites. The produced matrix was shown to have both high specificity and capacity [13]. The capture of IgG and elution at pH 5.5 is shown in the chromatogram in Fig. 2a and the high specificity of the capture step is demonstrated in Fig. 2b. This purification method based on the Z_{Ca} tetramer ligand can have a significant effect on the development of therapeutic antibodies since it allows for purification of acid-sensitive antibodies as well as Fc-fusion proteins. The protocol provided can be adjusted depending on the antibody to be purified, both regarding pH and EDTA concentration of the elution buffer.

2 Materials

2.1 Buffers

Prepare all buffers using deionized water and degas buffers to avoid air bubbles entering the column. All buffers are insensitive to light and can be stored at room temperature.

1. Running buffer: 50 mM Tris, 150 mM NaCl, 0.05% (v/v) Tween 20, 1 mM $CaCl_2$, pH: 7.5 (*see* **Note 1**).
2. Washing buffer: 5 mM NH_4Ac, 1 mM $CaCl_2$, pH: 5.5–6.
3. Elution buffer: 1×HBS (20 mM HEPES, 150 mM NaCl), 100 mM EDTA, pH: 7 (*see* **Note 2**).
4. Storage buffer: 50 mM Tris, 150 mM NaCl, 0.05% (v/v) Tween 20, 1 mM $CaCl_2$, 20% ethanol, pH: 7.5.

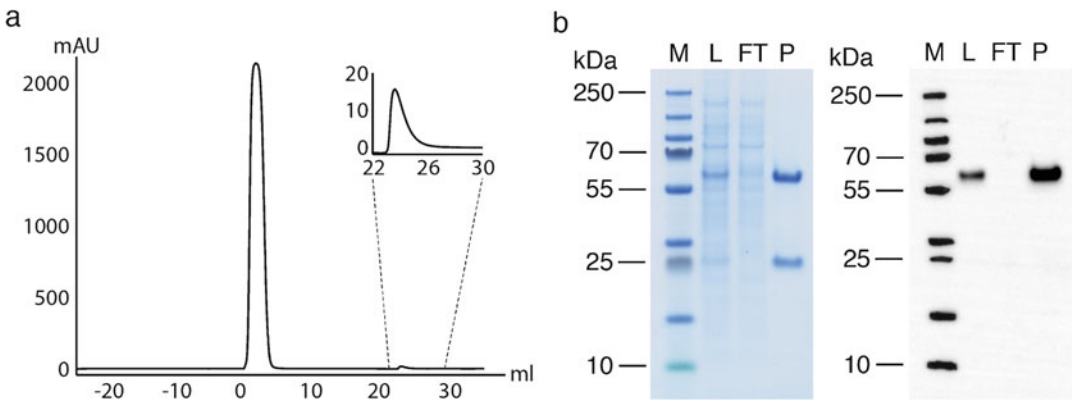

Fig. 2 Analysis of the purification of a cell culture supernatant with recombinantly produced IgG on a column with the tetrameric Z_{Ca} ligand. (**a**) A typical chromatogram displaying the purification using an elution buffer with 100 mM EDTA, 100 mM NH_4Ac (pH: 5.5). The left peak represents the flow through when the sample is added to the column and the right peak (zoomed in) shows the eluted antibody. (**b**) Representative results from SDS-PAGE and Western Blot analysis (detecting human IgG) of the loaded sample (L), the collected flow through (FT), and the eluted target protein (P) next to a molecular weight marker (M)

2.2 Chromatography Media and System

1. 1-ml HiTrap column (GE Healthcare) packed with resin with immobilized Z_{Ca} tetramer.
2. ÄKTA Pure chromatography system (GE Healthcare) or equivalent. A flow rate of 1 ml/min is used in this protocol.

3 Methods

1. Pulse a 1-ml Z_{Ca}-coupled HiTrap column with 6 column volumes (CV) of ultrapure water, 6 CV of running buffer, and 6 CV of elution buffer.
2. Equilibrate the column with 13 CV running buffer.
3. Load the antibody sample, with $CaCl_2$ added to a concentration of 1 mM, onto the column.
4. Wash the column with 13 CV running buffer followed by 5 CV washing buffer.
5. Elute the antibodies by adding 6 CV elution buffer and collect the eluate in fractions.
6. Monitor A_{280} in the chromatogram. A characteristic chromatogram is shown in Fig. 2a.
7. Examine the antibody purity in the eluted fractions by sodium dodecyl sulfate-polyacrylamide gel electrophoresis (SDS-PAGE). A representative SDS-PAGE gel is shown in Fig. 2b.
8. Regenerate the column by adding 3 CV elution buffer followed by 6 CV running buffer.
9. Add at least 2 CV ultrapure water to the column followed by at least 2 CV storage buffer (*see* **Note 3**). Store at 4–8 °C.

4 Notes

1. Do not use a phosphate buffer as there is a risk for calcium phosphate precipitation.
2. The EDTA concentration can be optimized for each target antibody and lower concentrations can likely be used.

   For purification of monoclonal IgG1 antibodies, an elution buffer with pH 5.5 should be used to achieve complete elution. Stepwise elution can be performed using 100 mM EDTA, 100 mM NH_4Ac (pH: 5.5). Gradient elution can be conducted using a linear gradient from 0 to 200 mM EDTA with 100 mM NH_4Ac (pH: 5.5), typically over 20 CV.

   Monoclonal IgG2 and IgG4 antibodies can also be purified using gradient elution over 20 CV from 0 to 200 mM EDTA with 1xHBS, at pH 7. Other buffering agents with buffer capacity at the desired pH can also be used, except for phosphate (*see* **Note 1**).
3. If the column is to be used again soon, up until the following day, it can also be stored in a buffer without ethanol.

References

1. Espiritu M, Collier A, Bingham J (2014) A 21st-century approach to age-old problems: the Ascension of biologics in clinical therapeutics. Drug Discov Today 19:1109–1113
2. Ecker DM, Jones SD, Levine HL (2015) The therapeutic monoclonal antibody market. MAbs 7:9–14
3. Gronemeyer P, Ditz R, Strube J (2014) Trends in upstream and downstream process development for antibody manufacturing. Bioengineering 1:188–212
4. Hober S, Nord K, Linhult M (2007) Protein a chromatography for antibody purification. J Chromatogr B 848:40–47
5. Boström T, Nilvebrant J, Hober S (2012) Purification systems based on bacterial surface proteins. In: Ahmad R (ed) Protein purification. INTECH Open Access Publisher, London
6. Shukla AA, Gupta P, Han X (2007) Protein aggregation kinetics during protein A chromatography. Case study for an Fc fusion protein. J Chromatogr A 1171:22–28
7. Vázquez-Rey M, Lang DA (2011) Aggregates in monoclonal antibody manufacturing processes. Biotechnol Bioeng 108:1494–1508
8. Paul AJ, Schwab K, Hesse F (2014) Direct analysis of mAb aggregates in mammalian cell culture supernatant. BMC Biotechnol 14:99
9. Liu B, Guo H, Xu J et al (2016) Acid-induced aggregation propensity of nivolumab is dependent on the Fc. MAbs 8:1107–1117
10. Mazzer AR, Perraud X, Halley J et al (2015) Protein A chromatography increases monoclonal antibody aggregation rate during subsequent low pH virus inactivation hold. J Chromatogr A 1415:83–90
11. Kanje S, Venskutonytė R, Scheffel J et al (2018) Protein engineering allows for mild affinity-based elution of therapeutic antibodies. J Mol Biol 430:3427–3438
12. Kaplon H, Reichert JM (2018) Antibodies to watch in 2018. MAbs 10:183–203
13. Julia Scheffel, Sara Kanje, Jesper Borin, Sophia Hober (2019) Optimization of a calcium-dependent Protein A-derived domain for mild antibody purification. mAbs 11 (8):1492–1501

Chapter 18

Macroporous Polymer Monoliths for Affinity Chromatography and Solid-Phase Enzyme Processing

E. G. Korzhikova-Vlakh, G. A. Platonova, and T. B. Tennikova

Abstract

Nowadays, monolithic stationary phases, because of their special morphology and enormous permeability, are widely used for the development and realization of fast dynamic and static processes based on the mass transition between liquid and solid phases. These are liquid chromatography, solid-phase synthesis, microarrays, flow-through enzyme reactors, etc. High-performance liquid chromatography on monoliths, including the bioaffinity mode, represents unique technique appropriate for fast and efficient separation of biological (macro)molecules of different sizes and shapes (proteins, nucleic acids, peptides), as well as such supramolecular systems as viruses.

In the edited chapter, the examples of the application of commercially available macroporous monoliths for modern affinity processing are presented. In particular, the original methods developed for efficient isolation and fractionation of monospecific antibodies from rabbit blood sera, the possibility of simultaneous affinity separation of protein G and serum albumin from human serum, the isolation of recombinant products, such as protein G and tissue plasminogen activator, respectively, are described in detail. The suggested and realized multifunctional fractionation of polyclonal pools of antibodies by the combination of several short monolithic columns (disks) with different affinity functionalities stacked in the same cartridge represents the original and practically valuable method that can be used in biotechnology. In addition, macroporous monoliths were adapted to the immobilization of such different enzymes as polynucleotide phosphorylase, ribonuclease A, α-chymotrypsin, chitinolytic biocatalysts, β-xylosidase, and β-xylanase. The possibility of use of immobilized enzyme reactors based on monoliths for different purposes is demonstrated.

Key words Proteins, Enzymes, Protein and peptide immobilization, Monoliths, Affinity chromatography, Fractionation, Enzyme reactors, Conjoint chromatography

1 Introduction

Currently, macroporous monolithic materials have become widely used in analysis and high-speed separation of small and macromolecules at different analytical processes (immunological, ecological, medical, and other types of analytical monitoring), preparative isolation of blood proteins from plasma and serum, as well as recombinant products directly from cell supernatants or lysates

Nikolaos E. Labrou (ed.), *Protein Downstream Processing: Design, Development, and Application of High and Low-Resolution Methods*, Methods in Molecular Biology, vol. 2178, https://doi.org/10.1007/978-1-0716-0775-6_18,

[1–3]. The monolithic sorbents are prepared via in situ synthesis in a mold of desirable size and shape. Contrary to the packed column, monolithic device represents a single-piece material pierced with interconnected flow-through channels (macropores). Due to the structural specialties of macroporous monoliths, these materials demonstrate unique hydrodynamic properties that are finally providing the fast separation at high flow rates and low operative back pressure [4]. The diversity of monolithic sorbents, which can be made from natural or synthetic polymers, inorganic or hybrid materials with various functionalities, allows the realization of separation process by the application of different HPLC modes.

In a wide range of protein isolation and purification techniques, affinity chromatography plays one of the key roles. This mode of chromatography is based on the noncovalent-specific interaction of a target protein being in solution to its natural biological complement—ligand—immobilized on the surface of the stationary phase [3, 5, 6]. In addition, bioaffinity pair formation on monoliths is very fast and the whole process of affinity separation can be realized within second time scale. Moreover, due the absence of steric limitations for the interaction of biomacromolecules inside the sorbent macroporous structure, affinity chromatography on monoliths provides the unique opportunity to investigate and quantitatively compare the biospecific pair formation under the close to physiological conditions.

In addition, macroporous monoliths are mostly adapted to the immobilization of enzymes and can serve as a base for the design of simple and convenient bioreactors for industrial purposes [7–9]. Solid-phase attachment of enzymes has a number of advantages compared to the application of soluble biocatalysts. An attachment of enzyme to a solid support provides the stabilization of enzyme, prevents its autolysis, facilitates the product removal, makes a biocatalyst reusable and stable for a long time period.

In addition, the combination of different chromatographic modes or biocatalytic and chromatographic techniques in a single run leads to the automation and simplification of the technological process. Such combination of several columns with different functionalities in a tandem-like (conjoint) mode can be easily performed for macroporous monoliths without the drastic increase of the operating back pressure [10–12].

This chapter gives some examples of effective affinity protein separations and fractionations, as well as heterogeneous biocatalysis realized with the use of macroporous polymethacrylate monoliths as stationary phases. The described protocols can be applied as they are or may be used as a base for the adaptation for similar practical tasks.

2 Materials

2.1 Monolithic Columns

1. Epoxy-bearing ultra-short macroporous monolithic columns of 12 mm i.d. × 3 mm, bed volume of 0.34 mL (CIM Epoxy disks, BIA Separations, Slovenia).
2. Epoxy-bearing ultra-short macroporous monolithic columns of 5 mm i.d. × 5 mm, bed volume of 0.1 mL (CIM Epoxy minidisks, BIA Separations, Slovenia).
3. Epoxy-bearing monolithic tube with bed volume of 8 mL (CIM Epoxy Tube, BIA Separations, Slovenia).
4. Analytical DEAE monolithic column of 12 mm i.d. × 3 mm, bed volume of 0.34 mL (CIM-DEAE disk, BIA Separations, Slovenia).
5. Epoxy-bearing macroporous monolithic columns of 4.6 mm id × 50 mm, bed volume of 0.84 mL, based on poly(glycidyl methacrylate-*co*-2-hydroxyethyl methacrylate-*co*-ethylene glycol dimethacrylate) (GMA-HEMA-EDMA) (*see* **Note 1**).

2.2 Chemicals and Biologicals Used for the Preparation of Affinity Sorbents and Immobilized Enzyme Reactors Based on Macroporous Monoliths

1. Monolithic column pretreatment solutions (before protein immobilization): ethanol, water/ethanol (50/50 v/v), and water.
2. Buffer and solutions preparations: analytical-grade chemicals and double distilled water are used to prepare the buffers for ligand immobilization and affinity chromatography. All solutions are purified by ultrafiltration through membrane filters with 0.2-μm pore size.
3. Buffer and solution storage: all buffers and solutions are stored at 4 °C in a dark glass.
4. Determination of protein concentration in solution: standard Lowry assay kit [13].
5. Washing buffer for affinity columns: 0.01 M sodium phosphate buffer containing 0.15 mmol/L of NaCl (0.01 M PBS), pH: 7.0.
6. Storage solution: 0.01 M PBS, pH: 7.0, containing 0.02% (w/v) of sodium azide is used for all affinity sorbents and immobilized enzyme reactors except those marked in additionally.

2.2.1 Immobilization of Peptides on Epoxy-Bearing Monolithic Columns

1. Affinity ligand: bradykinin (BK), pentadecapeptide and hexadecapeptide, representing part of C-chain of proinsulin and outside membrane loop of ATPase of P1-type, respectively.
2. Immobilization buffer: 0.1 M sodium borate buffer, pH: 10.

2.2.2 Immobilization of Proteins on Epoxy-Bearing Monolithic Columns

1. Affinity ligands:
   (a) for fractionation of a pool of polyclonal antibodies produced via immunization of rabbits with corresponding proteins and conjugate: (1) bovine serum albumin (BSA), (2) succinylated BSA (BSA-S), (3) BSA-S-BK.
   (b) for fractionation of IgG and HSA: (1) IgG-binding and (2) SA-binding Proteins G.
   (c) for isolation of protein G from *E. coli* cell lysate: IgG.
   (d) for isolation of t-PA: (1) monoclonal antibodies or (2) plasminogen.
2. Immobilization buffer: 0.1 M sodium carbonate buffer, pH: 9.3.

2.2.3 Immobilization of Proteins on Amino-Bearing Monolithic Columns

1. Solution for stationary-phase amination: 25% aqueous ammonium solution.
2. Immobilization buffer: 0.01 M sodium phosphate buffer, pH: 4.5.
3. Activation agent for protein carboxylic groups: Ethyl-3-(3-dimethylaminopropyl) carbodiimide.

2.2.4 Immobilization of Enzymes on Epoxy-Bearing Monolithic Columns

1. Enzymes: (a) polynucleotide phosphorylase from *Thermus thermophilus* (PNPase), (b) ribonuclease A (RNase), (c) α-chymotrypsin (ACHT).
2. Immobilization buffer: 0.02 M sodium carbonate buffer, pH of 9.3 for PNPase and 0.01 M sodium borate buffer, pH of 8.5 for RNase and ACHT.

2.2.5 Immobilization of Enzymes Through Aldehyde-Bearing Spacers

1. Enzymes: (a) Ribonuclease A (RNAse), (b) α-chymotrypsin (ACHT), (c) *Grindamyl* β-xylanase, (d) β-xylosidase from *Aspergillus awamori X-100, (e)* chitinase complex from *Clostridium paraputrificum* (strain J4).
2. Solution for stationary-phase amination: 25% aqueous ammonium solution.
3. Spacer: (a) short spacer—25% glutaraldehyde solution in water, (b) macromolecular spacer—oxidized *N*-methacrylamido-D-glucose (PMAG) (Mw 25,000) containing 28 mol% of aldehyde groups.
4. Immobilization buffer for spacer: 0.01 M PBS, pH: 7.0.
5. Immobilization buffer for proteins/enzymes: 0.01 M sodium phosphate, pH: 5.0, for β-xylanase /β-xylosidase, and 0.01 M sodium borate buffer, pH: 8.4, for others.
6. Reducing agent for imine bonds: sodium borohydride.

2.3 Chemicals and Biologicals for Affinity Chromatography and Flow-Through Heterogeneous Biocatalysis

2.3.1 Isolation/ Fractionation of Antibodies and Isolation of IgG and HSA from Blood Serum

1. Adsorption buffer: 0.01 M PBS, pH: 7.0.
2. Washing solution: 2.0 M NaCl in water.
3. Desorption solution: 0.01 M HCl, pH: 2.0.
4. Neutralization solution: 0.05 M NaOH or with 0.5 M Na_2HPO_4, pH: 9.0.
5. Biological samples: (1) redispersed in PBS pool of antibodies that were precipitated with 32–35% aqueous ammonium sulfate solution from rabbit blood sera [14], (2) human blood sera.

2.3.2 Isolation of Protein G

1. All buffers and solutions were the same as in Subheading 2.3.1.
2. Biological sample: *E. coli* cell lysate-containing protein G.

2.3.3 Enzymatic Synthesis and Phosphorolysis of Polyriboadenylate

1. Substrates: (a) Adenosine-5′-diphosphate (ADP) for biocatalytic synthesis, (b) polyriboadenylate (poly(A)) for biocatalytic hydrolysis.
2. Reaction mixture for the synthesis of polyriboadenylate: 0.2 M Tris–HCl buffer, pH of 8.0 + 6 mmol/L $MgCl_2$ + 1 mmol/L sodium salt of EDTA + 20 mmol/L ADP.
3. Reaction mixture for phosphorolysis of polyriboadenylate: 0.2 M Tris–HCl buffer, pH of 8.0 + 2 mmol/L sodium salt of EDTA + 14 mmol/L NaH_2PO_4 + 3 mmol/L $MgCl_2$ + 1.4 mmol/L poly(A).

2.3.4 Measurements of Activity of Immobilized Enzymes and Degradation of Macromolecular Substrates

ACHT

1. Substrate for activity determination: *N*-benzoyl-L-tyrosine ethyl ester (BTEE).
2. Reaction buffer: the mixture of 0.05 M Tris–HCl buffer, pH: 7.8, and methanol in ratio 1:1 (v/v).
3. Macromolecular substrate: Bovine serum albumin (BSA).

RNase

1. Substrate: Cytidine-2′,3′-cyclic monophosphate (CCM).
2. Reaction buffer: 10 mM Tris–HCl buffer, pH of 7.5, containing 2 mmol/L EDTA and 0.1 mol/L NaCl.
3. Macromolecular substrate: RNA from *Torula yeast*.

N-Acetyl-glucosaminidase

1. Substrate: for *N*-acetyl-glucosaminidase (presenting in complex of chitinases): 4-nitrophenol-*N*-acetyl-β-D-glucosaminide.
2. Reaction buffer: 0.1 M sodium phosphate buffer, pH of 6.0, with 5% of acetonitrile.
3. Standard for calibration plot building: 4-nitrophenol.

β-xylanase and β-xylosidase

1. Substrate: beechwoodxylan.
2. Reaction buffer: 20 mM sodium acetate buffer, pH: 5.0.
3. Xylose determination: Somogyi method [15].

2.4 Equipment

1. CIM housing suited for installation from 1 to 4 standard CIM disks (BIA Separations, Slovenia).
2. Chromatographic system consisting of high-pressure pump, spectrophotometric detector, column thermostat and computer provided with corresponding software to control the process. The low-pressure pump for the performance of recirculation of a solution through the monolithic column (heterogeneous biocatalysis).
3. UV-Vis spectrophotometer and system for vertical polyacrylamide gel-electrophoresis to determine the amount of isolated proteins, as well to control their purity.
4. Air thermostat working in the range from 30 to 65 °C for the performance of protein immobilization, biocatalytic synthesis, and degradation reactions.
5. Water thermostat working at 70 °C for synthesis of lab-made macroporous monolithic columns.

3 Methods

3.1 Preparation of Affinity Sorbents and Immobilized Enzyme Reactors Based on Macroporous Monoliths

The presence of original epoxy groups in monolithic CIM-material allows simple one-step reaction of covalent attachment of any amino-bearing molecules to the sorbent surface [14, 16–18]. Besides that, epoxy groups can be converted into many other functionalities, such as hydroxyl [19, 20], amino [21], aldehyde groups [21, 22], etc. The wide variety of possible surface modification allows also the immobilization of proteins through the spacers of different length. Usually, the introduction of a spacer complicates the immobilization procedure up to two-three steps. At the same time, protein immobilized through the spacer arm is distanced from the solid support surface and, as a result, the biomolecule is better accessible for affinity interaction. It is especially important for the case of immobilized enzymes involved in the biocatalytic reactions with macromolecular substrates.

The application of heterogeneous biocatalysts, i.e., enzymes, immobilized on a solid-phase surface [7, 23] is regarded as one of the most convenient and economic approaches of bioconversion of various raw materials. The localization of enzyme on the surface of a solid support promotes stabilization of its conformation, thus avoiding denaturation and a drop in catalytic activity.

3.1.1 Direct One-Step Immobilization of Peptides, Proteins, or Enzymes

1. (A) For CIM disks: Place macroporous monolithic CIM Epoxy disk of 12 mm i.d. × 3 mm or 5 mm i.d. × 5 mm in corresponding CIM housing to obtain column for installation into chromatographic system. (B) For lab-made columns: use as it is.
2. Install the column into a chromatographic system to wash consequently with 10 column volumes of ethanol, ethanol–water (50:50, v/v), water, and immobilization buffer with use of flow rate of 2 mL/min.
3. Prepare peptide, protein, or enzyme solution in immobilization buffer with concentration 2–3 mg/mL for peptides and 4–5 mg/mL for proteins/enzymes.
4. Disconnect the column from chromatographic system, connect the column to the Luer syringe filled with immobilization solution, and let pass 0.5 mL of solution through CIM mini-disc (5 × 5 mm), 1 mL of solution through CIM disk (12 × 3 mm), and 2 mL of solution through the column (4.6 × 50 mm).
5. Incubate the column filled with immobilization solution and closed from both ends by caps at 22–25 °C for 18–24 h or in air thermostat at 30 °C for 16 h without any stirring (static immobilization method) [14, 24–28].
6. After immobilization proceeded, install the column into a chromatographic system.
7. Remove the residual nonbound peptide or protein/enzyme by washing affinity support with immobilization buffer to reach a baseline detector signal. Collect solution to determine the amount of free ligand washed from pore space.
8. Lyophilize the washing fractions and then dissolve the dried samples in 0.5 mL of water to determine the amount of unbound peptide or protein/enzyme.
9. Calculate coupling efficiency (*see* **Notes 2** and **3**).
10. Install the column into chromatographic system and wash with 0.01 M PBS, pH: 7.0. If not use immediately, wash the column by pumping consequently water and storage buffer to reach the baseline signal. The washing flow rate is 2 mL/min.
11. Store columns at 4 °C until use. CIM disks are stored after being removed from housing and immersed into the container with storage buffer (*see* Subheading 2.2).

3.1.2 Immobilization of Proteins Via Their Carboxylic Groups on Amino-Bearing Surface

The proteins can be immobilized with the use of following *two-step method* [14]:

1. For CIM disks: (a) Place macroporous monolithic CIM Epoxy disk of 12 mm i.d. × 3 mm or 5 mm i.d. × 5 mm in

corresponding CIM housing to obtain column for installation into chromatographic system; (b) For lab-made columns: use as it is.

2. Install the column to a chromatographic system to wash consequently with 10 column volumes of ethanol, ethanol–water (50:50, v/v), water, and immobilization buffer with use of flow rate of 2 mL/min.
3. Prepare solution 25% aqueous ammonium solution for stationary-phase amination.
4. Connect the column to the Luer syringe filled with 25% aqueous ammonium solution and let pass 0.5 mL of solution through CIM minidisc (5 × 5 mm), 1 mL of solution through CIM disk (12 × 3 mm), and 2 mL of solution through the column (4.6 × 50 mm).
5. For surface modification, incubate closed from both ends with cups columns at 4 °C for 5 h without any stirring.
6. After reaction completed install the column into chromatographic system, wash the column with water and then with immobilization buffer up to baseline detector signal at a flow rate of 2 mL/min.
7. Prepare protein solution with concentration 4–5 mg/mL in immobilization buffer and add to this solution a 160-fold molar excess of activating agent for protein carboxylic groups (*see* Subheading 2.2.3).
8. Follow the protocol for one-step immobilization method (see earlier) starting from **steps 4** to **11**.

3.1.3 Immobilization of Proteins/Enzymes Through Aldehyde-Bearing Spacer

1. Follow the protocol for immobilization method described in Subheading 3.1.2 starting from **steps 1** to **6**.
2. After reaction is completed, install the column into chromatographic system and wash the column with water, and then with immobilization buffer for spacers (*see* Subheading 2.2.5) up to baseline detector signal at a flow rate of 2 mL/min.
3. Prepare a solution of spacer: (a) 25% aqueous glutaraldehyde or (b) aldehyde-bearing polymer, containing 28 mol% of aldehyde groups, (for example, ox.PMAG) with concentration 0.6 mg/mL in immobilization buffer for spacer (*see* **Note 4**).
4. Connect the column to the Luer syringe filled with spacer solution and let pass 0.5 mL of solution through CIM minidisc (5 × 5 mm), 1 mL of solution through CIM disk (12 × 3 mm), and 2 mL of solution through the column (4.6 × 50 mm).

5. For spacer immobilization, incubate closed columns at 22–25 °C for 1.5 h without any stirring (static immobilization method).
6. Install the column into chromatographic system and wash the column with water and then with immobilization buffer for proteins/enzymes up to baseline detector signal at a flow rate of 2 mL/min.
7. Prepare protein/enzyme solution in buffer for immobilization with concentration of 1 mg/mL for CIM minidisk, 3 mg/mL for CIM disk, and 5 mg/mL for monolithic column.
8. Remove the column from chromatographic system, connect the column to the Luer syringe filled with a solution of protein/enzyme, and force it through the column to fill the matrix inner space.
9. For protein/enzyme immobilization, incubate columns at 22–25 °C for 1.5 h without any stirring (static immobilization method).
10. Follow the protocol for one-step immobilization method described in Subheading 3.1.1 starting from **steps 7** to **9**.
11. Connect the column to the Luer syringe filled with an aqueous solution of sodium borohydrate with concentration 1 mg/mL and inject 0.5 mL of solution inside the stationary phase to reduce formed imine bonds and unreacted aldehyde functionality.
12. Follow **steps 10** and **11** of the protocol for one-step immobilization method described in Subheading 3.1.1.

3.2 Determination of Quantitative Parameters of Dynamic Adsorption Using Monolithic Disk Affinity Chromatography

The affinity characteristics of prepared monolithic sorbents, such as maximum adsorption capacity (Q_{max}) and apparent dissociation constants of affinity complex (K_{diss}), can be evaluated on the basis of the mathematical treatment of experimental adsorption isotherms resulting from the frontal analysis [14, 19, 29–31].

1. Install the monolithic column with immobilized peptide/protein ligand into a chromatographic system.
2. Equilibrate the column with adsorption buffer at a flow rate of 2 mL/min to reach a baseline at 280-nm wavelength.
3. Pass through the disk preliminary prepared solutions of protein, which has affinity to the immobilized peptide/protein ligand, with concentrations ranging from 0.1 to 1.5 mg/mL to reach the saturation (frontal elution) (*see* **Note 5**).
4. Wash the column with adsorption buffer to reach a baseline signal.
5. Wash the column with washing solution (2 M NaCl in water) to eliminate nonspecific adsorption and to reach a baseline signal.

6. Wash the column with adsorption buffer to reach a baseline signal.
7. Elute protein specifically bound to the immobilized affinity ligand with 0.01 M HCl, pH: 2.0, and collect desorbed fraction.
8. To prevent denaturation of the isolated protein, neutralize the collected fraction immediately using a neutralizing solution (*see* Subheading 2.3.1).
9. Measure the protein content in the eluted fraction using standard Lowry assay [13].
10. Follow **steps 10** and **11** of the protocol described in Subheading 3.1.1.
11. Use Excel or Origin software to plot the Langmuir-type adsorption isotherm in coordinates: *concentration of loaded IgG* (or HSA) (C), mg/mL—*amount of isolated IgG* (or HSA) (Q), mg (*see* **Note 6**).
12. Use the same software to plot the linearized form of isotherm in double reciprocal coordinates, e.g., $1/C - 1/Q$. From graph obtained, calculate the values of apparent dissociation constant (K_{diss}) and maximum adsorption capacity (Q_{max}) (*see* **Note 7**).

The examples of affinity parameters determined by this method are presented in Table 1.

3.3 Determination of Kinetic Parameters of Enzymes Immobilized on the Surface of Monolithic Materials

The measurements of kinetic parameters of immobilized enzymes, such as the apparent values of Michaelis constant (K_m) and maximum velocity of enzymatically catalyzed reaction (V_{max}), can be determined for immobilized enzymes by two experimental ways, namely, by substrate recirculation mode, and by zonal elusion mode. In both cases, kinetic parameters are calculated using a graphical approach based on plotting of the dependence of the hydrolysis velocity (V) on the substrate concentration ([S]) (Michaelis-Menten plot) and its subsequent linearization in double reciprocal coordinates, e.g., $1/[S] - 1/V$ (Lineweaver–Burk plot) [21, 32], or coordinates of $[S]/V - [S]$ (Hanes plot) [11, 27, 33].

3.3.1 Determination of Kinetic Parameters of Immobilized Ribonuclease A

In the recirculation mode, the bioreactor functions as a cyclic system, where the substrate solution recirculates through the monolithic column bearing covalently bound enzyme for a fixed time at a chosen flow rate. This approach allows the product accumulation in the reaction medium. To determine the RNase activity, cytidine-2′,3′-cyclic monophosphate (CCM) or uridine-2′,3′-cyclic monophosphate can be applied as specific substrates, respectively.

Table 1
The parameters of affinity bindings determined for some affinity pairs using affinity chromatography on macroporous monoliths

Affinity pair		Q_{ligand}, mg/mL of sorbent	K_{diss}, μm	Q_{max}, mg/mL sorbent	Size of CIM-epoxy disk (mm)	References
Immobilized ligand	Protein in solution					
IgG-binding protein G	IgG	2.5	0.7	0.5	12 × 3	[26]
HSA-binding protein G	HSA	2.3	0.7	3.5	12 × 3	[26]
Plasminogen	t-PA	4.7	0.9	0.3	12 × 3	[24]
Antibodies to t-PA	t-PA	3.5	0.2	0.9	12 × 3	[24]
Fibrinogen	t-PA	2.0	14.0	10.0	12 × 3	[24]
Bradykinin	Antibodies	5.0	2.6	1.4	12 × 3	[25]
BSA	Antibodies	5.9	2.4	4.2	12 × 3	[25]
Soybean trypsin inhibitor	Trypsin	2.6	0.8	0.4	12 × 3	[31]
Soybean trypsin inhibitor	Trypsin bound to polystyrene particles	3.2	1.0	0.2	12 × 3	[31]
Pentadecapeptide	Antibodies	2.6	1.9	0.4	25 × 2	[25]
Hexadecapeptide	Antibodies	5.9	1.1	1.5	25 × 2	[25]

The activity of RNase toward cytidine-based substrates is for several times higher than for uridine-based ones [34].

The determination of immobilized RNase activity in recirculation mode can be carried out in the following way:

1. Prepare operating buffer and cytidine-2,3-cyclic monophosphate solutions at the concentration of 0.01–0.30 mg/mL in operating buffer (*see* Subheading 2.3.3 for RNase).
2. Install the monolithic column with immobilized enzyme into a chromatographic system and equilibrate the column with the operating buffer at a flow rate of 2 mL/min to reach a baseline.
3. Pump 3 mL of substrate solution with different concentrations through the enzyme reactor for 10 min at 22 °C in a recirculation mode (Fig. 1). The optimal range of flow rates is 1–2 mL/min. The chosen flow rate must be kept constant. Between the recirculation of solutions with different concentrations, wash the column with 10 column volumes of operating buffer.

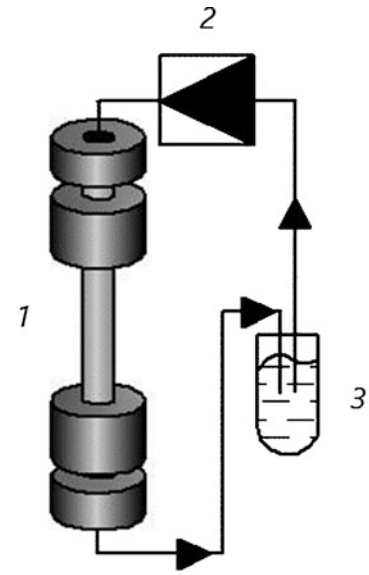

Fig. 1 Scheme of solution recirculation through monolithic column: (1) monolithic column, (2) low-pressure pump, (3) recirculated solution

4. After 10 min, take out the reaction medium for absorbance measurement at 286 nm to calculate the velocity of the biocatalytic reaction (*see* **Note 8**). Before measurement, set to zero the absorbance of the initial substrate solution with the same concentration to register ΔA.
5. At the end of work, wash the column by pumping storage buffer to reach the baseline signal. The washing flow rate is 2 mL/min.
6. Store columns at 4 °C until use. CIM disks are stored after being removed from housing and immersed into the container with storage buffer (*see* Subheading 2.2).
7. Using Excel or OriginPro software, build the Michaelis-Menten plot of the dependence of the velocity of hydrolysis (V) on the substrate concentration ([S]) and then linearize it in coordinates of $1/[S] - 1/V$ (Lineweaver–Burk plot) or $[S]/V - [S]$ (Hanes plot). Calculate K_m, V_{max}, and specific activity (*see* **Note 9**).

Immobilization capacities of RNase based on monolithic supports and apparent kinetic parameters for enzymatic hydrolysis of low-molecular substrate are presented in Table 2.

In contrast to recirculation, a zonal elution approach involves the application of a small, fixed amount of substrate solution to a column with the immobilized enzyme. The determination of immobilized RNase activity in zonal elution mode can be carried out as follows:

Table 2
Kinetic parameters determined for some reactions catalyzed by enzymes immobilized on macroporous monoliths

Immobilized enzyme	Immobilization approach	Monolith	Substrate	K_M, mM	A_{sp}, U/mg	References
RNase	Direct	CIM disk 12 × 3 mm	CCM	1.3	0.5	[39]
RNase	Through polymer spacer	CIM disk 12 × 3 mm	CCM	1.6	0.9	[39]
ACHT	Direct	CIM minidisk 5 × 5 mm	BTEE	0.9	8.3	[21]
ACHT	Through polymer spacer	CIM minidisk 5 × 5 mm	BTEE	2.2	23.2	[21]
Complex of chitinases	Through polymer spacer	CIM minidisk 5 × 5 mm	4-nitrophe-nyl-*N*-ace-tyl-β-D-glucos-aminide	28.9	0.4	[32]
β-Xylosidase	Through polymer spacer	Lab-made column 4.6 × 50 mm	Xylan	4.1	32.3	[11]
β-Xylanase	Through polymer spacer	CIM disk 12 × 3 mm	Xylan	1.0	517.0	[11]
PNPase	Direct	CIM disk 12 × 3 mm	Poly(A)	0.2	29.3	[17]

1. Follow **steps 1** and **2** of the protocol for recirculation mode (see earlier).
2. Set the wavelength on HPLC detector at 286 nm. Balance the chromatographic system with operating buffer (without column).
3. Inject 100 μL of substrate solutions with different concentrations to register "zero" absorbance. Using HPLC system software, calculate peak area for each injected sample.
4. Follow **steps 3** and **4** of the protocol for recirculation mode (see earlier).
5. Inject 100 μL of substrate solutions with different concentrations through the enzyme reactor at a flow rate of 0.5 mL/min.
6. Calculate the peak area for each hydrolyzed sample and find the difference between these values and corresponding peak area of the native substrate. To calculate the velocity of biocatalytic reaction, *see* **Notes 8** and **9**.

7. Follow **steps 7–9** of the protocol for recirculation mode (see earlier).

   The characteristics of some immobilized enzyme reactors are given in Table 2.

3.3.2 Determination of Kinetic Parameters of Immobilized α-Chymotrypsin

ACHT is a protease close to trypsin from the point of view of their molecular structure and mechanism of proteolysis. However, ACHT is more stable and demonstrates different cleavage specificity being active against peptide and ester bonds formed with aromatic amino acids such as tyrosine, phenylalanine, and tryptophan [35]. As specific low-molecular substrates, the different tyrosine derivatives are widely used. The activity of chymotrypsin-immobilized monolithic reactors can be carried out with the use of *N*-benzoyl-L-tyrosine ethyl ester (BTEE) as substrate [36].

1. Prepare the stock solution of the substrate (BTEE) in methanol with a concentration of 2 mg/mL.
2. Install the monolithic column with immobilized enzyme into a chromatographic system.
3. Equilibrate the column with a mixture of 0.05 M Tris–HCl, pH of 7.8, and methanol in ratio 1:1 (v/v) at a flow rate of 2 mL/min to reach a baseline.
4. Using the stock solution and 0.05 M Tris–HCl, pH of 7.8, prepare a solution of BTEE for enzymatic hydrolysis with substrate concentration in the range of 0.01–0.30 mg/mL. The ratio buffer/methanol in the final solution should be 1/1 (v/v). Each solution should be prepared before use and applied immediately.
5. Pump 3 mL of substrate solution with different concentrations through the enzyme reactor for 10 min at 22 °C (Fig. 1). The optimal range of flow rates is 1–2 mL/min. The chosen flow rate must be kept constant. Between the recirculation of solutions with different concentrations, wash the column with 10 column volumes of operating buffer.
6. After 10 min, take out the reaction medium for absorbance measurement at 256 nm to calculate the velocity of the biocatalytic reaction. The absorbance measurements should be performed immediately after hydrolysis. Before measurement, set to zero the absorbance of the initial substrate solution with the same concentration to register ΔA. The amount of the product is calculated using an extinction coefficient of the product (*N*-benzoyl-L-tyrosine) (*see* **Note 10**).
7. Follow **steps 7–9** of the protocol for RNase activity determination.

   The characteristics of some immobilized enzyme reactors are given in Table 2.

3.3.3 Determination of Kinetic Parameters of Immobilized N-Acetylglucosaminidase

Chitinases are used in biotechnology to produce chitooligosaccharides and *N*-acetyl-D-glucosamines, as well as for chitin waste processing [37]. It also facilitates the separation of reaction products and allows recycling of the biocatalyst. The activity of *N*-acetylglucosaminidase is determined with the use of low-molecular substrate 4-nitrophenol-*N*-acetyl-β-D-glucosaminide.

1. Prepare 0.1 M sodium phosphate buffer, pH of 6.0, with 5% of acetonitrile (operating buffer).
2. Prepare the solutions of 4-nitrophenol-*N*-acetyl-β-D-glucosaminide in operating buffer with concentrations in the range 0.01–0.30 mg/mL.
3. Follow **steps 3** and **4** of the protocol for RNase activity determination (Subheading 2.2.1).
4. Pump 3 mL of substrate solution with different concentrations through the enzyme reactor for 30 min at 40 °C (Fig. 1). The optimal range of flow rates is 1–2 mL/min. The chosen flow rate must be kept constant. Between the recirculation of solutions with different concentrations, wash the column with 10 column volumes of operating buffer.
5. After 15 min, take out the reaction medium for absorbance measurement at 288 nm to calculate the velocity of the biocatalytic reaction. Before measurement, set to zero the absorbance of the initial substrate solution with the same concentration to register ΔA.
6. Measure the absorbance of a product (4-nitrophenol) by offline UV detection at 410 nm and calculate the concentration of the product using the calibration curve made for 4-nitrophenol.
7. Follow **steps 7–9** of the protocol for RNase activity determination.

   The characteristics of some immobilized enzyme reactors are given in Table 2.

3.3.4 Determination of Kinetic Parameters of Immobilized β-Xylosidase or β-Xylanase

The activity of β-xylosidase or β-xylanase enzymes [11] immobilized on surfaces of monolithic disks and lab-made columns can be determined with the use of xylan as a substrate. Xylan is one of the main components of hemicellulose and the second most abundant polysaccharide in nature [38]. Products of its degradation, xylooligosaccharides and xylose, have important applications in the food industry as components of prebiotics and sweeteners.

1. Prepare 20 mM sodium acetate buffer, pH: 5.0 (operating buffer).
2. Prepare the solutions of xylan in operating buffer with concentrations from 0.1 to 2.0 mg/mL.

3. Follow **steps 3** and **4** of the protocol for RNase activity determination (Subheading 2.2.1).
4. Pass through the column with immobilized enzyme 3 mL xylan solution in the operating buffer for 10 min at 40 °C. The optimal range of flow rates is 1–2 mL/min. The chosen flow rate must be kept constant. Between the recirculation of solutions with different concentrations, wash the column with 10 column volumes of operating buffer.
5. After 10 min, take out the reaction medium for absorbance measurement at 220 nm to calculate the velocity of the biocatalytic reaction.
6. Follow **steps 7–9** of the protocol for RNase activity determination (*see* **Note 11**).

   The characteristics of some immobilized enzyme reactors are given in Table 2.

3.4 Affinity Chromatography and Heterogeneous Biocatalysis Based on Monoliths

The method of affinity chromatography on monoliths allows carrying out the isolation, purification, and fractionation of complex biological mixtures in fast elution mode [3, 5, 40]. In addition, macroporous monoliths are widely used for the immobilization of enzymes [41–43] and can serve as the base for the design of simple and convenient bioreactors for industrial purposes.

To test the prepared affinity sorbents regarding the nonspecific interactions between indifferent protein marker and polymer affinity matrix, the model experiments on adsorption of BSA were carried out. The absence of any eluted peak after the desorption step indicates the absence of binding of chosen marker to specific peptide ligands. All chromatographic experiments were carried out at room temperature.

1. Install monolithic column into a chromatographic system.
2. Equilibrate the column with adsorption buffer at 2 mL/min flow rate.
3. Prepare BSA solution in adsorption buffer with a concentration of 3 mg/mL.
4. Load to the column 200 μL BSA solution at 2 mL/min flow rate. Detection wavelength is 280 nm.
5. Wash the disk with adsorption buffer to reach the baseline.
6. Elute the probably adsorbed protein using 0.01 M HCl, pH of 2.0, at the same flow rate.
7. Determine the desorbed amount of BSA by spectrophotometry using established extinction coefficient, or by Lowry assay [13]. The absence of BSA in an eluted fraction confirms the absence of binding of the indifferent protein to affinity ligands.

8. Clean the column consequently with 10 column volumes of water and adsorption buffer at 2 mL/min flow rate.
9. Wash the column with storage buffer and disconnect it from the chromatographic system. Store the column at 4 °C.

3.4.1 Isolation of Antibradykinin Antibodies from Blood Serum

The fractionation of polyclonal antibodies expressed in vivo is currently an important task regarding the development of both practical and theoretical immunology. Mixtures of polyclonal antibodies were produced by immunization of a rabbit with complex antigen, namely, the conjugate BSA-S-BK [14, 25]. The affinity monolithic disk with immobilized hormone bradykinin was applied for fast isolation of antibodies from a blood serum preliminary purified by triple precipitation with 32–35% aqueous ammonium sulfate [44], as well as from a crude blood serum [14, 25]. In the first case, the chromatographic procedure includes the following steps:

1. Install the column with immobilized BK into a chromatographic system.
2. Pump adsorption buffer through the monolithic column at a flow rate of 2 mL/min to reach the baseline (detected signal at 280 nm).
3. Prepare a solution of preliminary purified and lyophilized pool of polyclonal anti-BK antibodies with a protein concentration of 0.6 mg/mL in adsorption buffer.
4. Load 1–2 mL solution on affinity disk at a flow rate of 2 mL/min.
5. Remove the ballast proteins by passing the adsorption buffer through the column.
6. Elute monospecific antibodies using 0.01 M HCl, pH of 2.0, at a flow rate of 2 mL/min. To prevent denaturation of isolated antibodies, it is necessary to neutralize immediately the eluted fraction using the neutralizing solution (Subheading 2.1, **item 2**) (*see* **Note 12**).
7. Regenerate affinity column consequently with 10 column volumes of water and with adsorption buffer for further use (flow rate is 2 mL/min).
8. Analyze eluted fraction relating to protein content using standard Lowry assay [13], as well as ELISA assay to measure the titers of eluted antibodies [45].
9. Wash the column with storage buffer and disconnect it from the chromatographic system. Store the column at 4 °C.

To isolate the specific antibodies from *crude blood serum*:

1. Follow **steps 1** and **2** of the previous protocol.

2. Prepare a solution of crude blood serum in adsorption buffer with protein concentration 15–20 mg/mL (*see* **Note 13**).
3. Follow **steps 4** and **5** of the previous protocol.
4. To accumulate the significant quantity of isolated antibodies, repeat the adsorption/washing process two or more times.
5. Follow **steps 6** and **9** of the previous protocol.

The test for affinity sorbent stability showed that monolithic column bearing BK as affinity ligand did not lose the efficiency for at least 12 months (recovery: 97–100%).

3.4.2 Multifunctional Fractionation of Polyclonal Pool of Antibodies

Conjoint chromatographic mode using CIM disks allows the combination of several monolithic disks (up to 4) with different affinity functionalities in the same cartridge [46]. The simplicity of commercially produced housing also allows easy rearrangement of disks sequence in a stack, as well as reinsertion of a single disk for subsequent desorption [14]. This type of affinity chromatography gives a possibility to fractionate polyclonal pools of antibodies against each part of conjugate used for immunization, as well as to evaluate the concentration of crossreactive antibodies that have the epitopes for complementary binding to all parts of complex antigen.

For example, for multifunctional fractionation of polyclonal pools of antibodies, each structural part of complex antigen, namely, BK, BSA, BSA-S, as well as the complete conjugate BSA-S-BK, is immobilized on the individual CIM disks [14]. The principle of the conjoint affinity chromatography is illustrated in Fig. 2. To perform the fractionation of a pool of polyclonal antibodies, the following protocol is applied:

1. Place three CIM disks with immobilized ligands corresponding to all three parts of complex immunogen conjugate, as well as the fourth disk with the immobilized conjugate, into one housing and install the device into a chromatographic system (*see* **Note 14**).
2. Pump adsorption buffer through the stack of disks at a flow rate of 2 mL/min to reach a baseline at 280-nm wavelength.
3. Prepare 1–2 mL solution of lyophilized polyclonal antibodies in adsorption buffer with a concentration of 2.0 mg/mL.
4. Load 0.5 mL of the prepared solution on the monolithic column at a flow rate of 2 mL/min.
5. Wash the column with adsorption buffer to reach a baseline signal.
6. Disconnect the housing. Left disk No. 1 in the housing, install a rearranged device into a chromatographic system and elute adsorbed monospecific antibodies using 0.01 M HCl, pH of 2.0, at 2 mL/min. Collect eluted protein fraction.

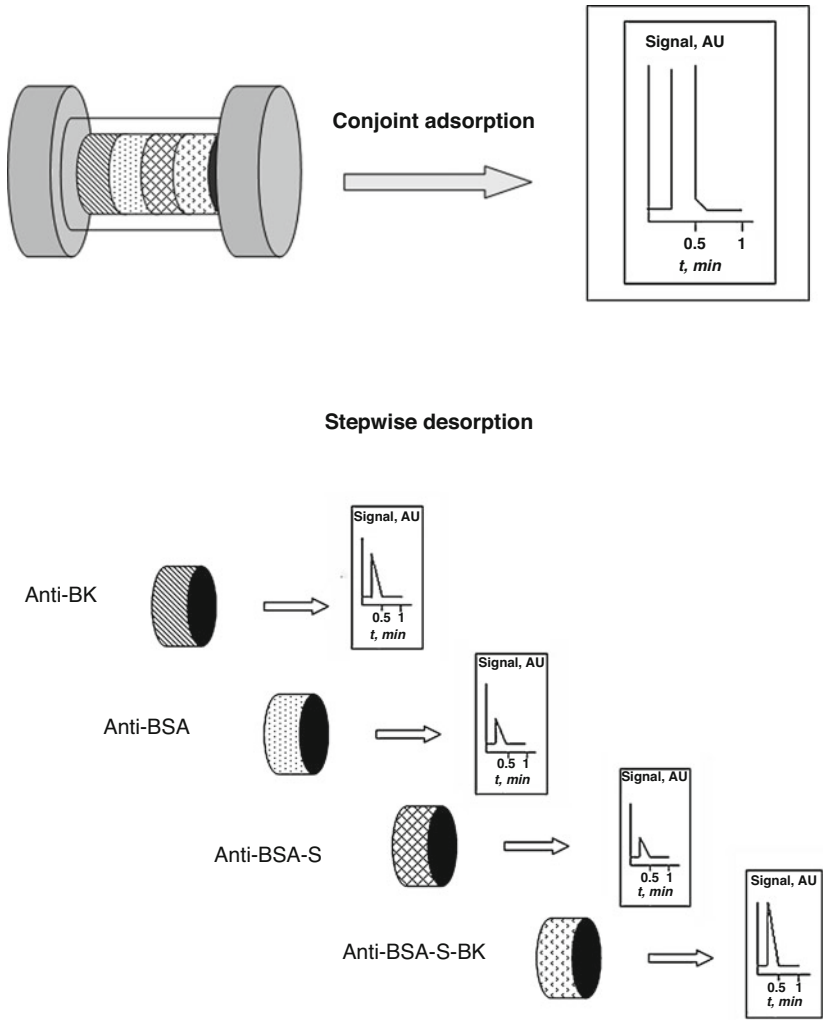

Fig. 2 The results of conjoin affinity chromatography on serum fractionation using CIM-epoxy disks with immobilized different parts of complex immunogen: (1) BK, (2) BSA, (3) BSA-S, (4) BSA-S-BK

7. Repeat this procedure with each disk.
8. To prevent denaturation of isolated antibodies, neutralize each fraction immediately using the neutralizing solution (*see* **Note 12**).
9. Follow **steps 8** and **9** for the protocol described in Subheading 3.4.1.

3.4.3 Semipreparative Isolation of IgG from Human Blood Serum

At present, to isolate IgG from a natural source, such as blood media, protein G is widely used as a specific affinity ligand [40]. The monolithic sorbents can be used successfully not only for analytical purposes but also for semipreparative protein recovery. There are two different experimental approaches allowing the

solution of such a problem. The first way is to stack several affinity disks of the same functionality (the same affinity ligand, namely, protein G). To perform the isolation of IgG using a stack of two protein G-disks from native human blood serum, the following procedure can be recommended:

1. Place two disks with immobilized ligand into housing and install the device into a chromatographic system.
2. Pump adsorption buffer through monolithic columns at a flow rate of 2.5 mL/min to reach the baseline at 280-nm wavelength.
3. Load on the column 1.0 mL of the human blood serum without any dilution.
4. Wash the column with adsorption buffer to reach the baseline at a flow rate of 2.5 mL/min.
5. Elute the adsorbed IgG using 0.01 M HCl, pH of 2.0, at 2.5 mL/min flow rate. Collect the eluted protein fraction.
6. Follow **steps 8** and **9** of the previous protocol (Subheading 3.4.2).

The complete experimental run, including loading, washing, and desorption steps, was performed within 10 min at 2.5 mL/min (Fig. 3a). The amount of isolated IgG was found to be equal to 2 mg [26].

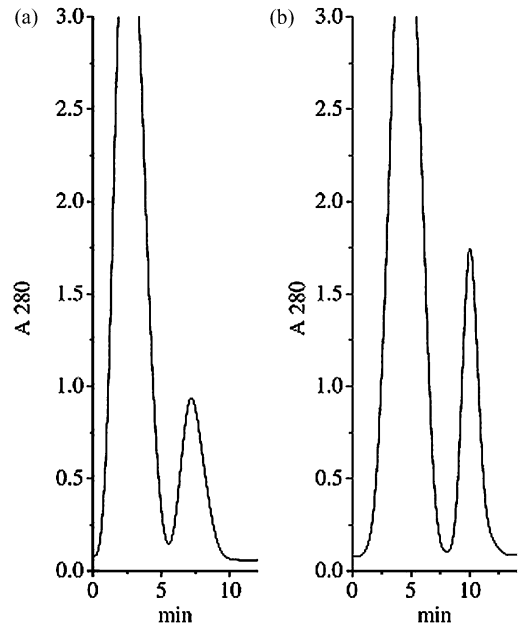

Fig. 3 Semipreparative extraction of immunoglobulin G from human sera by means of (**a**) two CIM disks with immobilized protein G installed into a single housing, and (**b**) protein G—CIM tube. (Reprinted with permission of Elsevier from [26])

Another way for semipreparative isolation of IgG from the same medium is the use of a tube with immobilized protein G. The procedure is mainly the same as that developed for two-disk stacked column, but the flow rate applied for separation can be elevated to 4 mL/min. The single experimental cycle for affinity tube is realized within 15 min (Fig. 3b). The amount of isolated IgG was 5 mg [26].

3.4.4 Simultaneous Isolation of IgG and SA Using Protein G Disks

To separate simultaneously IgG and SA from human blood serum, two disks with immobilized IgG-binding and SA-binding recombinant proteins G as affinity ligands are combined in one housing. The developed procedure of affinity isolation of IgG and SA is the following:

1. Place two disks with immobilized IgG-binding and SA-binding proteins G into a single housing and install the device into a chromatographic system.
2. Pump adsorption buffer through monolithic stacked column at a flow rate of 2.5 mL/min to reach a baseline at 280-nm wavelength.
3. Load on a column 0.2 mL of the human blood serum without any dilution.
4. Wash the column with adsorption buffer to reach a baseline at a flow rate of 2.5 mL/min.
5. Disconnect the housing. Left the disk No. 1 in the housing, install the rearranged device into a chromatographic system, and elute adsorbed IgG using 0.01 M HCl, pH of 2.0, at 2 mL/min flow rate. Collect eluted protein fraction.
6. Replace the disk No. 2 in the housing, install the device into a chromatographic system, and elute adsorbed SA using 0.01 M HCl, pH of 2.0, at 2 mL/min flow rate. Collect eluted protein fraction.
7. Follow **steps 8** and **9** of the protocol described in Subheading 3.4.2.

The whole operation requires about 15 min (Fig. 4).

3.4.5 Analytical-Scale Isolation of Protein G from *E. coli* Cell Lysate

It is known that the surface receptor of pathogenic *Streptococcus G*, e.g., protein G, recognizes the corresponding immunoglobulin of human and animal plasma and serum. To isolate recombinant protein G from *E. coli* cell lysate, the affinity monolithic matrix bearing IgG as a ligand is prepared. The developed and optimized protocol of affinity isolation of protein G using monolithic disk includes the following steps [47]:

1. Place the disk with immobilized IgG into housing and install the device into a chromatographic system.

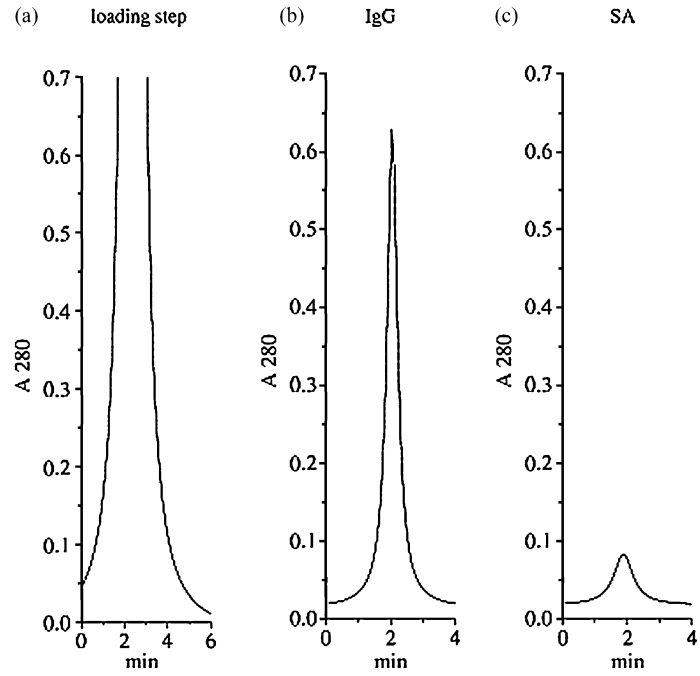

Fig. 4 Affinity fractionation of human sera on IgG-binding Protein G and SA-binding Protein G disks installed into the same housing. (Reprinted with permission of Elsevier Science from [26])

2. Pump adsorption buffer through the column at a flow rate of 3.0 mL/min to reach a baseline at 280-nm wavelength.
3. Load on a column 5 μL of 1:5 or 1:10 diluted by adsorption buffer cell lysate (*see* **Note 15**).
4. Wash the column with adsorption buffer for 2 min at a flow rate of 3.0 mL/min.
5. Elute adsorbed protein G using 0.01 M HCl, pH of 2.0, at 3.0 mL/min flow rate. Collect eluted protein fraction.
6. To prevent denaturation of the isolated protein, neutralize the collected fraction immediately using the neutralizing solution (*see* **Note 12**).
7. Measure the protein content in eluted fraction using standard Lowry assay [13]; to observe the level of probable impurities, use standard SDS-PAGE method [48].
8. Wash the column with storage buffer, disconnect it from the chromatographic system, and store at 4 °C.

The amount of isolated protein G corresponded exactly to its content in a loaded sample of crude lysate that was determined by ELISA assay. The purity level of isolated protein G is controlled by standard SDS-PAGE method.

3.4.6 Isolation of Recombinant t-PA from Animal Cell Supernatant

It is well known that the serine protease called tissue plasminogen activator (t-PA) efficiently dissolves blood clots [49, 50]. Thus, this protein seems to be extremely useful in clinical practice in the cases of heart attack victims. Nowadays, this protein is produced by recombinant technique and needs to be isolated from culture media. For isolation of t-PA, the affinity chromatography is based on monolithic sorbents containing monoclonal anti-t-PA antibodies or plasminogen [24, 29, 30]. The procedure of t-PA isolation from cell supernatant can be described as:

1. Place the disk with immobilized affinity ligand into the housing and install the device into a chromatographic system.
2. Pump adsorption buffer through the column at a flow rate of 2.0 mL/min to reach a baseline at 280-nm wavelength.
3. Load on a column 1.0 mL of cell supernatant with t-PA concentration from 6 to 30 μg/mL.
4. Wash the column with adsorption buffer for 2 min at a flow rate of 2.0 mL/min.
5. Repeat twice **steps 3** and **4**.
6. To elute the nonspecifically bound proteins, wash the disk with 2 M NaCl at 2.0 mL/min flow rate to reach a new baseline.
7. Wash the disk with adsorption buffer to reach at a flow rate of 2.0 mL/min the baseline again.
8. Elute adsorbed t-PA using 0.01 M HCl, pH of 2.0, at 2.0 mL/min flow rate. Collect eluted protein fraction.
9. To prevent denaturation of the isolated protein, neutralize the collected fraction immediately using the neutralizing solution (*see* **Note 12**).
10. Measure the protein content in eluted fraction using standard Lowry [13] and ELISA assays [45]; to observe the level of probable impurities, use standard SDS-PAGE method [48]. The efficiency of t-PA recovery from cell supernatant with a disk technology is about 90%.
11. Wash the column with storage buffer, disconnect it from the chromatographic system, and store at 4 °C.

3.4.7 Biocatalytic Synthesis and Hydrolysis of Polyribonucleotides with Immobilized Polynucleotide Phosphorylase

Synthetic polyribonucleotides has a wide range of effects on various immunological cells and functions [51]. They can enhance cellular and humoral immunity in both animals and humans. The enzymatically catalyzed synthesis of polyribonucleotides using immobilized PNPase is technologically and economically reasonable. Substrates for PNPase are ribonucleoside-5′-diphosphates that can also be obtained by the phosphorolysis of RNA catalyzed by immobilized PNPase.

Application of CIM disk with immobilized PNPase for the poly (A) synthesis gave the maximal substrate conversion equal to 32% [17]. The developed conditions for biocatalytic synthesis [17] can be scaled-up for industrial production of polyribonucleotides and nucleoside diphosphates under application of monoliths with large volume.

Synthesis of Polyriboadenylate

1. Prepare 0.2 M Tris–HCl buffer, pH of 8.0, containing 6 mmol/L $MgCl_2$, and 1 mmol/L EDTA sodium salt (operating buffer).
2. Prepare substrate solution: operating buffer + 20 mmol/L ADP.
3. Install the monolithic column with immobilized PNPase into a chromatographic system.
4. Equilibrate the column with the operating buffer to reach a baseline at 280 nm.
5. Pump 3 mL of substrate solution with different concentrations through the enzyme reactor for 10 min at 65 °C in a recirculation mode (Fig. 1). The optimal rate of flow rates is 1–2 mL/min. The chosen flow rate must be kept constant.
6. Detect the formation of inorganic phosphate in the reaction mixture using Fiske-Subbarow assay (*see* **Note 16**).
7. Monitor the macromolecular product formation using gel-chromatography with the use of column packed with Sephadex G-200 or other gel with similar characteristics. The elution time depends on column size and molecular weight of a product.
8. At the end of the procedure, wash the column by pumping storage buffer to reach the baseline signal. The washing flow rate is 2 mL/min.
9. Disconnect the housing from a chromatographic system. Store column at 4 °C until use. CIM disks are stored being removed from housing and immersed into the container with storage buffer (*see* Subheading 2.2).

Phosphorolysis of Polyriboadenylate

1. Follow **steps 1**, **3**, and **4** of the protocol for poly(A) synthesis with immobilized PNPase.
2. Prepare substrate solution: operating buffer + poly(A) with concentrations in the range of 0.5–5.0 mmol/L.
3. Follow **step 5** of the protocol for poly(A) synthesis with immobilized PNPase.
4. Detect the formation of ADP in the acid-soluble fraction (*see* **Note 17**).
5. Follow **steps 8** and **9** of the protocol for poly(A) synthesis with immobilized PNPase.

3.4.8 Biodegradation of Proteins with Immobilized α-Chymotrypsin

One of the powerful tools of proteome study is obtaining of peptide maps via protein digestion followed by peptide identification and data processing. The immobilized enzyme reactors (IMER) allow the performance of digestion in a few minutes and facilitate its integration into the system for *online* analysis. Currently, for peptide mapping, such immobilized proteases as trypsin [52] or chymotrypsin [20] are widely applied. An example of the protocol for digestion of BSA as a substrate is given.

1. Prepare 0.1 M sodium phosphate buffer, pH: 8.0 (operating buffer).
2. Prepare substrate solution: 0.5 mg/mL of protein in operating buffer.
3. Follow **steps 3** and **4** of the protocol for poly(A) synthesis with immobilized PNPase.
4. Expose the substrate solution at a water boiling bath for 1 min and then at 30 °C for 5 min.
5. Pump 3 mL of substrate solution through the enzyme reactor for 1–3 h at 30 °C in recirculation mode (Fig. 1) to achieve the different deepness of digestion. The optimal range of flow rates is 0.5–1.0 mL/min.
6. After the time is over, take out the reaction medium and analyze the formation of peptide digests using LC-MS or capillary electrophoresis provided with a spectrophotometric detector at 220 nm.
7. Wash the disk with operating buffer and then with storage buffer to reach a baseline. Disconnect the housing from a chromatographic system and store the column at 4 °C.

3.4.9 Biodegradation of RNA with Immobilized RNase

Currently, the widespread development of genetic engineering raises the challenge of obtaining highly purified DNA products that are free from RNA impurities. Typically, a method based on RNA degradation by ribonucleases is used to remove impurities of RNA from DNA samples. Ribonuclease A (RNase) catalyzes specific cleavage of phosphodiester bonds in single-stranded RNA and polynucleotides constructed from pyrimidine-containing nucleotides [34]. RNA destruction with RNase immobilized on monolithic columns can be carried both in recirculation mode with off-line monitoring of products [53] and in zonal elution mode followed by on-line monitoring of products [27].

RNA degradation with off-line monitoring of products:

1. Prepare 10 mM Tris–HCl, pH of 7.5, containing 2 mmol/L EDTA and 0.1 mmol/L NaCl (operating buffer).
2. Prepare the model mixture containing RNA, DNA and protein (concentration of each component is 0.5 mg/mL) in operating buffer to prove the column with immobilized RNase is functioned well.

3. Follow **steps 3** and **4** of the protocol for RNase activity determination (Subheading 3.3.1).
4. Pump 3 mL of the prepared model mixture through the RNase-bearing monolithic column for 15 min at 37 °C in a recirculation mode (Fig. 1). The optimal range of flow rates is 1–2 mL/min. The chosen flow rate must be kept constant.
5. After 15 min, take out the reaction medium for HPLC analysis of degradation products (*see* **Note 18**).
6. Follow **steps 7** and **8** of the protocol for RNase activity determination (Subheading 3.3.1).

The same protocol can be used for destruction of RNA in real samples with the control of RNA degradation by gel electrophoresis in agarose gel.

RNA degradation with on-line monitoring of products:

1. Follow **steps 1** and **2** of the protocol for RNA degradation with off-line monitoring of the products.
2. Install consequently the column with immobilized RNase and the monolithic CIM-DEAE disk into chromatographic system.
3. Equilibrate the columns with operating buffer (eluent A) at 260 nm using a flow rate of 1.5 mL/min.
4. Prepare 7 M urea in operating buffer (eluent B) and 1 M sodium chloride in eluent B (eluent C).
5. Inject the sample using a sample loop with a volume of 0.5 mL.
6. For RNA degradation and monitoring of products, use the following program: 0–5 min for eluent A (hydrolysis of RNA), 5–10 min for eluent B (column equilibration with buffer for the HPLC analysis), 10–35 min for 0–100% eluent B (HPLC analysis of the products of enzymatic hydrolysis).
7. Follow **steps 7** and **8** of the protocol for RNase activity determination (Subheading 3.3.1).

3.4.10 Conjoin Xylan Biodegradation with Immobilized β-Xylanase and β-Xylosidase

Synergistic action of exo- and endohydrolazes is preferred for effective destruction of biopolymers. The development of enzymatic monolithic reactors for the efficient degradation of xylan into xylooligosaccharides and xylose is presented in [11]. The optimized procedure of xylan hydrolysis with β-xylanase and β-xylosidase, immobilized on monolithic columns, followed by online HPLC monitoring of products can be described as follows:

1. Prepare 20 mM Na-acetate buffer, pH: 5.0 (operating buffer).
2. Prepare xylan solution in operating buffer with concentration 1 mg/mL.

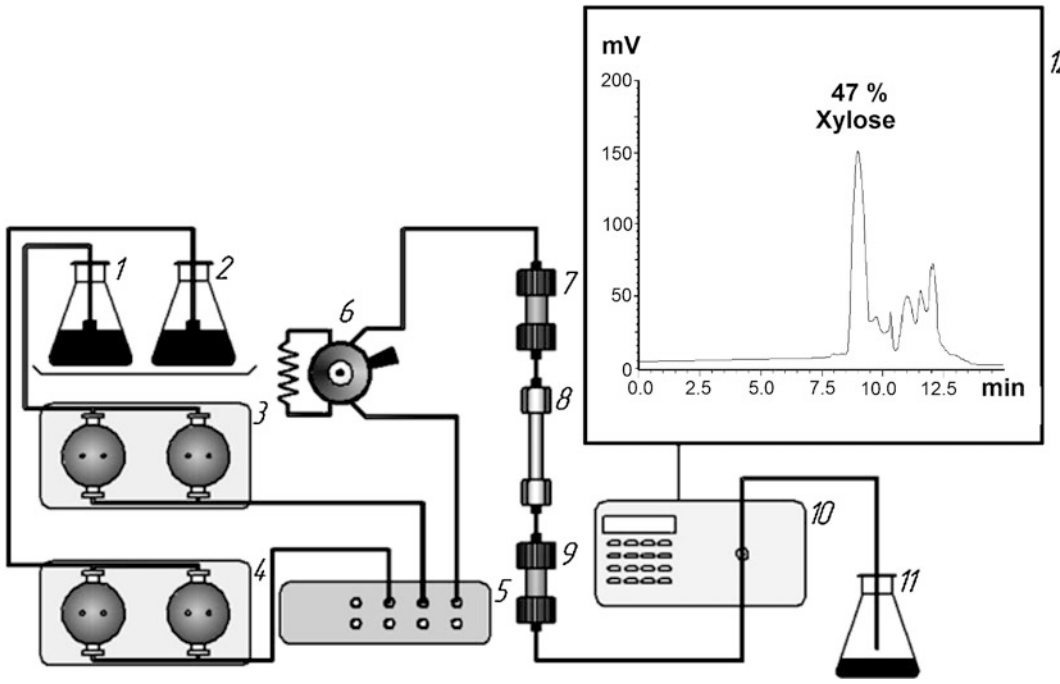

Fig. 5 Combination of β-xylanase disk and β-xylosidase column for effective xylan degradation with HPLC monitoring of the products. *Designations: 1, 2*—buffers A and B; *3, 4*—pumps; *5*—mixer; *6*—injector; *7*—β-xylanase disk IMER; *8*—β-xylosidase column IMER; *9*—analytical CIM DEAE disk; *10*—UV detector; *11*—outlet; *12*—chromatogram. (Reprinted with permission of Wiley from [11])

3. Install the columns with immobilized β-xylanase and β-xylosidase, as well as monolithic CIM-DEAE disk in a tandem-like mode into the chromatographic system (Fig. 5).
4. Equilibrate the system with operating buffer (eluent A) at 220 nm using a flow rate of 1.5 mL/min.
5. Prepare 2 M NaCl in 20 mM sodium acetate buffer, pH: 5.0 (eluent B).
6. Inject the sample using sample loop with a volume of 100 μL.
7. For xylan degradation and monitoring of products, use the following program: 0–5 min–100% eluent A (xylan hydrolysis), 5–20 min–100% eluent B (HPLC analysis of the products of enzymatic hydrolysis).
8. Wash the system with the operating buffer to reach a baseline at a flow rate of 1.5 mL/min.
9. Disconnect the β-xylanase and β-xylosidase columns and analytical DEAE disk from a chromatographic system and store monolithic supports at 4 °C in this buffer (*see* **Note 11**).

4 Notes

1. Macroporous polymer monoliths are synthesized in situ inside stainless steel housing (Supelco, USA) [27, 39]. GMA, HEMA, and EDMA are used as monomers. Dodecanol and cyclohexanol are the porogenic solvents. To prepare column with pore size 1.30 ± 0.05 μm and porosity 60 ± 2%, use the following polymerization mixture: GMA (14 vol%), HEMA (10 vol%), EDMA (16 vol%), dodecanol (50 vol%), and cyclohexanol (10 vol%). 2,2′-azo-*bis*-izobutyronitrile (AIBN) is an initiator (1% from mass of monomers). The polymerization was performed at 70 °C during 4 h. Each monolithic column was washed consequently with warm (45 °C) methanol, methanol/water (50:50 vol%), and finally with water. The control of monolithic material characteristics (average pore size and porosity) can be carried using the protocol published in [54].
2. For correct calculation of immobilized ligand amount, the initial concentration has to be determined by the same relative method as the concentration after the reaction. In the case of proteins/enzymes, the concentration can be determined by Lowry method [13] using a calibration curve preliminary build for the same protein. In the case of peptide ligands, their concentration can be measured using the preliminary established extinction coefficient and the results of UV-absorbance at 280 nm:

$$C = \Delta A_{280}/\varepsilon l, \tag{1}$$

where C is a concentration (mol/L), ΔA_{280} is an optical density of solution at 280 nm, ε is extinction coefficient of peptide determined at 280 nm (L/mol·cm), l is a cell thickness (cm).

3. Quantity of Peptide immobilized on the disk was determined from a difference in its concentration in the immobilization solution before and after coupling reaction. The ligand immobilization amount is calculated using the following equation:

$$Q_{\text{immob.}} = q_{\text{initial}} - q_{\text{after immob.}} - q_{\text{washing}}, \tag{2}$$

where $Q_{\text{immob.}}$ is the amount of ligand bound to the support (mg), q_{initial} is the amount of ligand in immobilization solution (mg), $q_{\text{after immob.}}$ is the amount of ligand in solution after reaction (mg), q_{washing} is the amount of ligand in washing solution (mg).

An amount of ligand in initial solution and solutions after reaction and washing can be calculated as follows:

$$q = VC, \tag{3}$$

where V is the volume of ligand solution (mL), C is the concentration of ligand solution determined using Lowry test or extinction coefficient.

4. Instead of PMAG, another polymer with 20–30 mol% of aldehyde groups can be utilized.
5. The volume needed for saturation depends on the applied flow rate. The higher flow rate, the larger volume of protein solution had to be loaded to reach the saturation.
6. The Langmuir adsorption isotherm is described by following equation:

$$Q = Q_{\max} C/(K_{\text{diss}} + C) \tag{4}$$

This equation can be rewritten in the linearized form:

$$C/Q = C/Q_{\max} + K_{\text{diss}}/Q_{\max} \tag{5}$$

or

$$1/Q = K_{\text{diss}}/Q_{\max} C + 1/Q_{\max} \tag{6}$$

The plot $1/C$ versus $1/Q$ yields a straight line that intercepts the x- and y-axes in points
$-1/K_{\text{diss}}$ and $1/Q_{\max}$, respectively.

7. The results can be counted as satisfied if the experimental data are linearized with regression coefficient $R \geq 0.98$.
8. When the substrate solution at a certain concentration is pumped through the enzyme reactor at a fixed flow rate, immobilized RNase hydrolyzes cytidine-2′,3′-cyclic monophosphate (CCP) that results in an increase of the absorbance at the column outlet because of 3′-cytidine monophosphate (CMP) formation. The velocity of CCP conversion into CMP catalyzed by RNase is determined using the following equation:

$$V = \mathrm{d}[\mathrm{P}]/\mathrm{d}t, \tag{7}$$

where V—the velocity of enzymatic reaction (μmol L^{-1} min^{-1}), d[P]—the change in product concertation (μmol/L), dt—the change in time (min).

$$\mathrm{d}[\mathrm{P}] = \Delta A_{296}/\Delta\varepsilon_{296} l, \tag{8}$$

where ΔA_{286} the an increment of absorbance after enzymatic reaction related to product formation, $\Delta\varepsilon_{286}$ is the ratio of CCP (substrate) and CMP (product) extinction coefficients, l is the spectrophotometer cuvette thickness; $\Delta\varepsilon_{286} = 516$ mol L^{-1} cm^{-1} [55].

9. The dependence of V (μmol L^{-1} min^{-1}) on [S] (mmol L^{-1}), representing the Michaelis-Menten curve, is built using experimental data. In the case of characterization of monolithic enzyme bioreactor operating in zonal elution mode, the

normalized values of initial substrate concentrations are used for the plotting [56]. Normalized substrate concentration is calculated using the following formula:

$$[S] = \left(C_{inj} V_{inj}\right)/V_b, \tag{9}$$

where C_{inj} and V_{inj} are injected substrate concentration and injected substrate volume, V_b is the pore volume of monolith, [S]—substrate concentration.

The graphical evaluation of nonlinear *Michaelis-Menten plot* to obtain kinetic parameters relies on accurate curve fitting. To calculate K_M and V_{max}, use a straight-line plot of $1/V$ versus $1/[S]$, known as *Lineweaver-Burk plot*. The intercepts of the straight line with *y*- and *x*-axes give $1/V_{max}$ and $-1/K_M$, respectively. *Hanes plot* includes the building of dependence of $[S]/V$ versus [S]. In this case, the intercept with *y*-axis gives K_M/V, whereas the intercept with *x*-axis allows the determination of $-K_M$.

Enzyme activity is expressed in moles of substrate converted per time unit. It can be calculated from V_{max} and reaction volume:

$$U = V_{max}\varphi, \tag{10}$$

where U is the activity of the enzyme (μmol min^{-1}), φ is the reaction volume (L).

The enzyme activity related to mg of enzyme represents *specific activity* (A_{sp}) (μmol min^{-1} mg^{-1}). Specific activity can be calculated using.

$$A_{sp} = U/m, \tag{11}$$

where m is the amount of enzyme used in the catalytic reaction and expressed in mg.

10. The activity of chymotrypsin is determined by monitoring of *N*-benzoyl-L-tyrosine (BT) formation at 256 nm. The BT extinction at 256 nm equal to 964 L mol^{-1} cm^{-1} is used for calculation of product amount.
11. In the case of immobilized chitinases, β-xylanase and β-xylosidase, 0.1 M sodium phosphate buffer, pH of 6.0, is used as a storage buffer. For other enzymes, the storage buffer for immobilized enzyme should be chosen keeping in mind pH range of the enzyme stability.
12. The quantitative desorption of bound proteins was achieved only under a strong acidic conditions; other typical buffers, such as 200 mM KSCN, pH of 7.4, or 100 mM glycine, pH of 3.0, did not desorb the proteins quantitatively. To prevent denaturation of isolated antibodies/proteins, it is necessary to neutralize the fraction immediately using neutralizing solution

0.5 M Na_2HPO_4, pH of 9.0, or 0.1 M NaOH (1 mL of collected fraction + 50 μL 0.5 M Na_2HPO_4, pH of 9.0, or 1 mL of collected fraction +10 μL 0.1 M NaOH). Since the exchange of a mobile phase inside short monolithic disk proceeds very quickly and complete desorption is achieved in a few seconds, inactivation of antibodies is negligible as confirmed by very high binding to antigen detected by ELISA.

13. The initial crude blood serum with the protein concentration 80 mg/mL is five times diluted by adsorption buffer.
14. The data present the results of fractionation of blood serum using conjoin separation on individual disks with immobilized different parts of the complex immunogen. The disk installed at the top of the stack adsorbs both its "own" Ab and also crossreactive immunoglobulins. Changing the sequence of disks in the housing makes possible to separate quantitatively all types of antibodies from whole serum fraction.
15. For semipreparative isolation of protein G 1:10 diluted cell lysate and scheme "three adsorption-one desorption" can be used. The volume of cell lysates loaded in one adsorption step was 1 mL. After each adsorption step, the washing with adsorption buffer is necessary.
16. The amount of enzyme providing for the elimination of 1 μmol of inorganic phosphate during 1 h at pH of 8.0 and 65 °C was taken as a unit of the enzyme activity. 1 mL of 2.5% solution of $HClO_4$ was added to 0.05 mL of samples and the precipitate was removed by centrifugation for 3 min at 16,000 × *g*. The amount of phosphate evolved is analyzed in the supernatant.
17. 1 mL of 2.5% solution of $HClO_4$ was added to 0.05 mL of samples and the optical density was measured in the supernatant at 259 nm (a maximum of absorption of ADP).
18. The bioreactors are characterized with high long-term storage. After 5 months, the loss of activity of immobilized enzymes was less than 10%.

Acknowledgments

The authors are very grateful to BIA Separations for long-term fruitful cooperation.

References

1. Groarke R, Brabazon D (2016) Methacrylate polymer monoliths for separation applications. Materials 9:446
2. González-González M, González-Valdez J, Mayolo-Deloisa K, Rito-Palomares M (2017) Monolithic chromatography: insights and practical perspectives. J Chem Technol Biotechnol 92:9–13
3. Pfaunmiller EL, Paulemond ML, Dupper CM, Hage DS (2013) Affinity monolith chromatography: a review of principles and recent analytical applications. Anal Bioanal Chem 405:2133–2145
4. Švec F, Tennikova TB, Deyl Z (2003) Monolithic materials : preparation, properties and applications. Elsevier, Amsterdam
5. Satzer P, Sommer R, Paulsson J, Rodler A, Zehetner R, Hofstädter K, Klade C, Jungbauer A (2018) Monolith affinity chromatography for the rapid quantification of a single-chain variable fragment immunotoxin. J Sep Sci 41:3051–3059
6. Lendero Krajnc N, Podgornik A, Štrancar A, Černigoj U, Nemec B, Vidic U, Vidič J, Gašperšič J (2016) Characterization of methacrylate chromatographic monoliths bearing affinity ligands. J Chromatogr A 1464:72–78
7. Naldi M, Tramarin A, Bartolini M (2018) Immobilized enzyme-based analytical tools in the -omics era: recent advances. J Pharm Biomed Anal 160:222–237
8. Han X, Xie Y, Wu Q, Wu S (2019) The effect of monolith properties on the digestion performance of monolith-based immobilized enzyme microreactor. J Chromatogr Sci 57:116–121
9. Vlakh EG, Tennikova TB (2013) Flow-through immme reactors based on monoliths: I. Preparation of heterogeneous biocatalysts. J Sep Sci 36:110–127
10. Ralla K, Anton F, Scheper T, Kasper C (2009) Application of conjoint liquid chromatography with monolithic disks for the simultaneous determination of immunoglobulin G and other proteins present in a cell culture medium. J Chromatogr A 1216:2671–2675
11. Volokitina MV, Bobrov KS, Piens K, Eneyskaya EV, Tennikova TB, Vlakh EG, Kulminskaya AA (2015) Xylan degradation improved by a combination of monolithic columns bearing immobilized recombinant β-xylosidase from Aspergillus awamori X-100 and Grindamyl H121 β-xylanase. Biotechnol J 10:210–221
12. Milačič R, Zuliani T, Vidmar J, Ščančar J (2016) Monolithic chromatography in speciation analysis of metal-containing biomolecules: a review. J Anal At Spectrom 31:1766–1779
13. Waterborg JH, Matthews HR (2009) The Lowry method for protein quantitation. In: Walker JM (ed) The protein protocols handbook. Humana Press INC, Totowa, NJ, USA, p 1984
14. Ostryanina ND, Vlasov GP, Tennikova TB (2002) Multifunctional fractionation of polyclonal antibodies by immunoaffinity high-performance monolithic disk chromatography. J Chromatogr A 949:163–171
15. Somogyi M (1952) Notes on sugar determination. J Biol Chem 195:19–23
16. Platonova GA, Vlakh EG, Ivanova ND, Tennikova TB (2009) A flow-through enzymatic bioreactor based on immobilized α-chymotrypsin. Russ J Appl Chem 82 (12):2182–2186
17. Platonova GA, Surzhik MA, Tennikova TB, Vlasov GP, Timkovskii AL (1999) The catalysis of polyriboadenylate synthesis and phosphorolysis by polynucltotide phosphorylase immobilized on a new type of carrier. Russ J Bioorgan Chem 25:166–171
18. Wang X, Xia D, Han H, Peng K, Zhu P, Crommen J, Wang Q, Jiang Z (2018) Biomimetic small peptide functionalized affinity monoliths for monoclonal antibody purification. Anal Chim Acta 1017:57–65
19. Vlakh E, Novikov A, Vlasov G, Tennikova T (2004) Solid phase peptide synthesis on epoxy-bearing methacrylate monoliths. J Pept Sci 10:719–730
20. Meller K, Pomastowski P, Szumski M, Buszewski B (2017) Preparation of an improved hydrophilic monolith to make trypsin-immobilized microreactors. J Chromatogr B 1043:128–137
21. Ponomareva EA, Kartuzova VE, Vlakh EG, Tennikova TB (2010) Monolithic bioreactors: effect of chymotrypsin immobilization on its biocatalytic properties. J Chromatogr B 878:567–574
22. Han W, Yamauchi M, Hasegawa U, Noda M, Fukui K, van der Vlies AJ, Uchiyama S, Uyama H (2015) Pepsin immobilization on an aldehyde-modified polymethacrylate monolith and its application for protein analysis. J Biosci Bioeng 119:505–510
23. Vlakh EG, Tennikova TB (2013) Flow-through immobilized enzyme reactors based on monoliths: I. preparation of heterogeneous biocatalysts. J Sep Sci 36:110–127

24. Vlakh EG, Platonova GA, Vlasov GP, Kasper C, Tappe A, Kretzmer G, Tennikova TB (2003) In vitro comparison of complementary interactions between synthetic linear/branched oligo/poly-L-lysines and tissue plasminogen activator by means of high-performance monolithic-disk affinity chromatography. J Chromatogr A 992:128–138
25. Platonova GA, Pankova GA, Il'ina IY, Vlasov GP, Tennikova TB (1999) Quantitative fast fractionation of a pool of polyclonal antibodies by immunoaffinity membrane chromatography. J Chromatogr A 852:129–140
26. Gupalova TV, Lojkina OV, Palagnuk VG, Totolian AA, Tennikova TB (2002) Quantitative investigation of the affinity properties of different recombinant forms of protein G by means of high-performance monolithic chromatography. J Chromatogr A 949:185–193
27. Vlakh EG, Volokitina MV, Vinokhodov DO, Tennikova TB (2014) Degradation of polyribonucleotides: biocatalysis and the monitoring of products. Appl Biochem Microbiol 50:600–607
28. Ponomareva EA, Kartuzova VE, Vlakh EG, Tennikova TB (2010) Monolithic bioreactors: effect of chymotrypsin immobilization on its biocatalytic properties. J Chromatogr B Anal Technol Biomed Life Sci 878:567–574
29. Vlakh E, Ostryanina N, Jungbauer A, Tennikova T (2004) Use of monolithic sorbents modified by directly synthesized peptides for affinity separation of recombinant tissue plasminogen activator (t-PA). J Biotechnol 107:275–284
30. Vlakh EG, Tappe A, Kasper C, Tennikova TB (2004) Monolithic peptidyl sorbents for comparison of affinity properties of plasminogen activators. J Chromatogr B Anal Technol Biomed Life Sci 810:15–23
31. Kalashnikova IV, Ivanova ND, Evseeva TG, Menshikova AY, Vlakh EG, Tennikova TB (2007) Study of dynamic adsorption behavior of large-size protein-bearing particles. J Chromatogr A 1144:40–47
32. Vlakh EG, Ponomareva EA, Tennikova TB (2014) A multienzyme bioreactor based on a chitinase complex. Appl Biochem Microbiol 50:441–446
33. Volokitina MV, Nikitina AV, Tennikova TB, Korzhikova-Vlakh EG (2017) Immobilized enzyme reactors based on monoliths: effect of pore size and enzyme loading on biocatalytic process. Electrophoresis 38:2931–2939
34. Raines RT, Ribonuclease A (1998) Chem Rev 98:1045–1065
35. Ma W, Tang C, Lai L (2005) Specificity of trypsin and chymotrypsin: loop-motion-controlled dynamic correlation as a determinant. Biophys J 89:1183–1193
36. By H, Bpn S (1975) Use of IV-benzoyl-L-tyrosine substrate Ester as a protease. J Biol Chem 250:7366–7371
37. Dahiya N, Tewari R, Hoondal GS (2006) Biotechnological aspects of chitinolytic enzymes: a review. Appl Microbiol Biotechnol 71:773–782
38. Sousa S, Ramos A, Evtuguin DV, Gamelas JAF (2016) Xylan and xylan derivatives—their performance in bio-based films and effect of glycerol addition. Ind Crop Prod 94:682–689
39. Ponomareva EA, Volokitina MV, Vinokhodov DO, Vlakh EG, Tennikova TB (2013) Biocatalytic reactors based on ribonuclease a immobilized on macroporous monolithic supports. Anal Bioanal Chem 405:2195–2206
40. Martinović T, Andjelković U, Klobučar M, Černigoj U, Vidič J, Lučić M, Pavelić K, Josić D (2017) Affinity chromatography on monolithic supports for simultaneous and high-throughput isolation of immunoglobulins from human serum. Electrophoresis 38:2909–2913
41. Vlakh EG, Tennikova TB (2013) Flow-through immobilized enzyme reactors based on monoliths: II. Kinetics study and application. J Sep Sci 36:110–127
42. Mao Y, Černigoj U, Zalokar V, Štrancar A, Kulozik U (2017) Production of β-Lactoglobulin hydrolysates by monolith based immobilized trypsin reactors. Electrophoresis 38:2947–2956
43. Masini JC, Svec F (2017) Porous monoliths for on-line sample preparation: a review. Anal Chim Acta 964:24–44
44. Kent UM (1999) Purification of antibodies using ammonium sulfate fractionation or gel filtration. In: Javois LC (ed) Methods in molecular biology: immunocytochemical methods and protocols. Humana Press Inc, Totowa, NJ, pp 11–18
45. Crowther JR (2009) The ELISA guidebook. In: Methods in molecular biology. Humana Press, Totowa, NJ, p 516
46. Strancar A, Barut M, Podgornik A, Koselj P, Josic D, Buchacher A (1998) Polymer based supports for fast separation of biomolecules. LC-GC Int 11:660–670
47. Kasper C, Meringova L, Freitag R, Tennikova T (1998) Fast isolation of protein receptors from streptococci G by means of macroporous affinity disks. J Chromatogr A 798:65–72

48. Kurien BT, Scofield RH (2012) Protein Electrophoresis. In: Methods in molecular biology. Humana Press, Totowa, NJ, p 869
49. Gravanis I, Tsirka SE (2008) Tissue-type plasminogen activator as a therapeutic target in stroke. Expert Opin Ther Targets 12:159–170
50. Thiebaut AM, Gauberti M, Ali C, Martinez De Lizarrondo S, Vivien D, Yepes M, Roussel BD (2018) The role of plasminogen activators in stroke treatment: fibrinolysis and beyond. Lancet Neurol 17:1121–1132
51. Khan AL, Heys SD, Eremin O (1995) Synthetic polyribonucleotides: current role and potential use in oncological practice. Eur J Surg Oncol 21:224–227
52. Naldi M, Černigoj U, Štrancar A, Bartolini M (2017) Towards automation in protein digestion: development of a monolithic trypsin immobilized reactor for highly efficient on-line digestion and analysis. Talanta 167:143–157
53. Volokitina MV, Vlakh EG, Platonova GA, Vinokhodov DO, Tennikova TB (2013) Polymer monoliths as efficient solid phases for enzymatic polynucleotide degradation followed by fast HPLC analysis. J Sep Sci 36:2793–2805
54. Vlakh EG, Maksimova EF, Tennikova TB (2013) Monolithic polymeric sorbents for high-performance chromatography of synthetic polymers. Polym Sci Ser B 55:55–62
55. Moussaoui M, Nogués MV, Guasch A, Barman T, Travers F, Cuchillo C (1998) The subsites structure of bovine pancreatic Ribonuclease a accounts for the abnormal kinetic behavior with Cytidine 2′,3′-cyclic phosphate. J Biol Chem 273:25565–25572
56. Bartolini M, Greig NH, Yu Q, Andrisano V (2009) Immobilized butyrylcholinesterase in the characterization of new inhibitors that could ease Alzheimer's disease. J Chromatogr A 1216:2730–2738

Chapter 19

Sample Displacement Batch Chromatography of Proteins

Laura Heikaus, Siti Hidayah, Manasia Gaikwad, Marta Kotasinska, Verena Richter, Marcel Kwiatkowski, and Hartmut Schlüter

Abstract

In downstream processing, large-scale chromatography plays an important role. For its development, screening experiments followed by pilot-plant chromatography are mandatory steps. Here we describe fast, simple, and inexpensive methods for establishing a preparative chromatography for the separation of complex protein mixtures, based on sample displacement batch chromatography. The methods are demonstrated by anion-exchange chromatography of a human plasma protein fraction (Cohn IV-4), including the screening step and upscaling of the chromatography by a factor of one hundred. The results of the screening experiments and the preparative chromatography are monitored by SDS-PAGE electrophoresis. In summary, we provide a protocol, which should be easily adaptable for the chromatographic large-scale purification of other proteins, in the laboratory as well as in the manufacturing of biopharmaceuticals. These protocols cover the initial piloting steps for establishing a large-scale sample batch chromatography. The results from the piloting steps may also be applied for packed columns for performing simulated-moving-bed (SMB) chromatography rather than batch chromatography.

Key words Sample displacement chromatography, Preparative chromatography, Anion exchange chromatography, Plasma proteins, Cohn fraction, SDS-PAGE, Simulated-moving-bed

1 Introduction

Preparative chromatography aims at separation and isolation of defined proteins but faces the challenges of product purity, high throughput, and fitting this process in a cost-effective frame. Preparative chromatography can be performed in either elution, frontal, or displacement modes [1]. The most widely used gradient elution-based preparative chromatography has the fundamental disadvantage of underutilization of column capacity and lower throughputs. The lesser-known displacement chromatography possesses the ability to concentrate and purify the protein feed simultaneously and thus promising for downstream processing [2].

Displacement chromatography is a chromatographic mode introduced by Tiselius in 1943 [3] and is being applied most

Nikolaos E. Labrou (ed.), *Protein Downstream Processing: Design, Development, and Application of High and Low-Resolution Methods*, Methods in Molecular Biology, vol. 2178, https://doi.org/10.1007/978-1-0716-0775-6_19,

often for preparative chromatography [1]. Chromatography in displacement mode requires a stationary phase, which separates molecules by adsorptive mechanisms. The sample application buffer must guarantee that the sample molecules will have a high affinity toward the stationary phase. As soon as the sample molecules are in close proximity to the stationary phase, they will compete for the binding sites. Driven by the competition for the binding sites, the sample molecules already arrange themselves according to their affinity at the column and organized in bands. The width of the bands is dependent on the total amount of each sample component and on its affinity toward the stationary phase.

Right after finishing sample feed, an eluent is pumped onto the column, which consists of the sample application buffer and contains the displacer molecule, which ideally should have a larger affinity to the stationary phase than any of the sample component. As soon as the displacer enters the top of the column, it will bind to the stationary phase, thereby displacing every sample component. As a result, the sample bands start to move down the column. The sample molecules with the most strong affinity displace their neighboring sample molecules, which have a lower affinity. The moving sample component bands driven by the displacer are termed displacement train. The displacement chromatography is finished as soon as the displacer molecule has completely saturated the stationary phase. The sample components moving directly in front of the displacer elute with the largest concentration, whereas the components with the lowest affinity elute with the lowest concentration. For deeper insight into displacement chromatography in the context of downstream processing, the reader is referred to the review article from Freitag and Horváth [4].

In the early nineties, success reports of ion-exchange displacement chromatography with novel displacers gathered interest [5, 6]. Recently, displacement chromatography has been used not only for purification of protein from complex proteins mixture but also for purification of some protein species (proteoforms). Zhang et al. [7] used displacement chromatography to isolate and characterize the therapeutic antibody charge variants. There were, however, only a few such reports of displacement chromatography in downstream processing of proteins as compared to elution-based preparative chromatography. Freitag & Breier proposed that the lack of suitable protein displacers as one of the reasons [4]. However, this problem has been successfully addressed already by Mazza et al. [8] and Tugcu [9], who developed a multiparallel high-throughput approach for screening for appropriate displacer molecules for protein purification. Nevertheless, some problems concerning the displacer may remain such as coelution with the target molecule.

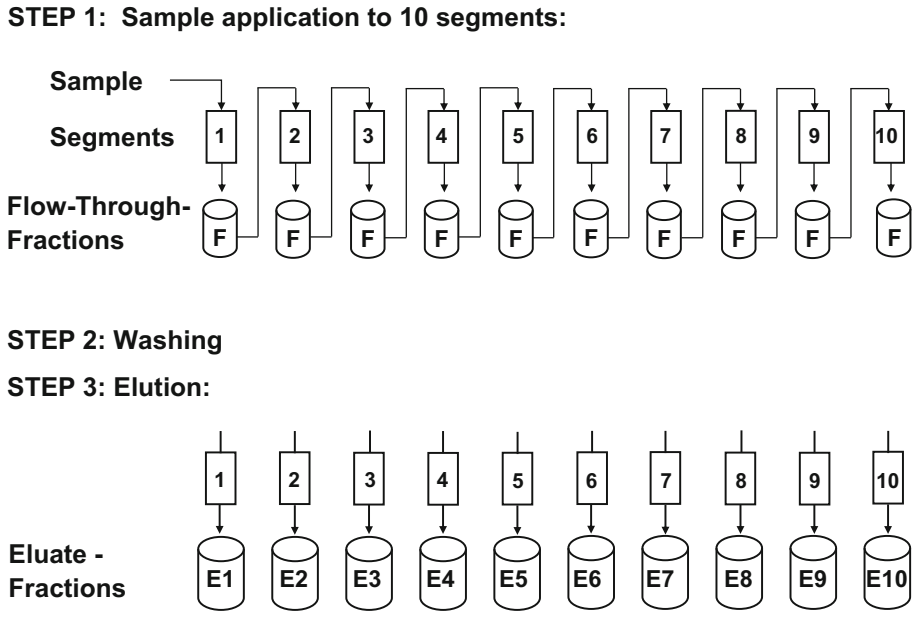

Fig. 1 Scheme of sample displacement batch chromatography. In sample displacement chromatography, the sample is moving from segment to segment (**a**), in this example from segment No. 1 to No. 10. Segments in this protocol are either spin columns in the case of the screening experiment or 50-mL tubes in the case of the pilot-plant scale. Each segment here contains an equal amount of the chromatography material. Sample application is finished as soon as the sample has passed the last segment. F: Flow-through. After sample application, each segment is washed (**b**). Then the adsorbed proteins are eluted from each individual segment (**b**) and the eluates (**e**) collected in tubes with numbers corresponding to the numbers of the segments

An alternative method in this case is sample displacement chromatography (SDC), which does not require any displacer molecule. SDC was first described by Hodges et al. in 1988 [10], who applied SDC for the separation of peptides. In SDC, the competition of the sample molecules toward the binding sites of the stationary phase is used for their separation. In contrast to conventional displacement chromatography, a segmented column system must be used (Fig. 1). The sample feed is pumped onto the columns, which are connected in series. Therefore, the first column segments are saturated with high-affinity sample components displacing the lower-affinity components to the next segments until all the column segments are completely saturated. Directly after sample application, the segments can be disconnected and the sample molecules can be eluted separately and with an appropriate eluent from each of the individual segment. A comprehensive review about SDC can be found from Srajer Gajdosik et al. [11] In 1991, Veeraragavan et al. [12] reported the use of SDC for the separation of proteins, while displacement chromatography was used not only for protein purification from complex protein mixtures but also for purification of protein species (proteoforms). Brgles et al. reported that using

SDC the column can be overloaded, resulting in the displacement of weakly binding high human abundant plasma proteins by the strongly binding low abundant proteins [13, 14]. Recently in 2018, Khanal et al. [15] described the possibility of using SDC for the separation of basic and acidic variants of monoclonal antibodies. These reports prove the potential of SDC in protein fractionation and purification.

This protocol focuses on the first steps in the development of a downstream processing procedure, including small-scale scouting trials and a scaling from laboratory to pilot plant involving a scale-up factor of 100-fold. As separation step for downstream processing, we describe SDC performed in the batch mode, since it is simple, fast, and the up-scaling is straightforward [16]. For an overview of further important aspects for the development of a down-stream procedure for protein purification, the reader is referred to Milne [17].

Plasma protein fraction (Cohn IV-4) is easily obtainable, relatively inexpensive, and, therefore, suitable for model experiments such as this. Nevertheless, the fraction contains a complex mixture consisting of a few abundant proteins and their species and lots of medium- as well as low-abundant proteins, which we already characterized in a previous proteomic study [18] Furthermore, chromatographic purification of plasma proteins in an industrial scale is an important topic in pharmaceutical biotechnology since many human plasma proteins have an important economic relevance. Approximately twenty different plasma protein therapeutics are applied for treating diseases or injuries, according to a review from Burnouf [19]. Nearly 30 million liters of human fresh frozen plasma from blood banks are fractionated per year worldwide, in batches of thousands of liters, in about seventy factories [20, 21].

2 Materials

1. Protein sample: Globulins Cohn fraction IV-4 (Sigma Aldrich).
2. Chromatography material: Fractogel EMD TMAE (M), 40–90 μm (Merck), abbreviated in this text as TMAE.
3. Sample application buffers: 20 mM piperazine, pH: 5; 20 mM potassium phosphate, pH: 7; 20 mM ethanolamine, pH: 9 (store at 4 °C in the refrigerator).
4. Elution buffers: Sample application buffers containing 1 M NaCl (stored at 4 °C in the refrigerator).
5. Spin column: Empty columns with a filter: Micro Bio-Spin Chromatography Columns with porous 30-μm polyethylene filter bed supports, 0.8-mL bed volume, include end cups and tip closures (Bio-Rad).

6. 2-mL tubes for equilibration and collecting flow-through, wash fractions, and eluates.
7. 50-mL tubes (Falcon tube, BD Biosciences) for pilot-plant experiment.
8. Centrifuge: Microcentrifuge (screening experiments), centrifuge for 50-mL tubes (pilot plant).
9. Vortex mixer.
10. Overhead rotor for 50-mL tubes.
11. Criterion XT Bis-Tris Gel, precast, 4–12% (Bio-Rad), 4× SDS sample buffer (Bio-Rad), MES running buffer (Bio-Rad), Coomassie Blue staining solution (50% H_2O, 40% methanol, 10% acetic acid, 0.025% Coomassie Blue R-250), destain solution (50% H_2O, 40% methanol, 10% acetic acid). All buffers listed were stored at room temperature.
12. Trypsin stock solution: 400 ng/μL (Promega). Sequencing grade-modified trypsin (Promega) with one vial 20-μg lyophilized powder and 1-mL resuspension buffer composed of 50 mM acetic acid was stored at −20 °C. Dissolve one vial of lyophilized trypsin in 50 μL of resuspension buffer in order to prepare a 400 ng/μL stock solution. Store excess of trypsin stock solution at −20 °C and avoid multiple freeze–thaw cycles.
13. Digest buffer: 50 mM NH_4CO_3, 10% acetonitrile (Merck) in water.
14. Digestion solution: Trypsin 10 ng/μL in digest buffer (Add trypsin directly before adding to samples to avoid self-digestion).
15. Swelling solution: 100 mM NH_4CO_3 in water.
16. Shrinking solution: 50 mM NH_4CO_3, 60% acetonitrile in water.
17. Peptide extraction solution: 65% acetonitrile, 5% formic acid (Fulka Analytical) in water.
18. 10 mM dithiothreitol (DTT, Sigma Aldrich) dissolved in swelling solution.
19. 50 mM iodoacetamide (Sigma Aldrich) dissolved in swelling solution.
20. Incubator, heating blocks, or water bath capable of maintaining 57 and 37 °C.
21. Vacuum centrifuge.
22. Reaction vial arrangement for trypsin digestion: Place glass vial (CS-Chromatography Service; ME G20 rund Borosilikatgalss) into a reaction vial (1.5 mL), and 1000 μL tip (cut of upper half so that it fits into your centrifuge) (Fig. 4).

23. Liquid chromatography-tandem mass spectrometry system (LC-ESI-IT-MS/MS): 1100 LC/MSD-trap XCT series system, equipped with a Chip Cube interface (Agilent Technologies). Large-capacity chip with 160-nL trap column and an analytical column (75 μm × 150 mm) filled with RP sorbent Zorbax 300 SB-C18 (Agilent Technologies).

3 Methods

One of the first steps in the development of a down-stream processing procedure is the screening for optimal parameters for the chromatographic purification of a target protein. A detailed overview of important chromatographic and nonchromatographic issues, which have to be considered during the development and also for choosing the fixed parameters for a chromatographic step is given in the review of Milne [14].

Here anion exchange chromatographic (AEX) material developed for protein purification (TMAE) was chosen for fractionation of the Cohn fraction IV-4 by SDC.

We exemplified the screening experiments by testing the effect of three different pH values on AEX-SDC of the Cohn fraction IV-4. The resulting fractions from SDC were analyzed by SDS-PAGE, offering the opportunity that the behavior of the target protein as well as abundant accompanying proteins can be observed. By the results from the screening experiments, a defined set of parameters can be chosen, which will be used for the pilot-plant experiments. In this study, an upscaling by a factor of 100 is demonstrated.

3.1 Screening Experiments for Determining Parameters for SDC

3.1.1 Calculation of the Amount of Chromatography Material Required for Sample Displacement Batch Chromatography Screening Experiments

1. Look for the binding capacity (*see* **Note 1**) of the chosen chromatography material given by the supplier: 1 mL TMAE binds 100-mg bovine serum albumin (BSA).
2. Choose the sample amount: 20-mg Cohn fraction IV-4.
3. Calculate the chromatography material required, approximately assuming that the binding capacities of the target proteins (Cohn fraction IV-4) are identical with the one given by the supplier: 200 μL.
4. Calculate the amount of chromatography material per segment. For 10 segments: 20-μL chromatography material/segment (*see* **Note 2**).

3.1.2 Equilibration of Chromatography Material

1. Suspend 300-μL TMAE (*see* **Note 3**) in 1.5-mL elution buffer by vortexing for 10 s. Centrifuge for 1 min at 13,000 × *g* and carefully discard the supernatant (*see* **Note 4**).

2. Wash by adding 1.5-mL sample application buffer and by suspending both components 10 s. Centrifuge and remove the supernatant (*see* **Note 4**). Repeat these steps three times.
3. After the third washing, do not centrifuge but sediment the material (*see* **Note 5**) and remove the supernatant carefully by aspiration.

3.1.3 Preparation of Segments

1. Suspend 300 μL chromatography material in 1.5-mL sample application buffer by vortexing.
2. Transfer immediately 100 μL of the homogeneous suspension to spin column No. 1 (*see* **Note 6**).
3. Suspend the remaining suspension from **step 1** by vortexing.
4. Transfer 100 μL to spin column No. 2.
5. Repeat **steps 3** and **4** until the suspension is transferred to spin column No. 15.
6. Carefully remove the buffer from the chromatography material.

3.1.4 Sample Application

1. Dissolve 20-mg protein sample in 400-μL sample application buffer.
2. Load the sample to spin column No. 1, close the column with the end cup.
3. Mix thoroughly by shaking for 30 min at 4 °C temperature.
4. After sedimentation of the chromatography material, snap off the tip at the bottom of the column (*see* **Note 7**) and place the column in a 2-mL microtube (*see* **Note 8**).
5. Centrifuge for 1 min at 1000 × *g* (*see* **Note 9**) and collect the flow-through fraction.
6. Load the flow-through fraction to spin column No. 2 and close the column with the end cup.
7. Repeat **steps 3**–**5**.
8. Continue this process, including application of the flow-through fraction to the next spin column and repeating **steps 3**–**5**, thereby moving with the flow-through fraction up to spin column 15 (*see* **Note 10**).

3.1.5 Washing the Chromatography Material of the Segments

1. Add 200-μL sample application buffer to spin column No. 1 (*see* **Note 11**) and suspend by aspirating.
2. Centrifuge for 1 min at 1000 × *g* and discard the washing fraction.
3. Repeat **steps 1** and **2** two times.
4. Repeat the washing procedure (**steps 1**–**3**) with spin column Nos. 2 to No. 15.

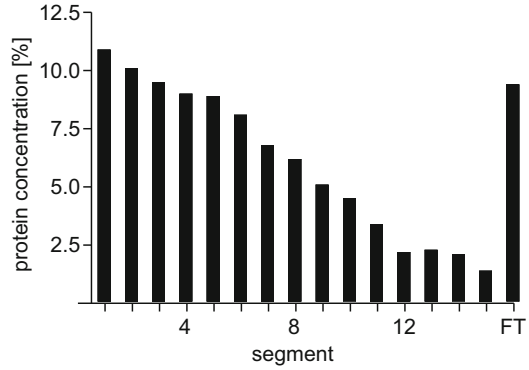

Fig. 2 Relative amounts of proteins in the fractions of sample displacement batch chromatography of the screening experiment performed with phosphate buffer, pH: 7. The initial sample amount (protein amount of 2 g Cohn IV-4 fraction) is equal to 100%

3.1.6 Elution of the Adsorbed Proteins from the Individual Segments

1. Add 150-µL elution buffer to spin column No. 1 (*see* **Note 11**) and suspend by aspirating for 10 s.
2. Centrifuge for 1 min at 1000 × *g*.
3. Collect the eluate of spin column No. 1 in a 2-mL microtube marked No. 1.
4. Repeat **steps 1–3** two times.
5. Repeat the elution procedure (**steps 1–4**) for all remaining spin columns.

3.1.7 Analysis of the Fractions

1. Measure the protein concentration of each eluate (Fig. 2).
2. Apply 20-µg protein of each elution fraction to the SDS-PAGE (Fig. 3a–c).

3.1.8 Sample Displacement Batch Screening Experiments

1. Repeat the steps from Subheadings 3.1.2–3.1.7 for every parameter, which has to be tested. Here, perform Subheadings 3.1.2–3.1.7 with the buffers for pH 5, pH 7, and pH 9.

3.2 Upscaling of Sample Displacement Batch Chromatography

Upscaling by a factor of 100 is performed. In this protocol, a sample displacement batch chromatography at pH 7 in pilot-plant scale is described.

3.2.1 Calculation of the Amount of Chromatography Material Required for Sample Displacement Batch Chromatography Pilot-Plant Experiment

1. Look at the results of the screening experiments for estimating the required segments.
2. Choose the sample amount: 2 g Cohn fraction IV-4.
3. Calculate the chromatography material required: For 2 g Cohn fraction IV-4, use 30 mL TMAE in total (*see* **Note 12**).

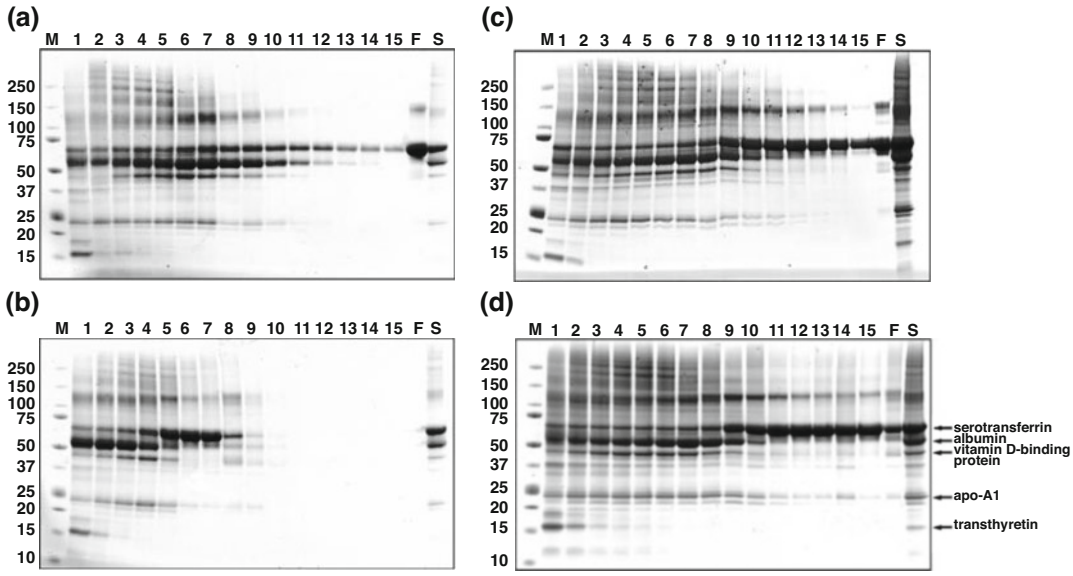

Fig. 3 SDS-PAGE analysis of the protein compositions of the fractions of the sample displacement batch chromatography. 20 μg of each fraction was applied to a SDS-PAGE. The gel was stained by Coomassie Blue. (**a**–**c**) Fractions from the screening experiments. (**a**) pH 7. (**b**) pH 5. (**c**) pH 9. (**d**) Fractions from the pilot-plant chromatography. *M* marker, *lines 1–15* eluates from segments 1 to 15, *F* flow-through fraction, *S* Sample. The identity of the proteins of the bands indicated by arrows was analyzed by tryptic digestion of the proteins in the SDS-PAGE bands and subsequent analysis with liquid-chromatography coupled to tandem mass spectrometry (LC-MS/MS) followed by database search of a protein database (SwissProt) by the search engine (MASCOT) as described in [9]

3.2.2 Equilibration of Chromatography Material

1. Distribute 10-mL portions of TMAE material in three 50-mL tubes (30 mL in total) and suspend each with 40-mL elution buffer (phosphate buffer, pH: 7 + 1 M NaCl) by vortexing for 20 s. Centrifuge for 1 min at 4000 × *g*. Remove carefully the supernatant by decanting followed by aspirating (*see* **Note 4**).
2. Wash the material with 40-mL sample application buffer (phosphate buffer, pH: 7), centrifuge, and discard the liquid (*see* **Note 4**).
3. Repeat this step three times.
4. Sediment the material by gravity (*see* **Note 5**) and discard carefully the buffer by aspiration.

3.2.3 Preparation of Segments

1. Suspend 10-mL chromatography material in 40-mL sample application buffer by vortexing.
2. Transfer immediately 10 mL of the homogeneous suspension to a 50-mL tube marked No. 1 (*see* **Note 13**).
3. Suspend the remaining suspension from **step 1** by vortexing.
4. Transfer immediately 10 mL to tube No. 2.

5. Repeat **steps 3** and **4** until the suspension is transferred to tube No. 15.
6. Sediment the material and carefully discard the buffer by aspiration.

3.2.4 Sample Application

1. Dissolve 2-g globulins Cohn fractions IV-4 in 40-mL phosphate buffer.
2. Load the sample to the tube No. 1, close the tube.
3. Mix thoroughly by overhead rotation for 30 min at 4 °C temperature.
4. Centrifuge for 1 min at 4000 × *g*.
5. Transfer carefully the supernatant to tube No. 2 (*see* **Note 14**).
6. Repeat **steps 2–4**.
7. Transfer carefully the supernatant to tube No. 3 (*see* **Note 14**).
8. Continue this process, including application of the flow-through fraction to the next tube and repeating **steps 3–5**, thereby moving with the supernatant up to tube No. 15 (*see* **Note 15**).

3.2.5 Washing of Chromatography Material of the Segments

1. Add 20 mL sample application buffer to tube No. 1 and suspend by vortexing.
2. Centrifuge for 1 min at 4000 × *g* and discard the washing fraction (*see* **Note 14**).
3. Repeat **steps 1** and **2** two times.
4. Repeat the washing procedure (**steps 1–3**) with tube Nos. 2 to No. 15.

3.2.6 Elution of the Adsorbed Proteins from the Individual Segments

1. Add 15 mL elution buffer to tube No. 1 and mix thoroughly for 20 s.
2. Centrifuge for 1 min at 4000 × *g*.
3. Transfer the supernatant to the tube marked No. 1 (*see* **Note 14**).
4. Repeat **steps 1–3** two times.
5. Repeat the elution procedure (**steps 1–4**) for all remaining tubes.

3.2.7 Analysis of the Fractions by SDS-PAGE

1. Measure the protein concentration of each eluate (Fig. 2).
2. Apply 20 µg of each elution fraction to the SDS-PAGE (Fig. 3d).

3.2.8 Tryptic Digestion of SDS-PAGE Gel Bands

1. Excise gel bands from SDS-PAGE, place bands into a 10-µL tip, and put this tip into reaction vial arrangement shown in Fig. 4 (according to Bertinetti et al. [14], modified).

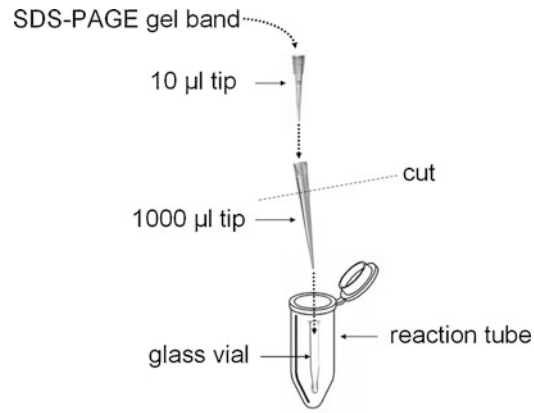

Fig. 4 Reaction vial and tip arrangement for trypsin digestion

2. Homogenize and transfer the gel to the glass vial by centrifugation at 16,000 × *g* for 5 min.
3. Add shrinking solution to generously cover the gel bands. This volume will vary from sample to sample, but on average ~200 µL is sufficient. Incubate for 5 min on a shaker at room temperature.
4. Remove shrinking solution, discard, add ~200 µL swelling solution, and incubate for 5 min. After 5 min, remove the swelling solution and discard it.
5. Repeat **steps 2** and **3** until appropriate destaining is achieved.
6. Add ~200 µL swelling solution, including DTT, and incubate for 10 min at 57 °C. Extract the supernatant and discard.
7. Add ~200 µL shrinking solution and incubate for 30 min on a shaker. Extract the supernatant and discard.
8. Add ~200 µL of the swelling solution, including iodoacetamide, and incubate for 30 min in the dark at room temperature.
9. Add ~200 µL shrinking solution and incubate for 10 min on a shaker. Extract the supernatant and discard.
10. Remove residual liquid and vacuum centrifuge for 15–20 min.
11. Add digest solution to just barely cover the gel pieces. This volume will vary from sample to sample depending on the gel band size, but on average 30 µL is sufficient.
12. Rehydrate the gel pieces on ice at 4 °C for at least 30 min. If gel pieces are not completely covered after 30 min, add digest buffer without trypsin to just cover the gel pieces and to keep them wet during digestion.
13. Incubate overnight at 37 °C.
14. Remove the sample from 37 °C and centrifuge the gel pieces and liquid condensate down.

15. Transfer the digest solution into a clean 1.5-mL reaction vial.
16. To the gel pieces, add 10 μL peptide extraction solution (enough to cover) and incubate for 10 min on a shaker. Add supernatant to the new tube.
17. Add 10 μL 100% acetonitrile and incubate for 10 min. Add supernatant to the new vial.
18. Spin extracted digests and vacuum centrifuge to dryness.
19. Resolve the pellet in 1 μL 30% CAN and add 10–15 μL 0.2% formic acid depending on protein concentration. The final concentration of acetonitrile should not exceed 5% for LC-MS analysis! Here the final sample volume was 15 μL.

3.2.9 Identification of Tryptic Peptides by Mass Spectrometric Analysis

1. Inject 5-μL sample into the LC-MS system.
2. Load the sample onto the enrichment column with a flow rate of 4 μL/min with a mixture of 98% solvent A (0.2% formic acid in water) and 2% solvent B (acetonitrile).
3. Run the chromatographic separation with flow rate of 400 nL/min with a gradient of 2–30% B in 2 min, maintaining 70% solvent B for 3.5 min.
4. Perform data acquisition with an automated data-dependent MS/MS mode by selecting the three most intense ions from each precursor MS scan for MS/MS analysis.
5. Generate a peak list from LC-MS data. Here, Data Analysis Software for 6300 Series Ion Trap LC/MS version 3.4 data interpretation was used.
6. Perform a protein database search with a search engine. Here, we used the online search engine MASCOT (version 2.4.00) Swissprot (2012_08) human protein database. Allow one missed cleavage in MASCOT search and include ad search parameters variable carbamidomethylation on cysteine residues and oxidation on methionine residues. Set the precursor ion mass tolerance to ±0.6 Da.

4 Notes

1. The binding capacity is an important parameter for SDC since the segmented columns or the segmented chromatography material in the case of batch SDC must be overloaded for making use of the sample displacement separation effect. An appropriate ratio of the total sample amount toward the total amount of the chromatography material must be chosen. If the sample amount is too low in relationship to the binding capacity of the chromatography material, the complete sample will adsorb at the first column segment and no separation will be

obtained. If the total sample amount exceeds significantly the total binding capacity of all column segments, this may also result in an insufficient separation because a part of the target protein might already get displaced from the last column segments.

The binding capacity can be roughly estimated from the binding capacities provided by the manufacturer. However, the given values can strongly differ from the binding capacity of the target protein. Additionally, the binding capacity is strongly dependent on chromatographic parameters like pH.

Since a screening experiment is performed first, it is not necessary to know the exact binding capacity of the target protein toward the stationary phase. Therefore, a rough estimation is adequate. This aspect is obvious in Fig. 3. In the presence of a sample loading buffer of pH 9 (Fig. 3b), most of the proteins already have bound to the stationary phase in the first 9 segments. In the presence of a sample loading buffer at pH 5 (Fig. 3a), a significant part of the proteins does not bind to the chromatography material as can be noticed in the lane of the flow-through fraction. At pH 7 (Fig. 3c, d), the amount of proteins in the flow-through fraction is considerably reduced, compared to pH 5. This effect can be explained by the increasing number of negatively charged proteins with increasing pH.

2. In the case of sample displacement batch chromatography, a single segment consists of chromatography material suspended in a buffer instead of a packed column. At least 10 segments are recommended. Since the binding capacity is only approximately estimated, further 5 segments should be added. Therefore, the total number of segments is 15 and the total amount of TMAE material is 300 µL.
3. For having a reference concerning the volume of 300 µL for the total amount of chromatography material, which has to be distributed to the segments, add 300 µL water to an empty 2-mL tube.
4. During equilibration, the chromatography material must sediment for 2 min, to avoid loss of chromatographic beads during removal of the buffer by aspiration.
5. The chromatography material must not be centrifuged but sediment by gravity to ensure correct estimation of its volume.
6. This step results in 20-µL chromatography material per spin column. To ensure equal distribution, it is mandatory to transfer immediately an aliquot of a homogeneous suspension to the segment (here spin column).
7. The tip at the end of the Micro-Bio-Spin Chromatography Columns should not be snapped off before application and incubation of the sample with the chromatography material.

If done otherwise, one can already loose some parts of the sample from the spin columns because of elution by gravity. During washing and elution step, a tip closure must be used for preventing loss of buffer.

8. Micro Bio-Spin Columns fit in 2-mL microtubes. Use these tubes for collection of the flow-through fraction, washing, and elution steps during centrifugation.
9. Using spin columns, avoid centrifugation at higher speed than recommended to prevent chromatography material passing the filter. The optimal speed for Micro Bio-Spin Chromatography Columns (Bio-Rad) is 1 min at 1000 × *g* or less.
10. The flow-through fraction of the last column (segment 15) is the flow-through fraction containing all proteins, which have not adsorbed to the stationary phase.
11. It is recommended to wash and elute the chromatography material directly after sample application to avoid drying of the chromatography material.
12. Thus 30 mL divided by 15 segments (here 50-mL tubes) result in 2-mL TMAE per tube.
13. This step results in 2-mL chromatography material per segment (50-mL tube). To ensure equal distribution, it is mandatory to transfer immediately an aliquot of a homogeneous suspension to the tube.
14. During transfer of the supernatant from the tube containing the chromatography material, some small parts of the chromatography material are transferred with the supernatant. Therefore, centrifuge the chromatography material twice to avoid taking it along during decanting or aspiration. For recovering those parts of chromatography material contaminating the supernatant, centrifuge the supernatant, separate the supernatant from the chromatography material sediment, and transfer the chromatography material back to the original tube.
15. The supernatant of the last tube (No. 15) is the flow-through fraction containing all proteins, which have not bound to the stationary phase.

References

1. Cramer S., Subramanian G., (1989) Preparative liquid chromatography of biomolecules-new directions, New Directions in Sorption Technology, Butterworths, Stoneham194-196
2. Cramer S, Subramanian G (1993) Preparative chromatography in biotechnology. Curr Opin Biotechnol 4:217–225
3. Tiselius A (1943) Displacement development in adsorption analysis. Ark Kemi Mineral Geol 16A:1–18
4. Freitag R, Horváth C (1996) Chromatography in the downstream processing of biotechnological products. Adv Biochem Eng Biotechnol 53:17–59
5. Gerstner J, Cramer S (1992) Cation-exchange displacement chromatography of proteins with protamine displacers: effect of induced salt gradients. Biotechnol Prog 8:540–545
6. Guhan J, Li Y, Moore J, Cramer S (1995) Ion-exchange displacement chromatography

of proteins dendritic polymers as novel displacers. J Chromatogr A 702:143–155

7. Zhang T, Bourret J, Cano T (2011) Isolation and characterization of therapeutic antibody charge variants using cation exchange displacement chromatography. J Chromatogr A 1218:5079–5086
8. Mazza CB, Rege K, Breneman CM, Sukumar N, Dordick JS, Cramer SM (2002) High-throughput screening and quantitative structure-efficacy relationship models of potential displacer molecules for ion-exchange systems. Biotechnol Bioeng 80:60–72
9. Tugcu N, Ladiwala A, Breneman CM, Cramer SM (2003) Identification of chemically selective displacers using parallel batch screening experiments and quantitative structure efficacy relationship models. Anal Chem 75:5806–5816
10. Hodges RS, Burke TW, Mant CT (1988) Preparative purification of peptides by reversed-phase chromatography. Sample displacement mode versus gradient elution mode. J Chromatogr 444:349–362
11. Srajer Gajdosik M, Clifton J, Josic D (2012) Sample displacement chromatography as a method for purification of proteins and peptides from complex mixtures. J Chromatogr A 1239:1–9
12. Veeraragavan K, Bernier A, Braendli E (1991) Sample displacement mode chromatography—purification of proteins by use of a high-performance anion-exchange column. J Chromatogr 541:207–220
13. Brgles M, Clifton J, Walsh R, Huang F, Rucevic M, Cao L, Hixson D, Muller E, Josic D (2011) Selectivity of monolithic supports under overloading conditions and their use for separation of human plasma and isolation of low abundance proteins. J Chromatogr A 1218:2389–2395
14. Josic D, Breen L, Clifton J, Srajer GM, Gaso-Sokac D, Rucevic M, Müller E (2012) Separation of proteins from human plasma by sample displacement chromatography in hydrophobic interaction mode. Electrophoresis 33:1842–1849
15. Khanal O, Kumar V, Westerberg K, Schlegel F, Lenhoff A (2018) Multi-column displacement chromatography for separation of charge variants of monoclonal antibodies. J Chromatogr A 9673:31499–31497
16. Heikaus L, Schlüter H (2014) Sample displacement chromatography for protein purification. Am Pharm Rev 17:2
17. Milne JJ (2011) Scale-up of protein purification: downstream processing issues. Methods Mol Biol 681:73–85
18. Ahrends R, Lichtner B, Bertsch A, Kohlbacher O, Hildebrand D, Trusch M, Schlüter H (2010) Application of displacement chromatography for the proteome analysis of a human plasma protein fraction. J Chromatogr A 1217:3321–3329
19. Burnouf T (2007) Modern plasma fractionation. Transfus Med Rev 21:101–117
20. Gaso-Sokac D, Kovac S, Clifton J, Josic D (2011) Therapeutic plasma proteins--application of proteomics in process optimization, validation, and analysis of the final product. Electrophoresis 32:1104–1117
21. Bertinetti D, Schweisberg S, Hanke SE, Schwede F, Bertinetti O, Drewianka S, Genieser HG, Herberg FW (2009) Chemical tools selectively target components of the PKA system. BMC Chem Biol 9:3

Chapter 20

Lectin Affinity Chromatography: An Efficient Method to Purify Horse IgG3

Salvatore G. De-Simone and David W. Provance Jr.

Abstract

Affinity chromatography is a separation method based on a specific binding interaction between an immobilized ligand and its binding partner. An important class of ligands for the effective separation and purification of biotechnologically important substances is lectins, a group of naturally occurring molecules widely found in plants that display a range of specificities to bind different sugars. As sugars are often added to proteins through the process of glycosylation, ~1/3 of all genetically encoded proteins are glycosylated, numerous cognate pairs of lectins with glycosylation groups have been discovered. Their specific binding interactions have not only allowed the development of numerous methodological strategies involving immobilized lectins to isolate molecules of interests but also for understanding the intermolecular interactions and alterations in glycosylation during a diverse set of biological phenomena, including tumor cell metastasis, intracellular communication, and inflammation. In this chapter, we describe a basic procedure for the separation of horse antibody classes by affinity chromatography based on differences in their glycosylation patterns. This procedure has been utilized for the purification of horse IgG3 (hoIgG3) from other six Ig from equine sera in a single step by using an *Artocarpus integrifolia* Jacalin column. This class of antibody comprises the therapeutic fraction generated in equine for passive antibody therapy and can serve as a biomarker for patient hypersensitivity. During the course of developing the protocol, the affinity interaction constant between the huIgE-hypersensitive immunoglobulin and the purified hoIgG3 was also determined.

Key words Affinity chromatography, Jacalin-sepharose, Horse IgG3, Purification, Human IgE, Thermophoresis

Abbreviations

EDTA	ethylenediaminetetraacetic acid
hoIgG3	horse immunoglobulin G3
HPLC	high-performance liquid chromatography
huIgE	human immunoglobulin E
Ig	immunoglobulin
IgE	immunoglobulin E
IgG	immunoglobulin G

Nikolaos E. Labrou (ed.), *Protein Downstream Processing: Design, Development, and Application of High and Low-Resolution Methods*, Methods in Molecular Biology, vol. 2178, https://doi.org/10.1007/978-1-0716-0775-6_20,

PAGE	polyacrylamide gel electrophoresis
PBS-NP40	phosphate buffer of pH 7.3 containing 150 mM NaCl and 0.1% Nonidet P-40
SDS	sodium dodecyl sulfate

1 Introduction

Lectins are proteins with a high degree of stereospecificity that are recognized by various sugar structures and can form reversible hydrostatic linkages with the carbohydrate groups on glycoconjugate complexes. The isolation, expression, and purification of native and recombinant proteins is an important aspect of the study of protein regulation, structure, and function. Normally, purification of proteins from a complex mixture is a daunting endeavor that, in spite of numerous attempts to streamline and simplify the process, often leads to unexpected results. While the reasons for such outcomes are numerous and diverse, one can minimize some major factors that affect yield, purity, and preservation of biological activity of the protein being purified through the use of lectin interactions. An important class of proteins whose purification for downstream applications can be greatly facilitated by lectin-based affinity chromatography are immunoglobulins (Ig).

This class of proteins is more commonly referred to as simply antibodies. They are important for basic research, industrial processes, and medicine. Antibodies can serve as biomarkers for a broad range of diseases, while their presence can serve as indicators for most pathogen infections. They are the keystones to the development of immunodiagnostics for the detection of foodborne pathogens, adulterants, toxins, and residues in food samples as well as environmental analysis/monitoring. In immunotherapeutics, antibodies are responsible for the targeting of drugs. The generation of antibodies is fundamental to methods for the isolation of a range of proteins and other molecules of interest as well as serving as the underlying therapy of immunoprophylaxis for treating acute conditions [1–11]. While a variety of simple and fast antibody purification strategies have been developed that can be applied to a wide range of classes of Igs from different animal species [12], very little has been described for purifying the therapeutic Igs prepared from horse serum that serves as important immunotherapeutics and immunoprophylaxis, collectively known as passive antibody therapies (PATs) [13].

The quintessential PATs, which are often indicated as a primary treatment, are antivenoms (e.g., snakes, scorpion, spider, and bees) and anti-infectious agents (e.g., diphtheria, botulinum, rabies). These immunobiological compounds consist of polyclonal antibodies that are raised against one or more venoms/infectious agent proteins principally in horses due to their large size [14]. Other

animals that serve as sources include sheep, goats, and donkey, according to a recent evaluation, but their lower yields can be cost prohibitive. The intravenous administration of an antivenom to patients with envenoming can rapidly prevent and even reverse clinical effect of the venom by the binding of the antibodies to circulating toxins, which neutralizes their activity and promotes their elimination [15]. The most severe, immediate side effect of a PAT generated in the horse is a classical IgE-mediated hypersensitivity reaction, which can be fatal and affects 1–40% of the recipients worldwide, depending on the preparation [16–25].

Traditionally, on a commercial scale for therapeutic applications, horse IgG (hoIgG) is concentrated by precipitation with ammonium sulfate [26] or by caprylic acid–based fractionation [27]. However, different techniques are utilized for the clear majority of Igs used at a research scale-like Protein-A, G, A/G, and L affinity chromatography. The performance of thiophilic chromatography has found an increasingly wider range of applications, especially in the case of industrial-scale purifications, where Protein A is the most preferred ligand of choice [28, 29]. Yet, the efficient recovery of a representative pool of antibodies can vary by methods (e.g., for human Igs, Protein A binds preferentially to IgM and IgG isotypes, although not the IgG3 subclass). Further, the phenotypic characteristic of Igs from the different animal species and the presence or not of the determined carbohydrate limits its applications. This is of interest for disease models in which the Ig acts as a marker as well as when the Ig may be associated with the protective immunity as is the case with antivenoms.

The horse IgG (hoIg) class of immunoglobulins comprises a mixture of seven subclasses (IgG1 > IgG3 > IgG4 > IgG7 > IgG2 = IgG5 > IgG6) that are present at different relative concentrations with IgG3 being the second most abundant hoIg in the sera [30]. This subclass is the key hoIg that provides antivenom protective and other therapeutics effects, but it is also the allergenic compound responsible for the observed hypersensitivities to antivenom sera therapy [31–34]. Altogether, the hoIgG antibodies are known to have important roles in the natural protection of horses against several diseases such as equine influenza virus [35] and equine Herpes virus [36]. Yet, the structure of the subclasses is poorly characterized. For hoIgG3, it was determined that it possesses O-linked as well as N-linked glycan attached to the heavy chain [30, 37]. This observation leads us to the use of Jacalin lectin for the affinity purification of hoIgG3 from the horse sera. Lectins have proven to be useful affinity reagents for the identification, enrichment, isolation, and characterization of many glycoconjugates that can detect the glycosylation fingerprint for the discrimination of various glycoproteins. Here, we show the application of Jacalin-Sepharose lectin-based affinity purification as a simple and suitable methodology that

could be a viable option for the large-scale production of hoIgG3, which is a key antigen in allergenic antivenom sera therapy. Besides, it was demonstrated that the hoIgG3-purified antigen presents a strong strength affinity ($10.6 \pm 0.6\%$) for the huIgE-hypersensitive antibodies.

2 Materials

2.1 Equipment

1. NanoDrop 2000 spectrophotometer (Thermo Scientific).
2. MicroScale Thermophoresis (MST) (NanoTemper Technologies GmbH, Germany).

2.2 Reagents

1. Sepharose CL-4B and Superdex 200 prep were purchased from GE Healthcare Life. Science (SP, Brazil).
2. Silver stain kit from Bio-Rad Laboratories, CA, USA.
3. Fluorescent dyes (NT-647, NT-532 or NT-488) and Monolith NT™ Protein Labeling. Kits were from NanoTemper Technologies GmbH (Germany).
4. Microwell plates for ELISA were from Nunc, New York, USA.
5. Rabbit anti-human IgG and goat anti-human IgE labeled with alkaline phosphatase or HRP were purchased from KPL (Kirkegaard & Perri Laboratories, USA).

3 Methods

3.1 Preparation of Jacalin-Sepharose

1. The Jacalin lectin was purified using a polyacrylate DEAE-HPLC (Shimadzu, Kyoto, Japan) column [38] and then conjugated to Sepharose CL4B beads (GE Healthcare Life Science, SP, Brazil) with carbodiimide (Sigma-Merck) according to the protocol described by the manufacturer to generate an affinity lectin column (GE Healthcare).

3.2 Jacalin-Based Affinity Chromatography Procedure

1. Immunoglobulins are glycoproteins and can, therefore, be purified using affinity chromatography based on immobilized lectin adsorbents. There are several examples in the literature using affinity chromatography for purifying classes and subclasses of Igs from various species, including human, mice [39], dog [40], and rabbit [41].
2. A column of Jacalin-Sepharose CL4B-column (3 cm × 1 cm, i.d.) was equilibrated overnight with Eq-buffer (Tris–buffer (175 mM Tris–HCl, pH: 7.4, containing 150 mM NaCl).
3. Horse serum (4 ml; supplied by Vital Brazil Institute, Niterói, RJ, Brazil) was mixed with an equal volume of Tris-buffer 2× (350 mM Tris–HCl, pH: 7.4, containing 300 mM NaCl) and passed through 0.45-μm filters.

4. The diluted, filtered horse serum was applied to the Jacalin-Sepharose column.
5. After washing with ≥25 ml of equilibration buffer Eq-Buffer, adsorbed proteins were eluted with 5 ml of 0.8 M α-D-Galactose prepared in Tris-buffer with a flow rate of 1 ml/min at room temperature (25 °C).
6. A single peak was observed for the material desorbed with 0.8 M α-D-Galactose (Fig. 1).
7. The yield of the recovered hoIgG3 protein was approximately 1.6–2.13% (E0.1% at 280 nm, 1-cm pathway = 1.36) of the total protein serum applied to the affinity matrix that correlated to 2.56–3.07 mg IgG3/column using 4 ml of sera (30–40 mg/ml) applied.

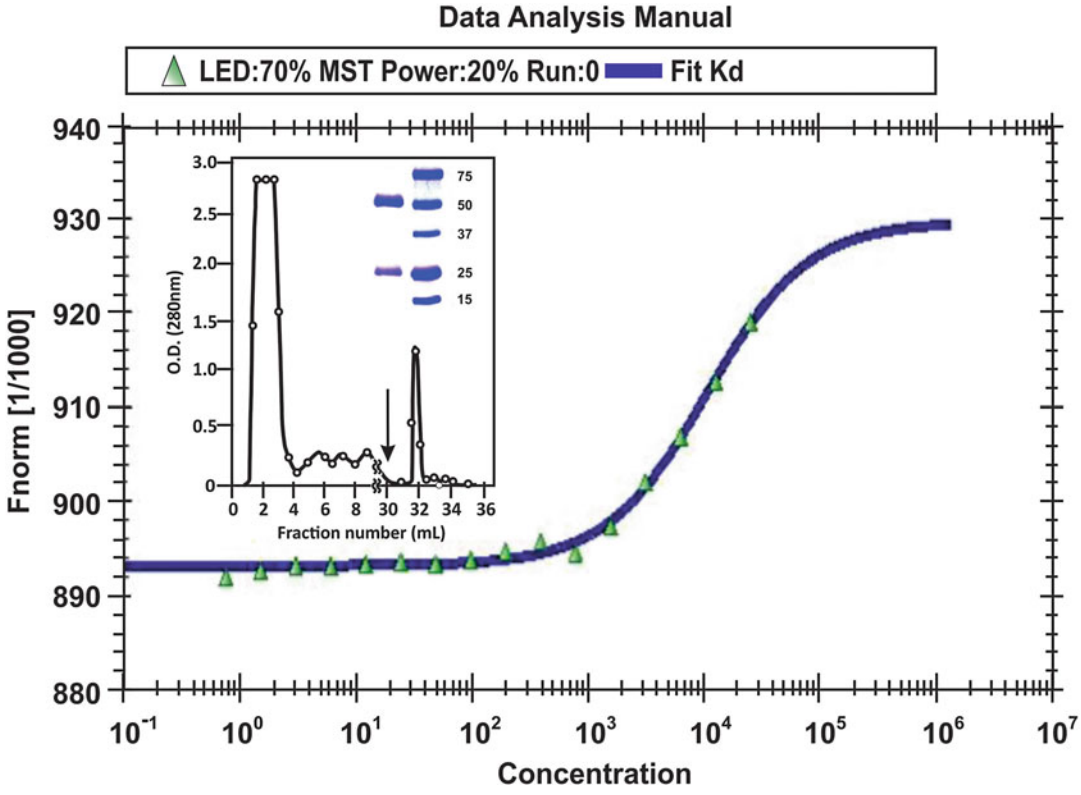

Fig. 1 Determination of the K_d of the interaction holgG3-IgE rich patient sera by MicroScale Thermophoresis (MST). For these experiments, the holgG3 was previously labeled with the NT. 647 fluorescent compound and a constant amount of holgG3-NT.647 mixed with different dilutions (25–0.001%) of IgE-rich patient sera. After a short incubation time, the samples were loaded into MST NT.115 standard glass capillaries and the MST analysis performed using the monolith NT-115. A K_d of 10.6 ± 0.6% was determined. Inset: Characterization of the holgG3 by SDS-PAGE (10%) under reducing conditions. The holgG3 sample (30 μg) was loaded into lane A and a standard weight maker in lane B. Proteins were revealed by Coomassie blue

8. This quantification was supported by measurements of the total bound and unbound proteins concerning the affinity chromatography.

3.3 Electrophoresis

1. Separation of the samples by discontinuous sodium dodecyl sulfate-polyacrylamide gel electrophoresis (SDS–PAGE [42]; 90 min/100 V/12% polyacrylamide gels) under reductive conditions showed that the hoIgG3 presented bands with an apparent molecular weight of 65 and 25 kDa for the heavy and light chain of IgG, respectively.
2. A molecular mass of 192 kDa was deduced for hoIgG3 (±11.5 kDa) by HPLC (data not shown).

3.4 MicroScale Thermophoresis (MST)

1. We further investigated the utility of the Jacalin-Sepharose resin for purifying a specific target, by determining the binding affinity of this target (hoIgG3) with antibodies IgE presents in the sera of a patient with allergy to anti-snake venom therapeutic horse sera, which would to better describe the observed selectivity and specificity of this ligand/binding partner. There are many ways to measure this interaction. Here, we have applied MST to measure the dissociation constant (K_d).
2. This methodology is based on the movement of molecules in a temperature gradient and has the advantage of performing fast measurements applicable to molecular interactions in solutions without requiring immobilization of one of the binding partners to a surface [43].
3. Purified hoIgG3 antigen was labeled with the fluorescent dye NT-647 using Monolith NT™ Protein Labeling Kits (cysteine-reactive) and mixed at different concentrations (25–0.001% in buffer) of a human hypersensitive-serum (*y*-axis).
4. The assay was performed in TSMT-buffer (50 mM Tris containing 150 mM NaCl, 10 mM $MgCl_2$, and 0.05% Tween® 20, pH: 7.6) and after a short incubation time, the samples were loaded into MST NT.115 standard glass capillaries.
5. The analysis was performed as described here in PBS and the K_d data were calculated using the NanoTemper software package.
6. A K_d of 10.6 ± 0.6% was determined (Fig. 1).
7. Originally it was reported that Jacalin primarily bound to the Galβ1-3GalNAcα- (Core1) structure [44, 45] and then that it had a wider binding specificity [46, 47].
8. More recently, it was demonstrated that among the Gal/GalNAc reactive lectins, Jacalin remains as a prime candidate for a serving as a tool to specifically select O-glycans. However, Jacalin does not bind to O-glycans with any C6-substituent at the reducing end GalNAc [48].

4 Notes

1. Affinity chromatography describes a type of liquid chromatography whereby a binding agent that has an "affinity" to interact with a target molecule is immobilized onto the stationary phase.
2. The retention of a solute or analyte is based on the specific and reversible interactions that occur between many biological binding agents and their targets [49].
3. This method can have high selectivity that allows for relatively simple separation protocols for isolating specific target molecules, even when the target is present within complex mixtures such as serum, urine, cell cultures, and food samples.
4. This method requires an appropriate binding agent for the given target.
5. Another requirement is the need for adequate techniques to immobilize the binding agent to the stationary phase along with the definition of conditions that can be used with this agent for the application and elution of the target for either its purification or analysis.
6. There are various ways that affinity ligands can be used in this method.
7. One common format is the on/off elution mode that is shown in Fig. 1.
8. In this format, a sample containing the target analyte is applied to an affinity column in the presence of an application buffer.
9. During this application step, nontarget components will not be retained by the binding agent and pass through the column, while the target analyte interacts with the binding agent and is retained on the stationary phase of the column.
10. The target analyte is then later eluted from the column by passing through an elution buffer that reverses the target/binding agent interaction followed by column regeneration.
11. This format is often used for binding agents that have strong retention for their targets (i.e., association equilibrium constants of roughly 10^6 M^{-1} or higher) as is the case of hoIgG3 for the lectin jacalin (K_d = 2.3 nM ± 0.3 nM = 0.43 nM; [13]).
12. The use of a strong binding interaction requires an elution buffer that weakens the interactions to promote target elution that can involve changes in pH, ionic strength, polarity, or the addition of agents to the mobile phase content such as chaotropic agents or competitive agents [50].

13. When the association equilibrium constant for the target with the immobilized binding agent is less than 10^5 to 10^6 M^{-1}, which describes a weak-to-moderate binding strength, elution conditions involve smaller changes such as isocratic displacement conditions that are employed in chiral separations or in the study of biological interactions.
14. The results shown in Fig. 1 definitely prove that the allergenic target in horse therapeutic sera was purified by lectin affinity column. The IgE present in the patient serum specifically binds to the target that was purified by the affinity column with strong binding strengths, $\sim 10^8$ M^{-1}.

Acknowledgments

We thank Dr. Daniel Maturana for assistance in the experiments with thermophoresis along with V.G. Mendes and K. Felisbino for support with technical laboratory analysis.

References

1. Sato S, Yanagida N, Ohtani K, Koike Y et al (2015) A review of biomarkers for predicting clinical reactivity to foods with a focus on specific immunoglobulin E antibodies. Curr Opin Allergy Clin Immunol 15:250–258
2. Kankeu-Fonkoua L, Yee NS (2018) Molecular characterization of gastric carcinoma: therapeutic implications for biomarkers and targets. Biomedicine 9:E32
3. Benzaquen J, Marquette CH, Glaichenhaus N et al (2018) The biological rationale for immunotherapy in cancer. Rev Mal Respir 35:206–222
4. Van Gasse AL, Sabato V, Bridts CH et al (2014) L'allergie au cannabis: bien plus qu'un voyage stupéfiant emerging allergens. Rev Fr Allergol 54:144
5. Drak CG, Lipson EJ, Brahmer JR (2014) Breathing new life into immunotherapy: review of melanoma, lung and kidney cancer. Nat Rev Clin Oncol 1:24–37
6. Welbeck K, Leonard P, Gilmartin N et al (2011) Generation of an anti-NAGase single-chain antibody and its application in a biosensor-based assay for the detection of NAGase in milk. J Immunol Methods 364:14–20
7. Dijkers ECF, de Vries EGE, Kosterink JGW et al (2008) Immunoscintigraphy as a potential tool in the clinical evaluation of HER2/neu targeted therapy. Curr Pharm Des 14:3348–3362
8. Subramanian A (2002) Immunoaffinity chromatography. Mol Biotechnol 20:41–47
9. Lipman NS, Jackson LR, Trudel LJ et al (2005) Monoclonal versus polyclonal antibodies: distinguishing characteristics, applications, and information resources. ILAR J 46:258–268
10. Ayyar BV, Aror S, Murphy C et al (2012) Affinity chromatography as a tool for antibody purification. Methods 56:116–129
11. Grom M, Kozorog M, Caserman S et al (2018) Protein A affinity chromatography of Chinese hamster ovary (CHO) cell culture broths containing biopharmaceutical monoclonal antibody (mAb): experiments and mechanistic transport, binding and equilibrium modeling. J Chromatogr B 1083:44–56
12. Arora S, Ayyar BV, O'Kennedy R (2015) Affinity chromatography for antibody purification. Methods Mol Biol 1129:497–516
13. De-Simone SG, Nascimento HJ, Prado I et al (2018) Purification of equine IgG3 by lectin affinity and an interaction analysis via microscale thermophoresis. Anal Biochem 561–562:27–31
14. Theakston RDG, Warrell DA (1991) Antivenoms: a list of hyperimmune sera currently available for the treatment of envenoming by bites and stings. Toxicon 29:1419–1470

15. Warrell DA (1996) Management of snakebite. In: Weatherall DJ, JGG L, Warrell DA (eds) Oxford Twbook of medicine, 3rd edn. Oxford University Press, Oxford, p 1135
16. Reddy PM, Nagaya H, Pascual HC et al (1978) Reappraisal of intracutaneous tests in the diagnosis of reagenic allergy. J Allergy Clin Immunol 61:36–41
17. Sutherland SK, Lovering KE (1979) Antivenoms: use and adverse reactions over a 12-month period in Australia and Papua New Guinea. Med J Aust 2:671–674
18. Malasit P, Warrell DA, Chanthavanich P et al (1986) Prediction, prevention, and mechanism of early (anaphylactic) antivenom reactions in victims of snake bites. Br Med J 292:17–20
19. Morais VM, Massaldi H (2009) Snake antivenoms: adverse reaction and production technology. J Venom Anim Toxins Incl Trop Dis 15:2–18
20. Chen JC, Bullard MJ, Chiu TF et al (2000) Risk of immediate effects from F(ab')2 bivalent antivenin in Taiwan. Wilderness Environ Med 11:163–167
21. Dart RC, McNally J (2000) Efficacy, safety, and use of snake antivenoms in the United States. Ann Emerg Med 37:181–188
22. LoVecchio F, Klemens J, Roundy EB et al (2003) Serum sickness following administration of antivenin (Crotalidae) polyvalent in 181 cases of presumed rattlesnake envenomation. Wilderness Environ Med 14:220–221
23. Ledin A, Arnemo JM, Liberg O, Hellman L (2008) High plasma IgE levels within the Scandinavian wolf population, and its implications for mammalian IgE homeostasis. Mol Immunol 45:1976
24. Thiansookon A, Rojnuckarin P (2008) Low incidence of early reactions to horse-derived F (ab'2) antivenom for snakebites in Thailand. Acta Trop 105:203
25. León G, Herrera M, Segura A, Villalta M, Vargas M, Gutiérrez JM (2013) Pathogenic mechanisms underlying adverse reactions induced by intravenous administration of snake antivenoms. Toxicon 76:63
26. Aj H (1948) The purification of antitoxic plasmas by enzyme treatment and heat denaturation. Biochem J 42:390
27. Rojas G, Jiménez JM, Gutierrez JM (1994) Caprylic acid fractionation of hyperimmune horse plasma: description of a single procedure for antivenom production. Toxicon 32:351
28. Raweerith R, Ratanabanangkoon K (2003) Fractionation of equine antivenom using caprylic acid precipitation in combination with cationic ion-exchange chromatography. J Immunol Methods 282:63
29. Ayyar BV, Arora S, Murphy C, O'Kennedy R (2012) Affinity chromatography as a tool for antibody purification. Methods 56:116
30. Lewis MJ, Wagner B, Woof JM (2008) The different effector function capabilities of the seven equine IgG subclasses have implications for vaccine strategies. Mol Immunol 45:818
31. De-Simone SG, Gomes LP, Gemal A, Quirino FS, Provance-Jr DW (2013) Determination of a linear B-cell epitope in equine IgG for improved detection in therapeutic preparations. J Biotechnol Lett 4:84
32. De-Simone SG, Napoleão-Pêgo P, Teixeira-Pinto LAL, Melgarejo AR, Aguiar AS, Provance-Jr DW (2014) IgE and IgG epitope mapping by microarray peptide-immunoassay reveal the importance and diversity of the immune response to the IgG3 equine immunoglobulin. Toxicon 78:83
33. Prado LC, Souza ALA, Rj C, Provance-Jr DW, De-Simone SG (2017) Ultrasensitive and rapid immuno-detection of human IgE anti-therapeutic horse sera using an electrochemical immunosensor. Anal Biochem 538:13
34. De-Simone SG, Souza ALA, Melgarejo AR, Aguiar AS, Provance-Jr DW (2017) Development of elisa assay to detect specific human IgE anti-therapeutic horse sera. Toxicon 138:37
35. Breathnach CC, Sturgill-Wright T, Stiltner JL, Adams AA, Lunn DP, Horohov DW (2016) Foals are interferon gamma-deficient at birth. Vet Immunol Immunopathol 112:199
36. Kydd JH, Townsend HG, Hannant D (2006) The equine immune response to equine herpesvirus-1: the virus and its vaccines. Vet Immunol Immunopathol 111:15
37. Raju TS, Briggs JB, Borge SM, Jones AJ (2000) Species-specific variation in glycosylation of IgG: evidence for the species-specific sialylation and branch-specific galactosylation and importance for engineering recombinant glycoprotein therapeutics. Glycobiology 10:477–486
38. De-Simone SG, Santos R, Araujo MF, Pinho RT (1994) Preparative isolation of the lectin jacalin by anion-exchange high-performance liquid chromatography. J Chromatogr A 68:357
39. Robertson ER, Kennedy JF (1996) Glycoproteins: a consideration of the potential problems and their solutions with respect to purification and characterization. Bioseparation 6:1
40. Peng Z, Arthur G, Simons FE, Becker AB (2013) Binding of dog immunoglobulins G,

A, M, and E to concanavalin A. Vet Immunol Immunopathol 36:83

41. Kabir S, Ahmed ISA, Daar AS (1995) The binding of jacalin with rabbit immunoglobulin G. Immunol Invest 25:725
42. Laemmli UK (1970) Cleavage of structural proteins during the assembly of the head of bacteriophage T4. Nature 227:680
43. Baaske P, Wienken CJ, Reineck P, Duhr S, Braun D (2010) Optical thermophoresis for quantifying the buffer dependence of aptamer binding. Angew Chem Int Ed Engl 49:2238
44. Tachibana K, Nakamura S, Wang H, Iwasaki H, Tachibana K, Maebara K et al (2006) Elucidation of binding specificity of Jacalin toward O-glycosylated peptides: quantitative analysis by frontal affinity chromatography. Glycobiology 16:46
45. Sastry MV, Banarjee P, Patanjali SR, Swamy MJ, Swarnalatha GV (1986) A. Surolia, analysis of saccharide binding to Artocarpus integrifolia lectin reveals specific recognition of T-antigen (β-DGal(1–3)D-GalNAc). J Biol Chem 261:11726
46. Ahmed JH, Chatterjee BP (1989) Further characterization and immunochemical studies on the carbohydrate specificity of jackfruit (Artocarpus integrifolia) lectin. J Biol Chem 264:9365
47. Jeyaprakash AA, Katiyar S, Swaminathan CP, Sekar K, Surolia A, Vijayan M (2003) Structural basis of the carbohydrate specificities of Jacalin: an X-ray and modeling study. J Mol Biol 332:217
48. Wu AM, Wu JH, Lin LH, Liu JH (2003) Binding profile of Artocarpus integrifolia agglutinin (Jacalin). Life Sci 72:2285
49. De-Simone SG, Netto CC, Silva-Jr FP (2006) Simple affinity chromatographic procedure to purify beta-galactoside binding lectins. J Chromatogr B Analyt Technol Biomed Life Sci 838:135
50. De-Simone SG, Correa-Netto C, Antunes OA, De-Alencastro RB, Silva-Jr FP (2005) Biochemical and molecular modeling analysis of the ability of two p-aminobenzamidine-based sorbents to selectively purify serine proteases (fibrinogenases) from snake venoms. J Chromatogr B Analyt Technol Biomed Life Sci 822:1

Chapter 21

Heparin-Binding Affinity Tag: A Novel Affinity Tag for Simple and Efficient Purification of Recombinant Proteins

Sanhita Maity, Musaab Al-Ameer, Ravi Kumar Gundampati, Shilpi Agrawal, and Thallapuranam Krishnaswamy Suresh Kumar

Abstract

Heparin, a polysulfated polyanionic member of the glycosaminoglycan family, is known to specifically bind to a number of functionally important proteins. Based on the available information on structural specificity of heparin–protein interactions, a novel heparin-binding peptide (HB) affinity tag has been designed to achieve simple and cost-effective purification of target recombinant proteins. The HB-fused recombinant target proteins are purified on a heparin-Sepharose column using a stepwise/continuous sodium chloride gradient. A major advantage of the HB tag is that the HB-fused target proteins can be purified under denaturing conditions in the presence of 8 M urea. In addition, polyclonal antibody directed against the HB tag can be used to specifically detect and quantitate the HB-fused recombinant protein(s). Herein, a step-by-step protocol(s) for the purification of different soluble recombinant target proteins is described. In addition, useful tips to troubleshoot potential problems and also suggestions to successfully adopt the HB-tag-based purification to a wide range of target proteins are provided.

Key words Recombinant proteins, Purification, Heparin Sepharose, Affinity tag, Denatured proteins

1 Introduction

Overexpression and purification of recombinant proteins is of immense interest in the pharmaceutical and biotechnological field [1]. Recombinant proteins have a diverse range of applications such as therapeutics, diagnostic tools, food processors, and instruments in proteomics [2–4]. Recent advances in recombinant DNA technology have facilitated the large-scale production of bioactive target proteins in suitable heterologous hosts [5]. Despite the exciting advances in recombinant DNA technology, the simple and cost-effective purification of target recombinant proteins still presents a complex challenge. In this context, affinity chromatography has emerged as the most efficient and selective method for the purification of recombinant proteins [6–8]. Selective affinity tags are fused

Nikolaos E. Labrou (ed.), *Protein Downstream Processing: Design, Development, and Application of High and Low-Resolution Methods*, Methods in Molecular Biology, vol. 2178, https://doi.org/10.1007/978-1-0716-0775-6_21,

to recombinant proteins of interest to facilitate the purification of target protein(s) by affinity chromatography [9, 10]. Typically, protein purification tags have some desirable properties such as (a) high specific binding to a resin, which is attached to one of the metal/substrate/protein affinity partner(s) (b) noninterference in the folding of the target recombinant protein; and (c) easy detachment from the target recombinant protein either by chemical or enzymatic cleavage methods.

Herein, we illustrate a simple, rapid, and cost-effective purification of target recombinant proteins from the soluble bacterial cell lysates by using a novel heparin-binding peptide affinity tag (HB tag) [11]. Heparin is a negatively charged polysulfated polyanionic member of the glycosaminoglycan family [12]. Heparin plays a multifunctional role and serves as a secondary receptor in several key cellular processes [13, 14]. Heparin has been recognized as a specific binder to a variety of proteins such as fibroblast growth factors, chemokines, fibronectin, antithrombin, laminin, thrombin, thrombospondin, to name a few [15–21]. Positively charged amino acids in the heparin-binding region of the heparin-binding proteins are involved in electrostatic interactions with the negatively charged heparin. Structural analyses reveal that some of the common heparin-binding segments of heparin-binding proteins are XBBXBX, XBBBXXBX, and XBBXXBBBXXBBX, wherein B is one of the three basic amino acids (arginine, lysine, or histidine) and X represents any of the other 17 natural amino acids [22, 23]. In particular, the heparin-binding specificity depends on the nature and number of the nonbasic amino acids (–X–) and the distribution among the positively charged amino acids (B) located in the heparin-protein-binding interface. Based on the structural information, a bacterial vector encoding a novel heparin-binding (HB) tag has been designed for overexpression and purification of recombinant proteins in *Escherichia coli* (*E. coli*) [24–26]. In principle, HB tag can be used as a protein affinity tag for the purification of nonheparin-binding target recombinant proteins to homogeneity employing heparin-Sepharose affinity chromatography [27]. DNA elements coding for heparin-binding (HB) affinity tag were fused with the target protein gene to generate the target protein fusion gene. Subsequent overexpression in *E. coli* resulted in the production of target recombinant proteins, which were successfully purified in a single step by heparin-Sepharose chromatography. Bound HB-fused target recombinant proteins can then be eluted by a using stepwise salt gradient. The HB tag can be separated from the target protein by selective enzyme-mediated cleavage to obtain the pure protein of interest [26].

1.1 Design and Characteristics of the HB Tag

Cardin and Weintraub identified potential heparin-binding motifs based on the analysis of the amino acid sequences of proteins that are known to possess strong heparin-binding affinity [28]. We identified consensus heparin-binding amino acid segments using a computer string search algorithm [29]. Our aim for designing the HB peptide was to achieve an asymmetric distribution of positive and uncharged amino acids in the three-dimensional structural models built for the consensus heparin-binding (HB) strings. The amino acid sequence of the synthetic HB was given as WASKAQKAQAKQAKQAQKA-. For optimal heparin binding, the HB sequence provided was repeated twice, with minor modifications, to yield a 32-amino acid HB (ASKAQKAQAKQWKQAQKAQKAQAKQAKQW***LVPRGS***) with an incorporated thrombin cleavage site, –LVPRGS–, located the C-terminal end of the affinity tag. The designed HB tag has the following specific characteristics:

1. The tag was designed so that 60% of the amino acids were polar to promote the overexpression of the HB-fused target protein in the soluble form.
2. The HB tag has the capability to form an amphipathic helix wherein the polar and nonpolar amino acids are located on the opposite surfaces of the helix.
3. The affinity tag contains positively charged lysine (K) and polar uncharged glutamine (Q) residues to facilitate electrostatic interaction(s) and H-bonding with the immobilized heparin on heparin-Sepharose matrix.
4. The construct has two tryptophan residues (W_{12} and W_{32}), one at each terminus at the (N- and C-termini) of the tag, to help monitor elution of HB-fused recombinant target proteins using absorbance at 280 nm.
5. Presence of a thrombin cleavage site (–LVPRGS–) at the C-terminal end of HB allows the cleavage and separation of the recombinant target protein from the affinity tag.
6. Far UV-circular dichroism spectrum of the HB tag suggested that it is primarily unfolded but transitions to form a partial helical conformation upon binding to heparin. Isothermal titration calorimetry results revealed that HB tag has a binding affinity with heparin in the high nanomolar range and the binding stoichiometry of HB with heparin is 1:1. Multidimensional NMR spectroscopy data established the noninterference of the HB tag with the folding of the recombinant target proteins [26].

   This chapter provides a step-by-step protocol(s) for the overexpression and purification of different soluble recombinant target proteins, including S100A13- a calcium-binding protein, C-terminal domain of the membrane protein Albino-3 and C2A domain of synaptotagmin using the HB tag.

1.2 Detection of the HB Tag

HB tag facilitates the overexpression of HB-fused recombinant proteins, including CAlb3, S100A13, and C2A domain of synaptotagmin in *E. coli* cells particularly as soluble forms. The soluble *E. coli* lysate was loaded on a heparin-Sepharose column and eluted in several fractions using a stepwise NaCl gradient. The purity of HB-fused recombinant protein(s) was assessed by SDS-PAGE analysis. The expression yields of HB-fused recombinant proteins were almost comparable with those observed for same target proteins fused to different protein affinity tags such as the glutathione S-transferase (GST) and polyhistidine tags. It was also observed that in few cases the expression yields of target recombinant proteins fused to the HB tag were in fact higher than compared to those achieved using other protein affinity tags. The HB tag has also been found to be conducive to purification of HB-fused recombinant proteins from their urea-denatured state(s). Polyclonal antibodies (HB-Ab) were raised in rabbit against the first 14 amino acids (QKAQKAQAKQAKQAC) of HB to specifically and quantitatively detect HB-tagged target recombinant proteins by Western blotting. Results of Western blot and ELISA revealed that polyclonal HB antibodies can successfully detect low concentrations (5–10 ng) of HB-fused target proteins [26].

1.3 Design of the Clone of the HB-Fused Target Protein(s)

The optimization of the yields of the target proteins is dependent on different steps starting from cloning all the way through to protein purification. A recombinant HB-pET22b™ expression vector was constructed, which can be extended to different types of expression vectors based on the compatibility of distinct expression hosts. The HB tag was cloned in the pET22b vector of the ribosome-binding site between NdeI and BamHI restriction sites. The stop codon is located downstream of the MCS site to terminate protein translation after the target protein sequence. To enable the elimination of the HB tag from the recombinant target protein, all HB-fused target protein-encoding DNA inserts are designed to contain a thrombin cleavage site interspread between the HB tag and the target protein. However, DNA inserts are flexible enough to be encoded for a specific polypeptide in frame with the HB tag using any available restriction site(s) on the vector. For example, factor Xa, enterokinase, and Tobacco Etch Virus (TEV) protease restriction protease sites can be optimally introduced. Because of the absence of methionine, asparagine, or glycine residues in the amino acid sequence of the HB tag, it is feasible to use chemical cleavage, such as cyanogen bromide and hydroxylamine reagents, to separate the HB tag from the target proteins, which lack potential sites that are vulnerable to cleavage by these chemical reagents.

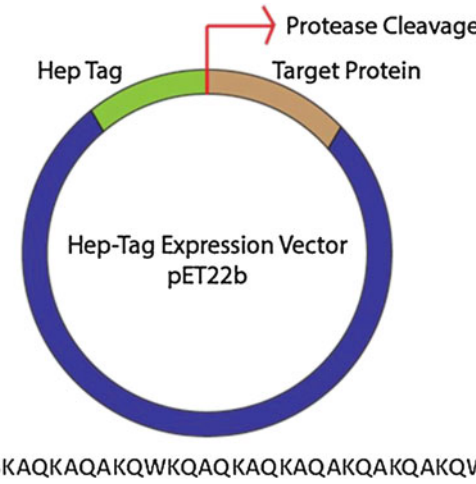

Fig. 1 The design of the pET22b vector containing the HB-tag-fused target protein insert. The arrow represents the location of the protease cleavage site. The single-letter amino acid sequence of the HB tag is shown at the bottom of the figure

1.4 Cloning, Overexpression, and Purification of HB-Fused Recombinant Target Protein (s)

PCR was used to amplify the gene-specific primers, which was later subjected to restriction enzyme digestion, and then followed by directional cloning in the MCS region. DNA sequencing was used to determine the accuracy of the plasmid. The pET-22b-HB plasmids were transferred into BL21(DE3) *E. coli* and the transformed bacterial cells were selected by ampicillin resistance property. Figure 1 shows the vector backbone and the components of HB-recombinant DNA construct. In a small volume of culture, a single isolated colony is grown, and subsequently the cells are induced by the addition of IPTG. Coomassie Brilliant Blue stained SDS-PAGE reveals the purity of expressed HB-fusion protein. HB-fusion protein can also be detected by Western blot using polyclonal antibodies. After successful small-scale expression, large-scale production of the HB-fused target protein(s) can be achieved by overexpression in *E. coli*. Flow chart depicting the steps involved in cloning and in the purification of the target recombinant protein(s) using the HB tag is shown in Figs. 2 and 3, respectively. Optimization of expression levels of the target proteins is critical to render an efficient and cost-effective purification process. Under certain circumstances, it is known that some fusion proteins are toxic to the host cell, which in turn can affect their expression levels [30]. In addition, detection of the target proteins among other contaminating proteins produced by the host is also challenging. This problem is overcome by performing Western blot to specifically detect HB-tagged recombinant proteins. The collected bacterial pellet is disrupted by using French press or ultrasonication. The whole-cell lysate is then centrifuged at high

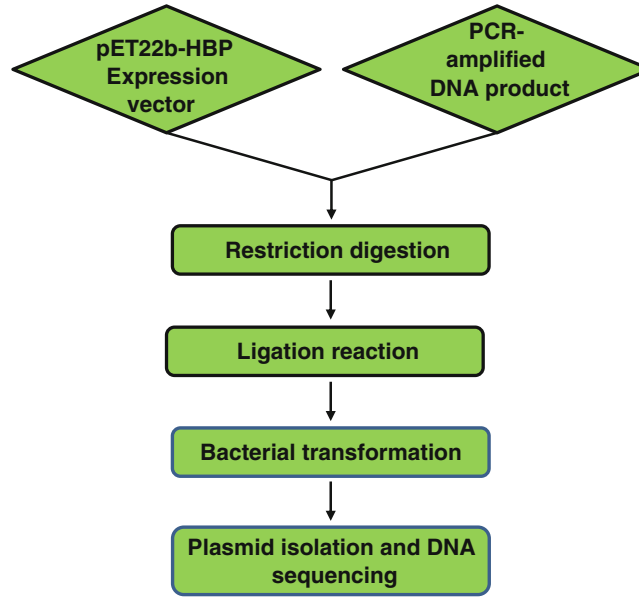

Fig. 2 Flowchart depicting the steps involved in cloning a coding sequence of a target protein of interest into the pET22b-HB expression vector

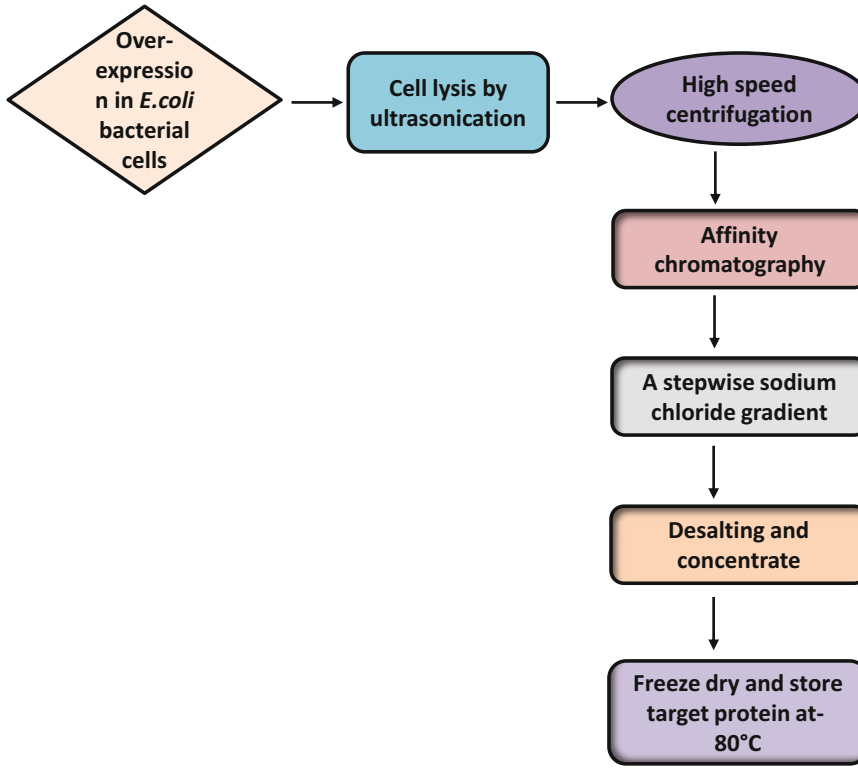

Fig. 3 Flowchart depicting the steps involved in the purification of an HB-fused protein(s)

speeds to obtain clear supernatant. By analyzing the SDS-PAGE, the overexpressed HB-fused target proteins are found in the soluble form.

The supernatant is loaded on a column of heparin-Sepharose and the bound proteins are eluted using a stepwise sodium chloride gradient. The HB-fused target proteins are eluted at NaCl concentrations greater than or equal to 500 mM. For example, HB-fused C2A domain is eluted as a single band in 500 mM NaCl and HB-CAlb3, HB-S100A13 are eluted at 1200 mM concentration of NaCl. In order to equilibrate the target protein(s) to the desired buffer and salt concentration, the fraction(s) containing the HB-fused target protein is subjected to desalting by size-exclusion chromatography and the volume is further concentrated down to 2–3 mL. Subsequently, the HB tag is cleaved from the target protein by selective restriction protease treatment and the protease-cleaved sample is reloaded onto the heparin-Sepharose column to separate the HB tag from target protein. A schematic representation of all the steps (overexpression till the cleavage of the tag) is shown in Fig. 4. The target protein is eluted in the wash buffer. Both the HB tag and thrombin, due to their strong binding affinity to heparin, are subsequently eluted at a higher salt concentration (>500 mM NaCl). The homogeneity of the target protein is verified independently by Coomassie blue and silver staining of the SDS-PAGE gels (Fig. 5). (This figure has been reproduced from

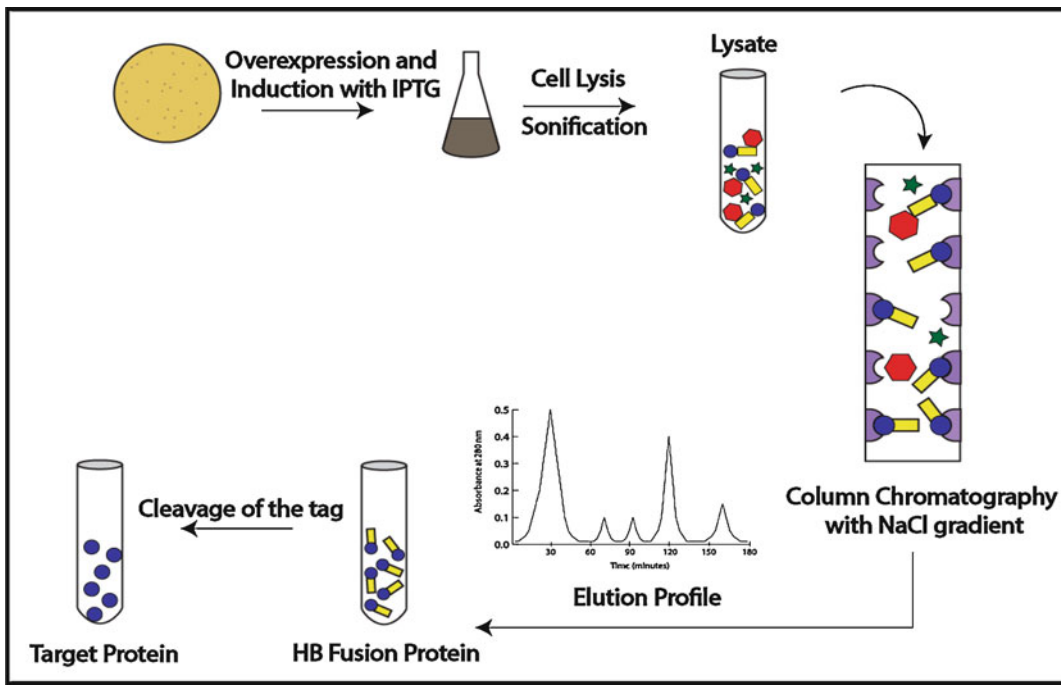

Fig. 4 Schematic representation of the steps involved in the purification of HB tag and the target recombinant proteins on heparin-Sepharose using a stepwise sodium chloride gradient

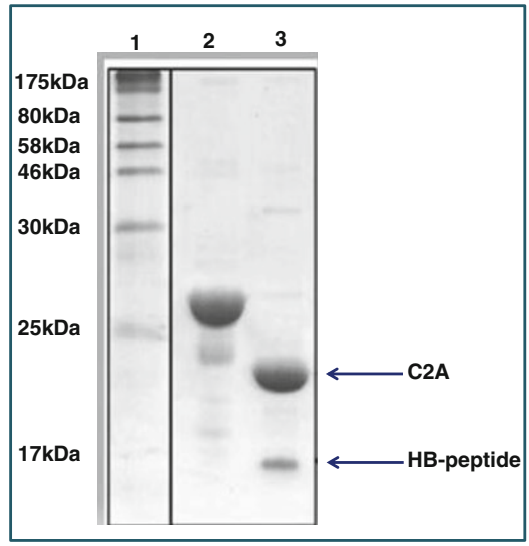

Fig. 5 Purification of HB-fusion proteins using heparin-Sepharose affinity chromatography. Coomassie blue-stained SDS-PAGE of the purified proteins: (Lane 1) represents the protein molecular-weight marker, (Lane 2) represents the band corresponding to HB-fused C2A domain of synaptotagmin, and (Lane 3) represents the thrombin-cleaved target protein (C2A domain of synaptotagmin). (This figure has been reproduced from Morris et al. with permission from Elsevier [11])

Morris et al. with permission from Elsevier [11]). The target protein was later dried and stored at −80 °C.

2 Materials

Prepare all the solutions using ultrapure (deionized) water and analytical-grade reagents. Prepare and store all the reagents at room temperature (except where mentioned).

2.1 Buffers

10 mM sodium phosphate buffer (PB), pH ~ 7.2: 19.2 g of sodium phosphate dibasic heptahydrate, 3.6 g of sodium phosphate monobasic monohydrate.

Lysis buffer: 10 mM sodium phosphate buffer (PB), pH ~ 7.2.

Elution buffer: Equilibration buffer [10 mM sodium phosphate buffer (PB), pH ~ 7.2] with stepwise gradient of NaCl (100 mM to 1.5 M).

Cleavage buffer: Same as equilibration buffer. $CaCl_2$ may be included in the buffer depending upon the conditions used.

Storage buffer: 100 mM NaCl in 10 mM sodium phosphate buffer (PB), pH ~ 7.2.

SDS-PAGE running buffer: 0.025 M Tris–HCl, 0.192 M Glycine, 0.1% SDS, pH: 8.3.

2.2 Media and Cells

LB medium: Dissolve 25 g of LB ready-made powder in 1 L of water. Dispense into flasks, cover with aluminum foil, and autoclave with liquid cycle for 15 min at 121.5 °C at 15-lb pressure.

LB agar plates.

Competent DH5α cells and BL21(DE3).

E. coli BL21-Pro cells containing HB-pET22b™.

2.3 Solutions

Ampicillin: 100 mg of ampicillin in 1 mL of 50% ethanol and store in −20 °C freezer.

Isopropyl-1-thio-B-D-galactopyranoside (IPTG): 238 mg of IPTG in 1 mL of water and store in −20 °C.

Glycerol stock of *E. coli* cells transformed with the HB-pET22b™ expression vector.

SDS–polyacrylamide gel electrophoresis (SDS-PAGE) set up: 30% polyacrylamide (29% acrylamide and 1% *N*,*N*-′-Methylenebisacrylamide), 1.5 M Tris–HCl (pH 6.8 for stacking gel and pH 8.8 for resolving gel), 10% ammonium per sulfate, *N*,*N*,*N*,*N*′-Tetramethyl-ethylenediamine.

Phenyl methyl sulfonyl fluoride (PMSF): 34.8 mg of PMSF in 1 mL of 100% ethanol and store in −20 °C freezer.

Bovine thrombin 1 U/μL.

Heparin-Sepharose™ resin.

2.4 Equipment

2-L Erlenmeyer flasks.

Temperature-controlled shaking incubator.

Mechanical device to disrupt *E. coli* cells (e.g., Ultrasonicator, French press, or cell homogenizer).

UV-Vis spectrophotometer.

Refrigerated centrifuge, and centrifuge bottles (500 mL and 50 mL).

Column with dimensions 1.6 cm × 20 cm can be used to pack heparin-Sepharose with a bed volume of ~15 mL.

UV monitor.

Low-flow peristaltic pump.

Oakridge tubes.

Ultrafiltration centrifugal concentrating devices (Centricon) with appropriate molecular-weight cut-offs.

Water bath.

3 Methods

3.1 Bacterial Overexpression, Purification, and Detection of Recombinant Heparin-Binding Peptide (HB) Fusion Proteins

3.1.1 Transformation of E. coli Cells

1. Take an aliquot (~100 μL) from the competent cell stock stored in a −80 °C freezer. Place the bacterial cells on ice to thaw for about 5 min.
2. Pipette 2 μL of plasmid DNA (HB-pET22b) and add to the thawed competent cells and incubate on ice for 30 min (*see* **Note 1**).
3. Heat shock the competent cells at 42 °C for 45 s. Place the heat-shocked cells on ice for 3 min.
   (a) After the heat-shock treatment, 900 μL of LB broth is added to the cells and kept on shaker at 37 °C for 1 h.
   (b) Spread the cells onto LB agar plates (usually 100 μL of culture). Make sure the plates have the appropriate antibiotic [ampicillin at 100 μg/mL (final concentration)]. Incubate the plate at 37 °C for about 14–16 h (overnight). Longer times of incubations will allow the satellite colonies to appear (*see* **Note 10**).

3.1.2 Overexpression of HB-Fused Target Protein

Preparation of Starter Culture

1. Prepare 50–100 mL of LB broth and sterilize the flask containing medium by autoclaving. Subsequently, add ampicillin [final concentration (100 μg/mL)] to the LB broth.
2. Pick a single colony from overnight LB agar plates using a sterile inoculation loop, a sterile pipette tip or a toothpick and, add to the LB broth containing ampicillin (*see* **Note 10**).
3. Incubate the bacterial culture in a shaker (250 rpm) overnight (12–15 h) at 37 °C.

Preparation of Large-Scale Bacterial Culture for Protein Overexpression

It is advisable to check the expression of the HB-fused target protein on a small scale (50-mL culture) to ensure that there is overexpression of the target protein.

1. Prepare 500-mL fresh, sterile LB broth in a 2-L Erlenmeyer flask, add 25 mL (5%) of the starter culture along with appropriate amounts of ampicillin.
2. Grow the cells under the same growth conditions of 37 °C and 250 rpm until the optical density at 600 nm reaches ~0.4 to 0.6 (*see* **Note 2**). Dispense 1 mL of bacterial cells from the flask, as a preinduction sample, for SDS-PAGE analysis.
3. Induce the culture to overexpress the HB-fused target protein by addition of 500 μL of 1 M IPTG stock solution to achieve a final concentration of 1 mM. Place the culture on the shaker at 37 °C (*see* **Note 2**).
4. Induction of HB-fused target protein usually takes 3–5 h. After induction, dispense 1 mL of bacterial cells from the flask, as a postinduction sample, for subsequent SDS-PAGE analysis. The

resulting gel should be expected to show a prominent band corresponding to the molecular size of the HB-fused target protein (*see* **Note 7**). Centrifuge the remaining bacterial cell culture in 500-mL centrifuge bottles at 6000 rpm (10,620 × *g*) for 25 min at 4 °C. Later carefully discard the supernatant without disturbing the bacterial cell pellet.

5. Transfer resuspended cells (cells suspended in 50 mL of freshly prepared 10 mM sodium phosphate buffer (PB), pH ~ 7.2) to a fresh falcon tube (50 mL) and again centrifuge at 6000 rpm (10,620 × *g*) for 15 min at 4 °C.
6. Discard the clear supernatant. Freeze the cell pellet at −80 °C for future use. When required, it can be thawed at room temperature and then placed on ice.

3.1.3 Column Packing

1. Efficient column packing is crucial for protein separation, especially when using gradient elution. A poorly packed column causes uneven flow, band broadening, and loss of resolution. Take 15 mL of a 50% slurry of heparin-Sepharose in 20% ethanol and degas (*see* **Note 5**).
2. Pour the degassed slurry into a column (1.6 cm × 20 cm) along the walls using a glass rod as a guide to avoid the formation of air pockets/bubbles.
3. Allow the heparin-Sepharose resin beads to settle by gravity flow for efficient packing. Wash the beads with equilibration buffer (starting buffer of purification, in most cases this buffer will be the same for cell lysis and for the first wash step) with a constant flow rate of 1–2 mL/min for at least 5 column volumes (CV) of buffer (*see* **Note 6**).

3.1.4 Bacterial Cell Lysis

1. Dispense the cell pellet from the freezer, add 30 mL of lysis buffer. Let it thaw for 20 min at room temperature and, subsequently, suspend the cell pellet until the suspension becomes turbid. Place the cell suspension on an ice bath.
2. Lyse the resuspended cells by ultrasonication (amplitude# 15 W output) with an alternate cycle of 10 s of ON and OFF (*see* **Note 4**).
3. To achieve higher efficiency of cell lysis, pass post-sonicated sample through a French press and spurge at 30,000 psi for 3 cycles.

3.1.5 Purification of the HB-Tag Fusion Protein Using Heparin-Sepharose Affinity Chromatography

1. Centrifuge the disrupted cell suspension for 30 min at 19,000 rpm (45,980 × *g*) at 4 °C. Filtering through 0.45-mm polyethersulfone membrane will help to remove residual particulates before loading onto the column.
2. Dispense a small aliquot of supernatant for SDS-PAGE analysis.

3. Apply the supernatant onto a column of heparin-Sepharose resin pre-equilibrated in 10 mM sodium phosphate buffer (pH ~ 7.2) at a constant flow rate of 1–2 mL/min. Wash the column with this buffer until a stable baseline is reached and then elute the bound fusion protein buffer followed with a stepwise gradient of sodium chloride to eliminate the bacterial contaminants (*see* **Note 6**). Pure HB-fusion protein typically elutes at 500 mM NaCl (in case of HB-C2A). But if the fusion partner has high density of positive charges, it might bind to heparin-Sepharose column more tightly and will be eluted at higher concentrations of sodium chloride. For example, we have observed that HB-fused C-Alb3, a positively charged protein (pI ~ 9.3), only eluted at 1200 mM NaCl concentration (*see* **Note 3**). Identify the fractions containing the HB-fused protein by SDS-PAGE.
4. Collect the fractions containing fusion protein(s), desalt and concentrate the sample with the storage buffer using Centricon (by centrifugation at 4500 rpm (7965 × *g*) for 10 min/cycle at 4 °C) with appropriate molecular-weight cut-off filter(s) (*see* **Note 6**). Repeat this process thrice.
5. Prepare 0.5-mL aliquots and flash-freeze with liquid nitrogen and store indefinitely at −80 °C.

3.2 Cleavage of HB Fusion Tag from the Target Protein

3.2.1 OFF-Column Cleavage

1. Perform the cleavage reaction outside the column in 10 mM sodium phosphate buffer (PB) at pH ~ 7.2 (OFF-column). Add restriction protease, thrombin, to the HB-fused target protein solution at a ratio of 1 U of thrombin to 250 μg of HB-fused target protein (*see* **Note 8**). Incubate the mixture at 37 °C for 2 h or at room temperature for 16 h with continuous mixing on a rotator.
2. Restrict the cleavage reaction by adding 1:1000 dilution of 0.2 M PMSF from the stock.
3. Reload the thrombin cleavage products onto heparin-Sepharose column under the same conditions and incubate the thrombin digestion products for 30 min. This step serves to adsorb the protein of interest, the HB-tag moiety, and any residual uncleaved fusion protein to the heparin-Sepharose column.
4. Wash the column with 10 mM sodium phosphate buffer (PB) containing 100 mM NaCl, pH ~ 7.2.
5. Collect the unbound (flow-through) fractions from the heparin-Sepharose column, which should contain the target protein free of the HB tag. Check the purity of the target protein by SDS-PAGE.

6. Subject the purified protein product(s) to desalting and concentration in storage buffer using ultrafiltration concentrator (s) of appropriate molecular-weight cut-off filter(s).

3.2.2 ON-Column Cleavage

1. Follow steps involved in Subheadings 3.1.1–3.1.5 (**steps 1–3**).
2. Reduce the contaminants from bacterial proteins by washing with less than 400 mM NaCl gradient.
3. Wash the column carefully with cleavage buffer containing restriction protease, thrombin.
4. To perform ON-column cleavage, add thrombin in larger amounts at a ratio of 1 U/125 μg of HB-fusion protein to get a higher cleavage efficiency in a shorter time interval (*see* **Note 8**).
5. Seal the top and bottom air tight with stop corks and mix the resin by placing on a rotator.
6. After incubation, elute the cleaved protein by passing 2 column volumes of 10 mM sodium phosphate buffer (PB) containing 100 mM NaCl, pH ~ 7.2.

3.3 Purification of HB-Fused Target Proteins Under Denaturing Conditions

1. Follow the steps from Subheadings 3.1.3, 3.1.4 and **step 1** from Subheading 3.1.5.
2. After centrifugation, the insoluble pellet is dissolved in the 10 mM sodium phosphate buffer (PB, pH ~ 7.2) containing 8 M urea with brief sonication for 5–10 min (*see* **Note 9**). The supernatant and the pellet fractions are analyzed by SDS-PAGE to monitor the expression of the target protein.
3. Spin down at 10,000 × *g* for 5 min and discard the supernatant. Repeat the same procedure once again. Centrifuge the urea-solubilized pellet at 19,000 rpm (45,980 × *g*) for 30 min at 4 °C. Carefully transfer the clear solution into a fresh falcon tube.
4. Check the supernatant for the HB-fused target protein by SDS-PAGE.
5. The supernatant-containing protein loaded onto a pre-equilibrated heparin-Sepharose column at a constant flow rate of 1–2 mL/min.
6. Wash the column with 10 mM sodium phosphate buffer (PB, pH ~ 7.2) containing 8 M urea until a stable baseline is reached and then elute the bound fusion protein (HB tag) with buffer followed by a stepwise gradient of NaCl to remove the bacterial contaminants. Pure HB fusion protein that elutes at 500 mM NaCl (in case of HB-C2A) is usually in the native well-folded conformation. Some HB-fused target proteins purified under denaturation conditions may elute at higher concentrations of NaCl. For example, HB-S100A13, a calcium-binding protein, elutes at slightly different NaCl concentrations when purified

under native and denatured conditions. Under native conditions of elution, HB-S100A13 was found to elute at 1200 mM NaCl concentration, but it elutes at 1000 mM NaCl under denaturing conditions. Monitor the presence of target protein in different fractions by performing SDS-PAGE.

7. Pool the fractions containing the HB-fused target protein. Subsequently, desalt and concentrate the sample using a centricon of appropriate molecular-weight cut-off (that is suitable for the molecular size of the fusion protein) by centrifugation at 4500 rpm ($7965 \times g$) for 10 min at 4 °C.
8. Prepare 0.5-mL aliquots and flash-freeze with liquid nitrogen and store at −80 °C indefinitely (*see* **Note 10**).

4 Notes

1. The choice of the expression host(s) is one of the most important parameters to be considered during cloning. Prokaryotes are preferred over eukaryotes for producing recombinant proteins because of their ease of handling, cost-effectiveness, and high doubling time.
2. The major parameters that affect the expression yields are growth temperature, aeration speed of the shaker, the generation time of bacteria (which can be evaluated by monitoring the bacterial growth curve). The time at which expression is induced and the concentration of the inducer (IPTG) are other important parameters that need careful consideration.
3. The binding affinity of the recombinant protein fused with HB to the heparin depends on the net charge of the recombinant protein, which in turn might vary with the change in the pH of the buffer. Therefore, the pI of the recombinant protein and the pH of the elution buffer are critical parameters to be considered for the purification of recombinant proteins using the HB tag. For example, a highly basic target protein ($pI > 7.0$) can increase the binding affinity of the recombinant protein to the heparin-Sepharose matrix. Therefore, it is strongly recommended that purification of HB-fused target proteins should be attempted on a smaller scale to optimize the elution under salt gradient conditions. Typically, it is advisable to incubate the heparin-Sepharose column with the clear cell lysate obtained after the centrifugation for at least 1 h at 4 °C to facilitate strong binding interaction. Such optimization of conditions is critical to achieve higher yields of the pure target proteins.
4. It is recommended that HB-fused target protein purification is performed at lower temperatures at 4 °C to slow down the rate of proteolysis and maintain the structural integrity of the target

protein. Alternatively, purification of HB-fused target proteins can be achieved at room temperature conditions with the addition of a cocktail of protease inhibitors to the lysis buffer to prevent protein degradation.

5. The efficiency of heparin-Sepharose matrix depends on proper maintenance and storage of the column. The most suitable solvent to store the column is in 20% ethanol with 1 mM sodium azide at 4 °C.
6. During the purification and desalting, the pH and concentration of salts in the buffer, and the temperature are extremely important factors. Minor change(s) in any of these factors can potentially increase the risk of aggregation of target recombinant protein(s) on the column.
7. Under certain circumstances, recombinant proteins might be expressed in very low amounts and therefore cannot be detected easily by regular Coomassie blue staining. In those cases, perform a western blot using polyclonal antibodies raised against HB tag for specific detection of HB-fusion proteins even at low concentrations (5–10 ng/mL) (*see* Fig. 6). (This figure has been reproduced from Morris et al. with permission from Elsevier [11]).
8. The affinity tag can be removed using two different methods: chemical method and enzymatic method. In a few specific cases, the affinity tag can be removed by harsh chemical

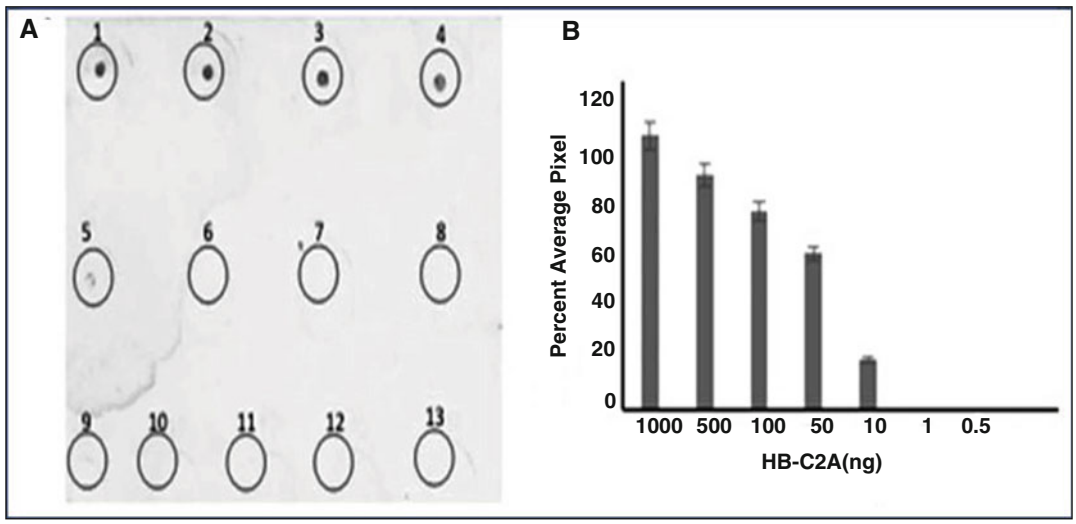

Fig. 6 (Panel A) Detection of HB-fused protein by dot blot analysis using polyclonal antibodies. The dot blots are labeled as circles 1–8. 1 μg (circle 1); 500 ng (circle 2); 100 ng (circle 3); 50 ng (circle 4); 10 ng (circle 5); 5 ng (circle 6); 1 ng (circle 7); 0.5 ng (circle 8); Circles 9–13 represent BSA: 1 μg (circle 9); 500 ng (circle 10); 100 ng (circle 11); 50 ng (circle 12); 10 ng (circle 13). (Panel B) Bar graph representing the densitometric scan of the dot blot by plotting concentration of HB-C2A on *x*-axis and percent average pixel on *y*-axis. (This figure has been reproduced from Morris et al. with permission from Elsevier [11])

treatment, such as cyanogen bromide or hydroxylamine. The harsher conditions used in the chemical-induced cleavage can potentially result in irreversible modification of the amino acids in the target proteins, which consequently cause denaturation of the overexpressed target protein. Therefore, chemical-induced cleavage of HB-fused target proteins is not a method of choice. Enzymatic methods are preferred over chemical methods due to the specificity and the milder conditions used in enzyme-induced cleavage. In this context, a plethora of restriction enzymes, such as thrombin, factor Xa, enterokinase, and aspartate protease, are available for the specific cleavage and separation of the HB tag from the target protein(s).

9. One major advantage of the HB tag is that the HB-fused target proteins can also be purified under denaturing conditions in the presence of 8 M urea. Circular dichroism spectroscopy analysis showed that the HB tag, in 10 mM sodium phosphate buffer (pH ~ 7.2) containing 100 mM sodium chloride, is a random coil. In addition, the HB tag binds strongly to heparin in the unfolded state(s). The presence of the denaturant, 8 M urea, does not affect the binding affinity of the HB-fused target protein to heparin-Sepharose. However, it is recommended that prior to purifying HB-fused target protein under denaturing conditions, care should be taken to ensure that the target protein exhibits reversible denaturant-induced unfolding. Figure 7 shows SDS-PAGE analysis of the purified protein

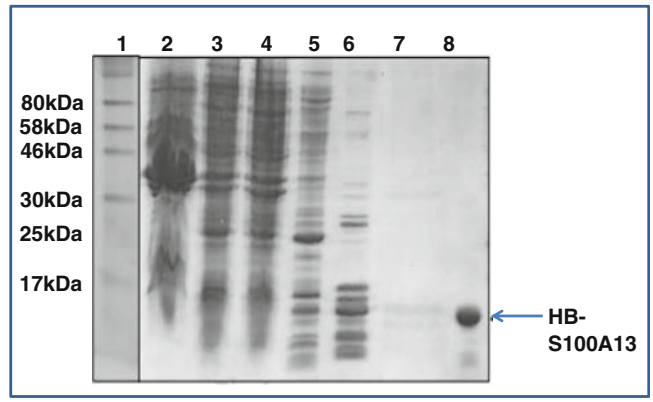

Fig. 7 Coomassie Blue stained SDS-PAGE of HB-S100A13 under denaturation conditions using 8 M urea. (Lane 1) shows protein molecular-weight marker; (Lane 2) shows insoluble fractions and (Lane 3) represents soluble fractions obtained from a 1-L culture; (Lane 4) shows 0 mM NaCl fraction; (Lane 5) shows 100 mM NaCl fraction; (Lane 6) shows 350 mM NaCl fraction; (Lane 7) shows 500 mM NaCl fraction; and (Lane 8) shows the 1000 mM NaCl fraction. 8 M urea was removed by a step dialysis to obtain the protein in a refolded form. (This figure has been reproduced from Morris et al. with permission from Elsevier [11])

Table 1
Depiction of time involved in the different steps involved in the transformation, overexpression, and purification of HB-fused target protein

Subprocess	Approximate time required
Bacterial transformation	2 h
Growth of transformants on plate	12–14 h
Colony pick up and growth of starter culture	14–16 h
Large-scale expression, induction, and harvesting	8 h
Sonication, centrifugation, and protein purification	8 h
Buffer exchange/desalting of the desired protein	1.5 h
Freeze drying	2 h

(HB-S100A13) under denaturing conditions using 8 M urea. (This figure has been reproduced from Morris et al. with permission from Elsevier [11]). In contrast, we found that HB-fused target proteins fail to show binding to heparin-Sepharose when guanidine hydrochloride is included in the elution buffer. Guanidine hydrochloride is an ionic denaturant that can potentially interfere with the electrostatic interaction (s) that occurs between the HB tag and the heparin-Sepharose resin.

10. Time Considerations: In general, the procedure from transformation to the final purification of the HB-fusion protein takes around 20 h. The entire process is broken into the following table (*see* Table 1).

References

1. Ferrer-Miralles N, Corchero J, Kumar P, Cedano J, Gupta K, Villaverde A, Vazquez E (2011) Biological activities of histidine-rich peptides; merging biotechnology and nanomedicine. Microb Cell Factories 10:1–5
2. Andersen DC, Krummen L (2002) Recombinant protein expression for therapeutic applications. Curr Opin Biotechnol 13:117–123
3. De Meyer T, Muyldermans S, Depicker A (2014) Nanobody-based products as research and diagnostic tools. Trends Biotechnol 32:263–270
4. Lesley SA (2001) High-throughput proteomics: protein expression and purification in the postgenomic world. Protein Expr Purif 22:159–164
5. Terpe K (2006) Overview of bacterial expression systems for heterologous protein production: from molecular and biochemical fundamentals to commercial systems. Appl Microbiol Biotechnol 72:211–222
6. Arnau J, Lauritzen C, Petersen G, Pedersen J (2006) Current strategies for the use of affinitytags and tag removal for the purification of recombinant proteins. Protein Expr Purif 48:1–13
7. Park N, Ryu J, Jang S, Lee H (2012) Metal ion affinity purification of proteins by genetically incorporating metal-chelating amino acids. Tetrahedron 68:4649–4654
8. Hunt I (2005) From gene to protein: a review of new and enabling technologies for multiparallel protein expression. Protein Expr Purif 40:1–22
9. Terpe K (2003) Overview of tag protein fusions: from molecular and biochemical fundamentals to commercial systems. Appl Microbiol Biotechnol 60:523–533

10. Martinez-Ceron M, Targovnik A, Urtasun N, Cascone O, Miranda M, Camperi S (2012) Recombinant protein purification using complementary peptides as affinity tags. New Biotechnol 29:206–210
11. Morris J, Jayanthi S, Langston R, Daily A, Kight A, McNabb DS, Kumar TKS (2016) Heparin-binding peptide as a novel affinity tag for purification of recombinant proteins. Protein Expr Purif 126:93–103
12. Gandhi NS, Mancera RL (2008) The structure of glycosaminoglycans and their interactions with proteins. Chem Biol Drug Des 72:455–482
13. Xu X, Dai Y (2010) Heparin: an intervenor in cell communication. J Cell Mol Med 14:175–180
14. Olczyk P, Mencner L, Komosinska-Vassev K (2015) Diverse roles of heparan sulfate and heparin in wound repair. Biomed Res Int 2015:1–7
15. Davis JE, Gundampati RK, Jayanthi S, Anderson J, Pickhardt A, Koppolu BP, Zaharoff DA, Kumar TKS (2018) Effect of extension of the heparin binding pocket on the structure, stability, and cell proliferation activity of the human acidic fibroblast growth factor. Biochem Biophys Rep 13:45–57
16. Pomin VH (2014) Heparin-binding proteins (chemokines and Defensins) and their complexes with glycosaminoglycans from the solution NMR perspective. Curr Protein Pept Sci 15:738–744
17. Tang NH, Chen YL, Wang XQ, Li XJ, Wu Y, Zou QL, Chen YZ (2010) N-terminal and C-terminal heparin-binding domain polypeptides derived from fibronectin reduce adhesion and invasion of liver cancer cells. BMC Cancer 10:552–564
18. Atha DH, Lormeau JC, Petitou M, Rosenberg RD, Choay J (1985) Contribution of monosaccharide residues in heparin binding to Antithrombin III. Biochemist 24:6723–6729
19. Kouzi-Koliakos K, Koliakos GG, Tsilibary EC, FurchtS LT, Charonis AS (1989) Mapping of three major heparin-binding sites on Laminin and identification of a novel heparin-binding site on the B1 chain. J Biol Chem 264:17971–17978
20. Carter WJ, Cama E, Huntington JA (2005) Crystal structure of thrombin bound to heparin. J Biol Chem 280:2745–2749
21. Tan K, Duquette M, Liu J, Zhang R, Joachimiak A, Wang J, Lawler J (2006) The structures of the thrombospondin-1 N-terminal domain and its complex with a synthetic pentameric heparin. Structure 14:33–42
22. Margalit H, Fischer N, Ben-Sasson S (1993) Comparative analysis of structurally defined heparin binding sequences reveals a distinct spatial distribution of basic residues. J Biol Chem 268:19228–19231
23. Weiler J, Linhardt R, Fromm PJ, Hileman R, Caldwell E (1997) Spacing of basic amino acids in heparin binding sites. Arch Biochem Biophys 343:92–100
24. Marty NJ, Rajalingam D, Kight AD, Lewis NE, Fologea D, Kumar TKS, Goforth RL (2009) The membrane-binding motif of the chloroplast signal recognition particle receptor (cpFtsY) regulates GTPase activity. J Biol Chem 284:14891–14903
25. Rajalingam D, Kumar TKS, Yu C (2005) The C2A domain of synaptotagmin exhibits a high binding affinity for copper: implications in the formation of the multiprotein FGF release complex. Biochemist 44:14431–14442
26. Sivaraja V, Kumar TKS, Rajalingam D, Graziani I, Prudovsky I, Yu C (2006) Copper binding affinity of S100A13, a key component of the FGF-1 nonclassical copper-dependent release complex. Biophys J 91:1832–1843
27. Jayanthi S, Gundampati RK, Kumar TKS (2017) Simple and efficient purification of recombinant proteins using the heparin-binding affinity tag. Curr Protoc Protein Sci 90:6–13
28. Cardin AD, Weintraub HJ (1989) Molecular modeling of protein-glycosaminoglycan interactions. Arterioscler Thromb Vasc Biol 9:21–32
29. Dempewolf C, Morris J, Chopra M, Jayanthi S, Kumar TKS, Li WN (2013) Identification of consensus glycosaminoglycan binding strings in proteins. Proceedings of the 4th international conference on Information Science & Applications, ISBN#—978-1-4799-0603-1/13/$31, pp 311–314
30. Rosano GL, Ceccarelli EA (2014) Recombinant protein expression in *Escherichia coli*: advances and challenges. Front Microbiol 5:172–188

Chapter 22

Expression and Purification of Recombinant Proteins in *Escherichia coli* Tagged with the Metal-Binding Proteins SmbP and CusF3H+

Jessica J. Gomez-Lugo, Bryan D. Santos, David A. Perez-Perez, Jorge M. Montfort-Gardeazabal, Megan M. McEvoy, and Xristo Zarate

Abstract

The bacterium *Escherichia coli* is still considered the first option as a microbial cell factory for recombinant protein production, and affinity chromatography is by far the preferred technique for initial purification after protein expression and cell lysis. In this chapter, we describe the methodology to express and purify recombinant proteins in *E. coli* tagged with the first two metal-binding proteins proposed as fusion partners. They are the small metal-binding protein SmbP and a mutant of the copper resistance protein CusF3H+. There are several advantages of using them as protein tags: they prevent the formation of inclusion bodies by increasing solubility of the target proteins, they enable purification by immobilized metal-affinity chromatography using Ni(II) ions with high purity, and because of their low molecular weights, excellent final yields are obtained for the target proteins after cleavage and removal of the protein tag. Here we also describe the protocol for the production of proteins in the periplasm of *E. coli* tagged with two SmbP variants that include the PelB or the TorA signal sequences for transport via the Sec or the Tat pathway, respectively. Based on these methods, we consider CusF3H+ and SmbP excellent alternatives as fusion proteins for the production of recombinant proteins in *E. coli*.

Key words SmbP, CusF3H+, *Escherichia coli*, Protein expression and purification, Metal-affinity chromatography, IMAC, Fusion protein, Affinity tag, Solubility tag

1 Introduction

Escherichia coli remains the first choice as a host microorganism for the expression of recombinant proteins; the use of strong, inducible promoters allows simple and rapid production, and considerable quantities of protein can be obtained using large-scale fermentation processes. Nevertheless, *E. coli* has its disadvantages, for example, sometimes the proteins do not fold correctly forming insoluble inclusion bodies and it lacks the capacity to perform some post-translational modifications [1].

Nikolaos E. Labrou (ed.), *Protein Downstream Processing: Design, Development, and Application of High and Low-Resolution Methods*, Methods in Molecular Biology, vol. 2178, https://doi.org/10.1007/978-1-0716-0775-6_22,

Fusion proteins have played a crucial role in recombinant protein expression and purification in *E. coli*. They work as solubility tags to decrease the formation of inclusion bodies or as affinity tags for protein purification using affinity chromatography [2]. Some fusion proteins show both features, for example, maltose-binding protein (MBP) and glutathione S-transferase (GST) [3, 4]. The most common affinity tag is the His-tag, six histidine residues included at either the N- or C-terminus of the target protein. This small modification enables the purification of proteins by means of immobilized metal-affinity chromatography (IMAC). There are numerous advantages to IMAC over other types of chromatography for protein purification, including low cost and great accessibility, and very often a high degree of protein purity can be obtained from this single chromatographic step. Several companies carry many different IMAC products like Ni(II) charged resins, magnetic beads, and ready-to-use prepacked columns for automated protein purification systems.

Recently, we have described two metal-binding proteins to be used as fusion partners to increase solubility and improve the purification of recombinant proteins in *E. coli*. The first is SmbP, a protein isolated from the periplasm of the Gram-negative bacterium *Nitrosomonas europaea* [5]. It is characterized by a series of 10 repeats of a seven amino acid motif and it contains an unusually high number of histidine residues; it binds different divalent metal ions like Cu, Ni, and Zn and it functions as a metal scavenger to protect the cell from high concentrations of metals, especially copper [6]. The second is CusF3H+, an enhanced version of the *E. coli* periplasmic protein CusF [7], which is part of the CusCFBA system that expels toxic Ag(I) and Cu(I) ions from the cell. By modifying its N-terminus to add three histidine residues, CusF3H+ binds Ni(II) ions during IMAC protein purification, yielding higher purity compared to the wild-type CusF, which binds only copper [8]. A crucial feature of both proteins is their low molecular mass, just 10 kDa, which allows high yields for the target protein after cleavage and removal of the metal-binding protein.

These two proteins are naturally found in the cell periplasm. They contain a signal sequence, sometimes referred to as signal peptide, at their N-termini for transport to the periplasmic space through the Sec pathway [6, 9]. Therefore, we usually work with constructs that lack the signal sequence for the expression of CusF3H+ or SmbP-tagged proteins in the cytoplasm of *E. coli*. Nevertheless, since periplasmic expression is crucial for proteins that contain disulfide bonds, it is sometimes preferred to have the signal peptide intact to ensure transport to the periplasm where proper folding can occur. We have effectively been able to express target proteins in the periplasm of *E. coli* using constructs that contain the full sequence of both fusion proteins. Nevertheless, for SmbP, we noticed very low periplasmic expression; therefore,

we exchanged its natural signal peptide with the signal peptides from CusF and the protein pectate lyase from *Erwinia carotovora* (PelB). These new SmbP constructs for periplasmic expression, CusF-SmbP and PelB-SmbP, made a considerable difference, increasing expression in the periplasm more than a 100-fold, especially PelB-SmbP [10]. Finally, one more version of SmbP was designed for high-level periplasmic protein expression: TorA-SmbP. This construct contains the signal sequence from the protein trimethylamine-N-oxide reductase, and it directs the transport of recombinant proteins to the cell periplasm via the twin-arginine (Tat) pathway, which works differently than the Sec in that it exports proteins to the periplasm after they have been folded in the cytoplasm [10]. This can be advantageous for target proteins that contain cofactors or can be misfolded in the periplasm.

Here, we describe a full protocol for the expression and purification of recombinant proteins in *E. coli* tagged with SmbP or CusF3H+. First, we describe how to create the DNA constructs necessary for cytoplasmic (Fig. 1) or periplasmic expression (Fig. 2); then a full description follows on how to transform *E. coli,* induce protein expression, and recover the cells. We include two lysis methods: whole-cell lysis using glass beads and a bead beater for cytoplasmic proteins; and a lysozyme/osmotic shock procedure to extract only the proteins from the cell periplasm. Finally, we describe the methods for protein purification using IMAC, cleavage with enterokinase, and tag removal to obtain pure target protein.

Fig. 1 Graphic representation of cytoplasmic constructs of CusF3H+ and SmbP

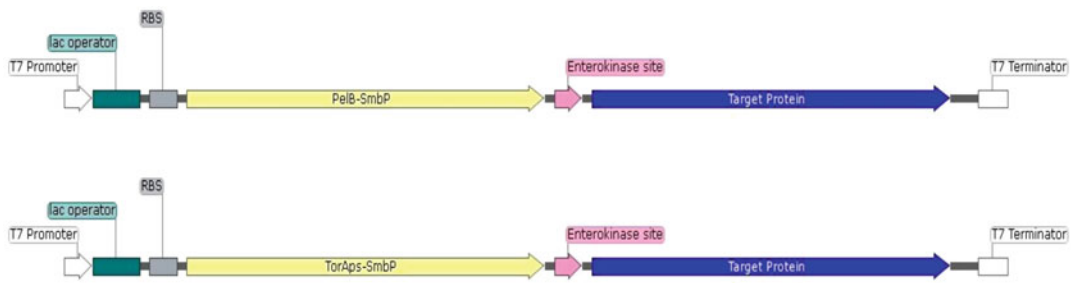

Fig. 2 Graphic representation of periplasmic constructs of PelB-SmbP and TorA-SmbP

2 Materials

Prepare all solutions with ultrapure water and analytical-grade reagents. All components and materials described here to produce recombinant DNA are readily available; different brands for the DNA polymerase and T4 DNA ligase can be used to achieve the final constructs.

2.1 Components for DNA Constructs

1. *Vent* DNA polymerase (New England Biolabs, Ipswich, MA) with its 10× reaction buffer. Store at −20 °C.
2. 10-mM dNTPs Mix. Store at −20 °C.
3. pET30a(+) vector (EMD Millipore, Burlington, MA) with the cloned fusion protein (CusF3H+, SmbP, PelB-SmbP, or TorA-SmbP) between the NdeI and KpnI restriction sites (*see* Table 1 for CusF3H+ sequence, used for cytoplasmic expression; *see* Table 2 for SmbP sequence, used for cytoplasmic expression; *see* Table 3 for PelB-SmbP sequence, used for periplasmic expression and transport via the Sec pathway; *see* Table 4 for the TorA-SmbP sequence, used for periplasmic expression and transport via the Tat pathway). Store at −20 °C.
4. Primers for the target gene. The forward primer should contain an NcoI restriction site and the reverse primer a XhoI site, both at the 5′ end. Store at −20 °C (*see* **Note 1**).
5. Thermal cycler.
6. QIAquick Gel Extraction Kit (Qiagen, Hilden, Germany).

Table 1
Encoding gene and amino acid sequence for CusF3H+

ATG	CAC	CAC	CAC	CAT	CAT	CAT	GAA	ACC	ATG	AGC	GAA	GCA	CAA	CCA	
M	H	H	H	H	H	H	E	T	M	S	E	A	Q	P	15
CAG	GTT	ATT	AGC	GCC	ACT	GGC	GTG	GTA	AAG	GGT	ATC	GAT	CTG	GAA	
Q	V	I	S	A	T	G	V	V	K	G	I	D	L	E	30
AGC	AAA	AAA	ATC	ACC	ATC	CAT	CAC	GAT	CCG	ATT	GCT	GCC	GTG	AAC	
S	K	K	I	T	I	H	H	D	P	I	A	A	V	N	45
TGG	CCG	GAG	ATG	ACC	ATG	CGC	TTT	ACC	ATC	ACC	CCG	CAG	ACG	AAA	
W	P	E	M	T	M	R	F	T	I	T	P	Q	T	K	60
ATG	AGT	GAA	ATT	AAA	ACC	GGC	GAC	AAA	GTG	GCG	TTT	AAT	TTT	GTC	
M	S	E	I	K	T	G	D	K	V	A	F	N	F	V	75
CAG	CAG	GGC	AAC	CTT	TCT	TTA	TTA	CAG	GAT	ATT	AAA	GTC	AGC	CAG	
Q	Q	G	N	L	S	L	L	Q	D	I	K	V	S	Q	90

Table 2
Encoding gene and amino acid sequence for SmbP constructs

ATG	AGC	GGC	CAC	ACC	GCG	CAC	GTG	GAC	GAG	GCG	GTT	AAG	CAC	GCG	
M	S	G	H	T	A	H	V	D	E	A	V	K	H	A	15
GAG	GAA	GCG	GTT	GCG	CAC	GGT	AAA	GAA	GGC	CAC	ACC	GAT	CAG	CTG	
E	E	A	V	A	H	G	K	E	G	H	T	D	Q	L	30
CTG	GAG	CAC	GCG	AAG	GAA	AGC	CTG	ACC	CAT	GCG	AAA	GCG	GCG	AGC	
L	E	H	A	K	E	S	L	T	H	A	K	A	A	S	45
GAA	GCG	GGT	GGC	AAC	ACC	CAT	GTG	GGT	CAC	GGC	ATC	AAG	CAC	CTG	
E	A	G	G	N	T	H	V	G	H	G	I	K	H	L	60
GAA	GAT	GCG	ATT	AAA	CAC	GGC	GAG	GAA	GGC	CAC	GTG	GGT	GTT	GCG	
E	D	A	I	K	H	G	E	E	G	H	V	G	V	A	75
ACC	AAG	CAC	GCG	CAA	GAG	GCG	ATC	GAA	CAC	CTG	CGT	GCG	AGC	GAG	
T	K	H	A	Q	E	A	I	E	H	L	R	A	S	E	90
CAC	AAA	AGC	CAC												
H	K	S	H												94

7. Restriction enzymes NcoI and XhoI with their 10× reaction buffer. Store at −20 °C.
8. T4 DNA ligase and its 10X buffer. Store at −20 °C.

2.2 Components for DNA Transformation and Screening

1. LB broth: Weigh 10 g of tryptone, 5 g of yeast extract, and 10 g of NaCl. Dissolve in 1 L of water; adjust the pH to 7.0 with 1 M NaOH. Sterilize in autoclave, 121 °C for 15 min. Store at 4 °C to avoid contamination.
2. Competent DH5α *Escherichia coli* cells (New England Biolabs, Ipswich, MA).
3. Water bath at 42 °C.
4. Orbital shaker incubator.
5. Plasmid mini-prep kit.

2.3 Components for Small-Scale Protein Expression

1. Competent *Escherichia coli* strain BL21(DE3) (New England Biolabs, Ipswich, MA) for protein expression in either the cytoplasm or periplasm. Store at −80 °C (*see* **Note 2**).
2. LB broth.
3. Kanamycin 1000× (30 mg/mL) solution: Weigh 0.3 g of kanamycin sulfate and dissolve it in 10 mL of water. Filter through a 0.22-μm membrane. Store in aliquots at −20 °C.
4. Orbital shaker incubator.

Table 3
Encoding gene and amino acid sequence for PelB-SmbP

ATG	AAA	TAC	CTG	CTG	CCG	ACC	GCT	GCT	GCT	GGT	CTG	CTG	CTG	CTG	
M	**K**	**Y**	**L**	**L**	**P**	**T**	**A**	**A**	**A**	**G**	**L**	**L**	**L**	**L**	15
GCT	GCT	CAG	CCG	GCT	ATG	GCT	AGC	GGC	CAC	ACC	GCG	CAC	GTG	GAC	
A	**A**	**Q**	**P**	**A**	**M**	**A**	S	G	H	T	A	H	V	D	30
GAG	GCG	GTT	AAG	CAC	GCG	GAG	GAA	GCG	GTT	GCG	CAC	GGT	AAA	GAA	
E	A	V	K	H	A	E	E	A	V	A	H	G	K	E	45
GGC	CAC	ACC	GAT	CAG	CTG	CTG	GAG	CAC	GCG	AAG	GAA	AGC	CTG	ACC	
G	H	T	D	Q	L	L	E	H	A	K	E	S	L	T	60
CAT	GCG	AAA	GCG	GCG	AGC	GAA	GCG	GGT	GGC	AAC	ACC	CAT	GTG	GGT	
H	A	K	A	A	S	E	A	G	G	N	T	H	V	G	75
CAC	GGC	ATC	AAG	CAC	CTG	GAA	GAT	GCG	ATT	AAA	CAC	GGC	GAG	GAA	
H	G	I	K	H	L	E	D	A	I	K	H	G	E	E	90
GGC	CAC	GTG	GGT	GTT	GCG	ACC	AAG	CAC	GCG	CAA	GAG	GCG	ATC	GAA	
G	H	V	G	V	A	T	K	H	A	Q	E	A	I	E	105
CAC	CTG	CGT	GCG	AGC	GAG	CAC	AAA	AGC	CAC						
H	L	R	A	S	E	H	K	S	H						115

The PelB signal sequence is displayed in bold text

5. 0.1-M IPTG solution: Dissolve 0.48 g of Isopropyl β-D-1-thiogalactopyranoside in 20 mL of water. Filter through a 0.22-μm membrane. Store in aliquots at −20 °C.
6. Lysis buffer 1: 50 mM Tris–HCl, pH: 8.0 buffer. Weigh 0.61 g Tris base, dissolve in 80 mL of water, adjust pH with HCl, and make up to 100 mL with water.
7. Glass beads, 0.1-mm diameter (BioSpec Products, Inc., Bartlesville, OK).
8. Sample buffer 4×: To prepare 10 mL, mix 4 mL of 100% glycerol, 2.4 mL of 1 M Tris buffer pH: 6.8, 0.8 g of SDS, 4 mg of bromophenol blue, 0.5 mL of beta-mercaptoethanol, and 3.1 mL of water. Store in aliquots at −20 °C.
9. 8-M urea solution: 50 mM Tris–HCl, 8 M urea, pH: 8.0. Weigh 96.1 g of urea and 1.21 g Tris base, dissolve in 180 mL water, adjust pH with HCl, and make up to 200 mL with water.

2.4 Components for Large-Scale Protein Expression

1. LB broth.
2. Kanamycin 1000× solution.
3. 5 mL of an overnight *E. coli* BL21(DE3) culture transformed with the target DNA construct as inoculum.

Table 4
Encoding gene and amino acid sequence for TorA-SmbP construct

ATG	AAC	AAC	AAC	GAC	CTG	TTC	CAG	GCG	AGC	CGT	CGT	CGT	TTC	CTG	
M	**N**	**N**	**N**	**D**	**L**	**F**	**Q**	**A**	**S**	**R**	**R**	**R**	**F**	**L**	15
GCG	CAA	CTG	GGT	GGC	CTG	ACC	GTG	GCG	GGT	ATG	CTG	GGT	CCG	AGC	
A	**Q**	**L**	**G**	**G**	**L**	**T**	**V**	**A**	**G**	**M**	**L**	**G**	**P**	**S**	30
CTG	CTG	ACC	CCG	CGT	CGT	GCG	ACC	GCG	AGC	GGC	CAC	ACC	GCG	CAC	
L	**L**	**T**	**P**	**R**	**R**	**A**	**T**	**A**	S	G	H	T	A	H	45
GTG	GAC	GAG	GCG	GTT	AAG	CAC	GCG	GAG	GAA	GCG	GTT	GCG	CAC	GGT	
V	D	E	A	V	K	H	A	E	E	A	V	A	H	G	60
AAA	GAA	GGC	CAC	ACC	GAT	CAG	CTG	CTG	GAG	CAC	GCG	AAG	GAA	AGC	
K	E	G	H	T	D	Q	L	L	E	H	A	K	E	S	75
CTG	ACC	CAT	GCG	AAA	GCG	GCG	AGC	GAA	GCG	GGT	GGC	AAC	ACC	CAT	
L	T	H	A	K	A	A	S	E	A	G	G	N	T	H	90
GTG	GGT	CAC	GGC	ATC	AAG	CAC	CTG	GAA	GAT	GCG	ATT	AAA	CAC	GGC	
V	G	H	G	I	K	H	L	E	D	A	I	K	H	G	105
GAG	GAA	GGC	CAC	GTG	GGT	GTT	GCG	ACC	AAG	CAC	GCG	CAA	GAG	GCG	
E	E	G	H	V	G	V	A	T	K	H	A	Q	E	A	120
ATC	GAA	CAC	CTG	CGT	GCG	AGC	GAG	CAC	AAA	AGC	CAC				
I	E	H	L	R	A	S	E	H	K	S	H				132

The TorA signal sequence is displayed in bold text

4. 0.1-M IPTG solution.
5. Orbital shaker incubator.
6. Centrifuge.

2.5 Components for Whole-Cell Lysis

1. Bead Beater with the 50-mL and 350-mL chamber attachments (BioSpec Products, Inc., Bartlesville, OK).
2. Glass beads, 0.1-mm diameter (BioSpec Products, Inc., Bartlesville, OK).
3. Lysis buffer 2: 50 mM Tris–HCl, 500 mM NaCl, pH: 8.0. Weigh 6.06 g Tris, 29.22 g NaCl, and dissolve them in water to a volume of 900 mL; adjust pH with HCl, make up to 1 L with water. Store at 4 °C (*see* **Note 3**).
4. Antifoam 204 (Sigma-Aldrich, St. Louis, MO).
5. Protease inhibitors cocktail (Sigma-Aldrich, St. Louis, MO).

2.6 Components for Lysozyme/ Osmotic Shock

1. Hypertonic buffer: 200 mM Tris–HCl, 20% sucrose, 0.5 mg/mL lysozyme, 2 mM EDTA, pH of 8.0: Weigh 200 g sucrose, 24.22 g Tris, 0.5 g lysozyme, and dissolve in 900 mL water,

add 4 mL of 0.5 M EDTA solution (pH: 8.0), adjust pH with HCl, and make up to 1 L with water. Store at 4 °C.

2. Ultrapure water.
3. Centrifuge.
4. Dialysis tubing.
5. Equilibration buffer: it is the same as Lysis buffer 2 (the same as component 3, Subheading 2.5).

2.7 Components for Protein Purification

1. ÄKTA system and a HiTrap FF column (GE Healthcare Bio-Sciences, Pittsburgh, PA) or any IMAC resin charged with Ni(II) (*see* **Note 4**).
2. Equilibration buffer: it is the same as Lysis buffer 2 (the same as component 3, Subheading 2.5).
3. Washing buffer: 50 mM Tris–HCl, 500 mM NaCl, 5 mM imidazole, pH of 8.0: Weigh 6.06 g Tris base, 29.22 g NaCl, 0.34 g imidazole, and dissolve them in water up to 900 mL, adjust pH with HCl, and make up to 1 L with water (*see* **Note 5**).
4. Elution buffer: 50 mM Tris–HCl, 500 mM NaCl buffer, 200 mM imidazole, pH of 8.0: Weigh 6.06 g Tris, 29.22 g NaCl, 13.61 g imidazole and dissolve them in water to a volume of 900 mL. Adjust pH with HCl. Make up to 1 L with water. Store at 4 °C.

2.8 Components for Enterokinase Cleavage and Tag Removal

1. Dialysis tubing.
2. Dialysis buffer: 50 mM Tris–HCl, 500 mM NaCl, pH of 8.0. Weigh 12.11 g of Tris base and 58.44 g of NaCl, dissolve in 1800 mL of water, adjust pH with HCl and make up to a final volume of 2 L with water.
3. Enterokinase light chain.
4. IMAC resin.

3 Methods

3.1 DNA Constructs

1. Prepare the PCR mix to amplify the target gene. It is strongly advised to use a high-fidelity polymerase in order to reduce mutations; an example of a PCR mix is shown in Table 5 (*see* **Note 6**).
2. Program thermal cycler, a routine PCR amplification is shown in Table 6.
3. Identify the amplicon using agarose gel electrophoresis.
4. Purify the PCR product using the gel-extraction kit.

Table 5
Example of PCR reactions

Component	20-μL reaction	50-μL reaction	Final concentration
Nuclease-free water	To 20 μL	To 50 μL	
10× polymerase buffer	2 μL	5 μL	1×
10-mM dNTPs	0.4 μL	1 μL	200 μM
10-μM forward primer (containing a NcoI site at the 5′ end)	1 μL	2.5 μL	0.5 μM
10-μM reverse primer (containing a XhoI site at the 5′ end)	1 μL	2.5 μL	0.5 μM
Template DNA	Variable	Variable	<250 ng
DMSO (optional)	(0.6 μL)	(1.5 μL)	3%
DNA polymerase	0.2 μL	0.5 μL	1.0 units/50 μL PCR

Table 6
Thermocycling conditions for routine PCR

Cycle step	Temp	Time	Cycles
Initial denaturation	95 °C	30 s	1
Denaturation, annealing, extension	95 °C, 45–65 °C, 72 °C	15–30 s, 15–60 s, 1 min per kb	30
Final extension	72 °C	5 min	1
Hold	4 °C	∞	–

5. Perform double digestion of the PCR product and the pET30a vector (which includes the fusion protein) with restriction enzymes NcoI and XhoI. Follow the enzyme manufacturer's instructions.
6. Determine the DNA concentration of the vector and insert.
7. Perform a DNA ligation using a T4 DNA ligase, following the manufacturer's instruction. For most standard cloning, a 3:1 insert-vector molar ratio is recommended.
8. Inactivate the ligase by incubating 10 min at 65 °C.

3.2 Heat-Shock Transformation and Screening

1. Thaw chemically competent DH5α cells on ice.
2. Mix 1–5 μL of the ligation reaction into 20–50 μL of competent cells. The volume of the ligation reaction added should be no more than 10% of the total mix volume.
3. Incubate the cells on ice for 20–30 min.

4. After incubation, submerge the tubes containing the competent cells in the 42 °C water bath for 45 s.
5. Place the tubes back on ice for 2 min.
6. Add 800 μL of sterile LB media (without antibiotic).
7. Incubate at 37 °C for 45–60 min in the shaker incubator.
8. Plate the transformed cells in an LB agar plate containing 30 μg/mL of kanamycin.
9. Incubate at 37 °C overnight (16 h).
10. Pick single colonies from the LB plate and inoculate 5 mL of LB broth containing 5 μL of kanamycin 1000× overnight.
11. Isolate the plasmid using a plasmid miniprep kit.
12. Perform a PCR reaction as in **steps 1** and **2**, Subheading 3.1, using the flanking primers for the target gene and the plasmid DNA isolated from the transformed cells as DNA template.
13. Run an agarose gel electrophoresis, look for expected band size that confirms the presence of the gene of interest in the plasmid.
14. Perform DNA sequencing to make sure that the DNA construct is correct.

3.3 Small-Scale Protein Expression

1. Transform chemically competent BL21(DE3) *E. coli* cells (or any other *E. coli* strain design for protein expression, *see* **Note 2**) with a plasmid that contains the gene for the target protein, selected from **steps 12–14**, Subheading 3.2.
2. After incubation for 16 h, select a few colonies and inoculate them separately in tubes containing 2 mL of LB broth with 2 μL of kanamycin 1000×.
3. Incubate them at 37 °C at 200 rpm until they reach an OD_{600} of 0.4–0.6 (*see* **Note 7**).
4. Once they reach the desire OD_{600}, let them cool for a few minutes and then add 2 μL of 0.1 M IPTG (final 0.1 mM IPTG concentration) and incubate them at 25 °C at 200 rpm for 16 h.
5. To obtain the soluble fraction: collect the cells by centrifugation at 16,250 × *g* for 2 min (use 2-mL Eppendorf tubes) and discard the supernatant. Add 120 μL of lysis buffer 1 and 150 μL of glass beads. Vortex for 4–5 min. Decant the glass beads, remove the lysate, and place it in a new tube. Centrifuge at 16,250 × *g* for 5 min, remove supernatant to a new tube, and add Sample buffer 4× (to a final concentration of 1×) and boil them for 10 min.
6. To obtain the insoluble fraction, wash the remaining pellet from the previous step by adding 120 μL of water, vortex, centrifuge, remove water, and repeat; then add 120 μL of

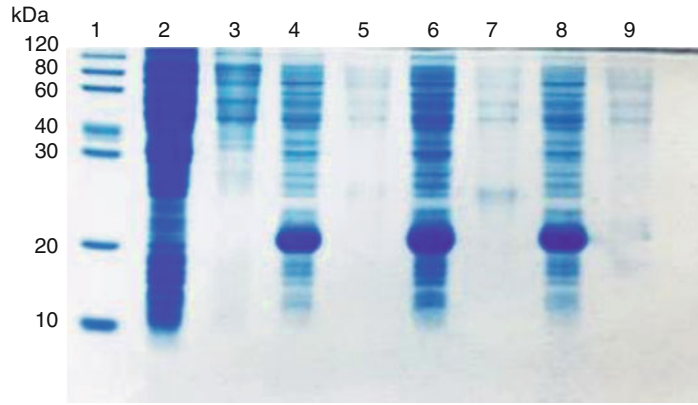

Fig. 3 15% SDS-PAGE analysis of small-scale expression of SmbP_Brazzein (16.8 kDa) in *E. coli* SHuffle. Lane 1: protein marker; lanes 2 and 3: soluble (SF) and insoluble (IF) fractions of *E. coli* SHuffle; lanes 4, 6, and 8: SF of SmbP_Brazzein clones; lanes 5, 7, and 9: IF of SmbP_Brazzein clones

8 M urea solution and resuspend the pellet using a vortex, boil the mix for 10 min, and then centrifuge at 16,250 × *g* for 10 min. Remove the supernatant and discard the cell pellet.

7. Load 2–3 μL of each fraction in different lanes of the SDS-PAGE.
8. Run the electrophoresis using a first step of 110 V for 20 min and a second step of 140 V for 1 h 20 min. Figure 3 shows the SDS-PAGE analysis of a small-scale expression of the protein Brazzein tagged with SmbP.

3.4 Large-Scale Protein Expression

1. Select a transformed colony and inoculate 5 mL of LB-Kan. Incubate at 37 °C at 200 rpm for 16 h.
2. Prepare 1 L of LB broth and dispense 125 mL into 8 baffled flasks and add 125 μL of Kanamycin 1000× to each.
3. Inoculate each flask with 125 μL of the overnight inoculum and incubate at 37 °C, 200 rpm until each they reach an OD_{600} of 0.4–0.6.
4. Let the flasks cool to room temperature and induce expression by adding 125 μL of the 0.1-M IPTG solution (final 0.1-mM IPTG concentration).
5. Incubate them at 25 °C at 200 rpm for 16 h.

3.5 Whole-Cell Lysis

This procedure is for cytoplasmic expression using constructs that include SmbP or CusF3H+.

1. Collect the cells by centrifugation at 17,000 × *g* for 10 min in a refrigerated centrifuge (*see* **Note 8**).

2. Fill at least half of the 50 mL Bead Beater small chamber with glass beads.
3. Resuspend the cell pellet in 30 mL of lysis buffer 2 and add it to the Bead Beater along with the glass beads.
4. Add 30 μL of antifoam 204 and 30 μL of protease inhibitor cocktail.
5. Place the small chamber inside the 350-mL large polycarbonate chamber prefilled with crushed ice and firmly screw them on the rotor assembly.
6. Run the Bead-Beater for 15 s, stop and let it stand 45 s to avoid heating, repeat 7 more times to complete 8 cycles (a total of 2 min).
7. Place the small chamber on ice and decant the glass beads.
8. Place the lysate in a centrifuge tube, wash the glass beads with more Lysis buffer 2 and add it to the lysate, centrifuge at 17,000 × *g* for 15 min at 4 °C to obtain a clear lysate.

3.6 Lysozyme/ Osmotic Shock

This procedure is for constructs that include PelB-SmbP or TorA-SmbP.

1. Collect the cells by centrifugation at 11,000 × *g* and 4 °C for 10 min and weigh the wet cell pellet.
2. Resuspend the cell pellet in 10 mL of Hypertonic buffer per gram of wet cells and incubate for 40 min at 4 °C.
3. Collect the cell pellet by centrifugation at 11,000 × *g* and 4 °C for 10 min. Keep the supernatant as the hypertonic fraction.
4. Resuspend the cell pellet from the previous step in ultrapure water, use 10 mL per gram of wet cells. Incubate for 40 min at 4 °C.
5. Recollect the cell pellet by centrifugation at 11,000 × *g* and 4 °C for 10 min. Store the supernatant as the hypotonic fraction.
6. Analyze both fractions by SDS-PAGE (*see* **Note 9**).
7. Dialyze the hypotonic fraction against equilibration buffer (*see* **Note 10**).

3.7 Protein Purification

1. Equilibrate the HiTrap column with 5 volumes of equilibrating buffer.
2. Load the clarified whole-cell lysate (or dialyzed hypotonic fraction), adjust the flow rate to avoid over pressure, follow the manufacturer's instructions (*see* **Note 11**).
3. Wash the column with washing buffer until absorption is either 0.1 or has achieved a steady baseline.
4. Elute target protein with elution buffer. Optionally, apply a gradient, usually 15 column volumes, to achieve higher purity.

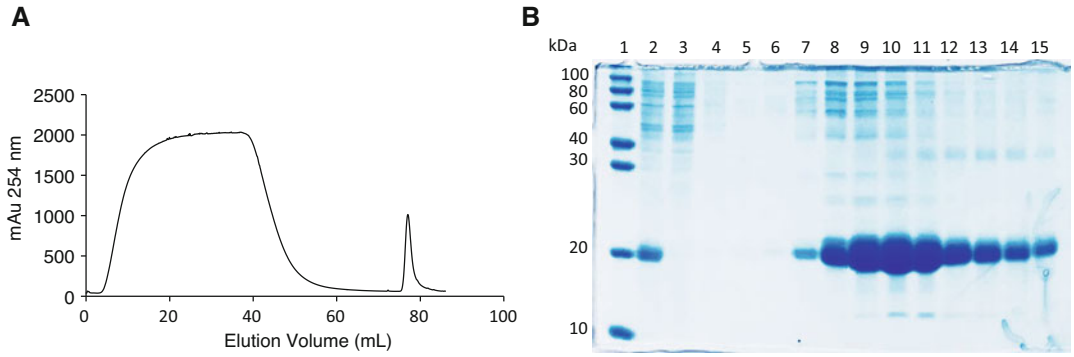

Fig. 4 IMAC purification of CusF3H+_Brazzein (17.09 kDa) using a one-step elution. (**a**) Chromatogram from the purification using the ÄKTA Prime Plus system with a 1-mL His-Trap FF column. The column was equilibrated with 50 mM Tris–HCl, 500 mM NaCl, 5 mM Imidazole, pH: 8, and washed with 50 mM Tris–HCl, 500 mM NaCl, 10 mM Imidazole, pH: 8, the elution was done with 50 mM Tris–HCl, 500 mM NaCl, and 200 mM imidazole, pH: 8. (B) 15% SDS-PAGE analysis of the eluted fractions, lane 1: protein marker; lane 2: lysate; lane 3: flow-through; lanes 4–6: washing fractions; lanes:7–15: elution fractions

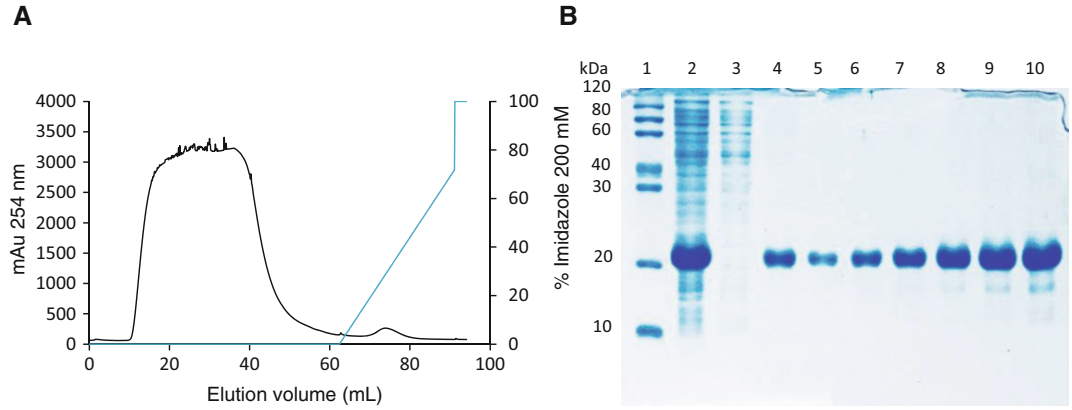

Fig. 5 IMAC purification of SmbP_Brazzein (16.8 kDa) using linear gradient elution. (**a**) Chromatogram from the purification using the ÄKTA Prime Plus system with a 1-mL His-Trap FF column. The column was equilibrated with 50 mM Tris–HCl, 500 mM NaCl, 5 mM Imidazole, pH: 8, and washed with 50 mM Tris–HCl, 500 mM NaCl, 10 mM Imidazole, pH: 8, the elution was done with 50 mM Tris–HCl, 500 mM NaCl, and 200 mM imidazole, pH: 8. (B) 15% SDS-PAGE analysis of the eluted fractions, lane 1: protein marker; lane 2: lysate control; lane 3: flow-through; lanes 4–10: elution fractions

5. Analyze all fractions elution fractions by SDS-PAGE. Figures 4 and 5 show the chromatograms and SDS-PAGE analysis for the purification of Brazzein. In Fig. 4, the target protein is tagged with CusF3H+ and the elution was done in one step. For Fig. 5, the same target protein is tagged with SmbP and elution was performed with a gradient.

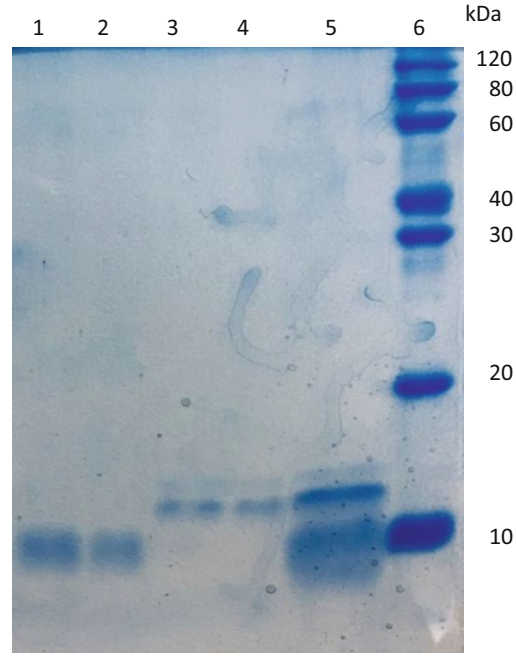

Fig. 6 15% SDS-PAGE analysis of Enterokinase cleavage and tag removal. Lanes 1–2: Brazzein (6.37 kDa); lanes 3–4: SmbP; lane 5: SmbP_Brazzein after enterokinase digestion; lane 6: protein marker

3.8 Enterokinase Cleavage and Tag Removal

1. Pool all elution fractions that contain the target protein and dialyze against dialysis buffer at 4 °C, change the buffer two times for complete dialysis.
2. For digestion with enterokinase, follow the manufacturer's instructions and monitor the reaction by taking samples every 2 h and analyzing them by SDS-PAGE (*see* **Note 12**).
3. Incubate reaction mixture with equilibrated IMAC resin for 1 h at 4 °C.
4. Centrifuge at 1,500 × *g* for 1 min.
5. Remove supernatant and analyze by SDS-PAGE. Figure 6 shows the cleavage of SmbP_Brazzein with Enterokinase and SmbP removal to yield pure Brazzein.

4 Notes

1. For efficient restriction reaction, 6–9 bp should be present at each side of the restriction site. For the NcoI restriction site consider the following sequence CCATGG**CT**; the last two nucleotides need to be added to not compromise the reading frame.

2. Other *E. coli* strains can be used like SHuffle(DE3) (New England Biolabs, Ipswich, MA) or Origami 2(DE3) (EMD Millipore, Burlington, MA) that are able to produce proteins with disulfide bonds in the cell's periplasm.
3. Using a 2–5 mM imidazole concentration range in Lysis buffer 2 avoids the binding of unwanted proteins to the column. Just make sure to add the imidazole before adjusting the final pH.
4. If an ÄKTA system is not available, use any commercial IMAC resin. For both HiTrap columns and resins, follow the manufacturer's instructions to charge the resin with nickel ions.
5. The imidazole concentration in the washing buffer can be increased up to 10 mM.
6. Depending on the polymerase used the quantities required may vary, follow the manufacturer's instructions.
7. Considering a sample of 2 mL of LB-Kan inoculated with a single colony, *E. coli* BL21(DE3) takes around 3–4 h to reach the OD_{600} of 0.4–0.6 and *E. coli* SHuffle takes between 6 to 7 h to reach the same OD_{600}.
8. Cell pellet can be stored at −20 °C until cell lysis.
9. Generally, periplasmic proteins are visualized only in the hypotonic fraction; although, sometimes, proteins are present in both fractions.
10. If both fractions (hypertonic and hypotonic) contain the target protein, pool them and dialyze against equilibration buffer.
11. If using an IMAC resin, follow the manufacturer's instructions for loading, washing, and elution steps.
12. For some target proteins, it may take up to 24 h to complete the enterokinase digestion.

References

1. Rosano GL, Ceccarelli EA (2014) Recombinant protein expression in *Escherichia coli:* advances and challenges. Front Microbiol 5:172. https://doi.org/10.3389/fmicb.2014.00172
2. Terpe K (2003) Overview of tag protein fusions: from molecular and biochemical fundamentals to commercial systems. Appl Microbiol Biotechnol 60:523–533. https://doi.org/10.1007/s00253-002-1158-6
3. di Guan C, Li P, Riggs PD, Inouye H (1988) Vectors that facilitate the expression and purification of foreign peptides in *Escherichia coli* by fusion to maltose-binding protein. Gene 67:21–30. https://doi.org/10.1016/0378-1119(88)90004-2
4. Smith DB, Johnson KS (1988) Single-step purification of polypeptides expressed in *Escherichia coli* as fusions with glutathione S-transferase. Gene 67:31–40. https://doi.org/10.1016/0378-1119(88)90005-4
5. Vargas-Cortez T, Morones-Ramirez JR, Balderas-Renteria I, Zarate X (2016) Expression and purification of recombinant proteins in *Escherichia coli* tagged with a small metal-binding protein from *Nitrosomonas europaea*. Protein Expr Purif 118:49–54. https://doi.org/10.1016/j.pep.2015.10.009
6. Barney BM, LoBrutto R, Francisco WA (2004) Characterization of a small metal binding protein from *Nitrosomonas europaea*. Biochemistry 43:11206–11213. https://doi.org/10.1021/bi049318k
7. Cantu-Bustos JE, Vargas-Cortez T, Morones-Ramirez JR et al (2016) Expression and purification of recombinant proteins in *Escherichia*

coli tagged with the metal-binding protein CusF. Protein Expr Purif 121:61–65. https://doi.org/10.1016/j.pep.2016.01.007

8. Vargas-Cortez T, Morones-Ramirez JR, Balderas-Renteria I, Zarate X (2017) Production of recombinant proteins in *Escherichia coli* tagged with the fusion protein CusF3H+. Protein Expr Purif 132:44–49. https://doi.org/10.1016/j.pep.2017.01.006
9. Loftin IR, Franke S, Roberts SA et al (2005) A novel copper-binding fold for the periplasmic copper resistance protein CusF. Biochemistry 44:10533–10540. https://doi.org/10.1021/bi050827b
10. Santos BD, Morones-Ramirez JR, Balderas-Renteria I et al (2019) Optimizing periplasmic expression in *Escherichia coli* for the production of recombinant proteins tagged with the small metal-binding protein SmbP. Mol Biotechnol 61(6):451–460. https://doi.org/10.1007/s12033-019-00176-4

Chapter 23

Antibody Aggregate Removal Using a Mixed-Mode Chromatography Resin

Tao Chen, Gaili Guo, Guoqing Tan, Ying Wang, and Yifeng Li

Abstract

In monoclonal antibody (mAb) production, aggregates represent a major class of product-related impurities that needs to be removed by the downstream process. Protein A chromatography is generally less effective at removing antibody aggregates under typical conditions, and in most cases aggregate removal relies on a subsequent polishing chromatography. Here we describe a procedure for effective removal of antibody aggregates using the mixed-mode chromatography resin Capto MMC ImpRes. Clearance of aggregates was confirmed by analytical size-exclusion chromatography (SEC) and native gel electrophoresis.

Key words Antibody aggregate, Capto MMC ImpRes, Native gel electrophoresis, Mixed-mode resin, Size-exclusion chromatography (SEC)

1 Introduction

In therapeutic monoclonal antibody (mAb) manufacturing, aggregates represent a major class of impurities that needs to be removed by the downstream process. The purification platform for mAbs typically employs three chromatographic steps: Protein A affinity chromatography followed by two polishing steps. Protein A chromatography under typical conditions is less effective at removing aggregates [1–5]. Thus, in most cases, aggregate removal relies on a polishing chromatography post Protein A. According to the literature, ion exchange, hydrophobic interaction, and mixed-mode chromatography can all effectively remove aggregates under appropriate conditions [1–14]. In this chapter, we describe a procedure for antibody aggregate removal using the mixed-mode resin Capto MMC ImpRes, whose ligand mediates ionic interactions, hydrophobic interactions, and hydrogen bonding [15, 16]. Compared to the related Capto MMC resin, MMC ImpRes has reduced bead size and ligand density, which renders the resin's improved selectivity

Nikolaos E. Labrou (ed.), *Protein Downstream Processing: Design, Development, and Application of High and Low-Resolution Methods*, Methods in Molecular Biology, vol. 2178, https://doi.org/10.1007/978-1-0716-0775-6_23,

between monomer and aggregates [15, 16]. We have previously shown that MMC ImpRes offers good aggregate clearance under typical conditions without the need for adding special additives (e.g., polyethylene glycol) to the mobile phase [5]. In this work, both linear gradient and stepwise elution were developed. The feed used in the current study is partially purified by Protein A and anion exchange (AEX) chromatography but still contains more than 20% aggregates. Capto MMC ImpRes under linear gradient and stepwise elution reduced the aggregates to 0.7% and 2.6%, respectively, according to analytical size exclusion chromatography (SEC) data. Clearance of aggregates by MMC ImpRes was also confirmed by native gel electrophoresis.

2 Materials

2.1 Equipment

1. AKTA pure 150 system installed with Unicorn software version 6.3 (GE Healthcare, Uppsala, Sweden).
2. SevenExcellence S470 pH/Conductivity Meter (Mettler-Toledo, Columbus, OH, USA).
3. NanoDrop One Spectrophotometer (Thermo Fisher Scientific, Waltham, MA, USA).
4. HPD-25 Diaphragm Vacuum Pump (Tianjin Hengao Technology Development, Tianjin, China).
5. PowerEase 300 W Power Supply (Thermo Fisher Scientific, Waltham, MA, USA).
6. ChemiDoc MP Imaging System (Bio-Rad Laboratories, Hercules, CA, USA).
7. TS-1 Decolorization Shaker (Haimen Kylin-Bell Lab Instruments, Jiangsu, China).
8. Corning LSE Vortex Mixer (Thermo Fisher Scientific, Waltham, MA, USA).

2.2 Chemicals

1. Ethanol, glycine, hydrochloric acid, sodium acetate trihydrate, sodium chloride, sodium hydroxide, and Tris base (Merck, Darmstadt, Germany).
2. Acetic acid and L-arginine hydrochloride (J. T. Baker, Phillipsburg, NJ, USA).
3. 30% acrylamide/bis-acrylamide solution (37.5:1) and TEMED (Bio-Rad Laboratories, Hercules, CA, USA).
4. Ammonium persulfate (APS), Coomassie blue R-250, glycerol, and bromophenol blue (Sigma-Aldrich, St. Louis, MO, USA).
5. NativeMark Unstained Protein Standard (Thermo Fisher Scientific, Waltham, MA, USA).

2.3 Protein, Chromatographic Media, and Buffers

1. The target mAb is an IgG1 (*see* **Note 1**).
2. Capto MMC ImpRes (GE Healthcare) (*see* **Note 2**).
3. Superdex 200 Increase 10/300 GL prepacked column (GE Healthcare) (*see* **Note 3**).
4. Buffers for Capto MMC ImpRes chromatography.
   (a) Sanitization buffer: 0.5 M NaOH.
   (b) Pre-equilibration buffer: 0.5 M NaAc-HAc, pH: 5.5.
   (c) Equilibration/wash 1 buffer: 50 mM NaAc-HAc, pH: 5.5.
   (d) Wash 2 buffer: 50 mM NaAc-HAc, 0.1 M NaCl, pH: 5.5.
   (e) Linear gradient elution buffer: 50 mM NaAc-HAc, 1 M NaCl, pH: 5.5.
   (f) Stepwise elution buffer: 50 mM NaAc-HAc, 0.3 M NaCl, pH: 5.5.
   (g) Strip buffer: 50 mM NaAc-HAc, 1 M Arg, pH: 5.5.
   (h) Storage buffer: 0.1 M NaOH.
5. Buffers for Superdex 200 column.
   (a) Rinse buffer: fresh ultrapure water at 18.2 MΩ cm.
   (b) Sanitization buffer: 0.5 M NaOH.
   (c) Equilibration/wash buffer: 50 mM NaAc-HAc, 0.15 M NaCl, pH: 5.0.
   (d) Storage buffer: 20% ethanol.
6. Buffers for native gel electrophoresis (*see* **Note 4**).
   (a) 10% APS (10 mL): weigh 1.0 g APS, transfer to a 15-mL tube and add deionized water to 10 mL (*see* **Note 5**).
   (b) Stacking gel buffer (4×): 0.5 M Tris–HCl, pH: 6.8.
   (c) Resolving gel buffer (4×): 1.5 M Tris–HCl, pH: 8.8.
   (d) Sample loading buffer (2×, 10 mL): 4 mg bromophenol blue, 2.5 mL 4× stacking gel buffer, 2 mL glycerol, and 1.5 mL deionized water.
   (e) Running buffer (10×): weigh 30 g Tris, 144 g glycine and add deionized water to 1 L (dilute to 1× before use).
   (f) Stain solution (1 L): 2.5 g Coomassie blue R-250, 300 mL ethanol, 100 mL acetic acid, and 600 mL deionized water.
   (g) Destain solution (1 L): 300 mL ethanol, 100 mL acetic acid, and 600 mL deionized water.

2.4 Other Material

1. Omnifit glass column (Diba Industries).
2. Electrophoresis chamber, short plates, spacer plates, 10-well combs (1.0 mm) casting stands, frames, gaskets, and gel releasers (Bio-Rad).
3. 0.22-μm Millipore Express PES membrane filters (Merck Millipore).
4. 0.22-μm bottle top vacuum filter (Corning).
5. Amicon Ultra-15 centrifugal filters, 30-kDa MWCO (Merck Millipore).
6. 15-mL centrifuge tubes (Jet Biofil).
7. Corning bottle (Corning).
8. Axygen 1.5-mL microtubes (Corning).

3 Methods

3.1 Capto MMC ImpRes Chromatography

1. Rinse the column with ultrapure water for 1 column volume (CV) (*see* **Note 6**).
2. Sanitize the column with 0.5 M NaOH for 3 CV.
3. Pre-equilibrate the column with 0.5 M NaAc-HAc, pH: 5.5, for 3 CV.
4. Equilibrate the column with 50 mM NaAc-HAc, pH: 5.5, for 5 CV.
5. Load the column at 25 mg of mAb per mL of resin (*see* **Note 7**).
6. Wash the column with 50 mM NaAc-HAc, pH: 5.5, for 5 CV. For stepwise elution, further wash the column with 50 mM NaAc-HAc, 0.1 M NaCl, pH: 5.5, for another 5 CV before elution (*see* **Note 8**).
7. Elute the bound mAb with linear salt gradient elution over 15 CV or stepwise salt elution. Figure 1 shows the chromatograms of runs under linear and stepwise gradient elution (*see* **Note 9**).
8. Strip the column with 50 mM NaAc-HAc, 1 M Arg, pH: 5.5, for 3 CV (*see* **Note 10**).
9. Sanitize the column with 0.5 M NaOH for 3 CV.
10. Store the column in 0.1 M NaOH.

3.2 Analytical SEC with Superdex 200

1. Rinse the column with ultrapure water for 1 CV (*see* **Note 11**).
2. Sanitize the column with 0.5 M NaOH for approximately 1.5 h.
3. Equilibrate the column with 50 mM NaAc-HAc, 0.15 M NaCl, pH: 5.0 (*see* **Note 12**).

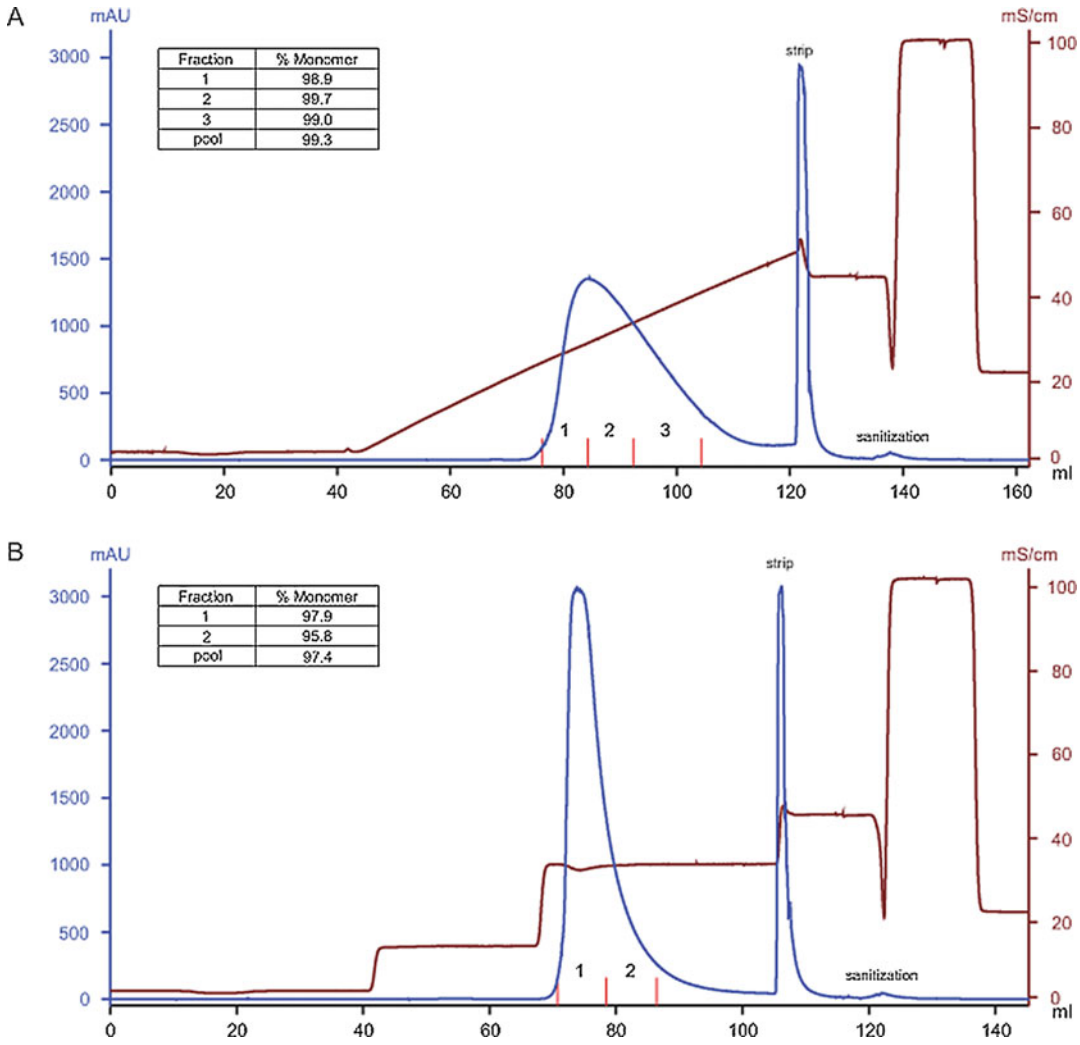

Fig. 1 Capto MMC ImpRes chromatograms of runs under (**a**) linear gradient elution and (**b**) stepwise elution. For linear gradient elution, mobile phase changed from 100% A (50 mM NaAc-HAc, pH: 5.5) to 50% B (50 mM NaAc-HAc, 1 M NaCl, pH: 5.5) over 15 CV. For stepwise elution, the bound mAb was eluted with 50 mM NaAc-HAc, 0.3 M NaCl, pH: 5.5

4. Load 100 μL of the sample using a 500-μL miniloop (*see* **Note 13**).
5. Run the column at a flow rate of 6 cm/h (approximately 0.08 mL/min) with 50 mM NaAc-HAc, 0.15 M NaCl, pH: 5.0, for 1.5 CV (*see* **Note 14**). Monitor the UV absorbance at 280 mM. Figure 2 shows the chromatograms of two runs loaded with samples before and post MMC ImpRes chromatography (*see* **Note 15**).
6. Sanitize and rinse the column with 0.5 M NaOH and ultrapure water, respectively.
7. Store the column in 20% ethanol.

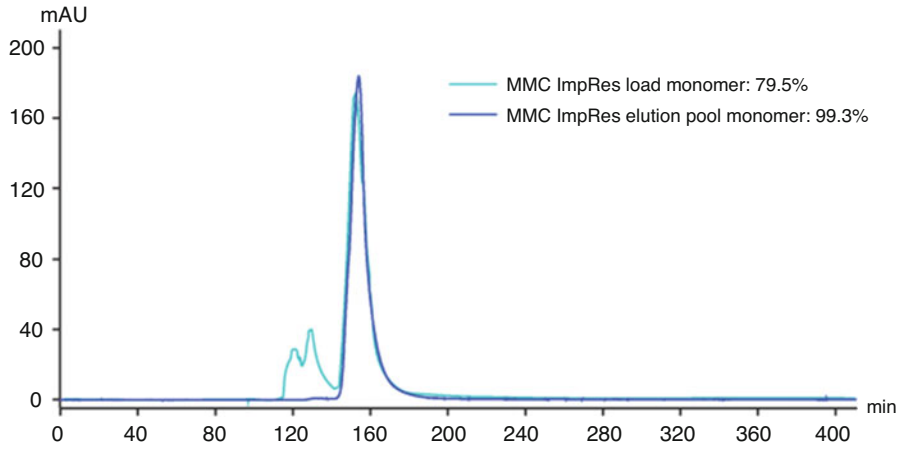

Fig. 2 Analytical SEC chromatograms of Capto MMC ImpRes load and elution pool under linear salt gradient elution. The load contains more than 20% aggregates and the amount of aggregates was reduced to less than 1% by MMC ImpRes chromatography

3.3 Native Gel Electrophoresis

1. Pour 8% resolving gel: mix the reagents in Table 1 in listed order with the indicated volumes, mix the solution gently and introduce proper amount into the gel casting chamber, allow the gel to polymerize for 20 min.
2. Pour stacking gel: mix the reagents in Table 2 in listed order with the indicated volumes, pipette the mixture on top of the resolving gel to fill the cast, insert the comb and allow the gel to polymerize for 20 min, remove the comb.
3. Transfer the casted gel into the gel apparatus, and fill the inner and outer reservoir with 1× running buffer.
4. Mix protein sample with an equal volume of 2× sample loading buffer, load sample into the wells (~4 μg per lane) along with a protein marker (*see* **Note 16**).
5. Connect the power pack and run at 180 V for 2.5 h.
6. After electrophoresis, incubate the gel in a container containing stain solution for 20 min with gentle shaking.
7. Decant the stain solution, rinse the gel with deionized water, and wash with destain solution until the desired background is achieved.
8. Take image of the gel using the ChemiDoc MP Imaging System. Figure 3 shows the native gel analysis of MMC ImpRes load and eluate from linear and stepwise gradient elution (*see* **Note 17**).

Table 1
Resolving gel composition

Reagents	Volume
30% acrylamide/bis-acrylamide	2.7 mL
4× resolving gel buffer	2.5 mL
H_2O	4.8 mL
10% APS	100 μL
TEMED	10 μL

Table 2
Stacking gel composition

Reagents	Volume
30% acrylamide/bis-acrylamide	0.8 mL
4× stacking gel buffer	1.25 mL
H_2O	2.95 mL
10% APS	50 μL
TEMED	5 μL

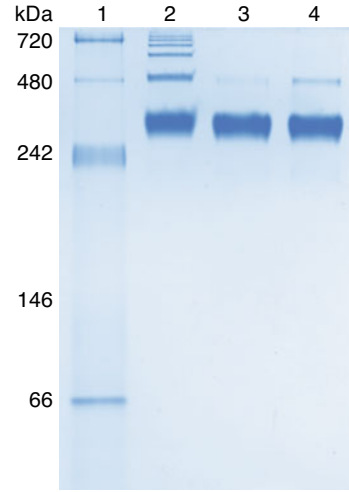

Fig. 3 Native gel analysis of protein sample before and post Capto MMC ImpRes chromatography. Lane 1: protein marker; Lane 2: MMC ImpRes load; Lane 3: MMC ImpRes eluate under linear gradient elution; Lane 4: MMC ImpRes eluate under stepwise elution

4 Notes

1. The target mAb is highly prone to aggregation owing to its inherent properties. It was expressed in CHO-K1 cells grown in HyClone ActiPro culture medium supplemented with Cell Boost 7a and 7b (the medium and feeding supplements were from GE Healthcare). The cell culture was allowed to grow for 14 days before harvest. The clarified harvest contains more than 20% aggregates according to size-exclusion chromatography-high-performance liquid chromatography (SEC-HPLC) analysis. The feed used in this study had been partially purified by Protein A and AEX chromatography (in flow-through mode). However, both Protein A and AEX failed to remove aggregates.
2. Capto MMC ImpRes is a multimodal cation exchanger. The resin was packed in a 0.66-cm-diameter glass column (Omnifit) with 15-cm bed height. The column's volume is approximately 5 mL.
3. This is a SEC column (inner diameter: 10 mm, length: 300 mm), which can be used for small-scale preparative purification and analytical purposes. The column's volume is approximately 24 mL.
4. As the purpose is to monitor antibody aggregates, native (non-denaturing) gel electrophoresis rather than sodium dodecyl sulfate polyacrylamide gel electrophoresis (SDS-PAGE) is used. Both the sample loading buffer and the gel running buffer should be prepared in the absence of SDS.
5. 10% APS is best prepared fresh. Although it can be stored at 4 °C, it may lose its effect if stored for longer than 2 weeks.
6. For all MMC ImpRes chromatography steps, the column was run at a follow rate of 180 cm/h (residence time: 5 min).
7. The feed was filtered with a 0.22-μm pore-size filter prior to loading.
8. Wash 2 is only required for stepwise elution. This wash step, with a low concentration of NaCl (i.e., 0.1 M), prevents aggregates from eluting at suddenly increased salt concentration used for stepwise elution.
9. Elution fractions and pools under both conditions (i.e., linear and stepwise gradient elution) were analyzed by SEC. Pools were also analyzed by native gel electrophoresis. Under linear gradient elution, monomer purity of the elution pool reaches 99.3%, suggesting aggregates in the load were almost completely removed. The total protein and monomer recovery under linear gradient elution were 73% and 91%, respectively. Stepwise elution was also developed to facilitate large-scale

production. Monomer purity of the elution pool under this condition is 97.4%, which is slightly lower than that of the pool from linear gradient elution. The total protein and monomer recovery under stepwise elution was 71% and 87%, respectively.

10. Arginine relaxes electrostatic, hydrophobic interactions, and hydrogen bonds, which are involved in MMC ImpRes-mediated binding [17]. 1 M arginine can effectively remove species (e.g., aggregates) tightly bound to the MMC ImpRes ligand.
11. For rinse, sanitization, and equilibration, the column was run at 12 cm/h (approximately 0.16 mL/min).
12. The column should be equilibrated until the conductivity and pH of the flow-through reach a steady state and become close to that of the equilibration buffer.
13. The two analytes are MMC ImpRes load and elution pool from a run under linear salt gradient elution. Prior to loading, the MMC ImpRes load was diluted with water, whereas the elution pool was concentrated using the Amicon Ultra centrifugal filter units at 2500 $\times$ *g* for 10 min. For both analytes, the load concentration was approximately 7 mg/mL.
14. As recommended, 150 mM NaCl was included in the column buffer to minimize weak ionic binding of proteins to ionic impurities in the resin [18]. The column was run at a slow rate to achieve good resolution.
15. Monomer purity was calculated by integrating the corresponding peak. As the data in Fig. 2 suggested, Capto MMC ImpRes under linear salt gradient (Fig. 1a) almost completely removed aggregates in the load. MMC ImpRes under stepwise elution (Fig. 1b) also removed most of the aggregates. The monomer purity of elution pool under stepwise elution is 97.4% (SEC chromatogram not shown).
16. The samples should not be heated or boiled.
17. The result is consistent with that of the analytical SEC. As indicated by lane 2, the load contains a relatively high percentage of aggregates with different sizes. Linear gradient elution removes aggregates more completely than stepwise elution.

Acknowledgments

We would like to thank Weichang Zhou and Peter (Keqiang) Shen for lending their support to this work.

References

1. Bonnerjea J, Brake RP, Davis MR, Kellerman K, Preneta A (2008) Ion exchange chromatography and purification of antibodies, United States patent application publication US 2008/0312425 A1
2. Vázquez-Rey M, Lang DA (2011) Aggregates in monoclonal antibody manufacturing processes. Biotechnol Bioeng 108:1494–1508
3. Hall T, Wilson JJ, Brownlee TJ, Swartling JR, Langan SE, Lambooy PK (2015) Alkaline cation-exchange chromatography for the reduction of aggregate and a mis-formed disulfide variant in a bispecific antibody purification process. J Chromatogr B 975:1–8
4. He X (2015) Mixed-mode chromatography for mAb S aggregate removal: comparison of CHT™ ceramic hydroxyapatite, capto adhere, and capto adhere impres. Bio-Rad Lab., Inc. Bull 6749
5. Zhang X, Chen T, Li Y (2019) A parallel demonstration of different resins' antibody aggregate removing capability by a case study. Protein Expr Purif 153:59–69
6. McCue JT, Engel P, Ng A, Macniven R, Thömmes J (2008) Modeling of protein monomer/aggregate purification and separation using hydrophobic interaction chromatography. Bioprocess Biosyst Eng 31:261–275
7. Lu Y, Williamson B, Gillespie R (2009) Recent advancement in application of hydrophobic interaction chromatography for aggregate removal in industrial purification process. Curr Pharm Biotechnol 10:427–433
8. McCue JT (2009) Theory and use of hydrophobic interaction chromatography in protein purification applications. Methods Enzymol 463:405–414
9. Gagnon P, Ng P, Aberrin C, Zhen J, He J, Mekosh H, Cummings L, Richieri R, Zaidi S (2006) A ceramic hydroxyapatite based purification platform: simultaneous removal of leached protein A, aggregates, DNA, and endotoxins. BioProcess Int 4:50–60
10. Gagnon P, Beam K (2009) Antibody aggregate removal by hydroxyapatite chromatography. Curr Pharm Biotechnol 10:440–446
11. Eriksson K, Ljunglöf A, Rodrigo G, Brekkan E (2009) MAb contaminant removal with a multimodal anion exchanger: a platform step to follow protein A. Bioprocess Int 7:52–56
12. Chen J, Tetrault J, Zhang Y, Wasserman A, Conley G, Dileo M, Haimes E, Nixon AE, Ley A (2010) The distinctive separation attributes of mixed-mode resins and their application in monoclonal antibody downstream purification process. J Chromatogr A 1217:216–224
13. Gao D, Wang LL, Lin DQ, Yao SJ (2013) Evaluating antibody monomer separation from associated aggregates using mixed-mode chromatography. J Chromatogr A 1294:70–75
14. Chmielowski RA, Meissner S, Roush D, Linden TO, Glowacki E, Konietzko J, Nti-Gyabaah J (2014) Resolution of heterogeneous charged antibody aggregates via multimodal chromatography: a comparison to conventional approaches. Biotechnol Prog 30:636–645
15. GE Healthcare Life Sciences (2013) Polishing of monoclonal antibodies using Capto™ MMC ImpRes in bind and elute mode. Application note 29-0373-49 AA
16. GE Healthcare Life Sciences (2015) Capto™ MMC ImpRes. Data file 29-0356-74 AB
17. Arakawa T, Ejima D, Tsumoto K, Obeyama N, Tanaka Y, Kita Y, Timasheff SN (2007) Suppression of protein interactions by arginine: a proposed mechanism of the arginine effects. Biophys Chem 127:1–8
18. Burgess RR (2018) A brief practical review of size exclusion chromatography: rules of thumb, limitations, and troubleshooting. Protein Expr Purif 150:81–85

Part IV

Assessing Protein Structural Integrity, Purity, and Stabilization

Chapter 24

Proteomic Analysisof Food Allergens by MALDI TOF/TOF Mass Spectrometry

Cosima D. Calvano, Mariachiara Bianco, Ilario Losito, and Tommaso R. I. Cataldi

Abstract

Matrix-assisted laser desorption/ionization (MALDI) mass spectrometry (MS) is largely recognized as an important tool in the analysis of many biomolecules such as proteins and peptides. The MS analysis of digested peptides to identify a protein or some of its modifications is a key step in proteomics. MALDI-MS is well suited for the peptide mass fingerprinting (PMF) technique, as well as selected fragmentation of various precursors using collisional-induced dissociation (CID) or post-source decay (PSD).

In the last few years, MALDI-MS has played a significant role in food chemistry, especially in the detection of food adulterations, characterization of food allergens, and investigation of protein structural modifications induced by various industrial processes that could be an issue in terms of food quality and safety.

Here, we present simple extraction protocols of allergenic proteins in food commodities such as milk, egg, hazelnut, and lupin seeds. Classic bottom-up approaches based on Sodium Dodecyl Sulphate (SDS) gel electrophoresis separation followed by in-gel digestion or direct in-solution digestion of whole samples are described. MALDI-MS and MS/MS analyses are discussed along with a comparison of data obtained by using the most widespread matrices for proteomic studies, namely, α-cyano-4-hydroxy-cinnamic acid (CHCA) and α-cyano-4-chloro-cinnamic acid (CClCA). The choice of the most suitable MALDI matrix is fundamental for high-throughput screening of putative food allergens.

Key words MALDI TOF/TOF, Mass spectrometry, Proteomics, Food, Allergens, Egg, Milk

1 Introduction

The introduction of "soft" ionization techniques as matrix-assisted laser desorption/ionization (MALDI) [1] and electrospray ionization (ESI) [2] has revolutionized mass spectrometry as a molecular characterization tool in many fields from proteomics [3, 4] to lipidomics [5, 6], food science and safety [7, 8]. Indeed, MALDI-MS has become a fundamental technique even in the analysis of low-molecular-weight compounds, including chlorophylls [9, 10],

Nikolaos E. Labrou (ed.), *Protein Downstream Processing: Design, Development, and Application of High and Low-Resolution Methods*, Methods in Molecular Biology, vol. 2178, https://doi.org/10.1007/978-1-0716-0775-6_24,

sugars [11–13], diols [14], vitamins [15, 16], and so on, by the introduction of novel rationally designed matrices [17, 18].

However, proteomic strategies still represent the workhorse of this analytical technique for clinical chemistry [4], microbiology [19], and food science [20]. In this area, MALDI represents a valuable analytical tool for food authentication [21], identification of food spoilers and food-borne pathogens [22], food allergen identification [23], control of the technological processes [3], impact on the chemical properties of food proteins and safety assessment of genetically modified foods [24].

Food allergy is nowadays regarded as a significant health problem in our society, which counts around 6–8% of children and up to 3% of adults affected. Allergic reactions are triggered by the immune system against food components and they can manifest by various symptoms from mild to fatal effects as anaphylaxis [25]. Until now, the only effective choice to avoid allergic reactions remains the strict avoidance of hurting foods. Conceivably, this requires clear classification and accurate labeling of the potential allergenic food ingredients. Ninety percent of food allergies are caused mainly by eight food groups referred to as "The Big 8," including egg, fish, milk, peanut, shellfish, soy, tree nuts, and wheat. It is recognized that food allergies are caused by proteins, also termed allergens, which are not generally considered damaging to the human body except for sensitized people [26]. About plant food allergens, the most relevant protein families are represented by 2S albumins, seed storage proteins, nonspecific lipid transfer protein, while for animal foods the most common protein families remain tropomyosin and EF-hand proteins [27]. Recently, it has been reported that lipids as well might represent an adjuvant for peanut allergens in sensitization via the skin [28] even if very few studies have been retrieved on this topic. Since it is recognized that even allergen amounts at ppm level can activate a negative reaction, it stays of paramount importance for the protection of allergic consumers to develop robust and sensitive analytical techniques, able to detect eventual residues of allergens contaminating foods, also referred to as "hidden" allergens. Current strategies use an antibody-based recognition as enzyme-linked immunosorbent assay (ELISA) or lateral flow devices [29, 30]. Some of these methods are commercialized and routinely used by industry and administration agencies because of their ease of use and limited technical requirements. However, they encounter several drawbacks, such as lack of accuracy and robustness due to crossreactivity phenomena, presence of interfering compounds in complex food matrices (false positives), allergen modification occurring during food processing or sample preparation that could mask the allergen itself (false negatives) [31–34]. Due to the high sensitivity, accuracy, and performance of last-generation mass analyzers, MS techniques really represent alternative powerful methods for the

sensitive and selective detection of allergens in food products [35]. MS may potentially turn into a high-throughput screening tool, able, within a single run, to quantify multiplex allergenic ingredients or traces in several food commodities at high molecular level of selectivity. The first step for their identification is the extraction of proteins from complex food samples by applying conventional protocols based on solid/liquid or liquid/liquid extraction with buffers as Tris–HCl, TRIZMA, or chaotropic agents, i.e., ammonium sulfate and sodium chloride [36]. Even if intact proteins can be analyzed, the choice to investigate peptides could be crucial since it allows to identify and localize minor modifications in the protein sequence, in order to obtain useful information for food authenticity [37, 38] or to discover unique diagnostic peptides related to hidden food allergens. So detection is usually achieved by a "bottom-up" approach analyzing peptides obtained after proteolytic digestion of the extracted proteins [39]. Proteins are usually first treated with reducing agents as dithiothreitol (DTT) to reduce any disulfide bridges and subsequently with iodoacetamide to block the SH groups before adding specific proteolytic enzymes such as trypsin, LysC, AspN, or Glu-C. Trypsin is the most used enzyme since it generates peptides within the mass range of 500–4000 Da that are easily suitable for successive investigation by liquid chromatography (LC)-MS or MALDI-MS. Masses of the generated peptides originate a characteristic dataset called peptide mass fingerprinting (PMF). According to this approach, experimental data are compared with in silico protein digest to find the best match that should identify the unknown protein. Moreover, it is possible also to recognize the amino acid sequence through MS/MS acquisitions and search on databases. If the digestion is performed on a single protein, as for example on a spot arising from a 2D gel electrophoresis separation, the output score will be higher compared to the same protein digested in a complex mixture [40]. However, consistent information can also be obtained by digesting a complex protein mixture and exploiting MS/MS analyses, with the great advantage of a considerable time saving. In the case of food allergens, it is critical to identify marker peptides since the robustness and sensitivity of the whole analytical method is strictly dependent on the reliability of the signature peptides (uniqueness, specificity, stability) reflecting the target offending proteins. The approach is usually developed on standard proteins or reference materials and then applied to processed food since it is known that food processing might affect the reliability of target peptides. The global scheme of the described approach is depicted in Fig. 1.

Here, we describe protocols for the treatment of some food commodities belonging to the "Big 8" group, such as milk, egg, hazelnut, and lupin seed flour, which are often employed as raw ingredients in several baked foods or can be present as hidden

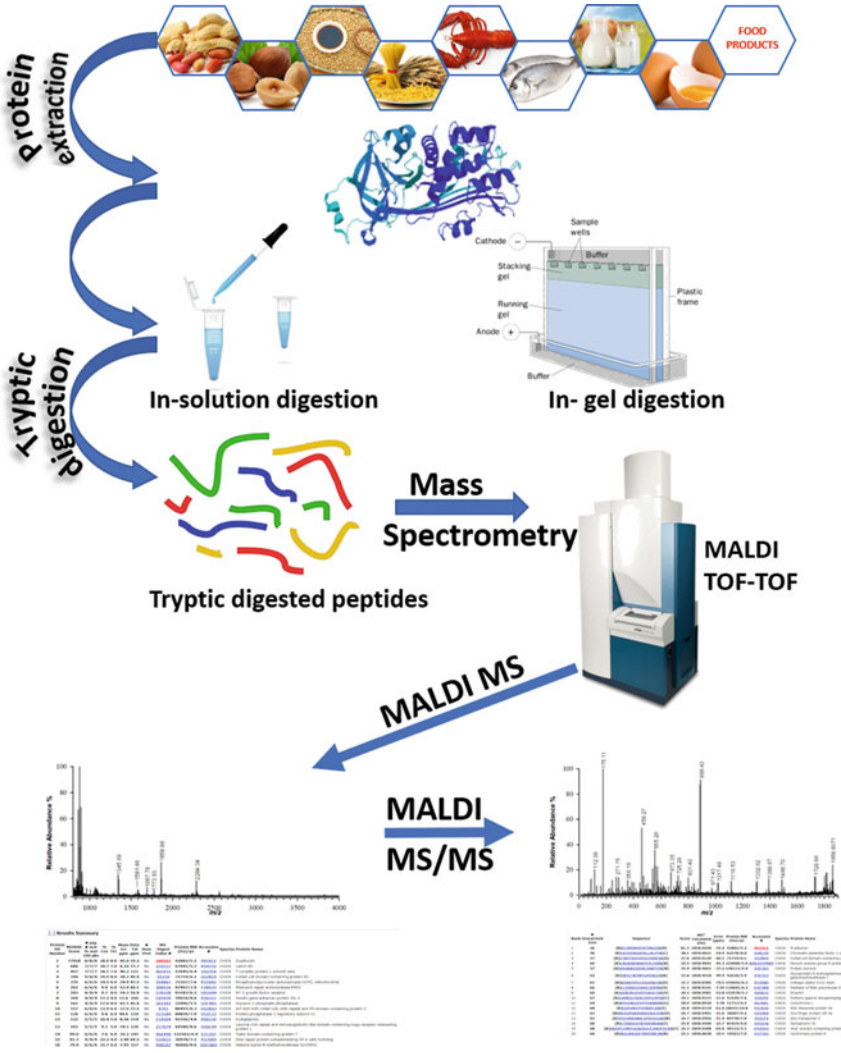

Fig. 1 Scheme of the whole bottom-up approach proposed for detection and characterization of allergen proteins from "Big 8" foods

allergens or contaminants due to their ubiquitous presence in many food industries. The proteins of milk can be grouped into three major classes, namely, caseins, milk fat globule membrane (MFGM), and whey proteins. Cow milk contains several proteins that are considered antigenic and responsible for inducing immune responses: lactoglobulins (β-LG), caseins (CN), and α-lactalbumin (ALA) are the major allergens, followed by minor proteins such as bovine serum albumin, lactoferrin, and immunoglobulins [41]. After cow's milk, hen's egg allergy is the second most common food allergy, with about 2% of prevalence in infants and children. The major allergens in egg white, containing more than 20 different proteins and glycoproteins, are ovomucoid (Gal d 1),

ovalbumin (Gal d 2), conalbumin (ovotransferrin) (Gal d 3), and lysozyme (Gal d 4), while in egg yolk the allergen responsible for syndrome has been identified in α-livetin (Gal d 5) [42].

As for the hazelnut proteome, at least five protein types of hazelnut appear to be involved in allergic reactions. The first major allergen, Cor a 1 (18 kDa, Bet v 1 family), is a typical pollen allergen. The second one, Cor a 2 (14 kDa), belongs to the profilin family and could be found in pollens and seeds. The other three ones belong to the seed storage protein family. Cor a 8 (9 kDa) is a nonspecific lipid transfer protein associated with severe allergic reactions to hazelnuts. The other major food allergens present in hazelnut are Cor a 9 (Corylin), a 59-kDa protein, which belongs to the legumin (11S globulin protein family) and Cor a 11 (48 kDa), which belongs to the 7S seed storage globulin family [43, 44]. Regarding the seed storage proteins of *Lupinus* species, conglutins are the major allergens. The two major fractions are β-conglutin (vicilin-like protein or acid 7S globulin) and α-conglutin (legumin-like protein or 11S globulin), whereas the two minor components are δ-conglutin (2S sulfur-rich albumin) and γ-conglutin (basic 7S globulin) [45].

Simple, rapid, and sensitive procedures for proteomic MALDI-MS/MS analysis of these foods are described in the following. A comparison between data obtained using two different matrices, namely, α-cyano-4-hydroxy-cinnamic acid (CHCA) and α-cyano-4-chloro-cinnamic acid (CClCA), is reported to underline their chief role in this field. The approach here described was able to identify the signature allergenic peptides actually available [36] for the selected foods.

2 Materials

Prepare all solutions using ultrapure water and analytical-grade reagents. Prepare and store all aqueous solutions at 4 °C and the organic solutions at room temperature. Store the reagents following the manufacturer's instructions. Diligently follow all waste disposal regulations when disposing of waste materials.

2.1 Protein Extraction

2.1.1 Protein Extraction from Milk [38]

1. Pyrex® glass centrifuge tube, tube capacity: 10 mL.
2. Acetic acid.
3. Centrifuge and centrifugal vacuum concentrator.
4. Pasteur pipettes.
5. Diethyl ether.
6. PVDF filters (0.45-μm porosity).

2.1.2 Protein Extraction from Hazelnut [23]

1. Porcelain pestle and mortar.
2. Eppendorf® test tube, tube capacity: 1.5 mL.
3. Aqueous isopropanol: 20% (v/v).
4. Centrifuge and centrifugal vacuum concentrator.
5. Pasteur pipettes.
6. Thermo shaker.
7. Cold acetone: 100%.

2.1.3 Protein Extraction from Egg

1. Pyrex® glass suitable container/beaker, volume capacity: 100 mL.
2. Falcon centrifuge tube, tube capacity: 25 mL.
3. Pure water.
4. Aqueous ethanol: 85% (v/v).
5. Centrifuge.
6. Pasteur pipettes.
7. Thermo shaker.
8. NaCl or $(NH_4)_2SO_4$: 10% (w/v).
9. HCl: 6 M.

2.1.4 Protein Extraction from Lupin Seed Flour [46]

1. Pyrex® glass centrifuge tube, tube capacity: 15 mL.
2. Eppendorf® test tube, tube capacity: 1.5 mL.
3. 0.2 M Tris–HCl buffer (pH: 8.2).
4. Centrifuge.
5. Pasteur pipettes.
6. Thermo shaker.
7. Filters made of 0.2-μm regenerated cellulose.

2.2 Protein Separation and Digestion

2.2.1 SDS Gel Electrophoresis [47]

1. Protein electrophoresis buffer: Dilute ten times with Millipore water the 10× Tris/Glycine/SDS buffer (Bio-Rad Laboratories, Hertfordshire, UK) (*see* **Note 1**).
2. Sample loading buffer: Laemmli sample buffer (Bio-Rad Laboratories) (*see* **Note 2**).
3. DTT solution: DL-Dithiothreitol 50 mM in ultrapure water (freshly prepared).
4. Thermo shaker.
5. Hamilton syringe.
6. 4–15% Mini-PROTEAN® TGX™ Precast Gels (Bio-Rad Laboratories, Hertfordshire, UK).
7. Molecular-weight marker "Precision Plus Protein™ Standards Dual Color" (Bio-Rad Laboratories).

8. Mini-PROTEAN® II Electrophoresis cell (Bio-Rad Laboratories).
9. Fixing solution: 50% (v/v) Millipore water, 40% (v/v) ethanol, 10% (v/v) acetic acid.
10. Staining solution: 0.116 g Blue Coomassie R250 in 100 mL of 67% (v/v) Millipore water, 25% (v/v) ethanol, 8% (v/v) acetic acid.
11. Destaining solution: 67% (v/v) Millipore water, 25% (v/v) ethanol, 8% (v/v) acetic acid.

2.2.2 In-Gel Digestion [48]

1. Sterile cutter.
2. 1.5-mL microfuge tubes.
3. Organic buffer A: NH_4HCO_3 200 mM in 40% (v/v) of ACN.
4. Organic buffer B: NH_4HCO_3 50 mM in 9% (v/v) of ACN.
5. Thermo shaker.
6. Centrifugal vacuum concentrator.
7. Trypsin solution in organic buffer B (Trypsin Proteomics Grade, Dimethylated, Sigma-Aldrich).
8. Aqueous 10% (v/v) trifluoroacetic acid (TFA).

2.2.3 In-Solution Digestion [49]

1. 0.5-mL microfuge tubes.
2. Aqueous buffer: 400 mM NH_4HCO_3 in 8 M urea (*see* **Note 3**).
3. DTT solution: DL-Dithiothreitol 50 mM in NH_4HCO_3 200 mM (freshly prepared).
4. IAA solution: iodoacetamide 150 mM in NH_4HCO_3 200 mM (freshly prepared).
5. Ultrapure water.
6. Trypsin solution in organic buffer B.
7. Aqueous 10% (v/v) TFA.

2.3 MALDI MS/MS Analysis

1. Matrix solution (*see* **Notes 4** and **5**).
2. Calibration peptide mixture: Mass standards kit for calibration was purchased from AB Sciex (Ontario, Canada) and contains Neurotensin, des-Arg^1-Bradykinin, angiotensin I, [Glu]^1-fibrinopeptide, ACTH fragments 18–39 (concentration ranging from 0.2 to 9.2 μg/vial) (*see* **Note 6**).
3. Acetonitrile, water, aqueous TFA 0.1% or formic acid 1% (v/v).
4. MALDI sample plate.
5. MALDI TOF/TOF mass spectrometer.

All experiments were performed using a 5800 MALDI ToF/-ToF analyzer (AB SCIEX, Darmstadt, Germany) equipped with a

neodymium-doped yttrium lithium fluoride (Nd:YLF) laser (345 nm) and operated in reflectron positive mode, with a typical mass accuracy of 5 ppm. In MS and MS/MS mode, 2000 laser shots were typically accumulated by a random rastering pattern, at a laser pulse rate of 400 and 1000 Hz, respectively. MS/MS experiments were performed setting a potential difference of 1 kV between the source and the collision cell; ambient air was used as the collision gas, with a medium pressure of 10^{-6} Torr. The delayed extraction (DE) time was set at 280 ns.

DataExplorer software 4.0 (AB Sciex) was used to control the acquisitions and to perform the initial elaboration of data, while SigmaPlot 11.0 was used to graph final mass spectra. ChemDraw Pro 8.0.3 (CambridgeSoft Corporation, Cambridge, MA, USA) was employed to draw chemical structures. Isotopic pattern contribution was achieved by Xcalibur 4.0 with Foundation 3.1 (Thermo Fisher Scientific). Any commercial MALDI mass spectrometer should be capable of obtaining data as discussed here.

3 Methods

3.1 Protein Extraction from Milk (See Notes 7 and 8)

1. Centrifuge 5 mL of milk samples at 5000 × *g* for 30 min at 4 °C.
2. Remove the film of fat formed at the top of the solution.
3. Add 250 μL of acetic acid in order to precipitate caseins.
4. Centrifuge at 5000 × *g* for 30 min.
5. Store the casein pellet.
6. Add an equal volume of diethyl ether to the remaining solution (containing whey proteins).
7. Remove lipid and filter whey proteins through PVDF filters (0.45-μm porosity).
8. Dry both casein and whey fractions in a centrifugal vacuum concentrator.
9. Redissolve in water (1 mg/mL) and subject to in-solution digestion or SDS-PAGE run.

3.2 Protein Extraction from Hazelnuts (See Note 8)

1. Ground into a fine powder 30 mg of roasted hazelnuts.
2. Add 1 mL of isopropanol 20% (v/v).
3. Shake for 60 min at 500 × *g*.
4. Centrifuge at 12,000 × *g* for 10 min at 4 °C.
5. Collect the supernatant and add 6 mL of cold acetone.
6. Vortex the mixture and incubate overnight at −20 °C.
7. Centrifuge at 3000 × *g* for 30 min.
8. Dry the pellet at room temperature (around 30 min).

3.3 Protein Extraction from Egg

1. Separate the yolk from the white by cracking the egg and collect them in two suitable container/beakers.
2. Prepare a 20% (w/v) solution of egg white in pure water (distilled or deionized).
3. Centrifuge at 3000 × *g* for 30 min.
4. Collect the supernatant (albumin fraction).
5. To 1 g of egg yolk, add about 2 mL of pure water (distilled or deionized).
6. Centrifuge at 4000 × *g* for 10 min.
7. To the precipitate, add 4 volumes of ethanol 85%, vortex and centrifuge at 4000 × *g* for 10 min.
8. Discard the supernatant if not necessary (it contains lipids).
9. Extract protein using 9 volumes of NaCl or $(NH_4)_2SO_4$ 10%.
10. Centrifuge at 4000 × *g* for 10 min and collect supernatant for successive purification (*see* **Note 9**) and enzymatic digestion.

3.4 Protein Extraction from Lupin Seed Flour (See Note 8)

1. Suspend 0.5 g of lupin seed flour in 12 mL of 0.2 M Tris–HCl buffer (pH: 8.2) (*see* **Note 10**).
2. Keep under magnetic stirring for 6 h at 60 °C.
3. Centrifuge at 10,000 × *g* for 20 min at 4 °C.
4. Filter on 0.2-μm regenerated cellulose filters.

3.5 SDS-Page

1. Mix a volume of 10 μL of each sample with 10 μL of Laemmli sample buffer (1:1, v/v).
2. Add 1 μL of DTT 50 mM and keep at 90 °C for 5 min in a thermo shaker.
3. Load a volume of 15 μL onto the gel using Hamilton syringe (*see* **Note 11**).
4. Run the gel with a constant voltage (200 V) and a variable current (run time ca. 25 min).
5. After the run, put the gel in the fixing solution for 30 min.
6. Stain the gel in the staining solution for 30 min.
7. Destain for 2 h in the destaining solution and then overnight in water.

3.6 In-Gel Digestion

1. Cut the bands in small pieces and put in 0.5-mL microfuge tubes.
2. Cover the pieces with 200 μL of organic buffer A.
3. Incubate samples at 37 °C for 30 s in a thermo shaker.
4. Repeat washing until the gel pieces are decolorized.

5. Dry the gel fragments in a centrifugal vacuum concentrator for 15 s.
6. Add porcine trypsin (0.05 μg/μL) and 50 μL of organic buffer B.
7. Incubate at 37 °C overnight.
8. Collect the liquid and acidify with aqueous TFA 10% (v/v).

3.7 In-Solution Digestion

1. Mix 10 μL of aqueous sample with 40 μL of aqueous buffer.
2. Add 5 μL of DTT solution and incubate for 40 min at 60 °C.
3. Chill at room temperature.
4. Add 5 μL of IAA solution and incubate in the dark at room temperature for 45 min.
5. Add 120 μL of water and 20 pmol of porcine trypsin (*see* **Note 12**).
6. Incubate overnight at 37 °C.
7. Stop the digestion with aqueous TFA 10% (v/v) (reach pH ca 2).

3.8 MALDI MS/MS Analysis

1. Mix the tryptic digests 1:1 (v/v) with the matrix.
2. Spot 1 μL of the sample/matrix solution and let drying in air.
3. Wash the spot twice with ultrapure water (*see* **Note 13**) and then analyze by MALDI-TOF-MS/MS.
4. Acquire spectra in reflectron positive ion mode.
5. For peptide analysis, the explored mass range is usually 700–4000 *m/z*; perform mass calibration using the appropriate peptide mixtures (*see* **Note 6**).

3.9 Protein Identification

For PMF analysis, the raw files relevant to tryptic digests were searched against the nonredundant database Swiss-Prot utilizing Mascot (Matrix Science Ltd., London, UK) or MS-Fit (Protein Prospector, California) database search engines (*see* **Note 14**). The search was performed against the taxonomies *Other Mammalia* (or *Bos Taurus*) for milk proteins, *Gallus gallus* for egg proteins, and *Green plants* for hazelnut and lupin seeds, setting an error of 20 ppm for mass accuracy. The following modifications were set: carbamidomethylation of cysteines as a fixed modification (for in-solution digestion), oxidation of methionines, and phosphorylation of serines, tyrosines and threonines as variable modifications. Up to three missed cleavages were accepted (*see* **Note 14**). For MS/MS analyses, the search was performed utilizing MS-Tag (Protein Prospector, California) and the same parameters except for error that was set to 0.1 Da for MS and 0.3 Da for MS/MS.

3.10 MALDI-MS and Tandem MS Analysis

Representative examples of mass spectra data obtained on some allergenic proteins extracted from food as described in the experimental section are discussed. In MALDI analyses, a key role to have a robust and sensitive detection of the unique, selective, and reliable signature peptides is played by the chosen matrix. Figure 2 reports a comparison of MALDI TOF spectra relevant to a tryptic digest arising from one SDS-PAGE spot of a commercial milk sample by using CHCA (Plot a) and CClCA (Plot b) as matrices. The PMF results from database search clearly indicate that β-casein was properly digested and positively identified irrespective of the matrix used, but the coverage was 21% (MOWSE score: 7066) for CHCA and 30% (MOWSE score: 54132) when CClCA was employed. As previously reported [16], CClCA shows a proton affinity lower than CHCA (198 vs. 201 kcal/mol), leading to an increased proton transfer to the analyte; the result is higher ionization efficiency for less basic peptides compared to CHCA. Then, it is likely that the positive effects detected in peptide mass fingerprint of β-casein (Fig. 2), i.e., enhancement in signal intensities and uniform instrumental response to peptides, no matter their amino acid composition, could be explained by the increased ion yield generated by the CClCA matrix, confirming its importance in detecting likely marker peptides. Notably, three phosphorylated peptides (*see* **label P** in Fig. 2b), which got undetected using CHCA, could also be identified. Indeed, phosphopeptides are challenging analytes (i.e., difficult to perceive without specific sample pretreatments) since they occur at low concentration, are suppressed during the ionization by nonphosphorylated peptides, and do not bind to C18 resin usually used for sample desalting. This observation suggests that the use of CClCA provides an enough enrichment of phosphopeptides directly on spot. To confirm the assignment of these peptides as potentially phosphorylated, MS/MS acquisitions were run on the native peptide at m/z 1981.7 (Fig. 3a) and the relevant phosphorylated form at m/z 2061.8 (Fig. 3b). Searching on the MS/MS database, the peptide at m/z 1981.7 was identified as FQSEEQQQTEDELQDK of β-casein by identifying the predominant *b*- and *y*-type ions [50] arising from the cleavage of the thermally labile C–N amide bonds of the polypeptide backbone. The peptide and precursor ion at m/z 2061.8 were instead identified as phosphorylated because the intense product ion at m/z 1963.9 is most likely due to the neutral loss of H_3PO_4 (=97.9 Da) used as a marker of fragmentation. Moreover, product ions *b*- and *y*-type explained by the database (labeled in plot 3b) correspond also to phosphorylated ion fragments, which allowed to assign the sequence as FQpSEEQQQTEDELQDK with phosphorylation on serine 35 [51].

While the aforementioned example was referred to an in-gel tryptic digest obtained from SDS PAGE purified sample, Fig. 4 shows the MALDI-TOF MS spectrum of an in-solution tryptic

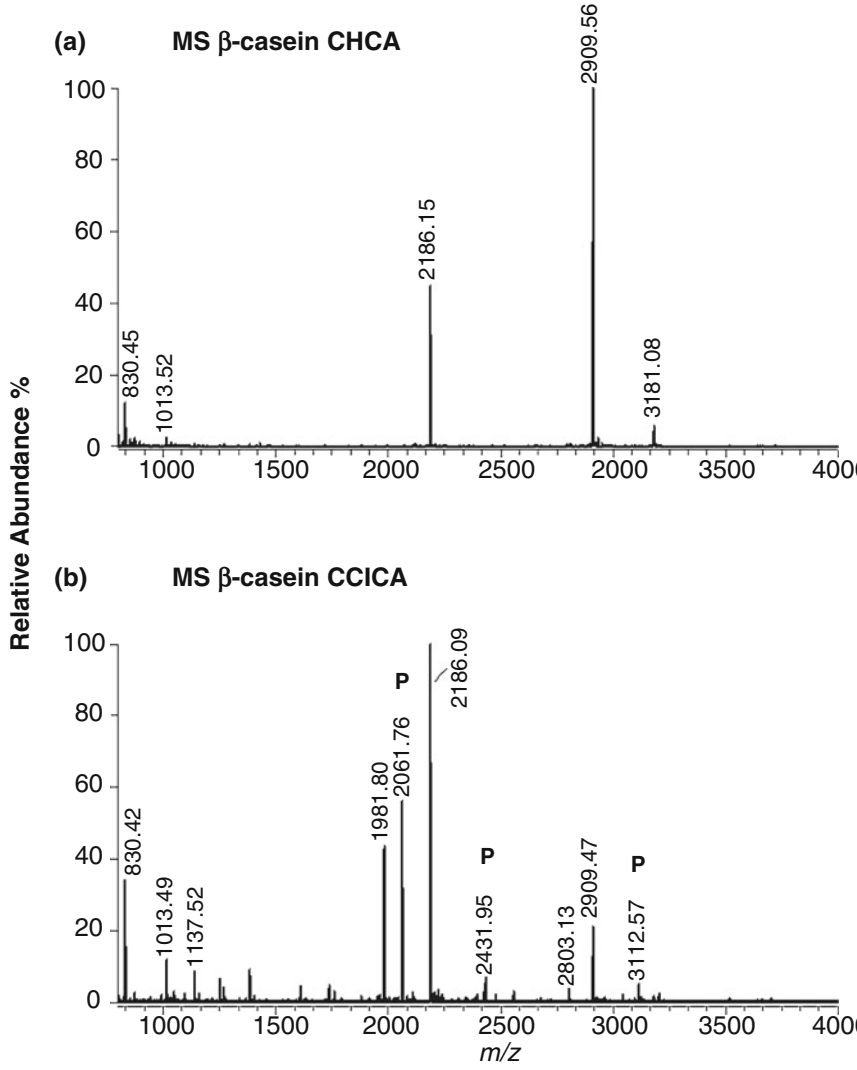

Fig. 2 MALDI TOF spectra of a tryptic digest arising from an SDS-PAGE spot of β-casein when a commercial milk sample was analyzed by CHCA (**a**) and CCICA (**b**) as matrices. Phosphopeptide species are labeled (P)

digest of lupin seed flour extract obtained following the method reported before by using CClCA as a matrix. The database search allowed to recognize the most abundant lupin seed proteins attributable to globulin family as β-conglutin 7 and β-conglutin 2. In this case, the MS spectrum exhibited many peaks, including minor peptides not predictable by PMF. A 2D gel separation could help in the characterization of lupin seed proteins. Alternatively, the MS/MS spectra carried out on selected peptides can also be useful to distinguish between different conglutin families. For instance, in Fig. 5 is reported the MS/MS spectrum of the precursor ion at *m/z* 1446.7 that was chosen since it is known to be a signature allergenic peptide to reveal the occurrence of lupin seed proteins. The *b*- and

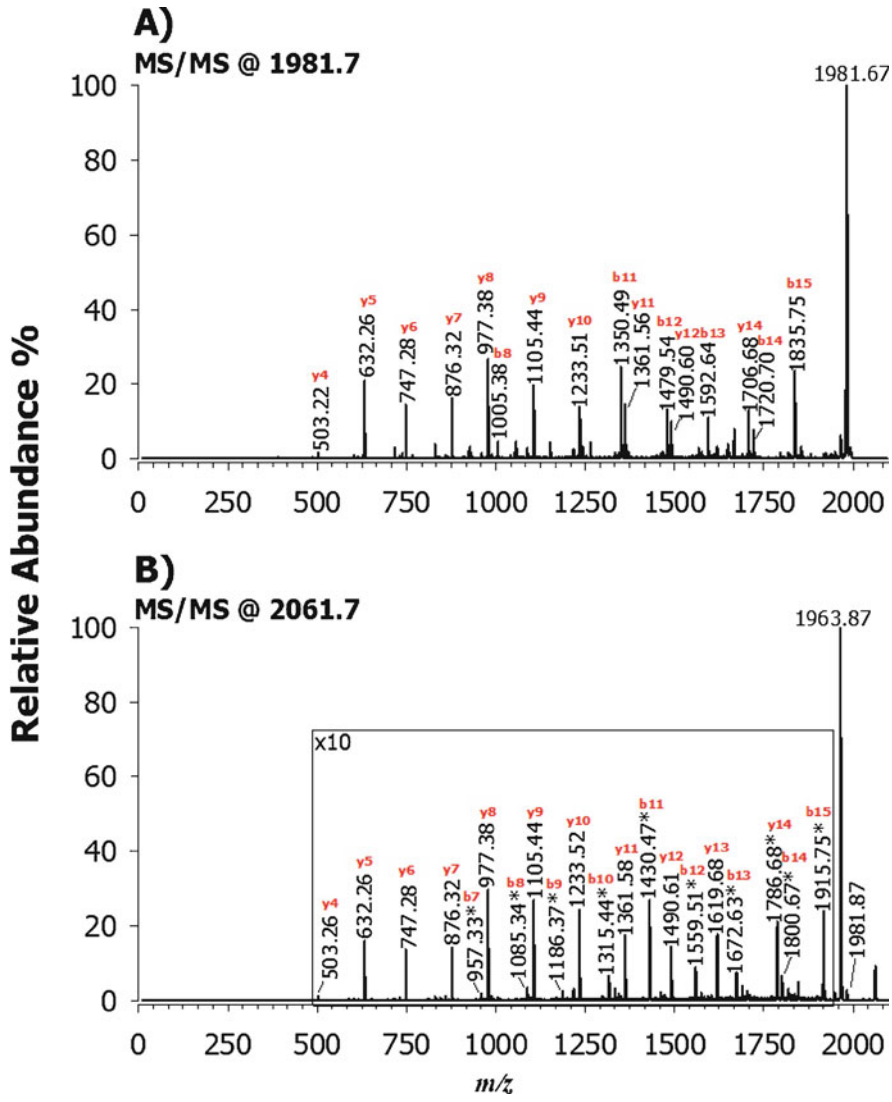

Fig. 3 MALDI TOF/TOF spectra relevant to the peptide FQSEEQQQTEDELQDK at *m/z* 1981.7 (**a**) and to the corresponding phosphorylated form at *m/z* 2061.76 (**b**) from β-casein digest. CCICA was used as a matrix. Phosphorylated fragments are labeled (∗)

y-type ions allowed to assign the peptide as LLGFGINADENQR, as previously described [36, 46]. Unfortunately, the high homology among various isoforms of β-conglutin did not allow to unambiguously identify the subspecies between β-conglutin 2, 3, 4, 5, and 6, but the peptide remains informative and stable to monitor the presence of lupin seeds.

Finally, also for another complex matrix such as egg white extract, the fragmentation of selected precursor ions enables the identification of the common allergens associated with this foodstuff. Figure 6 reports the tandem MS spectrum of the precursor

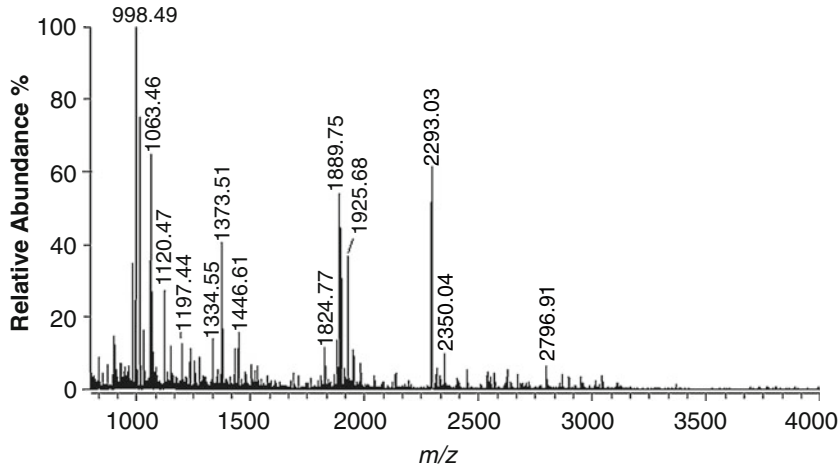

Fig. 4 MALDI TOF spectrum of a tryptic digest of proteins extracted from lupin seed flour, as described in the experimental section. MALDI matrix: CCICA

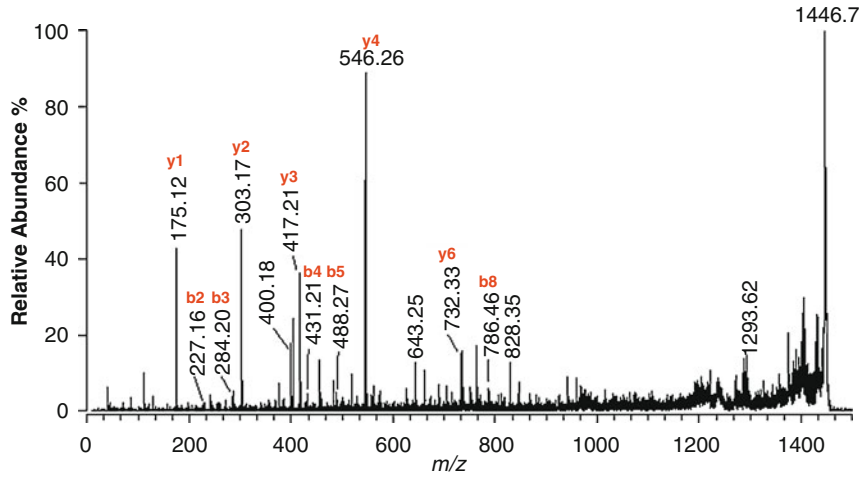

Fig. 5 MALDI TOF/TOF spectrum of the protonated peptide LLGFGINADENQR at *m/z* 1446.7 assigned to β-conglutin from lupin seed flour extract. The main *y* and *b* ions are reported. MALDI matrix: CCICA

ion at *m/z* 1858.8 identified as ELINSWVESQTNGIIR and well known to be an allergenic peptide of ovalbumin [36]. Therefore, if gel electrophoresis is not available, the tandem MS acquisition of MALDI-MS along with the right matrix choice is very important to search for the signature peptides of allergens introduced as hidden ingredients of foods.

4 Notes

1. The formulation of the commercial protein electrophoresis buffer 1× consists of 25 mM Tris–HCl, 192 mM glycine, 0.1% (w/v) SDS, pH = 8.3. A simple method of preparing

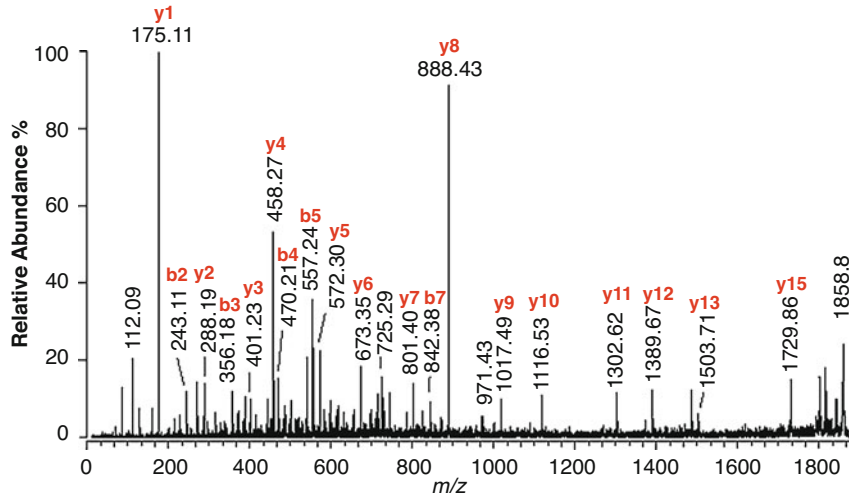

Fig. 6 MALDI TOF/TOF spectrum of the protonated peptide ELINSWVESQTNGIIR at *m/z* 1858.8 of ovalbumin from egg white. The main *y* and *b* ions are reported. MALDI matrix: CCICA

running buffer: Weigh 15.1 g of Tris, 71 g of glycine, and 0.5 g of SDS, mix, and make it to 500 mL with water.

2. The formulation of the commercial loading buffer consists of 62.5 mM Tris, pH = 6.8, 2% (w/v) SDS, 25% (v/v) glycerol, 0.01% (w/v) bromophenol blue. A simple method of preparing running buffer: Weigh 0.6 g of Tris and dissolve in 10 mL of water (pH 8.5). Take 2.5 mL of Tris buffer and add 0.31 g DTT, 0.4 g of SDS, 5.5 mL of water, 2 mL of glycerol, and a few crystals of bromophenol blue.
3. Alternatively, for complex samples, the denaturation can be performed by adding 40 μL of RapiGest™ (0.1% in 50 mM ammonium bicarbonate) reagent (Waters) instead of the aqueous buffer described. RapiGest™ SF Surfactant is a reagent used to enhance enzymatic digestion of proteins since it helps in solubilizing proteins, making them more susceptible to enzymatic cleavage without inhibiting enzyme activity. It is compatible with enzymes such as Trypsin, Lys-C, Asp-N, and Glu-C and other enzymes and it improves efficiency of digestion.
4. The matrix was usually prepared in ACN:H_2O 2:1 with 0.1% (v/v) TFA at a concentration of 10 mg/mL. The most common matrices for peptide analysis are α-cyano-4-hydroxycinnamic acid (CHCA) and α-cyano-4-chloro-cinnamic acid. For matrix recrystallization, *see* **Note 5**.
5. Recrystallization was carried out in 70% acetonitrile/30% (v/v) water. A saturated solution of the matrix in 70% acetonitrile/30% (v/v) water was heated until boiling. When the solid dissolved completely, the solution was cooled to room

temperature, then on ice until a precipitate was observed. Finally, the precipitate was filtered, and the procedure repeated in triplicate.

6. Instead of buying a specific kit, the mass calibration can also be carried out by manually preparing a mixture of standard peptides such as angiotensin I, $[Glu]^1$-fibrinopeptide, ACTH fragments 18–39, with decreasing concentration from the lightest to the heaviest peptide.
7. The in-solution tryptic digestion on whole milk samples originated MALDI mass spectra dominated by casein-related peptides, while whey proteins were almost absent. Thus, a preliminary procedure (see experimental) to separate caseins from whey fractions, which were then subjected to independent processing and analysis, was adopted.
8. All the described samples can be usually defatted using a 1:10 (w/v) sample/hexane mixture by end-over-end rotation at ambient temperature for 15 min. The hexane layer can be decanted, and the defatting process repeated two additional times. The defatted sample can be vacuum-dried and resuspended in the appropriate extraction buffer.
9. The purification step is a key phase in developing sensitive methods for the detection of allergens since it is necessary to concentrate proteins and eliminate interferences from the supernatant. Purification techniques usually involve solid-phase extraction (SPE), protein precipitation, ultrafiltration, and size exclusion chromatography (SEC) [52].
10. The same protocol can be applied to lupin seeds after grinding samples under liquid nitrogen to obtain a fine and homogeneous powder.
11. Centrifuging the samples prior to the run helps to remove insoluble debris, which could produce streaks in the protein lanes (revealed when stained with Coomassie Blue).
12. When using the common denaturants, such as SDS or urea, it is very important to dilute the sample before the addition of enzyme to avoid the denaturation of trypsin (or other proteolytic enzymes). This problem does not occur using *Rapi*Gest SF since it does not modify peptides or suppress protease activity.
13. If the concentration level of impurities is high, it could be nearly impossible to obtain useful signals. If you suspect that extraneous salts are interfering with data collection, a simple spot-washing step after cocrystallization of the sample and matrix may be useful. Simply apply a microliter of Milli-Q water to the spot and allow it to stand for several seconds. The water can then be removed with a pipette tip. Sometimes,

the wash on target is not enough to completely remove salts. In this case, a Zip Tip purification can be performed following the indications of the supplier Millipore. In the first step, the resin is washed and activated with acetonitrile (2 × 10 μL) and with TFA 0.1% (v/v) (2 × 10 μL). Then, the sample is loaded by taking up (ten times) the liquid containing the peptide mixture. Washing is performed with TFA 0.1% (v/v) (3 × 10 μL) in order to eliminate contaminants and finally the sample is eluted with 1–3 μL of matrix (*see* **Note 4**) directly on the target plate.

14. Often, modified peptides are not attributed to any theoretical protein and no database matching is obtained. For these reasons, a different approach can be followed. A number of well-known proteins normally present in food samples (for instance, in our case, globulin-like proteins, whey proteins, caseins) is created and the corresponding database codes are retrieved. Comparison of the experimental data with those related to peptides arising from these proteins is carried out by means of the FindPept software. In this search mode, one protein at a time was compared with the experimental *m/z* data in order to recognize unmodified as well as modified peptides. In this way, almost all signals of the mass spectra could be attributed to peptides and thus to proteins. This approach is very useful when investigations are carried out searching the modifications likely occurring during the heating processes, as deamidation, lactosylation, glycation.

Acknowledgments

This work was supported by Progetto di Ricerca di Interesse Nazionale—PRIN 2017YER72K—"Development of novel DNA-based analytical platforms for the rapid, point-of-use quantification of multiple hidden allergens in food samples."

References

1. Karas M, Bachmann D, Bahr U, Hillenkamp F (1987) Matrix-assisted ultraviolet laser desorption of non-volatile compounds. Int J Mass Spectrom Ion Process 78:53–68. https://doi.org/10.1016/0168-1176(87)87041-6
2. Fenn JB, Mann M, Meng CK, Wong SF, Whitehouse CM (1989) Electrospray ionization for mass spectrometry of large biomolecules. Science 246:64–71. https://doi.org/10.1126/science.2675315
3. Ortea I, O'Connor G, Maquet A (2016) Review on proteomics for food authentication. J Proteome 147:212–225. https://doi.org/10.1016/J.JPROT.2016.06.033
4. Greco V, Piras C, Pieroni L, Ronci M, Putignani L, Roncada P, Urbani A (2018) Applications of MALDI-TOF mass spectrometry in clinical proteomics. Expert Rev Proteomics 15:683–696. https://doi.org/10.1080/14789450.2018.1505510
5. Leopold J, Popkova Y, Engel KM, Schiller J (2018) Recent developments of useful MALDI matrices for the mass spectrometric characterization of lipids. Biomol Ther 8:1–25. https://doi.org/10.3390/biom8040173
6. Calvano CD, Picca RA, Bonerba E, Tantillo G, Cioffi N, Palmisano F (2016) MALDI-TOF

mass spectrometry analysis of proteins and lipids in *Escherichia coli* exposed to copper ions and nanoparticles. J Mass Spectrom 51:828–840. https://doi.org/10.1002/jms.3823

7. Yoshimura Y, Goto-Inoue N, Moriyama T, Zaima N (2016) Significant advancement of mass spectrometry imaging for food chemistry. Food Chem 210:200–211. https://doi.org/10.1016/j.foodchem.2016.04.096
8. Lu H, Zhang H, Chingin K, Xiong J, Fang X, Chen H (2018) Ambient mass spectrometry for food science and industry. TrAC Trends Anal Chem 107:99–115. https://doi.org/10.1016/J.TRAC.2018.07.017
9. Calvano CD, Ventura G, Cataldi TRI, Palmisano F (2015) Improvement of chlorophyll identification in foodstuffs by MALDI ToF/-ToF mass spectrometry using 1,5-diaminonaphthalene electron transfer secondary reaction matrix. Anal Bioanal Chem 407:6369–6379. https://doi.org/10.1007/s00216-015-8728-9
10. Calvano CD, Ventura G, Trotta M, Bianco G, Cataldi TRI, Palmisano F (2017) Electron-transfer secondary reaction matrices for MALDI MS analysis of Bacteriochlorophyll a in Rhodobacter sphaeroides and its zinc and copper analogue pigments. J Am Soc Mass Spectrom 28:125–135. https://doi.org/10.1007/s13361-016-1514-x
11. Calvano CD, Cataldi TRI, Kögel JF, Monopoli A, Palmisano F, Sundermeyer J (2017) Structural characterization of neutral saccharides by negative ion MALDI mass spectrometry using a superbasic proton sponge as deprotonating matrix. J Am Soc Mass Spectrom 28:1666–1675. https://doi.org/10.1007/s13361-017-1679-y
12. Calvano CD, Cataldi TRI, Kögel JF, Monopoli A, Palmisano F, Sundermeyer J (2016) Superbasic alkyl-substituted bisphosphazene proton sponges: a new class of deprotonating matrices for negative ion matrix-assisted ionization/laser desorption mass spectrometry of low molecular weight hardly ionizable analytes. Rapid Commun Mass Spectrom 30:1680–1686. https://doi.org/10.1002/rcm.7604
13. Korte AR, Lee Y-J (2014) MALDI-MS analysis and imaging of smallmolecule metabolites with 1,5-diaminonaphthalene (DAN). J Mass Spectrom 49:737–741. https://doi.org/10.1002/jms.3400
14. Monopoli A, Calvano CD, Nacci A, Palmisano F (2014) Boronic acid chemistry in MALDI MS: a step forward in designing a reactive matrix with molecular recognition capabilities. Chem Commun 50:4322. https://doi.org/10.1039/c4cc01185f
15. Qi Y, Müller M, Stokes CS, Volmer DA (2018) Rapid quantification of 25-hydroxyvitamin D3 in human serum by matrix-assisted laser desorption/ionization mass spectrometry. J Am Soc Mass Spectrom 29:1456–1462. https://doi.org/10.1007/s13361-018-1956-4
16. Calvano CD, Ventura G, Palmisano F, Cataldi TRI (2016) 4-Chloro-α-cyanocinnamic acid is an efficient soft matrix for cyanocobalamin detection in foodstuffs by matrix-assisted laser desorption/ionization mass spectrometry (MALDI MS). J Mass Spectrom 51:841–848. https://doi.org/10.1002/jms.3817
17. Corinti D, Crestoni ME, Fornarini S, Pieper M, Niehaus K, Giampà M (2019) An integrated approach to study novel properties of a MALDI matrix (4-maleicanhydridoproton sponge) for MS imaging analyses. Anal Bioanal Chem 411:953–964. https://doi.org/10.1007/s00216-018-1531-7
18. Calvano CD, Monopoli A, Cataldi TRI, Palmisano F (2018) MALDI matrices for low molecular weight compounds: an endless story? Anal Bioanal Chem 410:4015–4038. https://doi.org/10.1007/s00216-018-1014-x
19. Božik M, Cejnar P, Šašková M, Nový P, Maršík P, Klouček P (2018) Stress response of *Escherichia coli* to essential oil components-insights on low-molecular-weight proteins from MALDI-TOF. Sci Rep 8:13042. https://doi.org/10.1038/s41598-018-31255-2
20. Jagadeesh DS, Kannugundla U, Reddy RK (2017) Application of proteomic tools in food quality and safety. Adv Anim Vet Sci 5:213. https://doi.org/10.17582/journal.aavs/2017/5.5.213.225
21. Gallardo JM, Ortea I, Carrera M (2013) Proteomics and its applications for food authentication and food-technology research. TrAC Trends Anal Chem 52:135–141. https://doi.org/10.1016/J.TRAC.2013.05.019
22. de Koster CG (2016) MALDI-TOF MS identification and tracking of food spoilers and food-borne pathogens. Curr Opin Food Sci 10:76–84. https://doi.org/10.1016/J.COFS.2016.11.004
23. De Ceglie C, Calvano CD, Zambonin CG (2014) Determination of hidden hazelnut oil proteins in extra virgin olive oil by cold acetone precipitation followed by in-solution Tryptic digestion and MALDI-TOF-MS analysis. J Agric Food Chem 62:9401–9409. https://doi.org/10.1021/jf504007d

24. Ocaña MF, Fraser PD, Patel RKP, Halket JM, Bramley PM (2007) Mass spectrometric detection of CP4 EPSPS in genetically modified soya and maize. Rapid Commun Mass Spectrom 21:319–328. https://doi.org/10.1002/rcm.2819
25. Flores Kim J, McCleary N, Nwaru BI, Stoddart A, Sheikh A (2018) Diagnostic accuracy, risk assessment, and cost-effectiveness of component-resolved diagnostics for food allergy: A systematic review. Allergy 73:1609–1621. https://doi.org/10.1111/all.13399
26. Koeberl M, Clarke D, Lopata AL (2014) Next generation of food allergen quantification using mass spectrometric systems. J Proteome Res 13:3499–3509. https://doi.org/10.1021/pr500247r
27. Hoffmann-Sommergruber K (2016) Proteomics and its impact on food allergy diagnosis. EuPA Open Proteom 12:10–12. https://doi.org/10.1016/j.euprot.2016.03.016
28. Palladino C, Narzt MS, Bublin M, Schreiner M et al (2018) Peanut lipids display potential adjuvanticity by triggering a pro-inflammatory response in human keratinocytes. Allergy 73:1746–1749. https://doi.org/10.1111/all.13475
29. Ho MH-K, Wong WH-S, Chang C (2014) Clinical spectrum of food allergies: a comprehensive review. Clin Rev Allergy Immunol 46:225–240. https://doi.org/10.1007/s12016-012-8339-6
30. Asensio L, González I, García T, Martín R (2008) Determination of food authenticity by enzyme-linked immunosorbent assay (ELISA). Food Control 19:1–8. https://doi.org/10.1016/J.FOODCONT.2007.02.010
31. Scaravelli E, Brohée M, Marchelli R, van Hengel AJ (2009) The effect of heat treatment on the detection of peanut allergens as determined by ELISA and real-time PCR. Anal Bioanal Chem 395:127–137. https://doi.org/10.1007/s00216-009-2849-y
32. Downs ML, Taylor SL (2010) Effects of thermal processing on the enzyme-linked Immunosorbent assay (ELISA) detection of milk residues in a model food matrix. J Agric Food Chem 58:10085–10091. https://doi.org/10.1021/jf101718f
33. Fu T-J, Maks N (2013) Impact of thermal processing on ELISA detection of peanut allergens. J Agric Food Chem 61:5649–5658. https://doi.org/10.1021/jf304920h
34. Monaci L, Brohée M, Tregoat V, van Hengel A (2011) Influence of baking time and matrix effects on the detection of milk allergens in cookie model food system by ELISA. Food Chem 127:669–675. https://doi.org/10.1016/J.FOODCHEM.2010.12.113
35. Brockmeyer J (2018) Novel approaches for the MS-based detection of food allergens: high resolution, MS^3, and beyond. J AOAC Int 101:124–131. https://doi.org/10.5740/jaoacint.17-0402
36. Mélanie Planque TA, Gillard N (2018) Food allergen analysis: detection, quantification and validation by mass spectrometry Allergen, vol 2. Intech open, London, pp 8–41. https://doi.org/10.5772/32009
37. Calvano CD, Monopoli A, Loizzo P, Faccia M, Zambonin C (2013) Proteomic approach based on MALDI-TOF MS to detect powdered Milk in fresh Cow's Milk. J Agric Food Chem 61:1609–1617. https://doi.org/10.1021/jf302999s
38. Calvano CD, De Ceglie C, Monopoli A, Zambonin CG (2012) Detection of sheep and goat milk adulterations by direct MALDI-TOF MS analysis of milk tryptic digests. J Mass Spectrom 47:1141–1149. https://doi.org/10.1002/jms.2995
39. Monaci L, De Angelis E, Montemurro N, Pilolli R (2018) Comprehensive overview and recent advances in proteomics MS based methods for food allergens analysis. TrAC, Trends Analyt Chem 106:21–36. https://doi.org/10.1016/j.trac.2018.06.016
40. Gundry RL, White MY, Murray CI, Kane LA, Fu Q, Stanley BA, Van Eyk JE (2009) Preparation of proteins and peptides for mass spectrometry analysis in a bottom-up proteomics workflow. Curr Protoc Mol Biol. Chapter 10: Unit 10.25. https://doi.org/10.1002/0471142727.mb1025s88
41. Monaci L, Tregoat V, van Hengel AJ, Anklam E (2006) Milk allergens, their characteristics and their detection in food: a review. Eur Food Res Technol 223:149–179. https://doi.org/10.1007/s00217-005-0178-8
42. Urisu A, Kondo Y, Tsuge I (2015) Hen's Egg Allergy. Chem Immunol Allergy 101:124–130. https://doi.org/10.1159/000375416
43. Holzhauser T (2018) Protein or no protein. Opportunities for DNA-based detection of allergenic foods. J Agric Food Chem 66 (38):9889–9894. https://doi.org/10.1021/acs.jafc.8b03657
44. Lauer I, Foetisch K, Kolarich D, Ballmer-Weber BK, Conti A, Altmann F, Vieths S, Scheurer S (2004) Hazelnut (*Corylus avellana*) vicilin Cor a 11: molecular characterization of a glycoprotein and its allergenic activity.

Biochem J 383:327–334. https://doi.org/10.1042/BJ20041062

45. Guillamón E, Rodríguez J, Burbano C, Muzquiz M, Pedrosa MM, Cabanillas B, Crespo JF, Sancho AI, Mills ENC, Cuadrado C (2010) Characterization of lupin major allergens (*Lupinus albus* L.). Mol Nutr Food Res 54:1668–1676. https://doi.org/10.1002/mnfr.200900452
46. Mattarozzi M, Bignardi C, Elviri L, Careri M (2012) Rapid shotgun proteomic liquid chromatography-electrospray ionization-tandem mass spectrometry-based method for the lupin (*Lupinus albus* L.) multi-allergen determination in foods. J Agric Food Chem 60:5841–5846. https://doi.org/10.1021/jf302105r
47. Gallagher SR (2007) One-dimensional SDS gel electrophoresis of proteins. In: Current protocols in toxicology. John Wiley & Sons, Inc., Hoboken, NJ, USA, pp 1–38. https://doi.org/10.1002/0471140864.ps1001s68
48. Shevchenko A, Tomas H, Havli J, Olsen JV, Mann M (2007) In-gel digestion for mass spectrometric characterization of proteins and proteomes. Nat Protoc 1:2856–2860. https://doi.org/10.1038/nprot.2006.468
49. León IR, Schwämmle V, Jensen ON, Sprenger RR (2013) Quantitative assessment of in-solution digestion efficiency identifies optimal protocols for unbiased protein analysis. Mol Cell Proteomics 12:2992–3005. https://doi.org/10.1074/mcp.M112.025585
50. Roepstorff P, Fohlman J (1984) Letter to the editors. Biol Mass Spectrom 11:601–601. https://doi.org/10.1002/bms.1200111109
51. Mohammadi M, Xu C-F, Neubert TA, Ma J, Lu Y (2005) Identification of Phosphopeptides by MALDI Q-TOF MS in positive and negative ion modes after methyl esterification. Mol Cell Proteomics 4:809–818. https://doi.org/10.1074/mcp.t400019-mcp200
52. Labrou NE (2014) Protein purification: an overview. In: Methods in molecular biology (Clifton, N.J.). Humana Press, Inc, Totowa, New Jersey, pp 3–10. https://doi.org/10.1007/978-1-62703-977-2_1

Chapter 25

Protein Structure Analysis and Validation with X-Ray Crystallography

Anastassios C. Papageorgiou, Nirmal Poudel, and Jesse Mattsson

Abstract

X-ray crystallography is the main technique for the determination of protein structures. About 85% of all protein structures known to date have been elucidated using X-ray crystallography. Knowledge of the three-dimensional structure of proteins can be used in various applications in biotechnology, biomedicine, drug design, and basic research and as a validation tool for protein modifications and ligand binding. Moreover, the requirement for pure, homogeneous, and stable protein solutions in crystallizations makes X-ray crystallography beneficial in other fields of protein research as well. Here, we describe the technique of X-ray protein crystallography and the steps involved for a successful three-dimensional crystal structure determination.

Key words Protein structure, X-rays, Crystallization, Data collection, Structure determination

1 Introduction

Knowledge of the three-dimensional structure of proteins offers a great amount of information toward the better understanding of protein function and life processes. Visualization of protein structures at atomic resolution can provide suggestions for modifications, resulting, for example, in more efficient and stable enzymes and the design of new inhibitors as potential drugs. In addition, protein structure determination can help in validating protein preparations to optimize purification processes and storage conditions in order to avoid unwanted degradation pathways such as aggregation, deamidation, oxidation, or post-translational modifications. Moreover, protein structures can be used to validate biopharmaceuticals, either proteins or drugs bound to their protein/enzyme target. Crystal structures can also reveal new functions and novel ligand-binding modes.

X-ray crystallography is the most widely used method to obtain detailed three-dimensional structures of proteins. About 85% of all

Nikolaos E. Labrou (ed.), *Protein Downstream Processing: Design, Development, and Application of High and Low-Resolution Methods*, Methods in Molecular Biology, vol. 2178, https://doi.org/10.1007/978-1-0716-0775-6_25,

protein structures deposited in the Protein Data bank (PDB) have been elucidated using the technique of X-ray crystallography. Other methods used for structural information include nuclear magnetic resonance, electron microscopy, and neutron diffraction. In addition, complementary methods such as small-angle X-ray scattering have been proved useful in providing structural insights. Here, the technique of X-ray crystallography will be reviewed with an emphasis on practical issues during the process of determining and validating the structure of a new protein.

1.1 Steps in a Protein Crystal Structure Determination

A protein crystal structure determination involves seven major steps:

1. Protein expression and purification.
2. Crystallization.
3. Crystal characterization.
4. Data collection and processing.
5. Phasing.
6. Refinement and validation.
7. Structure analysis and deposition.

The first two steps are considered as the bottlenecks in any crystal structure determination because of their difficulties.

1.2 Protein Expression and Purification

Crystal structure determination by X-rays requires that the protein under study has been purified to >95% and in sufficient quantities (2–10 mg), enough for setting up initial crystallization tests. Most proteins are produced by recombinant technology using various expression systems and hosts. Protein production and purification have been greatly improved by the use of "tags," which can range in size from just a few residues to full-length proteins or domains [1]. The tags can be used to improve protein production, prevent insolubility, or to confer new properties that can be used for the characterization and study of the target protein. Sometimes, the term "fusion protein" is used for bigger tags, such as entire proteins, for example, glutathione transferase (GST) or maltose-binding protein (MBP). The simplest tag is the "His-tag" or 6xHis-tag. The His-tag binds via the histidine imidazole ring to nickel or cobalt atoms immobilized on metal affinity chromatography media. Subsequently, tagged proteins can be easily eluted using elution buffers with imidazole (100–250 mM) or low pH (4.5–6.0).

1.3 Crystallization

The major technique for protein crystallization is vapor diffusion, either in the sitting or in the hanging drop configuration (Fig. 1). In recent years, the sandwich technique for the crystallization of membrane and water-soluble proteins in the lipidic cubic phase has

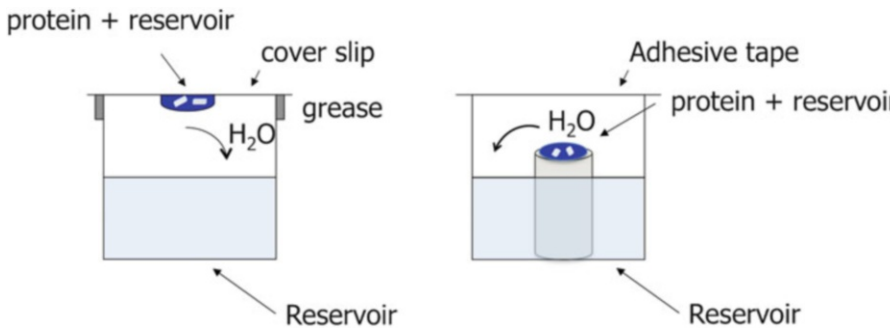

Fig. 1 The two main setups of the vapor diffusion method: hanging drop (left) and sitting drop (right)

been increasingly used [2]. In vapor diffusion, the protein solution is slowly driven to the supersaturation stage, where small nuclei are initially formed. Each protein behaves differently; thus, protein crystallization is an empirical process. Quick screening for crystallization conditions is carried out with commercial screens. Each screen usually contains 96 conditions through a combination of buffers, salts, organic solvents, and polyethylene glycols (PEGs) of various molecular weights.

The failure of a protein to produce crystals suitable for structure determination or no crystals at all may be caused by various reasons, such as:

1. Flexibility of the protein.
2. Unfavorable interactions.
3. Protein instability.
4. Denaturation.
5. Degradation.
6. Polydispersity.

In addition, tags may interfere with the crystallization; thus, provision must be made in the design of the expression constructs to include cleavage sites for the removal of tags (*see* **Note 1**) if problems arise. Removal of tags is especially important when fusion proteins such as GST or MBP are used, which should be removed before crystallizations. In special and difficult cases, fusion proteins can be kept as they might facilitate crystallization [3]. In case small molecules (e.g., ligands, substrates) can bind to the protein, they may improve the stability, reduce protein flexibility, and facilitate crystallization. Several other approaches have been proposed to improve the chances of obtaining crystals (*see* **Note 2**).

1.4 Crystal Characteristics and Basics of X-Ray Diffraction

Crystals are characterized by a high degree of order and internal symmetry, known as lattice symmetry. The smallest part in crystals that is repeated by lattice symmetry operations to build up the entire crystal is called a unit cell. The unit cell is a parallelepiped defined by three lattice translations with lengths a, b, c and three

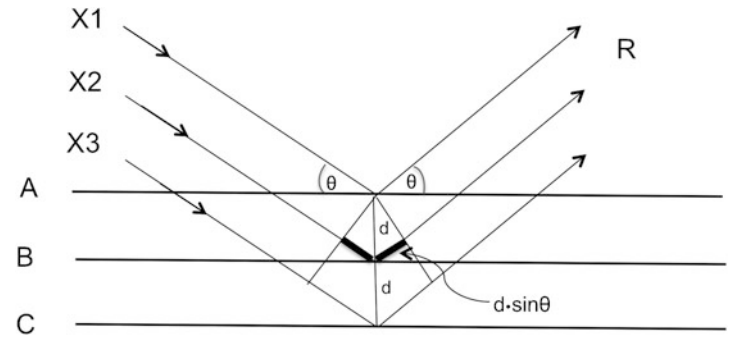

Fig. 2 Schematic diagram of Bragg's law. The incident X-rays are reflected by the lattice planes of the crystal. Diffraction is obtained in direction *R* when the thickened part is equal to a whole number of wavelengths. In this case, constructive interference occurs between the traveled waves

angles α, β, γ. The unit cell is further divided into smaller units, called asymmetric units, through a set of symmetry operations that define the space group. There are 230 space groups, but only 65 are possible for biological molecules owing to the presence of only L-amino acids in nature.

The diffraction of X-rays by crystals was first observed in 1912 by Max von Laue who suggested that the phenomenon could be explained in terms of diffraction by a three-dimensional grating. A year later, William H. Bragg and William L. Bragg (father and son) derived Bragg's law that explained the diffraction patterns obtained by crystals of ZnS, KCl, and NaCl as reflections by planes in the crystal lattice:

$$n\lambda = 2d \sin\theta$$

where n is an integer, λ the wavelength, d the distance between parallel planes in the crystal lattice, and θ the angle of the incident and reflected beam with the crystal plane (Fig. 2). The planes in the crystal lattice are defined by three integers h, k, l, known as plane indices or Miller indices.

1.5 Crystal Characterization

Once crystals of the protein being studied have been obtained, the next step is their characterization. A single crystal is exposed to an X-ray beam (Fig. 3). The crystal is mounted in either a thin-walled quartz capillary or in a loop (Fig. 4). The recording of a few diffraction images will provide the following information about the crystal after visual inspection of the diffraction:

1. Is it salt or protein crystal?
2. How far does it diffract?
3. What is the quality of diffraction?
4. Is there any disorder in the diffraction?
5. What are the unit cell dimensions?

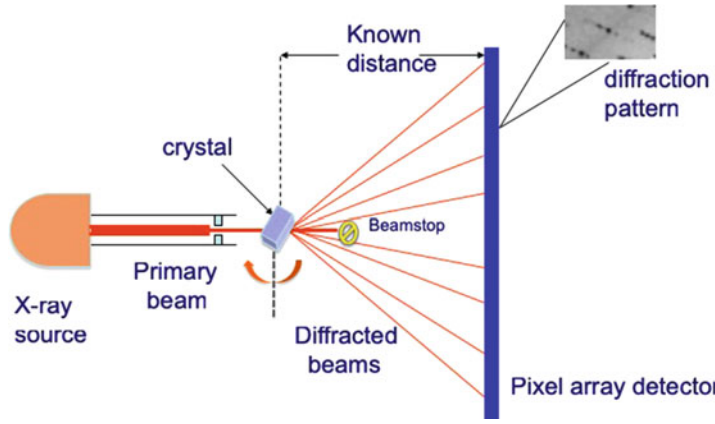

Fig. 3 Schematic representation of an X-ray diffraction experiment

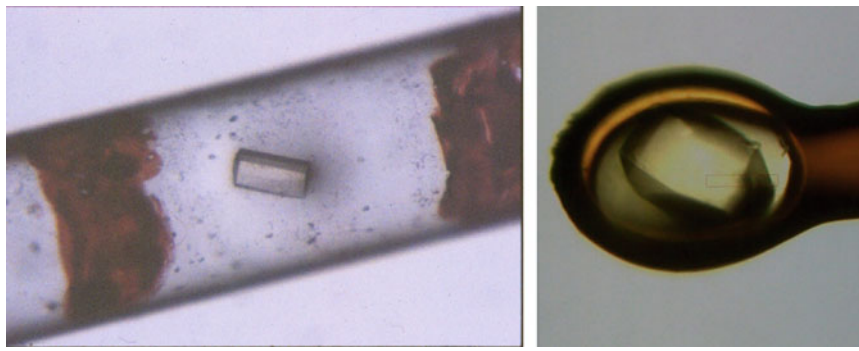

Fig. 4 Crystal mounting. Two methods can be used: either (**a**) a quartz capillary for data collection at room temperature or (**b**) a cryoloop for data collection at cryogenic temperatures (100 K)

It is preferable that crystals have been tested in-house so that their characteristics are already known and no valuable time is spent on the synchrotron beamlines for their characterization (*see* **Note 3**). Besides, the discovery that crystals traveled to synchrotrons are salt crystals can certainly create great disappointment! Several other tests that can give clues if the crystals contain salt or protein are available (*see* **Note 4**). However, the recording of a diffraction pattern will provide the definite answer.

It is advisable that images are recorded from different positions of the crystals, usually 90° apart from each other. The reason is that the crystals may have some anisotropy or disorder in one direction that could prevent the collection of a complete data set of good quality.

The crystals could be initially tested under cryogenic temperatures (*see* **Note 5**). However, a lack of diffraction in cryogenic temperatures does not necessarily mean that the grown crystals are unsuitable. An exposure at room temperature can give an

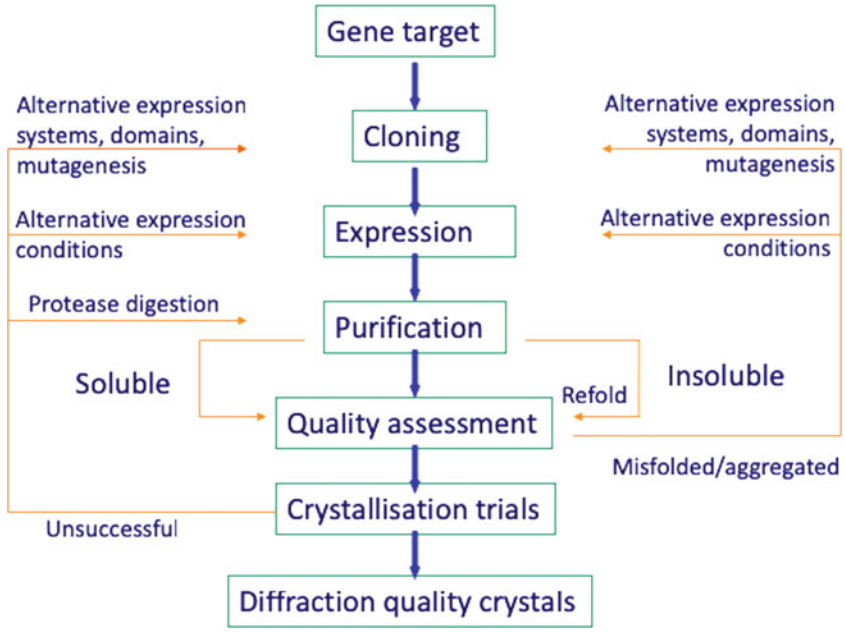

Fig. 5 A typical flowchart toward the successful crystallization of a new protein

answer in case that the cryoconditions used are not the right ones and another cryoprotectant has to be employed (*see* **Note 6**). For room temperature data, a single crystal has to be mounted inside a thin-walled quartz capillary.

Depending on the quality of the diffraction pattern and provided that several crystals have been tested, some decisions could be made at this stage:

1. No crystal optimization needed (i.e., diffraction is satisfactory).
2. Optimization of the crystallization conditions needed (e.g., small crystals, disorder).
3. Other crystallization conditions are required (e.g., large unit cell in the tested crystals).
4. Change/improvement of the purification protocol (e.g., protein purity not good).
5. New construct (e.g., protein unstable).

A typical flowchart of the steps required to obtain diffraction-quality crystals is given in Fig. 5 (*see* also **Note 7**).

1.6 Data Collection and Processing

If the diffraction is of good quality, then data collection can be carried out to obtain a full data set and proceed to the next steps of structure determination (Fig. 6). During X-ray data collection, the crystal is rotated in small steps (usually 0.05–1.0°) so that reflections from all lattice planes (Bragg reflections) and their associated intensities are recorded (*see* **Note 8**), preferably more than once.

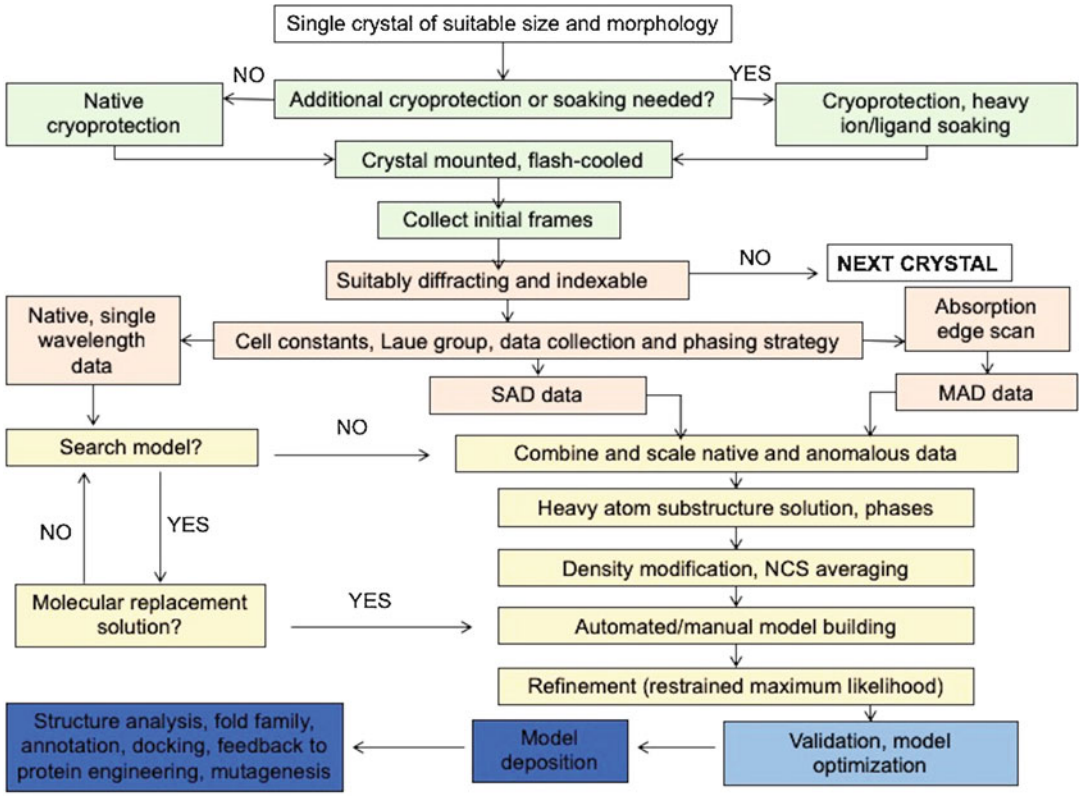

Fig. 6 Outline of data collection strategies and structure determination steps. For molecular replacement and ligand-binding studies, single-wavelength data sets are usually sufficient. (Figure adapted from [44])

For each *hkl*, the intensity I_{hkl} should be significant and accurate as judged by the signal-to-noise ratio $I/\sigma(I)$, where $\sigma(I)$ is the standard deviation. Ideally, the intensities of all the unique Bragg reflections should be measured, but this is not always the case owing to various reasons such as crystal orientation and radiation damage (see later). Moreover, it is especially important that the data at low resolution are complete with no overloads and that the higher-resolution shells contain enough intensities above the zero level, preferably $>2\sigma(I)$.

During data collection, recording of a few diffraction images (or even a single image) will initially provide information about the lattice and the unit cell dimensions of the crystal. Automated procedures are now implemented in synchrotron beamlines that allow initial characterization of the crystals, determination of a data collection strategy (e.g., rotation range, exposure time, resolution) depending on the type of the experiment and estimation of the anticipated radiation damage [4, 5].When the data processing programs have correctly predicted the crystal lattice and unit cell dimensions, the data are said to be autoindexed and data processing can be carried out for the entire data set. At the final stage, the

intensities for each *hkl* reflection will be accurately measured (=integrated) in each diffraction image, merged with the intensity of the same *hkl* reflection in other images or its symmetry pair $-h$, $-k$, $-l$ and finally scaled (*see* **Note 9**).

1.6.1 Radiation Damage

The use of third-generation synchrotron radiation sources for data collection has reduced the amount of time required for a complete data set. However, the intense beam can still create considerable damage to protein crystals even though the exposure times are usually short and despite the use of cryogenic temperatures. The so-called radiation damage can lead to difficulties in data collection and structure solution or even to alterations in the protein structure. Such alterations include:

1. The breaking of disulfide bonds.
2. Reduction in the oxidation stage of metals ions bound to structures.
3. Decarboxylation of Asp and Glu residues.
4. Removal of the methylthio group in Met residues.
5. Removal of the hydroxyl group in Tyr residues.

A strong indicator of radiation damage during data collection is the fading of high-resolution spots. The production of free radicals as a source of radiation damage has led to the use of various radical scavengers during data collection. Radical scavengers include small molecules, such as ascorbic acid, nicotinic acid, and most recently sodium nitrate [6]. However, the actual contribution of radical scavengers in the reduction of radiation damage has recently been questioned and some controversial results have been obtained [7].

To avoid/reduce the risk of radiation damage during data collection, care should be taken to ensure that a complete data set is collected in the minimum possible time and rotation range. Several software packages and data processing programs have options to calculate the best orientation of the crystal after a few images have been autoindexed and they will provide information for:

1. Maximum achievable resolution.
2. Total exposure time for a complete data set.
3. Starting crystal position.
4. Rotation width to avoid overlaps between diffraction spots (*see* **Note 10**).
5. Exposure time per image to avoid overloads at low resolution and to obtain acceptable intensities at the highest-resolution shell.

In addition, the strategy programs output the predicted final statistics of the data set, such as R_{merge}, $I/\sigma(I)$, and completeness.

1.7 Structure Solution

Before the coordinates of the protein atoms in the crystal are determined, an electron density map $\rho(x,y,z)$ throughout the unit cell has to be calculated. The peaks and features of the electron density will provide information about the location of atoms and hence their coordinates. The electron density $\rho(x,y,z)$ is a periodic function and can be described by a Fourier series of the structure factor amplitudes

$$\rho(x,y,z) = \frac{1}{V}\sum_h\sum_k\sum_l |F_{hkl}|e^{-2\pi i(hx+ky+lz)+i\alpha_{hkl}}$$

where $|F_{hkl}|$ are obtained from the intensity of the diffracted beam after application of certain correction factors: ${I_{hkl}}^{1/2} = |F_{hkl}|$. However, the phases α_{hkl} of the scattered beams cannot be measured in a diffraction experiment ("the phase problem"). Consequently, the method to proceed for a structure determination depends on the structural information available for the protein under study. If similar structures (preferably with sequence identity >30%) are available and deposited in the PDB, they can be used for the creation of suitable search models during molecular replacement. If no similar structures are available or the sequence identity is low (the sequence identity is related to the root mean square deviation between structures), the phases have to be determined experimentally. Even the presence of similar structures may not give a straightforward molecular replacement solution and experimental phasing may be more suitable in terms of time and effort.

1.7.1 Molecular Replacement

In molecular replacement (MR), initial phases are obtained from a structure of a homologous protein deposited with the PDB. The method is based on the observation that homologous proteins are structurally similar [8]. The procedure involves the placement of the known structure into the correct position in the crystal of the protein whose structure is unknown [9]. Molecular replacement is carried out in two separate and consecutive three-dimensional searches, known as rotation and translation:

$$M' = [\mathrm{R}]M + T$$

where R the rotation matrix and T the translation vector that have to be applied on the search molecule M to obtain the unknown M'. The two-step search reduces the computation time since only six parameters (three rotation angles and three translations) have to be determined. In case that there are N molecules in the asymmetric unit (*see* **Note 11**), the number of parameters is $6 \times N$.

The search is carried out through the Patterson function, which does not require any prior knowledge of the phases. In the rotation search, the interatomic distances of the search molecule are calculated, and the obtained Patterson function is compared to that of the real crystal (self-rotation function). Once an approximate

orientation of the molecule(s) has been obtained, the known molecule in its new approximate orientation is moved through the unit cell and an R-factor is calculated from the $|F_{\text{calc}}|$ and $|F_{\text{obs}}|$. Other criteria to identify top solutions include the calculation of a correlation coefficient or a Patterson correlation translation function.

1.7.2 Experimental Phasing

In the absence of a suitable model, the phases have to be calculated by experimental methods. Soaking of crystals with heavy atoms has been used until recently in multiple isomorphous replacement, which usually required the measurement of at least three X-ray diffraction data sets, a native and two or more derivatives. However, the possibility to express recombinant proteins with selenomethionine in the place of methionine and the availability of synchrotron radiation beamlines with tunable wavelengths have led to the use of anomalous scattering as a means to determine the phases and solve crystal structures through the multiple-wavelength anomalous dispersion (MAD) method. A single, well-ordered selenium site is sufficient to phase a 25–35 kDa protein and produce an excellent experimental electron density [10]. In recent years, further improvements in instrumentation and data processing have resulted in the use of only one wavelength in a method known as single-wavelength anomalous dispersion (SAD).

Anomalous dispersion or anomalous scattering is based on the scattering of atoms near their absorption edge and arises from resonance between beams of X-ray waves and electronic transitions from bound atomic orbitals. The scattering, in general, is a somewhat complex function consisting of two components: a major component and a minor component. The major component originates from normal Thompson scattering, it has a phase φ dependent on the atom's position and is wavelength independent. The second (minor) component is called the anomalous dispersion and consists of two anomalous scattering factors, one real (f') and one imaginary (f''), which are wavelength dependent. Thus, the radiation scattered by an atom is described by the following equation as a complex number:

$$f = f_0 + f' + if''$$

The imaginary anomalous component is 90° advanced in phase with respect to the real scattering component. In general, the anomalous component is very small, usually no more than 1% or less of the real scattering factor f_0. In some cases, however, it can be significant, leading to considerable changes in the diffraction pattern. The net consequence of the anomalous scattering is the breakdown of Friedel's law with the structure factor amplitudes $|F_{hkl}|$ and $|F_{-h,-k,-l}|$ no longer equal:

$$|F_{hkl}| \neq |F_{-h,-k,-l}|$$

The differences can be very small and within the expected statistical error of most X-ray diffraction experiments. However, careful data collection with high redundancy and optimum X-ray wavelength can provide the required differences for phase measurements.

1.8 Building and Refinement

When initial phases have been obtained, an electron density map will then be calculated. Based on the quality of the electron density map, a model of the protein may be constructed. Automated building is nowadays the first choice in crystal structure determinations. Various programs can incorporate the automated building with a simultaneous update of the structure and refinement to optimize the geometry of the model and its agreement with the experimental data (reflections). During refinement, the three positional parameters x, y, z and the temperature factor B (*see* **Note 12**) of all atoms in the structure are usually adjusted to minimize the following function:

$$E = E_{\text{chem}} + w_{\text{X-ray}}\left(E_{\text{X-ray}}\right)$$

where the stereochemical term E_{chem} is calculated as the difference between the values calculated from the model and the corresponding ideal values obtained from small molecules and peptides. The crystallographic term is calculated from the difference between the experimental structure factor amplitudes ($|F_{\text{obs}}|$) and the structure factor amplitudes calculated from the model ($|F_{\text{calc}}|$). An optimized weighting $w_{\text{X-ray}}$ of the X-ray terms relative to the geometric restraints has to be applied. Without the weighting term, the refinement could push the atoms to an unreasonable position in regard to geometry at medium resolution. However, at atomic resolution, for example, 1.0 Å, the electron density map will be able to give a more precise geometry of the structure. The crystallographic R-factor (R_{cryst}) has been routinely used to monitor the progress of the refinement:

$$R_{\text{cryst}} = \frac{\sum(|F_{\text{obs}}| - k|F_{\text{calc}}|)}{\sum|F_{\text{obs}}|} \times 100\%$$

It has been found, however, that the R_{cryst} could easily reach low values without improvement of the structure. Notably, some structures initially reported with low R_{cryst} were later discovered to be incorrect. For this reason, an additional calculation, namely, the free R-factor or R_{free}, was introduced in 1992 [11]. The calculation of R_{free} is the same as that of R_{cryst} with the key difference that only a subset (usually 5–10% of the total reflections) is used in the R_{free} calculations; these reflections are left aside during refinement; thus, the refined model can never "see" them. R_{free} values are typically higher than those of the R_{cryst}. The spread between R_{cryst} and R_{free} varies, but it is generally between 2% and 6% for well-refined

structures [12]. In higher/atomic resolution structures, the gap is smaller as the quality of the structures is improved. An increase in the gap indicates that either the quality of the model has deteriorated or the refinement strategy is incorrect.

1.9 Analysis and Validation of the Structure

A successful crystal structure determination will lead to a protein model that needs to satisfy certain quality criteria. Validation has become an important issue in structural biology following the realization that some early structures contained serious errors [13]. In addition, several recent cases of data fabrication have raised serious concerns in the structural biology community. Refinement and molecular graphics programs offer a variety of diagnostics to identify problematic regions in the protein for further inspection before deposition to the PDB. Among the most important indicators are:

1. (phi, psi) plot.
2. Standard deviation of bond lengths and bond angles.
3. R_{cryst} and R_{free} and their difference.
4. Average temperature factors for main-chain atoms, side-chain atoms, and water molecules.
5. Plot of temperature factors versus residue number.
6. Electron density correlation for each residue.
7. Coordinate error.
8. Clashscore.

New tools and guidelines for validation have been recently suggested [14], while several programs such as MOLPROBITY [14]and POLYGON [15] have been in use to improve the quality of the final structures.

2 Materials

2.1 Protein Preparation for Crystallization

1. Protein >95% pure.
2. Millipore Amicon ultracentrifugal filter units.
3. Centrifuge.
4. Falcon tubes.
5. Exchange buffer solution (e.g., Tris–HCl: 10 mM, pH: 8.0; HEPES: 10 mM, pH: 7.0). All buffers are stored at 4 °C.
6. Dithiothreitol solution (stored in aliquots of 0.2 mL at −20 °C as 1-M solutions).
7. Ice.

2.2 Initial Crystallization Screening

1. Concentrated protein solution >95% pure.
2. 96-well Corning crystallization microplates.
3. Optically clear adhesive sealing sheets.
4. Multichannel electronic pipette (0.2–2.5 μL).
5. Mettler Liquidator or a multichannel pipette (20–200 μL).
6. Styrofoam box filled with ice.
7. Crystallization screen with 96 solutions in deep-well blocks (*see* **Note 13**). The screen is stored at 4 °C.
8. Light stereomicroscope.
9. Eppendorf centrifuge.

2.3 Scale-Up of Crystallization

1. 24-well Linbro-style XRL plates.
2. Siliconized coverslips (square, 22 mm × 22 mm).
3. Modeling clay.
4. High-vacuum silicon grease.
5. Light stereomicroscope.
6. Gilson Microman pipette.

2.4 Cryoloop Mounting, Crystal Characterization, Data Collection

1. Ready-to-use cryoloops of various sizes (typically 0.1–0.4 mm) mounted on magnetic sample holders, preferably SPINE compatible for easy use in synchrotrons and robot mounting (*see* **Note 14**).
2. Various cryoprotectants (*see* **Note 6**).
3. Cryoprotectant solutions. Prepare each solution by mixing a suitable concentration of cryoprotectant (e.g., glycerol) with the mother liquor. A 20% v/v glycerol concentration is usually a good starting point.
4. Monochromatic X-ray beam, either from an in-house generator or synchrotron.
5. A goniostat equipped with a goniometer head for rotation of the crystal about a single axis during exposure.
6. A magnetic base fitted to the goniometer head for the easy attachment of the magnetic sample holder carrying the cryoloop.
7. A cryogenic cooling device for crystal cryoprotection.
8. A detector system.
9. XDS data processing software (freely available) (*see* **Note 15**) to measure intensities and their standard deviations from diffraction images [16].

2.5 Molecular Replacement

1. Linux workstations.
2. Internet access.

3. CCP4 suite, which includes many programs for all steps of a crystal structure determination (freely available) [17].
4. CCP4i2 GUI (the interface for the CCP4 suite of programs) [18].
5. PHASER for molecular replacement (freely available) [19].
6. COOT molecular graphics program for visualization of the structure/map and rebuilding (freely available) [20].

2.6 Experimental Phasing with Br-SAD

1. NaBr solution (5-M stock solution in water, prepared fresh).
2. Cryoprotectant solution.
3. Data processing software (XDS).
4. Tunable synchrotron beamline.
5. PHENIX package [21]for phasing and structure determination.

3 Methods

3.1 Protein Preparation for Crystallization

For crystallization, a protein concentration of approximately 10 mg/mL is ideal and preferable. However, this might not be achievable for several reasons, such as limited amount of protein expressed and solubility problems. Protein concentrations >5 mg/mL can be used and in difficult cases >2 mg/mL can also be useful.

1. Fill the filter with buffer. Avoid phosphate buffers as they interfere with crystallizations. Rinse the tube by spinning it down for a few minutes in fast cooling mode (4 °C) in the presence of water or exchange buffer. Use only one filter unit and do not split the protein in different filter units. The protein and the buffer should be kept on ice all the time.
2. If the protein contains free cysteines, add 1 mM of dithiothreitol (DTT) to the buffer solution to avoid the formation of disulfide bonds that may cause your protein to precipitate.
3. Add the protein sample into the filter unit. If the sample volume is large, add the protein sample in aliquots. Spin down to remove the original buffer and reduce the volume of the protein solution to ~0.2 mL. Add the remaining protein sample and repeat.
4. Next, add an appropriate amount of exchange buffer (~1 mL).
5. Centrifuge the filter unit at 4 °C for 15–45 min. Adjust the centrifugation time according to how fast the solution goes through the filter.
6. After each run, add a new volume of buffer. Always keep the flow-through in a Falcon tube until you are sure that there is no any leak in the filter. Repeat the process for 3–4 times.

7. To avoid clogging of the filter, carefully mix the protein solution using a pipette between spins.
8. After the concentration is finished, measure the new concentration.

3.2 Crystallization Screen

1. Pipette as much of the sample as you need to an Eppendorf tube. One screen with 96 conditions will require about 90 μL of protein.
2. Spin down the Eppendorf tube to separate precipitation and to remove dust particles from the protein solution.
3. Clean the crystallization plate using pressurized air before any pipetting.
4. Add 50 μL of screening solution to each well using a multichannel pipette or Liquidator 96 (Mettler Toledo).
5. Each well has a letter and a number written on the plate's edges. Always start from A1. The wells should be arranged as follows: A1–A12: solutions 1–12; B1–B12: solutions 13–24; C1–C12: solutions 25–36; and so on.
6. Pipette 0.75 μL of the protein to each subwell. Next, add an equal amount of solution from each well to the protein drop using a multichannel electronic pipette (*see* **Note 16**).
7. Put an adhesive transparent sheet on top of the plate. Press the adhesive sheet firmly to ensure a complete seal.
8. Place the plate in a 16 °C refrigerator. New plates should be placed in between old plates whose temperature is already at 16 °C to avoid condensation problems.
9. Check the plate using a light stereomicroscope (40×) after 2, 8, 24, 48 h, 3 days, 1 week, 2 weeks, 3 weeks, and then once every month. Automated imaging systems can also be used to inspect the crystallization screening plates in regular intervals. Photographs of the drops are taken and stored in a database.
10. Do not keep the plates outside for a long time. Up to 5 min are enough to observe all the subwells in a plate. Longer times outside the incubator can disturb the crystallization process and disrupt crystal growth.

3.3 Scale-Up and Optimization

1. Prepare the stock solutions needed for each condition to be used. Suitable conditions are found during the initial screening. For optimization, different pHs, concentrations of salts and PEGs, and temperatures may be needed.
2. Calculate the amount of salt, buffer, precipitant, and water needed for each well.
3. Put a small amount of modeling clay on each corner of the plate.
4. Grease the rims of the wells.

5. Pipette the solutions. Always start from the A1 well. First add water and leave volatile solutions (such as organic solvents) for the end. For viscous fluids, such as PEG 4000, use a special pipette, such as the Gilson Microman.
6. Mix the solutions by placing the plate on a plate shaker for a few minutes.
7. Pipette a suitable amount (1.5–3 μL) of protein onto a siliconized coverslip. After that, pipette an equal amount of precipitant solution from the well onto the protein drop. Use the same pipette tip for a single coverslip.
8. Carefully place the coverslip on top of the well, so the drop hangs above the well solution.
9. Make sure the well is airtight by pressing the coverslip with a plastic tip, so it is firmly attached to the grease. Do not press the middle of the coverslip because it might break.
10. After the coverslips are ready, place the cover over the plate and fix it tightly with the modeling clay.
11. Store the plate in the 16 °C refrigerator. Place it in between other plates to avoid condensation on the coverslips.
12. Examine the drops for crystals under a light stereomicroscope after 2, 8, 24, 48 h, 3 days, 1 week, 2 weeks, and then once every month.

3.4 Cryoloop Mounting

1. Check that the X-ray generator is working and the cryostream nozzle is in the right position using a nozzle alignment pin. This will ensure that the crystal remains in the coldest part of the stream to prevent ice formation. Make sure there is enough space around the goniometer head. If not, move the beam stop and the detector away.
2. Test the cryoprotectant solution. Dip a nylon cryoloop into a drop of the cryoprotectant solution and place the loop in the goniometer head for flash cooling by the stream of gaseous N_2. If a white cloud appears inside the loop, the concentration of the cryoprotectant is low. A much safer method is to take a short exposure and inspect the diffraction image for ice rings at 3.897, 3.669, 3.441, 2.671, and 2.249 Å resolution.
3. Observe the crystals and compare the size of the loop with the size of the crystals. Select the appropriate loop size depending on the size of the crystal.
4. Mark the wells that have crystals you want to use. Next, remove the cover of the crystallization plate and gently detach the coverslip that contains the crystal/s to be tested.
5. Place 2 μL of the cryoprotectant solution close to the drop with the crystal/s.

6. Scoop a single crystal up with the loop so that the crystal is placed inside the loop. Next, dip the loop with the crystal into the cryoprotectant solution for a few seconds and then mount it quickly on the goniometer head to flash cool the crystal in the cryostream (100 K).
7. Align the crystal in the X-ray beam using a goniometer key.
8. Move the beamstop back.
9. Put the crystallization plate with the remaining crystals back into the incubator.
10. Start collecting data and inspect carefully the first images. Adjust the data collection parameters, such as exposure time, crystal-to-detector distance (resolution), and rotation range for overlaps. Run data collection optimization programs (e.g., BEST [22]; http://www.embl-hamburg.de/BEST) to decide the optimum strategy.
11. Start data processing as soon as possible so that problems with the data can be identified at the early stages of data collection and corrected (e.g., change of the crystal). An XDS input file is provided (Fig. 7a). If the space group is not known, the SPACE_GROUP_NUMBER should change to 0 and the UNIT_CELL_CONSTANTS can either be replaced with 6 zeros or the line is commented out with an exclamation mark. The program will then automatically determine the space group.
12. Inspect the output file (CORRECT.LP) for data processing statistics (Fig. 7b).
13. Convert the measured intensities to structure factor amplitudes using XDSCONV as part of the XDS suite. The program will use the French and Wilson method [23] for the conversion and it will create a new file with the suffix .mtz.

3.5 Molecular Replacement (MR)

Before you start, check the completeness and quality of your data. High-resolution data would greatly help in cases where the solution is unclear.

1. Get the coordinates of a homologous protein from the PDB (http://www.rcsb.org; http://www.ebi.ac.uk/pdbe).
2. Start the CCP4i2 in your Linux workstation. If you use CCP4i2 for the first time, you have to set up a project. The project can have the name, for example, of the protein or the dataset.
3. When the interface starts, you select the project you have already set up from the drop-down menu (Projects) of the top bar.
4. Select "Bioinformatics including model preparation for Molecular Replacement" from the task menu and choose

```
MAXIMUM_NUMBER_OF_PROCESSORS=8
DETECTOR=MARCCD MINIMUM_VALID_PIXEL_VALUE=0      OVERLOAD=65000
DIRECTION_OF_DETECTOR_X-AXIS= 1.0 0.0 0.0
DIRECTION_OF_DETECTOR_Y-AXIS= 0.0 1.0 0.0
ROTATION_AXIS= 1.0 0.0 0.0
INCIDENT_BEAM_DIRECTION=0.0 0.0 1.0
POLARIZATION_PLANE_NORMAL= 0.0 1.0 0.0
FRACTION_OF_POLARIZATION=0.90
TRUSTED_REGION=0.0 0.99
NX=2048 NY=2048 QX=0.079092 QY=0.079092
ORGX=1025.008850 ORGY=1017.802053
DETECTOR_DISTANCE= 165.65
X-RAY_WAVELENGTH=0.900         !Angstroem
OSCILLATION_RANGE= 0.5
STARTING_ANGLE= 0.0
STARTING_FRAME= 1
SPACE_GROUP_NUMBER=20
UNIT_CELL_CONSTANTS=50.454   96.923   89.406   90.000   90.000   90.000
NAME_TEMPLATE_OF_DATA_FRAMES= GSTD9_BR_1_???.mccd DIRECT TIFF
DATA_RANGE= 25 700
SPOT_RANGE= 25 50
BACKGROUND_RANGE= 25 50
JOB= XYCORR INIT COLSPOT IDXREF DEFPIX INTEGRATE CORRECT
FRIEDEL'S_LAW=FALSE
```

SUBSET OF INTENSITY DATA WITH SIGNAL/NOISE >= -3.0 AS FUNCTION OF RESOLUTION

RESOLUTION LIMIT	NUMBER OF REFLECTIONS OBSERVED	UNIQUE	POSSIBLE	COMPLETENESS OF DATA	R-FACTOR observed	R-FACTOR expected	COMPARED	I/SIGMA	R-meas	Rmrgd-F	Anomal Corr	SigAno	Nano
5.27	17308	2642	2695	98.0%	1.7%	1.9%	17308	81.21	1.9%	1.0%	97%	7.018	1223
3.80	29216	4565	4572	99.8%	1.9%	1.9%	29216	83.29	2.1%	1.1%	92%	4.334	2187
3.12	35611	5703	5763	99.0%	2.3%	2.2%	35611	66.77	2.5%	1.5%	84%	3.063	2748
2.71	44335	6839	6839	100.0%	3.1%	3.4%	44335	46.95	3.4%	2.2%	76%	2.392	3324
2.43	50149	7759	7760	100.0%	4.8%	5.3%	50149	32.35	5.2%	3.6%	65%	1.843	3784
2.22	45644	7734	8578	90.2%	6.8%	6.4%	45644	25.53	7.5%	6.4%	71%	2.010	3748
2.06	58927	9192	9235	99.5%	9.8%	10.3%	58927	17.36	10.7%	8.2%	36%	1.175	4499
1.93	60282	9464	10037	94.3%	15.8%	16.3%	60282	11.28	17.2%	14.7%	25%	0.999	4615
1.82	53326	9459	10619	89.1%	22.2%	21.2%	53084	7.97	24.5%	23.3%	32%	1.076	4429
total	394798	63357	66098	95.9%	4.4%	4.5%	394556	32.94	4.8%	5.6%	66%	2.081	30557

Fig. 7 Data processing with XDS. (**a**) Basic information for the input file. The appropriate input file should be chosen depending on the type of the detector used for data collection. In the provided example, a CCD detector has been used. In automated implementations of XDS (e.g., in CCP4i2 as an option in the xia2 expert system of data processing [45]), all required information is extracted from the header of the first image in a data set. (**b**) Excerpt from the output. Information needed to assess the quality of the data set and the anomalous signal is underlined in red. R_{meas} is the $R_{r.i.m}$ (*see* **Note 9**)

SCULPTOR [24] to create a search model (Fig. 8). Residues that are not aligned in the two structures (gaps) are removed. Nonidentical residues are truncated to Cβ atoms and the coordinates of the resultant model are written out in a new .pdb file.

5. Check how many molecules are most likely present in the asymmetric unit using the program MATTHEWS_COEFF available through the task menu of the CCP4i2 (Reflection data analysis).

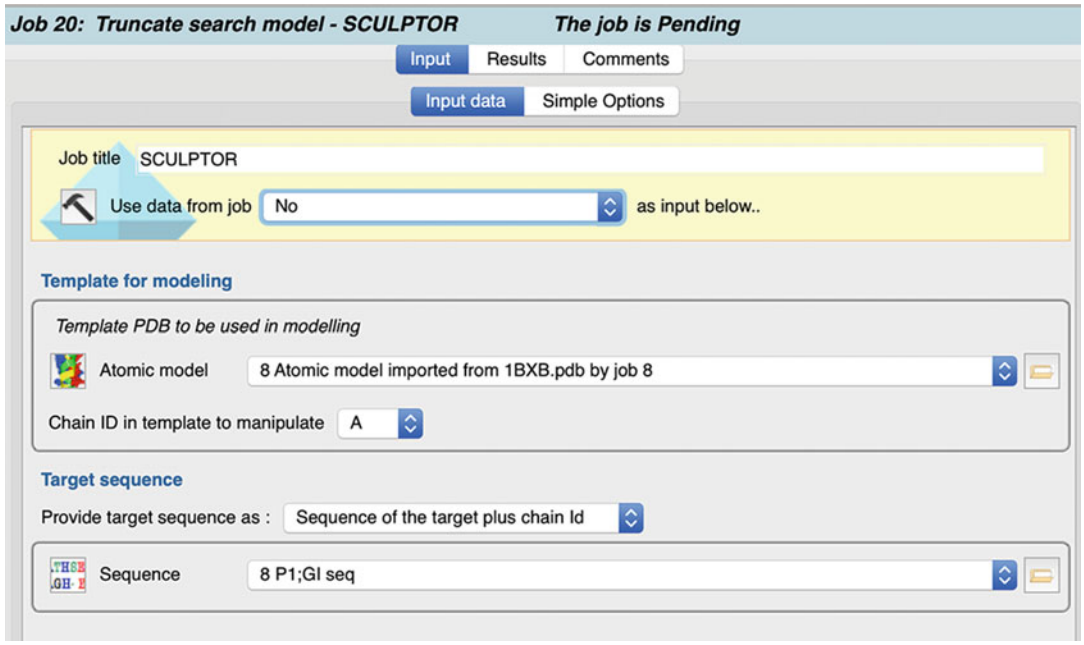

Fig. 8 Input for SCULPTOR. The PDB of the template structure and the target sequence are entered

6. Start PHASER from the CCP4i2 using the basic molecular replacement protocol (*see* **Note 17**). A new window appears (Fig. 9) and necessary information is entered:
7. The experimental data (diffraction measurements, i.e., the .mtz file from data conversion).
8. The number of molecules in the asymmetric unit and the sequence of your protein (as "Composition of the asymmetric unit").
9. The modified pdb file of the known structure (output file from SCULPTOR) (in the "Search model" section of the input).
10. Sequence identity (in the header of the modified coordinates file) with your protein (sequence identity is related to the root mean square deviation of the coordinates = how different the structures are expected to be).
11. Run PHASER from the CCPi2 to find the position of the 2 molecules in the provided example.
12. PHASER outputs the coordinate file of the best solution and a new reflection file with suffix .mtz that contains the original experimental structure factor amplitudes, their standard deviations, and phasing information. Coordinates for the 2 molecules will be present in the output .pdb file.

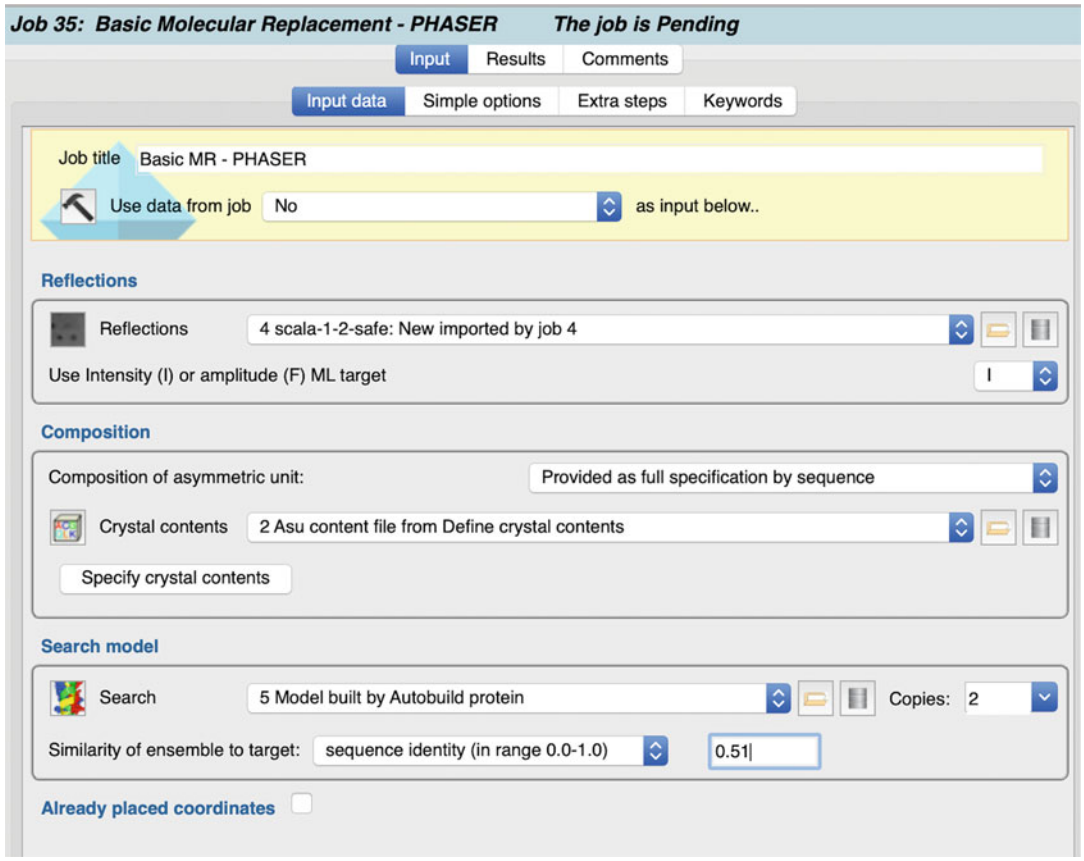

Fig. 9 Molecular replacement with PHASER. The input required is shown. In this example, the search will be carried out for 2 copies of the same protein in the asymmetric unit. The search model has 51% sequence identity with the target sequence and it has been created using SCULPTOR

13. Check the *Z*-score values in the log file (*see* **Note 18**). A *Z*-score > 6 indicates a possibly correct solution with the higher the *Z*-score, the better (*see* **Note 19**).
14. Start the molecular graphics program COOT to display the molecules and the electron density map. The .pdb and .mtz files written out by PHASER are loaded onto COOT.
15. Check the quality of the MR solution (*see* **Note 20**). Since a truncated model was used, you should be able to see electron densities for side-chains if the solution is right. Bulky residues, such as Phe/Trp or strong scatterers, such as the sulfur atom in Met and Cys residues should stand out. The packing of the molecules is another indicator of the correctness. A good MR solution should show no serious clashes between symmetry-related molecules.
16. After an initial solution has been obtained (*see* **Note 21**), the next step is to build as much of the structure as possible and to

start refinement. A safe procedure is to employ programs such as ARP/wARP [25]or BUCCANEER [26] for automated building (*see*, however, **Note 22**). Nevertheless, visual inspection is always necessary as mistakes can happen. Alternate cycles of manual rebuilding and refinement (e.g., REFMAC in CCP4) will improve the structure and lead to the final refined model.

3.6 Experimental Phasing with Br-SAD

1. Transfer a single crystal to a reservoir solution supplemented with 1-M NaBr.
2. Leave the crystal for 30 s to 1 min in the solution (you may need to try different times).
3. Transfer the crystal to the cryoprotectant solution. If the crystal is stable in the cryoprotectant solution, it can be transferred directly to a cryoprotectant solution containing 1-M NaBr.
4. If the cryoprotectant solution contains no NaBr, leave the crystal for 2 s in the cryoprotectant solution before flash-freezing in liquid nitrogen.
5. Collect data at 0.9-Å wavelength to get the anomalous signal from Br.
6. Process the data with XDS and use FRIEDEL'S LAW=FALSE. The data processing statistics could give an indication of the existence of anomalous signal owing to Br ions (Fig. 7b). High redundancy is required for accurate measurement of the anomalous signal.
7. Start PHENIX and from the GUI choose the Autosol option to locate the Br positions and obtain experimental phases (Fig. 9).
8. Examine the initial map, Br sites, and the density-modified map. All calculated maps and coordinate files can be loaded onto COOT through the GUI of PHENIX (Fig. 10).

4 Notes

1. Thrombin, Factor Xa, enterokinase, and TEV protease are among the most common proteases for the removal of tags, provided appropriate cleavage sites are present in the expressed construct.
2. New approaches to improve chances of getting crystals include the thermal stability assay [27] to estimate the crystallization likelihood of biological samples and recently in situ proteolysis [28].
3. Laboratory (in-house) X-ray sources are usually rotating anodes with a Cu or Mo target. Electrons produced by a heated

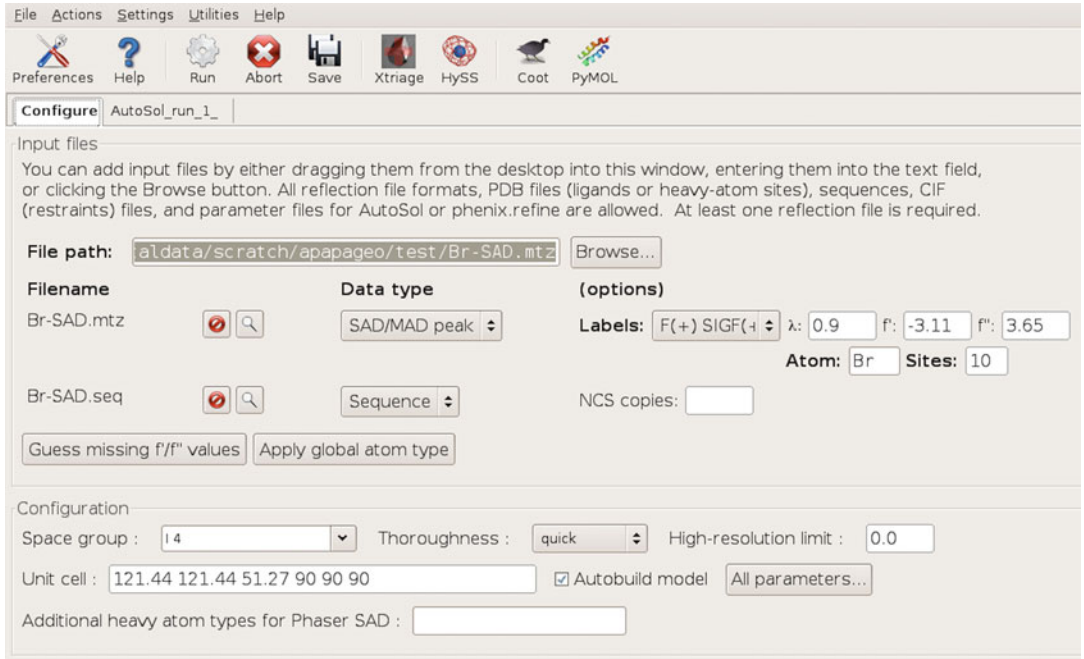

Fig. 10 Br-SAD with PHENIX. The required input is shown. In this example, automated building of the structure will be carried out after the initial phases have been calculated

tungsten filament are accelerated through a high potential toward the target. On collision with the target, the electrons are decelerated and X-rays are emitted. Synchrotrons are large infrastructures that produce electromagnetic radiation from far-UV to hard X-rays by an accelerated electron or positron beam that travels at relativistic speeds inside a storage ring. Bending magnets change the direction of the beam while insertion devices such as undulators and wigglers are used to produce more intense radiation. A key advantage of the synchrotron radiation compared to the laboratory sources is its wavelength tunability, which is needed for anomalous scattering experiments. In-house X-ray sources can also be used for anomalous scattering experiments but only for certain heavy atoms, such as zinc, iodine, and sulfur [29].

4. Strong colors under the light microscope using a polarized filter are an indication of salt crystals. The presence of zinc, calcium, or magnesium salts increases the chances of salt crystal formation. Traces of those metal ions could also be carried over from the purification steps. In case there are a few crystals available, other methods to test if the crystal is made of protein or salt include:
   (a) Running of an SDS-PAGE gel. The crystals should be washed first with the crystallization buffer several times

to ensure the complete removal of the protein from the solution.

(b) Staining of the crystals with specific dyes, such as the IZIT crystal dye (Hampton Research).

(c) Breaking the crystals with a needle. Salt crystals are hard to break in contrast to protein crystals that are soft and disintegrate easily even with a smooth touch of the needle.

(d) Mass spectroscopy using washed crystals.

(e) PX-scanner (Agilent Technologies) for in situ protein–crystal screening. The crystals are exposed to X-ray beam while they are still in the crystallization plate. In this case, the crystals remain undisturbed without being transferred outside the drop. A low-cost crystallization jig that can be attached to existent X-ray diffraction systems has also been developed [30].

5. The use of cryogenic temperatures is almost always the first choice as mounting a crystal in a loop is easier than in a capillary. In addition, if the crystal diffracts well, data collection can continue with the same crystal in order to obtain a full data set. The crystal can also be cryopreserved for high-resolution data collection, for example, in a synchrotron.
6. Some common cryoprotectants include glycerol, sorbitol, trehalose, sucrose, PEG 400, Paratone-N, and type NVH high-viscosity immersion oil.
7. Several techniques can be used to identify problems with the protein preparation when crystallizations have failed:
   (a) Protein stability: Differential scanning calorimetry [31], circular dichroism [32], thermal shift assay [27].
   (b) Protein purity: SDS-PAGE, size-exclusion chromatography, mass spectrometry [33].
   (c) Monodispersity, aggregation state: Size-exclusion chromatography/Multiangle laser light scattering [34], analytical ultracentrifugation [35].
   (d) Protein identification, post-translational modifications: Mass spectrometry [36].
   (e) Conformational state: Dynamic light scattering [37], analytical ultracentrifugation.
8. The charge-coupled detectors (CCDs) used for many years as a workhorse in synchrotron beamlines for data collection have now been replaced. New detectors, such as the PILATUS 6 M, which use two-dimensional hybrid pixel array technology, are now in use. These detectors have certain advantages compared to the old CCDs, including an essentially zero read-out time (i.e., in milliseconds range) and a superior signal-to-noise ratio.

More recently, the EIGER detectors, a new generation of pixel-array detectors, have been developed. Compared to PILATUS, the EIGER detectors features a smaller pixel size (75×75 μm), a shorter dead time (as low as 3.8 ms), a higher frame rate (up to 3000 Hz), and a fast 40 Gbit s^{-1} readout [38]. The combination of higher frame rates and shorter dead time allows the collection of high-quality data sets in a shorter time compared to PILATUS.

9. The quality of the data set is measured by several quality indicators [39], and two of them are as follows:

$$R_{\text{merge}} = \sum_{hkl}\sum_{i}\left|I_i(hkl) - \overline{I(hkl)}\right| / \sum_{hkl}\sum_{i}|I_i(hkl)|$$

$$R_{\text{r.i.m}} = \sum_{hkl}[N/(N-1)]^{1/2}\sum_{i}\left|I_i(hkl) - \overline{I(hkl)}\right| / \sum_{hkl}\sum_{i}|I_i(hkl)|$$

where R_{merge} the merging R-factor, $R_{\text{r.i.m}}$ the redundancy-independent merging R-factor (known also as R_{meas}), and N the redundancy of the data set. $I_i(hkl)$ is the ith observation of reflection hkl and $\overline{I(hkl)}$ is the weighted average intensity for all observations i of reflection hkl. Recently, a new statistic, CC$*$, was proposed to help in deciding which data could be used to improve model quality [40]. Special care should be taken in case that the crystals exhibit twinning problems. Identification of twinning could be done during data processing and analysis of the intensity distributions [41].

10. The spot overlapping depends on several parameters, including the beam cross section, the unit cell dimensions, the crystal size, the pixel size of the detector, the mosaicity of the crystal, and the crystal-to-detector distance. If the unit cell has a long axis, it is advantageous to mount the crystal in a way that the long axis is almost parallel to the rotation (spindle) axis. This setup, however, can be difficult with the use of cryoloops where the orientation of the crystal is hard to be dictated.

11. Calculation of the Matthews coefficient gives an estimation of the number of molecules in the unit cell. As proposed by Matthews in 1968 [42], the ratio V_{m} between the asymmetric unit volume (the unit cell volume divided by the number of the asymmetric units) and the molecular mass of the protein in the asymmetric unit is usually between 1.75 and 3.5 Å^3/Da. There are, however, cases of highly hydrated protein crystals (more than 70% hydration), and this calculation needs to be taken with caution as the V_{m} could be between 3.5 and 5.0 Å^3/Da. Accurate measurement of the Matthews coefficient can be carried out using density measurements of the protein crystals.

12. The temperature factor B provides a measure of the displacement of an atom from its mean position (also called atomic displacement factor):

$$B = 8\pi^2\overline{u}^2$$

where $\overline{u}^2$ the mean square displacement of the atomic vibration. If the vibration is the same in all directions, it is called isotropic.

13. Various commercial crystallization screens are available (e.g., INDEX from Hampton Research: http://www.hamptonresearch.com; JCSG-*plus* from Molecular Dimensions: http://www.moleculardimensions.com; the PACT suite from Qiagen: http://www.qiagen.com).

14. In SPINE-compatible sample holders, the length from the base to the loop is 22 mm. Check beforehand with the staff of the beamline, which sample holders are acceptable.

15. Documentation and further information on main programs mentioned here can be found at the following links: XDS: http://strucbio.biologie.uni-konstanz.de/xdswiki/index.php/Xds; CCP4: http://www.ccp4.ac.uk; PHASER: http://www.phaser.cimr.cam.ac.uk/index.php/Phaser_Crystallographic_Software; PHENIX: http://www.phenix-online.org; COOT: https://www2.mrc-lmb.cam.ac.uk/personal/pemsley/coot/. There are many other programs that can be used but, unfortunately, it is impossible to mention all of them.

16. For small amounts of proteins, the use of protein crystallization robots is recommended, where the protein volumes used could go down to 100 nL per drop.

17. Automated structure solutions using molecular replacement, such as MrBUMP [43], have also been developed and they are available through the CCP4i2.

18. PHASER implements maximum likelihood methods for the phasing of macromolecular crystal structures. The Z-score is computed as the log-likelihood gain (LLG) minus the mean LLG for a random sample of orientations divided by the RMS deviation of a random sample of LLG values from the mean.

19. A reason for an unsuccessful molecular replacement is sometimes the wrong space group. Most MR programs nowadays offer the option to check for alternative space groups of the same point group. The correct space group will show a higher Z-score in PHASER.

20. The success of molecular replacement usually depends on various factors, including:
    (a) completeness and quality of the data,
    (b) accuracy of the search model(s),

(c) number of molecules in the asymmetric unit (for two or more molecules),

(d) completeness of the search model (e.g., poly-Ala vs. full model, flexible regions omitted).

21. Although the success of molecular replacement can be evaluated by several criteria, the initial electron density map should always be inspected. Density for missing side-chains and for expected bound ligands or metals are good signs of a correct solution. A simulated annealing refinement protocol in PHENIX should be carried out as the next step. The *R*-factors (R_{cryst} and R_{free}) should drop below 50%, but if they go higher than 53%, this would be an indication of a wrong solution. The correctness can also be tested with the automated building using ARP/wARP or BUCCANEER.

22. For people new in X-ray crystallography, we strongly recommend that they first try themselves to build the model manually.

References

1. Derewenda ZS (2010) Application of protein engineering to enhance crystallizability and improve crystal properties. Acta Crystallogr D Biol Crystallogr 66:604–615. https://doi.org/10.1107/S090744491000644X
2. Caffrey M (2015) A comprehensive review of the lipid cubic phase or in meso method for crystallizing membrane and soluble proteins and complexes. Acta Crystallogr F Struct Biol Commun 71:3–18. https://doi.org/10.1107/S2053230X14026843
3. Suzuki N, Hiraki M, Yamada Y et al (2010) Crystallization of small proteins assisted by green fluorescent protein. Acta Crystallogr D Biol Crystallogr 66:1059–1066. https://doi.org/10.1107/S0907444910032944
4. Incardona M-F, Bourenkov GP, Levik K et al (2009) EDNA: a framework for plugin-based applications applied to X-ray experiment online data analysis. J Synchrotron Radiat 16:872–879. https://doi.org/10.1107/S0909049509036681
5. Svensson O, Malbet-Monaco S, Popov A et al (2015) Fully automatic characterization and data collection from crystals of biological macromolecules. Acta Crystallogr D Biol Crystallogr 71:1757–1767. https://doi.org/10.1107/S1399004715011918
6. De la Mora E, Carmichael I, Garman E (2011) Effective scavenging at cryotemperatures: further increasing the dose tolerance of protein crystals. J Synchrotron Radiat 18:346–357
7. Kmetko J, Warkentin M, Englich U, Thorne RE (2011) Can radiation damage to protein crystals be reduced using small-molecule compounds? Acta Crystallogr D Biol Crystallogr 67:881–893. https://doi.org/10.1107/S0907444911032835
8. Chothia C, Lesk AM (1986) The relation between the divergence of sequence and structure in proteins. EMBO J 5:823–826
9. Evans P, McCoy A (2008) An introduction to molecular replacement. Acta Crystallogr D Biol Crystallogr 64:1–10. https://doi.org/10.1107/S0907444907051554
10. Joachimiak A (2009) High-throughput crystallography for structural genomics. Curr Opin Struct Biol 19:573–584. https://doi.org/10.1016/j.sbi.2009.08.002
11. Brünger AT (1992) Free R value: a novel statistical quantity for assessing the accuracy of crystal structures. Nature 355:472–475
12. Wlodawer A, Minor W, Dauter Z, Jaskolski M (2008) Protein crystallography for non-crystallographers, or how to get the best (but not more) from published macromolecular structures. FEBS J 275:1–21. https://doi.org/10.1111/j.1742-4658.2007.06178.x
13. Branden CI, Jones TA (1990) Between objectivity and subjectivity. Nature 343:687–689. https://doi.org/10.1038/343687a0
14. Read RJ, Adams PD, Arendall WB et al (2011) A new generation of crystallographic validation tools for the protein data Bank. Structure

19:1395–1412. https://doi.org/10.1016/j.str.2011.08.006
15. Urzhumtseva L, Afonine PV, Adams PD, Urzhumtsev A (2009) Crystallographic model quality at a glance. Acta Crystallogr D Biol Crystallogr 65:297–300. https://doi.org/10.1107/S0907444908044296
16. Kabsch W (2010) XDS. Acta Crystallogr D Biol Crystallogr 66:125–132. https://doi.org/10.1107/S0907444909047337
17. Winn MD, Ballard CC, Cowtan KD et al (2011) Overview of the CCP4 suite and current developments. Acta Crystallogr D Biol Crystallogr 67:235–242. https://doi.org/10.1107/S0907444910045749
18. Potterton E, Briggs P, Turkenburg M, Dodson E (2003) A graphical user interface to the CCP4 program suite. Acta Crystallogr D Biol Crystallogr 59:1131–1137. https://doi.org/10.1107/S0907444903008126
19. McCoy AJ, Grosse-Kunstleve RW, Adams PD et al (2007) Phaser crystallographic software. J Appl Crystallogr 40:658–674. https://doi.org/10.1107/S0021889807021206
20. Emsley P, Cowtan K (2004) Coot: model-building tools for molecular graphics. Acta Crystallogr D Biol Crystallogr 60:2126–2132
21. Adams PD, Afonine PV, Bunkóczi G et al (2010) PHENIX: a comprehensive python-based system for macromolecular structure solution. Acta Crystallogr D Biol Crystallogr 66:213–221. https://doi.org/10.1107/S0907444909052925
22. Bourenkov GP, Popov AN (2010) Optimization of data collection taking radiation damage into account. Acta Crystallogr D Biol Crystallogr 66:409–419. https://doi.org/10.1107/S0907444909054961
23. French S, Wilson K (1978) On the treatment of negative intensity observations. Acta Cryst A 34:517–525. https://doi.org/10.1107/S0567739478001114
24. Bunkoczi G, Read RJ (2011) Improvement of molecular-replacement models with Sculptor. Acta Crystallogr D Biol Crystallogr 67:303–312. https://doi.org/10.1107/S0907444910051218
25. Morris R, Perrakis A, Lamzin V (2003) ARP/-wARP and automatic interpretation of protein electron density maps. Methods Enzymol 374:229–244. https://doi.org/10.1016/S0076-6879(03)74011-7
26. Cowtan K (2006) The Buccaneer software for automated model building. 1. Tracing protein chains. Acta Crystallogr D Biol Crystallogr 62:1002–1011. https://doi.org/10.1107/S0907444906022116
27. Dupeux F, Rower M, Seroul G et al (2011) A thermal stability assay can help to estimate the crystallization likelihood of biological samples. Acta Crystallogr D Biol Crystallogr 67:915–919
28. Wernimont A, Edwards A (2009) In situ proteolysis to generate crystals for structure determination: an update. PLoS One 4:e5094. https://doi.org/10.1371/journal.pone.0005094
29. Dodson E (2003) Is it jolly SAD? Acta Crystallogr D Biol Crystallogr 59:1958–1965
30. Hargreaves D (2012) A manual low-cost protein-crystallization plate jig for in situ diffraction in the home laboratory. J Appl Crystallogr 45:138–140. https://doi.org/10.1107/S0021889811052654
31. Privalov PL (2009) Microcalorimetry of proteins and their complexes. Methods Mol Biol 490:1–39. https://doi.org/10.1007/978-1-59745-367-7_1
32. Kelly SM, Jess TJ, Price NC (2005) How to study proteins by circular dichroism. Biochim Biophys Acta 1751:119–139. https://doi.org/10.1016/j.bbapap.2005.06.005
33. Morgner N, Robinson CV (2012) Linking structural change with functional regulation-insights from mass spectrometry. Curr Opin Struct Biol 22:44–51. https://doi.org/10.1016/j.sbi.2011.12.003
34. Ye H (2006) Simultaneous determination of protein aggregation, degradation, and absolute molecular weight by size exclusion chromatography-multiangle laser light scattering. Anal Biochem 356:76–85. https://doi.org/10.1016/j.ab.2006.05.025
35. Howlett GJ, Minton AP, Rivas G (2006) Analytical ultracentrifugation for the study of protein association and assembly. Curr Opin Chem Biol 10:430–436. https://doi.org/10.1016/j.cbpa.2006.08.017
36. Gheyi T, Rodgers L, Romero R et al (2010) Mass spectrometry guided in situ proteolysis to obtain crystals for X-ray structure determination. J Am Soc Mass Spectrom 21:1795–1801. https://doi.org/10.1016/j.jasms.2010.06.015
37. Papish AL, Tari LW, Vogel HJ (2002) Dynamic light scattering study of calmodulin-target peptide complexes. Biophys J 83:1455–1464. https://doi.org/10.1016/S0006-3495(02)73916-7
38. Casanas A, Warshamanage R, Finke AD et al (2016) EIGER detector: application in macromolecular crystallography. Acta Crystallogr D Struct Biol 72:1036–1048. https://doi.org/10.1107/S2059798316012304

39. Weiss MS (2001) Global indicators of X-ray data quality. J Appl Crystallogr 34:130–135. https://doi.org/10.1107/S0021889800018227
40. Karplus PA, Diederichs K (2012) Linking crystallographic model and data quality. Science 336:1030–1033. https://doi.org/10.1126/science.1218231
41. Parsons S (2003) Introduction to twinning. Acta Crystallogr D Biol Crystallogr 59:1995–2003
42. Matthews BW (1968) Solvent content of protein crystals. J Mol Biol 33:491–497
43. Keegan RM, Winn MD (2008) MrBUMP: an automated pipeline for molecular replacement. Acta Crystallogr D Biol Crystallogr 64:119–124. https://doi.org/10.1107/S0907444907037195
44. Rupp B (2009) Biomolecular crystallography: principles, practice, and application to structural biology. Garland Science, New York
45. Winter G (2010) xia2: an expert system for macromolecular crystallography data reduction. J Appl Crystallogr 43:186–190. https://doi.org/10.1107/S0021889809045701

Chapter 26

Measuring Binding Constants of His-Tagged Proteins Using Affinity Chromatography and Ni-NTA Immobilized Enzymes

Annette C. Moser, Benjamin White, and Frank A. Kovacs

Abstract

Affinity chromatography is one way to measure the binding constants of a protein–ligand interaction. Here, we describe a method of measuring a binding constant using Ni-NTA resin to immobilize a His-tagged enzyme and the method of frontal analysis. While other methods of immobilization are possible, using the strong affinity interaction between His-tagged proteins and Ni-NTA supports results in a fast, easy, and gentle method of immobilization. Once the affinity support is created, frontal analysis can be used to measure the binding constant between the protein and various analytes.

Key words Affinity chromatography, Frontal analysis, Binding constant, Enzyme immobilization

1 Introduction

One method of measuring binding constants of proteins is the use of frontal analysis affinity chromatography [1]. In this method, one portion of the affinity complex is immobilized onto a solid support while varying concentrations of the other component are applied to the column and allowed to bind. Based on the breakthrough volume (or time), the binding constant can be determined [2].

Frontal analysis affinity chromatography has previously been used to determine the binding constants of enzymes [3–7] as well as other affinity interactions including drug–protein binding constants [1, 8] and antibody–antigen binding constants [9]. Multiple methods of immobilization exist and include both covalent and noncovalent methods [3]. For both types of immobilization, it is important to verify the binding activity of the affinity ligand is not compromised [10, 11]. While covalent immobilization methods have the advantage of providing more stable supports, noncovalent methods tend to be gentler and can result in supports with higher activity.

Nikolaos E. Labrou (ed.), *Protein Downstream Processing: Design, Development, and Application of High and Low-Resolution Methods*, Methods in Molecular Biology, vol. 2178, https://doi.org/10.1007/978-1-0716-0775-6_26,

The use of biotin–streptavidin [12–14] and antibody–antigen [14] interactions are common methods of noncovalent site-directed immobilization. Here, we show how noncovalent immobilization using a metal ion support and frontal analysis affinity chromatography can be used to determine an enzyme–substrate binding constant. In this method, a nickel-nitrilotriacetic (Ni-NTA) affinity support was used to immobilize ascorbate peroxidase (APX), a His-tagged recombinant enzyme with a molecular mass of 29 kDa. While the physiological substrate for APX is ascorbate, it has also been observed to oxidize other nonphysiological substrates such as 2,2′-azino-bis(3-ethylbenzothiazoline-6-sulphonic acid (ABTS), guaiacol, and pyrogallol [15]. Using frontal analysis affinity chromatography, we were able to identify the presence of multisite binding in our enzyme substrate system and estimate the binding constant of the system using the method by described by Tweed et al. [16]. Other methods of determining binding constants include ultracentrifugation [17], NMR [18], and affinity capillary electrophoresis [19].

2 Materials

Prepare buffer fresh weekly in ultrapure water (18 MΩ resistivity reading at 25 °C) and store at 4 °C to minimize bacterial growth. Substrate should be prepared fresh daily or at the time of use depending on the sensitivity of substrate to degradation or oxidation. It is recommended that analytical-grade buffer salts and substrates be used.

1. Running Buffer: Prepare a buffer your protein (enzyme) is stable in and that mimics the conditions in which you want to determine the binding constant. The pH needs to be kept sufficiently high in order to keep the protein tightly bound to the Ni-NTA affinity support, typically pH > 7.5 (*see* **Note 1**).
2. Running Buffer with Analyte: Prepare buffered analyte (substrate) solutions in an appropriate range for estimated binding constant (*see* **Notes 2** and **3**).
3. Any column format can theoretically be used but a long narrow column is recommended. For example: Restek (Fisher) 250 × 2.1 mm i.d. × 0.25 in. o.d.
4. Ni-NTA chromatography resin: GE Healthcare Ni Sepharose 6 Fast Flow was used in this method (*see* **Note 4** for another alternative).
5. Chromatography system: The system must have the ability to (a) switch between two solvents, (b) detect at the absorbance of the molecule of interest, and (c) record absorbance over time and output data as text.

6. Affinity ligand: A sufficient quantity of 6×-Histidine-tagged recombinant protein to saturate the resin of the packed column is needed. It should be tested both before and after the binding study for activity with the appropriate assay.

3 Methods

3.1 Packing Affinity Column

There are a number of ways to pack the column that can be used. The following method was found to be effective for packing the small bore (2.1 mm i.d.): Restek column.

1. Mount empty Restek column to a clamp on a ring stand. The column should have the bottom fitting with frit attached.
2. Attach a luer-lock fitting to the bottom of the column along with a 10 mL syringe.
3. Attach the top column fitting *without frit* and attach a luer-lock fitting.
4. Attach a 10 mL syringe body (the syringe without the plunger) to the top luer-lock fitting *see* Fig. 1.

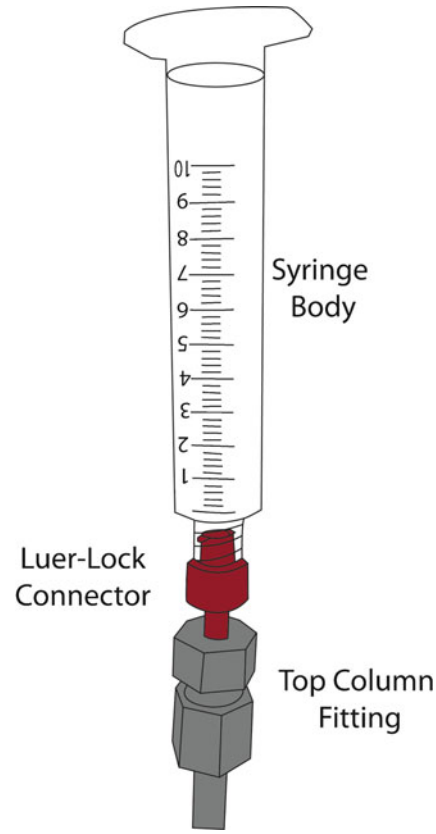

Fig. 1 Syringe reservoir configuration for column loading where syringe body is attached to the top fitting of the column via a luer-lock fitting

5. Add a dilute resin slurry to the top syringe reservoir.
6. Use the bottom syringe to draw resin slurry down into the column with care to keep the resin wet. The dilute resin slurry may be stirred periodically to prevent resin accumulation in the bottom of the top syringe reservoir.
7. Fill column completely with resin. Excess can be removed carefully with a spatula.
8. Attach column to chromatography pump and flow buffer through the column while monitoring pressure to keep the flow rate low below the pressure limit of the resin. The flow rate should be high enough to cause the resin to pack and will be limited by the resin type. The resin used in this protocol allowed for flow rates of 1–3 mL/min and has a pressure limit of 1.0 MPa.
9. Remove the top fitting to check the top of the column resin (*see* **Note 5**).
10. Add additional resin via syringe and needle with gentle suction supplied by the bottom syringe to pull the solution down into the column. Again care must be taken to not allow the resin to dry and air pulled into the resin. Excess resin can be removed by spatula.
11. Repeat **steps 8–10** until the column is packed as indicated by no drop in the top of the resin bed after using the chromatography pump in **step 8**.
12. Attach top fitting *with frit* to column.

3.2 Loading Protein onto Column

1. Desalt your purified protein using either dialysis or desalting column into a small volume of running buffer. In general, this volume is minimized to save time when loading the protein onto the column.
2. Determine the concentration of the desalted protein solution using an appropriate protein concentration assay for your protein. Use this initial concentration to calculate the amount of protein being added to the column.
3. Add protein to column and wash with running buffer while continuously monitoring absorbance. Collect all of the eluent until the absorbance reading returns back to baseline.
4. Determine the protein concentration of the eluent from **step 3** and calculate the total amount of protein eluted from the column using the concentration and volume.
5. Calculate the total immobilized protein on the column by subtracting the amount of eluted from the total amount loaded (*see* **Note 6**).

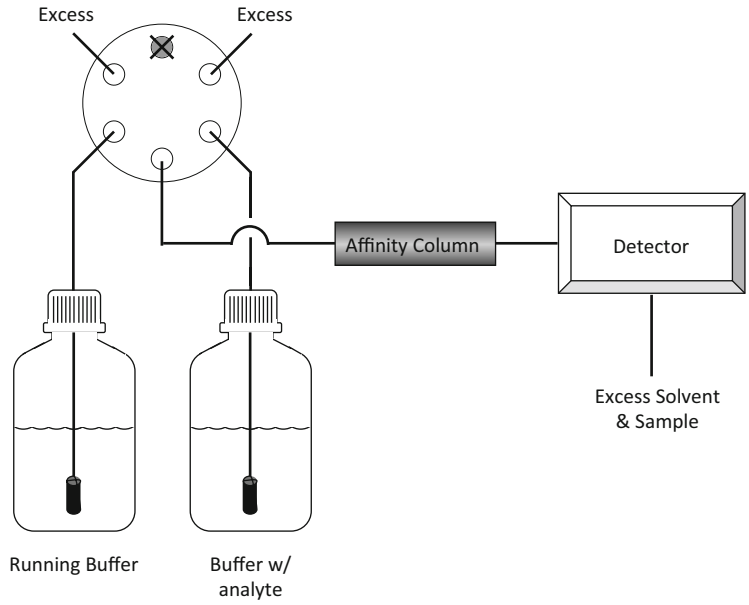

Fig. 2 Typical valve configuration involving two HPLC pumps, a 6-port 2-position valve and a detector

3.3 Frontal Analysis Affinity System

1. Set up the chromatography system as shown in Fig. 2 (*see* **Note 7**).
2. Connect the affinity column and equilibrate it with the running buffer.
3. Set up the operating system to switch the valve at time zero to apply the buffer containing the analyte (substrate) (*see* **Notes 8** and **9**).
4. The absorbance response should increase as the potential binding sites bind the analyte (substrate) and excess analyte is eluted. Eventually, the absorbance will level off and the valve should be switched and the running buffer allowed to flow through the column to reestablish the baseline (*see* **Note 10**).

3.4 Collection of Binding Data

Perform the following steps on the column both before (i.e., the blank column) and after the protein is added. Only the low and high substrate concentrations need to be run on the blank column to see if the column has affinity for the analyte (substrate) (*see* **Note 11**).

1. Equilibrate column with running buffer at a flow rate that does not generate pressure exceeding the limit for the resin.
2. Change flow rate to 0.25 mL/min (*see* **Note 12**).
3. At time zero, switch the valve to allow the substrate buffer to be applied (injected) onto the column while collecting absorbance data at the wavelength appropriate for your substrate.

4. Once the absorbance goes up and completely levels off (*see* **Note 10**), switch back to the running buffer to allow the substrate to dissociate and reestablish the baseline. Flow rate can be increased for washing and equilibration of the column for the next run. Keep the washing and equilibration time consistent between runs (*see* **Note 13**).
5. Repeat **steps 3** and **4** multiple times to collect a series of breakthrough curves at a variety of analyte (substrate) concentrations (*see* **Note 2**).
6. Determine the breakthrough times as described in Subheading 3.6.

3.5 Determining Void Volume of Affinity Column

1. In addition to determining breakthrough times for multiple analyte concentrations, the void breakthrough time of the column must also be determined (*see* **Note 14**).
2. Apply a dilute solution of the chosen non-retained compound.
3. This procedure should be performed on both the blank column (the column prior to adding any protein) and the protein column to ensure the support material does not interact significantly with the affinity ligand (substrate) (*see* **Note 11**).
4. Determine the breakthrough time as described in Subheading 3.6.

3.6 Data Analysis: Midpoint Determination

Data analysis of the binding data can be done using a number of different programs. Here is a simple method using a basic spreadsheet.

1. Import absorbance data into a spreadsheet as two columns, time and response.
2. Plot data so that to visualize the beginning and end of the breakthrough curve (Fig. 3).
3. Estimate the data points for the beginning (I_0) and end (I_N) of the frontal curve from the data and use I_0 and I_N as the baseline and topline values, respectively.
4. Estimate an initial midpoint (I_{MP}) and calculate area before the midpoint by summing the difference between Intensity (I_i) and I_0, starting with I_0 and ending at I_{MP}.

$$\text{Area}_{\text{Before}} = \sum_{i=0}^{\text{MP}} (I_i - I_0) \tag{1}$$

5. Calculate the area after the midpoint by summing the difference between I_N and I_i, starting with I_{MP} and ending with I_N.

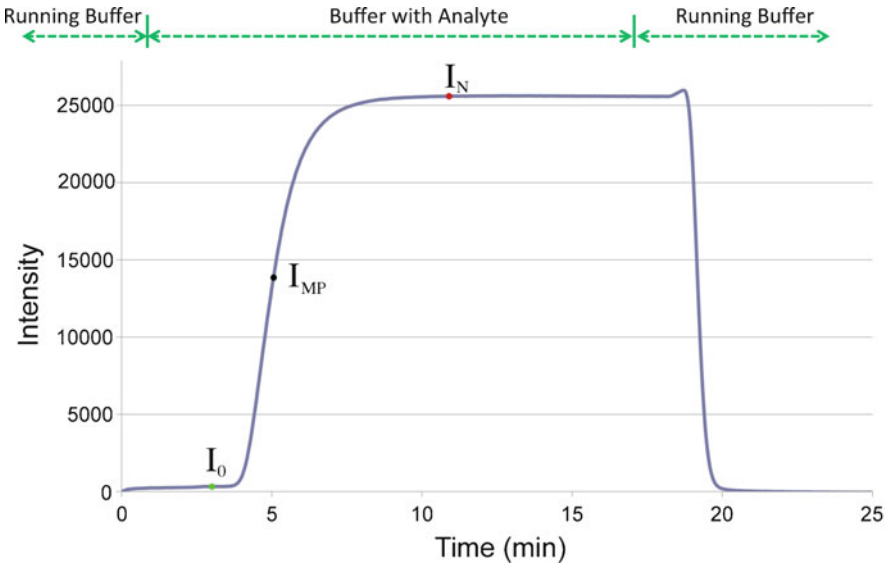

Fig. 3 Sample chromatogram. Shown here is a typical breakthrough curve along with the buffer switching times

$$\text{Area}_{\text{After}} = \sum_{i=MP}^{N} (I_N - I_i) \tag{2}$$

6. The midpoint is then found by finding the value where the absolute value of the difference between $\text{Area}_{\text{Before}}$ and $\text{Area}_{\text{After}}$ is minimized or where $\text{Area}_{\text{Before}} = \text{Area}_{\text{After}}$ (Fig. 4). This can be done by changing the I_{MP} until a minimum value is found for the difference.

3.7 Analysis of Midpoint Data

1. Once the midpoint of all of the substrate concentrations has been determined, a plot of $1/m_{\text{L,app}}$ versus $1/[\text{A}]$ must be constructed. The number of applied moles ($m_{\text{L,app}}$) can be calculated from the concentration, flow rate, and the midpoint time. For single-site binding, the predicted response takes the following form [1]:

$$\frac{1}{m_{\text{L,app}}} = \frac{1}{K_{\text{A}} m_{\text{L}} [\text{A}]} + \frac{1}{m_{\text{L}}} \tag{3}$$

2. If a linear calibration curve results from the plot, the affinity ligand (enzyme) has a single binding site. If the resulting plot is nonlinear (Fig. 5), then multisite binding is indicated (*see* **Note 15**) and the resulting plot takes the following form [16]:

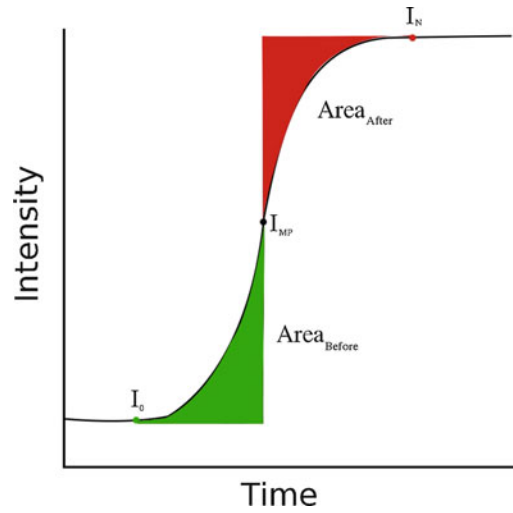

Fig. 4 Midpoint data analysis. Breakthrough curves are rarely symmetric, so identifying the midpoint is ***not*** as simple as finding the time point where the intensity is midway between the lowest (I_0) and the highest (I_N) absorbance readings. A good general method of finding the midpoint of the breakthrough curve is to find the point where the area before and below is equal to the area after and above

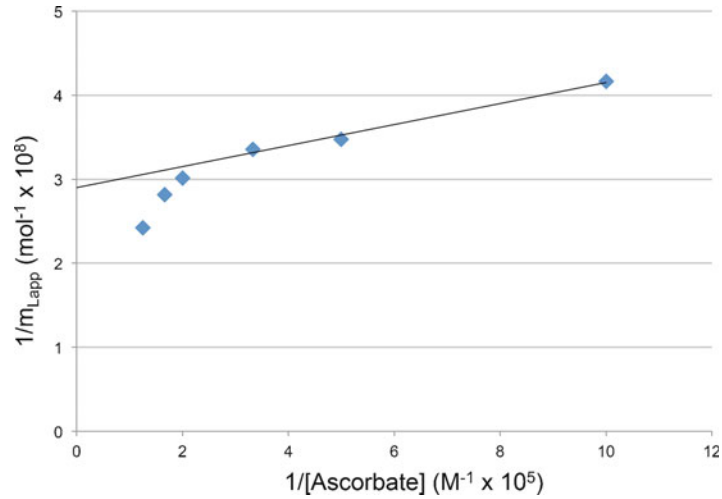

Fig. 5 Frontal analysis plot of APX–ascorbate binding. Note the curvature at the high concentrations (points 1–3), which indicates multisite binding. An estimate (within 10%) of the association constant can be obtained by taking the intercept divided by the slope of the best-fit line of the linear concentration range (i.e., low concentration range). The K_A for APX-ascorbate binding was found to be 2.3 ($\pm$0.3) $\times$ 10^6 M^{-1} in this experiment

$$\lim_{[A]\to 0}\frac{1}{m_{Lapp}} = \frac{1}{m_{Ltot}(\alpha_1+\beta_2-\alpha_1\beta_2)K_{a1}[A]} + \frac{\left(\alpha_1+{\beta_2}^2-\alpha_1{\beta_2}^2\right)}{m_{Ltot}(\alpha_1+\beta_2-\alpha_1\beta_2)^2} \quad (4)$$

where α_1 is the fraction of high-affinity binding sites and β_2 is the ratio of binding site affinity (K_{A1}/K_{A2}).

3. In either case, K_A can be determined by dividing the intercept by the slope. If multisite binding was present, the error in K_A will be less than 10% (*see* **Note 16**) for two binding sites.

4 Notes

1. Typically enzyme–substrate binding constants are measured under physiological conditions. In this protocol, we used a 20 mM potassium phosphate buffer, pH 7.6. When using Ni-NTA agarose resins, the matrix is stable over a wide range of pH (3–12). However, the His–Ni interaction (i.e., protein–resin interaction) will be most stable at pH's > 7.5. Significant protein loss from the column occurs at pH below 6.8.
2. The range of acceptable analyte concentrations used in frontal analysis affinity chromatography is limited by the association binding constant (K_A). To calculate concentrations, which can be used in the frontal analysis study, K_A·[A] should be between 0.1 and 10 to ensure a minimum of a 10% change [1]. For example, if the K_A value is ~5000, the analyte concentrations should be between 20 and 2000 μM. For enzyme–substrate interactions, K_A's are commonly in the range of 10^3 to 10^7 M^{-1}.
3. Generally, it is best to make a large batch of running buffer and then use portions of it to make the analyte containing buffer at the desired concentrations. This keeps the baseline more consistent and allows for a more accurate determination of the breakthrough times.
4. A good alternative to the use of nickel with the NTA resin as the immobilizing metal is cobalt. Initially, the cobalt is bound to the resin as Co^{2+} and allowed to bind the His-tagged protein. Then it is oxidized to Co^{3+} with H_2O_2 where it forms a highly stable and kinetically inert bond to the His-tag [20, 21]. This use of Co^{3+} has been recently demonstrated to be a way to immobilize His-tagged proteins on BLI biosensors with significantly higher stability [22].
5. After applying running buffer through the column, the resin tends to settle. More resin must be added until the column is completely packed for reproducible results.

6. Estimate the amount of protein added to column. In our experiments, approximately 1.0 μmole of APX was added to the column. If the breakthrough times are not significantly different from each other, larger amounts of protein may be necessary (along with a larger amount of stationary phase and a longer column). Another way to enhance the difference in the breakthrough times is the use of a slower flow rate to allow more time for binding to occur.
7. This protocol is designed for relatively weak affinity interactions (e.g., drug–protein interactions and enzyme–substrate interactions). If the affinity ligand–analyte interaction is sufficiently strong (e.g., antibody–antigen interactions), a denaturing buffer may be needed to disrupt the affinity interactions and elute the analyte. If this is the case, the affinity chromatography system will need to be set up so three separate buffers can be applied across the affinity column.
8. If the breakthrough times occur immediately after the analyte buffer is applied to the column, there may not be enough interaction between the affinity ligand and the analyte or an insufficient amount of immobilized protein. The column length and amount of support material can be increased or the flow rate decreased.
9. If changes in the breakthrough curves are visible, but it is difficult to identify the initial baseline of the chromatogram, delaying the valve switch for a minute or two may help in the data analysis. Any delay time must be accounted for when determining the final breakthrough time.
10. It is important to ensure that the peak absorbance fully plateaus to allow for accurate binding constant determination.
11. If the breakthrough times from the blank column vary with concentration, the analyte (substrate) does interact with the support material and breakthrough times for *each* of the concentrations must be determined for both the protein and blank columns. The difference between the protein breakthrough times and the blank breakthrough times can then be used to calculate moles of applied analyte ($m_{L,app}$) (each blank breakthrough time should be subtracted from the corresponding affinity column breakthrough time). The $m_{L,app}$ value can be calculated from the flow rate, concentration of analyte, and the change in breakthrough times.
12. Flow rates in frontal analysis chromatography should be relatively slow to ensure the binding between the affinity ligand and the analyte can occur. In addition, the flow rate can be adjusted based on the resulting breakthrough curves. If the breakthrough curves are too close together for varying concentration, slower flow rates have the ability to separate the

breakthrough curves. If a large shift between breakthrough curves exists, the flow rate can be increased to speed up the chromatography run times. Generally, flow rates between 0.10 and 0.50 mL/min are used for frontal analysis.

13. Once the breakthrough curve has leveled off, the substrate can be washed from the column and the column re-equilibrated with the original running buffer at a higher flow rate than that used for the actual frontal analysis. This is especially useful when doing several runs consecutively. Care should be used to not reach or exceed the maximum pressure for the resin.
14. A commonly used agent to determine void volume is sodium nitrate, but anything that does not interact with the immobilized protein and can be detected can be used. It is important to use a dilute solution of the non-retained compound to ensure the column is not being overloaded. Ideally, the void volume obtained using the non-retained compound is the same volume that was obtained from the blank column.
15. When multisite binding occurs, an estimate of the binding constant can be determined by looking at the linear range obtained from the lowest range of concentrations. This is possible since at very low concentrations, the highest affinity sites are bound first and it is only at high concentrations that secondary binding sites bind the analyte [16].
16. Since we are using a very uniform and gentle method of attachment of the protein to the chromatographic support, we can assume the distribution of the two binding sites is uniform and α_1 is equal to 0.5 and the error associated with the determination of K_{A1} is less than 10% based on the study by Tweed et al. [16].

Acknowledgments

This work was supported by the UNK Summer Student Research Program, the UNK Undergraduate Research Fellows Program, and the UNK Chemistry Department.

References

1. Hage DS (2002) High-performance affinity chromatography: a powerful tool for studying serum protein binding. J Chromatogr B 768:3–30
2. Loun B, Hage DS (1992) Characterization of thyroxine-albumin binding using high-performance affinity chromatography. I. Interactions at the warfarin and indole sites of albumin. J Chromatogr 579:225–235
3. Bertucci C, Bartonlini M, Gotti VA (2003) Drug affinity to immobilized target bio-polymer by high performance liquid chromatography and capillary electrophoresis. J Chromatogr B 797:111–129
4. Zhang B, Palcic MM, Schriemer DC et al (2001) Frontal affinity chromatography coupled to mass spectrometry for screening mixtures of enzyme inhibitors. Anal Chem 299:173–182

5. Nishikata M (1983) Affinity chromatography of chymotrypsin on a sepharose derivative coupled with a chymostatin analogue. J Biochem 93:73–79
6. Kasai K, Ishii S (1978) Studies on the interaction of immobilized trypsin and specific ligands by quantitative affinity chromatography. J Biochem 84:1061–1069
7. Ichinose H, Yoshida M, Kotake T et al (2005) An Exo-β-1,3-galactanase having a novel β-1,3-galactan-binding module from *Phanerochaete chrysosporium*. J Biol Chem 280:25820–25829
8. Hage DS, Anguizola JA, Jackson AJ et al (2011) Chromatographic analysis of drug interactions in the serum proteome. Anal Methods 3:1449–1460
9. Nelson MA, Moser AC, Hage DS (2010) Biointeraction analysis by high-performance affinity chromatography: kinetic studies of immobilized antibodies. J Chromatogr B 878:165–171
10. Kortt AA, Oddie GW, Iliades P et al (1997) Nonspecific amine immobilization of ligand can be a potential source of error in BIAcore binding experiments and may reduce binding affinities. Anal Biochem 253:103–111
11. Wilchek M, Bayer EA (1990) Introduction to avidin-biotin technology. Methods Enzymol 184:5–13
12. Wilchek M, Miron T (1987) Limitations of *n*-hydroxy-succimide esters in affinity chromatography and protein immobilization. Biochemistry 26:2155–2161
13. Turkova J (1999) Oriented immobilization of biologically active proteins as a tool for revealing protein interactions and function. J Chromatogr B 722:11–31
14. Gunaratna PC, Wilson GS (1990) Optimization of multienzyme flow reactors for determination of acetylcholine. Anal Chem 62:402–407
15. Raven EL (2003) Understanding functional diversity and substrate specificity in haem peroxidases: what can we learn from ascorbate peroxidase? Nat Prod Rep 20:367–381
16. Tweed SA, Loun B, Hage DS (1997) Effects of ligand heterogeneity in the characterization of affinity column by frontal analysis. Anal Chem 69:4790–4798
17. Arkin M, Lear JD (2001) A new data analysis method to determine binding constants of small molecules to protein using equilibrium analytical ultracentrifugation with absorption optics. Anal Biochem 299:98–107
18. Fielding L (2007) NMR methods for the determination of protein-ligand dissociation constants. Prog NMR Spectrosc 51:219–242
19. Hage DS, Tweed SA (1997) Recent advances in chromatographic and electrophoretic methods for the study of drug-protein interactions. J Chromatogr B 699:499–525
20. Wegner SV, Spatz JS (2013) Cobalt(III) as a stable and inert mediator ion between NTA and His6-tagged proteins. Angew Chem Int Ed Engl 52:7593–7596
21. Wegner SV, Schenk FC, Spatz J (2016) Cobalt (III) mediated permanent and stable immobilization of histidine-tagged proteins on NTA-functionalized surfaces. Chem Eur J 22:3156–3162
22. Auera S, Azizia L, Faschingerb F, Blazevicc V, Vesikaric T, Gruberb HJ, Hytönen VP (2017) Stable immobilization of his-tagged proteins on BLI biosensor surface using cobalt. Sens Actuators B Chem 243:104–113

Chapter 27

Stabilization of Proteins by Freeze-Drying in the Presence of Trehalose: A Case Study of Tubulin

Pavel Dráber, Vadym Sulimenko, Tetyana Sulimenko, and Eduarda Dráberová

Abstract

Microtubules, polymers of the heterodimeric protein αβ-tubulin, are indispensable for many cellular activities such as maintenance of cell shape, division, migration, and ordered vesicle transport. In vitro assays to study microtubule functions and their regulation by associated proteins require the availability of assembly-competent purified tubulin. However, tubulin is a thermolabile protein that rapidly converts into a nonpolymerizing state. For this reason, it is usually stored at −80 °C or liquid nitrogen to preserve its conformation and polymerization properties. In this chapter, we describe a method for freeze-drying of assembly-competent tubulin in the presence of nonreducing sugar trehalose, and methods enabling the evaluation of tubulin functions in rehydrated samples.

Key words Freeze-drying, Microtubules, Stability, Trehalose, Tubulin

1 Introduction

Freeze-drying (lyophilization), removal of water from biological samples under conditions of low temperature and vacuum, is a widely used technique in the areas of protein purification, protein reagent preparation, and manufacture of protein biomolecules for therapeutic and diagnostic applications. While single-chain proteins with a highly ordered tertiary structure may be freeze-dried with little difficulty, proteins with multiple domains forming protein complexes represent a far more tougher challenge to preserve their binding properties during the freeze-drying procedure [1]. The process of freeze-drying is split into three stages: freezing, primary drying at lower temperature when most of the water is removed, and secondary drying at ambient or higher temperature to minimize the final unbound water content. The theoretical basis of freeze-drying is well-described [2]. Previous studies have shown that sugars with known cryopreservative properties are capable of

Nikolaos E. Labrou (ed.), *Protein Downstream Processing: Design, Development, and Application of High and Low-Resolution Methods*, Methods in Molecular Biology, vol. 2178, https://doi.org/10.1007/978-1-0716-0775-6_27,

protecting proteins under dehydration-induced stress [3, 4]. In particular, the nonreducing disaccharide trehalose (α-D-glucopyranosyl-α-D-glucopyranoside) has a remarkable ability to preserve labile proteins during desiccation [5, 6] and subsequent storage at higher temperature [7]. Trehalose is highly soluble, nonreducing, nonhygroscopic, and belongs to the chemically most unreactive sugars [8, 9]. The favorable stabilization effect of trehalose during freeze-drying and prolonged storage at ambient temperature was documented for various proteins [10], including tubulins [11], the building components of microtubules, which represent dynamic polymers essential for many cellular functions.

Microtubules usually consist of 13 laterally associated protofilaments forming a cylinder with external diameter about 25 nm. Each protofilament is made up of αβ-tubulin dimers able to self-assemble in a head-to-tail fashion under the control of guanosine triphosphate (GTP). Within the cells, microtubules are anchored in microtubule-organizing centers such as centrosomes that contain γ-tubulin, a minor member of the tubulin family. Tubulin binds divalent ions and antimitotic drugs (e.g., Paclitaxel and nocodazole) as well as a large number of microtubule-associated proteins (MAPs). The maintenance of an appropriate three-dimensional structure of tubulin dimers is essential for assembling tubulin to microtubules, binding ligands, and associated proteins [12]. Since tubulin is a thermolabile molecule that converts to a nonpolymerizing state within several hours on ice [13], one of the essential steps in the preparation of tubulin for in vitro and in vivo studies is to assure the proper storage that preserves its polymerization capacity. Tubulin is usually rapidly frozen in liquid nitrogen and stored in small aliquots at −80 °C or in liquid nitrogen. However, repeated freeze–thaw cycles completely abolish the assembly properties of tubulin. Freeze-drying destroys the capacity of tubulin to polymerize [14].

Methods are described below for laboratory-scale freeze-drying of tubulins or microtubules and evaluation of tubulin functions in rehydrated samples.

2 Materials

2.1 Cells

Human osteosarcoma cells U2OS were obtained from American Type Culture Collection (Manassas, VA, USA). Cells are cultured in Dulbecco's modified Eagle's medium containing 10% fetal bovine serum, penicillin (100 units/mL), and streptomycin (0.1 mg/mL). Cells are grown at 37 °C in 5% CO_2 in air and passaged every 2 or 3 day using 0.25% trypsin/ 0.01% EDTA in PBS pH. 7.5.

2.2 Protein Preparation

Microtubule protein (MTP-2) is purified from porcine brain by two temperature-dependent cycles of assembly and disassembly [13]. A third polymerization step is performed in the presence of 500 mM Pipes and 10% DMSO to reduce the quantity of MAPs [15] that are subsequently removed by phosphocellulose chromatography [16]. Thermostable MAPs containing MAP2 and tau proteins are isolated from MTP-2 as described [17].

2.3 Antibodies

1. Mouse monoclonal antibody to β-tubulin TUB 2.1 conjugated with the indocarbocyanine dye (TUB 2.1-Cy3; Sigma-Aldrich; Cat. No. C4585).
2. Mouse monoclonal antibody to γ-tubulin TU-30 [18] conjugated with Alexa 488 (TU-30-Alexa 488; Exbio, Prague, Czech Republic).
3. Mouse monoclonal antibody to α-tubulin TU-01 [19] (Abcam; Cat. No. ab7750).
4. Mouse monoclonal antibody to α-tubulin DM1A (Abcam; Cat No. ab7291).
5. Mouse monoclonal antibody to α-tubulin TU-07 conjugated with biotin [20].
6. Antimouse antibody conjugated with horseradish peroxidase (Promega Biotec; W4021).

2.4 Chemicals

1. Guanosine 5′-triphosphate sodium salt hydrate (Sigma-Aldrich, Cat. No. G8877).
2. D-(+)-Trehalose dihydrate (Sigma-Aldrich; Cat. No. T5251).
3. Nocodazole (Sigma-Aldrich; Cat. No. M1404).
4. Paclitaxel (taxol; Sigma-Aldrich; Cat. No. T7402).
5. Poly(diallyldimethylammonium chloride) solution, 20% in water (PDDA; Sigma-Aldrich; Cat. No. 409014).
6. L-Glutamic acid, monosodium salt hydrate (Sigma-Aldrich; Cat. No. G1626).
7. Glutaraldehyde for electron microscopy, 50% in water (Fluka, Cat. No. 49628).
8. High molecular weight calibration kit for native electrophoresis (GE Healthcare, Cat. No. 17-0445-01).
9. Supersignal WestPico Chemiluminescent reagents (Thermo-Fisher Scientific, Cat. No. 34578).
10. Extravidin-horseradish peroxidase (Sigma-Aldrich; Cat. No. E2886).
11. ELAST ELISA Amplification System (PerkinElmer; Cat. No. NEP116001EA).

12. 3,3′,5,5′-tetramethylbenzidine (TMB) Liquid Substrate (Sigma-Aldrich; Cat. No. T8665).
13. Stop Reagent for TMB Substrate (Sigma-Aldrich; Cat. No. S5814).

2.5 Buffers

1. BRB80 buffer: 80 mM Pipes, adjusted with KOH to pH 6.8, 1 mM EGTA, 1 mM $MgCl_2$.
2. BRB80-GTP buffer: BRB80 supplemented with 1 mM GTP.
3. Column buffer: 100 mM Pipes, adjusted with KOH to pH 6.9, 1 mM EGTA, 1 mM $MgSO_4$, 1 mM DTT, 0.5 mM GTP.
4. Tris buffer solution (TBS; 10 mM Tris–Cl, pH 7.4, 150 mM NaCl) containing 0.05% Tween 20 (TBST).
5. 1% bovine serum albumin (BSA) in TBST (BSA/TBST).

2.6 Other Materials

1. Eight strip 0.2-mL PCR tubes with attached dome caps (Biotix; Cat. No. 3428.8S).
2. Thermoconductive platform CoolRack PCR96 (Biocision, Mill Valley, CA, USA; Cat. No. BSC-120).
3. Spectrophotometer quartz microcuvettes (Sigma-Aldrich; Cat No. C9917).
4. Round glass coverslips, 10 mm in diameter, No. 1 (Marienfeld GmbH & Co.KG, Lauda-Königshofen, Germany; Cat. No. 0111500).
5. Nitrocellulose, 0.45 μm (Schleicher & Schuell; Cat. No. 32-10402506).
6. High binding 96-well half-area polystyrene plates (Corning Inc.; Cat. No. 3690).

2.7 Equipment

1. Gilson Repetman with 1250 μL Distritips (Gilson International B.V., Limburg-Offheim, Germany).
2. Laboratory freeze dryer LyoQuest-80 (Telstar, Terrassa, Spain).
3. Microscope Olympus AX70 Provis equipped with 60× and 40× water-immersion objectives and a SensiCam cooled CCD camera (PCO IMAGING, Kelheim, Germany) for recording images.
4. Ultracentrifuge Optima L-70 with fixed angled rotor 70-Ti (Beckman Coulter Inc., Munich, Germany).
5. Table-top ultracentrifuge OptimaMax with fixed angled rotors MLA-80 and MLA-130 (Beckman Coulter Inc., Munich, Germany).
6. Milli-Q water purification system (Millipore S.A., Molsheim, France).

7. Spectrophotometer NanoDrop 1000 (Thermo Fisher Scientific, Wilmington, DE, USA).
8. Spectrophotometer Shimadzu UV-1800, with a temperature-controlled cuvette holder (Shimadzu, Canby, OR, USA).
9. Mini-PROTEAN vertical electrophoresis system (Bio-Rad Laboratories, Hercules, CA, USA).
10. Trans-Blot Turbo Transfer System system (Bio-Rad Laboratories, Hercules, CA, USA).
11. LAS 3000 imaging systém (Fujifilm, Düsseldorf, Germany).
12. Automatic washing device HydroFlex Platform (TECAN, Grödig, Austria).
13. Sunrise plate Reader (TECAN, Grödig, Austria).

3 Methods

3.1 Freeze-Drying of Tubulin and Microtubules

To get assembly-competent freeze-dried tubulin, it is necessary to recycle phosphocellulose purified tubulin before freeze-drying. Sodium glutamate is used for the stimulation of tubulin polymerization [21].

3.1.1 Recycling of Phosphocellulose Purified Tubulin

1. Supplement phosphocellulose purified tubulin in column buffer with GTP to 1 mM and add sodium glutamate (186 mg/mL) to a final concentration of 1.0 M; stir slowly until it is dissolved. Incubate in a water bath for 30 min at 37 °C.
2. Centrifuge at 185,000 × *g* for 15 min at 27 °C (Type 70-Ti rotor).
3. Resuspend pelleted microtubules five times their volume of BRB80 buffer supplemented with 0.1 mM GTP in a Teflon/glass homogenizer and incubate on ice for 30 min to allow microtubule depolymerization.
4. Centrifuge at 95,000 × *g* for 15 min at 4 °C (MLA80 rotor) and collect the supernatant.
5. Determine the concentration of tubulin by measuring the absorbance at 280 nm using an extinction coefficient at 280 nm of 115,000 M^{-1} cm^{-1} (*see* **Note 1**).

3.1.2 Preparation of Taxol-Stabilized Microtubules

Taxol-stabilized microtubules are prepared by stepwise polymerization of recycled phosphocellulose purified tubulin diluted to a concentration of 20 μM in BRB80 containing 1 mM DTT and 1 mM GTP. Tubulin is incubated at 37 °C with increasing concentrations of taxol from 2 μM to 200 μM as described (http://www.protocol-online.org/cgi-bin/prot/view_cache.cgi?ID=208).

3.1.3 Freeze-Drying of Tubulin and Microtubules

1. Dilute phosphocellulose purified, polymerization-competent tubulin to a concentration of 200 μM by cold BRB80 containing 0.1 mM GTP. In the case of taxol-stabilized microtubules, tubulin in the reaction mixture has a concentration of 8 μM. Keep solutions strictly on ice (*see* **Note 2**).
2. Add trehalose (in dry state) to protein solution to a final concentration of 0.25 M (95.57 mg trehalose dihydrate/mL). Keep on ice and stir to dissolve (*see* **Note 3**).
3. Immediately disburse 10–50 μL aliquots into 0.2 mL PCR thin-walled tubes and freeze them rapidly by insertion into a CoolRack PCR stand precooled in liquid nitrogen (*see* **Note 4**).
4. Insert uncapped tubes into a round-bottomed glass lyophilization flask (precooled at −80 °C). Lyophilization is performed in a freeze dryer at −75 °C, for 18 h, <40 μbar (*see* **Note 5**).
5. Gently release vacuum, carefully take out tubes from the lyophilization bottle, and cap them. Freeze-dried protein forms compact cake on the bottom.

3.1.4 Storage and Reconstitution of Tubulin and Microtubules

1. Store lyophilized samples in a vacuum desiccator in the dark at ambient temperature (~25 °C). Alternatively, samples can be stored in a vacuum desiccator at 4 °C (*see* **Note 6**).
2. Rehydrate tubulin samples with cold Millipore water at 4 °C to the original sample volume and incubate on ice for 20 min. Dilute in BRB80 supplemented with 0.1 mM GTP to the required concentration and centrifuge in an MLA 130 rotor at 300,000 × *g* for 5 min at 4 °C on a table-top ultracentrifuge to remove all aggregates. The tubulin concentration in supernatants is determined by measuring the absorbance at 280 nm. In the case of taxol-stabilized microtubules, rehydrate samples with distilled water to the original volume, for further dilution use BRB80 supplemented with 10 μM taxol (*see* **Note 7**).

3.2 Evaluation of the Properties of Rehydrated Tubulin and Microtubules

3.2.1 Turbidimetric Measurements

Turbidimetric measurements are rapid and reliable methods allowing us to follow the assembly kinetics of tubulin into microtubules in vitro. They are used in studies on the effect of drugs, proteins, nucleotides, and other factors on the microtubule assembly. The process is monitored with a recording spectrophotometer at 350 nm and 37 °C [22].

1. Prepare at 4 °C the assembly mixture containing rehydrated tubulin at a concentration of 15 μM in BRB80 buffer supplemented with GTP and glycerol at respective final concentrations 1 mM and 3.0 M. In order to evaluate the ability of rehydrated tubulin to bind antimitotic drugs, add nocodazole (10 μM), which inhibits microtubule polymerization, or paclitaxel (10 μM), which decreases the critical concentration and enhances the tubulin assembly. To assemble tubulin in the

absence of glycerol, prepare an assembly mixture containing 15 μM tubulin and 0.5 mg/mL porcine brain thermostable MAPs in BRB80 buffer supplemented with 1 mM GTP (*see* **Note 8**).

2. Transfer samples into a spectrophotometer with a temperature-controlled cuvette holder preheated to 37 °C.
3. Record absorbance at 350 nm for 30 min. To distinguish between turbidity caused by microtubule formation and that caused by nonmicrotubular aggregates, incubate polymerized microtubules for 15 min at 4 °C and record the turbidity.

A comparison of the assembly properties of the rehydrated tubulin freeze-dried in the presence or absence of trehalose and the control tubulin stored in liquid nitrogen is shown in Fig. 1a. Rehydrated tubulin freeze-dried in the absence of trehalose has a low capacity to form microtubules, while the inclusion of trehalose protects tubulin capability to assemble into microtubules after rehydration. Trehalose has a unique protective effect on tubulin stored at elevated temperature. Typical data for tubulin polymerization in samples freeze-dried in the presence or absence of trehalose and stored for 1 week at 50 °C are shown in Fig. 1b. The assembly properties are only preserved when freeze-drying is carried out in the presence of trehalose. The nonreducing disaccharide sucrose (β-D-fructofuranosyl-α-D-glucopyranoside) fails to protect tubulin at this temperature (*see* **Note 9**).

The effect of antimitotic drugs (nocodazole and taxol) on tubulin assembly is shown in Fig. 2a. While nocodazole at 10 μM completely inhibits microtubule formation, and taxol at 10 μM substantially enhances polymerization of both the reference tubulin stored in liquid nitrogen and rehydrated tubulin. To define the concentration of nocodazole that inhibits microtubule assembly by 50% (IC_{50}), tubulin assembly is carried out in the presence of nocodazole at lower concentrations (0.5–5 μM) (Fig. 2b).

Rehydrated tubulin forms microtubules not just because of a strong stimulatory effect of glycerol. Thermostable MAPs, in the absence of glycerol, also stimulate polymerization of rehydrated tubulin (Fig. 3). All in all, purified tubulin freeze-dried in the presence of trehalose is capable of assembling microtubules and binding antimitotic drugs after prolonged storage at ambient temperature.

3.2.2 Immunofluorescence Microscopy

Visual analysis of microtubules prepared from rehydrated tubulin can be performed by live video-enhanced differential interference contrast microscopy, by negative stain electron microscopy, or by immunofluorescence microscopy of fixed samples. Below are described three protocols for visualization of microtubules using immunofluorescence microscopy.

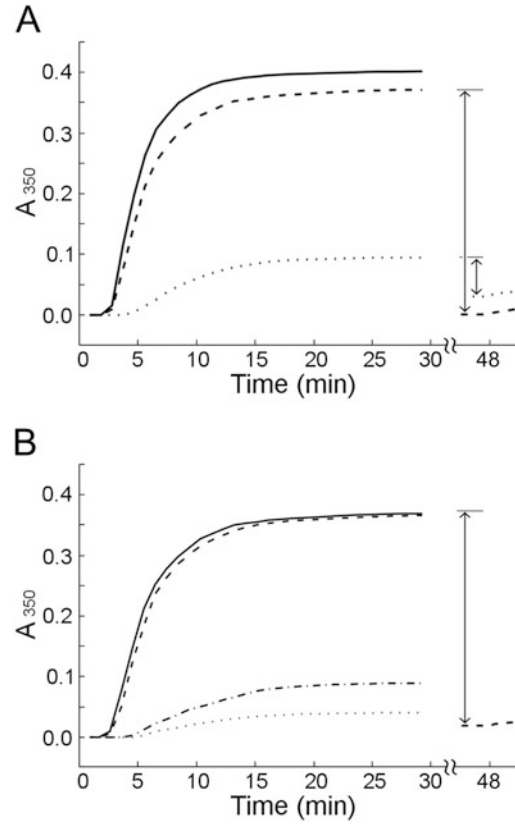

Fig. 1 Assembly properties of rehydrated tubulin in the presence of glycerol. (**a**) Comparison of tubulin assembly at 37 °C using tubulin stored in liquid nitrogen (——) and freeze-dried with (- - -) or without trehalose (. . . .). Drop in the assembly extent at 4 °C is depicted. Assembly at tubulin concentration 15 μM in the presence of 3.0 M glycerol. Freeze-dried samples were stored for 3 months at 25 °C. (**b**) Comparison of tubulin assembly in samples stored at different temperatures. Tubulin freeze-dried with trehalose and stored for 3 months at 25 °C; control (——). Tubulin freeze-dried with trehalose (- - -), sucrose (-.-.-) or without sugar (. . . .), and stored for 1 week at 50 °C. Assembly at a tubulin concentration of 15 μM. (Reproduced from [11] with permission from Elsevier)

Staining of Freeze-Dried Taxol-Stabilized Microtubules

1. Rehydrate freeze-dried taxol-stabilized microtubules in water and dilute in BRB80 with 10 μM paclitaxel.
2. Overlay glass coverslips, pretreated with 0.2% PDDA, with solution containing microtubules.
3. Incubate for 15 min at 25 °C.
4. Wash samples in BRB80 supplemented with 10 μM taxol and fix with 3% formaldehyde in BRB80.
5. Wash preparations with PBS and stain with TUB 2.1-Cy3 (dilution 1:600) to visualize microtubules.
6. Examine with a fluorescence microscope.

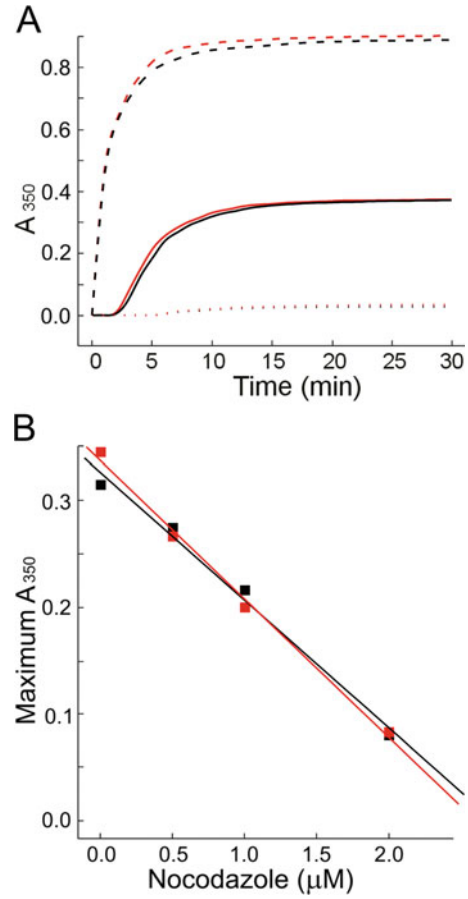

Fig. 2 Effect of antimitotic drugs on assembly of tubulin freeze-dried with trehalose (black lines) or stored in liquid nitrogen (red lines). (**a**) Control (——), 10 μM taxol (- - -), and 10 μM nocodazole (. . . .). (**b**) Effect of the increasing concentration of nocodazole on tubulin assembly. Maximum absorbance was recorded after 30 min of polymerization. Freeze-dried tubulin was stored for 3 months at 25 °C. Assembly at a tubulin concentration of 15 μM. The IC_{50} of tubulin stored in liquid nitrogen and tubulin freeze-dried with trehalose was, respectively, 1.26 and 1.40 μM. (Reproduced from [11] with permission from Elsevier)

An example of immunofluorescence staining of rehydrated taxol-stabilized microtubules is shown in Fig. 4. Microtubules are evident in preparations containing trehalose (Fig. 4a) but are lacking in preparations without trehalose (Fig. 4b).

Microtubule Spin-Down Assay

Spin-down assays make it possible to evaluate by immunofluorescence microscopy microtubules newly formed from rehydrated tubulin [23]. The whole procedure consists of several steps.

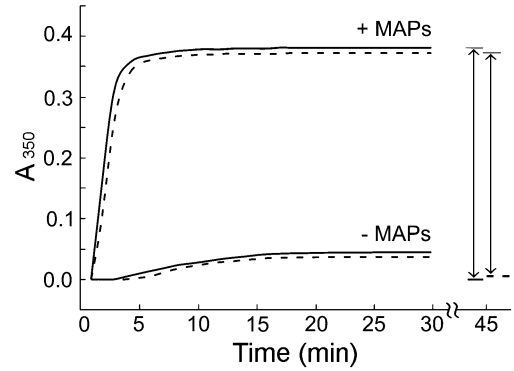

Fig. 3 Assembly properties of rehydrated tubulin in the presence of MAPs. Comparison of tubulin assembly at 37 °C using tubulin stored in liquid nitrogen (——) and freeze-dried with (- - -) trehalose in the presence (+MAPs) or absence (−MAPS) of thermostable microtubule-associated proteins. Drop in the assembly extent at 4 °C is depicted. Assembly, without glycerol, at a tubulin concentration of 15 μM in the presence of 0.5 mg/mL MAPs. Freeze-dried samples were stored for 3 months at 25 °C. (Reproduced from [11] with permission from Elsevier)

1. Polymerize rehydrated tubulin at a concentration of 18 μM in BRB80 buffer supplemented with 1 mM DTT and 1 mM GTP for 20 min at 37 °C.
2. Fix microtubules in solution with 1% glutaraldehyde and centrifuge through 10% glycerol cushion on glass coverslips.
3. Postfix microtubules attached on a glass coverslip in cold methanol.
4. Stain samples with anti-β-tubulin antibody TUB 2.1-Cy3 diluted 1:600.
5. Examine with a fluorescence microscope.

Typical results from spin-down assays are shown in Fig. 4c, d. Long microtubules are detected when tubulin freeze-dried with trehalose is rehydrated, polymerized, and spun-down on coverslips after fixation in solution (Fig. 4c). On the other hand, only a few short microtubules are observed in samples without trehalose (Fig. 4d).

Regrowth of Microtubules in Detergent-Extracted Cells

The stabilizing effect of trehalose is also demonstrable if freeze-dried tubulin is used in microtubule regrowth assay in detergent-extracted cells [24]. After depolymerization of microtubules in cells by reversible antimitotic drug nocodazole and cold, cytosolic tubulin is extracted by nonionic detergent, and exogenous tubulin is added at a subcritical concentration. New microtubules are formed from centrosomes at 37 °C. Microtubules are labeled by the anti-β-tubulin antibody and centrosomes by the anti-γ-tubulin antibody.

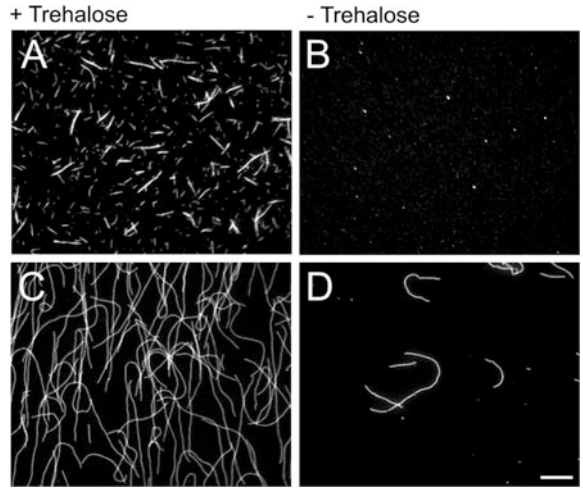

Fig. 4 Immunofluorescence analysis of microtubules. (**a**, **b**) Microtubules were prepared by taxol-driven polymerization and then freeze-dried at a tubulin concentration 8 μM in the presence (**a**) or absence (**b**) of trehalose. Microtubules were rehydrated, attached to coverslips and after fixation stained with the anti-tubulin antibody. (**c**, **d**) Tubulin freeze-dried in the presence (**c**) or absence (**d**) of trehalose was rehydrated and incubated at a concentration of 18 μM with 1 mM GTP for 20 min at 37 °C. Microtubules were fixed in solution, centrifuged onto coverslips, and used for immunostaining. Scale bar, 20 μm in all panels. (Reproduced from [11] with permission from Elsevier)

1. Incubate cells that grow on coverslips for 3 h at 37 °C with 10 μM nocodazole to disrupt microtubules.
2. Replace medium and wash off nocodazole at 4 °C for 30 min.
3. Extract cells for 2 min at 4 °C in 0.2% Triton X-100 in BRB80.
4. Wash cells three times for 3 min each in cold BRB80.
5. Overlay extracted cells with rehydrated tubulin at a final concentration of 5 μM (subcritical concentration) in BRB80 supplemented with 1 mM GTP (BRB80-GTP) and incubate for 7 min at 37 °C. Alternatively, incubate samples with BRB80-GTP alone (*see* **Note 10**).
6. Gently rinse preparations with BRB80-GTP.
7. Fix samples in 3% formaldehyde and postfix with methanol [18].
8. Perform double-label staining of samples with antibodies TUB 2.1-Cy3 (dilution 1:600) and TU-30-Alexa 488 (dilution 1:100).
9. Examine with a fluorescence microscope.

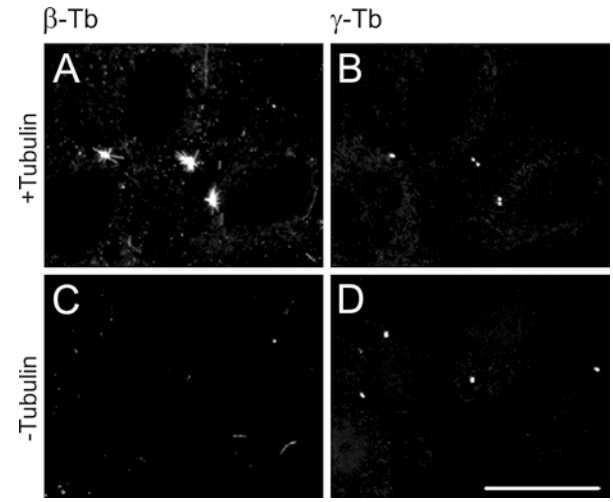

Fig. 5 Application of tubulin freeze-dried with trehalose in microtubule regrowth assay. Extracted cells were incubated with (**a**, **b**) or without (**c**, **d**) rehydrated tubulin (5 μM) in the presence of 1 mM GTP for 7 min at 37 °C. Preparations were fixed and double-label stained with antibodies to β-tubulin (**a**, **c**) and γ-tubulin (**b**, **d**). Scale bar, 20 μm in all panels. Photography E. Dráberová (Institute of Molecular Genetics, CAS , Prague)

An example of microtubule nucleation in detergent-extracted cells, using rehydrated freeze-dried tubulin, is shown in Fig. 5. Regrowth of microtubules from centrosomes is evident in cells incubated with exogenous tubulin (Fig. 5a), while only some nocodazole-resistant microtubules are detected in preparations lacking exogenous tubulin (Fig. 5c). No aster-like formation of microtubules occurs outside centrosomes (Fig. 5a).

3.2.3 Electrophoresis Under Nondenaturing Conditions

When tubulin is electrophoretically separated in polyacrylamide gel (PAGE) under nondenaturing conditions, it forms multiple oligomers [25–27]. After immunoblotting with an antitubulin antibody, typical "tubulin ladder" can be detected. Changes in oligomerization capability of tubulins stored under different conditions can be detected using this approach.

1. Prepare tubulin samples into electrophoresis loading buffer: 62.5 mM Tris/HCl, pH 6.8, 10% glycerol, and 0.01% Bromophenol Blue.
2. Separate samples on 7.5% polyacrylamide gel using the Laemmli separation system without SDS [28] and the Mini-PROTEAN vertical electrophoresis unit.
3. Transfer separated proteins onto nitrocellulose in a Trans-Blot Turbo Transfer System according to the manufacturer's directions.

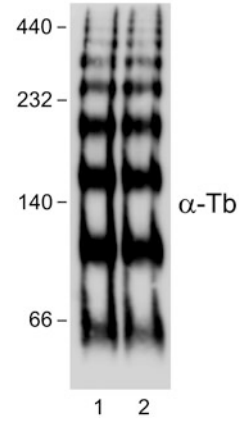

Fig. 6 Immunoblot analysis of purified tubulins separated by native PAGE. Tubulin stored in liquid nitrogen (lane 1), rehydrated tubulin freeze-dried in the presence of trehalose and stored 2 years at room temperature (lane 2). Aliquots of tubulin (5.7 μg) were separated on 7.5% gel. Molecular-mass markers (in kDa) are indicated on the left

4. Perform immunoblotting with primary and secondary antibodies and chemiluminescent detection using standard protocols [29, 30]. Dilute mouse monoclonal antibody TU-01 to α-tubulin in the form of hybridoma supernatant 1:10, and antimouse antibody conjugated with horseradish peroxidase 1: 10,000. Detect the peroxidase signal with SuperSignal West-Pico Chemiluminescent reagents and a LAS 3000 imaging System according to the manufacturer's directions.

As documented in Fig. 6, both tubulin stored in liquid nitrogen and tubulin stored in the freeze-dried form for 2 years at ambient temperature formed the same oligomers. The fastest migrating species of tubulin subunits reflect tubulin monomers [31, 32].

3.2.4 *Sandwich ELISA*

Freeze-dried tubulin is also suitable for generation of calibration curves in sandwich ELISA for quantification of tubulin using anti-tubulin antibodies that are directed to different epitopes [20]. For example, anti-α-tubulin monoclonal antibody DM1A can serve as the capture antibody, and biotinylated monoclonal TU-07 antibody to α-tubulin [33] is applied for detection of bound tubulin. Immobilized biotinylated antibody is then detected by extravidin-horseradish peroxidase, and the enzyme signal is augmented by biotinyl-tyramide amplification. The assay is performed in 96-well half-area plates. Washings throughout the assay (200 μL/well, four times per washing step, if not specified otherwise) are carried out using an automatic washing device with TBST buffer.

1. Coat wells of the plate with antibody DM1A at a concentration of 5 μg/mL in PBS (30 μL/well) overnight (~16 h) at 4 °C.
2. After washing, block the plates by adding 2% BSA in TBS (BSA/TBS) (185 μL/well) for 6 h at room temperature.
3. Wash the plates and incubate overnight (~16 h) at 4 °C with tubulin standards or tested samples diluted in 1% BSA in PBS (30 μL/well). The sample diluent serves as negative control.
4. Wash the plates and incubate for 1 h at room temperature with biotinylated anti-tubulin antibody TU-07 at a concentration of 1 μg/mL in BSA/TBST (30 μL/well).
5. Wash the plates and incubated for 45 min at room temperature with extravidin-horseradish peroxidase diluted 1:5,000 in BSA/TBST (30 μL/well).
6. Increase the sensitivity of the assay by biotinyl-tyramide signal amplification using the ELAST ELISA Amplification System according to the manufacturer's directions. Shortly, incubate plates with biotinyl-tyramide, diluted 1:500 in amplification diluent (30 μL/well) for 15 min at room temperature in the dark, wash (five times) and incubate with streptavidin-peroxidase diluted 1:1,000 in BSA/TBST (30 μL/well) for 30 min at room temperature in the dark.
7. Wash the plates (five times) and incubate with TMB Liquid Substrate (30 μL/well).
8. Stop the reaction after 13 min by adding Stop Reagent for TMB Substrate (30 μL/well).
9. Determine the absorption at 450 nm.

A typical calibration curve for tubulin obtained by sandwich ELISA with biotinyl-tyramide amplification is shown in Fig. 7. Absorbance at 450 nm was measured at different tubulin concentrations ranging from 2.5 to 150 ng/mL. No difference was observed when tubulin was stored in liquid nitrogen or freeze-dried in the presence of trehalose and stored for 2 years at ambient temperature. This documents that epitopes, recognized by the corresponding antibodies on the surface of tubulin molecule, are not damaged.

The paper presents a protocol for freeze-drying of porcine brain tubulin. However, tubulins isolated from various tissues of different species could be stabilized by the same procedure. Inclusion of trehalose as a stabilizer during freeze-drying preserves the biological activities of tubulin and allows its long-term storage at ambient temperature. The thermostability of such tubulin preparations facilitates their storage and transport. Trehalose-protected tubulin and microtubules can help standardize the assays and bio-nanodevices based on microtubules.

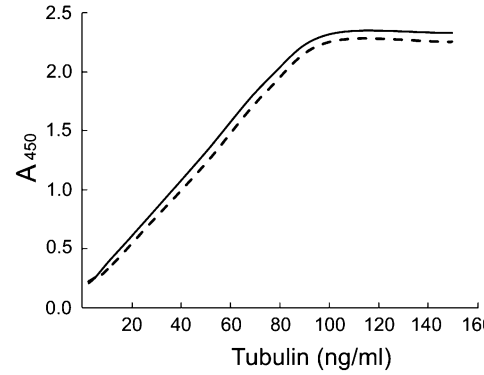

Fig. 7 Detection of tubulin at various concentrations by sandwich ELISA with biotinyl-tyramide amplification. Comparison of tubulin stored in liquid nitrogen (——) and tubulin freeze-dried in the presence of trehalose and stored for 2 years at ambient temperature1 (- - -)

It is relevant to stress that the unique thermostability conferred to biomolecules by trehalose has also been demonstrated for labile antibodies, enzymes, liposomes, human erythrocytes, or platelets [4, 34, 35]. It was also reported that freeze-drying in the presence of trehalose preserves integrity of DNA [36, 37]. The protective effect of 0.25 M trehalose during long-term storage of freeze-dried labile antitubulin monoclonal antibodies of IgM class is shown in Fig. 8. Microtubules are visualized by indirect immunofluorescence on fixed U2OS cells after application two mouse monoclonal antibodies: TU-07 to α-tubulin and TU-14 to β-tubulin [33]. A typical distribution of microtubules was observed with both freshly prepared supernatants (Fig. 8a, b) and supernatants freeze-dried in the presence of trehalose and stored for 2 years at ambient temperature (Fig. 8c, d). On the other hand, supernatants freeze-dried in the absence of trehalose and stored under the same conditions gave only unspecific staining (Fig. 8e, f).

4 Notes

1. Recycled phosphocellulose purified tubulin is highly concentrated (>40 mg/mL) and should be more than 98% pure, as determined by SDS-PAGE on overloaded gels. Prepared tubulin is immediately diluted and freeze-dried or stored in liquid nitrogen (control).
2. Tubulin concentration in samples used for freeze-drying affects the assembly properties. Samples stored at relatively high concentrations (400 and 200 μM) contain a proportion of active tubulin higher than those stored at tubulin concentrations 100 and 50 μM. Therefore, 200 μM tubulin is routinely used for freeze-drying.

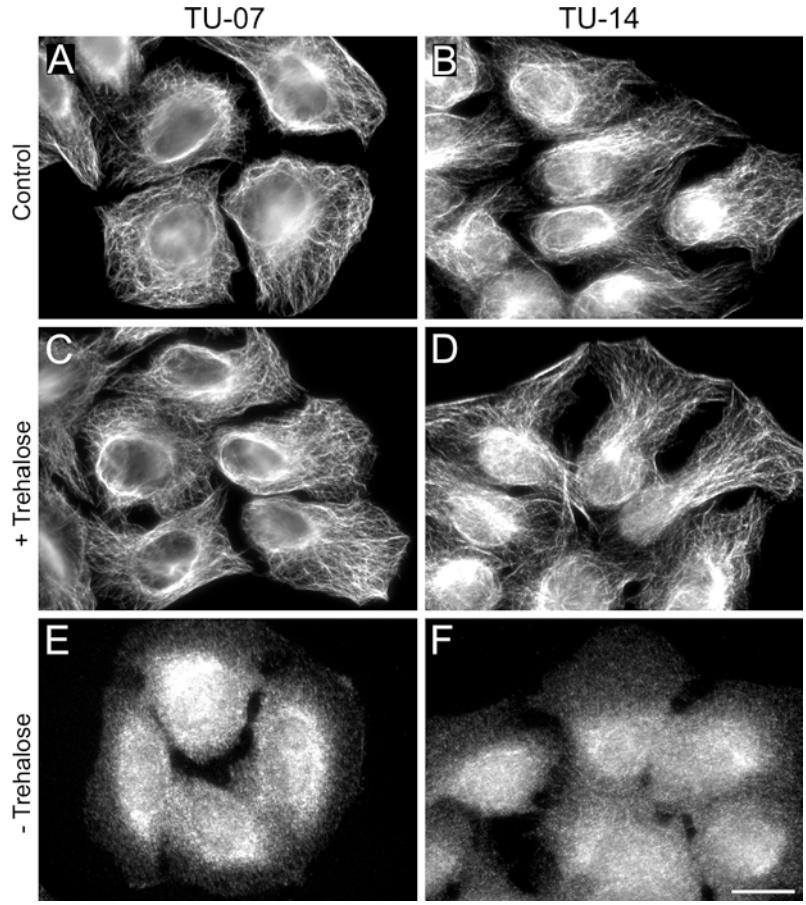

Fig. 8 Effect of trehalose on recovery of the binding activity of labile IgM monoclonal antitubulin antibodies. Binding of mouse monoclonal antibodies TU-07 (**a**, **c**, **e**) and TU-14 (**b**, **d**, **f**) to α-tubulin or β-tubulin, respectively, was detected by indirect immunofluorescence microscopy on formaldehyde fixed, Triton X-100 extracted U2OS cells as described [38]. (**a**, **b**) Freshly collected supernatants. (**c**, **d**) Supernatants freeze-dried in the presence of trehalose and stored for 2 years at ambient temperature. (**e**, **f**) Supernatants freeze-dried in the absence of trehalose. Scale bar, 20 μm in all panels. Photography E. Dráberová (Institute of Molecular Genetics, CAS, Prague)

3. Trehalose is added at a final concentration of 0.25 M. This concentration was previously found to be optimal for preserving the binding activities of labile IgM monoclonal antibodies during freeze-drying [34]. Antibodies of different subclasses freeze-dried in the presence of trehalose do not lose their binding activities even after 20 years of storage at 4 °C (E. Dráberová, unpublished results).
4. It is important to freeze tubulin aliquots rapidly. Tubulin can also be dispensed by dripping the ~50 μL aliquots directly into a Teflon beaker with liquid nitrogen, using an Eppendorf pipette and a standard yellow tip. As the viscous liquid in the

tip easily freezes in nitrogen vapors, the tip ends are cut off. The advantage is convenient manipulation and space saving during storage. On the other hand, the relatively large and nonstandard volume of aliquots may be a drawback.

5. When the freeze-dryer is equipped with shelves, the thermoconductive CoolRack PCR96 platform (precooled with liquid nitrogen) with PCR tubes containing frozen aliquots can be directly placed on precooled shelves. Tubulin in the form of frozen pellets can be transferred into a precooled round-bottomed glass lyophilization flask by pouring.
6. Freeze-dried samples containing trehalose are moisture-sensitive. For long-term storage, it is important to keep them in a vacuum desiccator. Transport of the freeze-dried samples at ambient temperature can be conveniently accomplished in the presence of desiccant packs. The favorable effect of trehalose on tubulin is evident even after 2 years of storage at ambient temperature.
7. In various in vitro assays, tubulin is most often used at concentrations ranging from 5 to 20 μM. For this, it is convenient to predilute rehydrated tubulin (~200 μM) to a concentration of ~40 μM, centrifuge it to remove aggregates, and determine the tubulin concentration in the supernatant using a Nanodrop spectrophotometer (measurement of 1–2 μL samples). Tubulin is then diluted to the final concentration. Usually, more than 96% of tubulin is soluble after rehydration and centrifugation.
8. To minimize the volume for turbidimetric measurements, use microcuvettes. The examined volume can be as small as 80 μL.
9. Sucrose is often used as a cheap protectant for freeze-drying of proteins. However, 0.25 M sucrose fails to protect the assembly activity of tubulin when stored at higher temperature. Sucrose in the presence of chemically reactive amino groups of proteins splits into reducing monosaccharides glucose and fructose. A prolonged storage of dried proteins in reactive sugars can thus lead to chemical damage of the proteins [7]. The chemical stability and nonreducing nature of trehalose may be the most decisive feature in the stability of freeze-dried tubulin at high temperatures. The maintenance of proper conformation of tubulin during freeze-drying in the presence of trehalose could be explained by the water replacement hypothesis, assuming that sugar molecules substitute for water from the protein hydration shell [9].
10. At tubulin dimer concentration exceeding the critical concentration, the dimers polymerize into microtubules. Critical concentration for particular tubulin preparation can be computed from turbidimetric measurements.

Acknowledgments

This work was supported in part by Grants 18-27197S and 19-20716S from the Czech Science Foundation, Grant LTAUSA17052 from Ministry of Education, Youth, and Sports of the Czech Republic, Project NAS-17-11 from Academy of Sciences of the Czech Republic, and by the Institutional Research Support (RVO 68378050).

References

1. Matejtschuk P (2007) Lyophilization of proteins. Methods Mol Biol 368:59–72
2. Adams G (2007) The principles of freeze-drying. Methods Mol Biol 368:15–38
3. Crowe JH, Carpenter JF, Crowe LM, Anchordoguy TJ (1990) Are freezing and dehydration similar stress vectors? A comparison of modes of interaction of stabilizing solutes with biomolecules. Cryobiology 27:219–231
4. Crowe JH, Crowe LM, Oliver AE, Tsvetkova N, Wolkers W, Tablin F (2001) The trehalose myth revisited: introduction to a symposium on stabilization of cells in the dry state. Cryobiology 43:89–105
5. Carpenter JF, Crowe JH (1988) Modes of stabilization of a protein by organic solutes during desiccation. Cryobiology 25:459–470
6. Israeli E, Shaffer BT, Lighthart B (1993) Protection of freeze-dried *Escherichia coli* by trehalose upon exposure to environmental conditions. Cryobiology 30:519–523
7. Roser B (1991) Trehalose drying: a novel replacement for freeze-drying. Biopharm 5:47–52
8. Crowe JH (2007) Trehalose as a "chemical chaperone": fact and fantasy. Adv Exp Med Biol 594:143–158
9. Cordone L, Cottone G, Cupane A, Emanuele A, Giuffrida S, Levantino M (2015) Proteins in saccharides matrices and the trehalose pecularity: biochemical and biopysical properties. Curr Org Chem 19:1684–1706
10. Ohtake S, Wang YJ (2011) Trehalose: current use and future applications. J Pharm Sci 100:2020–2053
11. Dráberová E, Sulimenko V, Sulimenko T, Böhm KJ, Dráber P (2010) Recovery of tubulin functions after freeze-drying in the presence of trehalose. Anal Biochem 397:67–72
12. Dráber P, Dráberová E (2012) Microtubules. In: Kavallaris M (ed) Cytoskeleton and human disease. Humana Press, New York: NY, pp 29–54
13. Shelanski ML, Gaskin F, Cantor CR (1973) Microtubule assembly in the absence of added nucleotides. Proc Natl Acad Sci U S A 70:765–768
14. Soifer D, Laszlo AH, Scotto JM (1972) Enzymatic activity in tubulin preparations. I. Intrinsic protein kinase activity in lyophilized preparations of tubulin from porcine brain. Biochim Biophys Acta 271:182–192
15. Mandelkow EM, Herrman M, Ruhl V (1985) Tubulin domains probed by limited proteolysis and subunit-specific antibodies. J Mol Biol 185:311–327
16. Weingarten MD, Lockwood AH, Hwo SY, Kirschner MW (1975) A protein factor essential for microtubule assembly. Proc Natl Acad Sci U S A 72:1858–1868
17. Fellous A, Francon J, Lennon AM, Nunez J (1977) Microtubule assembly in vitro—purification of assembly-promoting factors. Eur J Biochem 78:167–174
18. Nováková M, Dráberová E, Schürmann W, Czihak G, Viklický V, Dráber P (1996) γ-tubulin redistribution in taxol-treated mitotic cells probed by monoclonal antibodies. Cell Motil Cytoskeleton 33:38–51
19. Viklický V, Dráber P, Hašek J, Bártek J (1982) Production and characterization of a monoclonal antitubulin antibody. Cell Biol Int Rep 6:725–731
20. Dráberová E, Stegurová L, Sulimenko V, Hájková Z, Dráber P, Dráber P (2013) Quantification of alpha-tubulin isotypes by sandwich ELISA with signal amplification through biotinyl-tyramide or immuno-PCR. J Immunol Methods 395:63–70
21. Waterman-Storer CM (2001) Microtubule/organelle motility assays. Curr Protoc Cell Biol. Chapter 13:Unit 13.1

22. Gaskin F, Cantor CR, Shelanski ML (1974) Turbidimetric studies of in vitro assembly and disassembly of porcine neurotubules. J Mol Biol 89:737–755
23. Evans L, Mitchison T, Kirschner M (1985) Influence of the centrosome on the structure of nucleated microtubules. J Cell Biol 100:1185–1191
24. Brinkley BR, Cox SM, Pepper DA, Wible L, Brenner SL, Pardue RL (1981) Tubulin assembly sites and the organization of cytoplasmic microtubules in cultured mammalian cells. J Cell Biol 90:554–562
25. Correia JJ, Williams RC Jr (1985) Characterization of oligomers of tubulin by two-dimensional native electrophoresis. Arch Biochem Biophys 239:120–129
26. Sulimenko V, Sulimenko T, Poznanovic S, Nechiporuk-Zloy V, Böhm JK, Macurek L, Unger E, Dráber P (2002) Association of brain g-tubulins with ab-tubulin dimers. Biochem J 365:889–895
27. Chumová J, Trögelová L, Kourová H, Volc J, Sulimenko V, Halada P, Kučera O, Benada O, Kuchařová A, Klebanovych A, Dráber P, Daniel G, Binarová P (2018) γ-Tubulin has a conserved intrinsic property of self-polymerization into double stranded filaments and fibrillar networks. Biochim Biophys Acta, Mol Cell Res 1865:734–748
28. Laemmli UK (1970) Cleavage of structural proteins during the assembly of the head of bacteriophage T_4. Nature 227:680–685
29. Dráber P, Lagunowich LA, Dráberová E, Viklický V, Damjanov I (1988) Heterogeneity of tubulin epitopes in mouse fetal tissues. Histochemistry 89:485–492
30. Blume Y, Yemets A, Sulimenko V, Sulimenko T, Chan J, Lloyd C, Dráber P (2008) Tyrosine phosphorylation of plant tubulin. Planta 229:143–150
31. Kirchner K, Mandelkow EM (1985) Tubulin domains responsible for assembly of dimers and protofilaments. EMBO J 4:2397–2402
32. Montecinos-Franjola F, Schuck P, Sackett DL (2016) Tubulin dimer reversible dissociation: affinity, kinetics, and demonstration of a stable monomer. J Biol Chem 291:9281–9294
33. Dráber P, Dráberová E, Linhartová I, Viklický V (1989) Differences in the exposure of C- and N-terminal tubulin domains in cytoplasmic microtubules detected with domain-specific monoclonal antibodies. J Cell Sci 92:519–528
34. Dráber P, Dráberová E, Nováková M (1995) Stability of monoclonal IgM antibodies freeze-dried in the presence of trehalose. J Immunol Methods 181:37–43
35. Franze S, Selmin F, Samaritani E, Minghetti P, Cilurzo F (2018) Lyophilization of liposomal formulations: still necessary, still challenging. Pharmaceutics 10:e139
36. Zhang M, Oldenhof H, Sydykov B, Bigalk J, Sieme H, Wolkers WF (2017) Freeze-drying of mammalian cells using trehalose: preservation of DNA integrity. Sci Rep 7:e6198
37. Oldenhof H, Zhang M, Narten K, Bigalk J, Sydykov B, Wolkers WF, Sieme H (2017) Freezing-induced uptake of disaccharides for preservation of chromatin in freeze-dried stallion sperm during accelerated aging. Biol Reprod 97:892–901
38. Dráberová E, Dráber P (1993) A microtubule-interacting protein involved in coalignment of vimentin intermediate filaments with microtubules. J Cell Sci 106:1263–1273

Part V

Applications/Case Studies

Chapter 28

G-Protein-Coupled Receptor Expression and Purification

Karolina Corin, Lotta T. Tegler, and Sotirios Koutsopoulos

Abstract

G-protein-coupled receptors (GPCRs) are integral proteins of the cell membrane and are directly involved in the regulation of many biological functions and in drug targeting. However, our knowledge of GPCRs' structure and function remains limited. The first bottleneck in GPCR studies is producing sufficient quantities of soluble, functional, and stable receptors. Currently, GPCR production largely depends on the choice of the host system and the type of detergent used to extract the GPCR from the cell membrane and stabilize the protein outside the membrane bilayer. Here, we present three protocols that we employ in our lab to produce and solubilize stable GPCRs: (1) cell-free in vitro translation, (2) HEK cells, and (3) *Escherichia coli*. Stable receptors can be purified using immunoaffinity chromatography and gel filtration, and can be analyzed with standard biophysical techniques and biochemical assays.

Key words G-protein-coupled receptor (GPCR), Olfactory receptors, membrane proteins, Detergents, Surfactants

1 Introduction

GPCRs, the largest family of membrane proteins, are involved in processes ranging from sight to inflammation to smell (Fig. 1). They are also the target of ~50% of pharmaceutical drugs [1, 2]. In spite of their large numbers and importance, relatively little is known about how they function at the molecular level. This is primarily due to the difficulty of purifying and crystallizing these membrane proteins. Indeed, they are so difficult to work with that, as of March 2019, unique GPCR structures account for only 59 of the ~150,000 protein structures currently deposited in the Protein Data Bank [3, 4].

Large-scale expression and stabilization of GPCRs are necessary before structural or functional studies can be performed. However, this presents a daunting task. GPCRs are endogenously expressed at low levels while high expression in heterologous systems often results in protein misfolding or aggregation. Moreover, with the exception of rhodopsin, all crystallized GPCRs needed to

Nikolaos E. Labrou (ed.), *Protein Downstream Processing: Design, Development, and Application of High and Low-Resolution Methods*, Methods in Molecular Biology, vol. 2178, https://doi.org/10.1007/978-1-0716-0775-6_28,

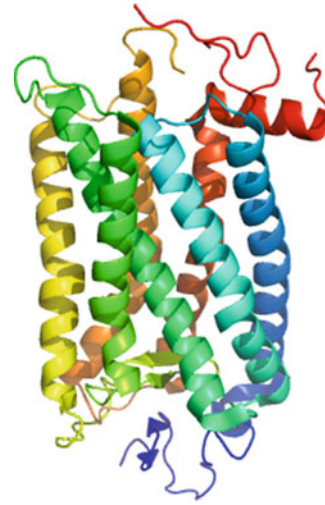

Fig. 1 Typical GPCR three-dimensional structure in which the seven transmembrane helices and the barrel conformation are shown. Currently, the resolved GPCR structures resemble the crystal structure of bovine rhodopsin, which was determined in 2000, PDB: 1F88 [3]

be modified to facilitate their expression, increase their solubility, or to enable crystallization. These modifications have included deletion of disorganized regions [5–35], addition of stabilizing mutations [7, 8, 12, 17, 18, 22, 26–29, 32, 33, 36–40], removal of posttranslational modification sites [6, 7, 16, 18, 23, 26, 41], and antibody-coupling [6] or insertion of fusion proteins to increase solubility and facilitate crystal packing [5, 8–20, 22–24, 26–42]. Insertion of T4-Lysozyme into the third intracellular loop in particular has facilitated a recent and relative explosion in GPCR structures [5, 8–14, 16, 23, 26, 36, 37, 40–42].

During the last three decades, research on membrane proteins and GPCRs has been intensified using a number of protein expression systems. These include cell-free synthesis [43], heterologous expression in mammalian cells [44], *Escherichia coli* (*E. coli*) [45, 46], insect cells [47, 48], *Drosophila* photoreceptor cells [49], transgenic *Xenopus laevis* photoreceptors [50], transgenic mouseretina [51], and *Saccharomyces cerevisiae* [52, 53]. We will briefly discuss these systems in the following paragraphs of this section.

GPCR expression in traditional systems, like eukaryotic or bacterial cells, often results in low yields, cell toxicity, protein degradation, protein inhomogeneity, and aggregation in internal compartments or inclusion bodies [47, 54–57]. Cell-free in vitro translation is a promising alternative, as it allows for rapid, cost-effective, high-yield GPCR expression [43, 58–61]. Cell-free expression is an established technology for soluble proteins, which can be adapted for membrane proteins by including an appropriate

detergent [43, 59–62]. With the right detergent, it is possible to use commercial cell-free expression kits to rapidly produce milligram quantities of GPCRs directly from plasmid DNA.

Mammalian cells are arguably a good system to express human GPCRs, as the environment they provide is closest to the native GPCR environment. They also have the necessary machinery to perform glycosylation and other posttranslational modifications. However, yields are typically low, and decrease with each cell passage after transient transfection. Moreover, the expressed proteins can be in various stages of expression or degradation. Such an inhomogeneous sample can inhibit crystallization and interfere with biochemical assays [55–57]. Inducible, stable cell lines can be used to overcome many difficulties associated with mammalian cell expression systems [44, 61, 66, 67]. Unlike transiently transfected cells, the gene of interest is incorporated into the genome of stably transfected cells, and expression does not decrease with each cell passage. When the gene is under an inducible promoter, cells can be grown before they are simultaneously induced. This makes the protein sample more homogeneous and reduces problems with cell toxicity resulting from high GPCR expression.

A widely used platform for GPCR overexpression is the Gram-negative bacterium *E. coli*, which provides a simple, cost-efficient, and robust system. High expression of membrane proteins can induce cell toxicity but this issue has been addressed and methods for producing milligram quantities of pure membrane proteins from *E. coli* have been developed [63]. Membrane protein expression in *E. coli* has been extensively reviewed and discussed previously [46, 54, 55, 64].

GPCR expression in Sf9 insect cells using the baculovirus infection system results in the production of much higher protein levels than that produced in mammalian cells [47, 48]. Furthermore, the functionality of GPCRs reconstituted in Sf9 cells is similar to the receptor properties expressed in mammalian cells. Sf9 insect cells can be grown in suspension culture, providing an inexpensive way of obtaining large amounts of GPCRs. Because of these advantages, this system has been used to express protein for most of the GPCRs crystallized to date.

GPCR overexpression in the retina of transgenic *Drosophila melanogaster* is based on the observation that photoreceptor cells are characterized by membrane stacks where rhodopsin (i.e., a model GPCR) resides [49]. *Drosophila* is a suitable system for this purpose because fly genetics are well studied and strategies have been developed to direct GPCR production to these membrane stacks and to isolate the target GPCR from there. This results in high expression yields of functional and homogeneous GPCRs. The metabotropic glutamate receptor was one of the first GPCRs expressed in *Drosophila* and the system is now successfully used for the production of a variety of membrane proteins.

The *Xenopus laevis* system has been used in pharmacology for drug screening and in the overexpression of GPCRs. It has been suggested that GPCR expression in *Xenopus laevis* retina allows for the production of large amounts of high-quality homogeneous proteins [50]. GPCR homogeneity is an important attribute that is missing in the standard mammalian cell expression systems utilized for membrane protein production.

Yeast provides an inexpensive GPCR expression system that is simple, robust, and amenable to genetic and biochemical manipulation. Furthermore, yeast contains GPCR signaling pathways similar to mammalian cells. Since the first report of functional coupling of the human β2 adrenergic receptor to the yeast pheromone-response pathway in 1990 [65], the technology has evolved and many heterologous GPCRs have been expressed in yeast. Yeast screens have also been used to identify GPCRligands.

In our laboratory, we have purified diverse GPCRproteins using three of the above systems: cell-free in vitro translation, human embryonic kidney-293 (HEK293) cells, and *E. coli* cells. Below, we present detailed protocols for the overproduction and purification of diverse GPCRs in these systems.

2 Materials

2.1 Cell-Free Expression System

2.1.1 Reagents for Cell-Free Expression of GPCRs

1. *E. coli*-based cell-free expression kits (cat # K9900-97 Invitrogen) containing *E. coli* cell lysates, the Reaction Buffer, and sterile, DNAse-free and RNAse-free water (*see* **Note 1**).
2. Brij-35 10% w/v (*see* **Note 2**).
3. Membrane protein gene ligated into the pIVex2.3 vector (Invitrogen) (*see* **Note 3**).

2.1.2 Immunoaffinity Purification of Cell-Free Expressed GPCRs

1. CNBr-activated Sepharose 4B beads (GE Healthcare) chemically linked to the rho1D4 monoclonal antibody (Cell Essentials, Boston, MA).
2. Dulbecco's phosphate buffer saline (DPBS: NaCl 137.93 mM, KCl 2.67 mM, KH_2PO_4 1.47 Mm, $Na_2HPO_4{\cdot}7H_2O$ 8.06 mM). The solution can be stored at 4 °C.
3. DNAse I 200 U/mL.
4. RNAse A 20 mg/mL.
5. Sterile filtered water (0.22 μm).
6. Wash Buffer: 0.2% w/v Fos-choline-14 (FC14, Anatrace/Affymatrix) in DPBS sterile filtered through 0.22 μm filters. This is made from a 10% w/v FC14 stock solution. The solution can be stored at 4 °C.

7. Elution Buffer: 800 μM elution peptide acetyl-TETSQVAPA-$CONH_2$ dissolved in Wash Buffer. The solution can be stored at 4 °C.
8. Amicon Ultra Centrifugal Filter Units with Ultracel membranes (Millipore).

2.1.3 Gel Filtration of Cell-Free Expressed GPCRs

1. Size exclusion HiLoad 16/60 Superdex 200 column (Akta Purifier FPLC system, GE Healthcare or similar).
2. Amicon Ultra Centrifugal Filter Units with Ultracel membranes (Millipore Sigma).
3. Wash Buffer: 0.2% w/v FC14 in DPBS, sterile filtered through 0.22 μm filters. The solution can be stored at 4 °C.
4. Gel filtration/Protein Storage Buffer comprised of 0.02% w/v FC14 in PBS, sterile filtered through 0.22 μm filters. The solution can be stored at 4 °C.
5. Sterile filtered water (0.22 μm).

2.2 HEK-Cell Expression System

2.2.1 Reagents for the Construction of Inducible Stable HEK Cell Lines Expressing GPCRs

1. Olfactory receptor ligated into the pcDNA4/TO vector (Invitrogen) (*see* **Note 3**).
2. HEK293S *N*-acetylglucosaminyltransferase I-negative cells (HEK293G) containing the pcDNA6/TR vector (Life Technologies) (*see* **Notes 4** and **5**).
3. Lipofectamine 2000.
4. DMEM F12 with Glutamax (*see* **Note 6**). The solution can be stored at 4 °C.
5. Fetal bovine serum. The solution can be stored at −20 °C.
6. HEPES buffer pH 7.0. The solution can be stored at 4 °C.
7. Nonessential amino acids.
8. Sodium pyruvate.
9. Penicillin and Streptomycin.
10. Zeocin.
11. Blasticidin.
12. Tetracycline.
13. Tissue culture dishes and flasks.
14. 6- and 24-well tissue culture plates.
15. DPBS.
16. Trypsin solution 0.05% w/v (*see* **Note 6**). The solution can be stored at 4 °C.
17. FC14.
18. Proteases inhibitors (Sigma Aldrich #04693132001).
19. Prepare the following growth and Selection media for the cells:

(a) Growth medium: DMEM F12 with GlutaMAX supplemented with 10% v/v fetal bovine serum, 15 mM HEPES, 0.1 mM nonessential amino acids, 0.5 mM sodium pyruvate, and 100 U/mL penicillin and 100 μg/mL streptomycin. The solution can be stored at 4 °C.

(b) Selection medium 1: Growth medium supplemented with 5 μg/mL of blasticidin and 50 μg/mL of zeocin. The solution can be stored at 4 °C.

(c) Selection medium 2: Growth medium supplemented with 5 μg/mL of blasticidin and 25 μg/mL of zeocin. The solution can be stored at 4 °C.

20. Prepare the following two Transfection media:
    (a) Transfection medium 1 (no antibiotics): DMEM F12 with GlutaMAX supplemented with 10% v/v fetal bovine serum, 15 mM HEPES, 0.1 mM nonessential amino acids, and 0.5 mM sodium pyruvate. The solution can be stored at 4 °C.
    (b) Transfection medium 2 (no serum or antibiotics): DMEM F12 with GlutaMAX supplemented with 15 mM HEPES, 0.1 mM nonessential amino acids, and 0.5 mM sodium pyruvate. The solution can be stored at 4 °C.
21. Sterile incubator maintained at 37 °C, 5% CO_2, and 95% relative humidity.
22. Tissue culture hood.
23. Pipettes.
24. Eppendorf tubes (1.5 mL centrifuge tubes).

2.2.2 Reagents for Immunocytochemical Analysis

1. Permeabilizing solution: acetone and methanol mixed in a 1:1 ratio. The solution can be stored at room temperature.
2. 10% neutral buffered formalin. The solution can be stored at room temperature.
3. Phosphate buffer saline (PBS: 137 mM NaCl, 2.7 mM KCl, 10 mM $Na_2HPO_4{\cdot}2H_2O$, 2 mM KH_2PO_4, pH 7.4). The solution can be stored at 4 °C.
4. Poly-L-lysine.
5. Glass coverslips.
6. Blocking solution: 0.2% w/v Tween-20, 0.3 M glycine, 4% v/v serum in PBS.
7. Primary antibody solution: 0.2% w/v Tween-20, 4% v/v serum, 1.6 μg/mL rho1D4 antibody in PBS.

8. Secondary antibody solution: Alexa-fluor-488 goat-anti-mouse conjugate diluted 1:3000 in PBS.
9. ProLong Gold Antifade with DAPI.
10. Shaker.
11. Kim wipes.
12. Aluminum foil.

2.2.3 Cell Extract Preparation

1. Tissue culture plates.
2. DPBS.
3. Pipettes.
4. Centrifuge tubes.
5. Tetracycline.
6. Sodium butyrate.

2.2.4 Detergent Screening

1. Protease inhibitors.
2. DPBS.
3. Detergents to be screened.
4. Rotator.
5. Centrifuge.
6. Eppendorf tubes.

2.2.5 Chromatographic Purification of HEK-Cell Expressed Receptors

1. 10% w/v FC14 solution in DPBS. The solution can be stored at 4 °C.
2. Cell pellets.
3. Protease inhibitors.
4. DPBS.
5. DNAse I 200 U/μL.
6. RNAse A 20 mg/mL.
7. Wash Buffer: 0.2% w/v FC14 in PBS. The solution can be stored at 4 °C.
8. Elution Buffer (800 μm of elution peptide TETSQVAPA in Wash Buffer). The solution can be stored at 4 °C.
9. Filter columns (Biorad).
10. Eppendorf tubes.
11. 50 mL tubes.
12. 50,000 MWCO filter column (Millipore).
13. Hi-Load 16/60 Superdex 200 column with an Akta Purifier HPLC system (GE Healthcare or similar).

2.3 E. coli-Based Expression System

2.3.1 Reagents for Expression of Membrane Proteins in E. coli

1. pEXP3-DEST expression vector containing gene of interest with N-terminal His6-tag.
2. C41(DE3)*E. coli* cells.
3. Lysogeny broth/Luria-Bertani medium (LB: 1.0% w/v Tryptone, 0.5% w/v Yeast Extract, 1.0% w/v NaCl, pH 7.0) containing 100 μg/mL Ampicillin (*see* **Note 7**). The solution can be stored at 4 °C.
4. LB Agar plates containing 100 μg/mL Ampicillin (*see* **Note 8**).
5. Terrific Broth (TB: 1.2% w/v Tryptone, 2.4% w/v Yeast Extract, 0.4% v/v Glycerol, 1.7 mM KH_2PO_4 and 7.2 mM K_2HPO_4) containing 100 μg/mL Ampicillin (*see* **Note 9**). The solution can be stored at 4 °C.
6. Isopropyl-β-D 1-thiogalactopyranoside (IPTG).

2.3.2 E. coli Cell Extract Preparation

1. Cell pellets.
2. Centrifuge.
3. French Press.
4. Ultracentrifuge.
5. 50 kDa molecular weight cutoff filter.
6. Tubes.

2.3.3 Detergent Screening

1. Overnight culture.
2. TB.
3. IPTG.
4. Centrifuge.
5. Tubes for centrifugation and lysis of cells.
6. Detergents to be used for screening (Table 1).

2.3.4 Chromatographic Purification of E. coli Expressed Receptors

1. Crude sample of solubilized protein.
2. Hitrap Chelating HP column 5 mL (GE Healthcare or similar).
3. Size exclusion column (HiLoad 16/60 Superdex 200 column, GE Healthcare, or similar) connected to FPLC system (AKTA purifier, GE Healthcare or similar).
4. Lysis Buffer (50 mM sodium phosphate pH 7.8, 200 mM NaCl, 100 mM KCl, 20% v/v glycerol, 10 mM EDTA, 2 mM DTT, 1 mM phenylmethylsulfonyl fluoride (PMSF, which is a serine protease inhibitor commonly used in the preparation of cell lysates; additional protease inhibitors may be needed), 50 mg/mL lysozyme, and DNase I to a final concentration of 1 μL/mL). The solution can be stored at 4 °C.

Table 1
Detergent screening for the solubilization of the CCR5 GPCR

#	Detergent	Type*	CMC(%)**	Conc.***	hCCR5 Spot Intensity
1	ANAMEG® -7	N	0.65	2%	
2	ANAPOE®-20	N	0.0072	1%	
3	ANAPOE®-35	N	0.001	1%	
4	ANAPOE®-58	N	0.00045	1%	
5	ANAPOE®-80	N	0.0016	1%	
6	ANAPOE®-$C_{10}E_6$	N	0.025	1%	
7	ANAPOE®-$C_{10}E_9$	N	0.053	1%	
8	ANAPOE®-$C_{12}E_8$	N	0.0048	1%	
9	ANAPOE®-$C_{12}E_9$	N	0.003	1%	
10	ANAPOE®-$C_{12}E_{10}$	N	0.2	1%	
11	ANAPOE®-$C_{13}E_8$	N	0.0055	1%	
12	ANAPOE®-X-100	N	0.015	1%	
13	ANAPOE®-X-114	N	0.011	1%	
14	ANAPOE®-X-305	N	-	1%	
15	ANAPOE®-X-405	N	0.16	1%	
16	ANZERGENT® 3-10	Z	1.2	2%	
17	ANZERGENT® 3-12	Z	0.094	1%	
18	ANZERGENT® 3-14	Z	0.007	1%	
19	Big CHAP	N	0.25	1%	
20	Big CHAP, deoxy	N	0.12	1%	
21	CHAPS	Z	0.49	2%	
22	CHAPSO	Z	0.5	2%	
23	Deoxycholic acid, sodium salt	A	0.24	1%	
24	Sodium cholate	A	0.41	2%	
25	C-DODECAFOS™	Z	0.77	2%	
26	CYCLOFOS™-4	Z	0.45	2%	
27	CYCLOFOS™-5	Z	0.15	1%	
28	CYCLOFOS™-6	Z	0.094	1%	
29	CYCLOFOS™-7	Z	0.022	1%	
30	CYGLU®-3	N	0.86	2%	
31	CYMAL®-4	N	0.37	1%	
32	CYMAL®-5	N	0.12	1%	
33	CYMAL®-6	N	0.028	1%	
34	CYMAL®-7	N	0.0099	1%	
35	2,6-Dimethyl-4-heptyl-β-D-maltopyranoside	N	1.2	2%	
36	2-Propyl-1-pentyl maltopyranoside	N	1.9	2%	
37	FOS-CHOLINE®-9	Z	1.2	2%	
38	FOS-CHOLINE®-10	Z	0.35	2%	
39	FOS-CHOLINE®-11	Z	0.062	1%	
40	FOS-CHOLINE®-12	Z	0.047	1%	
41	FOS-CHOLINE®-13	Z	0.027	1%	
42	FOS-CHOLINE®-14	Z	0.0046	1%	
43	FOS-CHOLINE®-15	Z	0.0027	1%	
44	FOS-CHOLINE®-16	Z	0.00053	1%	
45	FOS-CHOLINE®-ISO-9	Z	0.99	2%	
46	FOS-CHOLINE®-ISO-11	Z	0.9	2%	
47	FOS-CHOLINE®-ISO-11-6U	Z	0.87	2%	
48	FOS-CHOLINE®-UNSAT-11-10	Z	0.21	1%	
49	FOS-MEA®-8	A	0.59	2%	
50	FOS-MEA®-10	A	0.15	1%	
51	FOSFEN™-9	Z	0.014	1%	
52	MEGA-8	N	2.5	2%	
53	NOPOL-FOS™	Z	1.4	2%	
54	PMAL™-C8	Z	-	1%	
55	PMAL™-C10	Z	-	1%	
56	Decyltrimethylammonium chloride	C	0.07	1%	
57	Dodecyltrimethylammonium chloride	C	0.0012	1%	
58	Hexadecyltrimethylammonium chloride	C	0.000102	1%	
59	Tetradecyltrimethylammonium chloride	C	0.0009	1%	
60	n-Octyl-β-D-glucopyranoside	N	0.53	2%	
61	n-Nonyl-β-D-glucopyranoside	N	0.2	1%	
62	n-Octyl-β-D-maltopyranoside	N	0.89	2%	
63	n-Nonyl-β-D-maltopyranoside	N	0.28	2%	
64	n-Decyl-α-D-maltopyranoside	N	-	1%	
65	n-Decyl-β-D-maltopyranoside	N	0.087	1%	
66	n-Undecyl-α-D-maltopyranoside	N	0.029	1%	
67	n-Undecyl-β-D-maltopyranoside	N	0.029	1%	
68	n-Dodecyl-α-D-maltopyranoside	N	0.0076	1%	
69	n-Dodecyl-β-D-maltopyranoside	N	0.0087	1%	
70	n-Tridecyl-β-D-maltopyranoside	N	0.0017	1%	
71	n-Heptyl-β-D-thioglucopyranoside	N	0.85	2%	
72	n-Octyl-β-D-thiomaltopyranoside	N	0.4	2%	
73	n-Nonyl-β-D-thiomaltopyranoside	N	0.15	1%	
74	n-Decyl-β-D-thiomaltopyranoside	N	0.045	1%	
75	n-Undecyl-β-D-thiomaltopyranoside	N	0.011	1%	
76	n-Dodecyl-β-D-thiomaltopyranoside	N	0.0026	1%	
77	n-Decyl-N,N-dimethylglycine	Z	0.46	2%	
78	n-Dodecyl-N,N-dimethylglycine	Z	0.041	1%	
79	n-Dodecyl-β-iminodipropionic acid,monosodium salt	Z	-	1%	
80	Sodium dodecanoyl sarcosine	A	0.42	2%	
81	Hexaethylene glycol monooctyl ether (C_8E_6)	N	0.39	2%	
82	Octaethylene glycol monododecyl ether ($C_{12}E_8$)	N	0.0048	1%	
83	Pentaethylene glycol monodecyl ether ($C_{10}E_5$)	N	0.031	1%	
84	Tetraethylene glycol monooctyl ether (C_8E_4)	N	0.25	1%	
85	Sucrose monododecanoate	N	0.016	1%	
86	Dimethyldecylphosphine oxide	N	0.1	1%	
87	n-Tetradecyl-N,N-dimethylamine-N-oxide (TDAO)	Z	0.0075	1%	
88	n-Dodecyl-N,N-dimethylamine-N-oxide (DDAO)	Z	0.023	1%	
89	HEGA-10	N	0.26	1%	
90	NP-40	N	0.05-0.3	1%	
91	Digitonin	N	-	1%	
92	Digitonin (8%)+Cholate (2%)				
93	CHAPS (6%)+CHS (1.2%)+DDM (10%)				
94	CHAPS (10%)+CHS (2%)+DDM (2%)				
95	CHAPS (10%)+CHS (2%)				
96	CHAPS (10%)+OG (1%)				

Reproduced from Ref. 24. ∗ Detergent type: (A) anionic, (C) cationic, (N) nonionic, and (Z) zwitterionic detergent. ∗∗ (CMC) Critical Micelle Concentration of the detergent in H_2O (source www.anatrace.com). ∗∗∗ Concentration of the detergent used in the screening.

5. Membrane Wash Buffer (50 mM sodium phosphate pH 7.8, 500 mM NaCl, 100 mM KCl, 20% v/v glycerol, 10 mM EDTA, 1 mM PMSF). The solution can be stored at 4 °C.
6. Solubilization Buffer (50 mM sodium phosphate pH 7.8, 200 mM NaCl, 100 mM KCl, 20% v/v glycerol, 1% w/v FC14, 1 tablet of protease inhibitor per 10 mL). The solution can be stored at 4 °C.
7. Buffer A (Ni^{2+} chelating column Binding Buffer containing 50 mM sodium phosphate pH 7.8, 200 mM NaCl, 100 mM KCl, 0.02% w/v FC14, 25 mM imidazole). The solution can be stored at 4 °C.
8. Buffer B (Ni^{2+} chelating column Elution Buffer containing 50 mM sodium phosphate pH 7.8, 200 mM NaCl, 100 mM KCl, 0.02% w/v FC14, 500 mM imidazole). The solution can be stored at 4 °C.
9. Buffer C (gel filtration and purified protein Storage Buffer containing 0.02% w/v FC14 in PBS). The solution can be stored at 4 °C.

3 Methods

3.1 Cell-Free Expression

Commercial cell-free in vitro translation systems can be used to express milligrams of soluble and functional protein directly from plasmid DNA within hours. The receptors can be purified using immunoaffinity chromatography and gel filtration, and can be analyzed with standard techniques. An important factor affecting expression levels and solubility is the choice of detergent. The Brij family of detergents has repeatedly yielded high levels of receptors (Fig. 2), while Fos-Cholines (including FC14), which are optimal for purification from HEK293 cells (Fig. 3), result in almost no receptor expression [43, 59, 66, 67]. It should be noted that the detergents commonly used in cell-based production may not be optimal for use in cell-free systems and vice versa. In cell-based GPCR production systems, some detergents may inhibit transcription or translation by interfering with ribosomes or other synthesis machinery.

Using the cell-free system, factors like incubation temperature and time typically have small effects on expression. Although the optimal expression conditions must be validated for each protein of interest and the solubility and functionality of the expressed receptors should be analyzed, the following protocol has proven to be optimal for most of the receptors that we have tried to express in our lab.

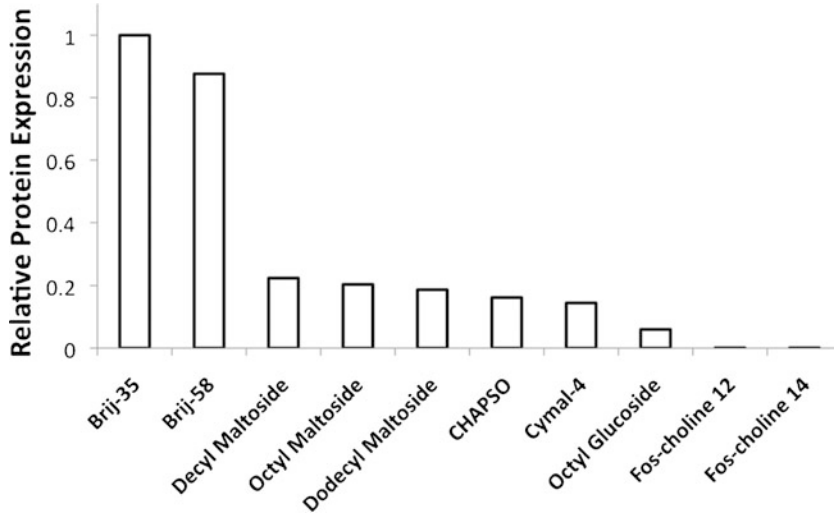

Fig. 2 Detergent screening for the cell-free production of the GPCR olfactory receptor hOR17-210. Brij-35 and Brij-58 yielded ~4–5 times more GPCR receptor compared to the next best detergent. Brij-35 consistently had slightly higher yields than Brij-58. Each bar represents the average of 2–3 experiments. The data are normalized to Brij-35. (Reproduced from ref. 20)

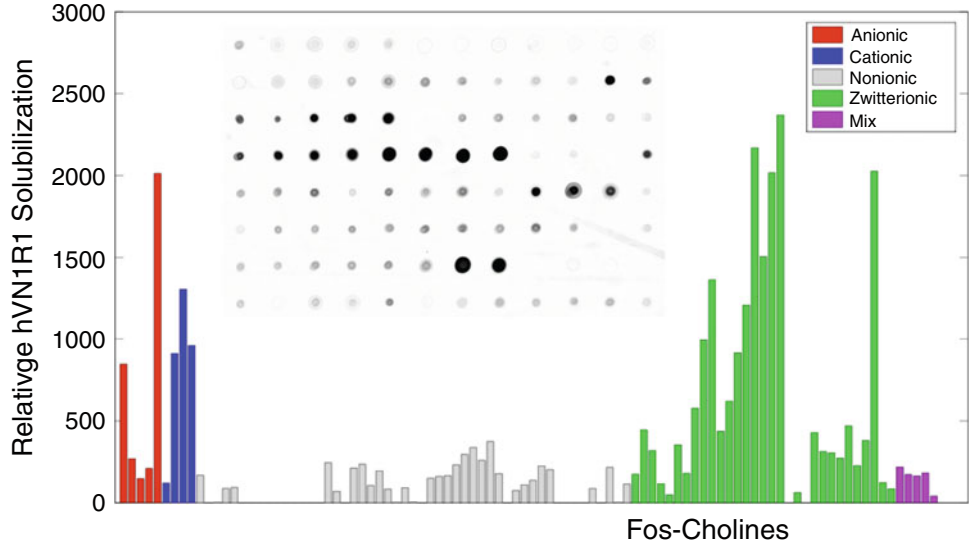

Fig. 3 Detergent screening for the solubilization of the hVN1R1 GPCR produced in HEK293 cells. Zwitterionic detergents typically solubilized a greater portion of the expressed protein compared to cationic and anionic detergents. Fos-choline detergents solubilized the highest amount of protein. (Reproduced with permission from Ref. 27)

3.1.1 Cell-Free Expression of Membrane Proteins

1. Thaw the *E. coli* extract, 2.5× IVPS Reaction Buffer, 2× IVPS Feed Buffer, amino acids, methionine, T7 Enzyme, and DNA on ice.

2. Add 200 μL of the *E. coli* extract, 200 μL of the 2.5× IVPS Reaction Buffer, 12.5 μL of the Amino Acids, 10 μL of the Methionine, and 10 μL of the T7 Enzyme Mix to a sterile, DNAse-free, RNAse-free Eppendorf tube (*see* **Note 10**).
3. Add the plasmid to the lysate so that the final DNA concentration is 10 μg/100 μL.
4. Add Brij-35 to a final concentration of 0.2% w/v.
5. Add DNAse-free and RNAse-free water so that the final volume of the cell-free reaction will be 500 μL.
6. Briefly spin down the Eppendorf tube.
7. Place the cell-free reaction in an Eppendorf rack in a shaking incubator at 33 °C and 250 rpm for 30 min (*see* **Note 11**).
8. During those 30 min, prepare the feed buffer. Add 250 μL of the 2× IVPS Feed Buffer, 12.5 μL of the Amino Acids, 10 μL of the Methionine to a sterile Eppendorf tube. Add Brij-35 to a concentration of 0.2%, and add water so that the final volume is 500 μL.
9. Add the Feed Buffer to the reaction.
10. Continue the reaction for 3–6 h.
11. After the reaction is complete, spin it down in a microcentrifuge for 5 min at 10,000 rpm.
12. Carefully transfer the supernatant to a fresh tube without disturbing the pellet. The supernatant contains solubilized receptor.
13. The synthesized receptors can be purified or run on an SDS-PAGE gel immediately, stored at 4 °C for 1–2 weeks, or stored at −20 °C for longer periods of time.

3.1.2 Detergent Screens

1. Detergents can be added directly to the reactions. A preliminary screen determined that the optimal detergent concentration was 0.2% w/v.
2. After the reactions are complete, the samples can be centrifuged at 10,000 rpm for 5 min. The supernatant containing the solubilized protein can be removed and stored.
3. The relative quantities of solubilized and precipitated protein can be determined with a western or dot blot. ImageJ (http://rsb.info.nih.gov/ij/) may be used to perform dot blot densitometry analyses and assess the amount of solubilized GPCR (Fig. 2).

3.1.3 Purification of Cell-Free-Produced Membrane Proteins

1. Add the antibody-coupled beads into a clean Amicon tube. Suspend the beads by gently shaking the tube suspension to ensure that they are distributed homogeneously.

2. Wash the beads with DPBS to remove excess Storage Buffer. Spin the beads down at 1400 × *g* for 1 min, and then let sit for 1 min to allow the beads to completely settle to the bottom of the tube. Using a pipette, slowly remove the supernatant without disturbing the bead pellet. Add one bead volume of DPBS to the pellet to resuspend the pellet. Repeat this process three times. After the last repetition, do not add more DPBS.
3. Add the supernatant from the cell-free reaction to the washed beads.
4. Add 1 μL of DNAse I (200 U/mL) and 1 μL of RNAse A (20 mg/mL) for each mL of the cell-free reaction volume.
5. Rotate the supernatant with the beads on a rotating platform overnight at 4 °C to capture the synthesized protein on the beads.
6. After the overnight rotation, spin the beads at 1400 × *g* for 1 min and let sit for 1 min to allow the bead pellet to settle. Remove the supernatant and transfer it to a tube labeled FT (Flow-Through). Save a small sample of the FT for analysis, and freeze the remaining at −80 °C in case the beads did not capture all of the synthesized receptors. Add one bead volume of Wash Buffer to the beads, and rotate at 4 °C on a rotating platform for 10 min.
7. Wash the GPCR-bound beads to remove any impurities. For each wash, after the tube has rotated for 10 min, spin it at 1400 × *g* for 1 min and allow it to sit for 1 min. Carefully remove the supernatant without disturbing the bead pellet, and transfer it to a clean tube (labeled Wash 1, Wash 2, etc.). Add 1 bead volume of Wash Buffer, and rotate on a rotating platform at 4 °C for 10 min. Repeat this process until the absorbance at 280 nm of the removed supernatant matches that of the Wash Buffer. Typically, 13–20 washes are required. The washes can be run overnight at 4 °C if necessary.
8. Elute the synthesized GPCRs from the beads. Add one bead volume of Elution Buffer to the beads and rotate on a rotating platform at room temperature for 1 h. Spin the beads at 1400 × *g* and let them sit for 1 min. Carefully remove the supernatant without disturbing the bead pellet and transfer it to a clean tube (labeled Elution 1, Elution 2, etc.). Repeat this process until the absorbance of the removed supernatant at 280 nm matches that of the Wash Buffer. There will be absorbance at ~215 nm due to the presence of the elution peptide. The supernatant contains the synthesized receptors. Typically, 5–7 elutions are required. The elutions can be run overnight at 4 °C if necessary.
9. The washes and elutions can be stored at 4 °C until they are ready for use.

10. The elutions can be pooled and concentrated in centrifugal units with 50 kDa molecular weight cutoff filters. If the protein will be analyzed by circular dichroism, it must be washed and concentrated with excess Wash Buffer to remove all residual elution peptide. 10 mL of Wash Buffer is usually sufficient to remove the elution peptide from a concentrated protein sample with a total volume of 300 μL. If the receptors will be run on a size exclusion column, they must be concentrated to a volume that will fit in the loading loop. The receptors should be concentrated immediately prior to being loaded on the column to minimize aggregation and precipitation.

3.1.4 Gel Filtration Chromatographic Purification of Cell-Free-Produced GPCRs

1. Equilibrate the gel filtration column with at least 1–2 column volumes of Wash Buffer. We use a HiLoad 16/60 Superdex 200 column.
2. Load the freshly concentrated GPCR sample onto the column.
3. Run the system at 0.3 mL/min, and monitor the UV absorbance at 215 nm and 280 nm. The monomeric form of our receptors typically exits the column after 60–65 mL (elution volume). Collect the first 40 mL in a clean bottle. Collect the rest in 384-well plates with 100 μL in each well to better separate the protein fractions.
4. Pool the appropriate fractions together based on the UV absorbance signal and western or dot blots.
5. Concentrate the pooled fractions to the necessary volume or concentration and store at 4 °C until they are ready for further analysis. Samples can be stored at −80 °C for long-term storage.

3.2 HEK Cell Expression System

The HEK293 cell line has been used for large-scale expression of rhodopsin, the olfactory receptor hOR17-4, the vomeronasal receptor hVN1R1, the human trace amine-associate receptor hTAAR5, and variants of these receptors [61, 66, 67]. Milligram quantities of homogenous receptors can be purified using immunoaffinity and size exclusion chromatography. The purified GPCR is properly folded and functional. Here, we will describe the protocol for producing a stable, inducible HEK293 cell line capable of expressing GPCRs and the protocol for purifying the protein.

3.2.1 Construction of Inducible Stable Cell Lines

1. Grow HEK293 cells so that there has been at least one passage since the cells were thawed and a sufficient number of them to cover a 150 mm tissue culture dish. Add 30 mL of growth medium to the 150 mm cell culture dish. Old media should be replaced with fresh media every 2–3 days. Unless otherwise noted, all volumes are for cells grown in 150 mm dishes.

2. The cells should be passaged when they are 90–95% confluent in the dishes.
   (a) Remove the old media.
   (b) Gently wash the adherent cells with 5 mL DPBS. Remove the DPBS (*see* **Note 12**).
   (c) Gently add 1 mL of 0.05% w/v trypsin solution and incubate at 37 °C for 3–5 min.
   (d) Gently tap the dish. If the cells do not release, incubate them for another 1–2 min. If the cells release from the culture dish, continue with passaging. Do not incubate cells in the trypsin solution for more than 10 min.
   (e) Deactivate the trypsin by adding 5 mL of growth media. Tip the flask and, using a 10 mL pipette, wash the bottom with the trypsin/growth media solution to break apart potential cell clumps and to completely detach the cells from the dish.
   (f) Split the trypsin/growth media solution containing cells into 2–10 fresh flasks, as desired.
   (g) Add fresh growth media to each new flask for a total volume of 30 mL. Place the newly passaged cells in the incubator.
3. The day before transfection, ensure that the cells are 90–95% confluent, passaging them if necessary. Replace the regular Growth medium with 30 mL of Transfection medium 1.
4. On the day of transfection, dilute 40 μg of the DNA into 2.5 mL of Transfection medium 2.
5. Dilute 100 μL of Lipofectamine 2000 into 2.5 mL of Transfection medium 2 and incubate at room temperature for 5 min. Longer incubation times may result in decreased activity.
6. Combine the diluted DNA and diluted Lipofectamine 2000 reagent, and incubate at room temperature for 20 min.
7. Remove the Growth medium from the cells. Wash them with DPBS and add 25 mL of Transfection medium 1.
8. Add the DNA-Lipofectamine reagent complex to the cells and mix by gently rocking the plate back and forth.
9. Incubate the cells at least 4–6 h, but up to 24 h, before removing the Transfection media and adding the Growth media.
10. Incubate the cells at least 24–48 h after transfection. Transient transgene expression can be assessed at this point. The following steps are necessary to create stable clones.
11. Passage the cells into three dishes at three different densities using Selection medium 1. A good starting point may be to

have 10% of the cells in one plate, 30% in the second, and the remaining 60% in the third. These values may need to be adjusted.

12. Replace the old media with fresh media every 2–3 days for 2–4 weeks. During this time, cells transiently expressing the gene will die and be removed with the old media. Stably transfected cells will grow and form colonies. These colonies should be spaced far enough apart to allow them to be individually picked without disturbing neighboring colonies.
13. When the stable colonies are 1–2 mm in diameter and visible to the eye, transfer them to a 24-well plate.
    (a) Gently wash the colonies in the tissue culture dish with PBS, ensuring that the colonies are not disturbed.
    (b) Add 100 μL of 0.05% w/v trypsin to each well of a 24-well tissue culture plate.
    (c) Using a 1000-μL pipette tip, aspirate a single colony and pipette it into one of the 24 wells. Continue this procedure until each well of the 24-well plate has a unique colony.
    (d) Pipette colonies up and down to break apart any cell clumps and to homogeneously suspend them in the trypsin solution. The colonies should not remain in the trypsin solution for more than 5 min (**steps c** and **d**) before proceeding to the next step.
    (e) Add 1 mL of Selection medium 1 to each well.
14. Allow the cells to grow until they are 95% confluent.
15. Split each confluent colony into 4 wells of a 12-well tissue culture dish. The first three wells should each contain 30% of the cells and should be labeled 0 (no induction), + (tetracycline induction), and ++ (tetracycline and sodium butyrate induction). The fourth well should contain the remaining 10% of the cells. This well will be used to expand the cell line should it be chosen. Add 3 mL of Selection medium 1 to each well. Replace the media every 2–3 days.
16. Induce gene expression when the cells are 90–95% confluent. Wash the cells with PBS first. In the well labeled 0, put 3 mL of Selection medium 1. In the well labeled +, put 3 mL of Selection medium 1 supplemented with 1 μg/mL tetracycline. In the well-labeled ++, put 3 mL of Selection medium 1 supplemented with 1 μg/mL tetracycline and 2.5 mM sodium butyrate (*see* **Note 13**).
17. After 48 h remove the Induction medium. Using cold PBS, resuspend the cells in each well by vigorous pipetting and transfer them to one or more clean Eppendorf tubes.

18. Spin the cells down at 10,000 rpm for 5 min at room temperature.
19. During the spinning process, prepare PBS with protease inhibitors. Each Roche mini tablet is good for 10 mL of PBS. Use cold PBS.
20. After spinning the cells, remove the PBS without disturbing the pellets. Resuspend each cell pellet in 120 μL of PBS with protease inhibitors.
21. Add 30 μL of 10% w/v FC14 to each tube (the final FC14 concentration should be 2% w/v). Do not pipette the cells up and down after adding detergent. If the cells are not suspended after adding FC14, vortex them (*see* **Note 14**).
22. Rotate the Eppendorf tubes at 4 °C for 60 min to solubilize the expressed receptors.
23. Spin the Eppendorf tubes at 13,000 rpm for 30 min at 4 °C to pellet any insoluble material.
24. Transfer the supernatant to a clean Eppendorf tube being careful not to disturb the pellet. The supernatant can be stored at −20 °C or analyzed immediately.
25. Use a dot blot to evaluate the relative protein expression of un-induced and induced samples for each clone. Select 2–3 of the highest expressing clones.
26. Run the supernatant of the selected clones on a western blot to assay for protein degradation or alternate expression constructs.
27. Select the clone that has the highest expression, least cell toxicity, and no extraneous bands in the western blot. Expand the cells from the untreated well of the selected clone from the 12-well plate (from **step 17**). Use Selection medium 2 from now on. The higher concentration of zeocin is necessary for selection, but the lower concentration is sufficient for maintenance (*see* **Note 15**).

3.2.2 Immunocytochemistry

1. Prepare a glass slide or coverslip to be seeded with cells.
   (a) Pipette enough poly-L-lysine solution on the glass coverslip to cover it without spilling over. (It may be helpful to place the slide on the bottom of a well in a 6-well plate.)
   (b) Incubate at room temperature for 30 min.
   (c) Pipette the excess solution off. It can be reused 1–2 more times.
   (d) Sterilize the coverslip under UV light overnight.
2. Seed the cells on the coverslip at a low density.
3. Incubate the cells on the slide overnight.

4. Remove the media.
5. Induce the cells by adding Selection medium 2 supplemented with 1 μg/mL tetracycline and 2.5 mM sodium butyrate.
6. One to two days after induction, remove the Induction medium and wash the cells with PBS (*see* **Note 16**).
7. Fix the cells in 10% neutral buffered formalin for 20 min at room temperature.
8. If the cells need to be permeabilized, incubate them in ice-cold permeabilizing solution for 3 min at −20 °C.
9. Block the cells in Blocking solution for 1 h at room temperature on a shaker.
10. Wash the cells with PBS.
11. Incubate the cells in the primary antibody solution overnight at 4 °C on a shaker.
12. Wash the cells three times in PBS on a shaker, 3–5 min each time.
13. Incubate the cells in the secondary antibody solution on a shaker. Cover the slides with foil to avoid exposure to light or do this step in a darkened room. In all subsequent steps, the slides should be covered or manipulated in a dim room to avoid light exposure.
14. Wash the slides with PBS three times, 5 min each time. Keep the slides covered during the washes to avoid exposure to light.
15. Carefully pick up one slide by the edge with tweezers and touch the edge to a Kim wipe to remove excess PBS.
16. Squeeze one drop of ProLong Gold Antifade with DAPI on top of the cells, and place a clean glass coverslip on top.
17. Allow the slides to sit overnight at room temperature.
18. Image the slides on a microscope or store them at 4 °C (Fig. 4).

3.2.3 Cell Extract Preparation

1. Grow the stable cell line expressing the gene of interest until sufficient cells are available. Typically, ten 150 mm tissue culture dishes can yield up to 2 g of cells, and high expressing clones can yield up to ~1 mg of protein per gram of cells.
2. When the cells are 90–95% confluent, induce gene expression with 1 μg/mL tetracycline and 2.5 mM sodium butyrate for 48 h (*see* **Note 17**).
3. Scrape harvest the cells and pool together. Alternatively, detach the cells by pipetting up and down with PBS. Centrifuge the cells for 5 min at 1000 rpm and remove the PBS without disturbing the pellet.
4. Use the cells immediately, or freeze and store the cells in liquid nitrogen until they are ready for experiments.

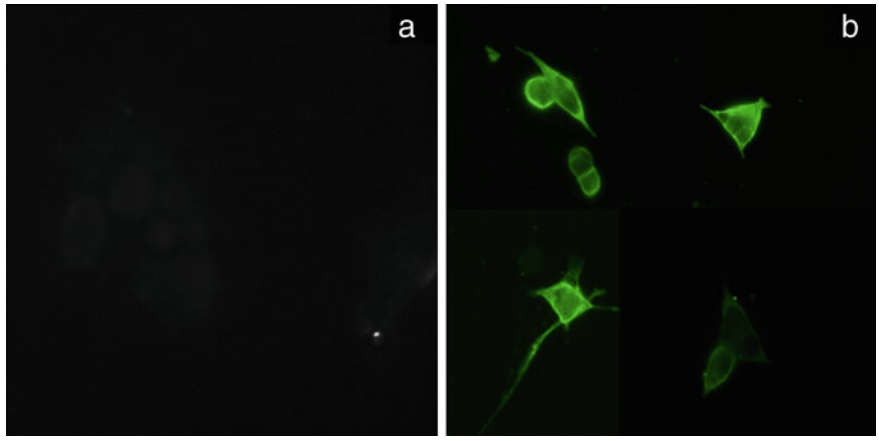

Fig. 4 (**a**) Non-induced HEK293 cells showed no staining. (**b**) Induced HEK293 cells stained with the rho1D4 antibody showed that the expressed GPCR receptor hVN1R1 was localized to the cell membrane. (Reproduced with permission from Ref. 27)

3.2.4 Detergent Screening

1. Use freshly prepared cell pellets, or thaw frozen cell pellets on ice.
2. Resuspend the cell pellets in DPBS with protease inhibitors. About 10 mL of DPBS is sufficient for each gram of cells.
3. Split the cell suspension into the desired number of tubes (one tube for each detergent to be tested).
4. Add detergent to a final concentration of 2% w/v. Do not pipette the cells after adding detergent.
5. Rotate the cells for 1 h at 4 °C to solubilize the protein.
6. Spin the cells at 13,000 rpm for 30 min to pellet any insoluble fractions.
7. Transfer the supernatant to a clean tube without disturbing the cell pellet.
8. Analyze the relative amounts of solubilized protein on a dot blot (Fig. 3).
9. The supernatants, which contain the protein, can be stored at −20 °C.

3.2.5 Receptor Purification

1. Use fresh cell pellets or thaw frozen cell pellets on ice.
2. Resuspend the cell pellet in PBS with protease inhibitors. Pipette the cells up and down until all cell clumps have been broken and the cells are homogeneously suspended.
3. Add 2.5 mL of 10% w/v FC14 for each gram of cell pellet (final concentration 2%). Do not pipette the cells after adding detergent (*see* **Note 18**).
4. Rotate the cells for 4 h at 4 °C to solubilize the protein.

5. Centrifuge the solubilized cells for 30 min at 30,000 × *g* and 4 °C.
6. Transfer the supernatant to Rho1D4-coupled CNBr-activated Sepharose 4B beads (binding capacity of 0.7 mg/mL).
7. Add 1 μL of DNAse I (200 U/mL) and 1 μL of RNAse A (20 mg/mL) for each mL of the supernatant-bead mixture.
8. Capture the solubilized GPCRs on the beads by rotating the mixture overnight at 4 °C.
9. Collect the beads by centrifuging them at 1400 × *g* for 1 min, or filtering them through a filter column. Save a sample of the supernatant (labeled "flow-through") for future analysis.
10. Resuspend the beads in one bead volume of Wash Buffer.
11. Rotate the beads for 10 min at 4 °C.
12. Collect the beads by centrifugation to perform the first wash. Measure the absorbance of the supernatant at 280 nm. Save the supernatant for future analysis (labeled "wash 1").
13. Repeat the washes until the absorbance at 280 nm is less than 0.01 mg/mL, indicating that all impurities have been removed.
14. Resuspend the pellets with one bead volume of Elution Buffer to perform the first elution, and rotate the beads at room temperature for 1 h.
15. Collect the beads by centrifugation to perform the first elution. Measure the absorbance of the supernatant at 280 nm. Save the supernatant containing the purified protein (labeled "elution 1"), and keep it on ice or at 4 °C.
16. Repeat the elutions until the absorbance at 280 nm is less than 0.1 mg/mL, indicating that all of the protein has been detached from the beads.
17. Pool the elutions. Using a 50 kDa molecular weight cutoff filter, concentrate them until the total volume is less than 1.7 mL. Centrifuge the protein at speeds 1000–2000 rpm.
18. Transfer the protein to a fresh tube, and load it on the size exclusion column pre-equilibrated with at least 1 column volume of Wash Buffer.
19. Run the protein through the column at 0.3 mL/min.
20. Collect the appropriate fractions, as determined by absorbance readings at 280 nm, and concentrate them to the desired concentration using, for example, an Amicon centrifuge tube with MWCO 10 kDa.
21. Analyze the fractions. Store the protein fractions at 4 °C for short-term storage, or at −80 °C for long-term storage.

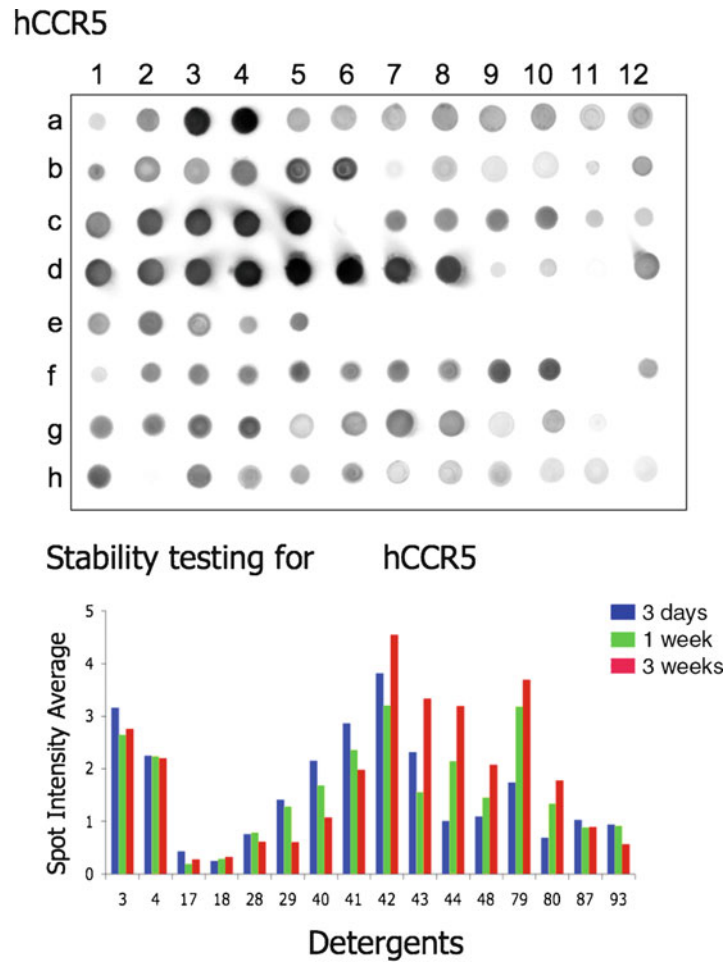

Fig. 5 Detergent screening for solubilization of the CCR5 GPCR expressed in *E. coli*. (*Top panel*) Dot blot showing the effectiveness of 96 different detergents (shown in Table 1) on solubilizing the CCR5 from cell lysates. Immunoblotting analysis was performed using a mouse anti-His_6-tag monoclonal antibody. (*Bottom panel*) Long-term stabilization of CCR5 solubilized in 16 of detergents (detergent numbers are shown in Table 1). The detergent effectiveness was tested at 4 °C for 3 days, 1 week, and 3 weeks using dot blot and a mouse anti-His_6-tag monoclonal antibody. (Adapted from Ref. 24)

3.3 E. coli-Based Expression System

To achieve high yields of functional membrane proteins, it is important to consider several factors such as the *E. coli* strain, the expression vector, fusion proteins to enhance expression or yields, purification tags, and the choice of detergent for solubilizing the expressed membrane proteins (Figs. 5 and 6). The *E. coli* host strain selected should show reduced cell toxicity from high-membrane protein expression. The "Walker" *E. coli* strains C41(DE3) and C43(DE3) [45] have been shown to increase the yield of some internal membrane and soluble proteins (Fig. 6). These strains are

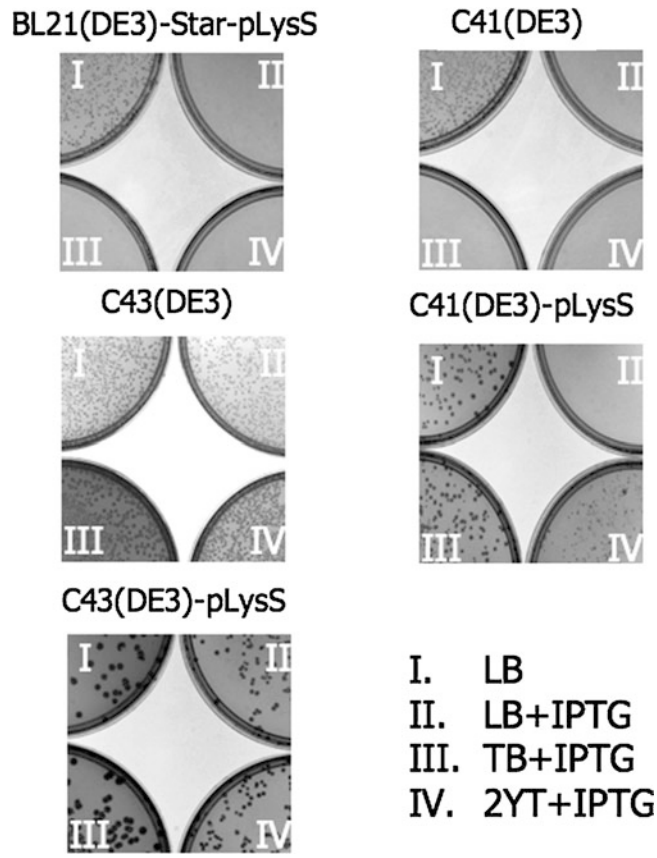

Fig. 6 Selection of *E. coli* strains for expression of the CCR5 GPCR. The vector containing the GPCR construct was transformed into 5 *E. coli* strains: BL21, C41, C43, C41-pLysS, and C43-pLysS. The cells were cultured on (I) LB-agar plates, (II) LB-agar-IPTG plates, (III) TB-agar-IPTG plates, and (IV) 2YT-agar-IPTG plates. The colonies were analyzed and the best GPCR expression conditions were selected. (Adapted from Ref. 24)

advantageous for GPCR overexpression compared to the standard BL21(DE3) strains because they are characterized by enhanced resistance to the toxicity caused by high-level expression of GPCRs.

The protocol described here uses the expression vector pEXP3-DEST, a high-copy plasmid with a T7 promoter, and a GPCR fused to a His-tag for purification with a Ni^{2+} column. The GPCR is expressed in the C41(DE3)*E. coli* strain and solubilized by FC14. This method has been tested and it was highly efficient for the solubilization of the chemokine receptors CCR3, CX3CR1, CXCR4, and CCR5 [63].

3.3.1 Expression of Membrane Proteins in E. coli

1. Transform the expression vector into C41(DE3)*E. coli* cells.
2. Plate the transformationreaction on LB agar plates and incubate overnight at 37 °C.

3. Prepare an overnight starter culture by incubating 5 colonies from the LB agar plates in sterile LB medium at 37 °C with shaking (250 rpm) for 12–16 h.
4. Cool 10 mL of the overnight culture on ice for 5 min prior to centrifugation (10 min, 3000 × *g*, 4 °C) to collect the cell pellet.
5. Dilute the cell pellet in 1 mL fresh sterile LB medium and inoculate into 1 L of fresh TB medium containing 100 mg/mL Ampicillin. Incubate at 37 °C with shaking at 220 rpm until cell concentration reaches an OD_{600} of 0.6 (*see* **Note 19**).
6. Lower temperature to 16 °C and continue shaking for 30 min.
7. Induce expression of the target protein by adding 0.3 mM IPTG and shake the culture for 24 h (*see* **Note 20**).
8. Harvest cells by centrifugation at 5000 × *g* for 20 min, and store the pellet at −20 °C until further use.

3.3.2 Detergent Screening

1. Inoculate 2 mL of overnight culture in 200 mL fresh TB media and culture at 37 °C and shaking at 220 rpm ~3 h, until the cell concentration reaches an OD_{600} of 0.6.
2. Lower temperature to 16 °C and continue shaking for 30 min.
3. Induce expression of the target protein by adding 0.3 mM IPTG and shake for 24 h.
4. Harvest cells by centrifugation at 5000 × *g* for 20 min.
5. Prepare 96 separate 1.5 mL centrifuge tubes marked 1–96.
6. Resuspend the pellet in 50 mL Lysis Buffer and pipet 180 μL into each 1.5 mL centrifuge tube.
7. Perform three freeze–thaw cycles at −80 °C and 42 °C.
8. Add 20 μL of 10% w/v or v/v solution of the detergent of choice in the 1.5 mL centrifuge tubes (Table 1), mix carefully, and incubate at 2–3 h at 4 °C.
9. Centrifuge the samples at 16,000 × *g* for 30 min.
10. Analyze the relative amounts of solubilized protein on a dot blot (Fig. 5).

3.3.3 Purification of E. coli-Produced Membrane Proteins

1. Collect membrane fractions by resuspending the pellet in 50 mL Lysis Buffer with added optimal detergent (in our case 2% w/v FC14) and perform three freeze–thaw cycles at −80 °C and 42 °C prior to passing the cells through a pre-cooled French press at 18,000 psi.
2. Centrifuge the cell lysate at 10,000 × *g* for 1 h to remove cell debris and inclusion bodies.
3. Collect the supernatant and ultracentrifuge at 100,000 × *g* for 1 h to collect the crude membrane fractions.

4. Wash the crude membrane fraction by carefully resuspending the pellet in 20 mL Membrane Wash Buffer followed by another ultracentrifugation step (100,000 × *g*, 1 h).
5. Solubilize the membrane protein by resuspending the crude membrane fractions in 10 mL Solubilization Buffer followed by gentle swirling at 4 °C overnight (*see* **Note 21**).
6. The following day, ultracentrifuge the solution at 100,000 × *g* for 1 h to remove non-solubilized protein.
7. Store the supernatant containing the protein at −20 °C.

3.3.4 Gel Filtration Chromatographic Purification of Membrane Proteins Produced in E. coli

1. Load the supernatant on a 5 mL Hitrap Chelating HP column ("ready-to-use" pretreated with chelated Ni^{2+}), equilibrated with Buffer A before use.
2. Wash the column with 15 column volumes of a mixture of 95% v/v Buffer A and 5% v/v Buffer B before eluting the protein with a linear gradient of 5–100% v/v Buffer B in Buffer A.
3. Pool fractions containing protein (determine the protein content of each fraction with absorbance reading at 280 nm, SDS-PAGE, or western blot) and concentrate with a 50 kDa molecular weight cutoff filter.
4. Load the concentrated protein on the size exclusion column (Superdex-200) pre-equilibrated with at least 1 column volume of Wash Buffer.
5. Run the protein solution through the column at 0.3 mL/min.
6. Collect the appropriate fractions as determined by absorbance readings at 280 nm, and concentrate them to the desired concentration.
7. Analyze the fractions, or store them at 4 °C for short-term storage or at −80 °C for long-term storage.

4 Notes

1. The lysate and buffer should be stored at −80 °C, thawed on ice, and used within 4 h of defrosting. It can be refrozen and thawed once for optimal results. Aliquots can be made for larger volumes. Kits from other companies are also available. Higher yields may be possible with lab-made lysates and buffers in overnight continuous exchange reactions, but sufficient yields are often achieved with commercial kits.
2. Brij-35 has been the optimal detergent in our experiments. However, other groups have found other detergents to be optimal for their GPCRs (e.g., polyoxyethylenes related to Brij-35) [9]. A preliminary detergent screen, in which the

volumes are scaled down to a total volume of 25–50 μL, may be necessary to find the best detergent for the specific GPCR to be produced.

3. GPCR genes have a 5′ NcoI site and a 3′ XhoI site for ligation. They also have a C-terminal rho1D4 epitope tag (TETSQVAPA) for purification followed by a double stop codon. Some have potential glycosylation sites removed. The pET24 and pET28 vectors can also be used for *E. coli*-based cell-free expression. A His-tag can be used for purification, but typically yields less pure protein, especially if the yields for a specific construct are lower. The rho1D4 tag usually yields purer protein preparations.
4. If the cells do not already contain the pcDNA6/TR vector, stable HEK293G cells expressing this vector must first be generated. This can be done using the same transfection protocol described here.
5. When working with expanding or induced HEK293 cells, all experiments should be done in a sterile hood. HEK cells should be grown in incubators kept at 37 °C, 5% CO_2, and 95% relative humidity.
6. Always warm the media, trypsin solution, and other reagents that will be used with HEK293G cells to 37 °C before beginning any protocols.
7. Autoclave on liquid cycle for 20 min at 15 psi. Allow solution to cool to 55 °C and add the antibiotic. Store at room temperature or at 4 °C for long-term storage.
8. Prepare LB medium, but add 15 g/L agar before autoclaving. Autoclave on liquid cycle for 20 min at 15 psi. After autoclaving, cool to 55 °C, add the antibiotic, and pour into plates. Let gel, then invert, and store at 4 °C, in the dark.
9. Add 12 g Tryptone, 24 g Yeast Extract, and 4 mL Glycerol to 900 mL distilled H_2O, sterilize by autoclaving. Allow to cool to room temperature and then adjust the volume to 1000 mL with 100 mL of filter-sterilized solution of 0.17 M KH_2PO_4 and 0.72 M K_2HPO_4.
10. The volumes listed here are for a total reaction volume of 1 mL. The volumes can be scaled up or down as necessary.
11. These are the optimal temperature, time, and rotation speed for the receptors we tested. Preliminary tests did not show significant differences in GPCR yields with rotation speeds up to 300 rpm, and at temperatures between 30° and 37 °C. However, the optimal conditions may vary with different receptors. In particular, lower temperatures can increase the yield of soluble receptors, while higher temperatures can increase the total receptor yield.

12. HEK293 cells are loosely adherent. All reagents should be gently pipetted down the sides of the cell culture dishes to avoid disturbing the cells.
13. Other concentrations of sodium butyrate may need to be used depending on the level of gene expression and cell toxicity. Higher concentrations can increase protein expression, but can also increase expression-related cell death.
14. If no results are seen with FC14, other detergents can be used to solubilize and extract the expressed membrane proteins. Once the clone with the highest expression is selected, the detergent can be optimized to minimize receptor damage.
15. It may be wise to expand the clone in a vented cap T75 flask to minimize the risk of infection. Also, samples of the clone should be frozen and stored in liquid nitrogen.
16. One day of induction is usually sufficient to observe protein expression, while 2 days of induction may result in optimal protein expression. If enough protein cannot be seen after 1 day, induce the cells for 2 days.
17. The amount of tetracycline and sodium butyrate as well as the time of induction may need to be optimized. Typically, optimal values range from 1–2 μg tetracycline, 1–5 mM sodium butyrate, and 1–2 days of induction.
18. FC14 has been the optimal detergent in our experiments. Depending on the GPCR, the detergent screen may yield another optimal detergent or concentration.
19. Carbenicillin is stable for long periods of time and can in some cases give a higher yield than Ampicillin.
20. Different timing, concentrations, and temperatures of the IPTG induction may affect the total yield of functional membrane protein. Optimization of gene expression can be performed by testing different conditions on small cultures prepared by inoculation of an overnight culture (1/100) in 5 mL fresh TB media containing 100 μg/mL Ampicillin, culture at 37 °C with shaking. Test induction at different cell concentrations (OD_{600}), IPTG concentrations, and temperatures. Pellet the cultures by centrifugation at 5000 × *g*. Analyze the samples for differences in expression level on a dot blot.
21. Systematic screening of detergents is recommended to achieve the highest yield of functional protein.

References

1. Klabunde T, Hessler G (2002) Drug design strategies for targeting G-protein-coupled receptors. Chembiochem 3:928–944
2. Lundstrom K (2005) Structural biology of G protein-coupled receptors. Bioorg Med Chem Lett 15:3654–3657
3. Protein Data Bank (2019). http://www.rcsb.org
4. Membrane Proteins of Known Structure run by the Stephen White Laboratory at UCI (2018). http://blanco.biomol.uci.edu/mpstruc/
5. Jaakola V-P et al (2008) The 2.6 Å crystal structure of a human A2A adenosine receptor bound to an antagonist. Science 322 (5905):1211–1217
6. Rasmussen SGF et al (2007) Crystal structure of the human β2 adrenergic G-protein-coupled receptor. Nature 450(7168):383–387
7. Warne T et al (2008) Structure of a β1-adrenergic G protein-coupled receptor. Nature 454 (7203):486–491
8. Wu B et al (2010) Structures of the CXCR4 chemokine receptor in complex with small molecule and cyclic peptide antagonists. Science 330(6007):1066–1071
9. Shimamura T et al (2012) Structure of the human histamine H1 receptor complex with doxepin. Nature 475(7354):65–70
10. Hanson MA et al (2012) Crystal structure of a lipid G protein-coupled receptor. Science 335 (6070):851–855
11. Kruse AC et al (2012) Structure and dynamics of the M3 muscarinic acetylcholine receptor. Nature 482(7386):552–556
12. Wu H et al (2012) Structure of the human κ-opioid receptor in complex with JDTic. Nature 485(7398):327–332
13. Manglik A et al (2012) Crystal structure of the μ-opioid receptor bound to a morphinan antagonist. Nature 485(7398):321–326
14. Granier S et al (2012) Structure of the δ-opioid receptor bound to naltrindole. Nature 485:400–404
15. Thompson AA et al (2012) Structure of the nociceptin/orphanin FQ receptor in complex with a peptide mimetic. Nature 485 (7398):395–399
16. Zhang C et al (2012) High-resolution crystal structure of human protease-activated receptor 1. Nature 492(7429):387–392
17. Tan Q et al (2013) Structure of the CCR5 chemokine receptor—HIV entry inhibitor Maraviroc complex. Science 341 (6152):1387–1390
18. Wang C et al (2013) Structure of the human smoothened receptor bound to an antitumour agent. Nature 497(7449):338–343
19. Wang C et al (2013b) Structural basis for molecular recognition at seratonin receptors. Science 340(6132):610–614
20. Siu FY et al (2013) Structure of the human glucagon class B G-protein-coupled receptor. Nature 499(7459):444–449
21. Burg JS et al (2015) Structural basis for chemokine recognition and activation of a viral G protein-coupled receptor. Science 347 (6226):1113–1117
22. Fenalti G et al (2014) Molecular control of d-opioid receptor signalling. Nature 506 (7487):191–196
23. Thal DM et al (2016) Crystal structures of the M1 and M4 muscarinic acetylcholine receptors. Nature 531(7594):335–340
24. Yin J, Mobarec JC, Kolb P, Rosenbaum DM (2015) Crystal structure of the human OX2 orexin receptor bound to the insomnia drug suvorexant. Nature 519(7542):247–250
25. Yin J et al (2016) Structure and ligand-binding mechanism of the human OX1 and OX2 orexin receptors. Nat Struct Mol Biol 23(4):293–299
26. Shihoya W et al (2016) Activation mechanism of the endothelin ETB receptor by endothelin-1. Nature 537(7620):363–368
27. Hua T et al (2016) Crystal structure of the human cannabinoid receptor CB1. Cell 167:750–762
28. Wacker D et al (2013) Structural features for functional selectivity at seratonin receptors. Science 340(6132):615–619
29. Hollenstein K et al (2013) Structure of class B GPCR corticotropin-releasing factor receptor 1. Nature 499(7459):438–443
30. Geng Y, Bush M, Mosyak L, Wang F, Fan QR (2013) Structural mechanism of ligand activation in human GABAB receptor. Nature 504 (7479):254–259
31. Wu H et al (2014) Structure of a class C GPCR metabotropic glutamate receptor 1 bound to an allosteric modulator. Science 344 (6179):58–64
32. Doré AS et al (2014) Structure of class C GPCR metabotropic glutamate receptor 5 transmembrane domain. Nature 511 (7511):557–562
33. Chrencik JE et al (2015) Crystal structure of antagonist bound human lysophosphatidic acid receptor 1. Cell 161:1633–1643

34. Zhang H et al (2015) Structure of the angiotensin receptor revealed by serial femtosecond crystallography. Cell 161:833–844
35. Byrne EFX et al (2016) Structural basis of smoothened regulation by its extracellular domains. Nature 535(7613):517–522
36. Chien YET et al (2010) Structure of the human dopamine D3 receptor in comlex with a D2/D3 selective antagonist. Science 330 (6007):1091–1095
37. White JF et al (2012) Structure of the agonist-bound neurotensin receptor. Nature 490 (7421):508–513
38. Zhang K et al (2014) Structure of the human P2Y12 receptor in complex with an antithrombotic drug. Nature 509(7498):115–118
39. Zhang D et al (2015) Two disparate ligand-binding sites in the human P2Y1 receptor. Nature 520(7547):317–321
40. Srivastava A et al (2014) High-resolution structure of the human GPR40 receptor bound to allosteric agonist TAK-875. Nature 513(7516):124–127
41. Haga K et al (2012) Structure of the human M2 muscarinic acetylcholine receptor bound to an antagonist. Nature 482(7386):547–551
42. Cherezov V et al (2007) High resolution crystal structure of an engineered human β2-adrenergic G protein-coupled receptor. Science 318 (5854):1258–1265
43. Klammt C, Schwarz D, Eifler N et al (2007) Cell-free production of G protein-coupled receptors for functional and structural studies. J Struct Biol 158:482–493
44. Reeves PJ, Thurmond RL, Khorana HG (1996) Structure and function in rhodopsin: high level expression of a synthetic bovine opsin gene and its mutants in stable mammalian cell lines. Proc Natl Acad Sci U S A 93:11487–11492
45. Miroux B, Walker JE (1996) Over-production of proteins in *Escherichia coli*: mutant hosts that allow synthesis of some membrane proteins and globular proteins at high levels. J Mol Biol 260:289–298
46. Wagner S, Klepsch MM, Schlegel S et al (2008) Tuning *Escherichia coli* for membrane protein overexpression. Proc Natl Acad Sci U S A 105:14371–14376
47. Hampe W, Voss RH, Haase W et al (2000) Engineering of a proteolytically stable human beta(2)-adrenergic receptor/maltose-binding protein fusion and production of the chimeric protein in *Escherichia coli* and baculovirus infected insect cells. J Biotechnol 77:219–234
48. Mouillac B, Caron M, Bonin H et al (1992) Agonist-modulated palmitoylation of b2-adrenergic receptor in Sf9 cells. J Biol Chem 267:21733–21737
49. Panneels V, Sinning I (2010) Membrane protein expression in the eyes of transgenic flies. Methods Mol Biol 601:135–147
50. Zhang L, Salom D, He JH et al (2005) Expression of functional G protein-coupled receptors in photoreceptors of transgenic *Xenopus laevis*. Biochemistry 44:14509–14518
51. Li N, Salom D, Zhang L et al (2007) Heterologous expression of the adenosine A1 receptor in transgenic mouse retina. Biochemistry 46:8350–8359
52. Sarramegna V, Muller I, Mousseau G et al (2005) Solubilization, purification and mass spectrometry analysis of the human mu-opioid receptor expressed in *Pichia pastoris*. Protein Expr Purif 43:85–93
53. Dowell SJ, Brown AJ (2002) Yeast assays for G-protein coupled receptors. Receptors Channels 8:343–352
54. Grisshammer R, Duckworth R, Henderson R (1993) Expression of a rat neurotensin receptor in *Escherichia coli*. Biochem J 295:571–576
55. Sarramegna V, Talmont F, Demange P et al (2003) Heterologous expression of G-protein-coupled receptors: comparison of expression systems from the standpoint of large-scale production and purification. Cell Mol Life Sci 60:1529–1546
56. McCusker EC, Bane SE, O'Malley MA et al (2007) Heterologous GPCR expression: A bottleneck to obtaining crystal structures. Biotechnol Prog 23:540–547
57. Tate CG, Grisshammer R (1996) Heterologous expression of G-protein-coupled receptors. Trends Biotechnol 14:426–430
58. Ishihara G, Goto M, Saeki M et al (2005) Expression of G protein coupled receptors in a cell-free translational system using detergents and thioredoxin-fusion vectors. Protein Expres Purif 41:27–37
59. Corin K, Baaske P, Ravel DB et al (2011) A robust and rapid method of producing soluble, stable, and functional G-protein coupled receptors. PLoS One 6:e23036
60. Corin K, Baaske P, Ravel DB et al (2011) Designer lipid-like peptides: a class of detergents for studying functional olfactory receptors using commercial cell-free systems. PLoS One 6:e25067
61. Wang XQ, Corin K, Baaske P et al (2011) Peptide surfactants for cell-free production of

functional G protein-coupled receptors. Proc Natl Acad Sci U S A 108:9049–9054

62. Koutsopoulos S, Kaiser L, Eriksson HM et al (2012) Designer peptide surfactants stabilize diverse functional membrane proteins. Chem Soc Rev 41:1721–1728
63. Ren H, Yu D, Ge B et al (2009) High-level production, solubilization and purification of synthetic human GPCR chemokine receptors CCR5, CCR3, CXCR4 and CX3CR1. PLoS One 4:e4509
64. Gubellini F, Verdon G, Karpowich NK et al (2011) Physiological response to membrane protein overexpression in *E. coli*. Mol Cell Proteomics 10:1–17
65. King K, Dohlman HG, Thorner J et al (1990) Control of yeast mating signal transduction by a mammalian beta-2-adrenergic receptor and Gs alpha-subunit. Science 250:121–123
66. Corin K, Baaske P, Geissler S et al (2011) Structure and function analyses of the purified GPCR human vomeronasal type 1 receptor 1. Sci Rep 1:172
67. Corin K, Pick H, Baaske P et al (2012) Insertion of T4-lysozyme (T4L) can be a useful tool for studying olfactory-related GPCRs. Mol BioSyst 8:1750–1759

Chapter 29

(Hyper)Thermophilic Enzymes: Production and Purification

Pierpaolo Falcicchio, Mark Levisson, Servé W. M. Kengen, Sotirios Koutsopoulos, and John van der Oost

Abstract

The discovery of thermophilic and hyperthermophilic microorganisms, thriving at environmental temperatures near or above 100 °C, has revolutionized our ideas about the upper temperature limit at which life can exist. The characterization of (hyper)thermostable proteins has broadened our understanding and presented new opportunities for solving one of the most challenging problems in biophysics: how are structural stability and biological function maintained at high temperatures where "normal" proteins undergo dramatic structural changes? In our laboratory, we have purified and studied many thermostable and hyperthermostable proteins in an attempt to determine the molecular basis of heat stability. Here, we present methods to express such proteins and enzymes in *E. coli* and provide a general protocol for overproduction and purification. The ability to produce enzymes that retain their stability and activity at elevated temperatures creates exciting opportunities for a wide range of biocatalytic applications.

Key words Thermozymes, Thermal stability, Heterologous production, Protein purification, His-tag, Immobilized metal affinity chromatography (IMAC), Size exclusion chromatography (SEC), Biocatalysis

1 Introduction

Living organisms can be grouped into four main categories as defined by the temperature range in which they thrive: psychrophiles (−15 to 20 °C), mesophiles (20–45 °C), thermophiles (45–80 °C), and hyperthermophiles (≥80 °C) [1]. The origin of extremophilic microorganisms has long been debated. One of the theories suggests that (hyper)thermophilic microorganisms actually appeared on Earth before mesophilic microorganisms [2]. Intuitively, this is in agreement with the environmental conditions on the surface of Earth when life emerged. According to this theory, all biomolecules evolved so as to be functional and stable at elevated temperatures, and subsequently adapted to lower temperature environments. However, another theory suggests that (hyper) thermophiles arose from mesophiles via adaptation to

Nikolaos E. Labrou (ed.), *Protein Downstream Processing: Design, Development, and Application of High and Low-Resolution Methods*, Methods in Molecular Biology, vol. 2178, https://doi.org/10.1007/978-1-0716-0775-6_29,

high-temperature environments. One of the arguments of the latter hypothesis is based on the supposition that RNA (the genetic material in emerging cellular life) is unstable at elevated temperatures [3, 4].

The first hyperthermophilic bacterium (*Thermus aquaticus*) was discovered in 1969 in hot acidic springs in Yellowstone National Park [5]. Since then, over 70 hyperthermophiles (both bacteria and archaea) have been isolated from the environments of extreme temperatures: near or above 100 °C. Examples of environments that, until recently, were considered as being hostile to life include volcanic areas rich in sulfur and "toxic" metals and hydrothermal vents in the deep sea (~4 km below sea level) of extremely high pressure [6]. Interestingly, hyperthermophilic microorganisms do not grow below temperatures of 50 °C and, in some cases, do not grow below 80–90 °C [7]. Yet, they can survive at ambient temperatures for prolonged times; the same way we can preserve mesophilic organisms in the fridge for prolonged times. Thermozymes and hyperthermozymes, in particular, are essentially inactive at moderate temperatures, but gain activity as temperatures increase [8].

Hyperthermozymes are not only active and stable at high temperatures, but are generally also more resistant to organic solvents, detergents, and high concentrations of chemical denaturants (e.g., GdHCl and urea), compared to their mesophilic counterparts [9]. These features may enable their use in a plethora of biotechnological applications. Therefore, it is important to develop technologies that allow the large-scale production and purification of such proteins. Purification of (hyper)thermophilic proteins expressed in a mesophilic host, such as *Escherichia coli*, is greatly facilitated by their intrinsic thermal stability. This generally allows a single-step purification, which involves removal of the vast majority of the host-cell proteins through heat-induced denaturation and subsequent aggregation and precipitation, while the structural integrity and function of the expressed (hyper)thermostable proteins remain intact. After heat treatment, the cell-free extract generally consists of about 90% of the expressed (hyper)thermophilic protein, which is often sufficient for most purposes including biochemical characterization and applications in biocatalysis. Although one or two additional chromatographic steps are usually sufficient to obtain pure protein, nowadays most recombinant proteins are expressed with an N- or C-terminal tag for affinity chromatography and protein detection. A commonly used tag is a polyhistidine (His-tag) tail for a single-step purification using immobilized metal affinity chromatography (IMAC).

In this chapter, we describe general procedures to produce (hyper)thermophilic proteins on the lab scale and to purify at least several mg of His-tagged (hyper)thermophilic protein. The described method has been developed in our lab during the last

20 years and has been successfully applied for the production and purification of various (hyper)thermozymes belonging to a number of enzymatic classes and subclasses, such as hydrolases [10–14], kinases [15–17], isomerases [18, 19], carboxylesterases [20, 21], aldolases [22, 23], dehydrogenases [24, 25], catalase-peroxidases [26], and oxidases [27].

2 Materials

Prepare all solutions using deionized water and analytical grade reagents. The materials are intended for the expression of a gene cloned in a pET24d vector (kanamycin resistant) in frame with a C-terminal His-tag and produced in BL21(DE3) cell (*see* **Note 1**).

2.1 Transformation

1. Electrocell manipulator system ECM 600 (BTX) and 2 mm gap electroporation cuvettes (Bio-Rad Laboratories).
2. pET24d (Novagen) plasmid DNA harboring the gene of interest, for example, the sequence encoding for a hyperthermostable esterase (pET24d-EstD) (*see* Subheading 3).
3. Electro-competent *E. coli* BL21(DE3) cells (Novagen) (*see* **Note 2**).
4. Tris–HCl and EDTA (TE) buffer: 10 mM Tris–HCl and 1 mM EDTA, pH 8.5. Sterilize by filtration through a 0.22-μm filter. Store at room temperature.
5. Super Optimal Broth with Catabolite repression (SOC) medium: 2% w/w tryptone, 0.5% w/w yeast extract, 10 mM NaCl, 2.5 mM KCl, 10 mM $MgCl_2$, 20 mM glucose, and pH 7.0. Dissolve 2 g of tryptone and 0.5 g of yeast extract in approximately 90 mL of water and transfer to a 100 mL graduate cylinder. Add 1 mL of 1 M NaCl, 0.25 mL of 1 M KCl, and 2 mL of 2 M $MgCl_2$. Mix and adjust the pH at 7.0 if necessary. Bring to a final volume of 100 mL with water. Autoclave the solution. Then, add 1 mL of filter-sterilized 2 M glucose. SOC medium can be stored in 5 mL aliquots at −20 °C.
6. Luria Bertani (LB) medium: 1% w/w peptone, 0.5% w/w yeast extract, 1% w/w NaCl, and pH 7.0. Dissolve 10 g of tryptone, 5 g of yeast extract, and 10 g of NaCl in 900 mL of water. Mix and adjust the pH at 7.0 if necessary. Bring to a final volume of 1000 mL. Autoclave the solution.
7. Luria Bertani (LB) agar: LB medium with 1.5% w/w agar. Add 7.5 g of agar to 500 mL of the LB medium and autoclave the solution.

8. Kanamycin stock solution (1000×): 50 mg/mL in water. Dissolve 500 mg of kanamycin in 10 mL of water and sterilize through a 0.22 μm syringe filter. Store at −20 °C (*see* **Note 3**).
9. LB-agar plates. Dispense the LB-agar medium supplemented with 50 μg/mL of kanamycin in Petri dishes.

2.2 Growth Medium and Inducer

1. Dispense 500 mL of the LB medium in four 2.5 L Erlenmeyer flasks and autoclave the solution.
2. Isopropyl-β-D-thiogalactopyranoside (IPTG) solution: 1 M solution in water. Sterilize through a 0.22 μm filter. Store the solution at −20 °C.

2.3 Solutions for Protein Preparation and FPLC Purification

1. Deoxyribonuclease I (DNaseI): prepare a solution containing 10 U/μL in lysis buffer.
2. Lysis buffer: 50 mM Tris–HCl, 300 mM NaCl, and pH 7.5. Dissolve 1.21 g of Tris and 3.5 g of NaCl in approximately 190 mL of water and transfer to a 250 mL graduate cylinder. Mix and adjust the pH at 7.5 with 6 M HCl. Bring to a final volume of 200 mL with water. Store at room temperature.
3. FPLC-IMAC Buffer A: 50 mM Tris–HCl, 300 mM NaCl, and pH 7.5. Dissolve 3.03 g of Tris and 8.77 g of NaCl in 480 mL of water and transfer to a 500 mL graduate cylinder. Mix and adjust the pH at 7.5 with 6 M HCl. Bring to a final volume of 500 mL with water. Filter the solution through a 0.45 μm filter and store at room temperature.
4. FPLC-IMAC Buffer B: 50 mM Tris–HCl, 300 mM NaCl, 500 mM imidazole, and pH 7.5. Dissolve 1.52 g of Tris, 4.39 g of NaCl, and 8.51 g of imidazole in 240 mL of water and transfer to a 250 mL graduate cylinder. Mix and adjust the pH at 7.5 with 6 M HCl. Bring to a final volume of 250 mL with water. Filter the solution through a 0.45 μm filter and store at room temperature.
5. FPLC-desalting column and FPLC-Size exclusion chromatography (SEC) buffer: 50 mM Tris–HCl, 150 mM NaCl, and pH 7.5. Dissolve 1.52 g of Tris and 2.2 g of NaCl in 240 mL of water and transfer to a 250 mL graduate cylinder. Mix and adjust the pH at 7.5 with 6 M HCl. Bring to a final volume of 250 mL with water. Filter the solution through a 0.45 μm filter and store at room temperature.

3 Methods

3.1 Gene Cloning into Expression Vector

The genes encoding the proteins of interest may be amplified from the microbial genomic DNA by the polymerase chain reaction (PCR). This approach is simple and inexpensive but does not allow the introduction of modifications in the coding sequence.

Although hyperthermozymes can be easily expressed in a mesophilic host, such as *E. coli*, sometimes the different codon usage between the native species and the production organism may result in poor protein expression. Currently, due to the decrease of the cost of synthetic DNA constructs, it is possible to design a gene with codons optimized for good expression in the host cell of choice. Most genes of interest are expressed after cloning in a pET series vector (Novagen) in frame with an N- or C-terminal His-tag for affinity chromatography and protein detection. These expression vectors are suitable for protein expression in *E. coli* strains, which express T7 RNA polymerase under control of the *lac* promoter, e.g. BL21(DE3), using IPTG as an inducer (see below).

3.2 E. coli BL21(DE3) Electrotransformation

1. Thaw the electrocompetent *E. coli* BL21(DE3) cells (which were stored at −80 °C) on ice (*see* **Note 4**).
2. In an ice cooled 1.5 mL polypropylene tube, mix 50 μL of the cell suspension with 1–2 μL of solution containing 1–2 μg of plasmid DNA in a low-ionic buffer such as TE buffer (*see* **Note 5**). Mix well and allow equilibration on ice for ~1 min.
3. Set the electro cell manipulator apparatus at 25 μF/2.5 kV. Set the pulse controller to 200 μΩ. Add the mixture of cells and plasmid to an ice-cooled 0.2 cm and make sure that the suspension is at the bottom of the cuvette. Push the cuvette in the safety chamber slide.
4. Apply one pulse using the above settings. This should produce a pulse with a time constant of ~5 μs (field strength should be 12.5 kV/cm). (Settings depend on the type of apparatus and therefore, optimization may be necessary).
5. Remove the cuvette from the chamber and immediately add 1 mL of 37 °C prewarmed SOC medium to the cuvette and gently mix by pipetting (*see* **Note 6**).
6. Transfer the cell suspension to a 14-mL polypropylene tube and incubate at 37 °C for 1 h while shaking the tube at 225 rpm to increase the recovery of the transformants.
7. Plate the cells on the LB agar medium supplied with 50 μg/mL kanamycin and incubate the plates overnight at 37 °C (*see* **Note 7**).

3.3 Protein Production and Purification

1. In a sterile atmosphere (flow chamber, or close to a flame), transfer a single colony of *E. coli* BL21(DE3) harboring the plasmid pET24d-EstD from the plate to a sterile tube containing 3 mL of the LB medium supplied with kanamycin. Incubate overnight in a shaking incubator at 37 °C.

2. The next day, again in a sterile atmosphere, transfer 0.5 mL of the overnight culture into each flasks containing 0.5 L of LB medium supplied with 50 μg/mL of kanamycin. Incubate in a shaking incubator (180 rpm) at 37 °C for 6 h (or until a cell suspension optical density at 600 nm of about 1.2–1.5).
3. Remove and store 1 mL culture sample before the induction for sodium dodecyl sulfate polyacrylamide gel electrophoresis gel analysis (SDS-PAGE) (*see* **Note 8**). Induce protein expression by adding, in a sterile atmosphere, IPTG to a final concentration of 0.5 mM. Incubate at 37 °C while shaking (150 rpm) for at least 16 h (*see* **Note 9**).
4. Harvest cells by centrifugation at 4 °C, 10,000 × *g* for 10 min. Resuspend the cell pellet in 25 mL of cell lysis buffer.
5. Pass the cell suspension twice through a French press at 110 MPa to lyse the cells. Add 1 μL of the DNaseI solution (10 U) to the crude cell extract and incubate for 20 min at room temperature to degrade the DNA and reduce the viscosity. Centrifuge the DNaseI-treated crude cell extract at 4 °C, 43,000 × *g* for 30 min. Transfer the supernatant (cell-free extract (CFE)), to a new tube and discard the pellet, which contains the cell debris. Incubate the CFE for 30 min at 70 °C to denature *E. coli* proteins (*see* **Note 10**). When correctly folded and present in the soluble fraction, this step should not affect the heterologously produced (hyper)thermostable protein. Centrifuge at 4 °C, 43,000 × *g* for 30 min to remove denatured biomolecules, which precipitate in the pellet. Transfer the supernatant, which represents the heat stable cell-free extract (HSCFE), to a new tube (*see* **Note 11**).
6. Filter the HSCFE through a 0.45 μm syringe filter, and use an ÄKTA FPLC protein purification system (GE Healthcare) to apply it to a 1 mL HisTrap column (GE Healthcare) equilibrated with Buffer A. Wash with Buffer A until the absorbance trace at 280 nm has returned to the baseline (*see* **Note 12**), and subsequently apply a linear gradient of 0–500 mM imidazole (Buffer B). All fractions are collected. Pool fractions containing the protein of interest (*see* **Note 13**).
7. Apply the collected fractions to a HiPrep 26/10 desalting column (GE Healthcare) equilibrated with 50 mM Tris–HCl buffer (pH 7.5) and 150 mM NaCl to remove the excess of imidazole.
8. Run a SDS-PAGE with samples collected during all the extraction and IMAC purification steps and measure the total protein content using for instance the Bradford assay [27] (*see* **Note 14**).

9. Apply the collected fractions to a HiPrep 26/10 desalting column (GE Healthcare) equilibrated with 50 mM Tris–HCl buffer (pH 7.5) and 150 mM NaCl to remove the excess of imidazole.
10. Apply the protein preparation to a Superdex-200 gel filtration column (GE Healthcare) equilibrated in 50 mM Tris–HCl buffer (pH 7.5) containing 150 mM NaCl to determine the native molecular weight of your protein.

3.4 Troubleshooting

1. Possible reasons for low protein yield:
   (a) IPTG in the stock solution may be degraded or the protein is toxic for the host. Protein is not properly folded with the consequent formation of inclusion bodies.
   (b) Incomplete resuspension of the pellet before the French Press processing, which may have resulted in the presence of significant amounts of protein in the pellet after centrifugation.
   (c) Incomplete lysis of the *E. coli* cells in the French Press.
   (d) Protein loss during chromatographic separation due to the nonaccessibility of the affinity tag.
   (e) No protein expression due to different codon usage bias.
2. Possible solutions for increasing the protein yield.
   (a) Use freshly made IPTG. Reduce the amount to a micromolar concentration to decrease the expression level and facilitate the correct protein folding.
   (b) Reduce the growth temperature during induction to 28 °C or 20 °C to facilitate correct protein folding and prevent the formation of inclusion bodies. At a lower temperature, the protein synthesis rate is lower giving more time to the neo synthetized protein to fold correctly and this may reduce protein aggregation.
   (c) To induce the expression of endogenous *E. coli* chaperone proteins, proteins that bind to unfolded proteins avoiding protein aggregation and facilitating protein folding, it is also possible to perform a cold shock before the IPTG induction, e.g. from 37 °C to 4 °C for a duration of 20–30 min.
   (d) If the protein is produced as stable and soluble at 37 °C only for a short time before aggregation, the induction time could also be reduced to 3–4 h although this step may result in reduced protein yield production. Consider to express your protein fused to a highly soluble protein, like Maltose Binding Protein (MBP) to facilitate the folding and to avoid the formation of inclusion bodies.

(e) Although proteins from (hyper)thermophilic organisms can be easily expressed in *E. coli* sometimes, the different codon usage bias between organisms can lead to failure in protein production. In this case, it is advisable to use *E. coli* strains containing a tRNA helper plasmid encoding several rare tRNAs to overcome the difference in codon usage.

4 Notes

1. Several affinity tags are available on different vectors from different suppliers. According to the type of vector, promoter/inducer combination, affinity tags, and antibiotic resistance gene may vary. For an overview of bacterial expression vector features, *see* Ref. 28.
2. *E. coli* BL21(DE3) strain expresses the T7 RNA polymerase under control of the lac promoter, using IPTG as an inducer. Several *E. coli* BL21(DE)3 strains are available for protein production, those may include strains containing plasmid coding for rare tRNA (BL21(DE3)pRIL), to overcome difference in codon usage bias, or for T7 lysozyme (BL21(DE3) pLys,) to reduce the background expression of toxic proteins.
3. It is important to apply antibiotic selection during all the stages of growth according to the resistance gene carried on your expression vector. Working concentrations of commonly used selection's antibiotics are: 100 μg/mL for ampicillin (Na-salt) and 50 μg/mL for kanamycin, streptomycin, and tetracycline-HCl.
4. Commercial electrocompetent cells gave the best results but several protocols are available for competent cell preparation. For a detailed general protocol, *see* Ref. 29.
5. DNA stored at −20 °C should be in low ionic strength buffer such as TE. A high ionic strength solution, containing a high concentration of salts, is conductive and can cause arcing under the high voltage conditions used in electroporation.
6. Quick addition of the SOC medium to the electroporation cuvette directly after the electric pulse is very important to maximize the recovery of the transformants.
7. Only the *E. coli* cells that contain the plasmid with the antibiotic resistance gene will survive.
8. For the SDS-PAGE protocol, *see* Ref. 30.
9. *E. coli* growth conditions may influence protein expression. When a low amount of soluble protein is produced or the protein aggregates as insoluble precipitates (inclusion bodies,

IB), culturing *E. coli* under suboptimal conditions (e.g. lower temperature and minimal medium) may improve protein expression. The amount of inducer and the duration of induction may also be changed to improve protein expression.

10. As standard conditions, a temperature of 70 °C and a duration time of 30 min are used. However, it is best to test different temperatures and incubation times using small portions of the CFE. Depending on the (hyper)thermozyme, better purification can be obtained optimizing the temperature and incubation time.
11. A biological assay should be used for monitoring the activity of the (hyper)thermozyme of interest during the extraction and the purification steps. When a specific assay is not available, it is possible to detect the presence of the protein of interest through immunoblotting techniques using anti-His-tag antibodies.
12. Optionally, the column can be washed with 10–20 mM imidazole (2–4% Buffer B) in the same Buffer A, and subsequently proteins can be eluted with a linear gradient of 10/20–500 mM imidazole. Washing may be necessary to remove contaminant proteins bound to the nickel column.
13. Generally, the presence of the affinity tag is enough to guarantee high purity. When contaminant proteins are present, it is possible to increase purity using other chromatographic techniques like hydrophobic interaction chromatography (HIC) and/or ion exchange chromatography (IEC).
14. SDS-PAGE analysis and measurements of the activity of the protein of interest can be used for the construction of a purification table.

References

1. Stetter KO (1996) Hyperthermophilic prokaryotes. FEMS Microbiol Rev 18:149–158
2. Woese CR (1998) The universal ancestor. Proc Natl Acad Sci U S A 95:6854–6859
3. Miller SL, Lazcano A (1995) The origin of life—did it occur at high temperatures? J Mol Evol 41:689–692
4. Forterre P (1996) A hot topic: the origin of hyperthermophiles. Cell 85:789–792
5. Brock TD, Brock KM, Belly RT, Weiss RL (1972) Sulfolobus: a new genus of sulfur-oxidizing bacteria living in low pH and high temperature. Arch Mikrobiol 84:54–68
6. Brock TD, Freeze H (1969) Thermus aquaticus, a nonsporulating extreme thermophile. J Bacteriol 98:289–297
7. Stetter KO (2006) History of discovery of the first hyperthermophiles. Extremophiles 10:357–362
8. Koutsopoulos S, van der Oost J, Norde W (2005) Temperature dependant structural and functional features of a hyperthermostable enzyme using elastic neutron scattering. Proteins 61:377–384
9. Chiaraluce R, Van Der Oost J, Lebbink JH, Kaper T, Consalvi V (2002) Persistence of tertiary structure in 7.9 M guanidinium chloride: the case of endo-beta-1,3-glucanase from Pyrococcus furiosus. Biochemistry 41:14624–14632
10. Gueguen YW, Voorhorst GB, van der Oost J, de Vos WM (1997) Molecular and biochemical

characterization of an endo-β-1,3-glucanase of the hyperthermophilic archaeon Pyrococcus furiosus. J Biol Chem 272:31258–31264

11. van Lieshout JF, Gutiérrez ON, Vroom W, Planas A, de Vos WM, van der Oost J, Koutsopoulos S (2012) Thermal stabilization of an endoglucanase by cyclization. Appl Biochem Biotechnol 167:2039–2053
12. Kaper T, Verhees CH, Lebbink JH, van Lieshout JF, Kluskens LD, Ward DE, Kengen SW, Beerthuyzen MM, de Vos WM, van der Oost J (2001) Characterization of beta-glycosylhydrolases from Pyrococcus furiosus. Methods Enzymol 330:329–346
13. Lebbink JH, Kaper T, Kengen SW, van der Oost J, de Vos WM (2001) Beta-Glucosidase CelB from Pyrococcus furiosus: production by *Escherichia coli*, purification, and in vitro evolution. Methods Enzymol 330:364–379
14. van Lieshout J, Faijes M, Nieto J, van der Oost J, Planas A (2004) Hydrolase and glycosynthase activity of endo-1,3-beta-glucanase from the thermophile Pyrococcus furiosus. Archaea 1:285–292
15. Kengen SW, Tuininga JE, Verhees CH, van der Oost J, Stams AJ, de Vos WM (2001) ADP-dependent glucokinase and phosphofructokinase from Pyrococcus furiosus. Methods Enzymol 331:41–53
16. Verhees CH, Koot DG, Ettema TJ, Dijkema C, de Vos WM, van der Oost J (2002) Biochemical adaptations of two sugar kinases from the hyperthermophilic archaeon Pyrococcus furiosus. Biochem J 366:121–127
17. de Geus D, Hartley AP, Sedelnikova SE, Glynn SE, Baker PJ, Verhees CH, van der Oost J, Rice DW (2003) Cloning, purification, crystallization and preliminary crystallographic analysis of galactokinase from Pyrococcus furiosus. Acta Crystallogr D Biol Crystallogr 59:1819–1821
18. Verhees CH, Huynen MA, Ward DE, Schiltz E, de Vos WM, van der Oost J (2001) The phosphoglucose isomerase from the hyperthermophilic archaeon Pyrococcus furiosus is a unique glycolytic enzyme that belongs to the cupin superfamily. J Biol Chem 276:40926–40932
19. Akerboom J, Turnbull AP, Hargreaves D, Fisher M, de Geus D, Sedelnikova SE, Berrisford JM, Baker PJ, Verhees CH, van der Oost J, Rice DW (2003) Purification, crystallization and preliminary crystallographic analysis of phosphoglucose isomerase from the hyperthermophilic archaeon Pyrococcus furiosus. Acta Crystallogr D Biol Crystallogr 59:1822–1833
20. Levisson M, van der Oost J, Kengen SW (2007) Characterization and structural modeling of a new of thermostable esterase from Thermotoga maritima. FEBS J 274:2832–2842
21. Levisson M, van der Oost J, Kengen SW (2009) Carboxylic ester hydrolases from hyperthermophiles. Extremophiles 13:567–581
22. Siebers B, Brinkmann H, Dörr C, Tjaden B, Lilie H, van der Oost J, Verhees CH (2001) Archaeal fructose-1,6-bisphosphate aldolases constitute a new family of archaeal type class I aldolase. J Biol Chem 276:28710–28718
23. Wolterink-van Loo S, van Eerde A, Siemerink MA, Akerboom J, Dijkstra BW, van der Oost J (2007) Biochemical and structural exploration of the catalytic capacity of Sulfolobus KDG aldolases. Biochem J 403:421–430
24. van der Oost J, Voorhorst WG, Kengen SW, Geerling AC, Wittenhorst V, Gueguen Y, de Vos WM (2001) Genetic and biochemical characterization of a short-chain alcohol dehydrogenase from the hyperthermophilic archaeon Pyrococcus furiosus. Eur J Biochem 268:3062–3068
25. Machielsen R, van der Oost J (2006) Production and characterization of a thermostable L-threonine dehydrogenase from the hyperthermophilic archaeon Pyrococcus furiosus. FEBS J 273:2722–2729
26. Kengen SWM, Bikker FJ, Hagen WR, de Vos WM, van der Oost J (2001) Characterization of a catalase-peroxidase from the hyperthermophilic archaeon Archaeoglobus fulgidus. Extremophiles 5:323–332
27. Kengen SWM, van der Oost J, de Vos WM (2003) Molecular characterisation of H_2O_2-forming NADH oxidases from Archaeoglobus fulgidus. Eur J Biochem 270:2885–2894
28. Terpe K (2006) Overview of bacterial expression systems for heterologous protein production: from molecular and biochemical fundamentals to commercial systems. Appl Microbiol Biotechnol 72:211–222
29. Sambrook J, Russell DW (2006) Transformation of *E. coli* by electroporation. Cold Spring Harb Protoc. https://doi.org/10.1101/pdb.prot3933
30. Sambrook J, Russell DW (2006) SDS-polyacrylamide gel electrophoresis of proteins. Cold Spring Harb Protoc. https://doi.org/10.1101/pdb.prot4540

Chapter 30

Screening of Recombinant Lignocellulolytic Enzymes Through Rapid Plate Assays

Anthi Karnaouri, Anastasia Zerva, Paul Christakopoulos, and Evangelos Topakas

Abstract

In the search for novel biomass-degrading enzymes through mining microbial genomes, it is necessary to apply functional tests during high-throughput screenings, which are capable of detecting enzymatic activities directly by way of plate assay. Using the most efficient expression systems of *Escherichia coli* and *Pichia pastoris*, the production of a high amount of His-tagged recombinant proteins could be thrived, allowing the one-step isolation by affinity chromatography. Here, we describe simple and efficient assay techniques for the detection of various biomass-degrading enzymatic activities on agar plates, such as cellulolytic, hemicellulolytic, and ligninolytic activities and their isolation using immobilized-metal affinity chromatography.

Key words Agar plate assay, Screening, Biomass-degrading enzymes, Glycoside hydrolases, Carbohydrate esterases, Oxidative enzymes, Immobilized-metal affinity chromatography

1 Introduction

The available genome sequence for an ever-increasing number of microorganisms allows the development of a complementary powerful tool for enzyme discovery. Bacterial and fungal microbial strains secrete lignocellulolytic enzymes that degrade cellulose and hemicellulose (Fig. 1) with an increasing number of applications in the industry [1]. Nowadays, biotechnology continuously searches for novel enzymes for use in various applications focused mainly in the energy and health sector. With the advent of recombinant DNA techniques and the use of cellular factories, such as *Escherichia coli* and *Pichia pastoris*, the isolation and screening of recombinant enzymes with industrial potential is faster and more efficient than ever before. *E. coli* is a prokaryotic expression system easy to handle, while the non-expressing eukaryotic proteins could be produced by the powerful expressing system of *P. pastoris* that is capable of

Nikolaos E. Labrou (ed.), *Protein Downstream Processing: Design, Development, and Application of High and Low-Resolution Methods*, Methods in Molecular Biology, vol. 2178, https://doi.org/10.1007/978-1-0716-0775-6_30,

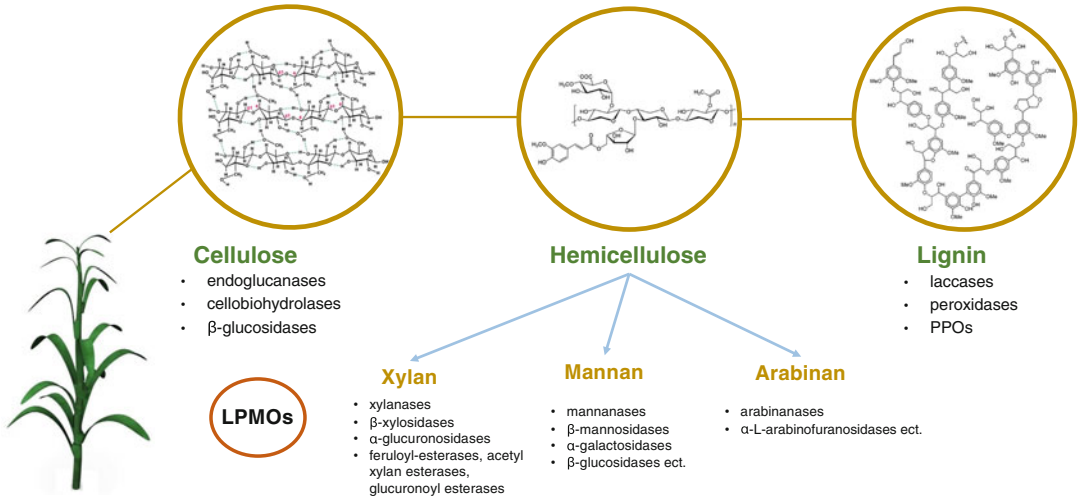

Fig. 1 Overall scheme of the various enzymatic activities implicated in the degradation of the lignocellulosic biomass

inducing all the necessary posttranslational modifications [2, 3]. The hexahistidine tagged (His-tag) recombinant proteins produced in the intra- or extracellular space are harvested prior to the one-step isolation process using immobilized-metal affinity chromatography (IMAC). IMAC provides a simple and fast purification by the chelation of His-tag to immobilized divalent metal ions, such as nickel or cobalt [4].

Screening assays that enable the functional confirmation of the enzyme before protein purification hold a key role in the production of recombinant enzymes, in order to screen the transformed strains and choose the best clone for further study. Despite the vast amount of different screening assays reported in the literature, choosing the most appropriate one that will provide accurate biochemical predictions for each different enzymatic activity remains a challenge. Qualitative and semiquantitative screening methods have to be simple, straightforward, cost-effective, reliable, and enable high-throughput screening compared with quantitative or chromatographic procedures. They are not that sensitive as the latter but provide an indication of enzymatic activity. Screening of transformants usually includes gel diffusion assays, which are based on synthetic substrates that consist of one group that can be cleaved after the activity of the enzyme (e.g., glycosides, acetate, and ferulate group) and another group that forms a detectable readout upon cleavage, easy to detect either upon visible color change (clear/colored halo), such as indoxyls (5-bromo-4-chloro-3-indolyl and 6-chloro-3-indolyl) [5], Remazol Brilliant Blue (RBB) [6], Ostazin Brilliant Red [7], and azurine [8] or upon UV irradiation, such as 4-methylumbelliferyllone [9]. Oxidative enzymatic activity,

Table 1
Summary of different commercially available substrates that can be used for the detection of activity of recombinant lignocellulosic enzymes

Class	Enzyme activity	Type of assay	Substrate
Cellulases	Endoglucanase	Chromogenic	CMC[a]/Congo red, AZO-HE-cellulose, AZCL[b]-HE cellulose, AZCL[b]-barley ß-glucan, AZCL[b]-xyloglucan
	Cellobiohydrolase	Fluorogenic, chromogenic	MeUmb[c]-cellobiopyranoside, MeUmb[c]-lactopyranoside, magenta[d]-cellobiopyranoside, CMC[a]/Congo red
	β-Glucosidase	Fluorogenic, chromogenic	MeUmb[c]-glycopyranoside, magenta[d]-glucopyranoside, esculin
Hemicellulases	Endoxylanase	Chromogenic	AZCL[b]-xylan, AZCL[b]-arabinoxylan, RBB[e]-xylan
	β-Xylosidase	Fluorogenic, chromogenic	MeUmb[c]-xylopyranoside, magenta[d]-xylopyranoside
	Endomannanase	Chromogenic	CMC[a]/galactomannan, CMC[a]/locust bean gum, AZCL[d]-glucomannan, magenta[d]-glucomannan
	Glucuronosidase	Chromogenic	magenta[d]-glucuronide
	β-Mannosidase	Fluorogenic, chromogenic	MeUmb[c]-mannopyranoside, magenta[d]-mannopyranoside
	Arabinanase	Chromogenic	AZCL[d]-debranched arabinan
	Arabinofuranosidase	Chromogenic	magenta[d]-arabinopyranoside
Esterases	Acetyl-xylan esterase	Fluorogenic	MeUmb[c] -acetate, α/β napthate, tributyrin
	Feruloyl esterase	Fluorogenic	MeUmb[c] -ferulate
Oxidative enzymes	LPMO	Chromogenic	PASC[f], CMC[a]
	Laccase	Chromogenic	ABTS[g]
	Peroxidase	Chromogenic	ABTS[g], H_2O_2

[a]CMC: Carboxymethyl-Cellulose
[b]AZCL: Azurine-Crosslinked
[c]MeUmb: 4-Methylumbelliferyl β-D
[d]Magenta: 5-Bromo-6-chloro-3-indolyl β-D
[e]RBB: Remazol rilliant lue
[f]PASC: Phopshoric Acid Swollen Cellulose
[g]ABTS: 2,2′-Azino-bis(3-ethylbenzothiazoline-6-sulfonate)

such as laccase, multicopper oxidase, and peroxidase activity, can also be detected by suitable substrates, offering color change upon oxidation, such as ABTS (2,2′-azino-bis-(3-ethylbenzothiazoline-6-sulphonic acid)) [10, 11]. There is a great variety of commercially available chromogenic and fluorogenic substrates with different solubility properties that offer great specificity, as described in Table 1. Chromogenic are generally more convenient than fluorogenic substrates, since the enzymatic activity can be monitored visually in the absence of any instrument. They can be incorporated in the agar media or added on the top of the agar plate after the

growth of the transformed strains [7, 12]. Colored indication dyes that interact with the carbohydrates, such as Congo Red, can be also used to detect the degradation zones [13].

In the present chapter, fast and easy qualitative plate assays are described for the screening of recombinant lignocellulolytic enzymes produced from both *E. coli* and *P. pastoris* expression systems prior to their purification using IMAC.

2 Materials

For the preparation of all solutions, ultrapure water (MilliQ, sensitivity of 18.2 MΩ cm at 25 °C) and analytical-grade reagents are to be used. All solutions should be prepared and stored at room temperature unless indicated otherwise. All waste disposal regulations have to be followed diligently when disposing of waste materials.

2.1 *E. coli* Agar Plates

For the preparation of approximately 20 Luria-Bertani (LB) agar plates (500 mL).

1. Add 250 mL of water to a graduated cylinder.
2. Weigh 5.0 g tryptone, 2.5 g yeast extract, 5.0 g NaCl, and 7.5 g agar. If required, weigh the appropriate amount of birchwood xylan (0.01% w/v) [14], CMC cellulose (0.4% w/v) [15], tributyrin (1% w/v) [16, 17], carob galactomannan (1% w/v) [18], esculin (0.5% w/v) [19], locust bean gum (0.5% w/v) [20], or any specific substrate that is incorporated in the agar medium (*see* **Note 1**).
3. Mix tryptone, yeast extract, and NaCl well in a 1 L beaker using a magnetic stirrer and when the solution is ready, add water to a total volume of 500 mL and finally transfer to 1 L Pyrex jar. Finally, add agar and the amount of substrate (if required), stir for 2 min and remove the stir bar.
4. Label the jar with autoclave tape and autoclave at 121 °C for 20 min with loosen top.
5. Leave agar to cool down to approximately 60 °C, which is a temperature that you are able to pick up the jar without burning your hands. Additives, such as 50 μL of 20 mg/mL antibiotics stock solution (add 200 mg of the antibiotic, e.g., ampicillin or kanamycin in 10 mL of water in a sterile vial (25 mL), mix thoroughly and store at 4 or −20 °C) and 40 μL of 100 mM IPTG stock solution (add 238 mg IPTG in 10 mL of water in a sterile vial (25 mL), mix thoroughly and store at −20 °C) should be added in this step, prior to pouring the plates. Also, temperature-sensitive chromogenic substrates should be added at this point, under sterile conditions (*see*

Note 2). After the addition, mix well in a circular motion while keeping the sterile jar on the bench, taking care that no foam or bubbles are created.

6. Pour a thin layer (~5 mm) of LB agar into sterile Petri dishes (85 mm diameter). Avoid lifting the cover off excessively to avoid contamination.
7. Let each plate to cool until it becomes solid and flip them in order to avoid condensation on the agar surface. The plates could be stored well in 4 °C for several months.

2.2 *P. pastoris* Agar Plates

For the preparation of approximately 20 Minimal Methanol (MM) agar plates (500 mL).

1. Weigh 7.5 g agar. If required, weigh the appropriate amount of birchwood xylan (0.01% w/v) [14], CMC cellulose (0.4% w/v) [15], tributyrin (1% w/v) [16, 17], carob galactomannan (1% w/v) [18], esculin (0.5% w/v) [19], locust bean gum (0.5% w/v) [20], or any specific chromogenic substrate that is incorporated in the agar medium (*see* **Note 1**).
2. Add agar in 400 mL of water in a 1 L Pyrex jar using a magnetic stirrer and when the solution is ready, remove the stir bar and label with autoclave tape.
3. Autoclave at 121 °C for 20 min with loosen top.
4. Leave agar to cool down to approximately 60 °C, which is a temperature that you are able to pick up the jar without burning your hands.
5. Under sterile conditions, add 50 mL of sterile 10× concentrated YNB stock solution, 1 mL of sterile 500× concentrated biotin, and 50 mL of sterile 10× methanol solution. For the preparation of stock solutions, see the following **steps 9–11**. Moreover, temperature-sensitive chromogenic substrates should be added aseptically at this step (*see* **Note 2**).
6. Mix well in a circular motion while keeping the sterile jar on the bench, taking care that no foam or bubbles are created.
7. Pour a thin layer of ~5 mm of MM agar into sterile Petri dishes (85 mm diameter). Avoid lifting the cover off excessively to avoid contamination.
8. Let each plate to cool until it is solid and flip them in order to avoid condensation on the agar surface. The plates could be stored well in 4 °C for several months.
9. Preparation of 10× YNB (13.4% w/v Yeast Nitrogen Base with ammonium sulfate without amino acids) stock solution: Add 134 g of YNB with ammonium sulfate and without amino acids in 1000 mL of water and heat the solution to completely dissolve YNB prior to filter sterilization. Alternatively, use

34 g of YNB without ammonium sulfate and amino acids and 100 g of ammonium sulfate. Store in 4 °C with a shelf life of approximately 1 year (adapted from the Invitrogen EasySelect *Pichia* expression kit manual).

10. Preparation of 500× biotin (0.02% w/v) stock solution: Add 20 mg of biotin in 100 mL of water and filter sterilize. Store in 4 °C with a shelf life of approximately 1 year (adapted from the Invitrogen EasySelect *Pichia* expression kit manual).
11. Preparation of 10× M (5% v/v methanol) stock solution: Add 5 mL of methanol in 95 mL of water and filter sterilize. Store in 4 °C with a shelf life of approximately 2 months (adapted from the Invitrogen EasySelect *Pichia* expression kit manual).
12. Preparation of ABTS substrate stock solution (10×): Prepare a fresh solution of ABTS at a final concentration of 20 mM (add 0.51 g in 50 mL ultrapure water) and filter sterilize. Keep on ice, in dark bottle until use.
13. Preparation of H_2O_2 solution (10×): Add 0.34 g H_2O_2 per liter of ultrapure water, to prepare a 10 mM stock solution of H_2O_2. Dilute ten times with ultrapure water before use. Keep in 4 °C and use it within 2 weeks.
14. Preparation of $CuSO_4$ stock solution (100×): Prepare a fresh solution of anhydrous $CuSO_4$ at a final concentration of 10 mM (add 79.8 mg in 50 mL ultrapure water) and autoclave, then add aseptically to the medium.
15. Preparation of $MnSO_4$ stock solution (100×): Prepare a fresh solution of $MnSO_4$ at a final concentration of 10 mM (add 75.5 mg in 50 mL ultrapure water) and autoclave, then add aseptically to the medium.

2.3 Congo Red Staining

Congo Red interacts with polysaccharides containing contiguous β-(1→4)-linked D-gluco or D-xylopyranosyl units yielding a vivid red color, leaving unstained the areas that contain cleaved oligosaccharides released by the activity of cellulases and hemicellulases [15]. Handling of Congo Red must be conducted with care as Congo Red is carcinogenic due to the presence of aromatic amine groups. Details of the supplier on the material safety data sheet should be taken into consideration prior to any experiment.

1. Congo Red solution: Add Congo Red in a final concentration of 1 mg/mL in H_2O. Vortex well to mix.
2. Destaining solution: 1 M NaCl.

2.4 Chromogenic Enzyme Substrates

The plate assays that involve the employment of chromogenic substrates have found widespread applications as they provide fast results and are easy to handle at a relatively low cost. These substrates contain polysaccharides that are covalently linked to

different dye molecules. When the substrate is degraded, the soluble reaction products diffuse into the gel, resulting in a change of color intensity in the degradation areas around the enzyme-producing strains. Azurine-crosslinked polysaccharides, indoxyl-glycosides, Ostazin Brilliant Red, and RBB substrates have been widely used in the literature. Moreover, a new generation of chromogenic polysaccharide hydrogel (CPH) substrates based on chlorotriazine dyes have been reported, where the different colors allow for the simultaneous screening and detection of different enzymatic activities [21].

2.4.1 Azurine-Crosslinked Polysaccharides (AZCL)

The enzyme activity of the proteins secreted from the recombinant clones can be tested against insoluble AZCL polysaccharides, incorporated into soft agar medium, and poured onto the petri dish. These substrates comprise of the polysaccharidic substrate in a crosslinked insoluble form and bound to blue copper-containing azurine molecules. Upon cleavage from cellulases and hemicellulases, azurine-dyed oligosaccharides are released into the gel leading to the formation of blue halos around the colonies. There is a great variety of substrates that are available, as depicted in Table 1, such as AZCL-HE-cellulose, AZCL-arabinoxylan, AZCL-barley β-glucan, AZCL-xylan either from beechwood or birchwood, AZCL-galactomannan, and others that allow the simple and fast detection of cellulolytic and hemicellulolytic activities [22, 23]. Plate assays employing AZCL substrates allow for high-throughput screening of multiple samples and are accurate, cost-effective, and easily performed.

1. For each screening plate, 6 mL of soft agar (7 mg/mL) containing 2 mg/mL of the azurine-linked substrate are required. For example, for 4 plates, we will need 24 mL of the final soft agar solution, containing 168 mg agar and 48 mg of the substrate. Firstly, weigh 48 mg of the substrate inside a 100 mL beaker (*beaker* ***#1***) and add a few drops of 96% ethanol (2–3 drops are enough). The substrate has to stay soaked with ethanol at least 10 min before further use, but do not exceed the time of 30 min.
2. To prepare the agar medium, add 0.12 g agar to 30 mL of water inside a 100 mL beaker (*beaker* ***#2***). Microwave the agar mix until it is completely dissolved and put it in a 60 °C water bath until the agar reaches the same temperature. When the agar solution had cooled down, pour the solution of beaker **#2** into that of beaker **#1** while stirring. The mixture needs to be cooled down to approximately 45 °C before it is poured directly to the grown recombinant colonies, in order to prevent heat deactivation and maintain recombinant enzymatic activity.

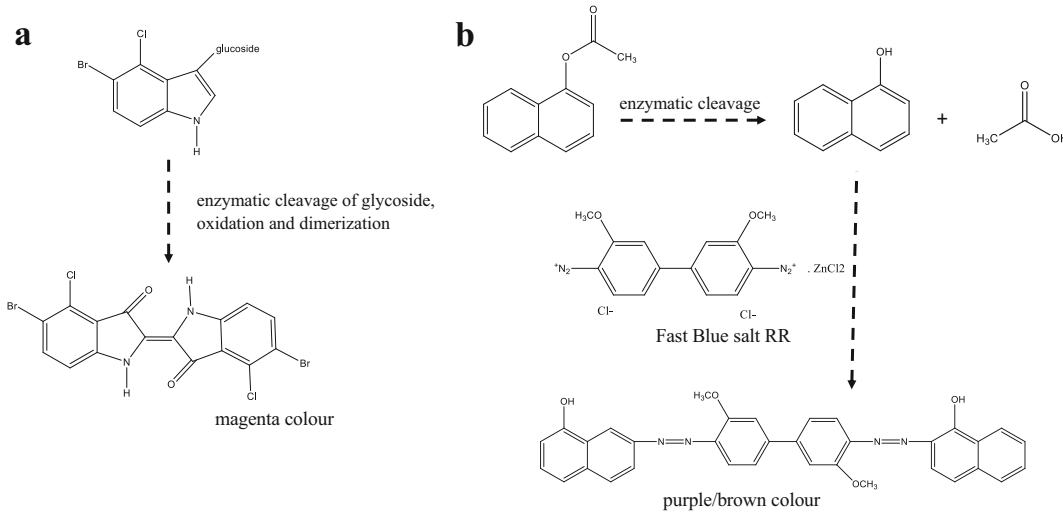

Fig. 2 (**a**) Indoxyl substrate and color formation for the detection of cellulases, hemicellulases activity and (**b**) β-napthyl substrate and color formation for the detection acetyl-xylan esterase activity

2.4.2 Indoxyl-Glycosides (5-Bromo-6-Chloro-3-Indolyl (Magenta) and Others)

Polysaccharidic substrates containing an indoxyl compound have found wide applications in diagnostic microbiology including their use in agar plate assays [24]. Indoxyl-glycosides of various monosaccharides have been reported and are readily available commercially. These substrates yield insoluble colored precipitates after enzymatic cleavage. The colored precipitate is derived mainly from two molecules of the cleaved aglycone, indoxyl, which combine via an oxidative process to form an indigo dye, as depicted in Fig. 2a [25]. The assay employing the 5-bromo-6-chloro-3-indolyl substrates has been reported in the literature for detecting the activity of various enzymes including β-glucosidase activity [5, 22, 26], arabinofuranosidase [27, 28], and others.

1. Prepare a stock solution of the 5-bromo-4-chloro-3-indolyl substrate in water at a concentration of 0.2 mg/mL in DMSO and store at room temperature until use.
2. For each screening plate, 6 mL of soft agar (7 mg/mL) containing 0.002 mg/mL of the chromogenic substrate (final concentration) are required. For example, for 4 plates, we will need 24 mL of the final soft agar solution containing 168 mg agar. Weigh the agar, add the water (*see* **Note 3**), then microwave the agar mix until it is completely dissolved and put it in a 60 °C water bath until the agar reaches the same temperature. When the agar solution had cooled down, add 10 μL of the chromogenic substrate stock solution (0.2 mg/mL) for every milliliter of top agar (a total of 60 μL per screening plate and 240 μL for 4 plates) and swirl lightly to disperse and avoid the formation of bubbles. The mixture needs to be cooled down to

approximately 45 °C before it is poured directly to the grown recombinant colonies, in order to prevent heat deactivation and maintain recombinant enzymatic activity.

2.4.3 Remazol Brilliant Blue R Substrates (RBB)

The plate assay based on covalently dyed RBB substrates has been reported to be more sensitive than Congo Red in the literature; therefore, it can be an attractive alternative in those cases that Congo Red assays fail to detect the hydrolytic activity of cellulases or hemicellulases [29]. The substrate is incorporated in a soft agar medium, poured onto the petri dish, and the enzyme activity is estimated by the formation of a clear halo around the colony.

1. For each screening plate, 6 mL of soft agar (7 mg/mL) containing 1% (w/v) of the chromogenic RBB substrate (final concentration) are required. For example, for 4 plates, we will need 24 mL of the final soft agar solution containing 168 mg agar. Weigh the agar, add the water, then microwave the agar mix until it is completely dissolved and put it in a 60 °C water bath until the agar reaches the same temperature.
2. Weigh the appropriate amount of the RBB substrate. For example, for 24 mL, we need 24 mg of the substrate. When the agar solution had cooled down, add the powder of the chromogenic substrate under stirring until the substrate is totally dissolved. The mixture needs to be cooled down to approximately 45 °C before it is poured directly to the grown recombinant colonies, in order to prevent heat deactivation and maintain recombinant enzymatic activity.

2.5 Ethyl Ferulate and Ethyl Acetate Soft Agar Substrate

1. Prepare a stock solution of ethyl ferulate, ethyl acetate, or ethyl butyrate (100 mg/mL) in dimethylformamide (DMF) and store at room temperature in a bottle wrapped with aluminum foil.
2. Each screening plate must be covered with 6 mL of molten soft agar (4 mg/mL) containing 1 mg/mL ethyl ferulate, ethyl acetate, or ethyl butyrate. For example, if we screen 4 plates for esterase activity, we add 96 mg agar to 24 mL of water inside a 100 mL beaker (*see* **Note 3**). Microwave the agar mix until it is completely dissolved and put it in a 60 °C water bath until the agar reaches the same temperature. Finally, we add 10 μL of the ethyl-containing substrate stock solution (100 mg/mL) for every milliliter of top agar (a total of 60 μL per screening plate) and swirl lightly to disperse and avoid the formation of bubbles. The mixture needs to be cooled down before it is poured directly to the grown recombinant colonies, in order to maintain recombinant enzymatic activity.

2.6 α- and β-Naphthyl Acetate

Both α- and β-naphthyl ester substrates are hydrolyzed by enzymatic action to α- and β-naphthol, which upon addition of Fast Blue RR salt forms a diazo dye complex with purple/brown color, Fig. 2b [30].

1. Prepare the mix of naphthyl substrate with Fast blue RR comprised of 18 mg/mL naphthyl substrate and 90 mg/mL Fast blue RR. Weigh 36 mg of substrate (α- or β-naphthyl ester) and 180 mg/mL Fast blue RR and dissolve them in 2 mL DMF. The solution must be always freshly prepared immediately prior to use.
2. For each screening plate, 6 mL of soft agar (5 mg/mL) containing 0.3 mg/mL of the naphthyl substrate and 1.5 mg/mL Fast Blue RR (final concentration) are required. For example, for 4 plates, we will need 24 mL of the final soft agar solution containing 120 mg agar. Weigh the agar, add the water (*see* **Note 3**), then microwave the agar mix until it is completely dissolved and put it in a 60 °C water bath until the agar reaches the same temperature. When the agar solution is cooled down, add 17 μL of the naphthyl-Fast blue RR mix (*see* **step 1**) for every milliliter of top agar (a total of 100 μL per screening plate and 400 μL for 4 plates) and swirl lightly to disperse and avoid the formation of bubbles. The mixture needs to be cooled down to approximately 45 °C before it is poured directly to the grown recombinant colonies, in order to prevent heat deactivation and maintain recombinant enzymatic activity.

2.7 Fluorescence Plate Assays Using 4-Methylumbelliferyl Substrates (MeUmb)

Various 4-methylumbelliferyl (MeUmb) substrates, such as MeUmb-dihydroferulate, MeUmb-acetate, MeUmb-butyrate, MeUmb-β-D-glucopyranoside, MeUmb-β-D-cellobioside, MeUmb-β-D-lactopyranoside, MeUmb-β-D-xylopyranoside, and MeUmb-β-D-mannopyranoside are appropriate for this plate assay methodology (Fig. 3). All aforementioned substrates are commercially available except MeUmb-dihydroferulate [31]. Fluorogenic substrates, such as MeUmb derivatives, have been used for many years to assay lignocellulolytic enzymes, by the release of 4-methylumbelliferone measured fluorometrically down to nanomolar concentrations. The low detection concentration limit results in a sensitive screening method with short incubation times. The hydrolysis of fluorogenic substrates release 4-methylumbelliferone that has an excitation peak at 365 nm with emission at 445 nm.

1. Prepare a 10 mM stock solution of MeUmb substrate in dimethyl sulfoxide (DMSO) and store at 4 °C.
2. Each screening plate must be covered with 6 mL of molten soft agar (10 mg/mL) containing 0.02 mM final concentration of MeUmb substrate. For example, if 4 plates are to be screened, add 240 mg agar to 24 mL of water inside a 100 mL beaker.

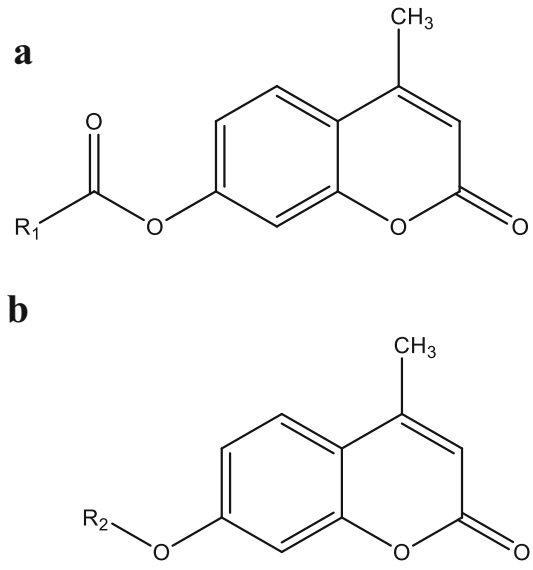

Fig. 3 (**a**) MeUmb-alkyl or hydroxycinnamoyl (R_1) esters and (**b**) MeUmb-glycosides (R_2) for the detection of various lignocellulolytic activities

Microwave the agar mix until it is completely dissolved and put it in a 60 °C water bath until the agar reaches the same temperature. Finally, add 2 μL of MeUmb substrate stock solution (10 mM) for every milliliter of top agar (a total of 12 μL per screening plate) and swirl lightly to disperse and avoid the formation of bubbles. The mixture needs to be cooled down before it is poured directly to the grown recombinant colonies, in order to maintain recombinant enzymatic activity.

2.8 Affinity Chromatography for the Purification of His-Tagged Recombinant Enzymes

The next step, after the production and detection of recombinant enzymatic activity produced by the heterologous hosts *E. coli* and *P. pastoris*, is the purification of His-tagged enzymes that will be carried out by the easy, fast, and well-documented method of IMAC. For the isolation of a recombinant protein using cobalt resin, such as TALON® Superflow Resin (Clontech, USA), the following buffers should be prepared prior to the equilibration of the affinity column:

1. Equilibration/wash buffer (50 mM Tris–HCl pH 8.0 with 300 mM NaCl):
   (a) For the preparation of 1 L of a ten-times (10×) concentrated stock solution (500 mM Tris–HCl with 3 M NaCl), add 60.57 g of Trizma Base and 175.32 g of NaCl in 900 mL water in a 2 L beaker.
   (b) Mix well using a magnetic stirrer and when the solution is ready, equilibrate the pH at 8 by adding the proper amount of fuming HCl (37%, w/w). Transfer the solution to a graduated cylinder and add water to a total volume of 1 L.

(c) In order to prepare the appropriate buffer concentration, dilute ten times. Both diluted and (10×) stock solution could be stored at room temperature with a shelf life of approximately 1 year.

2. Elution buffer (50 mM Tris–HCl pH 8.0 with 300 mM NaCl and 100 mM imidazole):
   (a) For the preparation of 1 L elution buffer, add 100 mL of the 10× equilibration/wash buffer with 6.8 g imidazole in 800 mL of water and mix well in a 2 L beaker using a magnetic stirrer.
   (b) When the imidazole is totally dissolved, transfer the solution to a graduated cylinder and add water to a total volume of 1 L. The elution buffer could be stored at room temperature with a shelf life of approximately 1 year.
3. TALON® Superflow Resin column packing and equilibration (adapted from TALON® Metal Affinity Resins User Manual):
   (a) Resuspend the resin thoroughly prior to pouring into the column (1.0 cm i.d., 15 cm length) and avoid introducing air bubbles.
   (b) Allow the resin to settle, assemble the top adaptor to the column and flow through equilibration/wash buffer with a peristaltic pump to speed up the packing process. Do not exceed a flow rate of 5 mL/min. If the resin volume is reduced, disassemble and add more resin up to the appropriate amount, which is dependent on the amount of protein to be isolated.
   (c) Equilibrate the column with equilibration/wash buffer, monitoring the eluent at 280 nm. The baseline should be stable after washing with 5–10 bed volumes. The column is now ready for the purification of a His-tagged recombinant protein.

3 Methods

3.1 Screening of Cellulase or Hemicellulose (Xylanase, Mannanase, and Arabinase) Producers Using Congo Red Plate Assay

The following procedure is suitable for qualitative display of cellulase or hemicellulase activity, depending on the polysaccharide added in the agar plate, using Congo Red that interacts with polysaccharides containing contiguous β-(1→4)-linked D-gluco or D-xylopyranosyl units [15]. In case of enzymes with lytic polysaccharide monooxygenase activity (LPMO), this assay can also be applied based on the weak endoglucanase activity of these enzymes, which was also the first indication of their action. In this case, LB or MM agar plates containing phosphoric acid swollen cellulose (PASC) or CMC-cellulose (*see* Subheadings 2.1 or 2.2) can be prepared and inoculated with the transformants. Staining with Congo Red can be used to detect the released reducing sugars [32] (*see* **Note 4**).

1. Make LB or MM agar plates containing CMC-cellulose, xylan, or other substrates (*see* Subheadings 2.1 or 2.2).
2. Using sterile toothpicks, patch more than 10 recombinant *E. coli* or *P. pastoris* colonies on two replica LB-IPTG or MM plates, respectively, at a density of approximately 1 colony/cm^2. For controls, make one patch from each of the strains that are transformed with the plasmid without the inserted gene (negative control).
3. Incubate the plates at 37 °C (*E. coli*) or at 28–30 °C (*P. pastoris*) for 16 h (overnight).
4. Add ~10 mL of Congo Red solution (*see* Subheading 2.3) to the top of one plate and keep the second replica plate as a reference (*see* **Notes 5** and **6**).
5. Incubate for 15 min at room temperature to stain the incorporated polysaccharide.
6. Discard Congo Red solution and add ~10 mL of 1 M NaCl (destaining solution).
7. Incubate for 5 min to destain the unbound regions and repeat **step 6** until clearing zones are observed around cellulase or hemicellulase positive colonies (Fig. 4a).
8. Use the replica plate to pick the corresponding recombinant colonies that were found positive in the enzymatic activity of interest prior to the purification process.

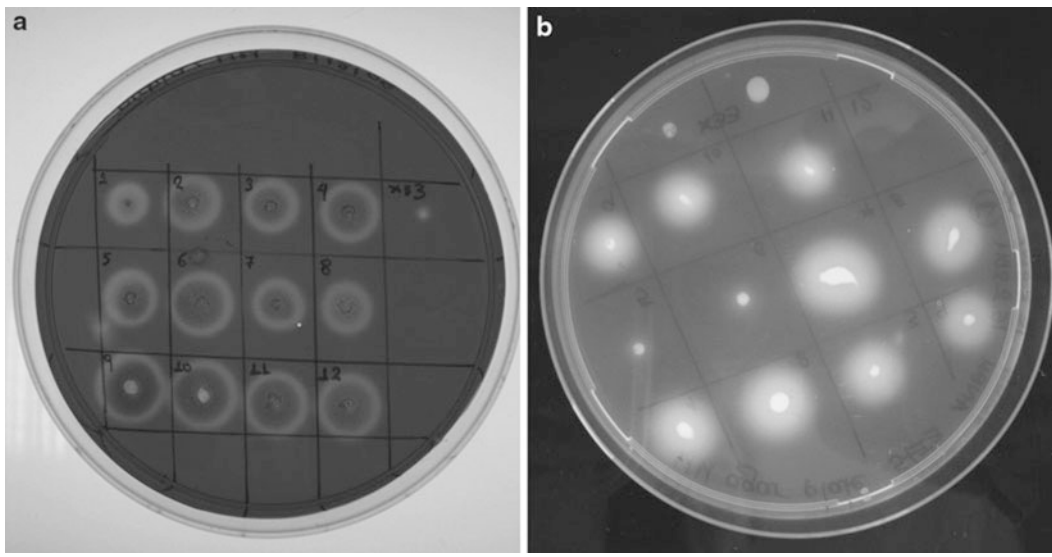

Fig. 4 (**a**) Congo Red and (**b**) 4-methylumbelliferyl fluorescence formed haloes surrounding positive recombinant colonies

3.2 Screening of Enzymatic Activities with AZCL, Indoxyl, and RBB Substrates

1. Prepare LB-IPTG or MM agar plates for screening *E. coli* or *P. pastoris* transformants, respectively (*see* Subheadings 2.1 or 2.2).
2. Using sterile toothpicks, patch more than 10 recombinant *E. coli* or *P. pastoris* colonies on two replica LB-IPTG or MM plates, respectively, at a density of approximately 1 colony/cm^2. For controls, make one patch from each of the strains that are transformed with the plasmid without the inserted gene (negative control).
3. Incubate the plates at 37 °C (*E. coli*) or at 28–30 °C (*P. pastoris*) for 16 h (overnight).
4. Prepare an appropriate amount of molten soft agar (7 mg/mL) containing 2 mg/mL of the azurine-linked substrate, 0.002 mg/mL of the indoxyl substrate, or 1 mg/mL of the RBB dyed substrates (*see* Subheading 2.4). Cool it down until the temperature reaches the thermostability range of the recombinant cellulase or hemicellulase.
5. Pour onto the grown recombinant colonies of one plate forming a cloudy top agar and keep the second replica plate as a reference.
6. Incubate plates at 30 °C for 2–4 h, until a colored zone around the colonies is formed, indicative of hydrolytic enzyme activity. Enzyme activity is visualized either by a clearing or a precipitate. In case of AZCL and indoxyl substrates, a blue and an indigo/magenta zone is formed, respectively, while in case of RBB substrates, the hydrolysis of the substrate leads to the formation of clear, decolorized areas around the transformed strains.
7. Use the replica plate to pick the corresponding recombinant colonies that were found positive in enzymatic activity prior to the purification process.

3.3 Screening of Laccase/ Multicopper Oxidase/ Peroxidase Activities Using the ABTS Assay

The oxidation of ABTS (2,2′-azino-bis-(3-ethylbenzothiazoline-6-sulphonic acid)) to its green-colored cation radical (Fig. 5a) [33] is a widely used assay for the detection of phenol-oxidation activity, and therefore can be used for the activity detection and screening of many different oxidative enzymes, including laccases, multicopper oxidases, peroxidases, some PPOs, and others. It has been used widely in the literature for screening purposes [10, 34–36], but also for the biochemical characterization of multicopper oxidases and peroxidases [11, 37–40]. ABTS, as a temperature-sensitive substrate, can be filter sterilized and added after the autoclave in agar plates. The oxidase-positive clones can be visualized by the appearance of a green halo around the colonies. For peroxidase enzymes, an additional step of H_2O_2 addition must be performed, while ABTS-mediated detection can be used for manganese-dependent

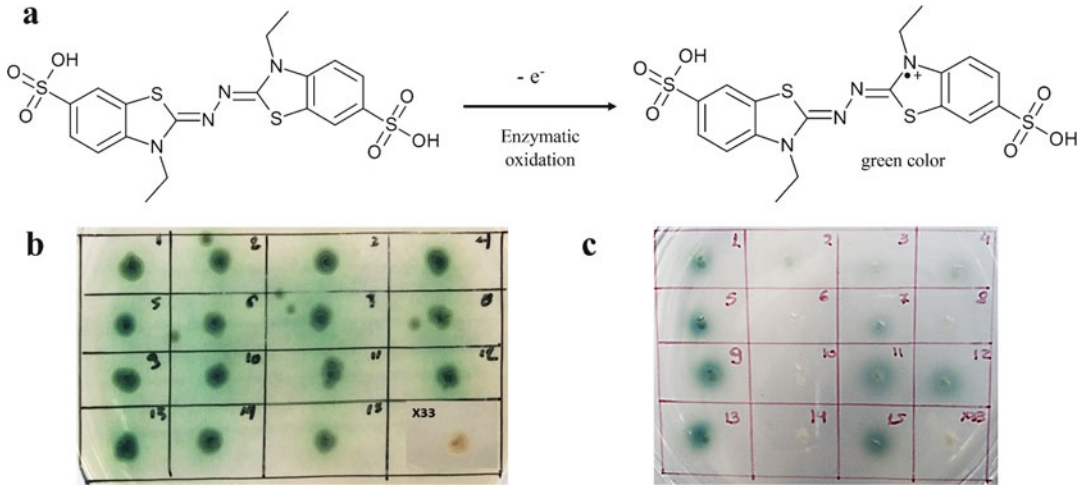

Fig. 5 (**a**) ABTS oxidation catalyzed by oxidative enzymes. Plate assays with ABTS as the substrate for monitoring the activity of (**b**) laccases and (**c**) peroxidases

(MnPs), manganese-independent (MiPs or lignin peroxidases, LiPs), versatile peroxidases (VPs), and dye-decolorizing peroxidases (DyPs). For the use of alternative substrates for the activity screening of ligninolytic enzymes, *see* **Note 7**.

1. Prepare LB-IPTG or MM agar plates for screening *E. coli* or *P. pastoris* transformants, respectively (*see* Subheadings 2.1 or 2.2), with filter-sterilized ABTS stock solution added after autoclave, at a final concentration of 2 mM (*see* **Note 2**). For laccase or multicopper oxidase activity detection, $CuSO_4$ at a final concentration of 0.1 mM has to be added in the medium (*see* **Note 2**). For manganese-dependent peroxidase activity, $MnSO_4$ has to be added in the medium, at a final concentration of 0.1 mM (*see* **Note 2**).
2. Under aseptic conditions, inoculate more than 10 recombinant *E. coli* or *P. pastoris* colonies on two replica LB-IPTG or MM plates, respectively, at a density of approximately 1 colony/cm^2. For controls, make one patch from a strain transformed with the plasmid without the inserted gene (negative control).
3. Incubate the plates at 37 °C (*E. coli*) for 16 h (overnight), or at 28–30 °C (*P. pastoris*) for 2–4 days, in a dark chamber. In some cases, the addition of small amounts of methanol on a daily basis can boost the enzyme production and enable the detection of the activity (*see* **Note 8**).
4. For oxidases using molecular oxygen (O_2) as an electron acceptor (such as laccases), the enzyme-producing clones can be visualized by the formation of a green halo around the positive clones (Fig. 5b).

5. For peroxidase activity detection, after the indicated incubation time, and the formation of visible colonies, overlay the colonies with a drop of H_2O_2 solution, at 1 mM concentration (*see* Subheading 2.2, **item 13**). Incubate for a further 20 min, in a dark chamber, at 30 °C, until the development of a green halo around the positive colonies (Fig. 5c).
6. Use the replica plate to isolate the corresponding recombinant clones that were found positive in oxidase/peroxidase activity prior to the purification process.

3.4 Screening of Ferulic Acid Esterase and Acetyl Xylan Esterase Activity Using the Ethyl Ferulate and Ethyl Acetate Plate Assay

Ferulic acid esterases are enzymes responsible for cleaving the ester link between ferulate and the side chains of hemicelluloses and are of great importance in biotechnology due to many industrial and medicinal applications [41]. Two agar plate assays are applicable for detecting such activity using ethyl ferulate [42, 43] or MeUmb-dihydroferulate [31, 44] as substrates. A similar assay can be used for acetyl xylan esterases by employing the ethyl-acetate or MeUmb-acetate as substrate [16, 45]. Acetyl xylan esterases are enzymes that act on the acetylated structures of hemicellulose and more specifically on acetylated xylans and xylo-oligosaccharides.

1. Prepare LB-IPTG or MM agar plates for screening *E. coli* or *P. pastoris* transformants, respectively (*see* Subheadings 2.1 or 2.2).
2. Using sterile toothpicks, patch more than 10 recombinant *E. coli* or *P. pastoris* colonies on two replica LB-IPTG or MM plates, respectively, at a density of approximately 1 colony/cm^2. For controls, make one patch from each of the strains that are transformed with the plasmid without the inserted gene (negative control).
3. Incubate the plates at 37 °C (*E. coli*) or at 28–30 °C (*P. pastoris*) for 16 h (overnight).
4. Prepare an appropriate amount of molten soft agar (4 mg/mL) containing 1 mg/mL of ethyl ferulate or ethyl acetate (*see* Subheading 2.5). Cool it down until the temperature reaches the thermostability range of the recombinant esterase.
5. Pour onto the grown recombinant colonies of one plate forming a cloudy top agar and keep the second replica plate as a reference (*see* **Note 9**).
6. Incubate plates at 30 °C for 2–4 h, until a clear zone around the colonies is formed, indicative of esterase activity.
7. Use the replica plate to peak the corresponding recombinant colonies that were found positive in esterase activity prior to the purification process.

3.5 Screening of Acetyl-Xylan Esterases with α- or β-Naphthyl Substrates

α- or β-naphthyl substrates are cleaved by the acetyl xylan esterases, producing α- or β-napthate that produces a colored halo when coupled to Fast Blue RR. This assay has been used in the literature, providing accurate results for different classes of acetyl xylan esterases [46, 47]. Esterases produce clear zones around the colony of naphthyl substrates that are visible even without any additional dye. However, the use of indicative dyes, such as Fast Blue RR, increases the sensitivity of the method and enable faster analysis.

1. Prepare LB-IPTG or MM agar plates for screening *E. coli* or *P. pastoris* transformants, respectively (*see* Subheadings 2.1 or 2.2).
2. Using sterile toothpicks, patch more than 10 recombinant *E. coli* or *P. pastoris* colonies on two replica LB-IPTG or MM plates, respectively, at a density of approximately 1 colony/cm^2. For controls, make one patch from each of the strains that are transformed with the plasmid without the inserted gene (negative control).
3. Incubate the plates at 37 °C (*E. coli*) or at 28–30 °C (*P. pastoris*) for 16 h (overnight).
4. Prepare an appropriate amount of molten soft agar (4 mg/mL) containing 18 mg/mL naphthyl substrate and 90 mg/mL Fast blue RR (*see* Subheading 2.6). Cool it down until the temperature reaches the thermostability range of the recombinant esterase.
5. Pour onto the grown recombinant colonies of one plate forming a cloudy top agar and keep the second replica plate as a reference (*see* **Note 9**).
6. Incubate plates at 30 °C for 2–4 h, until a color change around the colonies is visible, indicative of esterase activity.
7. Use the replica plate to pick the corresponding recombinant colonies that were found positive in esterase activity prior to the purification process.

3.6 Screening of Esterases with Tributyrin Plate Assay

Tributyrin agar assay was originally formulated by Anderson [48] for the detection of lipolytic microorganisms. It has been used for detecting the activity of acetyl xylan esterases [16, 17] by forming a zone of clearance around the transformants that produce the recombinant esterase.

1. Prepare LB-IPTG or MM agar plates containing 1% (w/v) tributyrin for screening *E. coli* or *P. pastoris* transformants, respectively (*see* Subheadings 2.1 or 2.2). Add 2.5 mM $CaCl_2$ and $MgSO_4$ (final concentration) to the culture media. The calcium and magnesium ions will improve the visualization of the result by intensifying the enzyme activity and stabilizing the substrate, respectively [17].

2. Using sterile toothpicks, patch more than 10 recombinant *E. coli* or *P. pastoris* colonies on two replica LB-IPTG or MM plates, respectively, at a density of approximately 1 colony/cm^2. For controls, make one patch from each of the strains that are transformed with the plasmid without the inserted gene (negative control).
3. Incubate the plates at 37 °C (*E. coli*) or at 28–30 °C (*P. pastoris*) for 16 h (overnight), until a clear zone around the colonies is formed, indicative of esterase activity.
4. Use the replica plate to pick the corresponding recombinant colonies that were found positive in esterase activity prior to the purification process.

3.7 Screening of β-Glucosidase with Esculin Plate Assay

Esculin can be efficiently used as a substrate for the detection of β-glucosidase activity. Around the strains that produce β-glucosidase, esculin is degraded to glucose and esculetin. The latter is conjugated to the ferric ions forming a brown halo around the transformants [26].

1. Prepare LB-IPTG or MM agar plates containing 0.5% (w/v) esculin for screening *E. coli* or *P. pastoris* transformants, respectively (*see* Subheadings 2.1 or 2.2). Add 0.1% (w/v) ammonium ferric citrate (final concentration) to the culture media. Upon the activity of β-glucosidase, a dark-brown color will be formed around the transformants that produce the recombinant enzyme.
2. Using sterile toothpicks, patch more than 10 recombinant *E. coli* or *P. pastoris* colonies on two replica LB-IPTG or MM plates, respectively, at a density of approximately 1 colony/cm^2. For controls, make one patch from each of the strains that are transformed with the plasmid without the inserted gene (negative control).
3. Incubate the plates at 37 °C (*E. coli*) or at 28–30 °C (*P. pastoris*) for 16 h (overnight), until a dark-brown zone around the colonies is formed, indicative of β-glucosidase activity.
4. Use the replica plate to pick the corresponding recombinant colonies that were found positive in esterase activity prior to the purification process.

3.8 Screening of Various Carbohydrate Active Enzymatic Activities Using 4-Methylumbelliferyl Fluorescence Agar Plate Assays

This fluorescence agar plate assay methodology provides a fast and sensitive detection of various cellulolytic and hemicellulolytic enzymatic activities including ferulic acid esterases (MeUmb-dihydroferulate), acetyl (xylan)esterase (MeUmb-acetate) (*see* **Note 10**), β-glucosidase (MeUmb-β-D-glucopyranoside), cellobiohydrolase (MeUmb-β-D-cellobioside and MeUmb-β-D-lactopyranoside), β-mannosidase (MeUmb-β-D-mannopyranoside), β-xylosidase (MeUmb-β-D-xylopyranoside), and cutinase or lipase (MeUmb-butyrate) activities. In addition to these substrates, it is possible to

use the following methodology for different MeUmb substrates that are not described in this report, allowing the detection of other biomass-degrading enzymatic activities.

1. Make LB-IPTG or MM agar plates for screening *E. coli* or *P. pastoris* transformants, respectively (*see* Subheadings 2.1 or 2.2).
2. Using sterile toothpicks, patch more than 10 recombinant *E. coli* or *P. pastoris* colonies on two replica LB-IPTG or MM plates, respectively, at a density of approximately 1 colony/cm^2. For controls, make one patch from each of the strains that are transformed with the plasmid without the inserted gene (negative control).
3. Incubate the plates at 37 °C (*E. coli*) or at 28–30 °C (*P. pastoris*) for 16 h (overnight).
4. Prepare an appropriate amount of molten soft agar (10 mg/mL) containing 0.02 mM final concentration of MeUmb substrate (*see* Subheading 2.7). Cool it down until the temperature reaches the thermostability range of the recombinant enzyme of interest.
5. Pour onto the grown recombinant colonies of one plate forming a clear top agar and keep the second replica plate as a reference.
6. Incubate plates at room temperature for 1–10 min depending on the enzymatic activity found. Inspect plates regularly under UV light at 312 nm on a transilluminator UV table for fluorescent haloes surrounding the recombinant colonies, which is indicative of MeUmb hydrolysis (Fig. 4b).
7. Use the replica plate to pick the corresponding recombinant colonies that were found positive in the enzymatic activity of interest prior to the purification process.

3.9 Purification of His-Tag Recombinant Enzymes Using IMAC

For the purification of the recombinant enzymes that exhibit an N- or C-terminal His-tag, IMAC procedure is the best and the easiest way to obtain a relatively pure protein in just one step. Resins charged with cobalt, such as TALON® (Clontech, USA), bind His-tagged recombinant proteins with higher specificity than nickel-charged resin, resulting in a less contaminated, by native host's proteins, enzyme [4]. According to the user manual of TALON® Superflow Resin, its binding capacity for individual proteins may vary from 5 to 20 mg/mL of resin. For the purification of a His-tagged recombinant protein, we need to apply the following steps:

1. Concentrate the culture supernatant (*P. pastoris* extracellular expression) or cell-free extract (*E. coli* or *P. pastoris* intracellular expression) down to approximately 5 mL using an Amicon ultrafiltration apparatus (Amicon chamber 8400 with membrane Diaflo PM-10, exclusion size 10 kDa or higher depending on the size of the recombinant protein), (Millipore, Billerica, USA).
2. Exchange the buffer of the concentrated protein solution overnight using dialysis tubes or cassettes with the appropriate MW cutoff at 4 °C against equilibration/wash buffer (20 mM Tris–HCl buffer containing 300 mM NaCl, pH 8.0).
3. Equilibrate a TALON® Superflow Resin column (*see* Subheading 2.8) with 5 bed volumes of equilibration/wash buffer. Start continuous monitoring of effluents at 280 nm for protein detection and start the separation when the baseline is stable.
4. Filter the crude enzyme extract through a 0.22 μm filter and load them onto the TALON® column at a flow rate of 0.5–1 mL/min to ensure His-tag binding to the resin (*see* **Note 11**).
5. Wash column with equilibration/wash buffer at a flow rate of up to 5 mL/min until the absorbance at 280 nm returns to baseline in order to remove non-bound proteins (*see* **Note 11**).
6. Apply a gradient from 0 to 100 mM imidazole (elution buffer) at a flow rate of up to 5 mL/min (*see* **Note 11**).
7. Collect fractions (2 mL) and search for the enzymatic activity of interest. Pool fractions, concentrate, and check the purity level qualitatively by sodium dodecyl sulphate-polyacrylamide gel electrophoresis (SDS-PAGE) according to the method of Laemmli [49].

   In the case of LPMOs, an additional step is required after purification in order to boost the activity of the enzyme (*see* **Note 12**).

4 Notes

1. The amount of CMC cellulose, xylan, or other substrates incorporated in agar for detecting cellulase or hemicellulase activity by Congo Red staining varies from 0.01% to 1% (w/v), as reported by different investigations published in the literature. We recommend 0.4% (w/v) and 0.01% (w/v) for CMC and xylan, respectively, 1% (w/v) and 0.5% (w/v) for galactomannan and locust bean gum, respectively, but the amount could be changed depending on the enzymatic activity detected.

2. Temperature-sensitive chromogenic substrates should be added after the mixture temperature has reached 60 °C, under sterile conditions. For the detection of oxidative enzymatic activity, 50 mL of filter-sterilized 10× ABTS solution should be added (prepare fresh stock solution 10× by mixing 0.51 g in 50 mL ultrapure water, and keep on ice, in dark bottle until use) (*see* Subheading 2.2, **item 12**) [11]. For the detection of laccase or multicopper oxidase activity, also add 5 mL of sterile $CuSO_4$ 100X solution (*see* Subheading 2.2, **item 14**) [10], while in case of manganese-dependent peroxidase activity, add aseptically 5 mL of sterilized $MnSO_4$ 100× solution (*see* Subheading 2.2, **item 15**).
3. In those cases that a specific pH value is required in order for the enzymatic activity to be detected, a buffer solution can be used instead of water. A concentration of 25–50 mM is recommended.
4. To detect the activity of LPMO on a plate assay based on its weak endoglucanase activity, a compound acting as a reducing agent that will provide electrons to support the activity of the enzyme is required. Different molecules, such as ascorbic acid, pyrogallol or gallic acid, can be used at an adequate concentration (1 to 5 mM or 0.1–0.5 mg for lignin, depending on its molecular weight). The reducing agent should be diluted in water (stock solution), filter sterilized, and added to the medium after autoclaving and cooling down to 50 °C.
5. In order to avoid diffusion of microbial colonies on agar plate when the top agar is flooded with Congo Red solution, it is recommended to wash off colonies prior to staining [50].
6. An alternative to Congo Red staining solution for screening cellulose-expressing hosts is the Gram's Iodine (Lugo's solution) staining that forms a bluish-black complex with cellulose, giving a distinct zone around microbial colonies faster compared with Congo Red staining [51]. Following the procedure described in Subheading 3.1, in **step 4**, Gram's iodine (2.0 g KI and 1.0 g iodine in 300 mL water) is added instead of Congo Red for 3–5 min.
7. Aside from the ABTS assay described here for the screening of recombinant laccase and peroxidase activities, numerous other plate assays have been described in the literature for the same purpose. Among them, the decolorization of different dyes, such as reactive black 5, Azure B [52], RBB, and Congo Red [53], and the oxidation of various phenolic compounds, such as guaiacol [52] and *O*- methoxyphenol [54], have been used as substrates for plate assays for oxidative enzyme activities in

their native hosts. However, due to the possible toxicity of such compounds to heterologous hosts usually employed for the recombinant expression of ligninolytic enzymes (*E. coli*, *P. pastoris*) and to the long incubation times required for the oxidation of such recalcitrant compounds, these protocols are not widely used for the screening of recombinant clones in the case of heterologous expression of laccase or peroxidase enzymes.

8. Multicopper oxidase and peroxidase expression in *P. pastoris* can often be impaired by many issues [11, 55] leading to low levels of heterologous protein expression, which can often make it impossible to detect the activity in plate assays. In order to circumvent this problem and obtain visible green halos as a positive indicator of activity, very strong induction of the *AOX1* promoter is necessary. This can be obtained by maintaining the gene induction throughout the 2–4-day incubation of the plates, by aseptically adding 100 μL liquid, filter-sterilized methanol to the cap of each petri dish every day. Due to methanol volatility, *P. pastoris* cells can have a similar feed as in the case of liquid cultures.
9. The ferulic acid esterase plate assay is adapted by Hassan & Pattat [42], changing the ethyl ferulate concentration in top agar from 0.05 mg/mL to the concentration reported by Donaghy et al. [56] 1 mg/mL in order to prepare a cloudy top agar layer, enhancing the detection of clear zones around the colonies. The use of agarose instead of agar is better for preparing the top agar layer not only in case of ethyl ferulate and ethyl acetate but also for naphthyl substrates and tributyrin, as it facilitates the formation of zones of clearance following the enzyme activity.
10. Acetyl xylan esterases belonging to CE4 family do not react on MeUmb-acetate and most probably, another assay is needed in order to verify the presence of the enzyme in the recombinant *E. coli* and *P. pastoris* cells. Sometimes these enzymes are active on acetylated natural substrates, so enzyme expression in shake flasks and activity tests of the supernatant is required.
11. The flow rate of TALON® Superflow Resin for loading, washing, and elution might be increased up to 5 mL/min/cm^2 in order to decrease the duration of the purification process. However, a decrease by 10–15% in capacity should be expected, depending on the recombinant protein.
12. Copper ions' saturation of the LPMO active site should be performed in the buffer that will be used in the subsequent experiments. This procedure will enable the efficient activity of the enzyme. The protocol is described in detail by Westereng et al. [57].

References

1. Bhat MK (2000) Cellulases and related enzymes in biotechnology. Biotechnol Adv 18:355–383
2. Baneyx F (1999) Recombinant protein expression in *Escherichia coli*. Curr Opin Biotechnol 10:411–421
3. Cereghino JL, Cregg JM (2000) Heterologous protein expression in the methylotrophic yeast *Pichia pastoris*. FEMS Microbiol Rev 24:45–66. https://doi.org/10.1111/j.1574-6976.2000.tb00532.x
4. Robichon C, Luo J, Causey TB et al (2011) Engineering *Escherichia coli* BL21(DE3) derivative strains to minimize *E. coli* protein contamination after purification by immobilized metal affinity chromatography. Appl Environ Microbiol 77:4634–4646. https://doi.org/10.1128/AEM.00119-11
5. Anbar M, Bayer EA (2012) Approaches for improving thermostability characteristics in cellulases. Methods Enzymol 510:261–271. https://doi.org/10.1016/B978-0-12-415931-0.00014-8
6. McCleary BV (1988) Soluble, dye-labeled polysaccharides for the assay of endohydrolases. Methods Enzymol 160:74–86. https://doi.org/10.1016/0076-6879(88)60108-X
7. Biely P, Mislovicova D, Toman R (1985) Soluble chromogenic substrates for the assay of endo-1,4-β-glucanase. Anal Biochem 144:142–146. https://doi.org/10.1016/0003-2697(85)90095-8
8. Thorn RG (1993) The use of cellulose azure agar as a crude assay of both cellulolytic and ligninolytic abilities of wood-inhibiting fungi. Proc Jpn Acad Ser B Phys Biol Sci 69:29–34. https://doi.org/10.2183/pjab.69.29
9. Karnaouri A, Topakas E, Paschos T et al (2013) Cloning, expression and characterization of an ethanol tolerant GH3 β-glucosidase from *Myceliophthora thermophila*. PeerJ 1:e46. https://doi.org/10.7717/peerj.46
10. Gu C, Zheng F, Long L et al (2014) Engineering the expression and characterization of two novel laccase isoenzymes from *Coprinus comatus* in *Pichia pastoris* by fusing an additional ten amino acids tag at N-terminus. PLoS One 9(4): e93912. https://doi.org/10.1371/journal.pone.0093912
11. Zerva A, Christakopoulos P, Topakas E (2015) Characterization and application of a novel class II thermophilic peroxidase from *Myceliophthora thermophila* in biosynthesis of polycatechol. Enzyme Microb Technol 75–76:49–56. https://doi.org/10.1016/j.enzmictec.2015.04.012
12. Neddersen M, Elleuche S (2015) Fast and reliable production, purification and characterization of heat-stable, bifunctional enzyme chimeras. AMB Express 5(1):122. https://doi.org/10.1186/s13568-015-0122-7
13. Vianna Bernardi A, Kimie Yonamine D, Akira Uyemura S et al (2019) A thermostable *Aspergillus fumigatus* GH7 endoglucanase over-expressed in *Pichia pastoris* stimulates lignocellulosic biomass hydrolysis. Int J Mol Sci 20:9. https://doi.org/10.3390/ijms20092261
14. Scheirlinck T, Meutter J, Arnaut G et al (1990) Cloning and expression of cellulase and xylanase genes in *Lactobacillus plantarum*. Appl Microbiol Biotechnol 33:534–541
15. Teather RM, Wood PJ (1982) Use of Congo red-polysaccharide interactions in enumeration and characterization of cellulolytic bacteria from the bovine rumen. Appl Environ Microbiol 4:777–780
16. Adesioye FA, Makhalanyane TP, Vikram S et al (2018) Structural characterization and directed evolution of a novel acetyl xylan esterase reveals thermostability determinants of the carbohydrate esterase 7 family. Appl Environ Microbiol 84:8. https://doi.org/10.1128/AEM.02695-17
17. Carrazco-Palafox J, Rivera-Chavira BE, Ramírez-Baca N et al (2018) Improved method for qualitative screening of lipolytic bacterial strains. Methods X 5:68–74. https://doi.org/10.1016/j.mex.2018.01.004
18. Katsimpouras C, Dimarogona M, Petropoulos P et al (2016) A thermostable GH26 endo-β-mannanase from *Myceliophthora thermophila* capable of enhancing lignocellulose degradation. Appl Microbiol Biotechnol 100 (19):8385–8397. https://doi.org/10.1007/s00253-016-7609-2
19. Mattéotti C, Bauwens J, Brasseur C et al (2012) Identification and characterization of a new xylanase from Gram-positive bacteria isolated from termite gut (*Reticulitermes santonensis*). Protein Expr Purif 83(2):117–127. https://doi.org/10.1016/j.pep.2012.03.009
20. Zhou C, Xue Y, Ma Y (2018) Characterization and high-efficiency secreted expression in *Bacillus subtilis* of a thermo-alkaline β-mannanase from an alkaliphilic *Bacillus clausii* strain S10. Microb Cell Factories 17(1):124. https://doi.org/10.1186/s12934-018-0973-0
21. Kračun SK, Schückel J, Westereng B et al (2015) A new generation of versatile chromogenic substrates for high-throughput analysis of biomass-degrading enzymes. Biotechnol

Biofuels 8:70. https://doi.org/10.1186/s13068-015-0250-y
22. Li LL, Taghavi S, McCorkle SM et al (2011) Bioprospecting metagenomics of decaying wood: mining for new glycoside hydrolases. Biotechnol Biofuels 4:23. https://doi.org/10.1186/1754-6834-4-23
23. Huang Y, Busk PK, Lange L (2015) Cellulose and hemicellulose-degrading enzymes in Fusarium commune transcriptome and functional characterization of three identified xylanases. Enzym Microb Technol 73–74:9–19. https://doi.org/10.1016/j.enzmictec.2015.03.001
24. Manafi M (1996) Fluorogenic and chromogenic enzyme substrates in culture media and identification tests. Int J Food Microbiol 31:45. https://doi.org/10.1016/0168-1605(96)00963-4
25. Cotson S, Holt SJ (1958) Studies in enzyme cytochemistry. IV. Kinetics of aerial oxidation of indoxyl and some of its halogen derivatives. Proc R Soc Lond B Biol Sci 148(933):506–519
26. Perry JD, Morris KA, James AL et al (2007) Evaluation of novel chromogenic substrates for the detection of bacterial b-glucosidase. Appl Microbiol 102(2):410–415. https://doi.org/10.1111/j.1365-2672.2006.03096.x
27. Arab-Jaziri F, Bissaro B, Dion M et al (2013) Engineering transglycosidase activity into a GH51 a-l-arabinofuranosidase. New Biotechnol 30:5. https://doi.org/10.1016/j.nbt.2013.04.002
28. Bissaro B, Durand J, Biarnés X et al (2015) Molecular design of non-Leloir furanose-transferring enzymes from an α-l-arabinofuranosidase: a rationale for the engineering of evolved transglycosylases. ACS Catal 5(8):4598–4611. https://doi.org/10.1021/acscatal.5b00949
29. Meddeb-Mouelhi F, Moisan JK, Beauregard M (2014) A comparison of plate assay methods for detecting extracellular cellulase and xylanase activity. Enzym Microb Technol 66:16–19. https://doi.org/10.1016/j.enzmictec.2014.07.004
30. Miller RB, Karn RC (1980) A rapid spectrophotometric method for the determination of esterase activity. J Biochem Biophys Methods 3(6):345–354
31. Leschot A, Tapia RA, Eyzaguirre J (2002) Efficient synthesis of 4-methylumbelliferyl dihydroferulate. Synth Commun 32:3219–3223. https://doi.org/10.1081/SCC-120013746
32. Dimarogona M, Topakas E, Olsson L et al (2012) Lignin boosts the cellulase performance of a GH-61 enzyme from *Sporotrichum thermophile*. Bioresour Technol 110:480–487. https://doi.org/10.1016/j.biortech.2012.01.116
33. Childs RE, Bardsley WG (1975) The steady-state kinetics of peroxidase with 2.2%-azino-di-(3-ethyl-benzthiazoline-6-sulphonic acid) as chromogen. Biochem J 145:93–103. https://doi.org/10.1042/bj1450093
34. Srinivasan C, Dsouza TM, Boominathan K et al (1995) Demonstration of laccase in the white rot basidiomycete *Phanerochaete chrysosporium* BKM-F1767. Appl Environ Microbiol 61(12):4274–4277
35. Yang Q, Zhang M, Zhang M et al (2018) Characterization of a novel, cold-adapted, and thermostable laccase-like enzyme with high tolerance for organic solvents and salt and potent dye decolorization ability, derived from a marine metagenomic library. Front Microbiol 9:2998. https://doi.org/10.3389/fmicb.2018.02998
36. Garg N, Bieler N, Kenzom T et al (2012) Cloning, sequence analysis, expression of *Cyathus bulleri* laccase in *Pichia pastoris* and characterization of recombinant laccase. BMC Biotechnol 12(1):1–12. https://doi.org/10.1186/1472-6750-12-75
37. Zerva A, Koutroufini E, Kostopoulou I et al (2019) A novel thermophilic laccase-like multicopper oxidase from *Thermothelomyces thermophila* and its application in the oxidative cyclization of 2′,3,4-trihydroxychalcone. New Biotechnol 49:10–18. https://doi.org/10.1016/j.nbt.2018.12.001
38. Johannes C, Majcherczyk A (2000) Laccase activity tests and laccase inhibitors. J Biotechnol 78(2):193–199
39. Sadhasivam S, Savitha S, Swaminathan K et al (2008) Production, purification and characterization of mid-redox potential laccase from a newly isolated *Trichoderma harzianum* WL1. Process Biochem 43(7):736–742. https://doi.org/10.1016/j.procbio.2008.02.017
40. Soden DM, O'Callaghan J, Dobson AD (2002) Molecular cloning of a laccase isozyme gene from *Pleurotus sajor-caju* and expression in the heterologous *Pichia pastoris* host. Microbiology 148(Pt 12):4003–4014. https://doi.org/10.1099/00221287-148-12-4003
41. Topakas E, Vafiadi C, Christakopoulos P (2007) Microbial production, characterization and applications of feruloyl esterases. Process Biochem 42:497–509. https://doi.org/10.1016/j.procbio.2007.01.007
42. Hassan S, Hugouvieux-Cotte-Pattat N (2011) Identification of two feruloyl esterases in *Dickeya dadantii* 3937 and induction of the major

feruloyl esterase and of pectate lyases by ferulic acid. J Bacteriol 193:963–970. https://doi.org/10.1128/JB.01239-10

43. Xu Z, He H, Zhang S et al (2017) Characterization of feruloyl esterases produced by the four *Lactobacillus* species: *L. amylovorus*, *L. acidophilus*, *L. farciminis* and *L. fermentum*, isolated from ensiled corn Stover. Front Microbiol 8:941. https://doi.org/10.3389/fmicb.2017.00941
44. Moukouli M, Topakas E, Christakopoulos P (2008) Cloning, characterization and functional expression of an alkalitolerant type C feruloyl esterase from *Fusarium oxysporum*. Appl Microbiol Biotechnol 79:245–254. https://doi.org/10.1007/s00253-008-1432-3
45. Mai-Gisondi G, Master ER (2017) Colorimetric detection of acetyl xylan esterase activities. Methods Mol Biol 1588:45–57
46. Rosenberg M, Roegner V, Becker FF (1975) The quantitation of rat serum esterases by densitometry of acrylamide gels stained for enzyme activity. Anal Biochem 66(1):206–212
47. Blum DL, Li XL, Chen H et al (1999) Characterization of an acetyl xylan esterase from the anaerobic fungus *Orpinomyces* sp. strain PC-2. Appl Environ Microbiol 65(9):3990–3995
48. Anderson JA (1934) The use of tributyrin agar in dairy bacteriology. J Bacteriol 27:69
49. Laemmli UK (1970) Cleavage of structural proteins during the assembly of the head of bacteriophage T4. Nature 227:680–685
50. Gilkes NR, Langsford ML, Kilburn DG et al (1984) Mode of action and substrate specificities of cellulases from cloned bacterial genes. J Biol Chem 259:10455–10459
51. Kasana RC, Salwan R, Dhar H et al (2008) A rapid and easy method for the detection of microbial cellulases on agar plates using gram's iodine. Curr Microbiol 57:503–507. https://doi.org/10.1007/s00284-008-9276-8
52. Casciello C, Tonin F, Berini F et al (2017) A valuable peroxidase activity from the novel species *Nonomuraea gerenzanensis* growing on alkali lignin. Biotechnol Rep 13:49–57. https://doi.org/10.1016/j.btre.2016.12.005
53. Falade AO, Eyisi O, Mabinya LV et al (2017) Peroxidase production and ligninolytic potentials of freshwater bacteria *Raoultella ornithinolytica* and *Ensifer adhaerens*. Biotechnol Rep (Amst) 16:12–17. https://doi.org/10.1016/j.btre.2017.10.001
54. Xu H, Guo MY, Gao YH et al (2017) Expression and characteristics of manganese peroxidase from *Ganoderma lucidum* in *Pichia pastoris* and its application in the degradation of four dyes and phenol. BMC Biotechnol 17(1):19. https://doi.org/10.1186/s12896-017-0338-5
55. Torres E, Ayala M, de Weert S et al (2010) Heterologous expression of peroxidases. In: Biocatalysis based on Heme peroxidases. Berlin Heidelberg, Springer, New York, pp 315–333
56. Donaghy J, Kelly PF, McKay AM (1998) Detection of ferulic acid esterase production by *Bacillus* spp. and *lactobacilli*. Appl Microbiol Biotechnol 50:257–260
57. Westereng B, Loose JSM, Vaaje-Kolstad G et al (2018) Analytical tools for characterizing cellulose-active lytic polysaccharide monooxygenases (LPMOs). In: Lübeck M (ed) Cellulases. Methods in molecular biology, vol 1796. Humana Press, New York, NY

INDEX

Nikolaos E. Labrou (ed.), *Protein Downstream Processing: Design, Development, and Application of High and Low-Resolution Methods*, Methods in Molecular Biology, vol. 2178, https://doi.org/10.1007/978-1-0716-0775-6,

C

D

E

F

G

H

I

J

K

L

M

N

O

P

Q

R

S

T

U

V

W

X

Z